## *Structural studies of novel hydrogen bonds by x-ray and neutron diffraction.*

Cowan, John Alexander

# Structural Studies of Novel Hydrogen Bonds by X-ray and Neutron Diffraction.

John Alexander Cowan.



*Submitted for the degree of Doctor of Philosophy, April 2002,*

*Department of Chemistry, University of Durham, Durham, U.K.*

*and*

*Institut Laue Langevin, Grenoble, France*

# Structural Studies of Novel Hydrogen Bonds by X-ray and Neutron Diffraction

*Submitted for the degree of Doctor of Philosophy, April 2002,*
*by John Alexander Cowan.*
*Department of Chemistry, University of Durham, Durham, U.K.*
*and*
*Institut Laue-Langevin, Grenoble, France.*

**Abstract**

The first set of measurements in this thesis discusses the hydrogen-bonding behaviour of 1,3-dimesitylimidazol-2-ylidene when co-crystallised with organic acids. 1,3-dimesitylimidazol-2-ylidene is an unusual molecule in which it is possible to have a carbon with a valence of two. In the co-crystals of 1,3-dimesitylimidazol-2-ylidene with pentafluorophenol, pentachlorophenol, 2(2-hydroxidophenyl)benzoxazole or 2,6-di-tert-butyl-4-methylpyridine the 1,3-dimesitylimidazol-2-ylidene becomes protonated and uncommonly short C-H···O hydrogen bonds are formed, the shortest has a C···O separation of 2.800(3)Å. In the 1:1 co-crystal of 1,3-dimesitylimidazol-2-ylidene and diphenylamine the first example of an N-H···C hydrogen bond is observed, with an N···C distance of 3.196(2)Å.

The 1:1, 1:2 and 2:1 co-crystals of 4,4'-bipyridine and benzene-1,2,4,5-tetracarboxylic acid (pyromellitic acid) have been studied by X-ray and neutron diffraction and the 1:1 and 1:2 co-crystals of 4,4'-bipyridine and benzene-1,2-dicarboxylic acid (phthalic acid) and the 1:2 co-crystal of bis-1,2-(2-pyridinium)ethane and benzene-1,2-dicarboxylic acid have been studied by X-ray diffraction. In the short N-H···O hydrogen bond observed in the 2:1 co-crystal of 4,4'-bipyridine and benzene-1,2,4,5-tetracarboxylic acid (N···O 2.5220(17)Å at 20K) the hydrogen atom was observed to change position with temperature; at 20K the hydrogen lies 1.207(3)Å from the nitrogen and 1.325(3)Å from the oxygen and at 296K it has moved across the hydrogen bond to lie 1.240(4)Å from the oxygen atom and 1.302(4)Å from the nitrogen atom.

The same phenomenon of temperature dependent proton migration has been observed by neutron diffraction in crystals of pyridine-3,5-dicarboxylic acid and upon deuteration of the hydrogen bonds the magnitude of the effect becomes greater. Solid-state density functional theory calculations have been used to provide theoretical models for the observed behaviour and to predict the inelastic-incoherent neutron-scattering spectra for pyridine-3,5-dicarboxylic acid in different degrees of deuteration.

John A, Cowan, 14th of April, 2002.

**Table of Contents**

**Table of Figures**

**1. Crystallography**



**2. The Co-crystals of N-Hetrocyclic Carbenes and Organic Acids.**

**3. Short Strong N-H···O / O-H···N Hydrogen Bonds in Co-crystals of Benzene-carboxylic Acids and Bipyridines.**

**4. Hydrogen Bonding in Pyridine-3,5-dicarboxylic acid.**



**5. Quantum Mechanical Modeling**

**Table of Tables**

**2. The Co-crystals of N-Hetrocyclic Carbenes and Organic Acids.**

**Supplementary Material.**

***ACKNOWLEDGEMENTS***

I would like to thank my two supervisors Professor Judith Howard and Dr. Garry McIntyre for their guidance, assistance, encouragement, patience and for their great good humour.

I am extremely grateful to the crystal producers, Dr. Ian Williams and Dr. Samuel Lo in Hong Kong, who produced the crystals used in sections 3 and 4 and Professor Matthew Davidson and Patrick Küpper for the crystals used in section 2.

Thanks also to Dr. Dean Myles, Prof. Clive Wilkinson, Dr. Sax Mason, Dr. Trevor Forsyth and Dr. Mark Johnson at I.L.L. for assistance with experiments and calculations, helpful advice and answers to questions. Similarly to Dr. Mike Leech and the group in Durham for assistance and help with X-ray diffraction experiments.

I would also like to thank the crystallography group in Durham for making it an enjoyable place to work and visit and go for a drink. Likewise to the gang in Grenoble, particularly Phil Callow, Charles and Mona Dewhurst, Julian Barratt, Judith Preston, Simon Levett, Ursula Lehnert, John and Lucy Stride and Matt Blakely for daft conversations at lunch and coffee times, skiing, cycling and going to O'Callaghans.

My warmest thanks to Stephanie Blair for love and affection throughout the last few years.

## 1. Crystallography

Crystallography – The scientific study of the structure and properties of crystals and their classification. *The Oxford English Dictionary.*

Early crystallographers were limited to studying the morphology and the macroscopic properties of crystals. With the demonstration by Friedrich, Knipping and Laue (1912) of the diffraction of X-rays by crystals and the solution of the crystal structure of sodium chloride by the Braggs (1913) from X-ray diffraction data, the science of crystallography began in earnest. The later demonstration of the diffraction of neutrons by a crystal by Mitchell and Powers (1936) opened up the new complementary field of neutron crystallography.

By careful measurement of the X-ray or neutron diffraction pattern from a crystal the crystallographer is able to determine accurately the average position of the atoms in the crystalline unit cell to within thousandths of an Ångstrom.

### 1.1 Diffraction Theory

X-rays and neutrons are diffracted by crystals. The diffraction pattern produced by shining light through two fine slits was observed and explained by Thomas Young in the early 19$^{th}$ century. The pattern can be explained by treating the incident light as a plane wave and each slit as a secondary point source. The interference pattern observed is produced by adding the phases of the waves at the screen (figure 1.1.1).

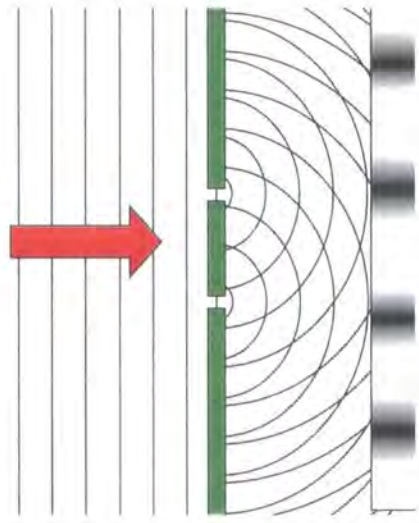

Figure 1.1.1. Diffraction from two slits. The plane wave of light is incident on the screen. The lines mark the wave crests. Each slit acts as a source of light. The screen shows an interference pattern where the circular waves add up constructively or destructively.

The diffraction pattern produced by shining X-rays or neutrons on a crystal can be treated in an analogous way. Each atom in the crystal is considered as a point source of waves. By considering the superposition of every wave scattered from every atom, the intensity of the scattering at every point in space can be calculated.

X-rays and neutrons can be produced with wavelengths of the same order of magnitude as the lattice spacing in crystals. X-rays are scattered by the electrons in a crystal while neutrons are scattered principally by the nuclei. The intensity of a reflection is given by the structure factor, $F(\mathbf{h})$ (equations 1a and 1b), which is the full expression for the sum of all the waves from all the atoms in the crystal.

$$F(\mathbf{h}) = \int \rho(\mathbf{r}) \exp(2\pi i \mathbf{r}.\mathbf{h})\, d\mathbf{r} \qquad \text{1a. For X-rays.}$$

The Fourier transform over all space $\mathbf{r}$, of the electron density $\rho(\mathbf{r})$ gives the structure factor for a specific reciprocal lattice vector, $\mathbf{h}$, which is equivalent to the position at which the structure factor is measured.

$$F(\mathbf{h}) = \sum_i b_i \exp(2\pi i \mathbf{r}_i.\mathbf{h}) \qquad \text{1b. For neutrons.}$$

The structure factor for neutrons is equivalent except as the nuclei are point particles it is only necessary to sum over all the nuclei, i, at positions $\mathbf{r}_i$ as there is no scattering density between the nuclei. $b_i$ is the scattering length of the nucleus, i.

In all the X-ray diffraction experiments in this work the atoms have been assumed to have spherical electron density centred at $\mathbf{r}_i$, and equation 1a becomes:

$$F(\mathbf{h}) = \sum_i f_i(\theta) \exp(-2\pi i \mathbf{r}_i.\mathbf{h}) \qquad 2.$$

$f_i(\theta)$, called the form factor, is equivalent to the scattering length for neutrons, but as the electron cloud of an atom has a shape X-rays reflected from different parts of the atom can interfere with each other, therefore the scattering length depends upon $\mathbf{h}$. If the atoms are assumed to be spherical the dependence on $\mathbf{h}$ can be simplified to just dependence on the scattering angle, $\theta$.

The scattered intensity is reduced by vibrational motion of the atoms. The structure factor is multiplied by a factor to account for this motion and becomes, for example for X-rays:

$$F(\mathbf{h}) = \sum_i f_i(\theta) \exp(2\pi i \mathbf{r}_i.\mathbf{h}) \exp(-T_j) \qquad 3.$$

Where

$$T_i = -8\pi^2 U^2 \sin^2\theta / \lambda^2 \qquad 4.$$

U is the isotropic mean-squared atomic displacement from the equilibrium position, $\lambda$ is the wavelength of the radiation used and $\theta$ is the scattering angle.

A crystal is made up of an effectively infinite three-dimensional repeating motif. The scattering need only be calculated for one unit of this motif, the unit cell. A consequence of this is that the scattered intensity is non-zero only at certain positions in space, called reflections.

$$n\lambda = 2d \sin\theta \qquad 5.$$

Bragg's law (equation 5) simplifies the above equations (equations 1,2 and 3) to describe the position of reflections in space. The atoms in the crystal are considered as being in planes, and the diffraction pattern is described by the reflection of the X-rays or neutrons from the planes. When Bragg's law is fulfilled the reflected waves interfere constructively and a reflection is observed. At all other positions the reflected waves interfere destructively and no scattering is observed.

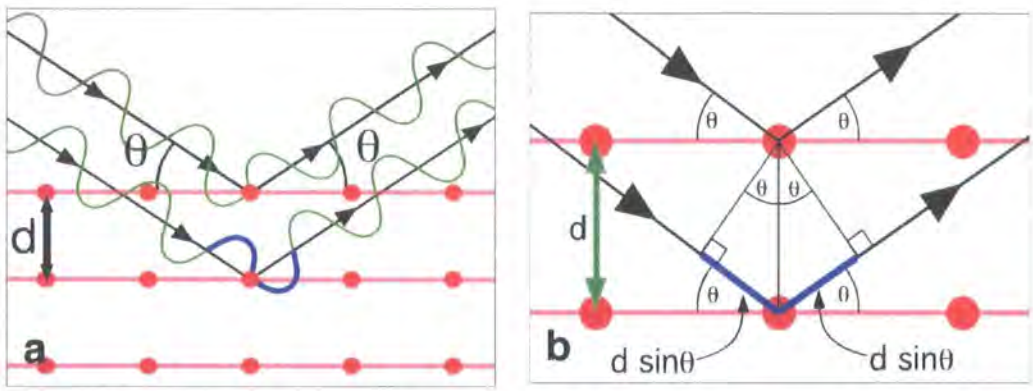


Figure 1.1.2.a and b. Bragg's Law. The waves are reflected at an angle $\theta$ from planes of atoms separated by distance d. The blue lines indicate the extra pathlength for waves which, when the path difference is one wavelength, equals $2d \sin\theta$.

n is an integer, $\lambda$ is the wavelength of the radiation, d is the spacing between the planes and $\theta$ is the angle of incidence and reflection of the radiation with respect to the planes (figure 1.1.2).

Bragg's law can also be described using vectors. Vectors can be used to describe the momentum of the incident and scattered particles (X-rays or neutrons), the change in the momentum of the particle upon scattering is called the scattering vector. The atomic planes

in a crystal can be described using a vector normal to the plane with magnitude inversely proportional to d, the separation of the planes, this vector is called a reciprocal lattice vector. A reflection can only be observed for a plane when the scattering vector is equal to the reciprocal lattice vector of that plane.

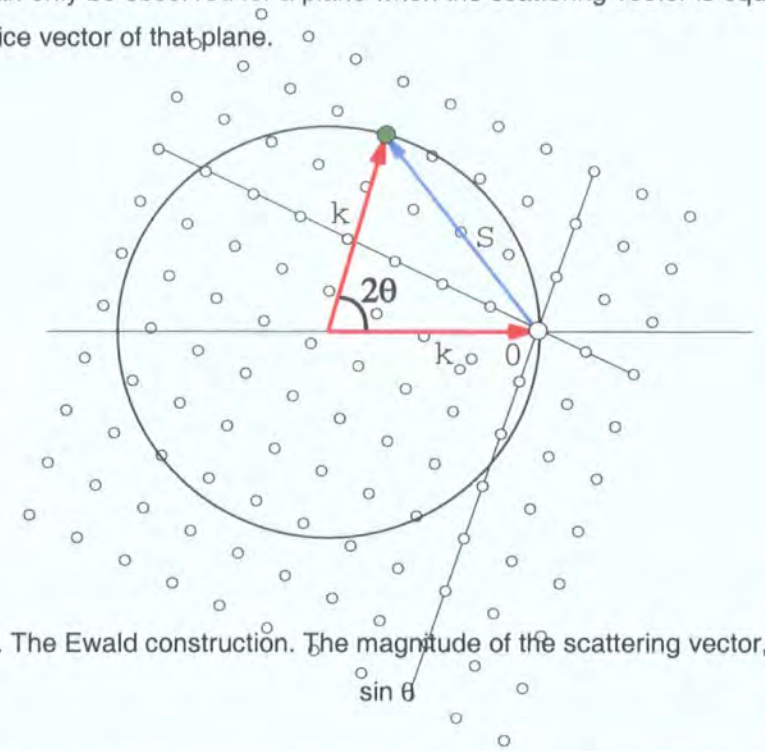


Figure 1.1.3. The Ewald construction. The magnitude of the scattering vector, S, equals 2k sin θ

The reflection condition can also be described using the Ewald construction (diagram 1.1.3). The incident beam, $k_0$, and scattered beam, k, are described by vectors with magnitude of $1/\lambda$. The origin of the reciprocal lattice, which describes all the possible planes in the crystal, is at the end of $k_0$. The vectors for the possible scattered beams describe a sphere in reciprocal space. A reflection will occur, for a particular orientation of the crystal, when a reciprocal lattice point intersects the sphere. Different reflections are obtained by rotating the reciprocal lattice until the required lattice point intersects the sphere.

The aim of a single crystal diffraction experiment is to determine accurately the electron density, with X-rays, or the nuclear density, with neutrons, inside the crystal. The structure factor is the Fourier transform of the scattering density therefore the density can be calculated using:

$$\rho(\mathbf{r}) = 1/V \sum_{h} F(\mathbf{h}) \exp(-2\pi i \mathbf{r}.\mathbf{h}) \qquad 6.$$

Where $\rho(\mathbf{r})$ is the scattering density, and V is the volume of the unit cell. The summation is over all **h**, i.e. over all reflections.

Therefore to recreate the scattering density as accurately as possible the maximum number of structure factors, F(**h**) must be determined.

### 1.2. X-rays and Neutrons

Neutrons for diffraction are produced using two different techniques, spallation and fission. At a spallation source, such as the U.K.'s ISIS, a pulse of high energy protons is bombarded against a stationary target, and the neutrons are smashed out of the nuclei in the target material. At a reactor source, such as the European High Flux Reactor at the Institut Laue Langevin (I.L.L.) in Grenoble, neutrons are produced during nuclear fission reactions in uranium. The neutron diffraction experiments in this work were all performed at the reactor source at the I.L.L.

The neutrons produced at both kinds of sources have much too high energies to be useful for diffraction purposes. Moderators are used to produce neutrons with the desired properties. The neutrons come to thermal equilibrium with the moderator and have wavelengths defined by that temperature. The kinetic energy of a neutron at temperature T is 3/2 kT, where k is the Boltzmann constant. The kinetic energy is also given by $p^2/2m$, where p is the momentum and m is the neutron mass. Using the deBroglie relationship $\lambda=h/p$, h is the Planck constant, produces the relationship:

$$\lambda^2 = h^2 / 3\,k\,T\,m$$

More usefully:

$$\lambda = 25.18 / \sqrt{T} \quad \text{in Ångstroms.}$$

Therefore thermal neutrons with a temperature ~300K have wavelengths of ~1.45Å. Hot neutrons have shorter wavelengths and cold neutrons have longer wavelengths.

An intense source of X-rays, can be produced from a sealed X-ray tube. Electrons are accelerated, using a large electric field, and then fired into a metal target. The incoming electrons knock inner core electrons from the atoms in the metal. The holes in the core are filled again producing X-rays of with characteristic wavelengths. Molybdenum and copper are the most commonly used anode materials producing X-rays of wavelength 0.71069Å and 1.5418Å respectively from the Kα lines. The X-ray diffraction data in this work have all been collected using molybdenum Kα radiation.

X-rays are scattered by the electrons is atoms and the scattering length of an atom at theta = 0° is proportional to the number of electrons in that atom. Neutrons are scattered by interactions with the nuclei and the variation in scattering length with atomic number cannot be explained easily. The neutron scattering length can vary wildly between isotopes for example the hydrogen has a scattering length of –3.74fm while deuterium has a scattering length of 6.67fm. Negative scattering lengths indicate a phase shift of $\pi$ on between the incident and scattered waves. Neutron scattering lengths can also be complex (these have been omitted from graph 1.2.1) which indicates a phase shift of $\varphi$ on scattering for a complex scattering length of $Ae^{i\varphi}$.

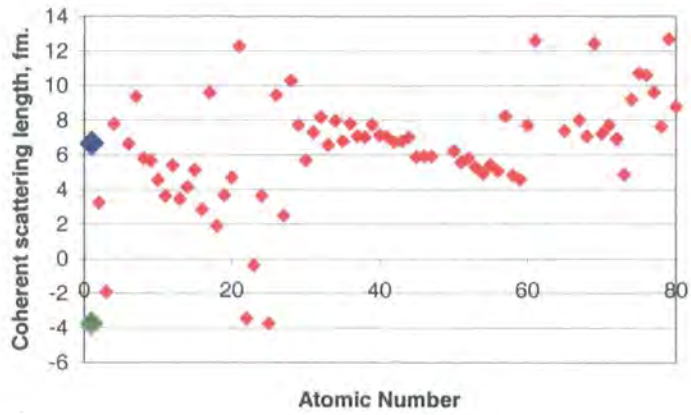


Graph 1.2.1. Bound coherent neutron scattering lengths (Sears, 1992). 1 fm = $10^{-15}$ metres. The scattering lengths are the values for the naturally occurring elements. The blue diamond is deuterium (6.67 fm), the green diamond is hydrogen (-3.74 fm).

The variation of neutron scattering length is an extremely useful property. Most heavy atoms have scattering lengths of between 5 and 15 fm, which means the light atoms, most importantly hydrogen, have comparable scattering lengths which are not dwarfed by the scattering from the heavy atom, as would occur for X-rays. Less importantly the variation in scattering length often produces greater contrast between atoms with similar numbers of electrons, which may be useful if chemical knowledge cannot be used to distinguish between different elements.

The neutron absorption cross-section of atoms shows wild variations that do not depend on the number of electrons. X-ray diffraction experiments can be severely hindered by very strong absorption by heavy atoms. Although there are some exceptions (gadolinium has an absorption cross section of 49700 barns compared with lead which has an absorption cross-section of 0.171 barns for neutrons with $\lambda$ = 1.798Å, 1 barn = $10^{-24}cm^2$) most atoms show negligible absorption for neutrons.

The effects of covalent bonding may significantly distort the electron cloud so that it is not centred upon the nucleus. Neutrons see the nuclear positions while X-rays see the electron cloud. This is especially important for hydrogen atoms. X-H bond lengths deduced from X-ray diffraction data are found to be consistently shorter than those found by neutron diffraction. In short strong hydrogen bonds where the electron cloud around the hydrogen atom may be distorted by the donor and acceptor atoms only neutron diffraction can accurately determine the hydrogen atom position.

### 1.3. Diffractometers

Four diffractometers have been used for the data collections in this work. All the X-ray experiments were carried out on the Bruker SMART-CCD diffractometer in Durham. The neutron experiments were carried out on the four-circle diffractometers D9 and D19 or the Laue diffractometer LADI at the I.L.L. in Grenoble.

#### 1.3.1. D9 and D19

D9 and D19 are four-circle diffractometers at the I.L.L. The instruments are very similar apart from a few details. A four-circle diffractometer has four circles, three to manipulate the crystal into the desired orientation (the Eulerian angles of classical mechanics) and one to move the detector. The crystal is placed at the centre of the diffractometer at the point where the axes of all of the circles intersect. The crystal is mounted on the end of the $\phi$-circle which is mounted upon the $\chi$-circle. The $\chi$-circle in turn is mounted upon the $\omega$-axis. The detector is mounted upon the $\gamma$-axis, which is coaxial with the $\omega$-axis, and for equatorial beam geometry can also be called the $2\theta$-axis.The four angles of these circles are called the diffractometer angles and are used to define the orientation of the crystal and the Bragg angle.

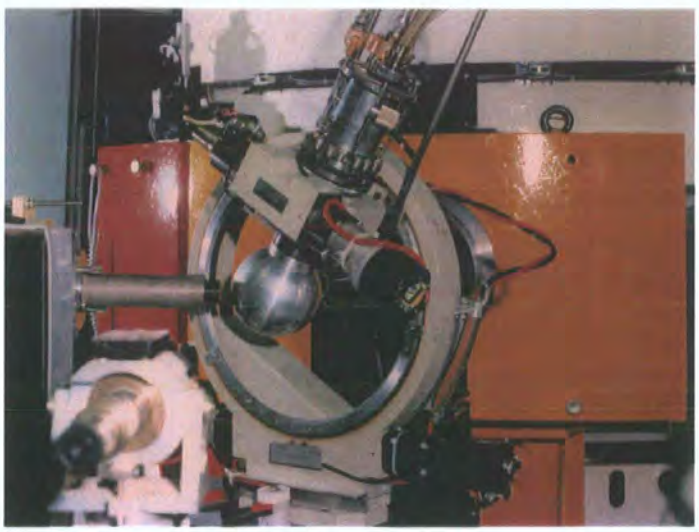

Figure 1.3.1. The D9 Eulerian cradle. The sample is mounted in the centre of the metallic sphere which is the outer aluminium heat shield of the Displex cryorefrigerator. This sphere is mounted upon the $\phi$-circle. The large circle nearly perpendicular to the page is the $\chi$-circle. The $\omega$-axis is parallel to the page and runs upwards through the centre of the $\chi$-circle. The neutrons approach the sample from behind the orange shielding. The grey horizontal tube close to the heat shield is the detector. The telescope used to centre the crystal is visible in the foreground.

The crystal can be cooled to as low as 15 K in both diffractometers using Displex closed cycle cryorefrigerators (Archer and Lehmann, 1986) mounted on the $\phi$-circles of the diffractometers. The crystal mounted on the Displex is enclosed in three heat shields, the inner shield is made from vanadium which has a very low coherent scattering length, the outer two shields on D9 (outermost is the sphere visible in figure 1.3.1) are made of aluminium. On D19 the innermost and outer shields are made from vanadium and the middle one made from aluminium. A correction for absorption by these heat shields is made at the data processing stage.

D9 usually receives its neutrons from a guide that is aimed at the hot neutron source near the reactor core. The hot neutron source was not present during the experiments in this work and the neutrons at the sample were thermal neutrons. A copper (2 2 0) monochromator was used to select neutrons of wavelength ~0.84Å from the guide and an erbium filter used to remove the $\lambda$ / 2 neutrons. The beam is then collimated using highly neutron-absorbing $B_4C$ to produce a beam slightly larger than the crystal, so that the entire volume of the crystal is always in the beam while the background is made as low as possible.

D19 is installed on a thermal neutron guide. Germanium (1 1 n) [where n is an odd number] or (3 3 5), copper (2 2 0) and graphite (0 0 2) monochromators are available, the germanium (1 1 5) reflection was selected during all the experiments in this work. $B_4C$ collimators are again used to obtain the optimal size for the beam.

D9 is equipped with 32 * 32 pixel position-sensitive detector (each pixel covers ~ 0.25° * 0.25°) which is mounted on the $\gamma$-circle in the equatorial plane. D19 has a 64° * 4° position-sensitive detector (Thomas et al. 1983) mounted with the long dimension vertical and therefore can measure reflections ±32° from the equatorial plane.

### 1.3.2. Bruker SMART-CCD

The Bruker SMART-CCD diffractometer uses molybdenum K$\alpha$ radiation, which has a wavelength of 0.71069Å, monochromated by a graphite (1 1 1) monochromator. Lead pinholes are used to collimate the beam. It is equipped with a large position-sensitive detector, which is made from a scintillating screen mounted in front of optical fibres that channel the scintillation produced on the screen by the X-rays onto a 1K CCD-chip (charge-coupled device). The crystal is mounted upon the $\phi$-circle of the diffractometer, which is fixed to the $\omega$-circle at an angle equivalent to 54° in $\chi$. The large position-sensitive detector is mounted on a $\gamma$-circle.

The temperature of the crystal is maintained using an Oxford Cryosystems Cryostream, which blows a stream of dry nitrogen gas over the crystal and can be used to obtain

temperatures between 90K and 370K. For very low temperatures an Oxford Cryosystems HELIX helium-flow device can be used to obtain temperatures down to 30K (Goeta et al. 1999).

### 1.3.3. LADI – LAue DIffractometer

The flux produced by a reactor source, unlike the X-rays produced by a sealed tube, has no preferred wavelengths. A broad spectrum is produced over a wide range of wavelengths, a monochromator selects only a small part of this spectrum. An old technique has been revived to exploit the total neutron flux. Laue diffraction is the use of a white beam and a stationary crystal and was the first type of X-ray diffraction observed (Freidrich et al. 1912).

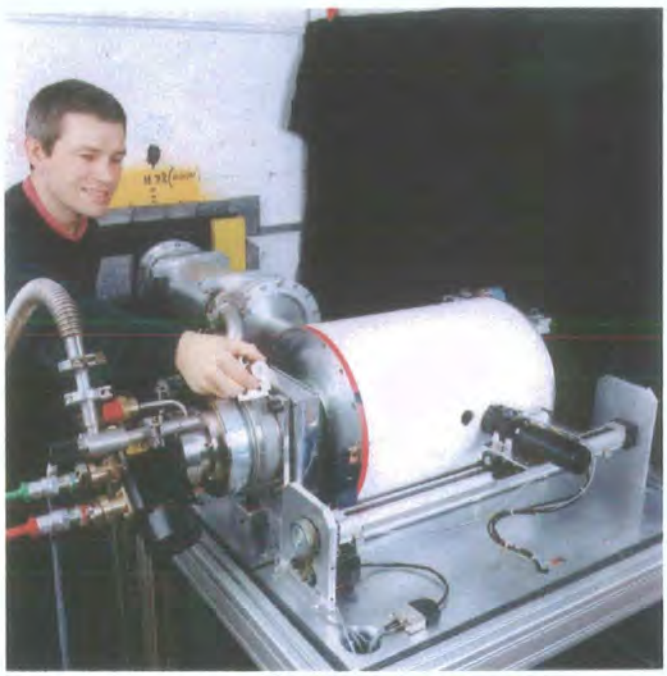

Figure 1.3.2. The instrument scientist, Dr. Dean Myles, attending to the LADI diffractometer. The crystal is mounted in the centre of the cylinder. The white image plates are on the outside of the cylinder. The laser and photomulitplier tube is seen at the front of the cylinder. A light-tight cover encloses the detector and scanner during operation.

The LADI instrument (Cipriani et al. 1996) was designed for protein crystallography and installed on a cold neutron beam. It was moved for test time to the thermal neutron guide H22 where we collected data.

The crystal is mounted at the centre of an aluminium drum, which is coated on the outside with neutron-sensitive image plates (Nimura et al. 1994). The neutrons illuminate the crystal and because of the white beam many reflections are observed simultaneously. The high flux and large area detector means that experiments can be performed on smaller crystals in considerably less time than for conventional neutron single-crystal diffraction experiments.

The beam from the guide tube is collimated using $B_4C$ pinholes to bathe the crystal entirely with neutrons. The crystal is mounted on a large aluminium baton which is inserted into the drum from one end. The only axis of rotation for the sample is about an axis parallel to the axis of the cylinder.

The drum has a radius of 160mm, therefore a circumference of 1000mm, and a length of 400mm. Four neutron images plates with area 400mm * 200mm cover 80% of the outside of the drum. The crystal is exposed while it and the detector are stationary. After an exposure the beam is closed and the detector drum spins at 350 r.p.m. The image is read from the image plates by a laser and photomultiplier tube which moves along the drum while it spins and scans the whole outer surface of the drum in a way analogous to an antique cylindrical phonograph. After reading the image to file from the image plate the residual image is erased by a fluorescent lamp shining on the spinning drum to be ready for the next exposure.

LADI is equipped with a Displex cryorefrigerator similar to the D9 and D19 examples which can reach temperatures as low as 15K.

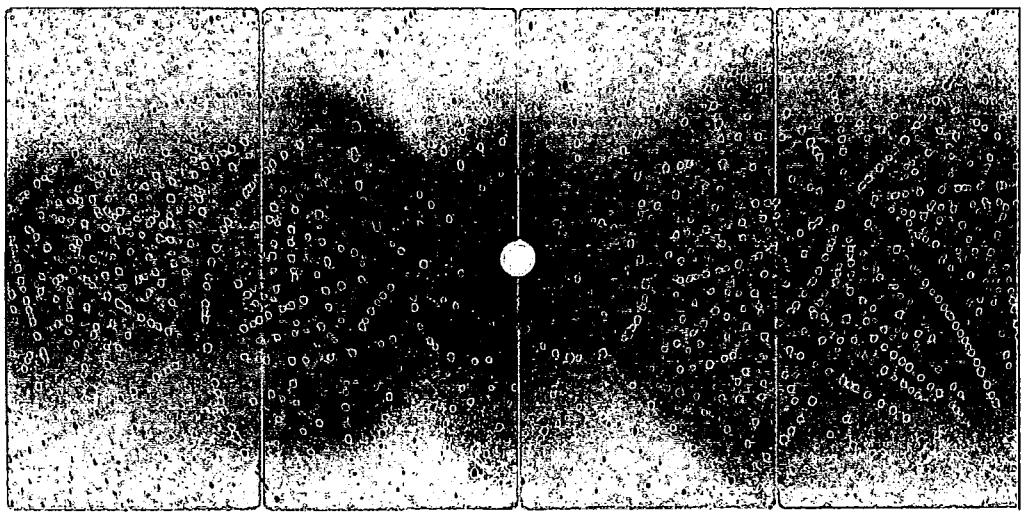

Figure 1.3.3. An example of a diffraction pattern from LADI. The crystal used was $CsV(SO_4)_2 \cdot 12D_2O$ with an exposure time of 45 minutes. The hole in the centre of the pattern is for the direct beam. The image plates are wrapped around the drum of the detector and the circumference of the drum runs horizontally across the page. The vertical white lines are the gaps between the four image plates. The broad streaks radiating out from the centre are caused by scattering from the cryostat heat shields.

### 1.4. Diffraction Experiments

#### 1.4.1 Preliminary Steps

Despite the differences between the diffractometers the experimental procedures are quite similar.

Perhaps the most consequential factor in the success of a single crystal experiment is the quality of the crystal. The crystal chosen should, if possible, be the optimum size and shape according to its absorption and the dimensions of the radiation beam. The crystal should be slightly smaller than the dimensions of the uniform cross section of the beam so that a constant volume, the entire crystal, is always diffracting. If possible, to reduce the effects of absorption and facilitate the correction, the crystal should be isotropic. When rotated between two polarisers on a polarising microscope, the total crystal should totally extinguish polarised light in a small angle; failure to do so can indicate a poor mosaic spread or a twinned crystal.

The mounting procedures for the neutron diffraction experiments are similar. For neutrons the crystal is attached to a vanadium pin using Kwikfil, a car bodywork filler with good properties at very low temperatures.

The crystals used in the X-ray experiments were mounted in degassed oil upon a hair inserted into the end of a syringe needle. The crystals were all flash frozen in the nitrogen stream which freezes the oil, firmly attaching the crystal to the hair. The coating of oil around the crystal seals it from the air and moisture to which some of the crystals were sensitive.

The crystal is centred on the diffractometer so that upon rotation about any axis its centroid remains stationary. On D9, D19 and the SMART the crystal is mounted upon the diffractometer and the position refined using perpendicular translations with the aid of a telescope. It is impossible to see the crystal when it is mounted upon LADI therefore the crystal is centred upon a specially built mounting stage which has perpendicular telescopes focussed upon the ideal crystal position.

Although the crystal may appear to be good quality when examined with a microscope it may not be good enough for an experiment. A truer test is to observe the Bragg peaks. This is most easily done on the SMART, where a few short exposures can be taken and the shapes of any Bragg peaks observed within a minute. If Bragg peaks are present and of compact shape then a short data collection can be performed to determine the unit cell and orientation of the crystal; this procedure is known as indexing. The unit cell obtained can be checked to verify that the crystal is of the desired compound and if necessary against the

structures in Cambridge Crystallographic Database (Allen and Kennard, 1993). The shape of the Bragg peaks in the ω-direction can indicate the quality of the mosaic spread of the crystal. If the crystal has too broad a mosaic spread and a long cell edge, reflections may overlap and integration of the reflections made difficult.

In principle it is possible to index an unknown crystal from scratch using the four-circle neutron diffractometers however neutron diffraction experiments are rarely performed on unknown samples. With knowledge of the unit cell and an educated guess at the orientation of the crystal from observing the crystal morphology indexing can be performed quickly and the peak shapes observed to establish the crystal quality.

On LADI a single diffraction pattern should allow indexing and evaluation of the crystal quality. No moving of the crystal is required and the mosaic spread can be evaluated from the size of the Bragg peaks, courtesy of the white beam.

The crystals on the SMART were all flash cooled. The Displex cryorefrigerators do not allow easy flash cooling and the low temperatures in the neutron experiments were achieved by slow cooling at a rate of ~2Kmin$^{-1}$ while monitoring a strong reflection to observe any change in the unit cell, orientation or crystal quality. On LADI 10-20 minute exposures were taken during cooling to observe any temperature-dependent changes.

Precise measurement of the unit cell before data collection is essential on D9 and D19, though less important on LADI and the SMART, as D9 and D19 have small area detectors compared with the other two instruments. The orientation is needed in order to be able to position the diffractometer so that the reflections are observed fully on the detector. The data collection strategy depends upon the crystal lattice system. This is most important for the four-circle diffractometers in order to measure the maximum number of unique reflections and to minimise the time spent between reflections. The crystal system also affects the data collection strategy for LADI, and for the SMART, though less critically.

### 1.4.2. Data Collection

The reflections are collected on D9 one-by-one. The crystal system determines how many unique reflections are required, for example only one quarter of the total reflections are required in monoclinic systems as $|F(hkl)| = |F(h\bar{k}l)| = |F(\bar{h}\bar{k}\bar{l})| = |F(\bar{h}k\bar{l})|$. A few other reflections are measured, usually in the low-angle region, to verify the crystal system and space group. During the data collection two or three test reflections are repeatedly measured to check for crystal deterioration. The reflections are almost always collected in constant monitor mode, the monitor being a low-efficiency detector in the incident beam. Collecting for

a constant count on the monitor compensates for any variation in the reactor power or any variation in flux caused by other instruments.

The data collection on D19 is similar to D9, except D19 mostly works in normal-beam geometry. The detector on D9 is in the equatorial plane and the crystal must be oriented to place the reflections in the equatorial plane. D19's detector extends ±32° out of the equatorial plane which means a more efficient data collection strategy may be followed. The detector is held at constant $\gamma$ and the crystal rotated about $\omega$ at constant $\phi$ and $\chi$ to bring the reflections quasi simultaneously into the diffracting position at different positions on the detector. The optimum choice of $\phi$, $\chi$ and ranges of $\omega$ are worked out with the aid of the program HKLGEN (ILL Program).

On the SMART the data-collection strategy requires less consideration. The data are collected by scanning $\omega$ at constant $\phi$ and $\chi$ ($\chi$ cannot be changed) in the same way as for D19 in normal-beam geometry. The size of the detector means that normally only four $\phi$ settings and one detector setting are required to collect a complete set of data up to 55° in $2\theta$, equivalent to a d-spacing of 0.77Å for molybdenum radiation. Collecting a full sphere or hemisphere of data using the standard programmed settings can compensate for any uncertainty over the crystal system. Indeed this is a wise strategy as the frames can be archived for later reference if any problems come to light during the structure solution and refinement stages.

On LADI the data collection strategy is straightforward, as there is only one axis of rotation for the crystal. A data set collected on LADI requires a great deal of redundancy to facilitate the wavelength normalisation. Steps in the rotation angle of ~25° are optimal to give overlap of reflections for the relative scaling of the images and to obtain good coverage of unique reflections. Some reflections are lost through the ends of the drum, for high-symmetry systems these may be measured in other regions of the detector, but often the crystal needs to be remounted to collect these reflections.

The crystal is oriented for a reflection in equatorial-plane mode with the scattering vector in the equatorial plane, the scattering plane in the crystal can be rotated 360° around the scattering vector and the same plane will diffract, this is known as a $\psi$ rotation. During data collections on D9 and D19 a scan of one reflection at different $\psi$ angles, which give different path lengths for the beam inside the crystal, is very useful to check the corrections for absorption and extinction. Similar information can be determined from the over measurement of reflections in LADI and SMART.

## 1.5. Data Processing

### 1.5.1. Unit-Cell Dimensions

To obtain the most accurate integrated intensities the integration programs need to be able to find the reflections in the data, therefore the most accurate orientation and unit-cell dimensions must be determined.

On the SMART, D9 and D19 the procedures are very similar, a preliminary integration is performed to find the reflections. The SMART software (Bruker, 1998) is used to select 1000 of the strongest high-angle reflections from different regions of the data set, the unit-cell dimensions and orientation are determined and refined to get the optimum agreement between the predicted and observed reflection positions. D9 and D19 use the orientation matrix used in the data collection to perform the integration over all the measured reflections, from the strongest reflections the unit cell is refined iteratively using the programs RAFD9 and RAFD19 (Filhol, 1998) respectively.

The Bragg equation can be rewritten as $\sin\theta = n\lambda / 2d$. On LADI only $\theta$ is measured therefore only the ratio of $\lambda/d$ can be determined. The wavelength of the neutrons in a given reflection on LADI is determined from the unit-cell parameters. Therefore the unit-cell dimensions can not be refined absolutely, but only the cell angles and the relative cell dimensions can be refined. The detector is unlikely to be a perfect cylinder and parameters are also refined in the indexing to account for distortions in the shape, however these may mask or be correlated with errors in the orientation or unit cell. Further on in the processing the wavelengths attributed to the reflections are used to deduce the incident flux spectrum, and therefore any errors introduced by poor indexing may propagate and introduce more errors later. Although the unit-cell dimensions cannot be determined accurately the best fitting unit cell parameters for integration are still required and are calculated using the program LAUEGEN (Campbell, 1995)

On LADI the approximate values for the minimum and maximum wavelengths and the minimum d-spacing that produce observable reflections must be determined. If these are incorrect reflections that are observable may not be integrated, reflections that are made from one wavelength of neutrons may be believed to be made up of two or more wavelengths in which case they will be discarded, or reflections made up of two or more wavelengths may be indexed as being made up of one wavelength introducing errors. The wavelength range and d-spacing range are determined within the program LAUEGEN (Campbell, 1995) following the procedure of Hao et al. (1995).

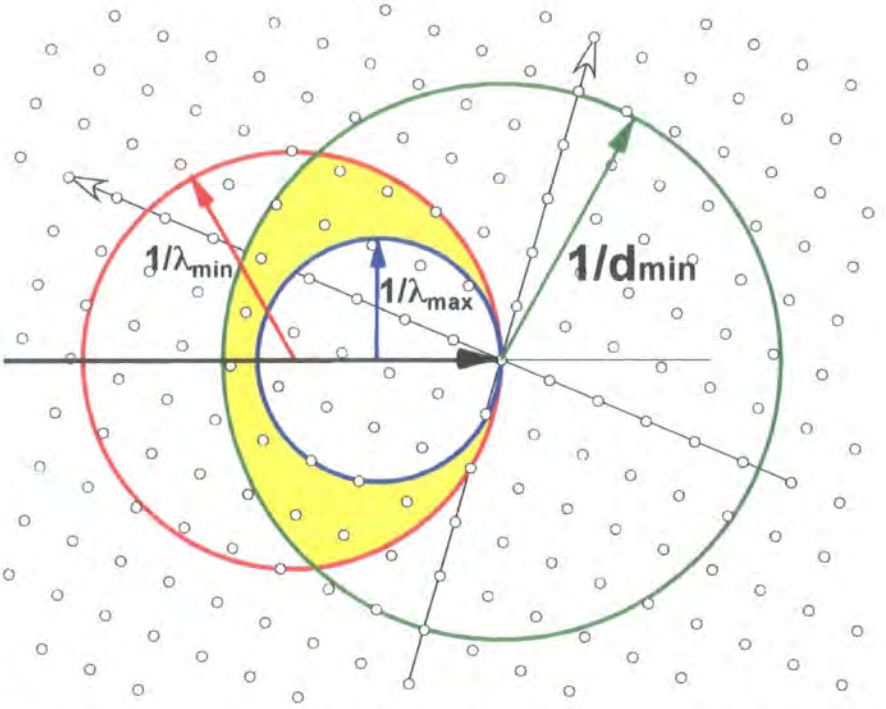


Figure 1.5.1. Ewald construction for Laue diffraction. Reflections can in principle be observed from wavelengths between $\lambda_{min}$ and $\lambda_{max}$, between the blue and the red circles. The observable reflections are in practise observed out to a resolution limit of $d_{min}$, the green circle, that depends mainly upon the crystal quality.

### 1.5.2. Data Reduction

The intensity of a reflection is proportional to the square of the structure factor for that reflection.

$$I(\mathbf{h}) = I_o(\lambda)\,|F(\mathbf{h})|^2\,L\,P\,A\,E\left(\frac{\lambda^3 V}{V_c^{\,2}}\right) \qquad 7.$$

The intensity of a reflection I(**h**) is given by equation 7. $I_o(\lambda)$ is the wavelength dependent incident intensity. L is the Lorentz factor, a geometrical factor that depends on the manner in which the reflection is measured. P is the polarisation factor which is only necessary for X-rays. A is the correction for absorption by the crystal. E is the extinction correction. V and $V_c$ are the volumes of the crystal and the unit cell respectively.

The data from D19 and D9 are integrated using different versions of the same program, RETREAT on D19 and the modification RACER (Wilkinson et al. 1988) on D9. The data from LADI are integrated using a two-dimensional implementation of the same algorithm using the program INTEGRATE+. The data from the SMART are integrated using the program SAINT (Bruker, 1998).

Lorentz corrections (McIntyre and Stansfield, 1988) are applied in RACER, RETREAT and SAINT after integration. SAINT also applies the polarisation correction to account for any polarisation of the X-rays. The equivalent to the Lorentz correction, which takes into account the wavelength range in a reflection, is applied in the wavelength normalisation program for the LADI data.

The absorption of radiation on passing through a crystal is given by Beer's law (equation 8)

$$I = I_0 e^{-\mu t} \qquad 8.$$

where $\mu$ is the absorption coefficient, t is the pathlength in the crystal, I is the observed intensity and $I_0$ the initial intensity. The contributions from all of the crystal must be summed and the overall absorption factor, A, for a reflection is given by:

$$A = 1/V \int_V e^{-\mu t} dV \qquad 9.$$

In the experiments on D19 and D9 the face separations, therefore the volume of the crystal, are measured and the absorption correction is computed with DATAP (Coppens, 1970) for D9 and D19ABS (Matthewman et al. 1982) for D19 which both use the Gaussian integration method of Busing and Levy (1957). If there is significant absorption the X-ray data are corrected using the program SADABS (Sheldrick, 1996) which uses the equivalence between reflections to calculate an effective crystal shape, this requires no face indexing. No absorption correction was applied to the data from LADI.

A correction for attenuation of the beam by the cryostat heat shields is applied on D19 and D9. Any reflections, which pass through the ends of the cylindrical heat shields, are discarded.

Neutron absorption coefficients are calculated from the tabulated values in Neutron News, (Sears, 1992). The neutron absorption by hydrogen is estimated using the empirical formula of Howard et al. (1987).

Any isotropic extinction effects, which were mostly negligible in the crystals discussed in this work, were corrected for in the structural refinement program. There are two types of extinction, in each the crystal described as being made up of small, slightly misaligned sub crystals in a mosaic. Primary extinction occurs when the mosaic blocks are closely aligned and interference effects between crystals scattered from different blocks cause reduction in the observed intensity. Secondary extinction occurs when the intensity of the incident beam on a mosaic block is reduced because an earlier similarly aligned block has already diffracted significant intensity from the beam.

The incident flux on LADI is determined by using the internal agreement between reflections, which is why a large amount of redundancy is required. In general only reflections between

1-2 Å are used in the normalisation as the reflections outside of this range are too weak or too few. The procedure is performed by the program LAUENORM (Campbell et al. 1996). Scale factors are determined and applied between images to account for the different exposure times and any variation of the crystal volume in the beam.

A good indication of the quality of the data comes from Rint and R(σ). These figures have more value for SMART and LADI data where more equivalent data are measured compared with D9 and D19 where the time taken to measure a data set means that few equivalent reflections are measured. Low values for Rint and R(σ) indicate good quality data. Rint is a measure of the agreement between observations of equivalent reflections. R(σ) is a measure of the strength of the reflections compared to the uncertainty of their value, a low R(σ) indicates strong well-measured data, a high R(σ) indicates that the data contain a lot of weak reflections.

$$R\text{int} = \frac{\sum_{h}\sum_{i=1}^{n}\left\langle I(h)\right\rangle - I(h)_i}{\sum_{h}\sum_{i=1}^{n} I(h)_i}$$

where n is the number of observations of reflection h.

$$R(\sigma) = \frac{\sum_{h}\sigma(F_o(h))^2}{\sum_{h}(F_o(h))^2}$$

where $\sigma(F_o)$ is the estimated uncertainty in the measurement of $F_o$.

### 1.6. Structure Solution and Refinement

The structures in this work have all been solved by direct methods from X-ray diffraction data. Since the intensity of a reflection is proportional to $|F(\mathbf{h})|^2$, the phase of $F(\mathbf{h})$ is lost and cannot be recovered experimentally in a normal diffraction experiment. Two assumptions are made: that the scattering density is positive everywhere in the crystal and that the scattering is from discrete points. Various mathematical "tricks" are then used to deduce the probable phases and rule out the improbable phases of as many structure factors as possible, the remaining few are guessed until a reasonable trial solution is found. Although direct methods could work with neutron-diffraction data in practice X-ray diffraction data are more commonly used to solve the structure. The cost of neutron-diffraction facillities means neutron-diffraction experiments are rarely allowed to be performed on crystals with unknown structures.

Once a trial structure has been created the model is refined using least squares to minimise the differences between the calculated and the measured structure factors. The refinement is continued until there is no further improvement. In general for each atom nine parameters were refined, three positional parameters and six anisotropic displacement parameters. Only an isotropic displacement parameter could be refined for the hydrogen atoms in the X-ray refinements. All the structure solutions and refinements were carried out using SHELX programs (Sheldrick, 1997).

The quantity minimised in the least squares refinement is the weighted R-factor, with each reflections weighted by a factor, w, according to its expected accuracy.

$$wR2 = \frac{\sum_h [w(F_o(h)^2 - F_c(h)^2)^2]}{\sum_h [w(F_o(h)^2)^2]}$$

The R-factor, R1, and the goodness of fit, GoF (sometimes known as S) are other indicators to the quality of the refinement.

$$R1 = \frac{\sum_h (F_o(h) - F_c(h))}{\sum_h F_o(h)}$$

$$G.o.F = S = \left[ \frac{\sum_h w[(F_o(h)^2 - F_c(h)^2)^2]}{(n-p)} \right]^{1/2}$$

where n is the number of observations and p is the number of parameters refined.

## 1.7. References


Allen, F.H., Kennard. O. (1993) Chem. Des. Autom. News, **8**, 31-37.

Bragg, W.H., Bragg, W.L. (1913). Proceedings of the Royal Society London. **A88.** 428-438.

Bruker (1998). SMART and SAINT. Bruker AXS. Inc. Madison, Wisconsin, USA.

Busing, W.R., Levy, H.A. (1957). Acta Cryst. **10.** 180-182.

Campbell, J.W. (1995). J. Appl. Cryst. **28.** 228-236.

Campbell, J.W., Habash, J., Helliwell, J.R., Moffat, K. (1996). Quarterly for Protein Crystallography, 18.

Cipriani, F, Castagna, J.-C., Wilkinson, C., Oleinek, P., Lehmann, M. (1994). J. Neutron. Research, **4.** 79-85.

Coppens, P. (1970). Crystallographic Computing. Edited by Ahmed, F.R. Munksgaard International Booksellers and Publishers Ltd. 255-270.

Filhol, A. (1998). RAFD19 and RAFD9. Institut Laue Langevin, Grenoble, France.

Freidrich, W., Knipping, P., von Laue. M. (1912). Sitzungsberger. Math. Nuturwiss. Kl. Bayer. W. München, 303-322.

Goeta, A.E., Thompson, L.K., Sheppard, C.L., Tandon, S.S., Lehmann, C.W., Cosier, J., Webster, C., Howard, J.A.K. (1999). Acta Cryst. **C55**, 1243-1246.

Hao,Q., Harding, M.M., Campbell, J.W. (1995). J. App. Cryst. **28.** 447-450.

Howard, J.A.K., Johnson, O., Schultz, A.J., Stringer, A.M. (1987). J. Appl. Cryst. **20.** 120-122.

McIntyre. G.J., Stansfield, R.F.D. (1988). Acta Cryst. **A44.** 257-262.

Matthewman, J.W., Thompson, P., Brown, P.J. (1982). J. Appl. Cryst. **15.** 167-173.

Mitchell, D.P., Powers, P.N. (1936). Phys. Rev. **50.** 486-487.

Niimura, N. Karasawa, Y., Tanaka, I., Miyahara, J., Takahashi, K., Saito, H., Koizumi, S., Hidaka, M. (1994). Nucl. Instrum. Meth. **A 349.** 521-525.

Sears, V.F. (1992). Neutron News. Vol 3. No 3. 26-37.

Sheldrick, G.M. (1996). SADABS. University of Göttingen, Germany.

Sheldrick, G.M. (1997). SHELXL97 and SHELXS97. University of Göttingen, Germany.

Thomas, M., Stansfield, R.F.D., Berneron, M., Filhol, A., Greenwood, G., Jacobé, J., Feltin, D., Mason, S.A. (1983). Position Sensitive Detection of Thermal Neutrons, edited by Convert, P. and Forsyth, J.B. Academic Press, 344-350.

Wilkinson, C., Khamis, H.W., Stansfield, R.F.D., McIntyre, G.J. (1988). J. Appl. Cryst. **21.** 471-478.

## 2. The Co-crystals of N-Heterocyclic Carbenes with Organic Acids; A Study of Weak Intermolecular Interactions

We have studied co-crystals of a variety of weak organic acids with 1,3-dimesitylimidazol-2-ylidene by low temperature X-ray diffraction. 1,3-dimesitylimidazol-2-ylidene contains a stable carbene atom, a divalent carbon atom with two non-bonding electrons and no formal charge. Unusual intermolecular interactions are observed involving this carbene atom or the protonated imidazolium ion, including an N-H···C hydrogen bond and extremely short C-H···O hydrogen bonds.

### 2.1. Supramolecular Chemistry

Supramolecular chemistry has been described as chemistry beyond the molecule (Lehn, 1988, Desiraju, 2001). It describes the study of the interactions between molecules and the use of this knowledge to create useful structures from combinations of molecules (Desiraju, 1995, Prins et al. 2001).

The most accomplished supramolecular chemist is nature. The commonest illustration is the binding of a substrate by an enzyme. The active site of the enzyme is finely adapted in shape and environment to select and attract the desired substrate from solution. The same forces, although not strictly supramolecular, control the conformation of large biological molecules such as DNA and proteins.

#### 2.1.1. Applications

Supramolecular chemistry has potential applications and real challenges over a broad spectrum of scientific disciplines.

Chemistry: Predicting polymorphism, which can alter the efficacy and even toxicity, of drugs (Desiraju, 2001). Creating nanoporous solids to act as efficient and stable catalysts (Brunet at al 1997). Creating working supramolecular machines on surfaces (Chia et al. 2001)

Physics: The design of solid state structures with novel properties, for example non-linear optical properties (Gangopadhyay and Radhakrishnan, 2001) or of liquid crystals (Lee et al. 2001)

Biology: The understanding of protein folding and conformation. Understanding the processes at binding sites and the mechanisms of enzymes.

Hence supramolecular chemistry is a rising and fashionable discipline in science. In a search of the literature database 'Web of Science' for the words dinosaur, organometallic and supramolecular, dinosaur and organometallic had an approximately constant frequency of

occurrences, while the number of occurrences of supramolecular has grown exponentially over the past twenty years. And an issue of Angewandte Chemie rarely passes without 'molecular recognition', 'self-assembly' or 'supramolecular' figuring prominently in the key words for articles.

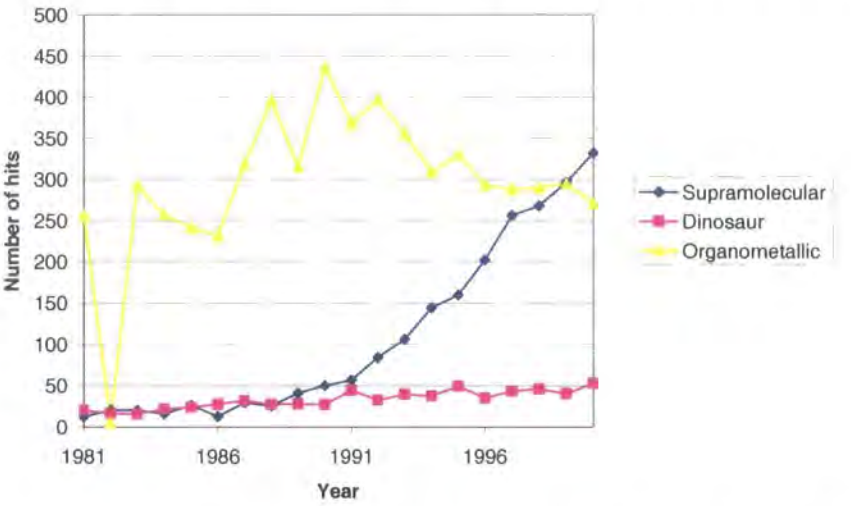


Graph 2.1. Number of occurrences per year in article titles from 'Web of Science'. The graphs are normalised to the total number of database entries. Bizarrely in 1982 there were only five hits for organometallic.

One of the many challenges for supramolecular chemistry is the understanding of the weak non-covalent interactions between molecules. These weak interactions such as hydrogen bonds, halogen-halogen interactions, and van der Waals forces are unpredictable and sensitive to subtle changes in the chemistry. Studying simple crystals, in which there are a smaller number of variables, should help us pin down the elusive nature of these interactions.

### 2.1.2. Hydrogen bonds

Hydrogen bonding plays a critical role in chemistry, often controlling structure and reactivity and serving as a basis for molecular recognition. Exceptional hydrogen bonds test the limits of our theories about the mundane hydrogen bonds and also may bring to light hitherto unrecognised properties of hydrogen bonds.

A general hydrogen bond can be described as $A^{\delta-}\text{-}H^{\delta+}\cdots B^{\delta-}$. The positive hydrogen atom in the A-H dipole is attracted to a region of negative charge on the B atom (Hibbert and Emsley, 1990). Atom A must be significantly electronegative to polarise the A-H bond. Atom B also must be electronegative to attract the positive charge on the hydrogen atom. A and B are most commonly oxygen, nitrogen or fluorine. A can also be carbon if it is attached to electron-withdrawing groups. B does not have to be a single atom but can be the $\pi$-electron cloud in an unsaturated bond, for example.

The presence of a hydrogen bond in a crystal structure is inferred from the A-H, H···B and A···B distances and the A-H-B angle. As the proton position is difficult to determine accurately for X-ray diffraction results, the most common parameter used is the A···B distance. If this distance is lower than the sum of the Van der Waals radii of the two atoms then a hydrogen bond is expected, although some form of hydrogen bonding cannot be ruled out if the distance is longer.

### 2.1.3. C-H···X Hydrogen Bonds

Hydrogen bonds can also be formed from hydrogen atoms bonded to carbon atoms if the hydrogen atom can become partially positively charged (Steiner, 1997). The acceptor for this kind of hydrogen bond can be any region of negative charge on an atom or in a delocalised electron cloud.

The role of weak C-H···O hydrogen bonds in crystal chemistry has been widely investigated (Steiner, 1997, Berkovitch-Yellin and Leiserowitz, 1984). Often they do not play an important role in determining the molecular packing and conformation, especially when stronger hydrogen bond donors are present, but conversely they can often be decisive in directing intermolecular interactions in crystals. H···O separations in C-H···O bonds can range from 2.92Å (Steiner et al. 1998) to 1.935(5)Å (Davidson et al. 2000) and the C-H-O angles can range from ~120º to 180º. C-H···N hydrogen bonds with similar properties and dimensions also have been observed (Berkovitch-Yellin and Leiserowitz, 1984).

C-H···π, O-H···π and N-H···π hydrogen bonds where the π-electron clouds can be in C=C, C≡C bonds or delocalised aromatic systems are also known (Allen at al. 1996, Allen et al. 1996a, Hanton et al, 1992, Viswamitra et al, 1993).

### 2.1.4. Halogen···Halogen Interactions

The intermolecular interactions between halogen atoms in organic crystals, where the distance between the atoms is less than the sum of the Van der Waals radii, have been categorised by Sakurai et al. (1963) and further discussed by Desiraju and Parthasarathy (1989). They describe two distinct types of interaction: type 1 where the C-X···X angles are equal; type 2,where one C-X···X angle is close to 180º and the other 90º. Desiraju and Parthasarathy also conclude that these interactions are significant for chlorine, iodine and bromine, and insignificant for fluorine.

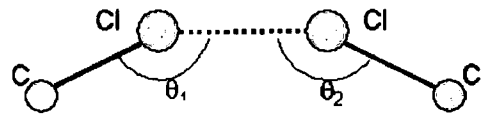


Type 1 Cl···Cl Interaction. $\theta_1 \approx \theta_2$.

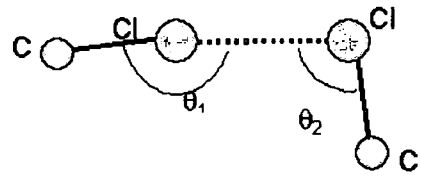


Type 2 Cl···Cl Interaction. $\theta_1 \approx 180^\circ$, $\theta_2 \approx 90^\circ$.

The causes of Cl···Cl interactions have been investigated in detail using database studies and molecular modelling by Price et al. (1994). They conclude that the interaction is a combination of electrostatic and dispersive contributions and that the anisotropy is caused by the anisotropic charge distribution around the chlorine atoms.

### 2.1.5. π-π Interactions

Attractive interactions between the delocalised π-electron systems in crystal structures of aromatic compounds have long been recognised (Robertson, 1951) and are characterised by perpendicular distances of ~3.4Å between aromatic rings.

Two obvious and important examples of π-π stacking interactions are in DNA helices (Blackburn and Gait, 1996), where the mean separation of base pairs along the DNA molecule is 3.4(5)Å and in graphite, in which the hexagonal carbon layers are held together by the π-π interactions. The separation between the layers in graphite is 3.355Å and the offset between the hexagonal ring centres is 1.423Å in the plane of the ring (Trucano and Chen, 1975).

Hunter and Sanders (1990) explain π-π interactions by treating the π-electron system and the σ-system, in which they include the nuclei and the σ-electrons, as separate and considering just the electrostatic interactions between them (Hunter et al. 2001). In this way they can explain the offset between delocalised systems (Diagram 2.1.1) observed in the crystal structures (Desiraju and Gavezzotti, 1989).

In certain cases the attraction can also be explained by charge transfer between the highest occupied molecular orbital (HOMO) of one molecule and the lowest unoccupied molecular orbital (LUMO) of the other molecule (Mulliken, 1950, Mayoh and Prout, 1971). This interaction is verifiable by UV-visible absorption spectroscopy (Hunter et al. 1989).

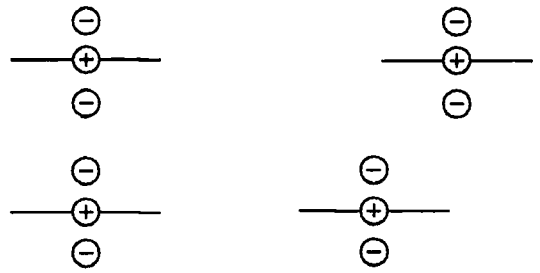

Diagram 2.1.1. (A). Face to face π-π stacking results in repulsion between the negative π-electron systems. (B) Offset stacking allows attractive π-σ electrostatic interactions.

The aromatic π-π interactions in this chapter are tabulated by: A. the distance between the ring centroids; B. the angle between the planes of the two rings; C. the shorter perpendicular distance from the centroid of one ring to the plane of the other ring. (Diagram 2.1.2)

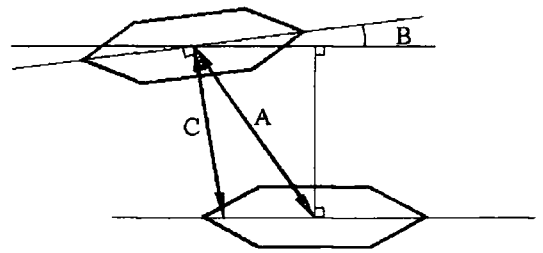


Diagram 2.1.2. Parameters in π-π interactions.

### 2.1.6. N-Hetrocyclic Carbenes

We have studied six different crystals, each containing 1,3-dimesitylimidazol-2-ylidene (1,3-bis(2,4,6-trimethylphenyl)imidazol-2-ylidene) (DMIY) in different environments. Carbon C1 is a carbene, a two-coordinate carbon atom with two non-bonding electrons and no formal charge. Carbenes are highly reactive and usually have lifetimes under 1 second (March, 1985).

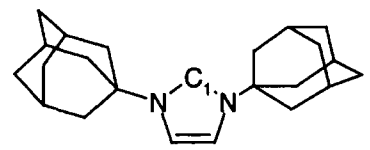


1,3-di-adamantyl-imidazol-2-ylidene.

A stable 'bottle-able' carbene has long been a goal of organic chemists (Regitz, 1991). A stable crystalline carbene was first produced as 1,3-di-adamantyl-imidazol-2-ylidene (Arduengo et al. 1991). A class of compounds has subsequently been produced with different side groups including the compound we have studied 1,3-dimesitylimidazol-2-ylidene. The N-C=C-N structural subunit stabilises the carbene in these structures. The large side groups offer some protection to the central unit, but still allow access to the carbene atom.

The structures containing DMIY that have already been determined are mostly organometallics (Arduengo et al. 1992a, 1993, 1994, Abernethy et al. 1999, Voges et al. 1999). The uncommon electronegative properties of the carbon atom mean it can accept hydrogen bonds, or, if it becomes protonated, act as a donor. Co-crystallisation with different weak organic acids is expected to produce novel C-H...X or X-H···C hydrogen bonding. Indeed, in the structure of DMIY and its protonated imidizolium salt with $PF_6$ and with $CF_3SO_3$, a C-H···C hydrogen bond has been observed (Arduengo et al, 1995).

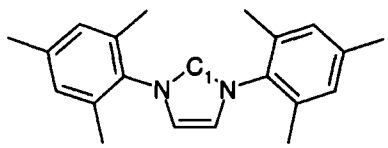


1,3-dimesitylimidazol-2-ylidene

## 2.2. Studying hydrogen bonds by diffraction.

Neutron diffraction is the ideal technique for studying hydrogen atoms in crystals (section 3), but where neutron diffraction experiments are impossible due to the size of the crystal or the availability of the neutrons, accurate low-temperature X-ray diffraction experiments can often be nearly as useful for determining proton positions. In long and weak hydrogen bonds that are almost entirely electrostatic the proton position can be deduced reasonably accurately from X-ray experiments. The conformation of the molecules, the bond lengths and angles, can also be used to deduce the proton positions reliably.

### 2.2.1. Assigning proton positions bonded to C1.

The motivation for this series of experiments is to investigate the interactions of carbon atom C1. It is important to know if C1 is or is not protonated. In structure determinations of small organic molecules from accurate low-temperature X-ray data there is often no problem locating and refining proton positions. In these experiments, in which the whole interpretation of the structure depends on the state of C1, great care must be used in determining the proton positions.

### 2.2.2. The Difference Fourier Map

The most revealing evidence for the existence of a hydrogen atom lies in the difference Fourier maps. A peak of residual electron density of 0.5-1.0 $eÅ^{-3}$ around 1 Å from C1 would indicate the existence of a hydrogen atom, provided it was in a chemically reasonable position. The scattering from hydrogen atoms may be swamped in crystals that contain more powerful X-ray scattering elements, for example chlorine; the Fourier maps will be unreliable for placing the hydrogen atoms.

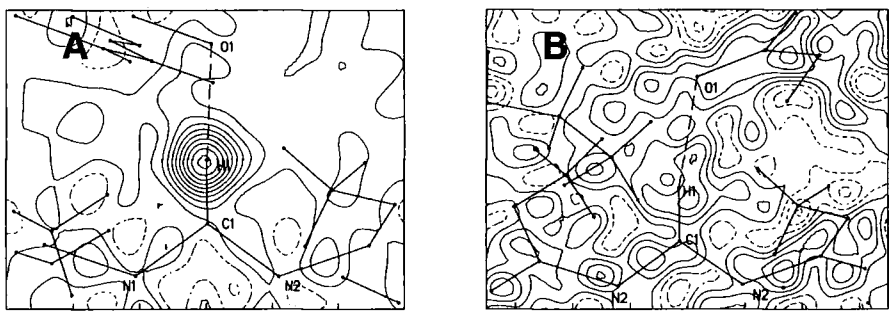


Figures 2.2.1.a. and b. Difference Fourier maps from the structures of 1,3-dimesitylimidazol-2-ylidene with 2(2-hydroxyphenyl)benzoxazole (A , section 2.5) and pentachlorophenol (B, section 2.8). The maps were calculated without the hydrogen atom H1, which has been indicated in the diagram. The contours are at 0.1$eÅ^{-3}$. In A the hydrogen position is obvious. In B, which contains several chlorine atoms, the difference Fourier map is too noisy to reveal hydrogen atom positions.

### 2.2.3. Observations of Other Molecules

The protonation state can also be deduced from the states of the other molecules in the crystal. Five of the structures studied in this chapter are co-crystals of weak organic acids and DMIY, a weak base. If the counter molecule in the co-crystal is obviously deprotonated then DMIY must have become protonated.

### 2.2.4. Comparison with other molecules

If a proton cannot be easily located attached either to C1 of DMIY or to the counter molecule, then the proton position must be deduced from the conformations and orientations of the molecules in the crystal. For example the C-O distance in a hydroxyl group is a reliable indicator of the protonation state of the oxygen, if the hydroxyl group has become deprotonated the C-O distance will be significantly shorter than the expected value. The expected values of C-O bond lengths for different varieties of hydroxyl groups, and many other bond lengths, are tabulated in the International Tables for Crystallography (Allen et al, 1992).

#### 2.2.4.1. The Cambridge Structural Database

A more comprehensive source of data for the expected conformations of molecules is the Cambridge Structural Database, CSD (Allen and Kennard, 1993). The database contains 233218 (April, 2001) organic and organometallic crystal structures. The database can be searched for molecules or fragments of molecules, and the relevant bond lengths, bond angles, torsion angles, etc. can be extracted. The estimated standard deviation taken from the CSD is standard deviation calculated from the spread of the values found.

The unprotonated central pentagon of DMIY is quite rare, a search of the CSD returned just 19 results. The much more common protonated fragment is part of imidizole and the nucleotides guanine and adenosine and yields 2093 results. To make the search more relevant to DMIY the two nitrogen atoms in the pentagon were required to be bonded to three carbon atoms and this yielded 79 results. The mean C1-N bond lengths and N1-C1-N2 bond angles are tabulated below.

Table 2.2.1, CSD Results.

| | C1-N distance | N1-C1-N2 Angle | Number of observations |
|---|---|---|---|
| Unprotonated | 1.366(4) Å | 102.0(8)º | 19 |
| Protonated | 1.324(14) Å | 109.1(8)º | 79 |

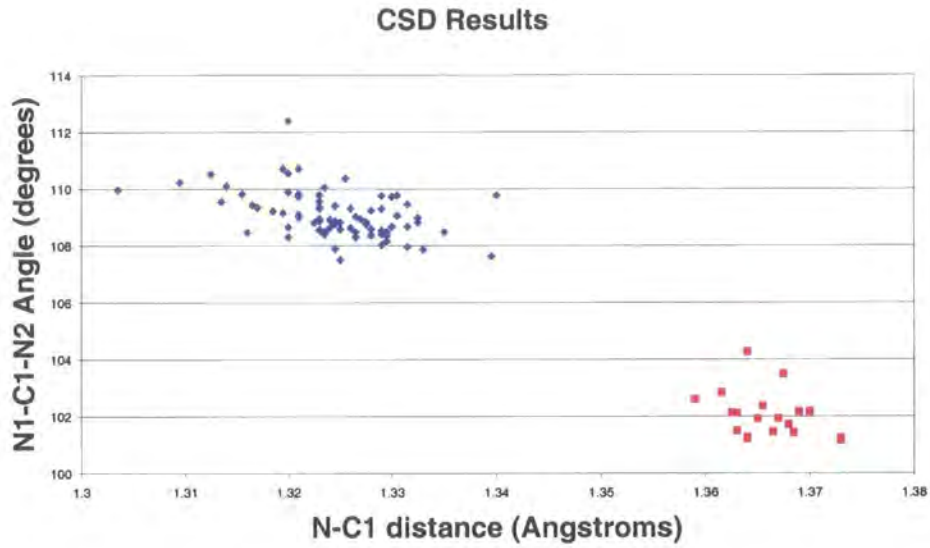


Graph 2.2.1. C-N bond lengths and N-C-N bond angles for the central pentagon of DMIY from the CSD. Red points indicate unprotonated fragments and blue points indicate protonated fragments.

The results from the CSD show a clear distinction between the conformations of the protonated and unprotonated pentagon. The protonated fragments (blue marks) have C-N bond lengths of 1.31 Å – 1.34 Å and a N-C-N bond angle of 108º - 111º. The unprotonated fragments (red marks) have C-N bond lengths of1.36 Å – 1.37 Å and a N-C-N bond angle of 101º - 104º.

### 2.2.4.2. Comparision with Theoretical Molecules, Density Functional Theory Calculations

Density-functional-theory quantum-mechanical calculations were performed on the neutral DMIY molecule and the protonated ion using the program DMol$^3$ (Delley, 2000). The program calculates the electronic wavefunctions of a molecule and hence calculates the energy of and the forces on each atom. The geometry of the molecule is optimised starting from an approximate structure by calculating iteratively the forces on the atoms then moving the atoms to minimise the forces.

Starting from the X-ray diffraction derived structures, the geometry was optimised on the DMIY molecule. Four separate geometry-optimisation calculations were performed beginning from different input structures. The four input structures were:

1. The neutral molecule conformation.
2. The protonated positive ion conformation.
3. The protonated positive ion conformation with the proton on C1 and charge removed.
4. The neutral molecule conformation with a proton added to C1 and a charge of +1.

Calculations 3 and 4 were performed to confirm that the geometry was moving to a minimum of the potential energy surface in each case.

Table 2.2.2. Density-Functional Calculation Input.

| | N1-C1-N2 Angle | N1-C1 distance (Å) | C1-N2 distance (Å) |
|---|---|---|---|
| Neutral conformation | 101.5º | 1.369 | 1.373 |
| Protonated conformation | 107.8º | 1.334 | 1.339 |

Table 2.2.3. Density-Functional Calculation Output.

| | N1-C1-N2 Angle | N1-C1 distance (Å) | C1-N2 distance (Å) |
|---|---|---|---|
| Case 1 | 101.7º | 1.357 | 1.359 |
| Case 2 | 108.4º | 1.333 | 1.333 |
| Case 3 | 101.6º | 1.357 | 1.359 |
| Case 4 | 108.4º | 1.333 | 1.333 |

The results are consistent with the observed structures from the Cambridge Structural Database (Allen and Kennard, 1993). If the DMIY molecule is neutral the N-C-N angle is expected to be ~101.7º with C1-N bond lengths of ~1.358Å. If the DMIY molecule has become protonated the N-C-N angle is expected to be ~108.4º with C1-N bond lengths of ~1.333Å.

## 2.3. Experimental Procedure

All the X-ray experiments were performed on a Bruker SMART-CCD diffractometer (Bruker, 1998). The Bruker SMART-CCD is a popular commercial diffractometer system equipped with a large position sensitive area detector. It is a simplified four-circle diffractometer with the chi-circle removed and the phi-circle mounted at a fixed chi of 54º. Molybdenum Kα radiation, which has a mean wavelength of 0.71073Å, is used in the Durham set up. This is ideal for the instrument as a routine data set complete to $\theta = 25º$ (equal to $\sin\theta / \lambda = 0.6$ Å$^{-1}$ or a resolution of 0.833 Å), the value recommended for publication in Acta Crystallographica, can be collected with one detector position.

In each experiment a crystal of size suitable for X-ray diffraction was mounted using degassed oil, onto a hair that was inserted into the end of a fine syringe needle on a goniometer head, which was then mounted on the diffractometer. The degassed oil forms a film around the air-sensitive crystal that hardens at low temperatures to hold the crystal firmly to the hair. The crystal was flash cooled using a nitrogen gas flow cryostream to 100K, at which temperature the data were collected.

The diffracted intensities are recorded in frames collected at fixed phi and omega settings. After each frame the crystal is rotated about omega, usually by ~0.3º, and the next frame is measured. Data are collected at four specific phi-angles to yield around 2000 frames in each data collection.

The frames are combined to yield the intensities and positions of the reflections. From the positions of the strongest high-angle reflections the orientation matrix for the crystal is calculated (Bruker-SMART, 1998). This is then used during the integration to predict the centres of the reflections (Bruker-SAINT, 1998).

The structures were solved by direct methods using the program SHELXS (Sheldrick, 1997) and refined using full-matrix least squares with the program SHELXL (Sheldrick, 1997). The figures were produced with SHELXP (Bruker, 1998) and PLATON (Spek, 1990) has been used to help analyse the structures.

## 2.4. The Crystal Structure of 1,3-Dimesitylimidazol-2-ylidene

The 1,3-dimesitylimidazol-2-ylidene (1,3-bis(2,4,6-trimethylphenyl)imidazol-2-ylidene, DMIY) molecule forms the basis of our study. It is one of a series of stable carbenes originally produced by Arduengo et al. (1991, 1992, 1995)

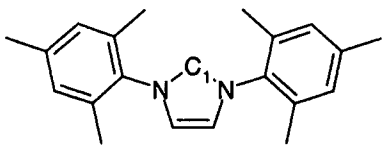


**[DMIY]**

The crystal structure of the pure compound has been solved by Arduengo et al (1992). We have also collected data on DMIY to compare this structure with the others in this series.

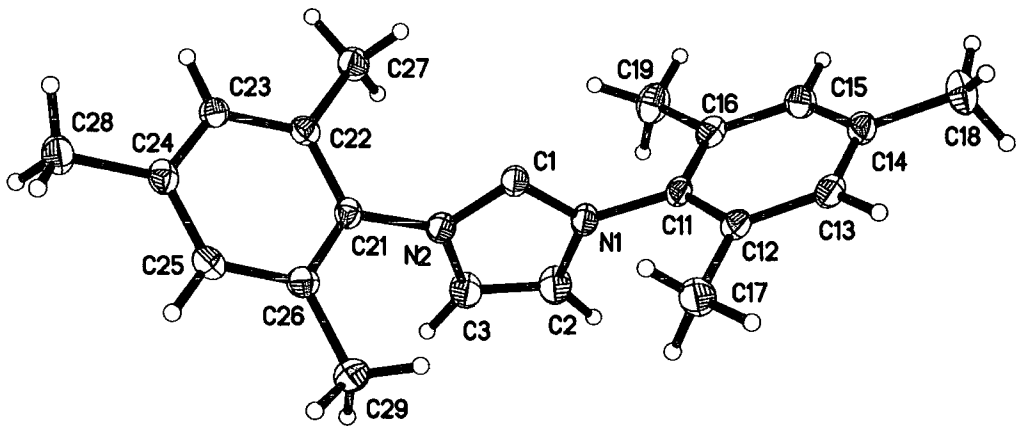


Figure 2.4.1. 50% Thermal ellipsoid plot of DMIY.

For the crystal to be neutral C1 should not be protonated. The C1-N1 and C1-N2 bond lengths of 1.369(2) Å and 1.373(2) Å and the N1-C1-N2 bond angle of 101.48(12)º agree with the previously observed and calculated values for the neutral molecule. In the difference Fourier map there is electron density near C1. The highest peak of residual electron density in the structure (0.29 $eÅ^{-3}$) is the centre of a delocalised bond. The second-highest peak (0.23 $eÅ^{-3}$) occurs 0.87Å from C1. This could be the hint of a proton or the lone pair electron density of the carbene. This electron density can be seen clearly in the Fourier map below.

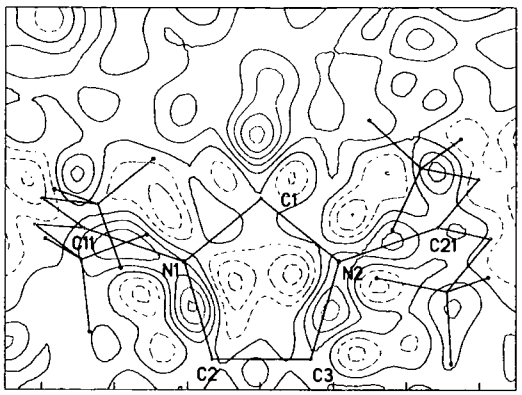


Figure 2.4.2. Difference Fourier map of DMIY in the plane of C1, C2, C3, N1 and N2. The contours are at 0.05 eÅ$^{-3}$. The blue contours indicate negative electron density and red contours indicate positive electron density.

The twist angles of the plane of the mesityl groups related to the imidazol-2-ylidene plane [81.16(6)º for ring 1 and 70.53(7)º for ring 2] are optimised in the crystal to minimise the mutual interference of the methyl groups with the imidazol-2-ylidine ring and to optimise weak C-H···π and π···π intermolecular interactions.

The packing is dominated by weak C-H···π interactions. Two C-H···π hydrogen bonds, C2-H2···Ring 2 and C3-H3···Ring 1, combine to link the molecules together in zig-zag chains parallel to the b-axis (Figure 2.4.3).

Table 2.4.1. C-H···π Interactions

| | C – Ring Centre | C-H | H - Ring Centre | C-H-Ring Angle |
|---|---|---|---|---|
| C2-H2-Ring 2$^{ii}$ | 3.6054(17) | 0.98(3) | 2.64(3) | 170(2)º |
| C3-H3-Ring 1$^{i}$ | 4.1496(17) | 0.94(2) | 3.23(2) | 166(2)º |

Ring 1 = C11-C12-C13-C14-C15-C16; Ring 2 = C21-C22-C23-C24-C25-C26.
Symmetry Codes: (i) –x, -0.5+y, 1-z, (ii) –x, 0.5+y, 1-z,

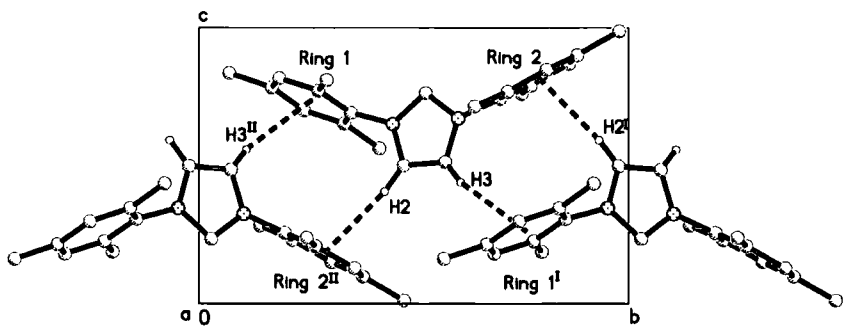


Figure 2.4.3. Packing diagram of DMIY viewed along the a-axis. All the hydrogen atoms except H2 and H3 have been omitted for clarity. (I = -x,-0.5+y,1-z; II = -x, 0.5+y, 1-z). The CH-π interactions are denoted by dotted lines.

The zig-zag chains fit together via close $\pi$-$\pi$ contacts, to create corrugated sheets perpendicular to the a-axis. The centres of the Ring 1 and Ring $2^{i}$ (i = -x, 0.5 +y, -z) are 3.7985(5)Å apart and the perpendicular distance from ring 1 to ring $2^{i}$ is 3.4548(12)Å. The angle between the planes of ring 1 and ring 2 is 11.34(7)º.

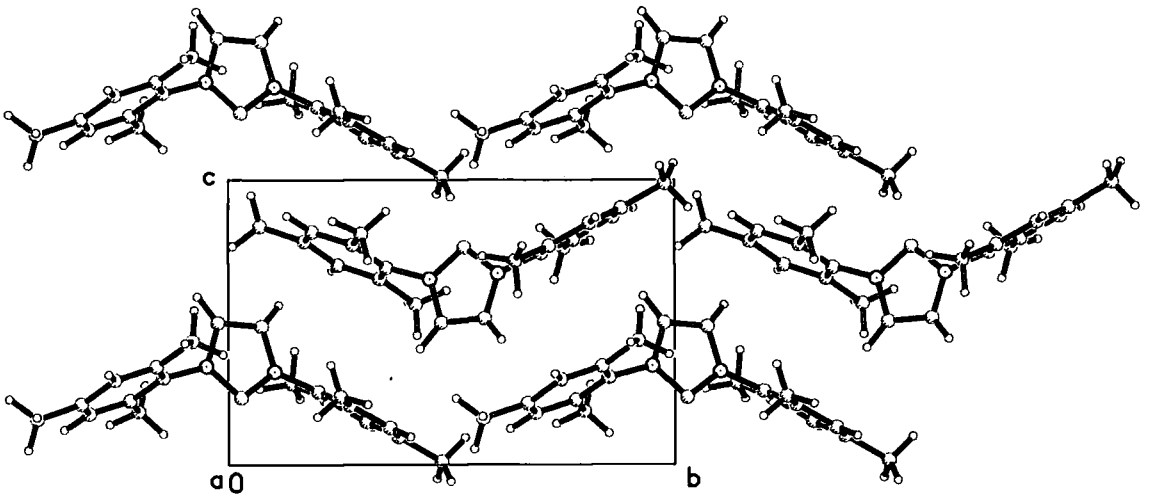


Figure 2.4.4. Packing diagram of DMIY viewed along the a-axis perpendicular to the corrugated sheets of molecules.

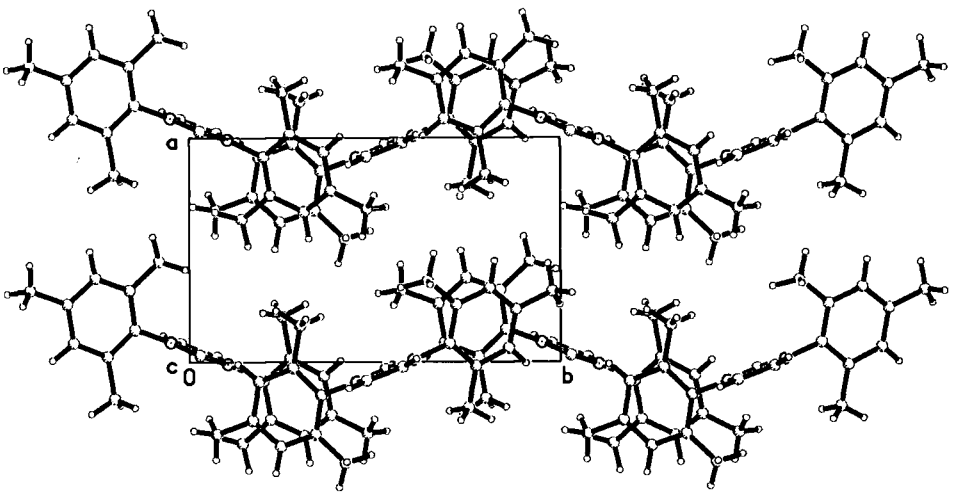


Figure 2.4.5. Packing diagram of DMIY viewed along the c-axis in the plane of the corrugated molecular sheets.

**Experimental details.**

Table 2.4.cry. Crystal parameters of DMIY.

| Formula | $C_{21}H_{24}N_2$ | Formula Weight | 304.42 |
|---|---|---|---|
| Crystal System | Monoclinic | Space Group | $P2_1$ |
| a (Å) | 8.3365(11) | α (°) | 90 |
| b (Å) | 12.9536(17) | β (°) | 110.172(2) |
| c (Å) | 8.8058(12) | γ (°) | 90 |
| Volume $(Å)^3$ | 892.6(2) | Z | 2 |
| Density (Mg $m^{-3}$) | 1.133 | Colour | Colourless |
| Crystal Shape | Plate | Dimensions (mm) | 0.5 * 0.35 * 0.1 |

Table 2.4.data. Data collection details for DMIY.

| Radiation | Mo Kα | λ (Å) | 0.71073 |
|---|---|---|---|
| Temperature (K) | 100(2) | | |
| Reflections | 7923 | Independent reflections | 4068 |
| Reflections I > 2σ(I) | 3790 | | |
| Rint | 0.0775 | Rsigma | 0.0597 |
| h | -11 → 11 | k | -16 → 17 |
| l | -11 → 10 | $\theta_{max}$ | 28.49º |

Table 2.4.ref. Refinement details for DMIY.

| $R[F^2 > 2\sigma(F^2)]$ | 0.0417 | $wR^2(F^2)$ | 0.1054 |
|---|---|---|---|
| S | 1.025 | Data / Parameters | 4068 / 304 |
| $\Delta\rho_{max}$ (e $Å^{-3}$) | 0.290 | $\Delta\rho_{min}$ (e $Å^{-3}$) | -0.184 |
| $(\Delta/\sigma)_{max}$ | 0.001 | $\Delta\rho_{rms}$ (e $Å^{-3}$) | 0.042 |

Cell parameters were determined from 946 strong reflections with θ = 13.54 – 27.73º Anisotropic thermal parameters of all non-hydrogen atoms were refined. All the hydrogen atoms were located in the difference Fourier maps and refined with isotropic displacement parameters. The C-H distances (C-H = 0.93(2)Å –1.03(4)Å ) all refined to within standard ranges and there were no anomalous values of $U_{iso}$.

## 2.5. The 1:1 Co-crystal of 2(2-hydroxyphenyl)benzoxazole and 1,3-Dimesitylimidazol-2-ylidene

2(2-hydroxyphenyl)benzoxazole and 1,3-dimesitylimidazol-2-ylidene crystallise in a 1:1 ratio as a molecular salt, $C_{21}H_{25}N_2^+ \cdot C_{13}H_8NO_2^-$ in space group $P2_1/c$. 2(2-hydroxyphenyl)benzoxazole has been deprotonated to 2(2-hydroxyphenoxide)benzoxazole (HPOB-) and 1,3-dimesitylimidazol-2-ylidene has been protonated to become 1,3-dimesitylimidizolium (DMI+). The DMI+ molecules and the HPOB- molecules are connected by C-H···O hydrogen bonds and pack to form infinite, one-dimensional columns parallel to the b-axis.

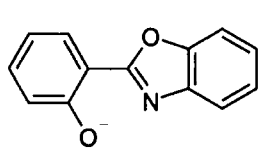


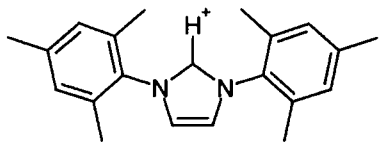


**[HPOB-]** **[DMI+]**

2(2-hydroxyphenyl)benzoxazole (HPB) is commonly used as a ligand in organometallic chemistry and all of the structures in the Cambridge Structural Database (Allen and Kennard, 1993) which contain it are organometallics.

There are no significant residual electron density peaks near O1 that could indicate the presence of a hydrogen atom in the hydroxyl group of HPOB-. The largest peak of residual electron density in the difference Fourier maps is 0.27 $eÅ^{-3}$ and lies near C18. The O1-C46 bond length of 1.2876(14)Å, which is much shorter than the average C-O distance of 1.362Å in phenols (International Tables for Crystallography, 1992), also indicates that O1 has become deprotonated.

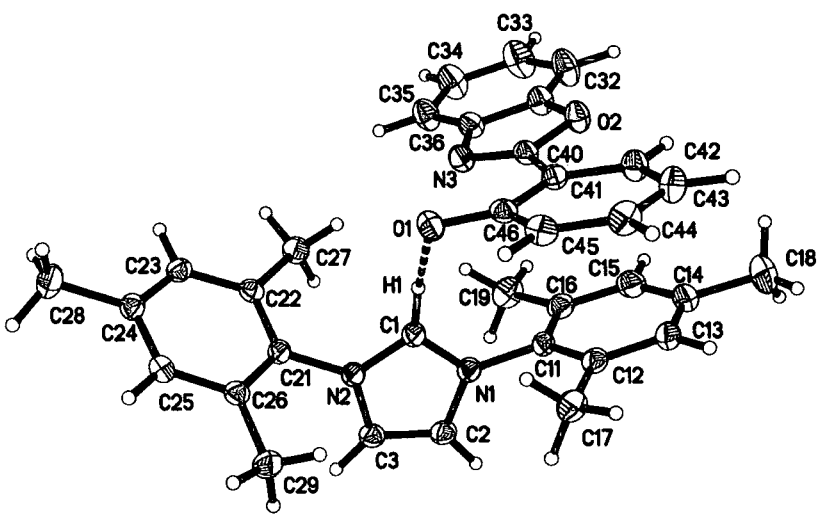


Figure 2.5.1. 50% Thermal ellipsoid plot of the HPOB- and DMI+. The dashed line indicates a short C-H···O hydrogen bond.

The HPOB- molecule is almost planar with only 6.73(2)° between the phenoxide and the benzoxazole planes. The C40-C41 bond length of 1.454(2)Å is shorter than comparable C-C bonds in bipyridine or biphenyl and suggests that the delocalised electron systems at each end of the molecule, have spread throughout the molecule.

A hydrogen atom was found in the difference Fourier map bonded to C1 in the DMI+ moity, which agrees chemically with the deprotonation of HPOB-. The N1-C1-N2 angle of 107.8(1)° and the C1-N1 and C1-N2 distances of 1.3341(15)Å and 1.3385(15)Å confirm that this is an imidizolium ion rather than a carbene.

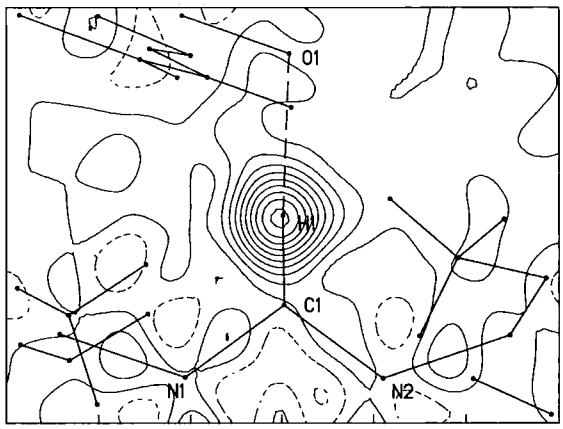


Figure 2.5.2. Difference Fourier map of HPOB- and DMI+ calculated after omitting H1. The position of H1 has been indicated in the diagram. The contours are at 0.1 eÅ$^{-3}$ The peak at H1 is 0.83 eÅ$^{-3}$.

The anisotropic displacement parameters of C18 are anomalously large, suggesting rotational disorder around the C14-C18 bond. It was impossible to refine hydrogen atom positions bonded to C18 satisfactorily and a rigid-rotor model has been used for the methyl group, in which the C-H bond lengths and H-C18-H and C14-C18-H angles are fixed at idealised values, but the group is allowed to rotate around the C14-C18 bond.

The dominant interactions for the packing are C-H···O hydrogen bonds and π-π interactions. Two short C-H···O hydrogen bonds are formed: C1-H1··· O1 and C2-H2···O1, which link the molecules into columns.

Table 2.5.1. C-H···O Hydrogen Bonds.

| | C–O distance (Å) | C-H distance (Å) | H–O distance (Å) | C-H-O Angle |
|---|---|---|---|---|
| C1-H1···O1 | 2.896(2) | 0.96(2) | 2.00(2) | 152(1)º |
| C2-H2···O1$^{i}$ | 3.133(2) | 0.96(2) | 2.39(2) | 133(1)º |

Symmetry code (i) x, y+1, z

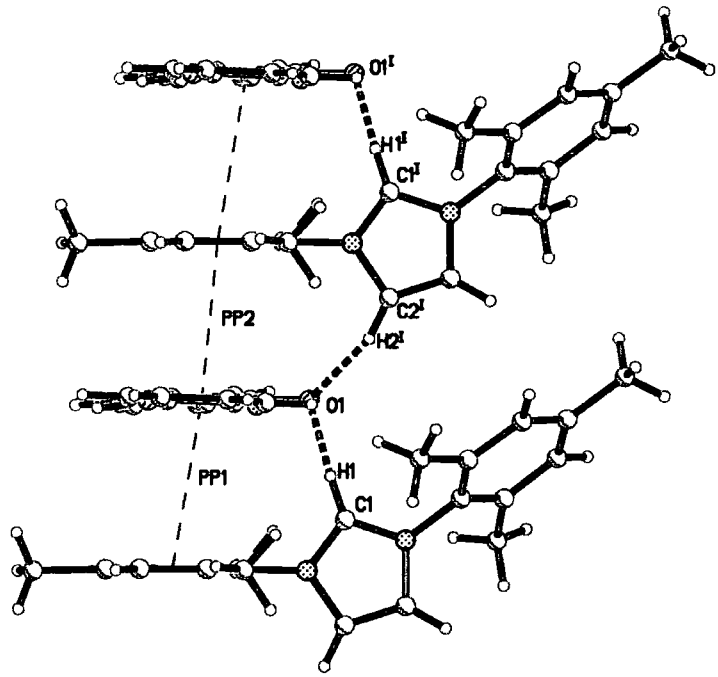


Figure 2.5.3. Packing diagram of HPOB- and DMI+ showing the hydrogen bonded columns and the complementary $\pi$-$\pi$ interactions. C-H···O bonds are indicated by the heavy dashed lines. The thin dashed lines join the centre of the C11-C16 ring to the centre of the C41-C40 bond, and indicate two $\pi$-$\pi$ interactions (PP1 and PP2). (Symmetry code: I = x, y-1, z)

The HPOB- molecule and the mesityl ring containing C11 are almost co-planar; the angle between the two planes is 0.37(2)°. The centre of the C40-C41 bond lies almost directly under the centre of the C11 ring. There are two $\pi$-$\pi$ interactions one in parallel with the C1-H1···O1 hydrogen bond (PP1 in figure 2.5.3), and the other in parallel with the C2-H2···O1 hydrogen bond (PP2 in figure 2.5.3).

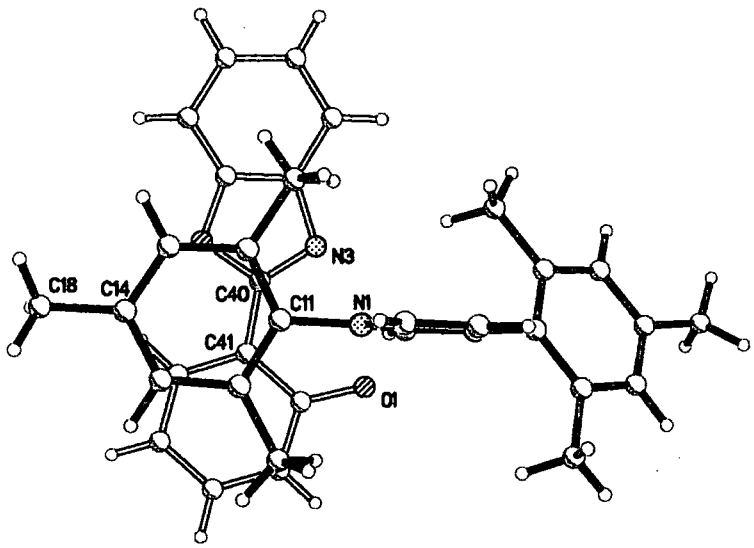


Figure 2.5.4. The asymmetric unit of HPOB- and DMI+ viewed down the b-axis. The centre of the C40-C41 bond lies almost directly below the centre of the C11-C16 mesityl ring.

Table 2.5.2. π-π Interactions.

| | Centre-to-centre distance (Å) | Angle between planes | Shortest perpendicular distance (Å) |
|---|---|---|---|
| PP1 | 3.5220(5) | 0.36(2)º | 3.4708(6) |
| PP2 | 3.4283(4) | 0.36(2)º | 3.3507(6) |

In table C5.2 the centre-to-centre distances are measured between the centroid of the C40-C41 bond and the ring C11-C12-C13-C14-C15-C16. The angles are measured between the plane of the ring and the plane of the whole HPOB- molecule.

The C-H···O and π-π interactions combine to pack the molecules in columns parallel to the b-axis.

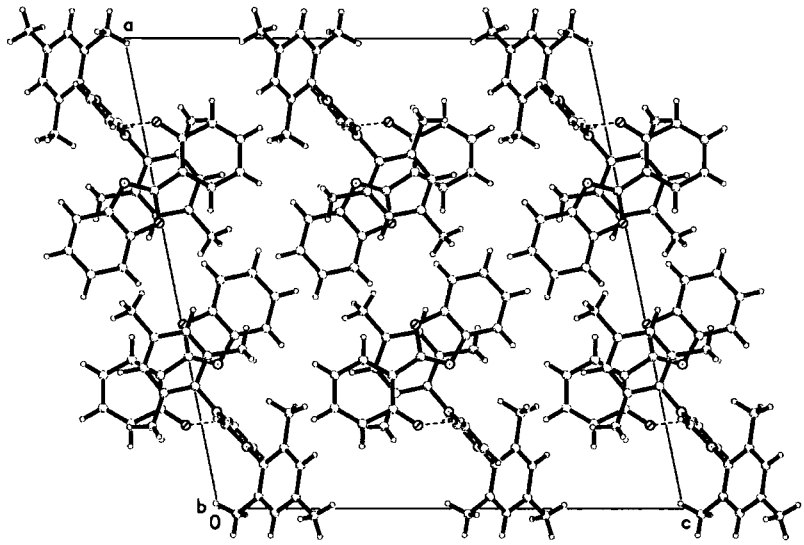


Figure 2.5.5. Packing diagram of HPOB- and DMI+ viewed down the b-axis, in the direction of the molecular columns.

**Experimental Details**

Table 2.5.cry. Crystal parameters for HPOB- and DMI+.

| Formula | $C_{21}H_{25}N_2^+ \cdot C_{13}H_8O_2N_1^-$ | Formula Weight | 515.63 |
|---|---|---|---|
| Crystal System | Monoclinic | Space Group | $P2_1/c$ |
| a (Å) | 20.443(3) | $\alpha$ | 90º |
| b (Å) | 6.9412(9) | $\beta$ | 101.378(2)º |
| c (Å) | 19.742(3) | $\gamma$ | 90º |
| Volume $(Å)^3$ | 2746.3(6) | Z | 4 |
| Density (Mg $m^{-3}$) | 1.247 | Colour | Pale green |
| Crystal Shape | Block | Dimensions (mm) | 0.5 * 0.45 * 0.35 |

Table 2.5.data. Data collection details for HPOB- and DMI+.

| Radiation | Mo K$\alpha$ | $\lambda$ (Å) | 0.71073 |
|---|---|---|---|
| Temperature (K) | 120(2) | | |
| Reflections | 23904 | Independent reflections | 6269 |
| Reflections I > 2$\sigma$(I) | 5115 | | |
| Rint | 0.0262 | Rsigma | 0.0198 |
| H | -26 → 23 | K | -9 → 8 |
| I | -25 → 25 | $\theta_{max}$ | 27.49º |

Table 2.5.ref. Refinement details for HPOB- and DMI+.

| $R[F^2 > 2\sigma(F^2)]$ | 0.0401 | $wR^2(F^2)$ | 0.1045 |
|---|---|---|---|
| S | 1.051 | Data / Parameters | 6269 / 473 |
| $\Delta\rho_{max}$ (e $Å^{-3}$) | 0.275 | $\Delta\rho_{min}$ (e $Å^{-3}$) | -0.210 |
| $(\Delta/\sigma)_{max}$ | 0.001 | $\Delta\rho_{rms}$ (e $Å^{-3}$) | 0.041 |

Cell parameters were determined from 952 strong reflections $\theta$ = 14.68 – 29.37º. Anisotropic thermal parameters for all non-hydrogen atom were refined. All hydrogen atoms, except those bonded to C18, were found in the difference Fourier maps and refined with isotropic displacement parameters.

## 2.6. The Co-crystal of Diphenylamine and 1,3-Dimesitylimidizol-2-ylidene

Diphenylamine (DPA) and 1,3-dimesitylimidizol-2-ylidene (DMIY) crystallise in a 1:1 ratio as a neutral molecular adduct in space group $P\bar{1}$. A unique N-H···C hydrogen bond is formed between N3 and the lone pair of electrons on C1. Originally we performed this experiment at 100K using the nitrogen cryostream and the proton, H1, was found bonded to N3. The experiment was repeated at 30K using the Oxford Cryosystems HELIX helium-flow device to confirm and enhance the results. Only the 30K results will be discussed.

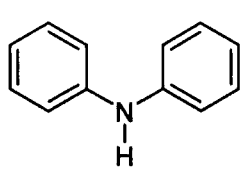

**[DPA]**

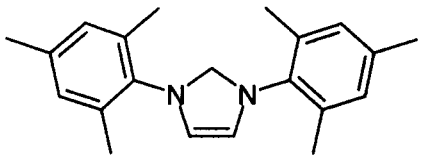

**[DMIY]**

Diphenylamine (DPA) is a weak organic acid and in all its occurrences in the Cambridge Structural Database (Allen and Kennard, 1993) it is protonated. In the difference Fourier map calculated omitting H1 the largest peak of residual electron density is 0.83 $eÅ^{-3}$ situated 0.806Å from N3, the next largest peak is 0.26 $eÅ^{-3}$ in the centre of the C16 to C19 bond.

No proton was found on C1 of the DMIY, which is consistent with N3 remaining protonated. The N1-C1-N2 angle of 101.7(1)° and the C1-N1 and C1-N2 distances of 1.3700(16)Å and 1.3730(16)Å agree with the values for the unprotonated carbene and with other examples of similar molecules in the Cambridge Structural Database (Allen and Kennard, 1993).

Consequently we can conclude that a unique N-H···C hydrogen bond has been formed between C1 and N3.

Table 2.6.1. N-H···C Hydrogen Bonds Parameters

| | D···A (Å) | D-H (Å) | H···A (Å) | D-H-A |
|---|---|---|---|---|
| N3-H1···C1 | 3.196(2) | 0.90(2) | 2.29(2) | 179.1(16)º |

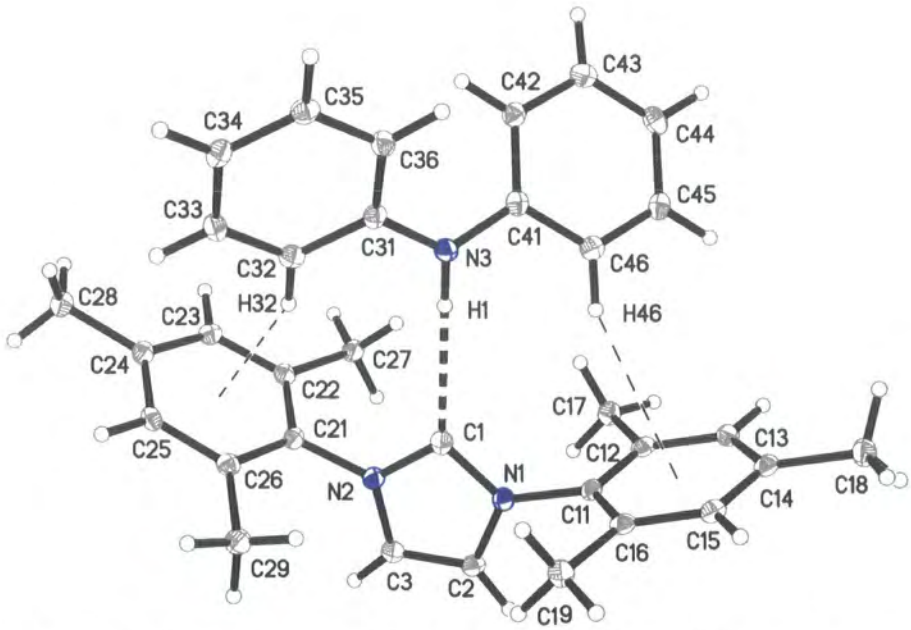


Figure 2.6.1. 50% Thermal ellipsoid plot of DPA and DMIY. The N-H···C hydrogen bond is indicated by the heavy dashed line. C-H···π hydrogen bonds are indicated by the thin dashed lines.

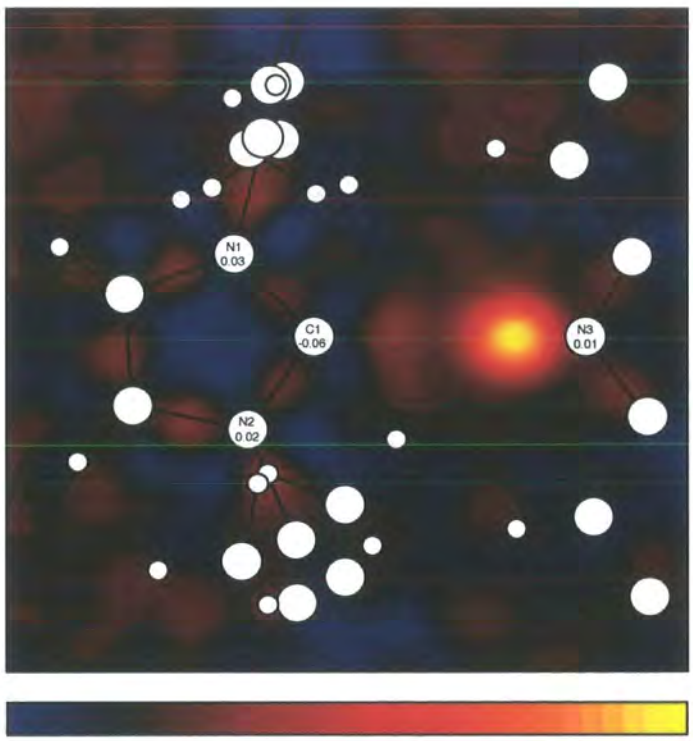


Figure 2.6.2. Difference Fourier map of DPA and DMIY through the plane of C1, N1, N2, N3 after least-squares refinement with the hydrogen H1 removed. There is a large peak of electron density (0.83eÅ$^{-3}$) 0.806Å from N3. It is clear where the hydrogen atom is located. Yellow indicates +0.8eÅ$^{-3}$ and blue indicates –0.2eÅ$^{-3}$.

In the solid state structure the two phenyl rings of DPA are twisted at an angle of 50.97(5)° with respect to each other to optimise weak C-H···π bonds to the mesityl groups of DMIY [C32-H32···Ring2 and C46-H46···Ring1]. These combine with the N-H···O hydrogen bond to link the DMIY and DPA molecules into weakly bound dimers.

Table 2.6.2. C-H···π bonds

| | C···Ring centre distance | H···Ring centre distance | C-H-Ring centre angle |
|---|---|---|---|
| C32-H32···Ring2 | 3.4366(14) | 2.518(15) | 156.0(11)º |
| C46-H46···Ring1 | 3.8077(19) | 2.902(15) | 155.6(11)º |
| C43-H43···Ring3$^{I}$ | 4.191(2) | 3.247(16) | 160.1(11)º |
| C3-H3···Ring4$^{II}$ | 3.7248(15) | 2.946(15) | 140.1(11)º |
| C36-H36···Ring2$^{III}$ | 4.0510(16) | 3.199(15) | 147.0(11)º |

Ring1 = C11-C12-C13-C14-C15-C16; Ring2 = C21-C22-C23-C24-C25-C26.
Ring3 = C31-C32-C33-C34-C35-C36. Ring4 = C41-C42-C43-C44-C45-C46.
Symmetry codes: (i) 2-x, -y, -z. (ii) x-1, y, z. (iii) 1+x, y, z.

Two DPA molecules also link together in C-H···π bonded dimers [C43-H43···Ring3], which link two DPA·DMIY dimers "back to back" (Figure 2.6.3).

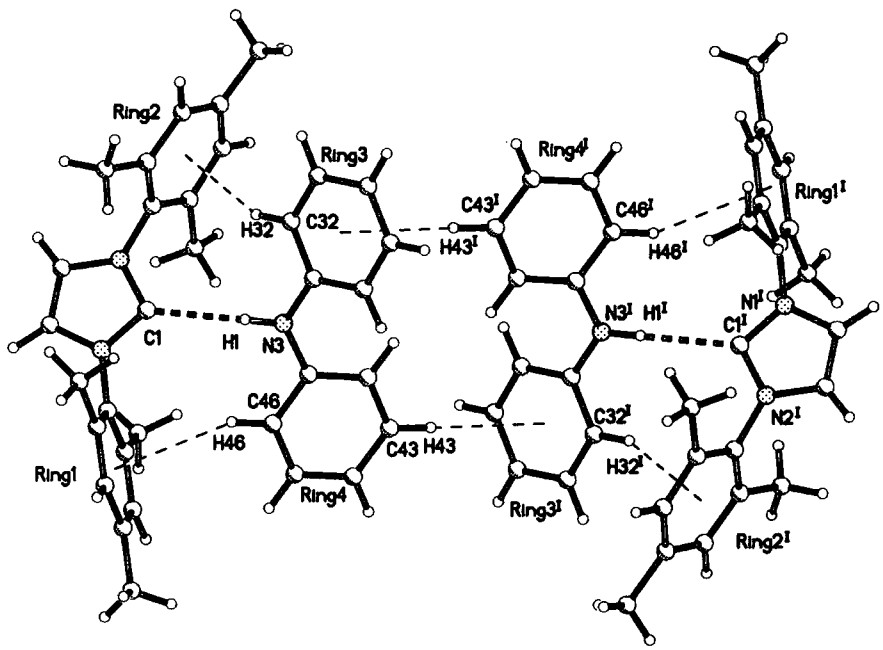


Figure 2.6.3. Packing diagram of DPA and DMIY illustrating C-H···π bonds. The heavy dashed lines indicate C-H···O hydrogen bonds. The thin dashed lines indicate C-H···π bonds. Symmetry Code I = 2-x, -y, -z.

Two other weak C-H···π hydrogen bonds [C35-H35···Ring2 and C3-H3···Ring4] connect the molecules in columns parallel to the a-axis.

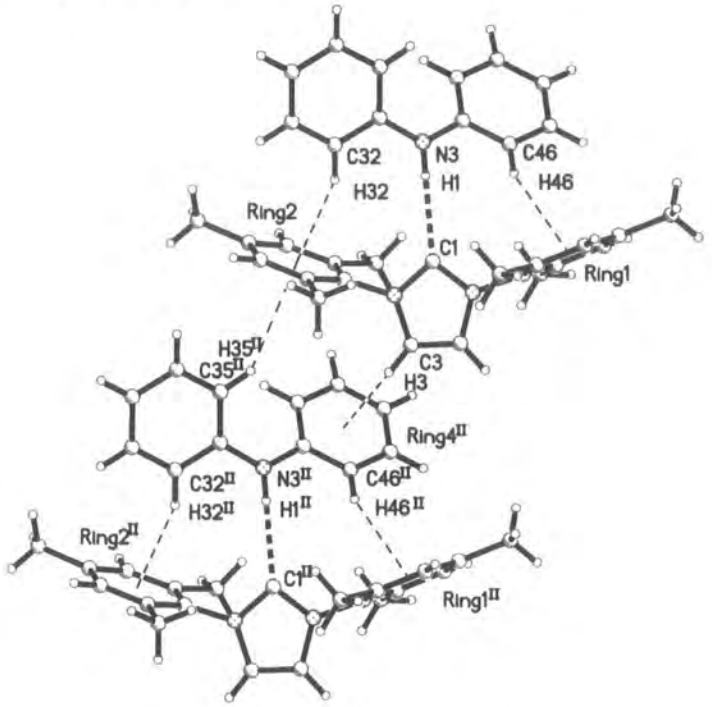


Figure 2.6.4. Packing plot of DPA and DMIY illustrating C-H···π bonds indicated by thin dashed lines. Symmetry Code II = x-1, y, z.

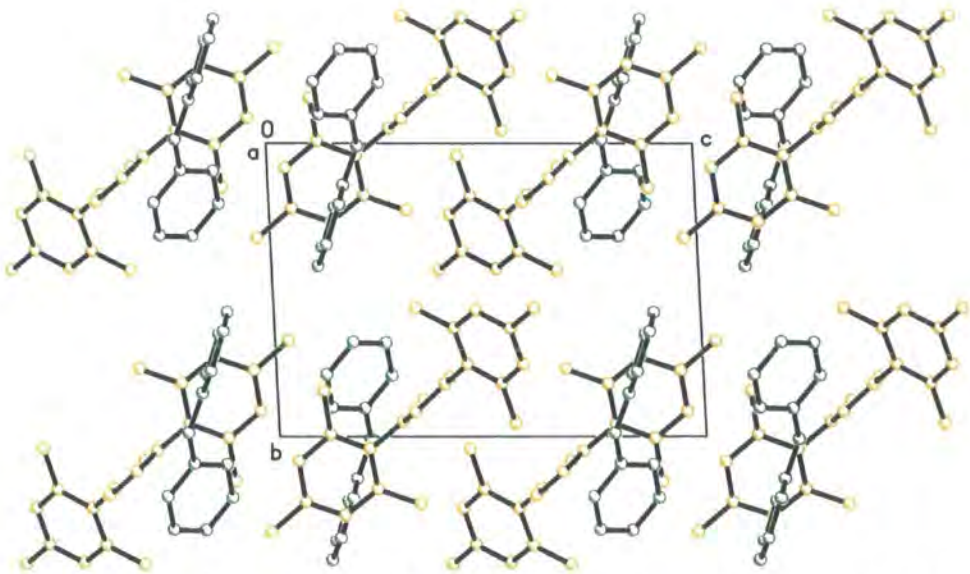


Figure 2.6.5. Packing diagram of DPA and DMIY viewed down the a-axis, parallel to the columns in figure 2.6.4. DMIY molecules are yellow and DPA molecules are green. The hydrogen atoms have been omitted for clarity.

**Experimental Details**

Table 2.6.cry. Crystal details for DPA and DMIY.

| Formula | $C_{21}H_{24}N_2 \cdot C_{12}H_{11}N$ | Formula Weight | 473.64 |
|---|---|---|---|
| Crystal System | Triclinic | Space Group | P-1 |
| a (Å) | 9.6629(19) | α | 80.60(3)º |
| b (Å) | 10.578(2) | β | 71.68(3)º |
| c (Å) | 14.967(3) | γ | 67.72(3)º |
| Volume $(Å)^3$ | 1342.3(5) | Z | 2 |
| Density (Mg $m^{-3}$) | 1.172 | Colour | Yellow |
| Crystal Shape | Needle | Dimensions (mm) | 0.48 * 0.26 * 0.16 |

Table 2.6.data. Data collection details for DPA and DMIY.

| Radiation | Mo Kα | λ (Å) | 0.71073 |
|---|---|---|---|
| Temperature (K) | 30(2) | Independent reflections | 5307 |
| Reflections | 11025 | | |
| Reflections I > 2σ(I) | 4412 | | |
| Rint | 0.0285 | Rsigma | 0.0313 |
| h | -12 → 11 | k | -13 → 13 |
| l | -18 → 19 | $\theta_{max}$ | 27.17º |

Table 2.6.ref. Refinement details for DPA and DMIY.

| $R[F^2 > 2\sigma(F^2)]$ | 0.0376 | $wR^2(F^2)$ | 0.0991 |
|---|---|---|---|
| S | 1.029 | Data / Parameters | 5307 / 465 |
| $\Delta\rho_{max}$ (e $Å^{-3}$) | 0.257 | $\Delta\rho_{min}$ (e $Å^{-3}$) | -0.207 |
| $(\Delta/\sigma)_{max}$ | 0.000 | $\Delta\rho_{rms}$ (e $Å^{-3}$) | 0.041 |

Cell parameters were determined from 751 strong reflections θ = 13.73 – 27.16º
Anisotropic thermal parameters for all non-hydrogen atoms were refined. All the hydrogen atoms were found in the difference Fourier maps and refined with isotropic displacement parameters. The C-H distances (C-H = 0.95(2)Å –1.02(2)Å ) all refined to within standard ranges and there were no anomalous values of $U_{iso}$.

## 2.7. The Co-Crystal Structure of 2,6-Di-tert-butyl-4-methylphenol and 1,3-Dimesitylimidazol-2-ylidene

2,6-di-tert-butyl-4-methylphenol and 1,3-dimesitylimidizol-2-ylidene crystallise in a 1:1 ratio as a molecular salt, $C_{21}H_{25}N_2^+ \cdot C_{15}H_{23}O_1^-$ in space group P-3. The 1,3-dimesitylimidizol-2-ylidene has been protonated to become 1,3-dimesitylimidizolium (DMI+) and correspondingly 2,6-di-tert-butyl-4-methylphenol has become deprotonated to form 2,6-di-tert-butyl-4-methylphenoxide (DTPO-). DMI+ and DTPO- are linked by a short C-H···O hydrogen bond to form dimers. There are two independent DMI+·DTPO- dimers in the asymmetric unit that also contains a molecule of toluene and a molecule of unidentified solvent, modelled as n-hexane disordered around a 3-fold axis.

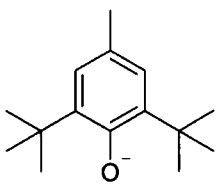


**[DTPO-]**

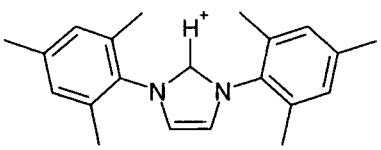


**[DMI+]**

Hydrogen atoms were found in the difference Fourier map to be bonded to C1 and C1A in the DMI+ molecules. The C31-O1 and C31A-O1A bond lengths in DTPO- of 1.310(2)Å and 1.307(2)Å are much shorter than the average value of 1.362Å for phenol (International Tables for Crystallography, 1992), which also suggests that the DTPO- molecules have become deprotonated. The N-C1 and N-C1A bond distances of 1.331(3)Å, 1.343(3)Å, 1.334(3)Å and 1.340(3)Å and the N1-C1-N2 and N1A-C1A-N2A bond angles of 107.3(2)º and 107.2(2)º, all agree with the conformation for a DMI+ ion rather than the conformation for the ylide.

The DMI+ molecules are linked to the DTPO- molecules by short C-H···O hydrogen bonds [C1-H1···O1 and C1A-H1A···O1A] to form two similar, but not identical, dimers. The C···O separations in the two DMI+.DTPO- dimers of 2.800(3)Å and 2.841(3)Å are much shorter than the shortest C-H···O hydrogen bond previously observed (Bock et al. 1993), which has a C···O separation of 2.937(1)Å.

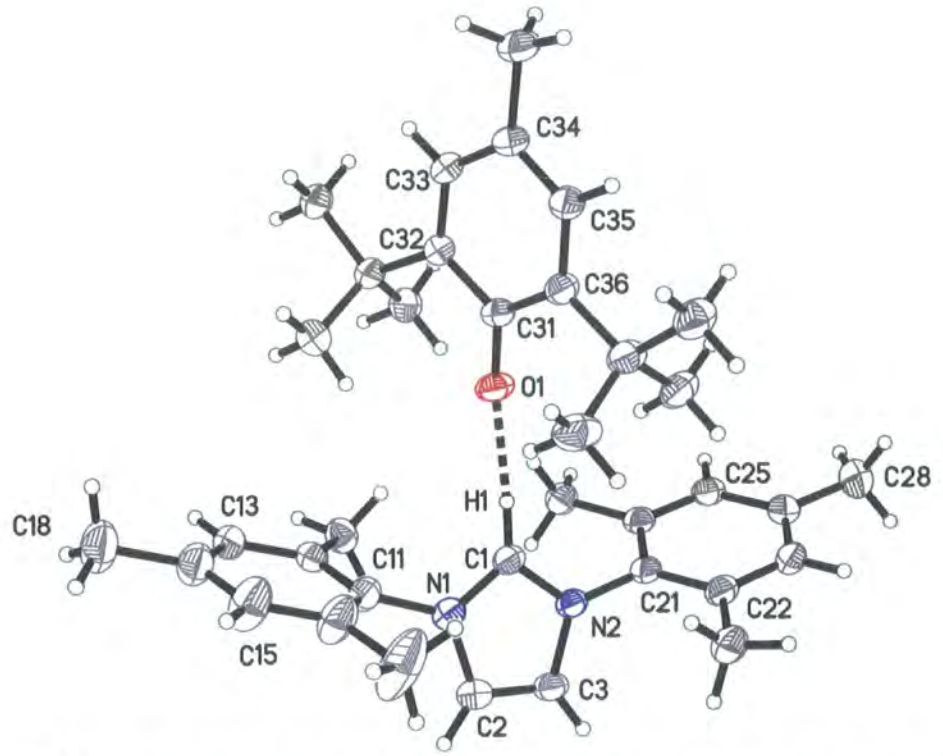


Figure 2.7.1. 50% thermal-ellipsoid plot of the first of the DMI+·DTPO- dimers. The dashed line indicates the short C-H···O hydrogen bond. [C1···O1 2.800(3)Å]

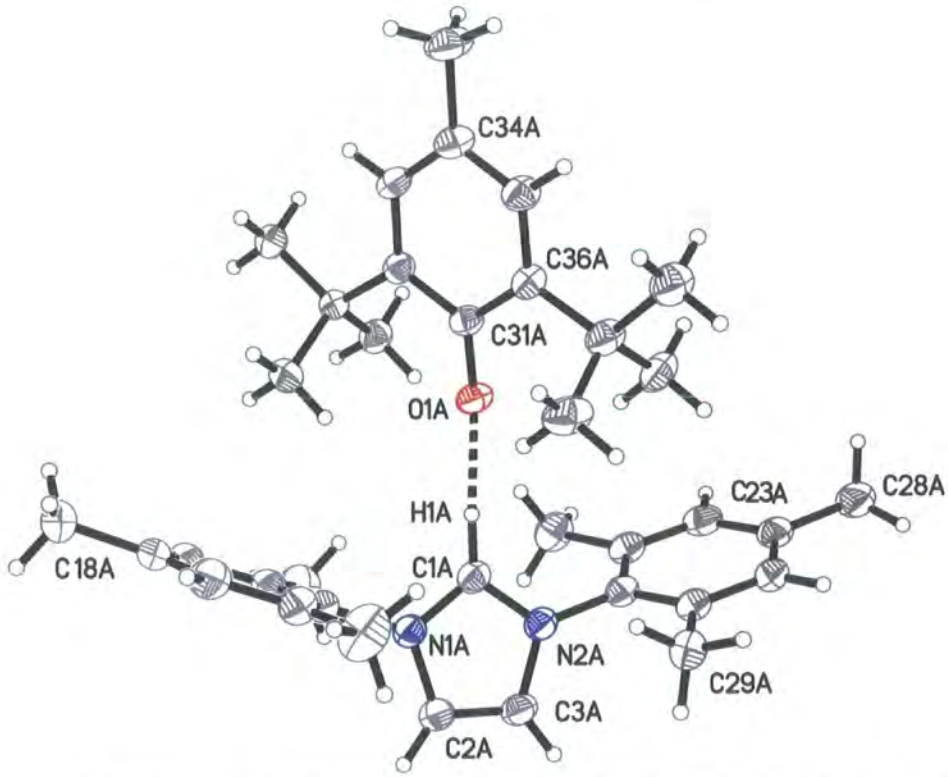


Figure 2.7.2. 50% thermal-ellipsoid plot of the second of the DMI+·DTPO- dimers. The dashed line indicates the short C-H···O hydrogen bond. [C1A···O1A 2.841(3)Å]

There are four main intermolecular interactions and two independent occurrences of each one. The short C-H···O hydrogen bonds connect the DMI+ and DTPO- molecules in dimers, the other interactions connect crystallographically independent dimers together into weakly hydrogen bonded 6 membered rings around the 3-fold axes at (2/3 1/3 0) (figure 2.7.4).

Table 2.7.1. C-H···O hydrogen bonds.

| | C-O | C-H | H-O | C-H-O |
|---|---|---|---|---|
| C1-H1-O1 | 2.800(3) | 0.94(3) | 1.86(3) | 175(2)º |
| C1A-H1A-O1A | 2.841(3) | 0.96(3) | 1.87(3) | 168(2)º |
| C3-H3-O1A$^{i}$ | 3.544(3) | 0.93 | 2.82 | 136º |
| C3A-H3A-O1$^{ii}$ | 3.656(3) | 0.93 | 2.98 | 131º |

Table 2.7.2. C-H···π hydrogen bonds.

| | C-Ring centre (Å) | C-H distance (Å) | H-Ring centre (Å) | C-H-Ring centre |
|---|---|---|---|---|
| C2-H2-Ring3A$^{i}$ | 3.041(2) | 0.93 | 2.19 | 151º |
| C2A-H2A-Ring3$^{ii}$ | 3.185(2) | 0.93 | 2.31 | 156º |
| C25-H25-Ring2A$^{iii}$ | 3.760(2) | 0.93 | 2.84 | 170º |
| C23A-H23A-Ring2$^{iv}$ | 3.871(3) | 0.93 | 2.99 | 159º |

Ring2 = C21-C22-C23-C24-C25-C26. Ring3 = C31-C32-C33-C34-C35-C36.
Ring2 = C21A-C22A-C23A-C24A-C25A-C26A. Ring3 = C31A-C32A-C33A-C34A-C35A-C36A.
Symmetry codes. i = y, -x+y, 1-z. ii = 1+ y, -x+y, 1-z. iii = -1-x-y, -1+x, 1-z. iv = -x-y, x, 1-z.

The disordered hexane solvent molecule lies very close to the a-axis and fills a space produced where the hydrogen-bonded rings do not intersect. It has been refined with an occupation of 0.75. The toluene molecule lies in three positions close to the (1/3, 2/3, 0) axis in the ab-plane and in a gap between the hydrogen-bonded rings.

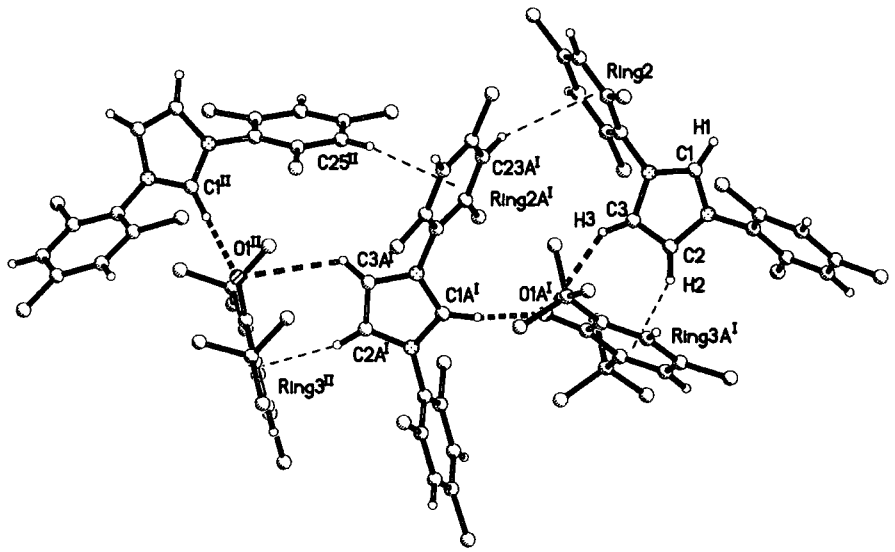


Figure 2.7.3. The intermolecular interactions between the DMI+ and DTPO- molecules. The heavy dashed lines indicate C-H···O hydrogen bonds. The thin dashed lines indicate C-H···π hydrogen bonds. The methyl group hydrogen atoms have been omitted for clarity. (Symmetry codes. I = y, -x+y, 1-z. II = -x+y, -x-1, z)

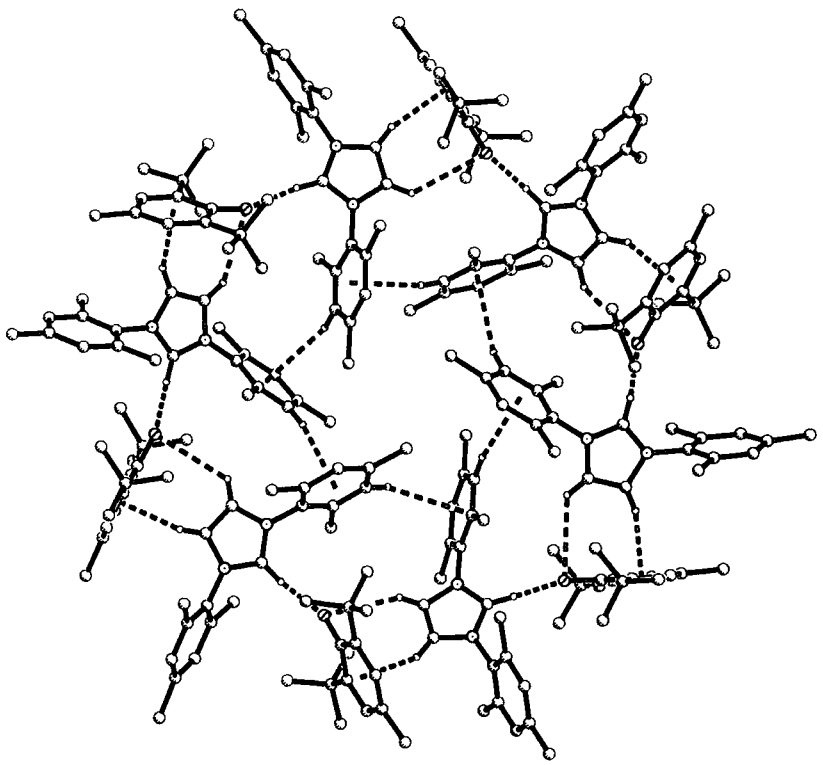

Figure 2.7.4. Packing of the DMI+ and DTPO- molecules in a ring around the (2/3 1/3 0) 3-fold axis. C-H···π and C-H···O bonds are indicated by dashed lines.

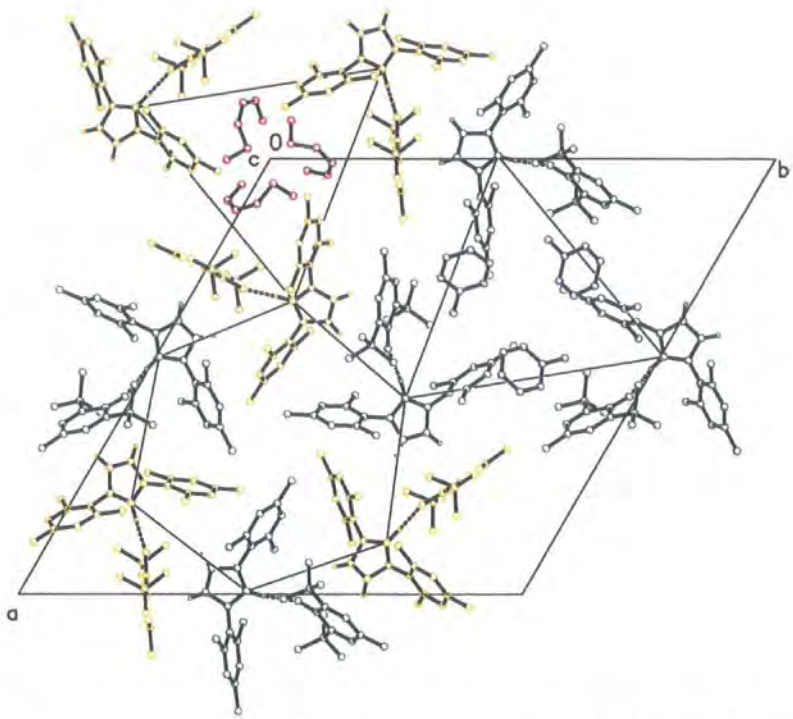


Figure 2.7.5. Packing of a layer of molecules viewed parallel to the c-axis. The hexane solvent is red and lies around the 3-fold axis at (0 0 0). The toluene solvent is purple and around the 3-fold axis at (1/3 2/3 0). The crystallographically identical DMI+ and DTPO- molecules are the same colour, either yellow or green. The hexagon illustrates the fragment from figure 2.7.4.

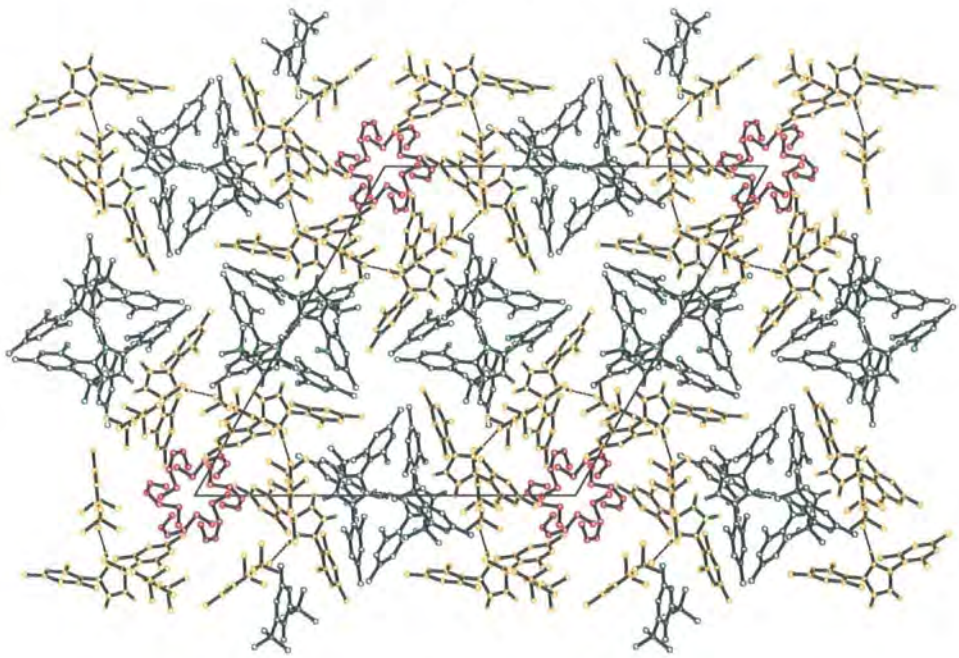

Figure 2.7.6. Packing diagram viewed parallel to the c-axis. The molecules are colour coded in the same way as in figure 2.7.5.

**Experimental details**

Table 2.7.cry. Crystal data for DTPO- and DMI+.

| | | | |
|---|---|---|---|
| Formula | $2[C_{21}H_{25}N_2^+]\cdot 2[C_{14}H_{23}O\text{-}]\cdot C_7H_8\cdot 0.75C_6H_{14}$ | Formula Weight | 603.15 |
| Crystal System | Trigonal | Space Group | P-3 |
| a (Å) | 27.008(9) | $\alpha$ | 90º |
| b (Å) | 27.008(9) | $\beta$ | 90º |
| c (Å) | 17.684(9) | $\gamma$ | 120º |
| Volume $(Å)^3$ | 11171(8) | Z | 12 |
| Density (Mg $m^{-3}$) | 1.078 | Colour | Colourless |
| Crystal Shape | Block | Dimensions (mm) | 0.2 * 0.2 * 0.1 |

Table 2.7.data. Data collection details for DTPO- and DMI+.

| | | | |
|---|---|---|---|
| Radiation | Mo K$\alpha$ | $\lambda$ (Å) | 0.71073 |
| Temperature (K) | 100(2) | | |
| Reflections | 121938 | Independent reflections | 17075 |
| Reflections I > 2$\sigma$(I) | 11562 | | |
| Rint | 0.0557 | Rsigma | 0.0324 |
| h | -35 → 35 | K | -35 → 35 |
| l | -22 → 22 | $\theta_{max}$ | 27.48 |

Table 2.7.ref. Refinement details for DTPO- and DMI+.

| | | | |
|---|---|---|---|
| $R[F^2 > 2\sigma(F^2)]$ | 0.0603 | $wR^2(F^2)$ | 0.1869 |
| S | 1.012 | Data / Parameters | 17075 / 840 |
| $\Delta\rho_{max}$ (e $Å^{-3}$) | 0.773 | $\Delta\rho_{min}$ (e $Å^{-3}$) | -0.410 |
| $(\Delta/\sigma)_{max}$ | 0.001 | $\Delta\rho_{rms}$ (e $Å^{-3}$) | 0.049 |

Cell parameters were determined from 979 strong reflections $\theta$ = 15.74 – 20.97º. Anisotropic thermal parameters for all non-hydrogen atoms were refined. All the hydrogen atoms, except H1 and H1A, were refined with a riding model with thermal parameters dependent upon the ridden atom. H1 and H1A, because of their importance in the structure, were refined freely with an isotropic thermal parameter resulting in realistic values for positional and thermal paramaters.

## 2.8. Co-Crystals of Pentachlorophenol and 1,3-Dimesitylimidazol-2-ylidene

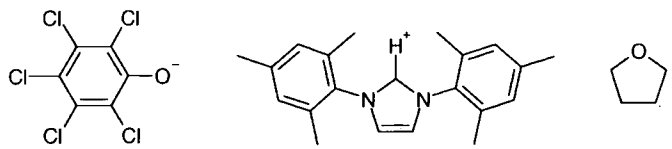


[PCPO-] [DMI+] [THF]

Pentachlorophenol and 1,3-dimesitylimidazol-2-ylidene crystallise in 1:1 ratio as a molecular salt with one molecule of tetrahydrofuran (THF) solvent, $C_{21}H_{25}N_2^+ \cdot C_6Cl_5O_1^- \cdot C_4H_8O$, in space group $P2_1$. Pentachlorophenol has been deprotonated to become pentachlorophenoxide (PCPO-) and 1,3-dimesitylimidazol-2-ylidene has been protonated to become 1,3-dimesitylimidizolium (DMI+). The molecules interact through C-H···O hydrogen bonds and $\pi$-$\pi$ stacks to form columns parallel to the a-axis.

The chlorine atoms, with 17 electrons each, in PCPO-, dominate the X-ray scattering consequently the difference Fourier map is unreliable for finding hydrogen atoms. The root mean squared deviation of the residual electron density from zero is 0.100 $eA^{-3}$, which is twice the value found in the other structures in this series. The hydrogen atoms were all placed by geometric considerations and refined with a riding model.

The pentachlorophenol molecule has become deprotonated, which its conformation reflects. In a search of the Cambridge Structural Database (Allen and Kennard, 1993) the structures of PCPO-are more distorted from a regular hexagon than the structures of pentachlorophenol and the average C-O bond length is, as expected, shorter in the PCPO- (figure 2.8.1). The molecule in this structure, with internal angles ranging from 113.5(3)º to 123.6(3)º and a C-O distance of 1.274(4)Å, closely fits the PCPO- template.

C1 in the DMIY molecule has become protonated, which agrees chemically with the deprotonation of PCP. The N1-C1-N2 angle of 108.1(3)° and the C1-N1 and C1-N2 distances of 1.337(4)Å and 1.338(4)Å confirm that this is the imidizolium ion rather than the carbene.

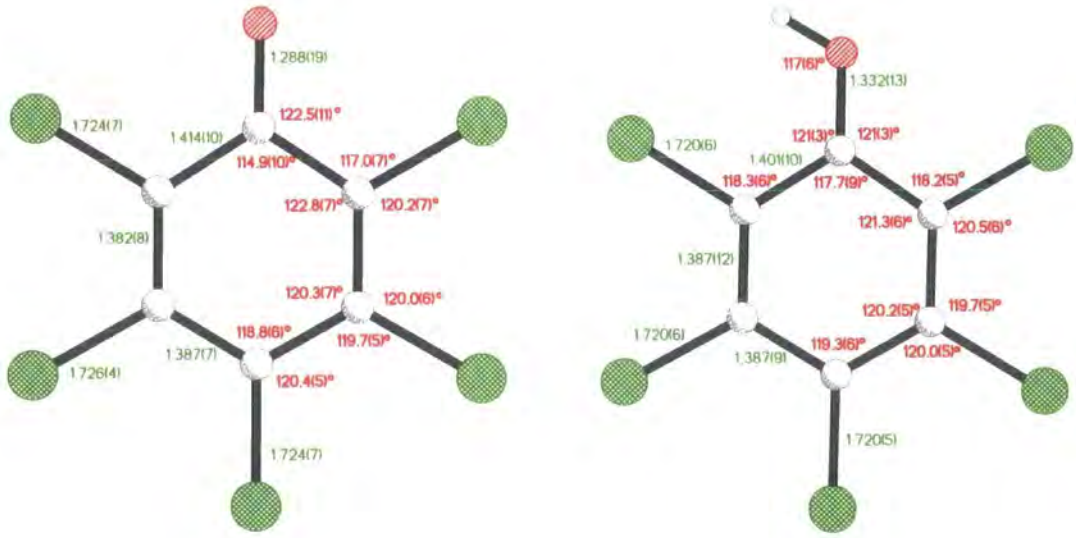


Figure 2.8.1. The average bond lengths and angles in PCP and PCPO- from the Cambridge Structural Database. Bond lengths in Ångströms are in green and bond angles are in red. Chlorine atoms are green, the oxygen atom red and the carbon atoms are white.

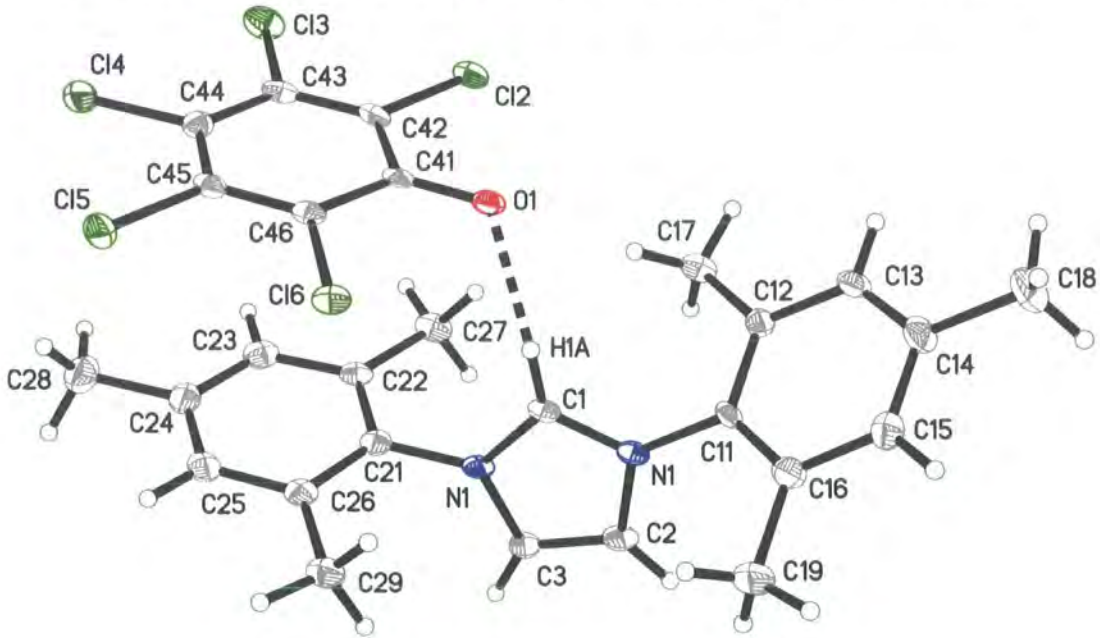


Figure 2.8.2. 50% thermal-ellipsoid plot of PCPO- and DMI+. The dashed line indicates a hydrogen bond.

The PCPO- and DMI+ molecules pack to form C-H···O hydrogen bonded and π-π stacked columns parallel to the a-axis. Two C-H···O bonds are formed [C1···O1, C3···O1$^{i}$] between PCPO- and DMI+ to link the molecules into chains. Longer C-H···O hydrogen bonds connect DMI+ and THF solvent molecules in the same columns [C13···O1S$^{iii}$, C2···O1S$^{ii}$].

Table 2.8.1: C-H···O Hydrogen Bond Parameters.

| | D···A (Å) | H···A (Å) | D-H-A |
|---|---|---|---|
| C1-H1···O1 | 2.916(4) | 2.031 | 154.3° |
| C3-H3···O1$^{I}$ | 3.031(4) | 2.154 | 153.0° |
| C2-H2···O1S$^{II}$ | 3.165(5) | 2.557 | 122.1° |
| C13-H13···O1S$^{III}$ | 3.471(5) | 2.536 | 168.4° |

Symmetry Codes: (i) x – 1, y, z, (ii) x, y, z + 1, (iii) x + 1, y, z + 1.

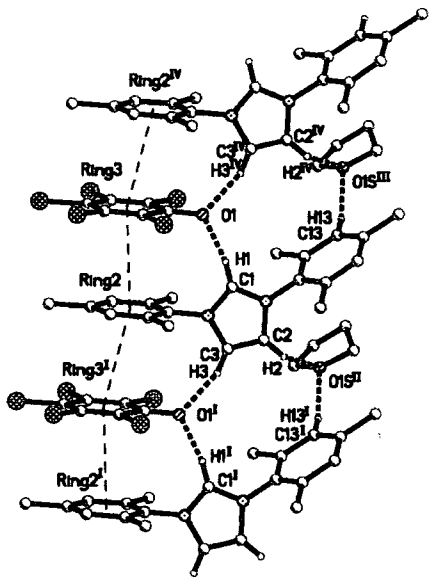


Figure 2.8.3. Packing diagram showing the columns of PCPO- and DMI+ molecules. Heavy dashed lines indicate C-H···O hydrogen bonds. Thin dashed lines indicate π-π interactions. (Symmetry codes correspond to the table 1. IV = 1+x, y, z. Ring 1 = C11-C16, Ring 2 = C21-C26. Ring 3 = C41-C46)

The mesityl rings twist with respect to the imidazolium ring by 63.15(10)° for ring 1 and 78.89(11)° for ring 2 to optimise the C-H···O hydrogen bonds and the π-π interactions. Two π-π interactions, both between ring 2 and ring 3, complement the C-H···O hydrogen bonds between DMI+ and PCPO+.

Table 2.8.2. π-π Interactions.

| | Centre-to-centre distance (Å) | Angle between planes | Shortest perpendicular distance (Å) |
|---|---|---|---|
| Ring2-Ring3 | 3.8004(11) | 1.75(11)° | 3.406(3) |
| Ring2-Ring3$^{II}$ | 3.7080(11) | 1.75(11)° | 3.433(2) |

Weak halogen-halogen interactions link the PCPO- molecules into chains along the [1 0 1] direction. Halogen-halogen interactions are classified into two types depending on the C-Cl-Cl angles (Desiraju and Parthasarathy, 1989, Sakurai et al, 1963), in type 1 both C-Cl-Cl angles are equal, in type 2 one C-Cl-Cl angle is expected to be 180º and the other is expected to be 90º. The Cl2-Cl5 interaction corresponds to a type 1 interaction. The Cl2-Cl6 and Cl3-Cl5 interactions are almost identical frustrated type 2 interactions with one angle close to 180º and the other angle ~120º. This frustration must optimise the overall strength of the three interactions.

Table 2.8.3. Halogen···Halogen Interactions.

| | Cl···Cl distance (Å) | C-Cl-Cl Angle | Cl-Cl-C Angle |
|---|---|---|---|
| C42-Cl2···Cl5$^{III}$-C45$^{III}$ | 3.5638(13) | 121.1(1)º | 121.67(1)º |
| C42-Cl2···Cl6$^{III}$-C46$^{III}$ | 3.5448(13) | 167.5(1)º | 121.90(1)º |
| C43-Cl3···Cl5$^{III}$-C45$^{III}$ | 3.5427(14) | 122.2(1)º | 164.66(1)º |

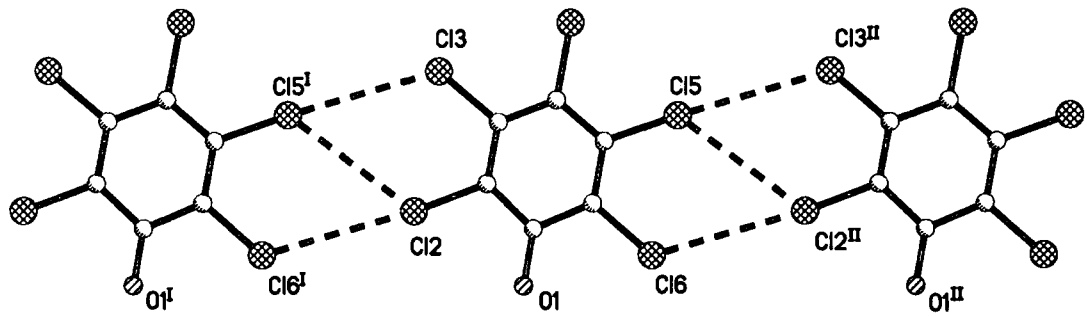


Figure 2.8.4. Cl···Cl Interactions between the PCPO- molecules.

The molecules pack to form columns perpendicular to the a-axis. The columns pack in layers linked by the Cl···Cl interactions.

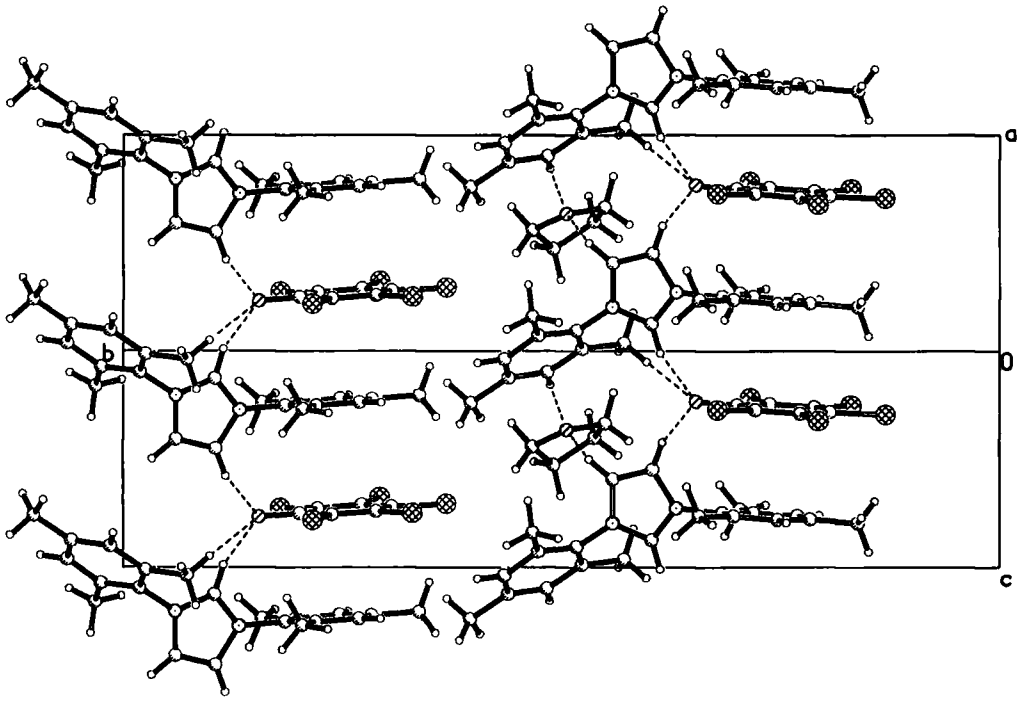


Figure 2.8.5. Packing diagram of PCPO- and DMI+ viewed perpendicular to the molecular columns.

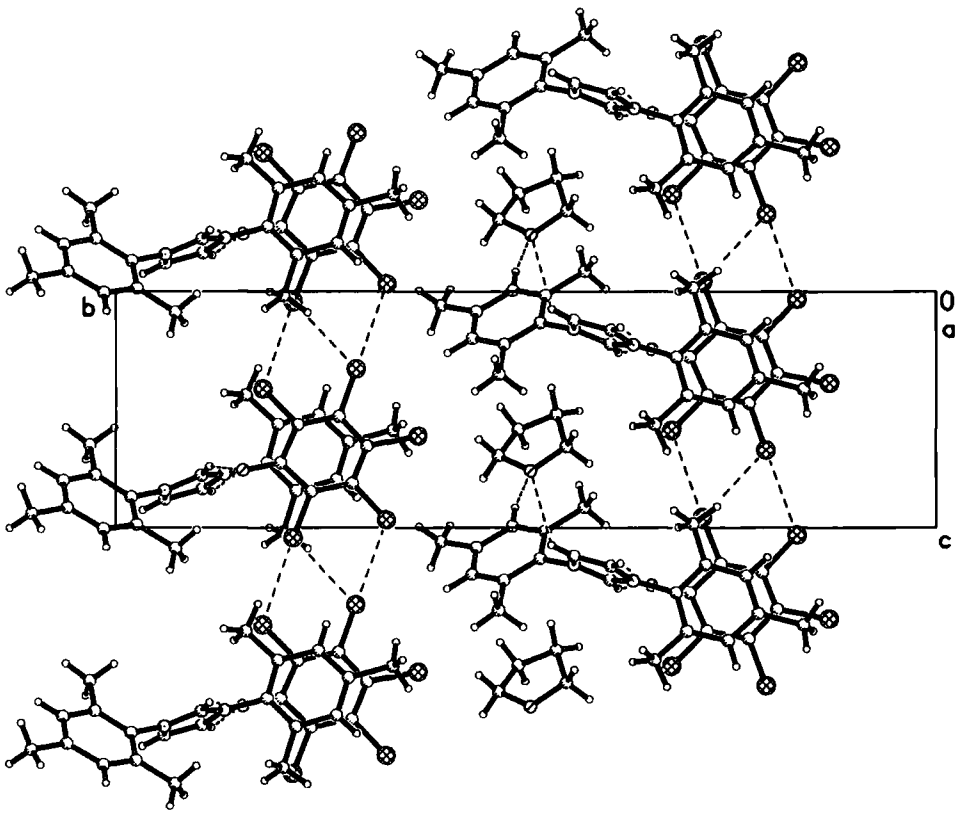


Figure 2.8.6. Packing diagram of PCPO- and DMI+ viewed parallel to the a-axis, looking down the $\pi$-stacked molecular columns.

**Experimental Details**

Table 2.8.cry. Crystal parameters for PCPO- and DMI+.

| Formula | $C_{21}H_{25}N_2^+.C_6Cl_5O^-$ $\cdot C_4H_8O$ | Formula Weight | 642.84 |
|---|---|---|---|
| Crystal System | Monoclinic | Space Group | $P2_1$ |
| a (Å) | 7.422(2) | α | 90º |
| b (Å) | 26.875(8) | β | 114.838(4)º |
| c (Å) | 8.567(3) | γ | 90º |
| Volume $(Å)^3$ | 1550.9(8) | Z | 2 |
| Density (Mg $m^{-3}$) | 1.377 | Colour | Colourless |
| Crystal Shape | Plate | Dimensions (mm) | 0.6 * 0.3 * 0.05 |

Table 2.8.data. Data collection details for PCPO- and DMI+.

| Radiation | Mo Kα | λ (Å) | 0.71073 |
|---|---|---|---|
| Temperature (K) | 100(2) | | |
| Reflections | 19264 | Independent reflections | 8424 |
| Reflections I > 2σ(I) | 7200 | | |
| Rint | 0.0590 | Rsigma | 0.0615 |
| h | -10 → 10 | K | -36 → 36 |
| l | -12 → 12 | $\theta_{max}$ | 30.49º |

Table 2.8.ref. Refinement details for PCPO- and DMI+.

| $R[F^2 > 2\sigma(F^2)]$ | 0.0540 | $wR^2(F^2)$ | 0.1301 |
|---|---|---|---|
| S | 1.076 | Data / Parameters | 8424 / 367 |
| $\Delta\rho_{max}$ (e $Å^{-3}$) | 0.703 | $\Delta\rho_{min}$ (e $Å^{-3}$) | -0.507 |
| $(\Delta/\sigma)_{max}$ | 0.001 | $\Delta\rho_{rms}$ (e $Å^{-3}$) | 0.100 |

Cell parameters were determined from 845 strong reflections θ = 14.57 – 24.14º.
An absorption correction was applied with the multi-scan program SADABS (Sheldrick, 1993), μ = 0.499 $mm^{-1}$, Maximum transmission = 1.00, minimum transmission = 0.6745.
Anisotropic thermal parameters of all non-hydrogen atoms were refined. All the hydrogen atoms were refined with a riding model with thermal parameters dependent upon the ridden atom.

## 2.9. The Co-Crystal of Pentafluorophenol and 1,3-Dimesitylimidazol-2-ylidene

Pentafluorophenol and 1,3-dimesitylimidazol-2-ylidene crystallise in a 2:1 ratio as a molecular salt, i.e. $C_6F_5OH{\cdot}C_6F_5O^-{\cdot}C_{21}H_{25}N_2^+$ in space group $P2_1/c$. One pentafluorophenol (PFP) molecule has been deprotonated to become pentafluorophenoxide (PFPO-) and the 1,3-dimesitylimidazol-2-ylidene has been protonated to become 1,3-dimesitylimidizolium (DMI+). The PFP and PFPO- molecules are linked by a short O-H···O hydrogen bond. A C-H···O hydrogen bond connects DMI+ to the PFP·PFPO- dimer.

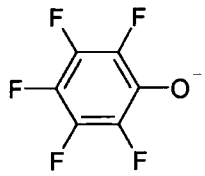


**[PFPO-]**

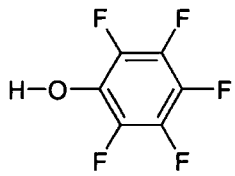


**[PFP]**

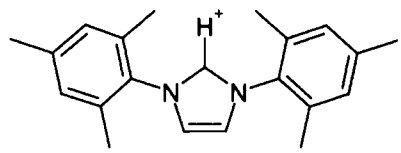


**[DMI+]**

There are only six occurrences of PFP in the Cambridge Structural Database (CSD, Allen and Kennard, 1993) and three occurrences of PFPO-. The internal angle [C46-C41-C42] in PFPO- is 114.14(15)º, which agrees with the average value observed in the CSD of 114.2(2)º for PFPO-. The internal angle [C32-C31-C36] in PFP is 116.4(2)º, which agrees with the average value observed in the CSD of 116.6(7)º for PFP.

The average values in the CSD for the C-O bond lengths are 1.305(8)Å for PFPO- and 1.342(5)Å for PFP, the values observed here are 1.318(2)Å for PFPO- and 1.330(3)Å for PFP. The differences of the C-O values from the average values can be explained by the strength of the O-H···O hydrogen bond.

Table 2.9.1. O-H···O Hydrogen Bond Parameters.

| | O···O distance (Å) | O-H distance (Å) | H···O distance (Å) | O-H-O angle |
|---|---|---|---|---|
| O31-H100···O41 | 2.443(2) | 1.12(4) | 1.35(4) | 162(3)º |

The proton position measured by X-ray diffraction is unreliable in short-strong hydrogen bonds. Neutron diffraction measurements on similar short hydrogen bonds show the lengthening of the O-H bond as the O-O distance gets shorter. The O-H bond length is quite long but agrees with the neutron diffraction measured O-H bond length for a strong O-H···O bond with an O···O separation of ~2.45Å (Graph 2.9.1).

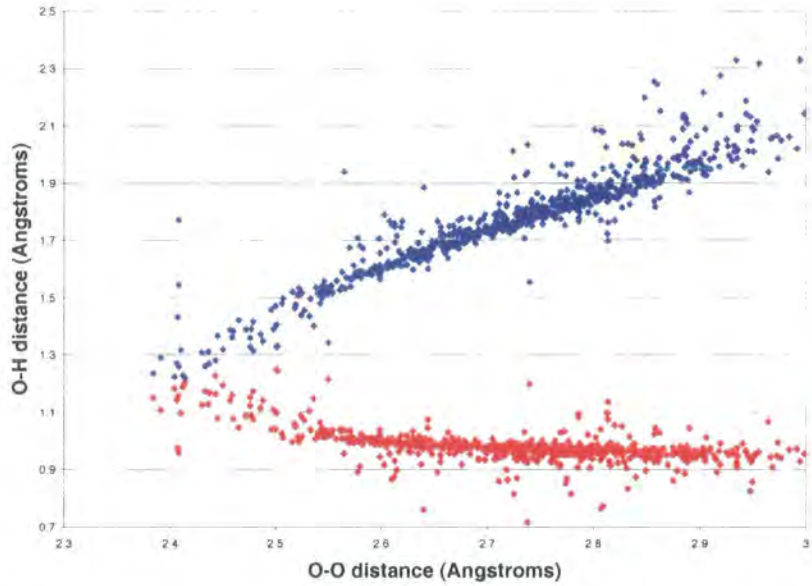


Graph 2.9.1. O-H···O hydrogen bonds from the CSD studied by neutron diffraction. The O-H distances are in pink. The H···O distances are in blue.

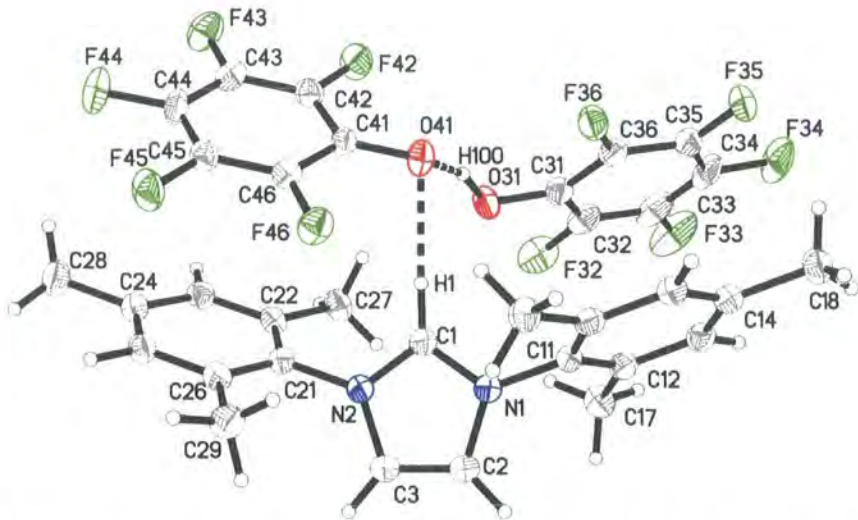


Figure 2.9.1. 50% thermal-ellipsoid plot of the asymmetric unit of PFP, PFPO- and DMI+. The dashed lines indicate hydrogen bonds. The minor part of the disordered molecule has been omitted.

A proton was found in the difference Fourier map bonded to C1 in the DMI+, which agrees chemically with the deprotonation of one molecule of PFP. The N1-C1-N2 angle of 108.3(1)° and the C1-N1 and C1-N2 distances of 1.336(2)Å and 1.340(2)Å confirm that this is the imidizolium ion rather than the carbene.

The PFP molecule is rotationally disordered and has been modelled on two positions with occupations of 81% and 19%. The major component has been refined freely with anisotropic

displacement parameters, the minor component has been restrained to have a similar geometry to the major component and refined with isotropic displacement parameters. The geometries of both components are unreliable because of the disorder and the large thermal ellipsoids.

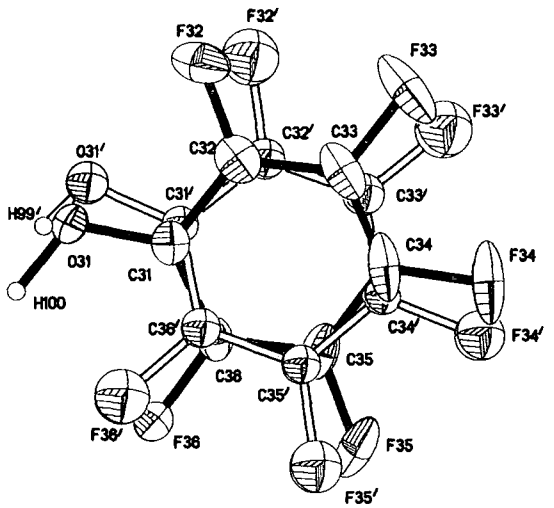


Figure 2.9.2. The disordered PFP molecule. The minor component is drawn with hollow bonds.

A C-H···O hydrogen bond and two π-π interactions link DMI+ to the PFP·PFPO- dimer. A short C-H···O hydrogen bond is formed between C1 and O41 [C1···O41 3.068(2)] and π-π interactions are formed between the PFP and PFPO- molecules and the mesityl rings of the DMI+ to link all the molecules in the asymmetric unit (figure 1). A further π-π bond and a C-H···F hydrogen bond [C2···F32 3.120(3)Å] link the asymmetric units into π-stacked columns parallel to the a-axis (figure 2.9.3).

Table 2.9.2. C-H···O hydrogen bond parameters.

| | C···O distance (Å) | C-H distance (Å) | H···O distance (Å) | C-H-O angle |
|---|---|---|---|---|
| C1-H1···O41 | 3.068(2) | 0.98(2) | 2.09(2) | 178(2)º |
| C3-H3···O41$^{I}$ | 3.109(2) | 0.97(2) | 2.53(2) | 118(2)º |

Table 2.9.3. C-H···F hydrogen bond parameters.

| | C···F distance (Å) | C-H distance (Å) | H···F distance (Å) | C-H-F angle |
|---|---|---|---|---|
| C2-H2···F32$^{II}$ | 3.120(3) | 0.97(2) | 2.42(2) | 128(2)º |
| C3-H3···F36$^{I}$ | 3.379(2) | 0.97(2) | 2.50(2) | 149(2)º |

Table 2.9.4. C-H···π hydrogen bond parameters.

| | C···ring centre distance (Å) | C-H distance (Å) | H···ring centre distance (Å) | C-H-ring centre angle |
|---|---|---|---|---|
| C15-H15···Ring 2$^{iii}$ | 3.704(2) | 0.98(2) | 2.77(2) | 160.1(16)º |

Table 2.9.5. π-π Interactions.

| | Centre to centre distance (Å) | Angle between planes | Shortest perpendicular distance (Å) |
|---|---|---|---|
| Ring1-Ring3 | 4.0507(12) | 1.8(2)º | 3.4931(19) |
| Ring2-Ring4 | 3.7660(10) | 13.07(3)º | 3.4398(18) |
| Ring1-Ring3$^{ii}$ | 4.0109(11) | 1.8(2)º | 3.4459(17) |

Ring 1 = C11-C12-C13-C14-C15-C16. Ring 2 = C21-C22-C23-C24-C25-C26.

Ring 3 = C31-C32-C33-C34-C35-C36. Ring 4 = C41-C42-C43-C44-C45-C46.

Symmetry code. i = 1-x, -0.5+y, 0.5-z. ii = x-1, y, z. iii = 1-x, 0.5+y, 0.5-z.

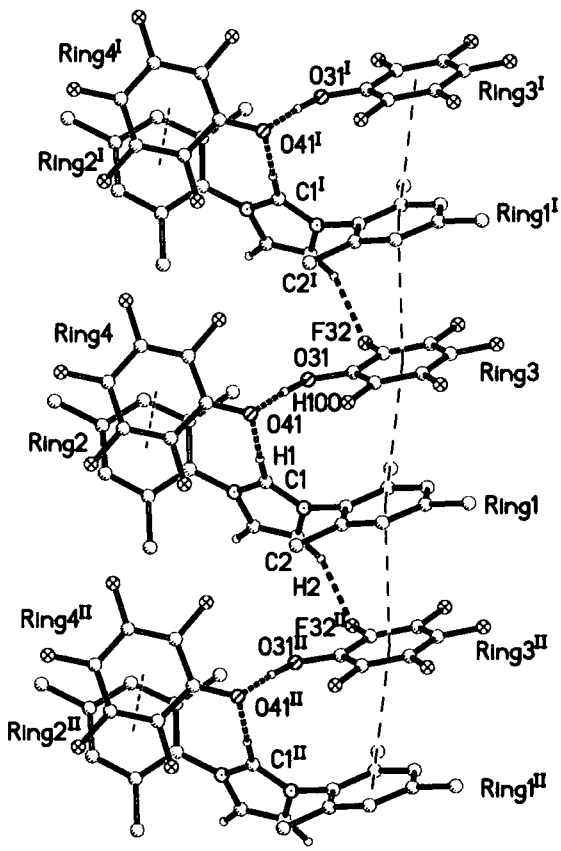


Figure 2.9.3. Packing diagram of PFP, PFPO- and DMI+ illustrating the molecular columns along the a-direction. Hydrogen bonds are indicated by heavy dashed lines. π-π interaction are indicated by thin dashed lines. (Symmetry codes i = 1+x, y, z, ii = x-1, y, z)

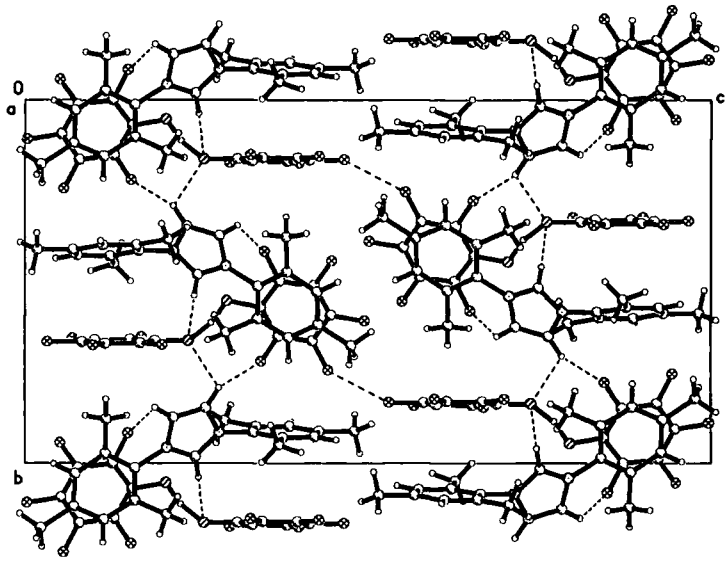


Figure 2.9.4. Packing diagram of PFP, PFPO- and DMI+ viewed parallel to the a-axis. Looking along the molecular columns in figure 2.9.3.

C-H···π [C15···Ring2], C-H···O [C3···O41] and C-H···F [C3···F36] hydrogen bonds connect adjacent molecular columns (figure 2.9.5) and also form a second molecular chain in the b direction.

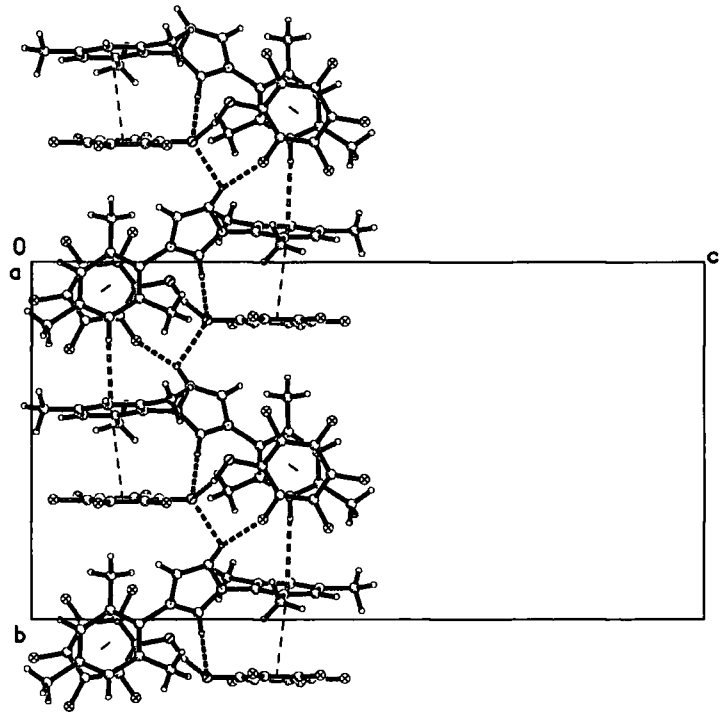


Figure 2.9.5. Packing diagram of PFP, PFPO- and DMI+ illustrating an alternative molecular chain. Heavy dashed lines indicate C-H···F and C-H···O hydrogen bonds. Hollow dashed lines indicate C-H···π hydrogen bonds. Thin dashed lines indicate π-π interactions.

**Experimental details**

Table 2.9.cry. Crystal parameters for PFP, PFPO- and DMI+

| Formula | $C_{21}H_{25}N_2^+ \cdot C_6F_5O^- \cdot C6HF5O$ | Formula Weight | 672.56 |
|---|---|---|---|
| Crystal System | Monoclinic | Space Group | $P2_1/c$ |
| a (Å) | 8.159(2) | α | 90º |
| b (Å) | 14.293(4) | β | 93.191(4)º |
| c (Å) | 26.863(8) | γ | 90º |
| Volume $(Å)^3$ | 3127.9(15) | Z | 4 |
| Density $(Mg\ m^{-3})$ | 1.428 | Colour | Colourless |
| Crystal Shape | Block | Dimensions (mm) | 0.45 * 0.35 * 0.25 |

Table 2.9.data. Data collection details for PFP, PFPO- and DMI+.

| Radiation | Mo Kα | λ (Å) | 0.71073 |
|---|---|---|---|
| Temperature (K) | 100(2) | | |
| Reflections | 22777 | Independent reflections | 6012 |
| Reflections I > 2σ(I) | 4950 | | |
| Rint | 0.0504 | Rsigma | 0.0311 |
| H | -9 → 9 | K | -17 → 17 |
| I | -33 → 33 | $\theta_{max}$ | 26.60º |

Table 2.9.ref. Refinement details for PFP, PFPO- and DMI+.

| $R[F^2 > 2\sigma(F^2)]$ | 0.0430 | $wR^2(F^2)$ | 0.1091 |
|---|---|---|---|
| S | 1.027 | Data / Parameters | 6012 / 567 |
| $\Delta\rho_{max}$ (e $Å^{-3}$) | 0.242 | $\Delta\rho_{min}$ (e $Å^{-3}$) | -0.261 |
| $(\Delta/\sigma)_{max}$ | 0.000 | $\Delta\rho_{rms}$ (e $Å^{-3}$) | 0.052 |

Cell parameters were determined from 912 strong reflections θ = 13.72 – 27.43º. Anisotropic thermal parameters were refined for all non-hydrogen atoms excluding the minor disordered component. All the hydrogen atoms were found in the difference Fourier maps and refined with isotropic displacement parameters, except the hydrogen atoms in the methyl group bonded to C28 which were refined with a rigid rotor model. The C-H distances all refined to within standard ranges and there were no anomalous values of $U_{iso}$.

## 2.10. Discussion

The five new structures of co-crystals of 1,3-dimesitylimidazol-2-ylidene with weak organic acids reported in this chapter have produced novel and interesting weak hydrogen bonding, including an N-H···C hydrogen bond and very short C-H···O hydrogen bonds.

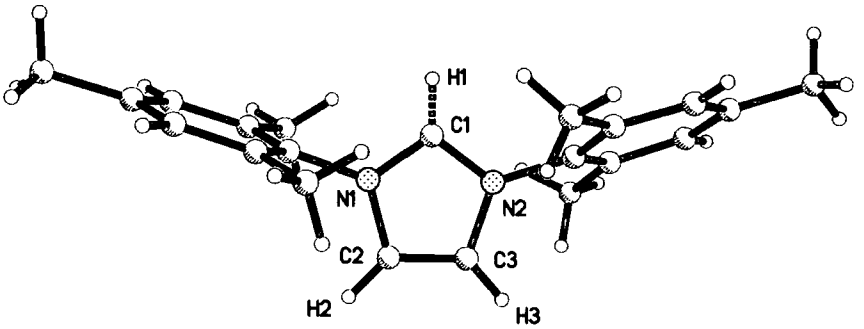


Diagram 2.10.1. The numbering scheme around the central pentagon.

### 2.10.1. Density Functional Theory Calculations

Density functional theory quantum mechanical calculations using the program DMol$^3$ (Delley, 2000) were performed on the molecules of DMIY and the protonated ion, DMI+, to calculate the charge density and the electrostatic charges around the free molecules. Although the results of these calculations are not exactly applicable to the molecules confined in crystals they should produce a good approximation for the charge distribution in the solid state.

The results of these calculations are shown graphically in figures 2.10.1 and 2.10.2. The charge density surface has been calculated at a level of 0.02eÅ$^{-3}$ and the electrostatic charge has been mapped onto this surface. In figures 2.10.1A, B and C the DMIY molecule has been shown in different orientations and in figures 2.10.2A, B and C the DMI+ molecule has been shown. The red indicates regions of positive electrostatic charge and the blue indicates regions of negative electrostatic charge. The scales for the colouring are not the same to indicate the variations over the surface more clearly. The total range of charge in DMIY is from –0.12e (blue) to +0.17e (red), while the maximum charge in DMI+ is +0.36e (red).

The largest difference between the two calculated electrostatic charges is around C1. In the neutral DMIY molecule the region around C1 has a small negative charge while in the DMI+ ion this region is the most positively charged part of the surface. On both the DMIY and the DMI+ surfaces the regions close to H2 and H3 are significantly positively charged. The C-H bonds around the central pentagon are therefore strongly polarised and if C1 becomes protonated the C1-H1 bond is also strongly polarised, which facilitates C-H···X hydrogen bond formation.

Figure 2.10.1. Electrostatic charge mapped on to the charge density surface at $0.02eÅ^{-3}$ of the DMIY molecule. Green represents approximately neutral and red represents a positive charge and blue represents a negative charge.

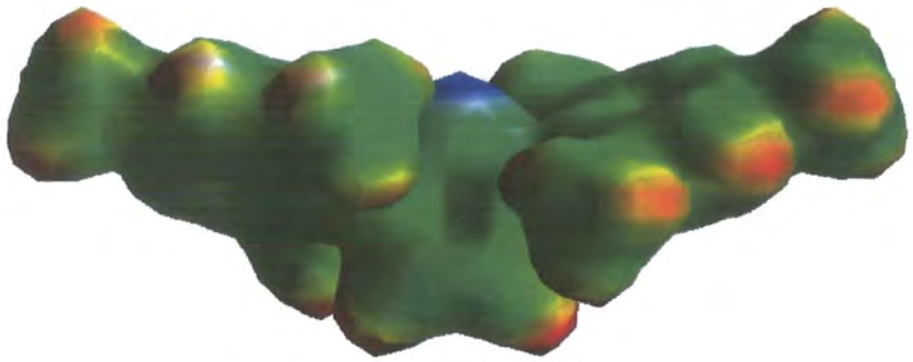

Figure 2.10.1.A. Side view.

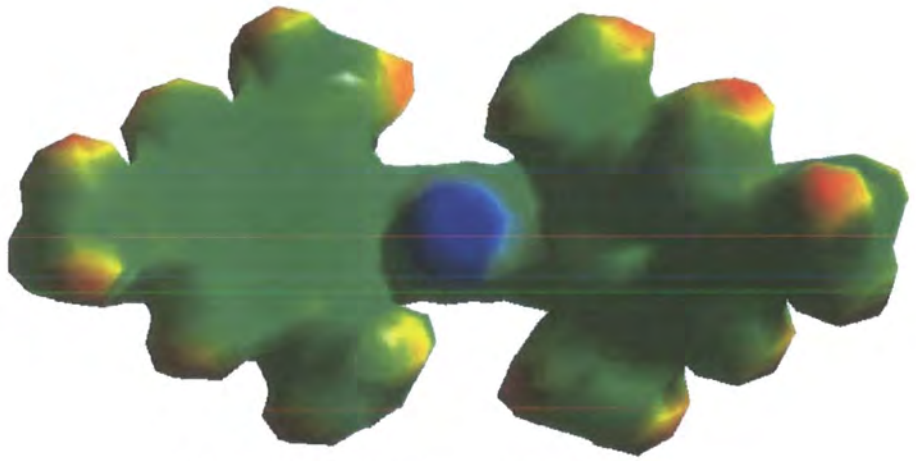

Figure 2.10.1.B. View looking down upon C1.

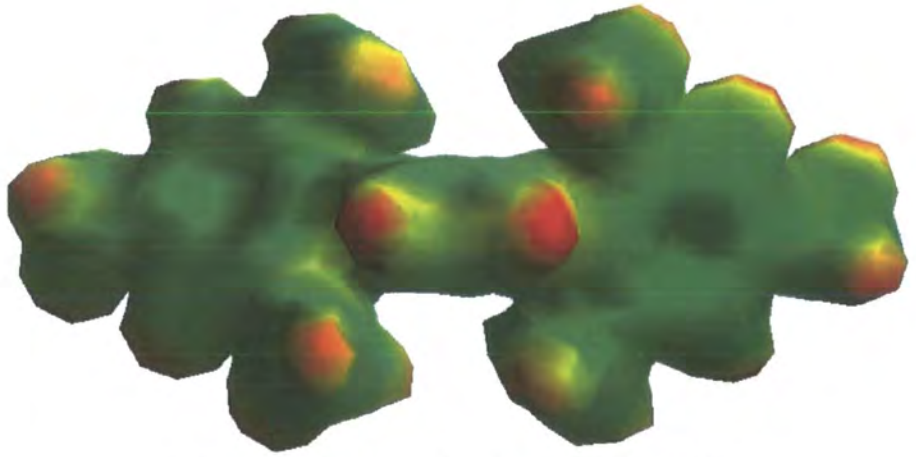

Figure 2.10.1.C. View looking up on H2 and H3.

Figure 2.10.2. Electrostatic charge mapped on to the charge density surface at 0.02eÅ$^{-3}$ of the imidazolium ion. Green represents approximately neutral and red represents a positive charge.

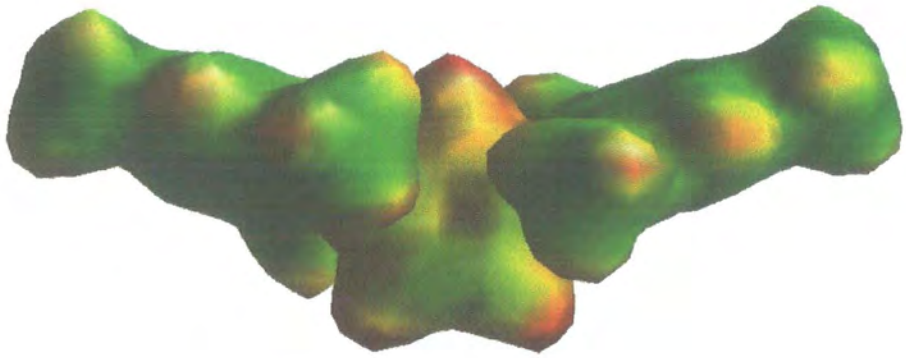

Figure 2.10.2.A. Side view

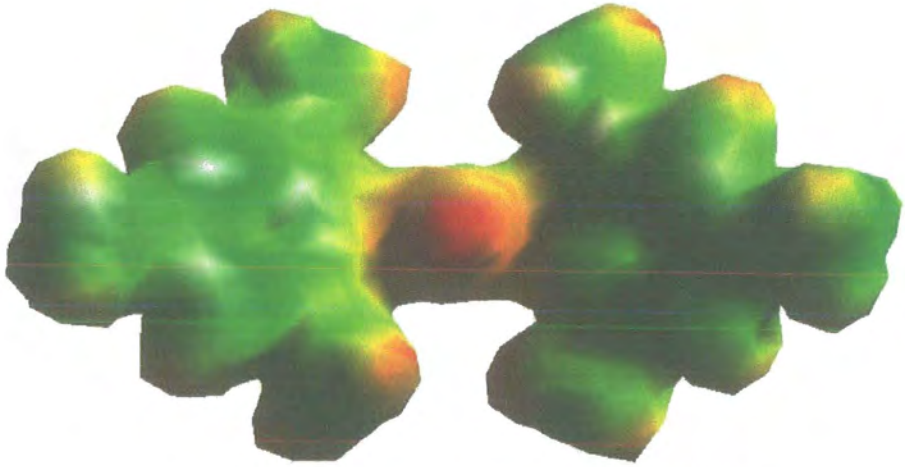

Figure 2.10.2.B View looking down on C1 and H1.

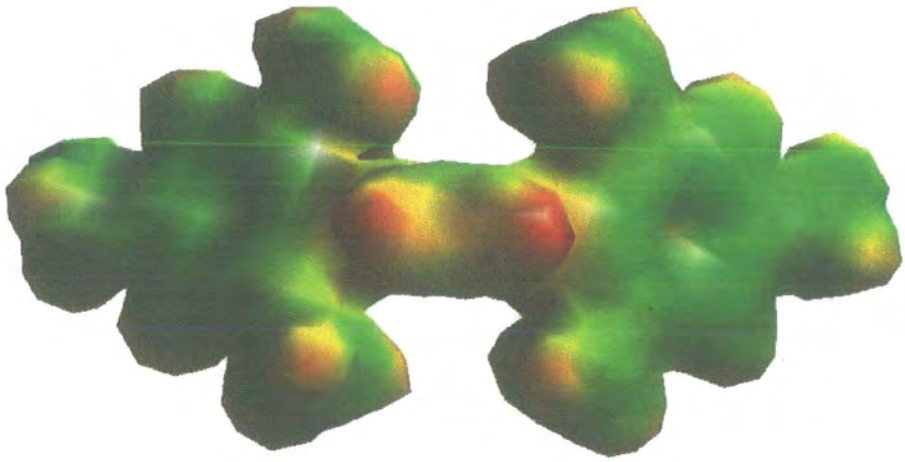

Figure 2.10.2.C. View looking down on H2 and H3.

### 2.10.2. C-H···O Bonds

All of the C-H···O hydrogen bonds in this set of structures are from the DMI+ ion. Only one of these hydrogen bonds does not involve the central imidizolium pentagon. The hydrogen bonds that arise from C1-H1 are shorter and more linear than the hydrogen bonds arising from C2-H2 or C3-H3 (Graphs 2.10.1 and 2.10.2). The strengths of the hydrogen bonds can be related to the calculated electrostatic charges on the molecules, the stronger C1-H1···O bonds come from a larger positive charge on H1 than on H2 or H3.

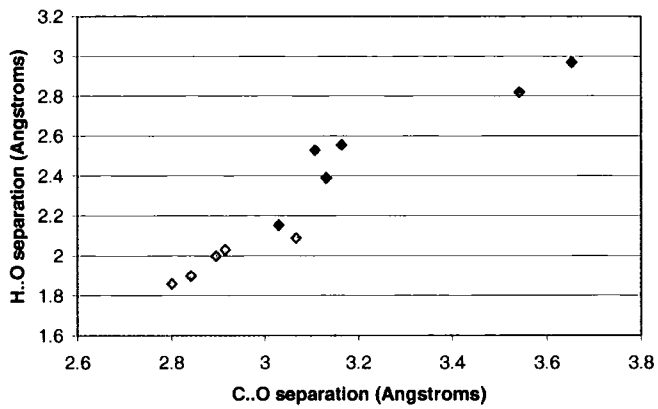


Graph 2.10.1. C··O separations vs. O··H separations in the C-H···O hydrogen bonds observed in this chapter. The red points are hydrogen bonds from C1 and the blue points are hydrogen bonds from C2 or C3.

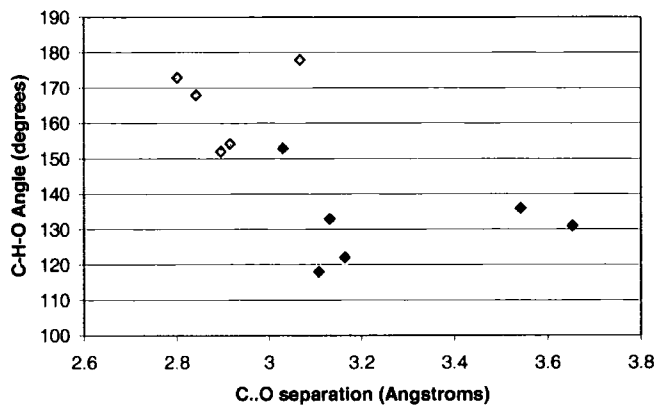


Graph 2.10.2. C··O separations vs. C-H-O angles in the C-H···O hydrogen bonds observed in this chapter. The red points are hydrogen bonds from C1 and the blue points are hydrogen bonds from C2 or C3.

The C1-H1···O hydrogen bonds are all extremely short, with C···O < 3.1Å. The shortest, C1-H1···O1 in the co-crystal of DMI+ with DTPO-, the C···O separation is 2.800(3)Å is significantly shorter than any previously reported C-H···O hydrogen bonds (Steiner, 1997, Davidson et al. 2000)

### 2.10.3. The N-H···C Hydrogen Bond

In the co-crystallisation of DMIY with DPA the DMIY molecule has remained unprotonated and an unprecedented N-H···C hydrogen bond has been formed. A C-H···C hydrogen bond has been observed in DMIY·DMI+ dimers (Arduengo et al. 1995). This is the first interaction observed from an electronegative strong hydrogen bond donor atom to a carbon atom.

### 2.10.4. Recognition Patterns Between DMIY and Phenols

Four of the structures in this chapter involve modified phenoxide molecules (PCPO-, PFPO-, DTBO- and HPOB-) and all apart from DTPO- show similar packing motifs. A C-H···O hydrogen bond forms, assisted by a $\pi$-$\pi$ interaction between one half of the DMI+ ion and the planar counter ion or solvent.

The C··O-C angle, $\theta$, in this motif should be ~110º if the C-O bond and the pentagon are planar, the hexagons are then parallel and can still be offset from one another and can still rotate about an axes parallel to the C-O bond.

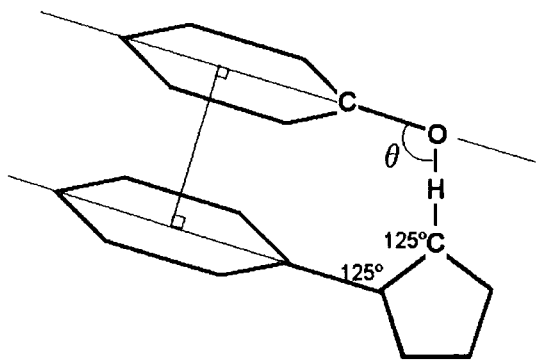


Diagram 2.10.2. The C-O-C angle in DMI+·phenoxide structures. The 125º angles are taken from the DMol$^3$ optimised structure.

Table 2.10.1. C-O-C angles in DMI+·phenoxide structures.

| Structure | Atoms | C-O-C Angle, θ (º) |
|---|---|---|
| DMI+.HPOB- | C1-O1-C46 | 111.79(7) |
| DMI+·DTPO- | C1-O1-C31 | 153.65(13) |
| DMI+·DTPO- | C1A-O1A-C31A | 151.38(12) |
| DMI+·PCPO- | C1-O1-C41 | 117.7(2) |
| DMI+·PFPO- | C1-O1-C41 | 102.66(10) |

The packing motif is further enhanced in DMI+·HPOB- and DMI+·PCPO- where the counter ion also forms a π-π interaction 'underneath' the DMI+ and is linked with a C-H···O hydrogen bond from C2-H2 or C3-H3, and the molecules pack in infinite C-H···O + π-π stacked columns.

The exception to this packing motif is DMI+·DTPO-. Perhaps the tertiary butyl groups hinder π-π stacking or perhaps the extra C-H···π interactions in this structure are optimised preferentially.

### 2.10.5. C-H···π Hydrogen Bonds

C-H···π hydrogen bonds are also common in these crystal structures and undoubtedly play an important role in the packing of DMIY, DMIY·DPA and DMI+·DTBO-. The hydrogen bonds arising from the electropositive H2 or H3 atoms seem to be slightly stronger than those that arise from the hydrogen atoms in the mesityl rings and in the counter ions.

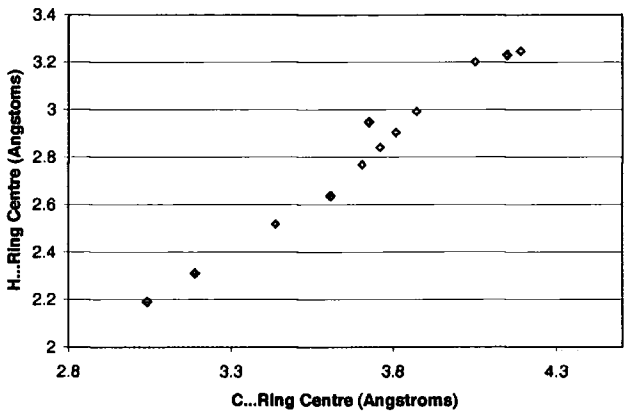


Graph 2.10.3. C···Ring centre distance vs H···Ring centre distance in C-H···π hydrogen bonds. The blue points are hydrogen bonds that arise from C2 or C3 and the green points arise from other C-H groups.

The parameters tabulated for C-H···π bonds are unreliable, especially from X-ray results where the hydrogen atoms positions are not very accurate, as it is difficult to say unambiguously where the hydrogen bond points to, the centre of a C-C bond or the centre of the ring.

## 2.11. References


Abernathy, C.D., Clyburne, J.A.C., Cowley, A.H., Jones, R.A. (1999). J. Am. Chem. Soc. 121, 2329-2330.

Allen, F.H., Kennard, O., Watson, D.G., Brammer, L., Orpen, A.G. & Taylor, R. International Tables for Crystallography. (1992). Volume C, Table 9.5.1.1. 685-706.

Allen, F.H. & Kennard. O. (1993). Chem. Des. Autom. News, 8, 31-37.

Allen, F.H., Lommerse, J.P.M., Hoy, V.J., Howard, J.A.K., Desiraju, G.R. (1996). Acta. Cryst. B52, 734-745.

Allen, F.H., Howard, J.A.K., Hoy, V.J., Desiraju, G.R., Reddy, D.S., Wilson, C.C., (1996a). J. Am. Chem. Soc. 118. 4081-4084.

Arduengo III, A. J., Harlow, R.L., Kline, M. (1991). J. Am. Chem. Soc. 113, 361-363.

Arduengo III, A.J., Dias, H.V.R., Harlow, R.L., Kline, M. (1992). J. Am. Chem. Soc. 114, 5530-5534.

Arduengo III, A.J., Dias, H.R.V., Calabrese, J.C., Davidson, F. (1992a). J. Am Chem. Soc. 114, 9724-9725.

Arduengo III, A.J., Dias, H.R.V., Calabrese, J.C., Davidson, F. (1993). Organometallics. 12, 3405-3409.

Arduengo III, A.J., Gamper, S.F, Calabrese, J.C., Davidson, F. (1994). J. Am. Chem. Soc. 116, 4391-4394

Arduengo III, A.J., Gamper, S.F., Tamm, M., Calabrese, J.C., Davidson, F., Craig, H.A. (1995). J. Am. Chem. Soc. 117, 572-573.

Berkovitch-Yellin, Z., Leiserowitz, L. (1984). Acta. Cryst. B40, 159-165.

Blackburn, G.M., Gait, M.J. (1996). Nucleic acids in chemistry and biology. pp 39-42. Oxford University Press.

Bock, H., Dienelt, R., Schödel, H., Havlas, Z. (1993). Chem. Commun. 1792-1793.

Bruker (1998). SMART and SAINT. Bruker AXS Inc., Madison, Wisconsin, USA.

Brunet, P., Simard, M., Weust, J.D. (1997) J. Am. Chem. Soc. 119. 2737-2738.

Chia, S., Cao. J., Stoddart, J.F., Zink, J.I. (2001) Angew. Chem. Int. Ed. 40. 2447-2451.

Davidson, M.G., Goeta, A.E., Howard, J.A.K., Lamb, S., Mason, S.A. (2000). New J. Chem. 24, 477-479.

Delley, B. (2000). J. Chem. Phys. 113, 7756-7764.

Desiraju, G.R., Gavezzotti, A. (1989). Chem. Commun. 621-623.

Desiraju, G.R., Parthasarathy, R. (1989). J. Am. Chem. Soc. 111, 8725-8726.

Desiraju, G.R. (1995). Angew.Chem. Int. Ed. Engl. 34, 2311-2327.

Desiraju. G.R. (2001). Nature 412, 397-400.

Flack H.D. (1983). Acta Cryst. A39, 876-881.

Gangopadhyay, P., Radhakrishnan, T.P. (2001). Angew. Chem. Int. Ed. 40. 2451-2455.

Hanton, L.R., Hunter, C.A., Purvis, D.H. (1992) Chem. Commun. 1134-1136.

Hibbert, F., Emsley, J. (1990). Advances in Physical Organic Chemistry. 26. 255-379.

Hunter, C.A., Sanders, J.K.M., Stone, A.J. (1989). J. Chem. Phys. 133. 395-404.

Hunter, C.A., Sanders, J.K.M. (1990). J. Am. Chem. Soc. 112. 5525-5534.

Hunter, C.A., Lawson, K.R., Perkins, J., Urch, C.J. (2001) J. Chem. Soc. Perkin. Trans. 2. 651-669.

Lee, H.-K., Lee, H., Ko, Y.H., Chang. Y.J., Oh, N.-K., Zin, W.-C. (2001) Angew. Chem. Int. Ed. 40. 2669-2671.

Lehn, J.M. (1988). Angew. Chem. Int. Ed. Engl. 27, 89-112.

March, J. (1985). Advanced Organic Chemistry, 3rd Edition. pp. 170-173. John Wiley & Sons.

Price, S.L., Stone, A.J., Lucas, J., Rowland, R.S., Thornley, A.E. (1994). J. Am. Chem. Soc. 116, 4910-4918.

Prins, L.J., Reinhoudt, D.N., Timmerman, P. (2001). Angew, Chem. Int. Ed. 40. 2382-2426.

Regitz, M. (1991). Angew. Chem. Int. Ed. Engl. 30. 674-676.

Robertson, J.M. (1951). Proc. R. Soc. London Ser. A. 207, 101-110.

Sakurai, T., Sundarlingham, M., Jeffery G.A., (1963). Acta Cryst. 16, 354-363.

Sheldrick, G.M. (1997). SHELXL97 and SHELXS97. University of Göttingen, Germany.

Spek, A.L. (1990). PLATON. Acta Cryst. A46, C-34

Steiner, T. (1997). Chem. Commun. 727-734.

Steiner, T., Lutz, B., Van der Maas, J., Schreurs, A.M.M., Kroon, J., Tamm, M. (1998). Chem. Commun. 171-172.

Trucano, P., Chen, R. (1975). Nature. 258. 136-137.

Viswamitra, M.A., Radhakrishnan, R., Bandekar, J., Desiraju, G. (1993). J. Am. Chem. Soc. 115, 4868-4869.

Voges, M.H., Romming, C., Tilset, M. (1999) Organometallics. 18, 529-533.

## 3. Short Strong N-H···O / O-H···N Hydrogen Bonds in Co-crystals of Bipyridines and Benzene-carboxylic Acids.

Co-crystals of benzene-polycarboxylic acids and bipyridines have been used to study strong N-H···O hydrogen bonding by neutron and X-ray diffraction. Varying the ratio of carboxylic acid groups to pyridine groups alters the patterns of hydrogen bonding. In the 1:2 co-crystal of benzene-1,2,4,5-tetracarboxylic acid and 4,4'-bipyridine a very short N··H··O hydrogen bond is observed in which the hydrogen atom changes position between 20K and 296K.

### 3.1. Short Strong Hydrogen Bonds and Neutron Diffraction.

X-rays are scattered by the electrons in crystals. For most atoms it is adequate to place the nuclear position at the maximum of the electron density. Hydrogen only has one electron and when hydrogen is covalently bonded its electron density is shifted into the covalent bond. Therefore X-H bond lengths derived from X-ray diffraction results are known to be consistently too short. Also as hydrogen has only one electron its X-ray scattering power is much weaker than other elements. As hydrogen is the lightest element and because of the positions it occupies in molecules it often has the largest thermal motion and its scattering power is further reduced.

Neutrons are scattered by the nuclei of atoms. The neutron scattering length of an atom does not depend upon only its atomic number, but also upon the number of neutrons in its nucleus. Hydrogen has a neutron scattering length comparable to carbon, oxygen and nitrogen. In very short hydrogen bonds where the hydrogen electron-density is significantly distorted only neutron diffraction can determine accurately the hydrogen atom nuclear positions.

There have been many studies of short O-H···O hydrogen bonds by neutron diffraction, with many examples of centred or almost centred proton positions (Wilson, 2000, Hibbert and Emsley, 1990, Graph 3.1.1.). Until recently there were no neutron diffraction studies of very short N-H···O or O-H···N hydrogen bonds (Graph 3.1.2). Steiner et al. (2000 and 2001) have studied the short N-H···O hydrogen bonds in co-crystals of 4-methylpyridine with pentachlorophenol and 4-methylpyridine with pentafluorophenol, which have produced the shortest N···O hydrogen bonds studied by neutron diffraction (the green points in graph 3.1.2.). In the shortest of these bonds the hydrogen atom position was observed to change with temperature, at low temperature the hydrogen lies ~1.3Å from the oxygen atom and 1.2Å from the nitrogen; at 300K the situation is reversed with the hydrogen atom lying 1.3Å from the nitrogen atom and 1.2Å from the oxygen atom.

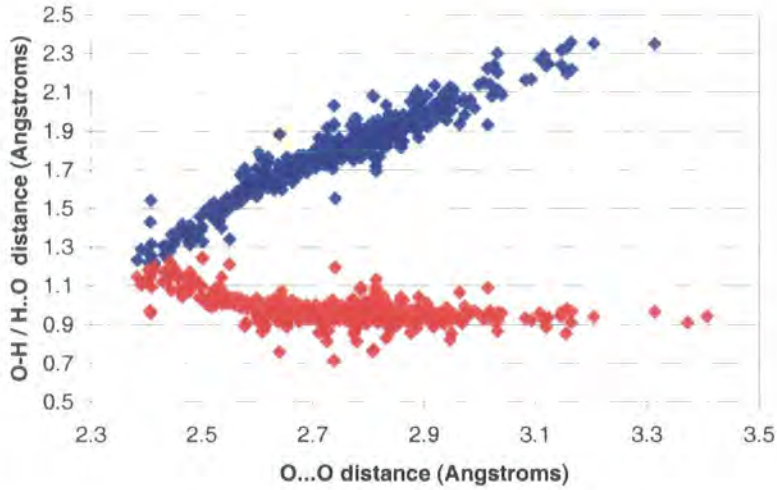


Graph 3.1.1. O-H···O hydrogen bonds measured by neutron diffraction taken from the Cambridge Structural Database. Red points indicate the O-H distance and blue points indicate the H···O distance.

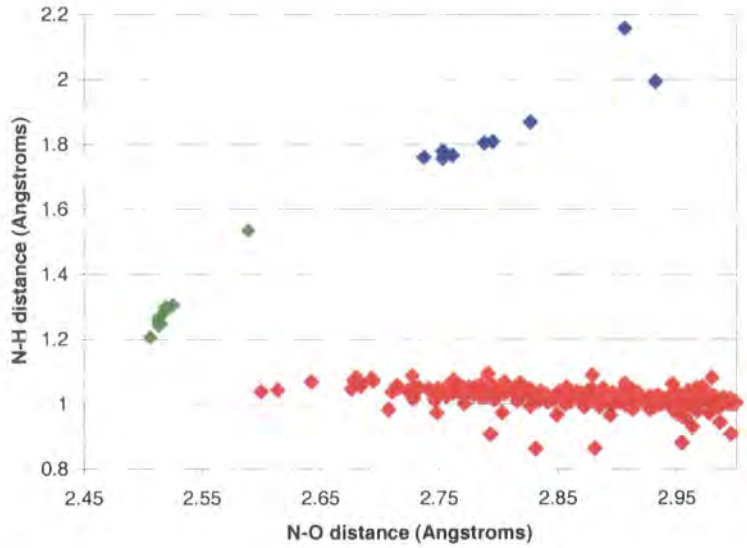


Graph 3.1.2. N-H···O / O-H···N hydrogen bonds studied by neutron diffraction from the Cambridge Structural Database. Red points indicate N-H···O hydrogen bonds, blue points indicate O-H···N hydrogen bonds. The green points are taken from Steiner et al. (2000 and 2001).

Co-crystallisations of benzene-polycarboxylic acids and pyridines provide good opportunities for strong hydrogen bonds to form. In a study of benzene-1,2,4,5-tetracarboxylic acid and various organic bases (Biradha and Zaworotko, 1998) zero, one, two and three dimensional networks were formed by PMA2- molecules all including lots of hydrogen bonding. In the 1:2 co-crystal of benzene-1,2,4,5-tetracarboxylic acid and 4,4'-bipyridine (Lough et al 2000) there are two short N···O hydrogen bonds, one very short N-H···O hydrogen bond (N···O = 2.5236(12)Å) and one slightly longer O-H···N hydrogen bond (N···O = 2.6146(12)Å). These

two hydrogen bonds form in almost identical chemical environments. Small changes in intermolecular environment cause significant changes the hydrogen bonds.

It has been suggested that short strong hydrogen bonds play an important part in stabilising intermediate states in certain mechanisms of enzymatic catalysis (Cleland and Kreevoy, 1994, Hibbert and Emsley, 1990). For example in serine protease (diagram 3.1.1.) it is postulated that an N-H···O hydrogen bond becomes modified by a change in its local intermolecular environment and becomes a very short N··H··O hydrogen bond, stablising the intermediate state so that the substrate can become bound to the protein. The dynamic changes in intermolecular environment in the enzyme can be compared with the static differences in the intermolecular environments in the co-crystals.

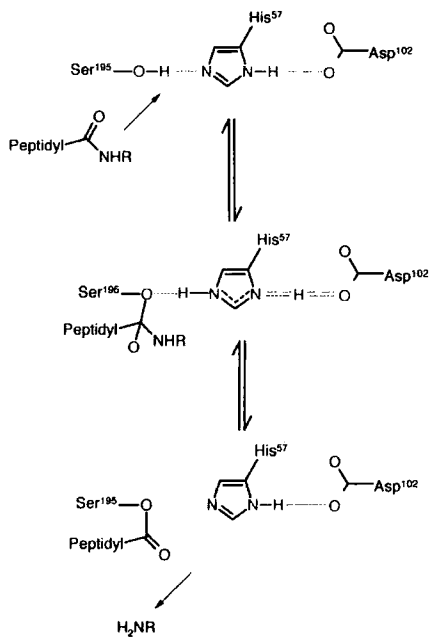


Diagram 3.1.1. Postulated catalytic mechanism in serine protease enzymes. The intermediate state is stabilised by conversion of the red N-H···O hydrogen bond into a short strong N··H··O hydrogen bond.

### 3.2. The Neutron Structure of 4,4'-Bipyridinium Dihydrogen Pyromellitate (2-) Hydrate at 215K.

4,4'-bipyridine and benzene-1,2,4,5-tetracarboxylic acid (pyromellitic acid) crystallise in a 1:1 ratio as a molecular salt, with two molecules of water, in space group $P\bar{1}$. The 4,4'-bipyridine molecule has been doubly protonated to become 4,4'-bipyridinium$^{+2}$ (BPY2+) and the pyromellitic acid has been doubly deprotonated to become dihydrogen pyromellitate$^{-2}$ (PMA2-). The BPY2+ and PMA2- molecules are linked by strong N-H···O hydrogen bonds to form infinite one-dimensional chains, which stack in columns along the a-axis. The disordered water molecules lie in a channel along the a-axis and link parallel chains together with O-H···O hydrogen bonds. Neutron diffraction data were collected on D19 at the ILL at 215K.

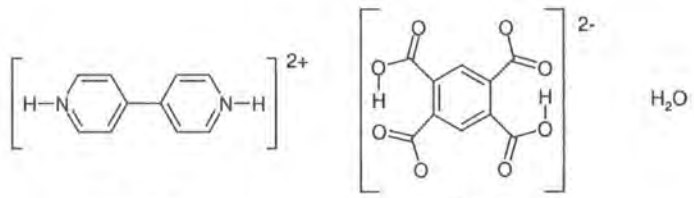


[BPY2+] [PMA2-]

The PMA2- molecule lies around an inversion centre at (½ ½ 0) and therefore only half of the molecule is in the asymmetric unit. There is one independent carboxylic acid group in the molecule and one independent carboxylate group. The C-O bond lengths for a carboxylic acid group attached to a phenyl ring taken from the International Tables for Crystallography (Allen et al. 1992) are 1.305(20)Å for the single bond and 1.226(20)Å for the double bond, in a carboxylate group attached to a phenyl ring both C-O bond lengths are expected to be 1.255(10)Å. The bond lengths in the carboxylic acid group agree perfectly with these [ C10-O11 = 1.300(2)Å, C10-O12 = 1.215(2) ] as do the bond lengths in the carboxylate group [ C20-O21 = 1.247(2)Å, C20-O22 = 1.247(2)Å ].

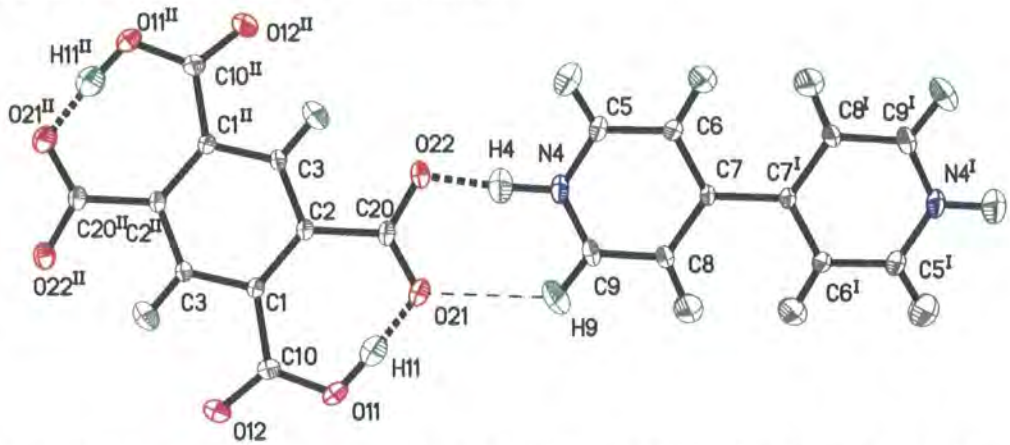


Figure 3.2.1. 50% thermal-ellipsoid plot of PMA2- and BPY2+. The heavy dashed lines indicate strong hydrogen bonds, the thin dashed line indicates a weak C-H···O hydrogen bond. Symmetry codes: I = -x-1, -y, 1-z. II = 1-x, 1-y, -z.

A very short intramolecular hydrogen bond is formed (O...O 2.422(3)Å) between the carboxylic acid group and the carboxylate group. The torsion angles between the carboxyl groups and the phenyl ring are O12-C10-C1-C2 = 172.1(2)º and O21-C20-C2-C1 = 5.7(3)º and the ring of C1-C10-O11-H11-O21-C20-C2 is nearly planar (RMS deviation from the plane of 0.0342Å). Even though the O···O separation is very short for an O-H···O hydrogen bond the hydrogen atom is asymmetrically positioned, more asymmetrically positioned than would be expected from neutron diffraction measurements of similar length O-H···O hydrogen bonds (graph 3.2.1). There is no evidence of disorder in the Fourier map (figure 3.2.2).

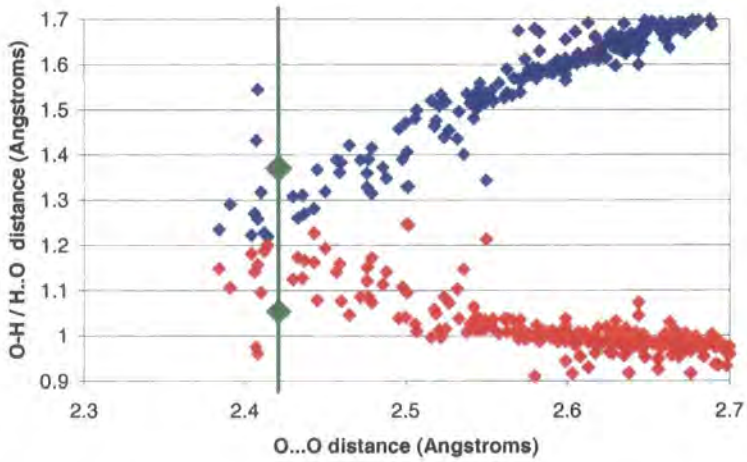


Graph 3.2.1. O-H···O hydrogen bonds measured by neutron diffraction from the Cambridge Structural Database (Allen and Kennard, 1993). The vertical green line marks an O···O distance of 2.42Å and the green points mark the O11-H11 and H11···O21 bond distances.

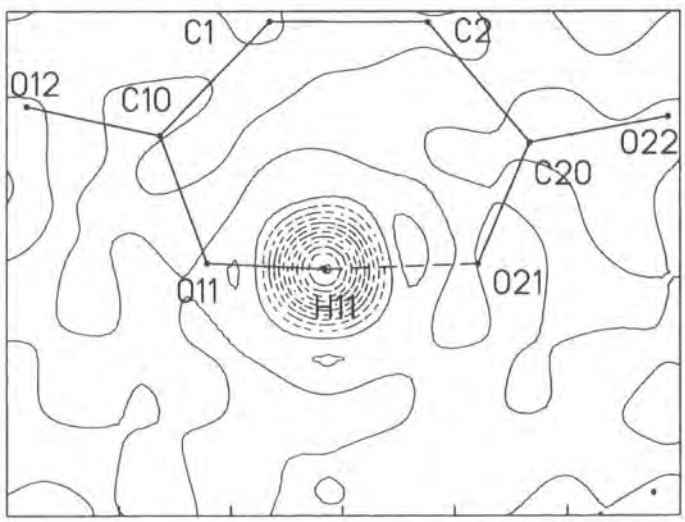


Figure 3.2.2. Difference Fourier map of PMA2- calculated on omitting H11, which has been indicated in the diagram. The contours are at a nuclear scattering density of 1.0 fm $Å^{-3}$. Negative contours are indicated by dashed lines.

The 4,4'-bipyridine molecule has been doubly protonated to become 4,4'-bipyridinium$^{+2}$ (BPY2+). The BPY2+ molecule lies across an inversion centre at (-½ 0 ½) and only half of the molecule lies in the asymmetric unit, which constrains the pyridyl rings within the molecule to be co-planar.

A strong charge-assisted N-H···O hydrogen bond (N4-H4···O22) (Gilli et al, 1994), complemented by a weak C-H···O hydrogen bond (C9-H9···O21), links the BPY2+ molecules and the PMA2- molecules into one-dimensional chains along the [2 1 –1] direction (figure 3.2.3).

Table 3.2.1: Strong Hydrogen Bond Parameters.

| | D···A (Å) | D-H(Å) | H···A (Å) | D-H-A |
|---|---|---|---|---|
| N4-H4···O22 | 2.605(2) | 1.097(3) | 1.511(3) | 174.7(3)º |
| O11-H11···O21 | 2.421(3) | 1.053(4) | 1.370(4) | 175.0(4)º |

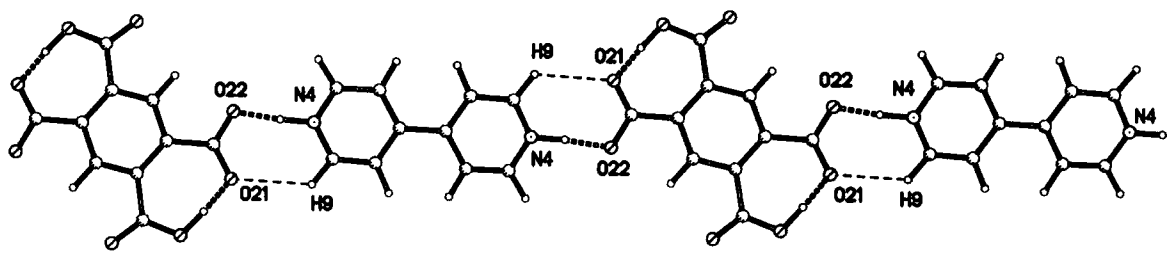


Figure 3.2.3. Chain of PMA2- and BPY2+ molecules along the [2 1 –1] direction.

Weak C-H···O hydrogen bonds link parallel chains together to form planes perpendicular to the [1 –2 0] direction. The chains link together to form two hydrogen bonded rings (figure 3.2.4).

Table 3.2.2: C-H···O Hydrogen Bond Parameters.

| | D···A (Å) | C···H (Å) | H···A (Å) | D-H-A |
|---|---|---|---|---|
| C6-H6···O12$^{i}$ | 3.199(2) | 1.078(3) | 2.253(4) | 145.3(4)º |
| C8-H8···O12$^{ii}$ | 3.362(2) | 1.082(3) | 2.402(4) | 147.1(4)º |
| C9-H9···O21 | 3.303(2) | 1.080(3) | 2.593(4) | 122.6(3)º |

Symmetry Codes: i = x-2, y-1, z. ii = 1-x, 1-y, 1-z.

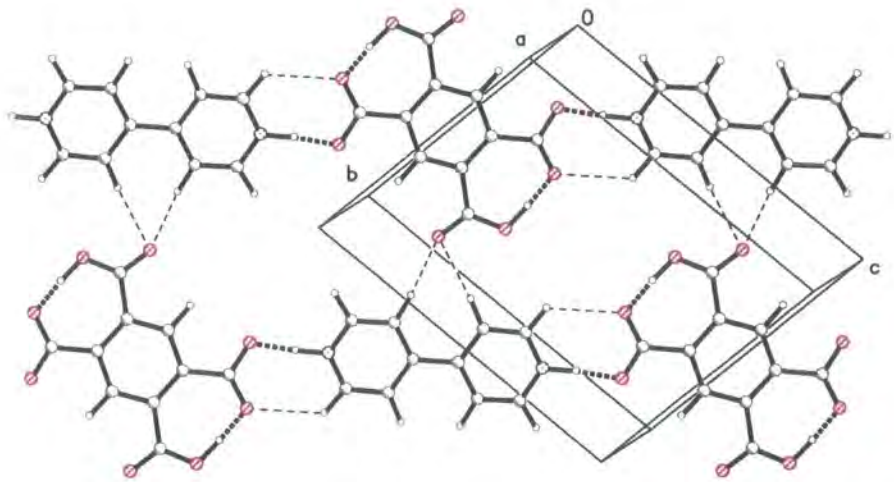


Figure 3.2.4. Planes of PMA2- and BPY2+ pack together to form two hydrogen-bonded rings.

The molecules are arranged in π-π stacked columns along the a-axis. The angles between the π-π stacked rings are identically 0º because the rings are related by translation symmetry and the distance between the centres of the rings is identical to a (figure 3.2.6). A disordered chain of water molecules threads through the tunnel formed by the larger hydrogen bonded ring (figure 3.2.5).

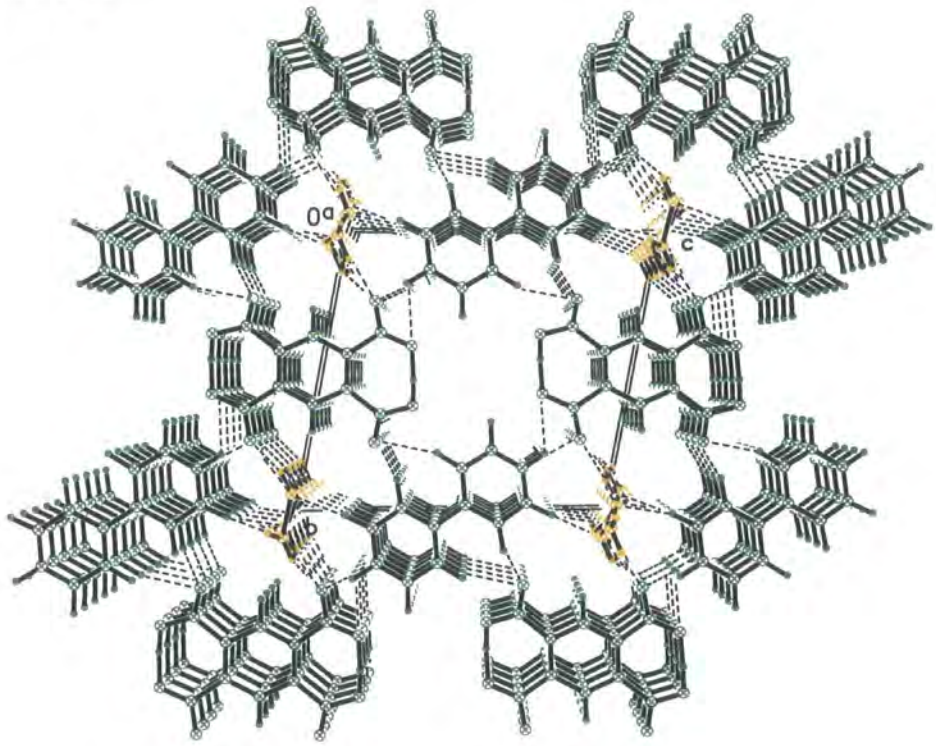


Figure 3.2.5. Packing diagram of PMA2- and BPY2+ with the unit cell viewed along the a-axis. The π-π stacked molecular columns are easily seen. The disordered water molecules (yellow) are shown in the tunnel along the a-axes.

Table 3.2.3. π-π Interactions.

| | Centre-to-centre distance (Å) [≡a] | Angle between planes | Shortest perpendicular distance (Å) |
|---|---|---|---|
| Ring1-Ring1$^{i}$ | 3.7747(2) | 0º | 3.3875(16) |
| Ring2-Ring2$^{i}$ | 3.7747(2) | 0º | 3.4000(18) |

Ring 1: C1-C2-C3-C1$^{ii}$-C2$^{ii}$-C3$^{ii}$. Ring 2: N4-C5-C6-C7-C8-C9.

[Symmetry codes: (i) 1+x, y, z. (ii) = 1-x, 1-y, -z.]

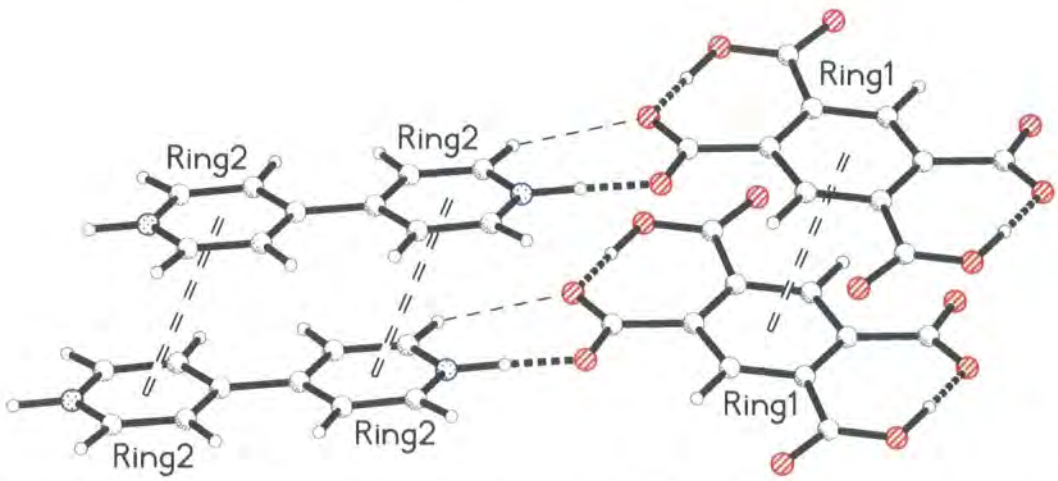


Figure 3.2.6. The π-π stacking interactions between PMA2- and BPY2+ along the a-axis are indicated by hollow dashed lines.

The water molecules have been modelled as disordered over four positions and have been refined with the O-H bond lengths and the H-O-H bond angle restrained. Most of the residual un-modelled nuclear-density left after refinement lies around the water molecules and the model only approximates the true disorder. The occupation factors of each water molecule were refined and then fixed close to the refined value so that with a reasonable isotropic thermal parameter the overall occupation added up to two per unit cell. It was not possible to refine anisotropic displacement parameters for any of the atoms in the water molecules. O-H···O hydrogen bonds are formed to O22 from all of the water molecules.

Table 3.2.4: Water Hydrogen Bond Parameters.

| | D···A (Å) | D···H (Å) | H···A (Å) | D-H-A |
|---|---|---|---|---|
| O1A-H1A···O22 | 2.792(14) | 0.96(2) | 1.867(16) | 160(2)º |
| O2A-H2A···O22 | 2.838(12) | 0.93(2) | 1.940(13) | 162(1)º |
| O3A-H3A···O22 | 2.927(15) | 0.96(1) | 2.073(17) | 147(2)º |
| O4A-H4A···O22 | 2.880(16) | 0.90(2) | 2.12(2) | 141(3)º |

**Experimental Details**

Neutron diffraction data were collected on D19 at the ILL. A rod like pale brown crystal was mounted on a vanadium pin using Kwikfill glue, car bodywork filler that has good low temperature properties. The pin was attached to a Displex cyrorefrigerator and cooled at 2K per minute while monitoring the strong 1 –1 1 reflection. Near 200K the peak broadened significantly, evidence of the crystal deteriorating. The cooling was stopped and the crystal warmed to 215K, where the peak narrowed to its original width. The rest of the experiment was carried out at this temperature.

Data were collected up to 100° in 2θ, and a few reflections up to 110°. Cell parameters were determined from 1196 strong reflections. Initial co-ordinates for the refinement were taken from the room temperature X-ray results.

Table 3.2.cry. Crystal parameters for BPY2- and BPY2+.

| | | | |
|---|---|---|---|
| Formula | $[C_{10}H_4O_8^{-2}]\cdot[C_{10}H_{10}N_2^{+2}].2[H_2O]$ | Formula Weight | 446.0 |
| Crystal System | Triclinic | Space Group | P-1 |
| a (Å) | 3.7747(2) | α | 99.626(3)º |
| b (Å) | 10.8587(5) | β | 97.726(3)º |
| c (Å) | 11.9519(6) | γ | 95.515(3)º |
| Volume $(Å)^3$ | 475.07(4) | Z | 2 |
| Density $(Mg\ m^{-3})$ | 1.559 | Colour | Brown |
| Crystal Shape | Rod | Dimensions (mm) | 2.0 * 0.8 * 0.5 |

Table 3.2.data. Data collection details for PMA2- and BPY2+.

| | | | |
|---|---|---|---|
| Radiation | Neutron | λ (Å) | 1.31080 |
| Temperature (K) | 215(2) | | |
| Reflections | 1983 | Independent reflections | 1654 |
| Reflections I > 2σ(I) | 1426 | | |
| Rint | 0.0175 | Rsigma | 0.0360 |
| H | -2 → 4 | k | -13 → 13 |
| l | -14 → 14 | $\theta_{max}$ | 55 |

Table 3.2.ref. Refinement details for PMA2- and BPY2+.

| | | | |
|---|---|---|---|
| $R[F^2 > 2\sigma(F^2)]$ | 0.0361 | $wR^2(F^2)$ | 0.0588 |
| S | 1.511 | Data / Parameters | 1654 / 244 |
| $\Delta\rho_{max}$ (e $Å^{-3}$) | 0.448 | $\Delta\rho_{min}$ (e $Å^{-3}$) | -0.470 |
| $(\Delta/\sigma)_{max}$ | 0.000 | $\Delta\rho_{rms}$ (e $Å^{-3}$) | 0.100 |

### 3.3. Crystal Structure of 4,4'-Bipyridinium bis-Trihydrogen Pyromellitate

4,4'-Bipyridine and benzene-1,2,4,5-tetracarboxylic acid crystallise in a 1:2 ratio as a molecular salt, i.e. $2C_{10}H_5O_8^- \cdot C_{10}H_{10}N_2^{2+}$, in the space group Cc. Both benzene-1,2,4,5-tetracarboxylic acid molecules have been deprotonated to become trihydrogen pyromellitate (PMA-) and 4,4-bipyridine has been doubly protonated to become 4,4'-bipyridinium (BPY2+). The PMA- molecules are connected by O-H···O hydrogen bonds in a two dimensional mesh. The BPY2+ molecules thread through gaps in the mesh and via N-H···O hydrogen bonds, connect the layers together.

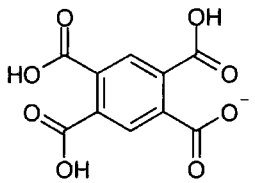

**PMA-**

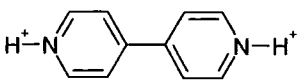

**BPY2+**

X-ray diffraction data on this crystal were collected first at room-temperature in Hong Kong and the structure solved in space group C2/c, however the thermal parameters of the molecules were unrealistic and the refined R-factor was only ~10%. On refinement in space group Cc no significant improvement in the thermal parameters and R-factors could be obtained. Since great care must be taken when choosing between these two space groups (Baur and Kassner, 1992; Marsh, 1997) the higher symmetry space group, C2/c, was chosen.

Neutron-diffraction data were collected at 20K on the diffractometer D19 at the ILL. These more accurate data shows that there are two independent, slightly different, PMA- molecules in the asymmetric unit. The structure must be solved in Cc, a space group with the same systematic absences but less symmetry. When the room-temperature X-ray data were refined again, in Cc, starting from the neutron derived atomic co-ordinates, the results were much better, R1 = 0.0418 and the thermal parameters realistic. Using low-temperature X-ray data collected at 30K on the HELIX-SMART the structure could be solved immediately in Cc but could not be solved in C2/c.

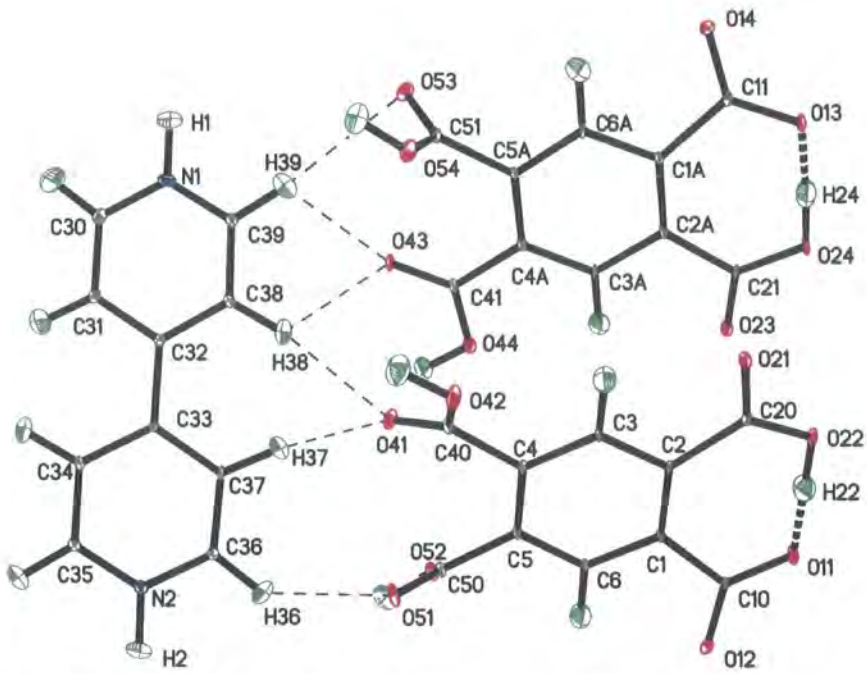


Figure 3.3.1. 50% Thermal ellipsoid plot of the asymmetric unit of the 2:1 co-crystal of PMA- and BPY2+ from the 20K neutron structure.

**Structure Discussion**

Unless otherwise specified all the parameters for the discussion are taken from the 20K neutron data.

There are two very similar PMA- molecules in the asymmetric unit, both have been deprotonated. A short intramolecular hydrogen bond is formed between the deprotonated carboxylate group and the adjacent carboxylic acid group in both PMA- molecules. Both intramolecular hydrogen bonds are quite asymmetric and the O-H and O···H distances lie at the outer edges of the range expected for O-H···O hydrogen bonds with similar O···O separations (graph 3.3.1).

Table 3.3.1. Intramolecular O-H···O hydrogen bonds.

| | O···O distance (Å) | O-H distance (Å) | H···O distance (Å) | O-H-O angle. |
|---|---|---|---|---|
| O22-H22···O11 | 2.404(3) | 1.078(5) | 1.331(5) | 172.6(4)º |
| *O22-H22···O11** | *2.4092(18)* | *0.97(2)* | *1.45(2)* | *169(2)°* |
| O24-H24···O13 | 2.419(3) | 1.076(5) | 1.347(5) | 173.2(4)º |
| *O24-H24···O13** | *2.4278(19)* | *0.89(3)* | *1.54(3)* | *173(2)°* |

* The results derived from the X-ray experiments at 30K.

The X-ray results give approximately the same O-O distances. But the O-H distances do not agree to within three standard uncertainties (s.u.). The X-ray difference Fourier maps (figures 3.3.2.a and b), calculated from the 30K data, are misleading and show the electron density not the nuclear positions. The Neutron Fourier maps (figures 3.3.4.a and b) leave no room for doubt on the location of the hydrogen atoms.

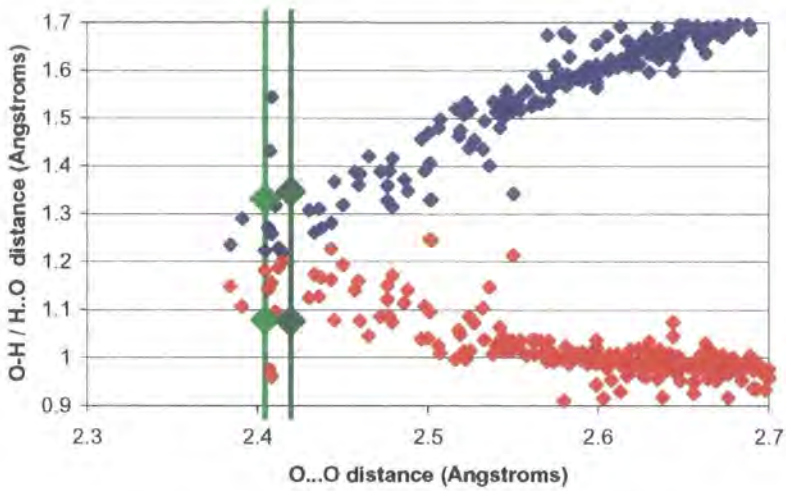


Graph 3.3.1. O-H···O hydrogen bonds measured by neutron diffraction from the Cambridge Structural Database (Allen and Kennard, 1993). The vertical green lines mark the O···O distances in the intramolecular hydrogen bonds and the green points mark the O-H and H···O bond distances.

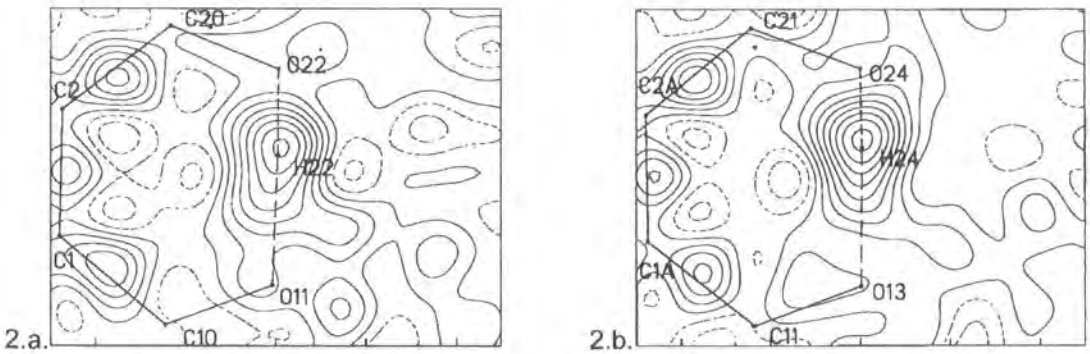


Figures 3.3.2.a and 3.3.2.b. The X-ray difference Fourier maps calculated on omitting H22(3a) and H24(3b). The contours are at 0.05 $eA^{-3}$. The dashed lines indicate negative density. Covalent bonding between the carbon atoms is also evident.

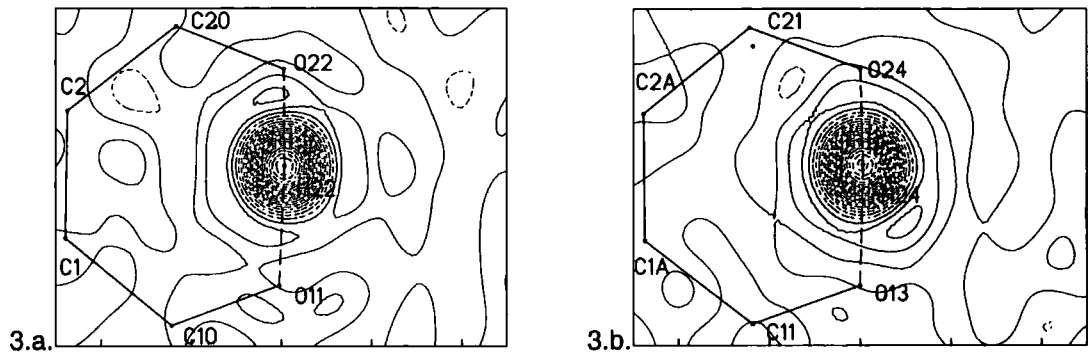


Figures 3.3.3a and 3.3.3.b. The neutron difference Fourier maps calculated on omitting H22(3a) and H24(3b). The contours are at nuclear scattering densities of 0.5 fm $A^{-3}$. The dashed lines indicate negative density.

If the structure adopted space group C2/c then the carboxylate group involving C10 would be equivalent to the carboxylate group involving C11. In the same way the carboxylic groups involving C20 would be equivalent to the one involving C21, the one with C40 equivalent to the one with C41 and the one with C50 equivalent to the one with C51. The differences between the two independent PMA- molecules are the torsion angles of the carboxyl groups. The torsion angles between the carboxyl group and phenyl ring are very similar for the groups involved in the intramolecular O-H···O hydrogen bonds, the torsion angles are not related for the other carboxylic acid groups. In C2/c the torsion angles of the carboxylic acid groups of the two PMA- molecules would be the same.

Table 3.3.2. Carboxyl Torsion angles.

| PMA- Torsion angles | | PMA- (A) Torsion angles | |
|---|---|---|---|
| O12 - C10 - C1 - C2 | 164.7(2)º | O14 - C11 - C1A - C2A | 161.4(2)º |
| O21 - C20 - C2 - C1 | -174.5(2)º | O23 - C21 - C2A - C1A | -171.9(2)º |
| O41 - C40 - C4 - C5 | -37.7(3)º | O43 - C41 - C4A - C5A | -1.3(3)º |
| O51 - C50 - C5 - C4 | -54.4(3)º | O53 - C51 - C5A - C4A | -90.7(2)º |

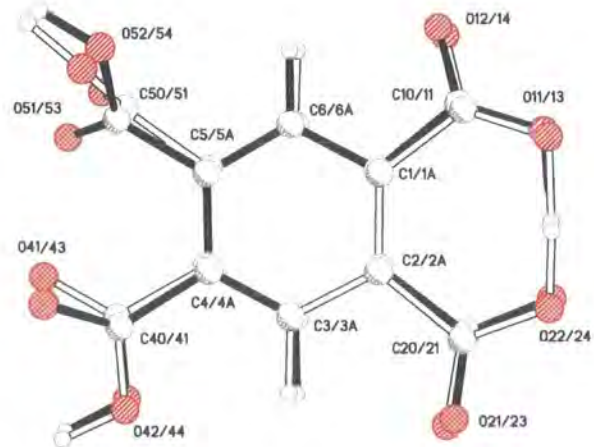


Figure 3.3.4. The two PMA- molecules superimposed as if they were in space group C2/c. The molecule containing C1A has been inverted and translated so that the centroids of the two molecules are coincident. The main differences between the two molecules are the torsion angles of the carboxyl groups.

The PMA- molecules are connected together by O-H···O hydrogen bonds (table 3.3.3) to form infinite two-dimensional networks. Each network is made up of only one type of PMA- molecule (figures 3.3.5.a and 3.3.5.b). The PMA- molecules are polar, there is one hydrogen bond accepting end, which also contains the intramolecular O-H···O hydrogen bond and one hydrogen bond donating end (figure 3.3.6).

Table 3.3.3. Intermolecular O-H···O hydrogen bonds.

| | O···O distance (Å) | O-H distance (Å) | H···O distance (Å) | O-H-O angle. |
|---|---|---|---|---|
| O42-H42···O11$^{IV}$ | 2.613(3) | 1.011(5) | 1.612(5) | 169.8(4)º |
| O52-H52···O21$^{III}$ | 2.717(3) | 1.002(5) | 1.718(4) | 174.7(4)º |
| O44-H44···O13$^{III}$ | 2.630(3) | 1.009(4) | 1.636(4) | 167.2(4)º |
| O54-H54···O23$^{IV}$ | 2.739(3) | 1.002(5) | 1.741(5) | 173.2(4)º |

Symmetry codes: III = -½ + x, -½ + y, z; IV = ½ + x, -½ + y, z.

The intermolecular hydrogen bonds are similar for the different PMA- molecules but not identical to within the s.u.'s.

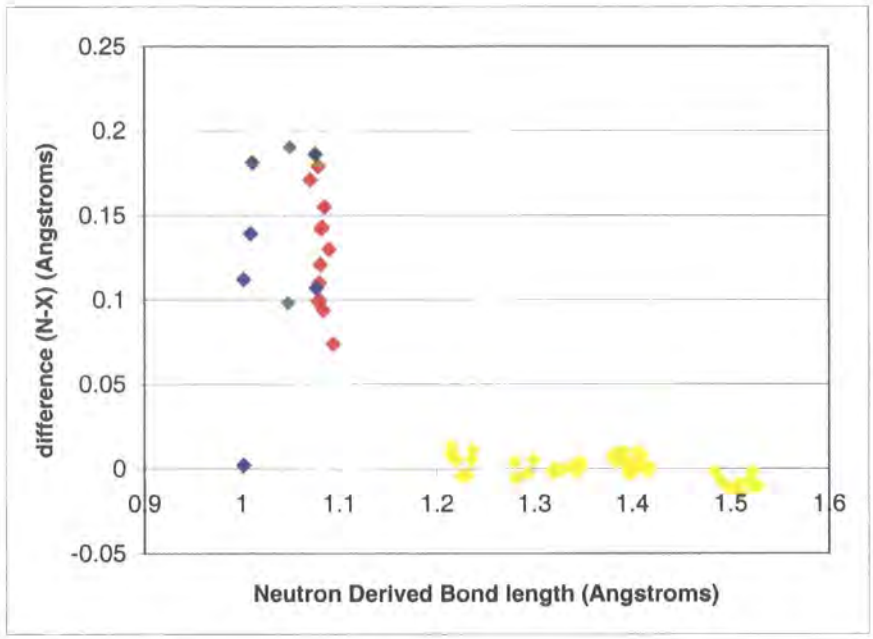


Graph 3.3.2. The difference between X-ray derived bond lengths and neutron derived bond lengths. Yellow points mark C-C, C-O and C-N bonds, red points mark C-H bonds, green points N-H bonds and blue points mark O-H bonds.

The x-ray and neutron derived bond lengths agree well for the bonds between the heavy atoms (graph 3.3.2, yellow points). The X-H bond lengths derived from the X-ray data are all underestimated and spread over a wide range. Only one X-H bond length from the X-ray data agrees with the neutron derived data to within three s.u.'s.

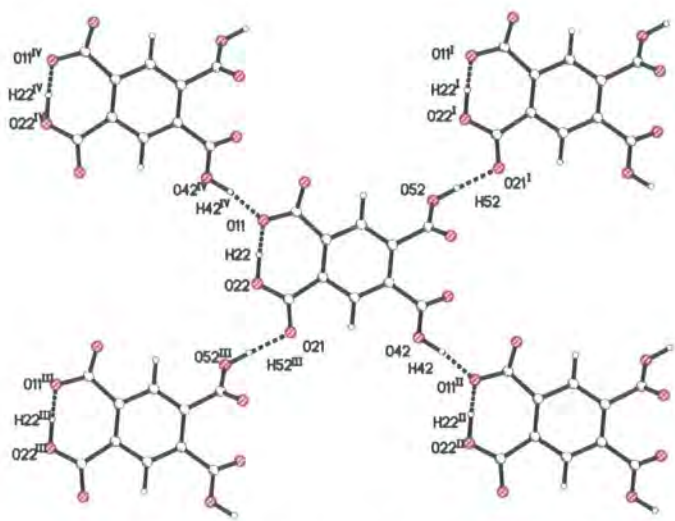


Figure 3.3.5.a. Intermolecular network made up from the PMA molecule that contains C1.

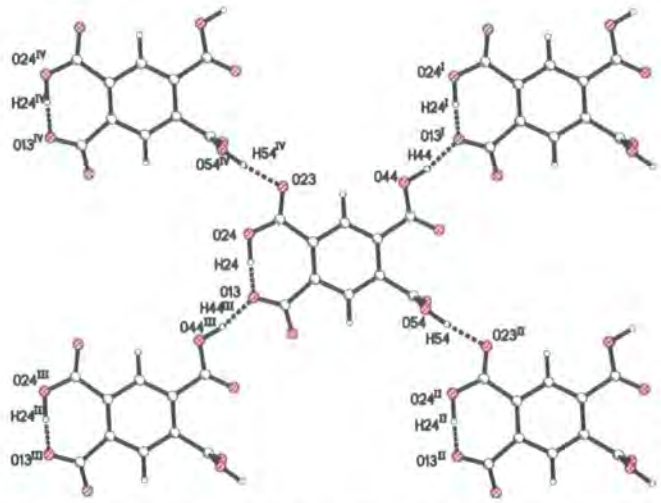


Figure 3.3.5.b. Intermolecular network made up from the PMA molecule that contains C1A.

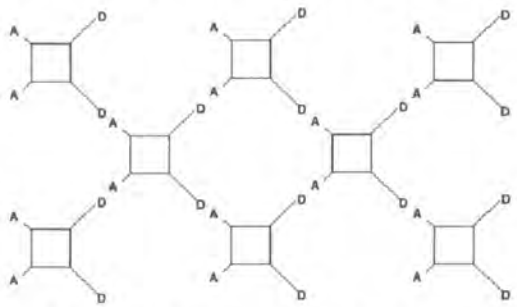


Figure 3.3.6. A schematic diagram of the PMA- molecule packing.

The 4,4-bipyridine molecule has been doubly protonated to become 4,4-bipyridinium (BPY2+). The planes are 21.36(9)º apart. The pyridyl groups are twisted 21.36(9)º with respect to each other to satisfy weak C-H···O hydrogen bonds (figure 3.3.7).

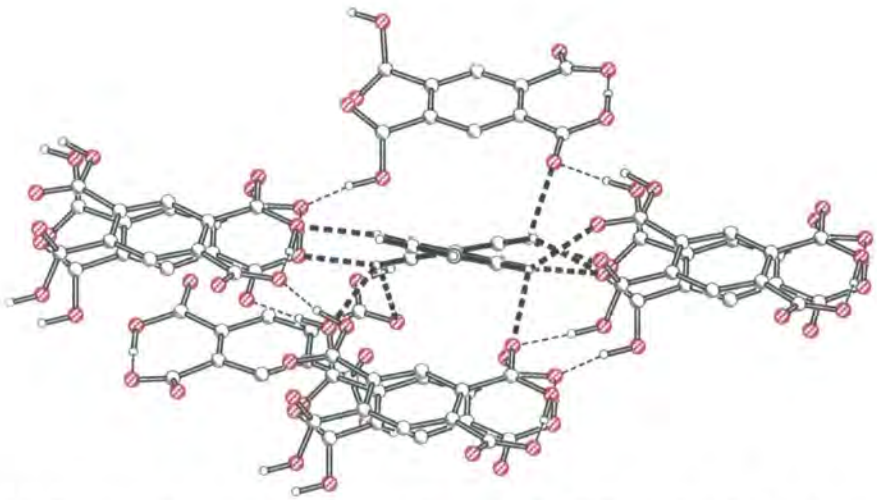

Figure 3.3.7. Packing diagram viewed along the axis of BPY2+ molecule. The heavy dashed lines indicate C-H···O hydrogen bonds. It can be seen how the twist in the BPY2+ molecules optimises these weak hydrogen bonds.

Table 3.3.4. C-H···O hydrogen bond parameters.

| | C-O distance (Å) | H-O distance (Å) | C-H-O Angle |
|---|---|---|---|
| C31-H31···O24$^{VI}$ | 3.191(3) | 2.228(5) | 146.7(4)º |
| C34-H34···O52$^{VII}$ | 3.414(3) | 2.482(5) | 143.9(4)º |
| C34-H24···O22$^{VI}$ | 3.154(3) | 2.465(4) | 120.6(3)º |
| C35-H35···O22$^{VI}$ | 3.154(3) | 2.549(5) | 115.0(3)º |
| C35-H35···O43$^{V}$ | 3.043(3) | 2.494(4) | 110.8(3)º |
| C36-H36···O51 | 3.219(3) | 2.363(5) | 134.9(3)º |
| C36-H36···O21$^{IIX}$ | 3.134(3) | 2.415(5) | 122.7(3)º |
| C37-H37···O41 | 3.140(3) | 2.194(5) | 144.7(4)º |
| C38-H38···O41 | 3.420(3) | 2.351(4) | 169.6(3)º |
| C38-H38···O43 | 3.045(3) | 2.564(4) | 106.0(3)º |
| C39-H39···O23$^{VII}$ | 3.108(3) | 2.594(5) | 108.3(3)º |
| C39-H39···O43 | 2.994(3) | 2.493(5) | 107.1(3)º |
| C39-H39···O53 | 3.739(3) | 2.693(5) | 163.1(4)º |

Symmetry codes: V = x, 1 – y, ½ + z; VI = x, 1+ y, z;
VII = ½ + x, ½ + y, z; IIX = x – ½, ½ + y, z.

Two strong charge-assisted N-H···O hydrogen bonds link the BPY2+ molecules to the PMA- molecules. These hydrogen bonds would be equivalent in C2/c but are very different in Cc.

Table 3.3.5. Intermolecular N-H···O hydrogen bonds.

| | N···O distance (Å) | N-H distance (Å) | H···O distance (Å) | N-H-O angle. |
|---|---|---|---|---|
| N1-H1···O12$^{I}$ | 2.674(2) | 1.048(4) | 1.636(4) | 169.8(4)º |
| N2-H2···O14$^{II}$ | 2.638(2) | 1.050(4) | 1.664(4) | 152.0(3)º |

Symmetry codes: I = ½ + x, ½ - y, -½ + z; II = -½ + x, ½ - y, ½ + z.

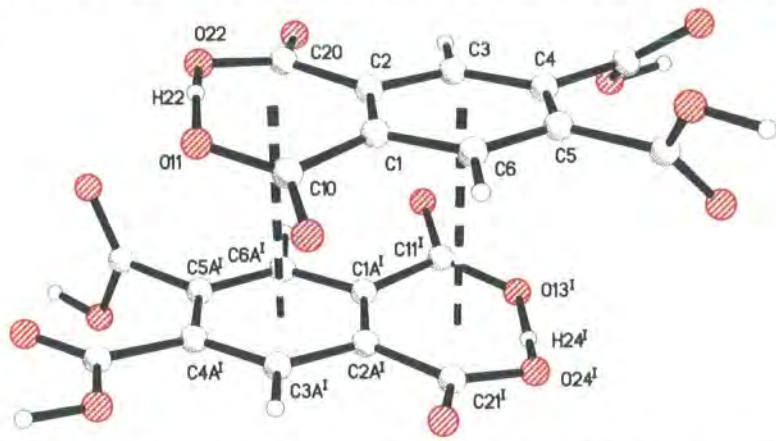


Figure 3.3.8. The π-"π" interactions between the independent PMA- molecules. Symmetry code I = x, -y, 0.5+z.

Table 3.3.6. Pseudo π-π interactions

| | Centre-to-centre distance (Å) | Angle between planes |
|---|---|---|
| Ring1-Ring4$^{I}$ | 3.541 | 7.54(7)° |
| Ring2$^{I}$-Ring3 | 3.491 | 4.76(7)° |

Ring 1 = C1, C2, C3, C4, C5, C6. Ring 2 = C1A, C2A, C3A, C4A, C5A, C6A.

Ring 3 = C1, C10, O11, H22, O22, C20, C2. Ring 4 = C1A, C11, O13, H24, O24, C21, C2A.

Symmetry code. I = x, -y, 0.5+z.

The two independent PMA- molecules pack together to form a pseudo-π···π stacked pair. The phenyl ring of one PMA- molecule lies directly over the ring formed by the intramolecular hydrogen bond in the other PMA- molecule (figure 3.3.8).

The PMA- molecules pack together to form negatively charged two-dimensional networks (figures 3.3.5.a and 3.3.5.b) perpendicular to the c-axis. The networks pack alternately to leave channels along the [0 0 1] direction in which the BPY2+ molecules fit (figure 3.3.9). There are two different spacings between the layers, one spanned by the BPY2+ molecules and one defined by the pseudo-π···π interaction. The BPY2+ molecules span two layers and form N-H···O hydrogen bonds that connect layers three spacings apart (figure 3.3.10). The spacing spanned by the BPY2+ molecules (marked A in figure 3.3.10) is ~3.95Å wide perpendicular to the layers and ~4.27Å parallel to the c-axis. The spacing between the π···pseudo-π stacked layers is ~3.09Å perpendicular to the layers and ~3.34Å parallel to the c-axis.

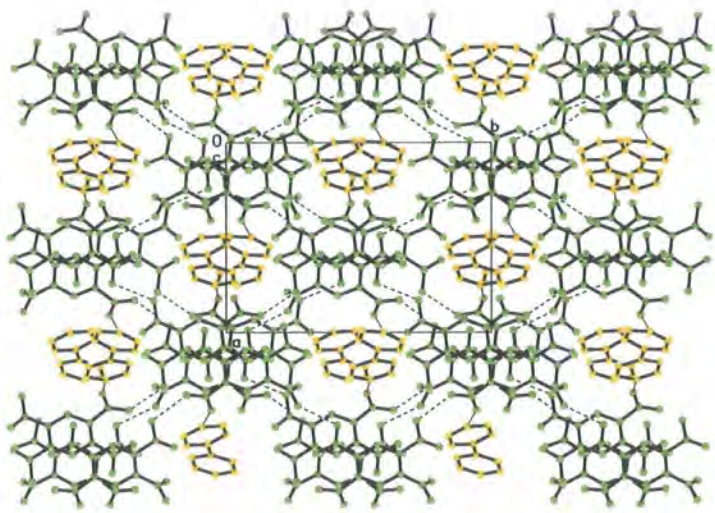


Figure 3.3.9. Packing diagram viewed along the c-direction. The BPY2+ molecules are yellow and the PMA- molecules are green. The hydrogen atoms have been omitted for clarity. The two dimensional PMA- network is parallel to the page and the BPY2+ molecules thread though the gaps.

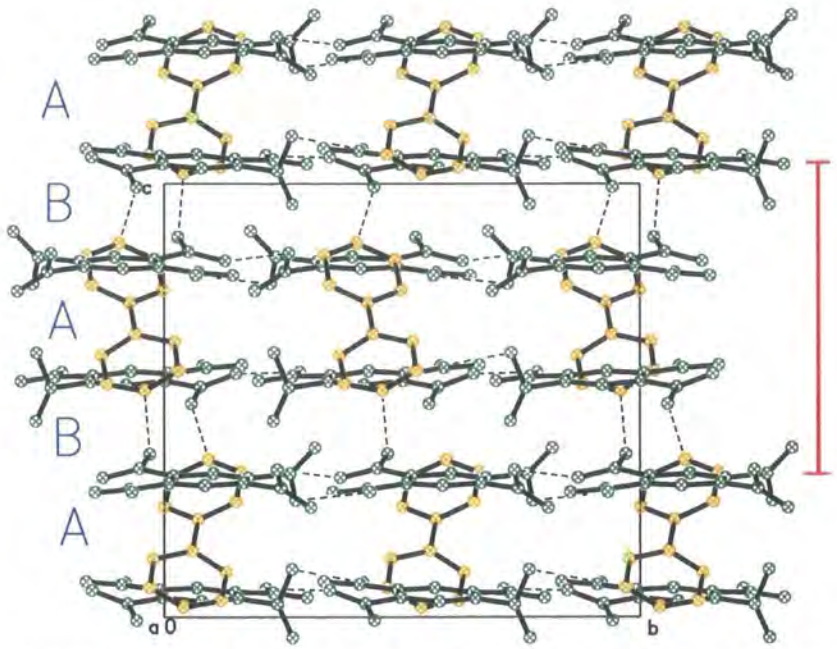


Figure 3.3.10. Packing diagram viewed along the a-direction. The BPY2+ molecules are yellow and the PMA- molecules are green. The hydrogen atoms have been omitted for clarity. The red line indicates the distance one BPY2+ molecule spans to hydrogen-bond layers three spacings apart. The letters indicate the different layer spacings.

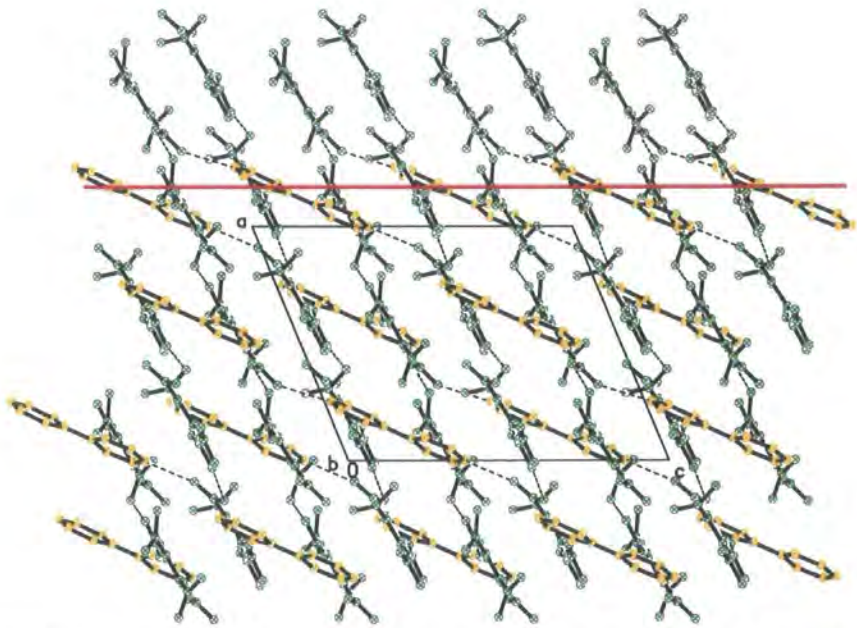


Figure 3.3.11. Packing diagram viewed along the b-direction. The BPY2+ molecules are yellow and the PMA- molecules are green. The hydrogen atoms have been omitted for clarity. The red line parallel to the c-axis marks one of the tunnels through the structure and illustrates how the BPY2+ molecules lie at an angle to the tunnels.

**Experimental Details**

X-ray data were collected on a Bruker-SMART diffractometer, using a HELIX helium-flow cryostream to cool the crystal to 30K.

Neutron diffraction data were collected on D19 at the ILL. A pale yellow crystal was attached to a vanadium pin using Kwikfill glue and attached to a Displex cryorefrigerator mounted on D19. No signs of deterioration in the crystal was observed during cooling to 20K, at which temperature data were collected. Data up to $2\theta = 70°$ were collected in equatorial geometry, further data up to $2\theta = 100°$ were collected in normal beam geometry. Cell parameters were determined from 3055 strong reflections. Initial co-ordinates for the refinement were taken from the low-temperature X-ray results.

Table 3.3.cry. Crystal parameters for PMA- and BPY2+

| | | | |
|---|---|---|---|
| Chemical Formula | $2\cdot[C_{10}H_5O_8^-]\,[C_{10}H_{10}N_2^{2+}]$ | Formula Weight | 664.48 |
| Crystal Setting | Monoclinic | Space Group | Cc |
| Z | 4 | | |

Table 3.3.data. Data collection and refinement details for PMA- and BPY2+.

| | | |
|---|---|---|
| Diffractometer | D19 | Bruker SMART-HELIX |
| Radiation | Neutron | X-ray Mo-K$\alpha$ |
| Wavelength (Å) | 1.3108(1) | 0.71073 |
| Temperature (K) | 20 | 30 |
| a (Å) | 12.0090(10) | 12.037(2) |
| b (Å) | 15.4840(10) | 15.484(2) |
| c (Å) | 15.2210(10) | 15.215(2) |
| beta (º) | 112.270(10) | 112.336(2) |
| Volume (Å$^3$) | 2619.2(3) | 2623.0(6) |
| No of reflections for cell parameters | 3055 | 999 |
| $\theta$ range | 5-50 | 12.00-20.79 |
| $\mu$ (mm$^{-1}$) | 0.1428 | 0.140 |
| Crystal Shape | Bar | Block |
| Crystal Colour | Yellow | Yellow |
| Crystal Dimensions | 2.2*1.0*0.7 | 0.4*0.25*0.2 |
| Absorption Correction | Gaussian, D19ABS. | None |
| T min | 0.8406 | - |
| T max | 0.8911 | - |
| No. of reflections | 3741 | 6670 |
| Independent reflections | 2647 | 3949 |

Table 3.3.data. *continued.*

| No. of reflections $I > 2\sigma$ | 2628 | 3856 |
|---|---|---|
| R int | 0.0187 | 0.0202 |
| R sigma | 0.0254 | 0.0186 |
| θ max | 55.16 | 27.32 |
| h | -4→14 | -14→15 |
| k | -19→13 | -17→18 |
| l | -19→17 | -18→19 |
| $R[F^2 > 2\sigma(F^2)]$ | 0.0219 | 0.0261 |
| $wR(F^2)$ | 0.0433 | 0.0671 |
| S | 1.631 | 1.669 |

### 3.4. The 2:1 Co-crystal of 4,4-bipyridine and Pyromellitic acid.

4,4'-bipyridine and benzene-1,2,4,5-tetracarboxylic acid (pyromellitic acid) crystallise in a 2:1 ratio as a molecular salt, i.e. $C_{10}H_5O_8^{2-}\cdot 2C_{10}H_{10}N_2^{+}$, in the space group P-1. The benzene-1,2,4,5-tetracarboxylic acid molecules have been deprotonated to become dihydrogen pyromellitate (PMA2-) and 4,4-bipyridine has been protonated to become 4,4'-bipyridinium (BPY+). A strong N··H··O and a strong O-H···N hydrogen bond connect the molecules in infinite chains along the [0 1 -2] direction. The position of the proton in the N··H··O hydrogen bond changes with respect to temperature, at room temperature the N-H distance is ~1.3Å, at 20K the N-H distance is ~1.2Å, while the N···O distance remains at ~2.5Å.

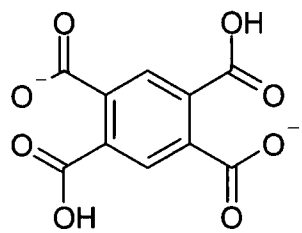

**PMA2-**

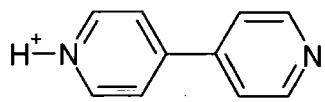

**BPY+**

**X-Ray Results.**

Dr. Toby Mak in Hong Kong first collected room temperature X-ray data and solved the structure of this compound. Although the hydrogen atom positions were not reliable something odd could be seen. There was one short strong O-H···N hydrogen bond and a very short N···O hydrogen bond in which the proton appeared to lie equidistant from the nitrogen and the oxygen atoms.

Table 3.4.1. Room temperature, X-ray derived, hydrogen bond parameters.

| | D···A (Å) | D-H(Å) | H···A (Å) | D-H-A |
|---|---|---|---|---|
| N1-H1···O22 | 2.5319(16) | 1.28(2) | 1.28(3) | 163(2)º |
| O12-H2···N2$^{II}$ | 2.6129(15) | 1.06(3) | 1.56(3) | 172(2)º |

Symmetry codes: II 1-x, 2-y, -2-z.

To measure accurate hydrogen atom positions neutron diffraction was proposed. In preparation for the neutron-diffraction experiments low-temperature X-ray diffraction experiments were performed in Durham at 100K and 30K. This structure has since been reported by Lough et al. (2000) also at 100K.

Table 3.4.2. Low-temperature, X-ray-derived, hydrogen-bond parameters.

| | D···A (Å) | D-H(Å) | H···A (Å) | D-H-A |
|---|---|---|---|---|
| N1-H1···O22, 100K | 2.5236(12) | 1.20(2) | 1.34(2) | 167(2)º |
| N1-H1···O22, 30K | 2.541(2) | 1.15(2) | 1.40(2) | 170(2)º |
| O12-H2···N2$^{II}$, 100K | 2.6146(12) | 1.03(2) | 1.59(2) | 172(2)º |
| O12-H2···N2$^{II}$, 30K | 2.632(2) | 1.00(2) | 1.64(2) | 172(2)º |

The compound cools to 30K without deterioration and there are no phase transitions. According to the X-ray results the hydrogen atom position in the shortest N-H···O hydrogen bond seems to move closer to the nitrogen atom as the temperature is lowered.

**Neutron Experiments**

Three neutron diffraction experiments were performed on this crystal. The experiments at 20K and 296K were performed on the monochromatic diffractometer D19 at the ILL. The 200K data were collected on the Laue diffractometer LADI during tests of the instrument on a thermal neutron beam.

**Structure Discussion**

Unless otherwise specified all the discussion is taken from the 20K neutron data.
The PMA2- molecule lies around an inversion centre at (½ ½ 0) therefore only half of the molecule is in the asymmetric unit. There is one independent carboxylic acid group in the molecule and one independent carboxylate group. The C-O bond lengths for a carboxylic acid group attached to a phenyl ring taken from the International Tables for Crystallography (Allen et al. 1992) are 1.305(20)Å for the single bond and 1.226(20)Å for the double bond, in a carboxylate group attached to a phenyl ring both C-O bond lengths are expected to be 1.255(10)Å. The bond lengths in the carboxylic acid group of the PMA2- agree very well with these [ C10-O11 = 1.219(2), C10-O12 = 1.312(2)Å]. The bond lengths in the carboxylate group [ C20-O21 = 1.235(2)Å, C20-O22 = 1.284(2)Å ] are between the ideals values for carboxylate and carboxylic groups. Although the PMA2- molecule is deprotonated no intramolecular hydrogen bonds are formed.

The geometry of the BPY+ molecule agrees with other singly protonated BPY+ molecules in the CSD (Allen and Kennard, 1993). The C11-N1-C15 angle of 120.2(1)º agrees with the average value for fully protonated BPY of 121.4(9)º. The C21-N2-C25 angle of 118.2(1)º agrees with the average value for unprotonated BPY of 116.3(16)º. The angle between the planes of the pyridyl and pyridinium rings is 2.98(6)º.

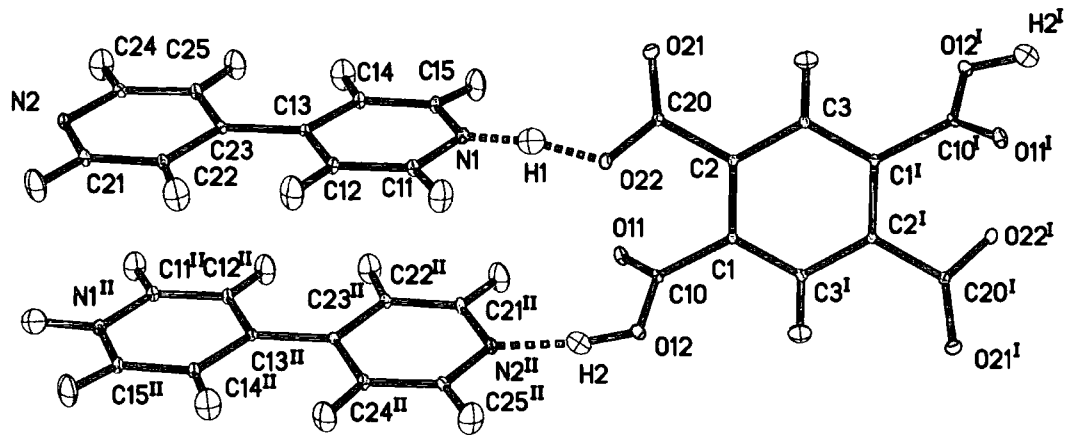


Figure 3.4.1. 50% Thermal ellipsoid plot of the 1:2 co-crystal of PMA2- and BPY+ at 20K. Hydrogen bonds are indicated by the dashed lines. [Symmetry codes: (I) 1-x, 1-y, -z. (II) 1-x, 2-y, -2-z.]

The BPY+ molecules are each bound to two PMA2- molecules by strong hydrogen bonds. A strong O-H···N hydrogen bond [O12-H2···N2] joins the carboxylic acid group to the unprotonated end of the BPY+ molecule. This is very short, with an O···N separation of 2.610(2)Å, there has been only one shorter O-H···N hydrogen bond studied by neutron diffraction (Steiner et al. 2000) which has an O···N separation of 2.588(3)Å. The proton position in the bond agrees with that found in the X-ray diffraction results.

The protonated end of the BPY+ molecule forms a strong N-H···O hydrogen bond with the carboxylate group. Again there has been only one shorter similar N-H···O hydrogen bond studied by neutron diffraction (Steiner et al. 2001) which has an N···O separation of 2.506(2)Å at 20K. The extremely long N-H distance of 1.207(3)Å agrees with the N-H separation found by Steiner et al. (2001) of 1.206(6)Å in the co-crystal of pentachlorophenol and 4-methylpyridine. Correspondingly the H···O distance of 1.325(3) is also very short.

The O-H···N hydrogen bond is strengthened by a weak C-H···O hydrogen bond, C21-H21···O11. The stronger N-H··O is not aided by a C-H···O hydrogen bond as the carboxylate group is twisted too far from the plane of the pyridyl ring.

Table 3.4.3: Strong Hydrogen Bond Parameters at 20K.

| | D···A (Å) | D-H(Å) | H···A (Å) | D-H-A |
|---|---|---|---|---|
| N1··H1··O22 | 2.5220(17) | 1.207(3) | 1.325(3) | 169.7(3)° |
| O12-H2···N2$^{II}$ | 2.6104(17) | 1.068(3) | 1.551(3) | 170.2(3)° |

Symmetry codes: II = 1-x, 2-y, -2-z.

The BPY+ molecules form π-π stacked columns along the [1 0 0] direction. Complementary C-H···O hydrogen bonds, C3-H3···O21 and its symmetry equivalent, link the PMA2- molecules edge to edge in the same direction (figure 3.4.4).

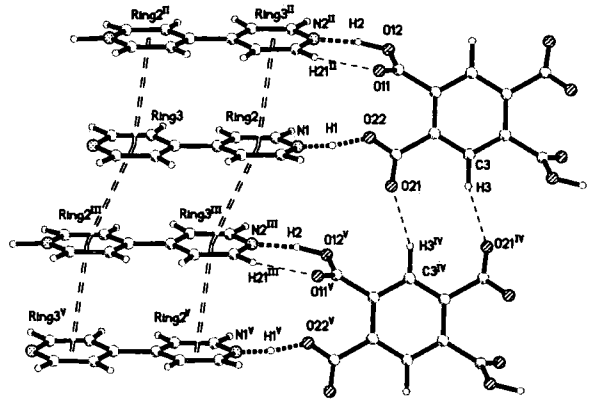


Figure 3.4.2. Packing diagram of PMA2- and BPY+ illustrating the C-H···O and π···π interactions linking the molecules together. [Symmetry codes: (II) 1-x, 2-y, -2-z. (III) –x, 2-y, -2-z. (IV) –x, 1-y, -z. (V) –1+x, y, z.]

Table 3.4.4. π-π Interactions.

| | Centre-to-centre distance (Å) | Angle between planes | Shortest perpendicular distance (Å) |
|---|---|---|---|
| Ring2···Ring3$^{II}$ | 3.7449(11) | 2.99(6)º | 3.3743(10) |
| Ring2···Ring3$^{III}$ | 3.7451(11) | 2.99(6)º | 3.4058(11) |

Two small, almost identical, rings are formed from N···O and C···O hydrogen bonds (figures 3.4.4.a and 3.4.4.b), each with four hydrogen bonds each and an inversion centre in the middle of each ring containing ten atoms. Two large rings also with four hydrogen bonds each, although one of these requires that C22-H22···O11 is a long, weak and bent hydrogen bond. The large rings each contain sixteen atoms.

Table 3.4.5. C-H···O Hydrogen Bond Parameters.

| | D···A (Å) | C···H (Å) | H···A (Å) | D-H-A |
|---|---|---|---|---|
| C3-H3···O21$^{IV}$ | 3.280(2) | 1.093(3) | 2.248(3) | 156.5(2)° |
| C11-H11···O22$^{VI}$ | 3.243(2) | 1.091(3) | 2.178(3) | 164.8(3)° |
| C14-H14···O21$^{X}$ | 3.231(2) | 1.091(3) | 2.164(3) | 165.3(3)° |
| C21-H21···O11$^{VIII}$ | 3.106(2) | 1.089(3) | 2.282(3) | 130.9(2)° |
| C22-H22···O11$^{VII}$ | 3.309(2) | 1.080(3) | 2.595(3) | 122.9(2)° |
| C24-H24···O21$^{X}$ | 3.365(2) | 1.091(3) | 2.282(3) | 172.1(3)° |
| C25-H25···O12$^{IX}$ | 3.426(2) | 1.089(3) | 2.428(3) | 151.6(3)° |

Symmetry codes: (IV) x, 1-y, -z (VI) 1-x, 1-y, -1-z; (VII) x, -y, z-1; (VIII) –1-x, 2-y, -1-z; (IX) x-1, y+1, z+1; (X) –x, 2-y, -2-z.

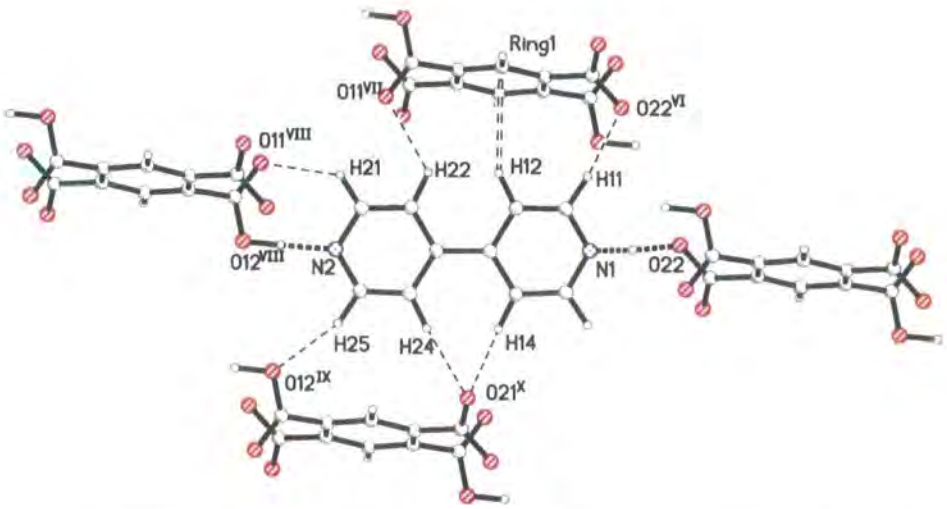


Figure 3.4.3. C-H···O and C-H···π bonds around the BPY+ molecules. [Symmetry codes: (IV) x, 1-y, -z (VI) 1-x, 1-y, -1-z; (VII) x, -y, z-1; (VIII) –1-x, 2-y, -1-z; (IX) x-1, y+1, z+1; (X) –x, 2-y, -2-z. ]

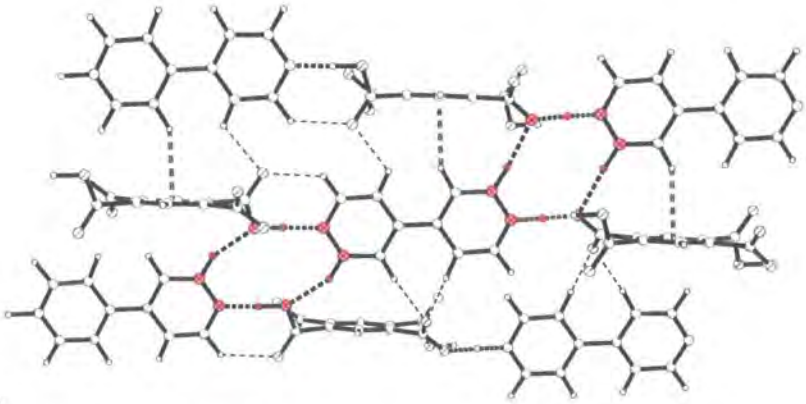

4.a.

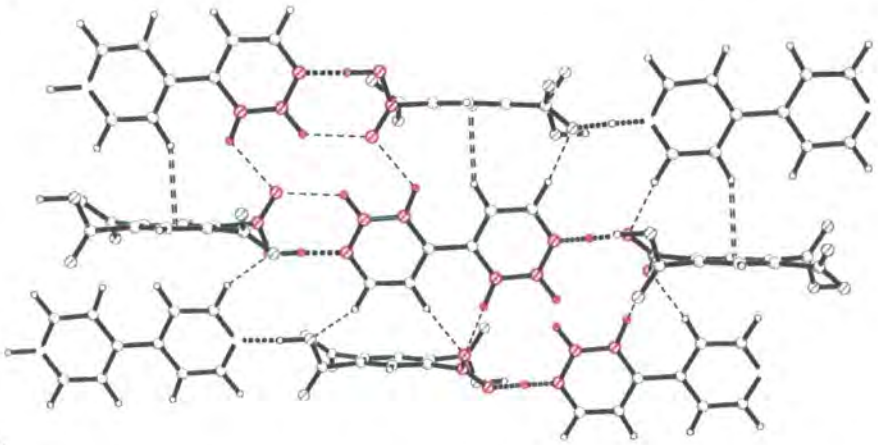

4.b.

Figures 3.4.4.a and 3.4.4.b. Hydrogen bonded rings in PMA2- and BPY+. The atoms in the hydrogen-bonded rings are marked in red. The ten membered rings are highlighted in A and the sixteen membered rings are highlighted in B.

Table 3.4.6. C-H···π Hydrogen Bond Parameters.

| | D···A (Å) | C···H (Å) | H···A (Å) | D-H-A |
|---|---|---|---|---|
| C12-H12···Ring1$^{XI}$ | 3.6521(12) | 1.086(3) | 2.668(3) | 150.4(2)° |

Symmetry code: (XI) x, y, -1+z.

The PMA2- and BPY+ molecules linked by the N-H···O and O-H···N hydrogen bonds form one-dimensional chains along the [0 1 –2] direction (figure 3.4.5). The chains are linked together in the a-direction by C-H···O and π-π interactions to form molecular layers (figure 3.4.6). The layers pack together linked in the bc-plane by C-H···O and C-H···π hydrogen bonds (figure 3.4.3) to form a chequered pattern of BPY+ and PMA2- columns (figure 3.4.6).

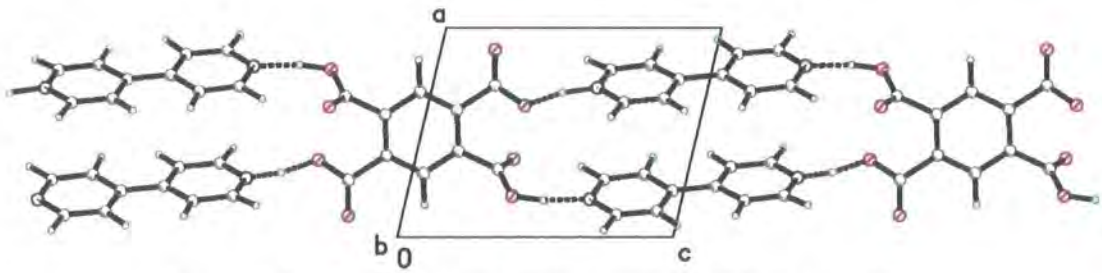


Figure 3.4.5. The hydrogen bonded chains in PMA2- and BPY+.

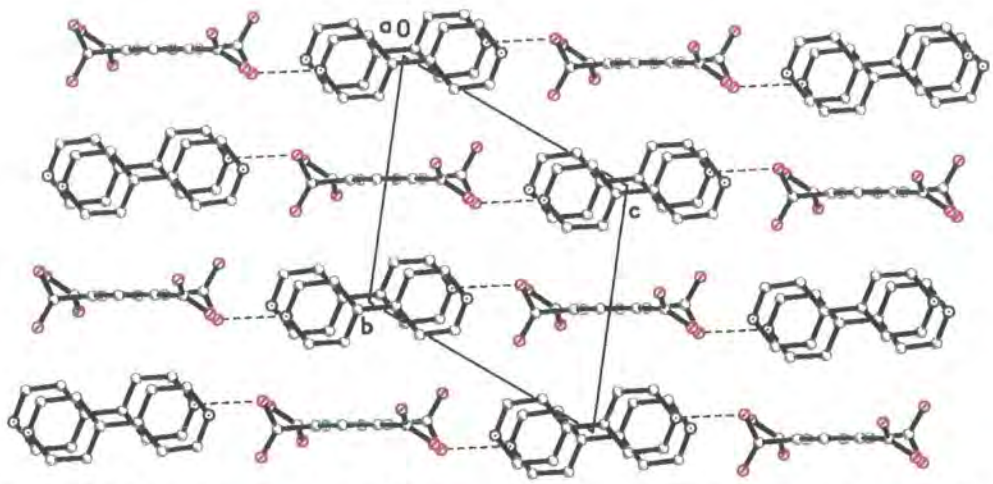


Figure 3.4.6. Packing diagram of PMA2- and BPY+ viewed along the a-direction. The hydrogen atoms have been omitted for clarity. The BPY·PMA chains can be seen running across the page.

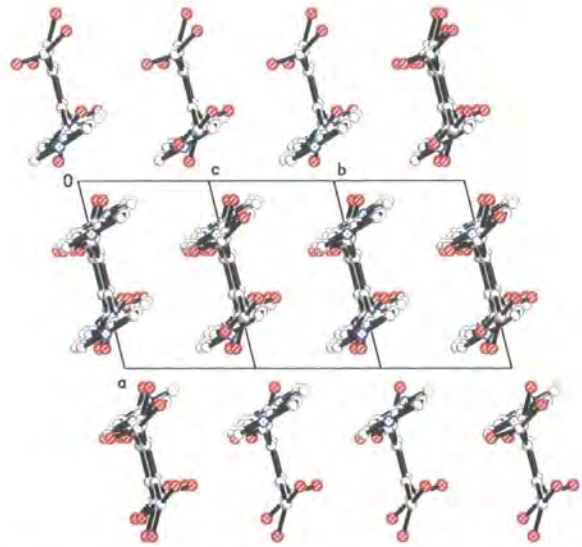


Figure 3.4.7. Packing diagram of PMA2- and BPY+ viewed along the molecular chains. The hydrogen atoms have been omitted for clarity.

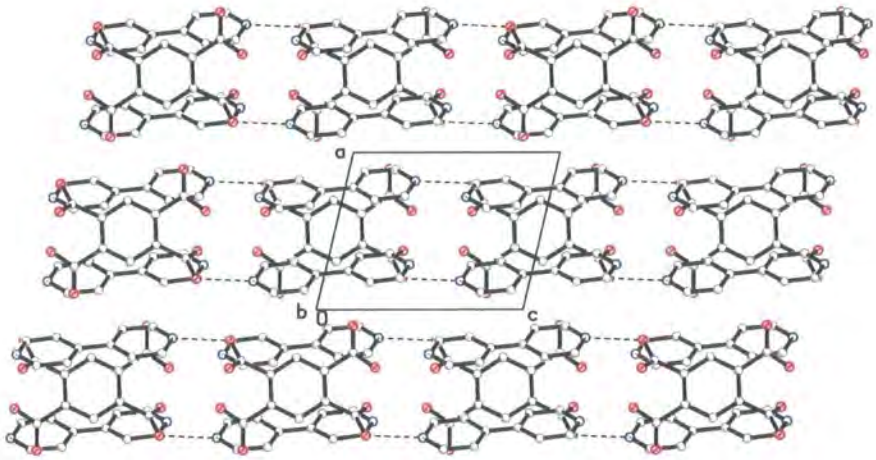


Figure 3.4.8. Packing diagram of PMA2- and BPY+ viewed along the b-axis. The hydrogen atoms have been omitted for clarity. The molecular chains again run across the page.

**Experimental Details**

The 100K and 30K X-ray data were collected in Durham on the Bruker-SMART diffractometer. The crystal was cooled to 30K using a HELIX helium flow cryostream. The crystal was cooled in the 100K experiment using an Oxford cryosystems nitrogen flow device. Dr. Samuel Lo in Hong-Kong using a SIEMANS P4 diffractometer collected the room-temperature data.

The room-temperature and 20K neutron diffraction data were collected on the 4-circle diffractometer D19, at the ILL. The 200K data were collected on the Laue diffractometer LADI also at the ILL.

**D19 Experiments**

A crystal suitable for neutron diffraction was mounted on a vanadium pin inserted into an aluminium mount, which was then mounted on the 4-circle diffractometer D19. Data were collected using monochromatic thermal neutrons with a wavelength of 1.3108(1)Å from a Ge(115) monochromator in a combination of normal-beam and equatorial-plane geometry.

Data first were collected at room temperature up to $2\theta = 110°$. Then the crystal was cooled to 20K using a Displex cryorefrigerator (Archer & Lehmann, 1986), where data were again collected up to $2\theta = 110º$. Unit-cell dimensions were refined using the program RAFD19 (Filhol, 1988) the results are summarised in table 3.4.data below. Data were reduced to integrated intensities using the ILL program RETREAT (Wilkinson et al. 1988) which also applies a Lorentz correction. The intensities were corrected for attenuation by the crystal by Gaussian integration (Matthewman et al. 1982) and for absorption by the aluminium and vanadium heat shields where used.

**LADI Experiment**

A small crystal was mounted on the Laue diffractometer, LADI (Wilkinson & Lehmann, 1991; Cipriani et al. 1995) while it was installed for trials on a thermal beam. The crystal was cooled using a Displex cryorefrigerator (Archer & Lehmann, 1986) to 200K where data were collected. 15 exposures of 2 hours each were collected. The images were indexed using LAUEGEN (Campbell, 1995) and reduced to integrated intensities using the ILL program INTEGRATE+ based upon the same algorithm as RETREAT (Wilkinson et al. 1988). Cell dimensions were estimated by linear interpolation between the monochromatic 20K and room temperature results, as dimensions refined from LADI are inaccurate. The data were normalised for the wavelength spectrum using the program LAUENORM (Campbell et al. 1996), only reflections with wavelengths between 1.0Å and 1.9Å were accepted for normalisation.

Table 3.4.data. Crystal, data collection and refinement details for PMA2- and BPY+.

| Diffractometer | D19 | LADI | Bruker SMART | Bruker SMART | D19 |
|---|---|---|---|---|---|
| Temperature (K) | 296 | 200 | 100 | 30 | 20 |
| Radiation | Neutron | Neutron | X-ray Mo-Kα | X-ray Mo-Kα | Neutron |
| Wavelength (Å) | 1.3108(1) | 1-2 | 0.71073 | 0.71073 | 1.3108(1) |
| a (Å) | 7.5011(3) | 7.541(1) | 7.3960(3) | 7.401(5) | 7.3561(2) |
| b (Å) | 9.7868(3) | 9.715(1) | 9.6390(4) | 9.645(7) | 9.5856(2) |
| c (Å) | 10.2303(3) | 10.204(1) | 10.1899(4) | 10.212(7) | 10.1478(3) |
| alpha (°) | 64.140(3) | 64.51(1) | 64.922(2) | 65.263(8) | 65.203(2) |
| beta (°) | 71.682(3) | 72.03(1) | 72.420(2) | 72.687(9) | 72.699(3) |
| gamma (°) | 75.516(3) | 76.08(1) | 76.763(2) | 77.066(9) | 77.099(3) |
| Volume ($Å^3$) | 635.93(4) | 628.9(12) | 622.93(4) | 627.9(8) | 616.16(3) |
| No of reflections for cell parameters | 2509 | N.A. | 896 | 880 | 2325 |
| θ range | 0-55° | 0 - 140° | 14.71-30.31 | 11.97-27.74 | 0-55° |
| μ ($mm^{-1}$) | 0.1672 | 0.1672 | 0.112 | 0.111 | 0.1672 |
| Crystal Shape | Bar | Plate | Block | Block | Bar |
| Crystal Colour | Colourless | Colourless | Colourless | Colourless | Colourless |
| Crystal Dimensions | 4.5*1.2*0.75 | 1*0.5*0.2 | 0.4*0.2*0.1 | 0.5*0.35*0.15 | 4.5*1.2*0.75 |
| Absorption Correction | Gaussian, D19ABS. | None | None | None | Gaussian, D19ABS |
| T min | 0.602 | - | - | - | 0.602 |
| T max | 0.892 | - | - | - | 0.892 |
| No. of reflections | 3096 | 6363 | 7323 | 5958 | 2988 |

Table 3.4.data. *continued.*

| Diffractometer | D19 | LADI | Bruker SMART | Bruker SMART | D19 |
|---|---|---|---|---|---|
| Temperature (K) | 296 | 200 | 100 | 30 | 20 |
| Independent reflections | 2145 | 1958 | 3280 | 2549 | 1866 |
| No. of reflections $I > 2\sigma$ | 1894 | 1193 | 2756 | 2126 | 1743 |
| R int | 0.0276 | 0.1180 | 0.0282 | 0.0380 | 0.0230 |
| R sigma | 0.0287 | 0.1234 | 0.0268 | 0.0322 | 0.0233 |
| $\theta$ max (°) | 55.51 | 70 | 29.91 | 27.43 | 56.27 |
| h | -9→9 | -7→7 | -8→10 | -9→9 | -9→9 |
| k | -12→4 | -12→13 | -13→13 | -12→12 | -12→6 |
| l | -12→12 | 0→14 | -13→14 | -12→12 | -12→12 |
| $R[F^2 > 2\sigma(F^2)]$ | 0.0351 | 0.0493 | 0.0392 | 0.0432 | 0.0329 |
| $wR(F^2)$ | 0.0822 | 0.1067 | 0.0975 | 0.0889 | 0.0774 |
| S | 1.552 | 1.262 | 1.863 | 1.657 | 1.660 |
| Qmax* | 0.425 | 0.680 | 0.348 | 0.340 | 0.518 |
| Qmin* | -0.443 | -0.678 | -0.290 | -0.218 | -0.579 |
| RMS Q* | 0.100 | 0.164 | 0.058 | 0.048 | 0.129 |
| Shift ($\Delta/\sigma$) | 0.000 | 0.000 | 0.000 | 0.000 | 0.005 |

* The units of Q, the residual unmodelled densities are $eÅ^{-3}$ for X-rays and fm $Å^{-3}$ for neutrons.

## 3.5. Temperature Dependence in the Structure of the 2:1 Co-crystal of 4,4-Bipyridine and Benzene-1,2,4,5-Tetracarboxylic acid

### 3.5.1. The Unit Cell

The unit-cell dimensions contract as the temperature is lowered. The 20K cell edge lengths and angles change by approximately 2% of the room-temperature values, the lengths decrease and the angles increase. The volume at 20K is 97% of the room-temperature value.

The cell dimensions in the 200K neutron experiment could not be measured accurately, therefore they have been derived by a least-squares fit of a straight line through the measured cell dimensions with weights of $1/\sqrt{esd}$. The esd's from the least squares calculation were much too small considering the small number of observations and the assumption that the change in cell parameters in a linear function of temperature, so the esd's have been estimated to be equal to the original room temperature X-ray esd's.

Table 3.5.1. Temperature dependence of the unit cell dimensions

| | a (Å) | b (Å) | c (Å) | α (º) | β (º) | γ (º) | Volume (Å$^3$) |
|---|---|---|---|---|---|---|---|
| 296K (X) | 7.503(1) | 9.784(1) | 10.231(1) | 64.11(1) | 71.67(1) | 75.49(1) | 635.73(12) |
| 296K (N) | 7.5011(3) | 9.7868(3) | 10.2303(3) | 64.140(3) | 71.682(3) | 75.516(3) | 635.93(4) |
| 100K (X) | 7.3960(3) | 9.6390(4) | 10.1899(4) | 64.922(2) | 72.42(2) | 76.763(2) | 622.93(4) |
| 100K* (X) | 7.3974(3) | 9.6352(4) | 10.1688(3) | 64.872(2) | 72.375(2) | 76.612(2) | 620.92(4) |
| 30K (X) | 7.401(5) | 9.645(7) | 10.212(7) | 65.263(8) | 72.687(9) | 77.066(9) | 627.9(8) |
| 20K (N) | 7.3561(2) | 9.5856(2) | 10.1478(3) | 65.203(2) | 72.699(3) | 77.099(3) | 616.16(3) |
| *200K** (N)* | *7.451(1)* | *9.715(1)* | *10.204(1)* | *64.51(1)* | *72.03(1)* | *76.08(1)* | *628.9(12)* |

* Cell Dimensions taken from the structure determination by Glidewell et al. (2000).

** The 200K cell dimensions have been estimated from a least-squares fit of a straight line through the other measurements.

The hydrogen bonded chains are along the [0 1 –2] direction, the largest component of the hydrogen bonding is therefore in the c-direction (figure 3.4.6), which is the direction with the smallest thermal expansion. The thermal expansion is greatest along the a and b directions, which are the directions of the weak π-π, C-H···O and C-H···π interactions.

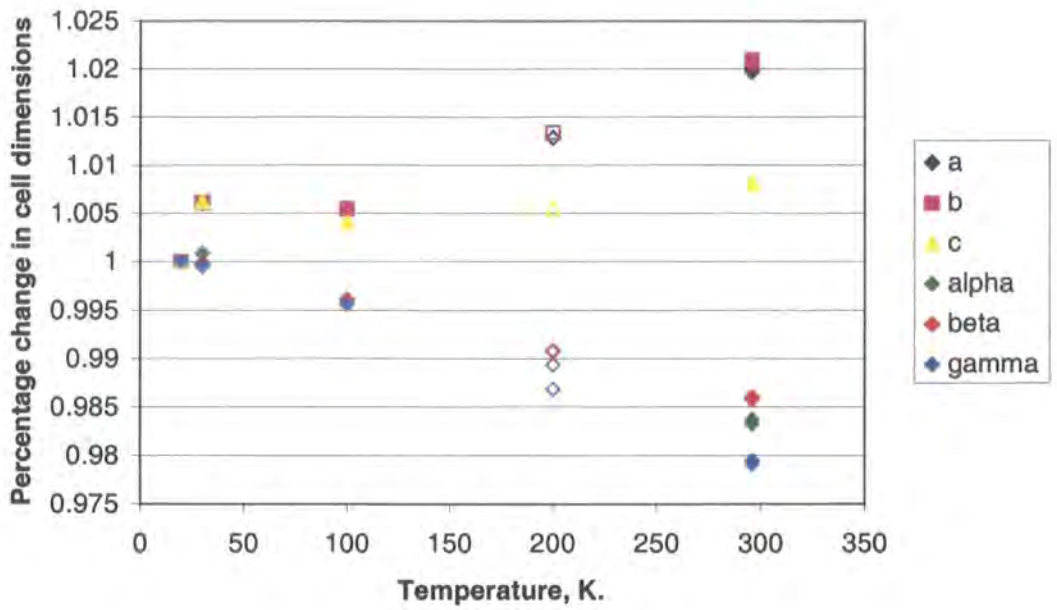


Graph 3.5.1. Percentage change in the cell dimensions from the 20K values over the temperature range.

### 3.5.2. Temperature Dependence of the Thermal Parameters

The change in thermal parameters of the atoms is approximately linear over the temperature range as expected by theory (Blessing, 1995). The X-ray derived parameters are consistently slightly larger than the neutron ones as is often observed (Blessing, 1995). In general absorption reduces the intensities of low angle reflections more than high-angle ones, which reduces the apparent thermal motions, however the 20K and 296K neutron-diffraction data have been corrected for absorption and the X-ray data left uncorrected. Extinction, which is more significant for neutron diffraction data, reduces the intensities of strong low-angle data with respect to the high-angle data, which will tend to reduce the apparent thermal motions (Willis and Pryor, 1975). The effect of inelastic thermal-diffuse scattering is more pronounced for neutrons than X-rays and also tends to reduce the apparent thermal parameters.

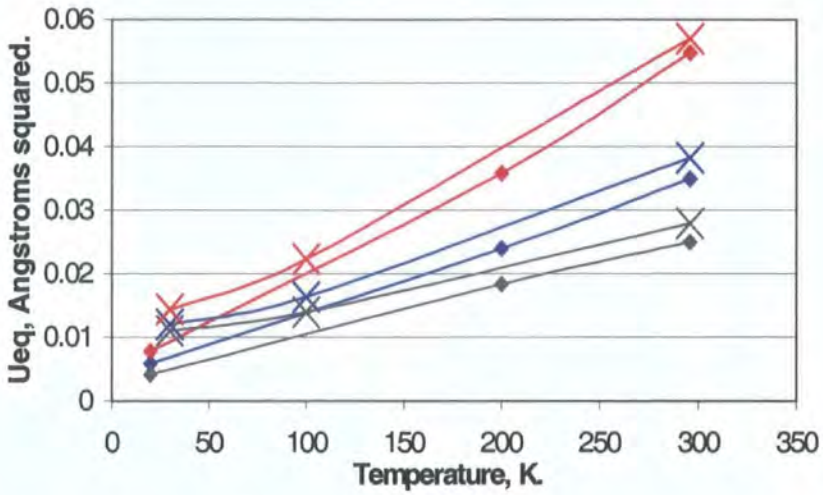


Graph 3.5.2. The variation in Ueq for C1 (grey), N1 (blue) and O11 (red). The values derived from X-ray results are marked with 'X' and the values from the neutron results are marked with a diamond. The lines are smoothed fits to emphasise the trends.

However in general the neutron diffraction data more accurately measures the thermal parameters. The atoms in a SHELX refinement are considered to be spherical and the electron or neutron scattering density is modelled accordingly. The scattering of neutrons from the nucleus is spherical and the refined anisotropic-displacement parameters should accurately represent the true atomic motions in the crystal.

X-rays are scattered from the electron cloud of an atom. In a molecule some electrons are often redistributed around the molecule, for example in delocalised phenyl rings (figure 3.5.1), the electron density of the atom-core is therefore reduced. The intensity of the X-rays scattered from an atom increases with the number of its electrons and decreases with the amount of thermal vibration. The spherical-atom in the model therefore must be made to vibrate more to fit the intensity scattered from the atom with the reduced number of electrons. The X-ray derived anisotropic displacement parameters also take into account any anisotropic changes in the electron cloud.

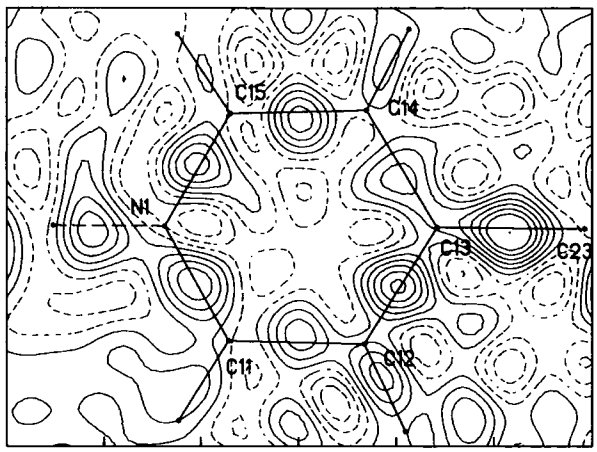


Figure 3.5.1. Difference Fourier map through the phenyl ring in part of the BPY+ molecule from the 30K X-ray data. The contours are at 0.05 $eÅ^{-3}$. Dashed lines indicate negative contours. There are clear peaks of electron density between the atoms in the ring.

### 3.5.3. Hydrogen Bond Lengths and Angles

There are two extremely similar hydrogen bonds in the structure. The O12-H2···N2 hydrogen bond parameters are identical within the standard uncertainties at all temperatures (Table 3.5.2). In the N1··H1··O22 hydrogen bond at 20K the proton is 1.325(3)Å from the oxygen atom and 1.207(3)Å from the nitrogen atom, at 296K the proton position has moved along the bond to be 1.240(4)Å from the oxygen atom and 1.302(4)Å from the nitrogen atom. The N1···O22 separation changes by ~0.01Å from 2.5220(17)Å at 20K to 2.5315(16)Å at 296K. At 200K the proton is close to the centre of the hydrogen bond. By interpolation the proton should be centred, ~1.265Å from the nitrogen and the oxygen atoms, at ~210K. The proton motion was observed in results of the X-ray experiments (table 3.4.1 and table 3.4.2) but with incorrect N-H and O-H bond lengths.

Table 3.5.2. The Temperature Dependence in the O12-H2···N2 Hydrogen Bond

| | O12···N2 distance (Å). | O12··H2 distance (Å) | H2··N2 distance (A) | O12-H2-N2 Angle (°) |
|---|---|---|---|---|
| 296K | 2.6095(17) | 1.078(4) | 1.542(3) | 169.6(3) |
| 200K | 2.609(3) | 1.062(5) | 1.556(5) | 170.5(7) |
| 20K | 2.6104(17) | 1.068(3) | 1.551(3) | 170.2(3) |

Table 3.5.3. The Temperature Dependence in the N1··H1··O22 Hydrogen Bond

| | O22···N1 distance (Å). | O22··H1 distance (Å) | H1··N1 distance (A) | O22-H1-N1 Angle (°) |
|---|---|---|---|---|
| 296K | 2.5315(16) | 1.240(4) | 1.302(4) | 169.4(3) |
| 200K | 2.520(3) | 1.280(6) | 1.251(6) | 169.4(6) |
| 20K | 2.5220(17) | 1.325(3) | 1.207(3) | 169.7(3) |

In the co-crystal of pentachlorophenol and 4-methylpyridine (Steiner et al. 2001) an identical phenomenon is observed in a short N··H··O hydrogen-bond. The N···O separation at 20K is 2.506(2)Å and 2.525(4)Å at 200K. The proton position at 20K is 1.206(6)Å from the nitrogen atom and 1.309(7)Å from the oxygen atom. At 200K the proton is 1.306(11)Å from the nitrogen and 1.228(11)Å from the oxygen atom. The proton is observed in the centre of the bond at 80K.

### 3.5.4. X-Ray Diffraction Derived Difference Fourier Maps

The X-ray diffraction data cannot give good hydrogen atom positions, but they can be used to calculate Fourier maps to show the electron density in the crystal. Refinement on omitting H1 results in a peak of unmodelled electron-density in the difference Fourier map. The peak position does not depend on the temperature, but the peak becomes more pronounced at low temperature. The peak shape observed in the difference Fourier maps (Figures 3.5.2.a, 3.5.2.b and 3.5.2.c) does not appear to change, but it becomes higher at low temperatures.

The proton position placed from the X-ray data is not at the peak of the electron density but is offset to a position where the residual electron-density is minimised.

Table 3.5.4. Peaks of residual electron density after refinement omitting H1

| | N-Peak distance (Å) | O-Peak distance (Å) | Peak Height ($eÅ^{-3}$) |
|---|---|---|---|
| 296K | 0.98 | 1.55 | 0.50 |
| 100K | 0.90 | 1.64 | 0.59 |
| 30K | 0.97 | 1.59 | 0.67 |

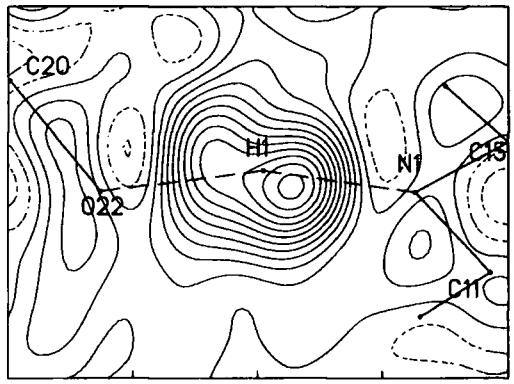


2.a. Room Temperature.

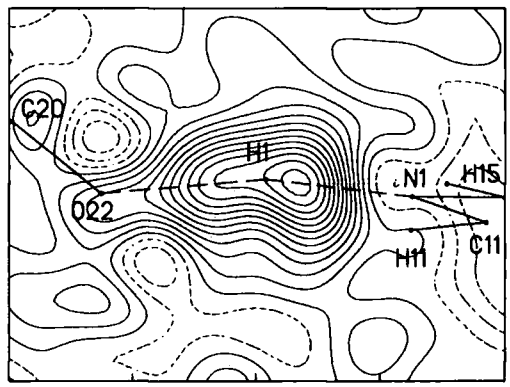


2.b. 100 K.

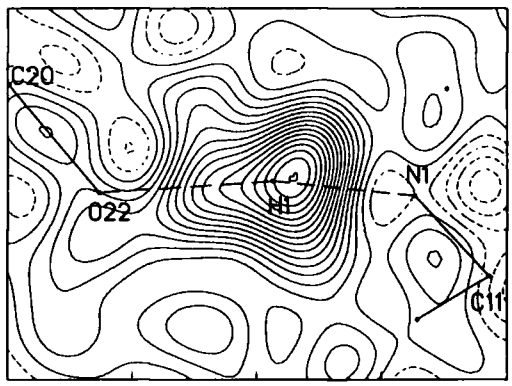


2.c. 30K

Figures. 3.5.2.a, 3.5.2.b and 3.5.2.c. Difference Fourier maps calculated from the X-ray data on omitting H1, which has been indicated in the diagram. The contours are at 0.05 $eÅ^{-3}$.

The shape of the electron density peak suggests that the electron cloud is distorted and that there is significant covalent character in the bond. In the difference Fourier map calculated with all the atoms at 30K, there is significant electron-density between the proton position and the nitrogen and the oxygen atoms (Figure 3.5.3).

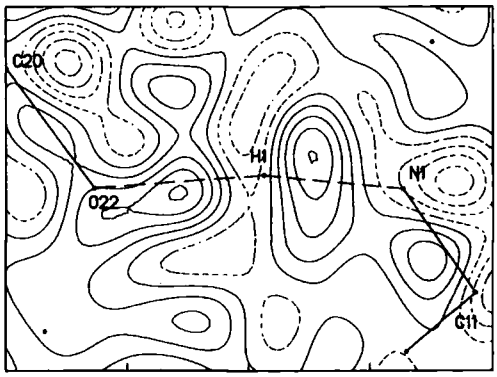


Figure 3.5.3. The difference Fourier map calculated from the 30K X-ray data. The contours are at 0.05eÅ$^{-3}$. Negative contours are indicated by dashed lines.

### 3.5.5. Neutron Fourier Maps

The proton positions are unambiguously seen in the neutron diffraction derived difference Fourier maps.

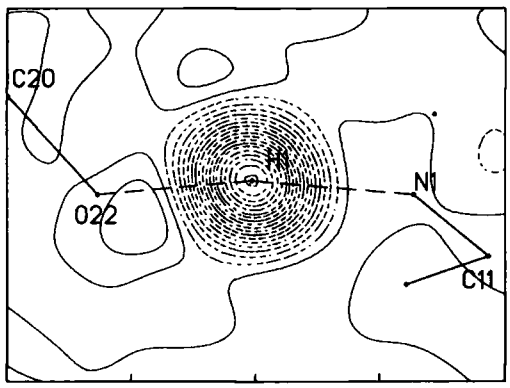


4.a. Room Temperature.

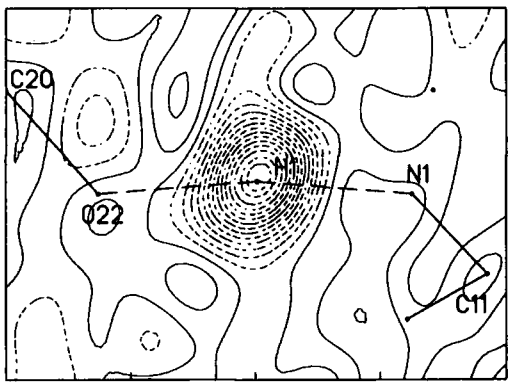


4.b. 200 K.

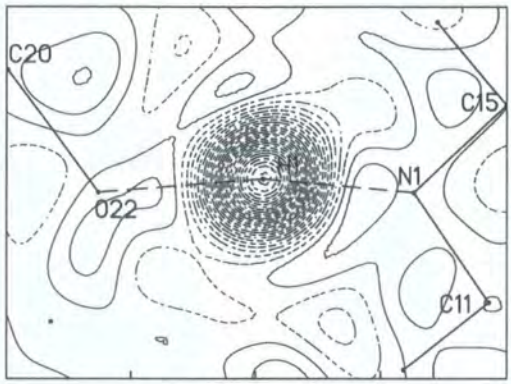


4.c. 20K.

Figures 3.5.4.a., 3.5.4.b and 3.5.4.c. Difference Fourier maps calculated from the neutron diffraction data. The contours are at nuclear scattering density of 0.5 fm $Å^{-3}$.


5.a. Room Temperature

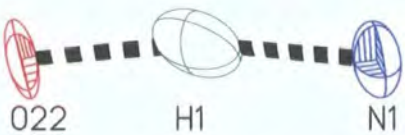


5.b. 200K


5.c. 20K.

Figures 3.5.5.a, 3.5.5.b and 3.5.5.c. 50% thermal-ellipsoid plots of the atoms in the hydrogen bond.

Disorder in the hydrogen bond, between O-H···N and N-H···O configurations with different occupancies cannot be ruled out by the X-ray diffraction results, but there is no hint of disorder in the neutron diffraction Fourier maps. The thermal parameters are well defined and show no evidence of excessive distortion, which could indicate disorder, along the N···O direction.

### 3.5.6. Other Bond Lengths and Angles

The most conspicuous change in bond lengths and the reason for the investigation of the temperature dependence is the proton migration in the hydrogen bond N1-H1···O22. The C20-O22 bond length and the C11-N1-C15 angle are the parameters that should be most affected by the change in the hydrogen bond. In the O12-H2···N2 hydrogen bond the C-O distance is 1.312(2)Å and the C21-N2-C25 angle is 118.2(1)° while in the shortest similar N-H···O hydrogen bond (section A.2) the C-O distance is 1.247(2)Å and the C-N-C angle is 121.75(12)°. As the hydrogen bond changes from approximately O-H···N to roughly N-H···O the C20-O22 distance may be expected to decrease and the C11-N1-C15 angle increase.

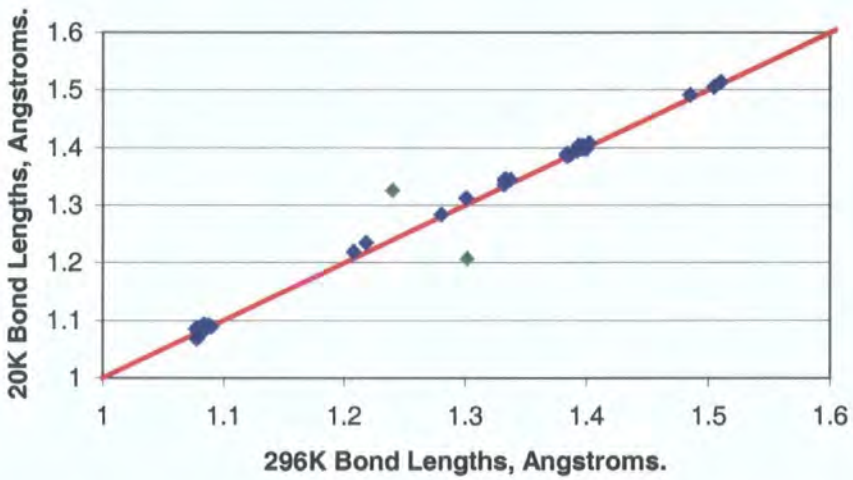


Graph 3.5.3. Room-temperature bond lengths vs. Low-temperature bond lengths. The red line corresponds to no change. All the points lie very close to the line. The green points are the O22-H1 and N1-H1 bond lengths.

There is very little change in any of the bond lengths between 20K and 296K, the only large change is the N1-H1 and O22-H1 bond distances (the green points in graph 3.5.3). The C11-N1-C15 angle increases by ~1° from ~119.2° at room temperature to 120.2° at 20K (graph 3.5.4) as the hydrogen bond changes from O-H···N to N-H···O.

The C20-O22 distance seems to increase slightly with temperature but the s.u's are large compared to the change over the temperature range (graph 3.5.5). The changes in the bond lengths could be accounted for by librational motion, although PLATON (Spek, 1990) calculates only a 0.0021Å increase in the C20-O22 bond length for the 296K neutron structure and a 0.0002Å increase in the 20K neutron structure.

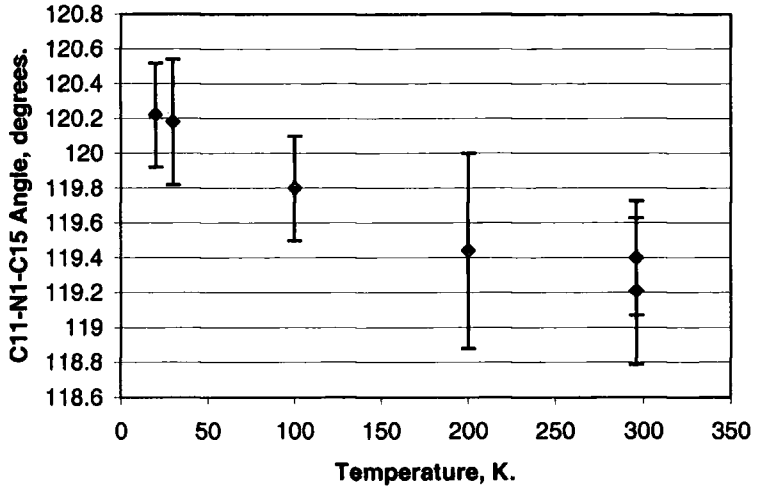


Graph 3.5.4. The C11-N1-C15 angle with respect to temperature. The error bars are at 3 s.u's.

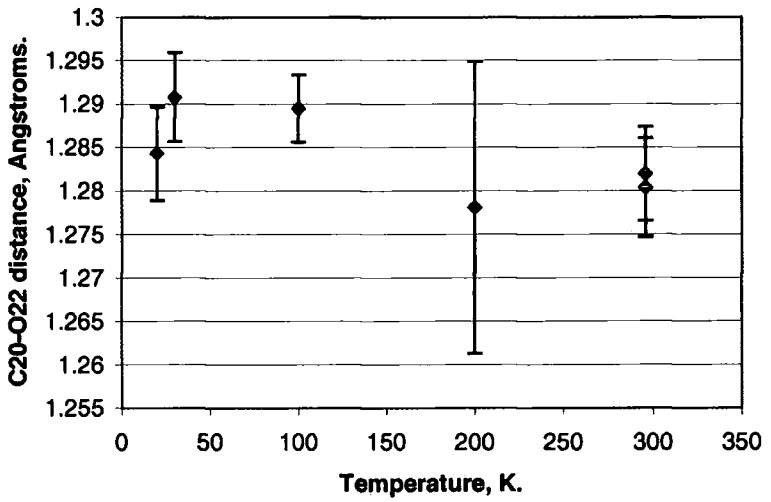


Graph 3.5.5. The C20-O22 bond length with respect to temperature. The error bars are at 3 s.u's.

### 3.6. The X-ray Structure of the 1:2 Co-crystal of 4,4'-Bipyridinium and Hydrogen Phthalate at 153K

4,4'Bipyridine and benzene-1,2-dicarboxylic acid (phthalic acid) crystallise in a 1:2 ratio as a molecular salt in space group C2/c. The 4,4'-bipyridine molecule has been doubly protonated to become 4,4'-bipyridinium$^{+2}$ (BPY2+) and the phthalic acid has been deprotonated to become the hydrogen phthalate$^{-1}$ anion (PHT-). Strong charge-assisted N-H···O hydrogen bonds link two PHT- molecules and a BPY2+ molecule into a linear trimer. The trimers are linked together by weak C-H···O and C-H···π interactions.

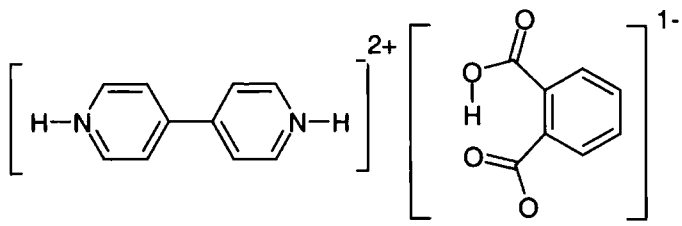


**[BPY2+]** **[PHT-]**

In the PHT- ion a short intramolecular hydrogen bond is formed between the carboxylic acid group and the carboxylate group. The hydrogen atom, H2, was found in the electron density difference Fourier map to be bonded to O12 (figure 3.6.1). On refinement after omitting H2 the largest peak of residual electron density is 0.38eÅ$^{-3}$ at 1.08Å from O12 and 1.31Å from O21, the next largest peak is 0.22eÅ$^{-3}$ at 0.40Å from O22 but not between O12 and O22. On refinement with H2 the largest peak of residual electron density is 0.20eÅ$^{-3}$ in the centre of the C2-C20 bond.

The C10-O bond lengths [ C10-O11 = 1.216(2)Å and C10-O12 = 1.306(2)Å ] agree with the standard values tabulated in the International Tables of Crystallography (Allen et al. 1992) for a carboxylic acid group attached to a phenyl ring. The C20-O bond lengths [C20-O21 = 1.272(2)Å and C20-O22 = 1.247(2)Å ] which are of more similar lengths are characteristic of a carboxylate group. The position of the hydrogen atom, H2, is in agreement with these bond lengths.

The long O-H bond length in the hydrogen bond agrees with neutron diffraction measurements of similar short O-H···O hydrogen bonds. However the difference Fourier map, although indicating the presence of a hydrogen atom, is not of good enough quality to be used to deduce the proton position accurately.

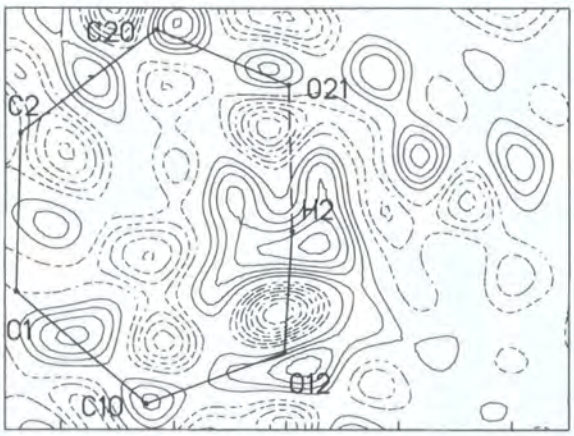


Figure 3.6.1. X-ray difference Fourier map calculated on omitting H2, which has been replaced in the diagram. The highest peak of electron density is close to H2. The contours are at 0.1eÅ$^{-3}$.

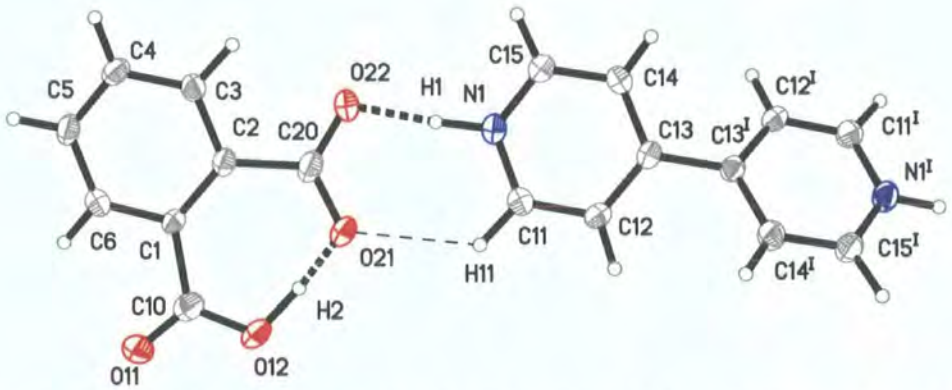


Figure 3.6.2. 50% Thermal ellipsoid plot of the molecules. Strong hydrogen bonds are indicated by heavy dashed lines. The thin dashed line indicates a weak C-H···O hydrogen bond. [Symmetry code (I) –x, y, -0.5-z]

The BPY2+ molecule lies across a two-fold axis at (0 y -¼) and only half of the molecule lies in the asymmetric unit. The pyridyl rings of the BPY2+ molecule are twisted at angle of 30.75(3)° with respect to each other, which optimises intermolecular C-H···O hydrogen bonding (figure 3.6.3) and reduces the steric interference between the BPY2+ hydrogen atoms (H12 and H14$^{I}$, H14 and H12$^{I}$).

The hydrogen atom, H1, was found in the difference Fourier map. The C11-N1-C15 bond angle of 121.18 (5)° agrees with the average bond angle for 4,4-bipyridinium$^{+2}$ of 121.5° taken from a search of the Cambridge Structural Database (Allen and Kennard, 1993), compared to 116.5° for the neutral molecule. A strong charge-assisted N-H···O hydrogen bond is formed between the BPY2+ and the PHT-, (N1-H1···O22).

This strong N-H···O hydrogen bond is complemented by a weak C-H···O hydrogen bond (C11-H11···O21) which holds the pyridyl ring approximately in the same plane as the carboxylate group (figure 3.6.3). The torsion angle between a line joining the two oxygen atoms, O21 and O21, and a line joining H11 and N1, through an axis along the strong N-H···O hydrogen bond, (H11-N1-O22-O21) is 1.0(4)°.

Table 3.6.1: Strong Hydrogen Bond Parameters.

| | D···A (Å) | D-H(Å) | H···A (Å) | D-H-A |
|---|---|---|---|---|
| N1-H1···O22 | 2.6273(16) | 1.03(2) | 1.60(2) | 175(2)° |
| O12-H2···O21 | 2.4141(15) | 1.10(2) | 1.32(2) | 171(2)° |

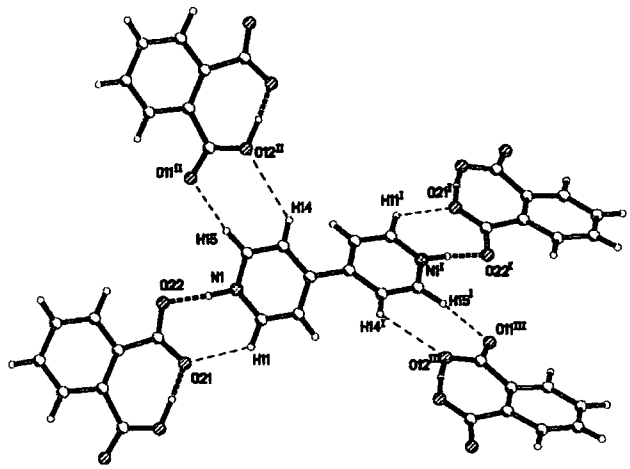

Figure 3.6.3. The intermolecular interactions that define the twist angle in the BPY2+ molecule. The molecular trimer can be seen linked by the strong N-H···O hydrogen bonds. The pyridinium rings are each in approximately the same plane as two PHT- molecules. [Symmetry codes (I) –x, y, -0.5-z. (II) –0.5+x, 0.5+y, z. (III) 0.5-x, 0.5+y, -0.5-z.]

Table 3.6.2: C-H···O Hydrogen Bond Parameters.

| | D···A (Å) | C···H (Å) | H···A (Å) | D-H-A |
|---|---|---|---|---|
| C4-H4···O21$^{III}$ | 3.304(2) | 1.000(13) | 2.575(13) | 129.6(10)° |
| C5-H5···O12$^{III}$ | 3.306(2) | 0.991(13) | 2.598(13) | 128.4(9)° |
| C11-H11···O21 | 3.153(2) | 1.037(13) | 2.411(13) | 127.7(9)° |
| C14-H14···O12$^{II}$ | 3.596(2) | 0.940(12) | 2.940(12) | 128.0(10)° |
| C15-H15···O11$^{II}$ | 3.219(2) | 1.031(13) | 2.199(14) | 170.1(11)° |

Symmetry codes: (II) –0.5+x, 0.5+y, z. (III) x, 2-y, 0.5+z.

Two PHT- molecules and one BPY2+ form strongly hydrogen bonded trimers, which are linked together by weak C-H···O, C-H···π and π···π interactions. C-H···O hydrogen bonds (C4···O21 and C5···O12) link the PHT- molecules into linear chains along the c-direction

(figure 3.6.4) and C-H···π interactions link them into perpendicular chains along the b-direction (figure 3.6.5).

Table 3.6.3: C-H···π Hydrogen Bond Parameters.

| | C-Ring centre (Å) | C-H (Å) | H-Ring centre (Å) | C-H-Ring centre |
|---|---|---|---|---|
| C3-H3···Ring1$^{V}$ | 3.5782(18) | 1.029(13) | 2.800(13) | 132.7(9)° |

Ring1 = C1-C2-C3-C4-C5-C6. Symmetry code: (V) 0.5-x, 0.5+y, 0.5-z.

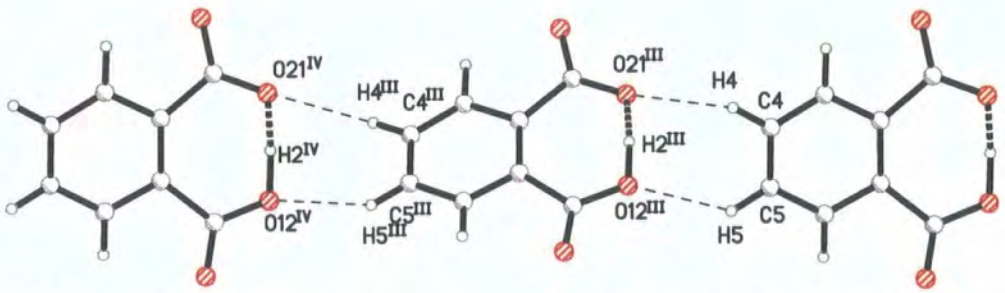


Figure 3.6.4. C-H···O hydrogen bonded chains of PHT- ions along the c-direction. [Symmetry codes (III) x, 2-y, 0.5+z. (IV) x, y, 1+z.]

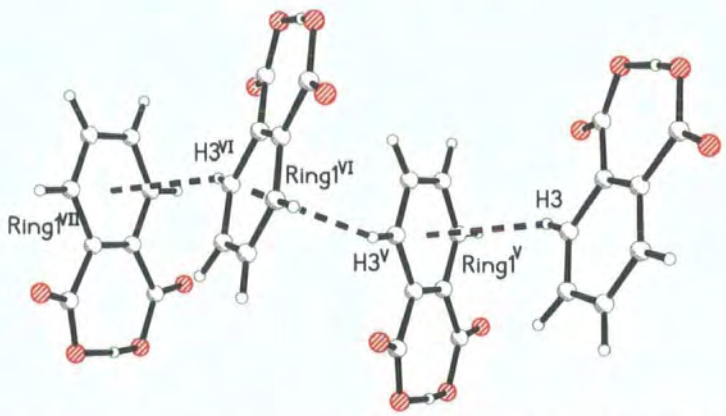


Figure 3.6.5. C-H···π chains along the b-direction. [Symmetry codes: (V) 0.5-x, 0.5+y, 0.5-z. (VI) x, 1+y, z. (VII) 0.5-x, 1.5+y, 0.5-z.]

Table 3.6.4. π-π Interactions.

| | Centre-to-centre distance (Å) | Angle between planes | Shortest perpendicular distance (Å) |
|---|---|---|---|
| Ring2···Ring1 | 3.8158(4) | 14.50(6)° | 3.3061(14) |

Ring1 = C1-C2-C3-C4-C5-C6. Ring2 = N1-C11-C12-C13-C14-C15.

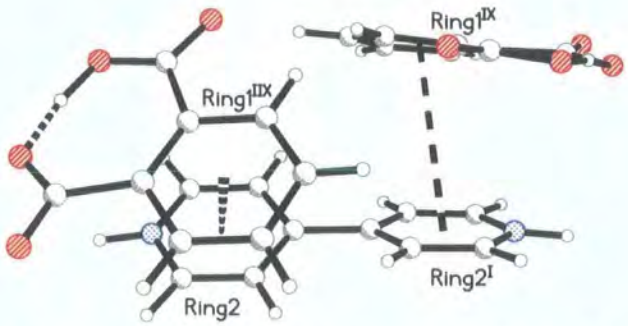


Figure 3.6.6. The π-π interactions indicated are symmetry equivalent. [Symmetry codes: (I) –x, y, -0.5-z, (IIX) 0.5-x, 2.5-y, -z, (IX) –0.5+x, 2.5-y, -0.5+z]

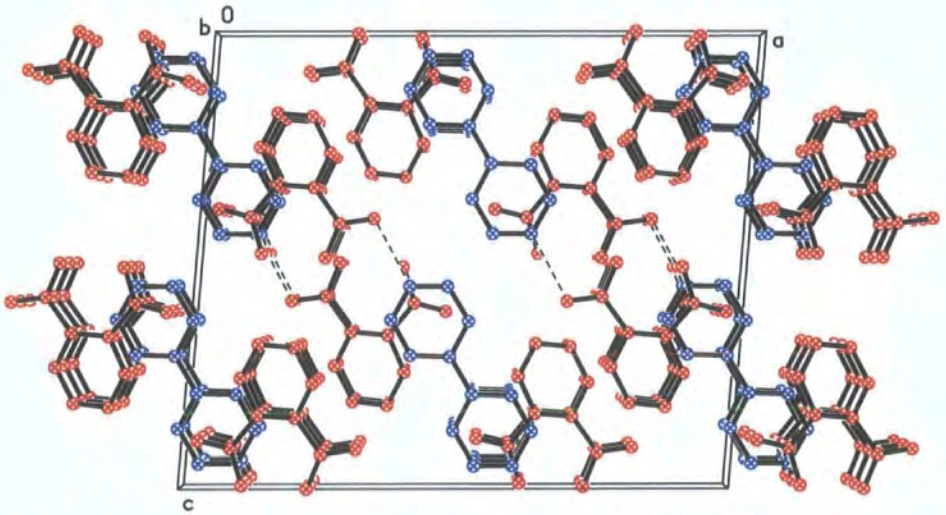


Figure 3.6.7. Packing diagram viewed along the b-axis. The PHT- molecules are red and the BPY2+ molecules are blue. The hydrogen atoms have been omitted for clarity.

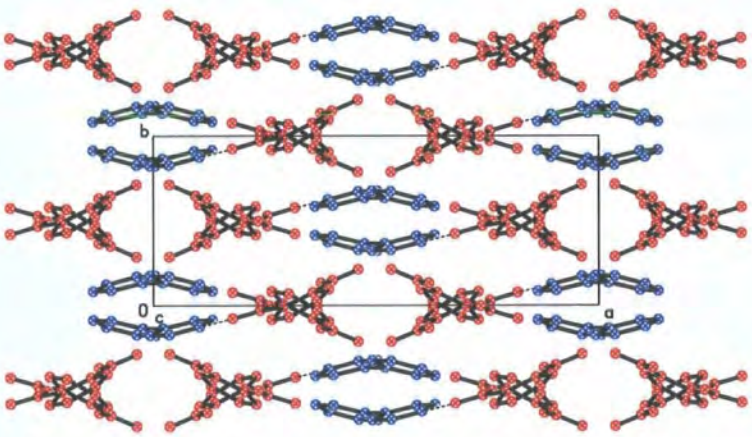


Figure 3.6.8. Packing diagram viewed along the c-axis parallel to the C-H···O hydrogen bonded chains of PHT- molecules. The PHT- molecules are red and the BPY2+ molecules are blue. The hydrogen atoms have been omitted for clarity.

**Experimental**

Data were collected on a Bruker-SMART diffractometer using an Oxford Cryosystems nitrogen flow device to cool the crystal.

Table 3.6.cry. Crystal parameters for PHT- and BPY2+.

| | | | |
|---|---|---|---|
| Formula | $C_{10}H_{10}N_2^{2+}\cdot 2[C_8O_4H_5^-]$ | Formula Weight | 488.44 |
| Crystal System | Monoclinic | Space Group | C2/c |
| a (Å) | 18.983(3) | α | 90° |
| b (Å) | 7.2140(11) | β | 94.897(8) |
| c (Å) | 15.792(2) | γ | 90° |
| Volume $(Å)^3$ | 2154.7(5) | Z | 4 |
| Density (Mg $m^{-3}$) | 1.506 | Colour | Colourless |
| Crystal Shape | Block | Dimensions (mm) | 0.35*0.25*0.1 |

Table 3.6.data. Data collection details for PHT- and BPY2+.

| | | | |
|---|---|---|---|
| Radiation | Mo Kα | λ (Å) | 0.71073 |
| Temperature (K) | 153 | | |
| Reflections | 12409 | Independent reflections | 2994 |
| Reflections I > 2σ(I) | 1274 | | |
| Rint | 0.0768 | Rsigma | 0.1461 |
| h | -26→26 | k | -9→9 |
| l | -21→22 | $\theta_{max}$ | 30.42 |

Table 3.6.ref. Refinement details for PHT- and BPY2+.

| | | | |
|---|---|---|---|
| $R[F^2 > 2\sigma(F^2)]$ | 0.0411 | $wR^2(F^2)$ | 0.1284 |
| S | 0.938 | Data / Parameters | 2994 / 203 |
| $\Delta\rho_{max}$ (e $Å^{-3}$) | 0.199 | $\Delta\rho_{min}$ (e $Å^{-3}$) | -0.221 |
| $(\Delta/\sigma)_{max}$ | 0.001 | $\Delta\rho_{rms}$ (e $Å^{-3}$) | 0.045 |

Cell parameters were determined from 998 strong reflections $\theta = 7.86 - 20.44^{\circ}$.
All non-hydrogen atom anisotropic thermal parameters were refined. All the hydrogen atoms were found in the difference Fourier maps and refined with isotropic thermal parameters. The C-H distances (C-H = 0.940(12)Å - 1.037(13)Å ) all refined to within standard ranges and there were no anomalous values of Uiso. The values of Uiso for the two hydrogen atoms in the strong hydrogen bonds were much larger than those of the other hydrogen atoms. As we are interested in the behaviour of the hydrogen atoms with respect to any hydrogen-bonded networks, it would be artificial to add any constraints to this stable and converged refinement.

### 3.7. The X-ray Structure of the 1:1 Co-crystal of 4,4'-Bipyridine and Phthalic acid at 200K

4,4'Bipyridine (BPY) and benzene-1,2-dicarboxylic acid (phthalic acid, PHT) crystallise in a 1:1 ratio as a neutral molecular adduct in space group C2/c. The BPY and PHT molecules are linked by strong O-H···N and weak C-H···O hydrogen bonds to form infinite two-dimensional sheets.

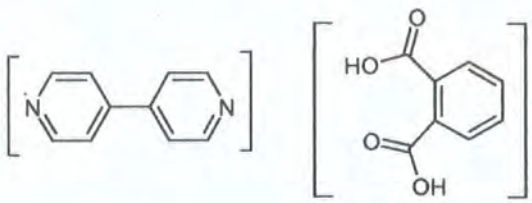


[BPY] [PHT]

The PHT molecule, of which only half is in the asymmetric unit, lies on a 2-fold axis along (0 y ¼). The C-O bond lengths of the carboxylic acid group of 1.2093(15)Å and 1.3089(15)Å agree with the standard values tabulated in the International Tables for Crystallography (Allen et al. 1992) of 1.305(20)Å and 1.226(20)Å for a carboxylic acid group attached to a phenyl ring. The torsion angle between the carboxyl group and the C1-C1$^{I}$ bond in the phenyl ring is 41.6(2)°.

The BPY molecule lies across an inversion centre at ( ¼ -¼ 0 ) and only half of the molecule lies in the asymmetric unit. The two pyridyl rings of the BPY are constrained to be planar by the inversion centre. The C-N-C bond angle [C20-N1-C24 = 116.7(1)°] agrees well with the average value of 116.5° for neutral bipyridine molecules taken from the Cambridge Structural Database (Allen and Kennard, 1993). This parameter along with the conformation of the carboxylic acid group in the PHT molecule accords with H1 being bound to O12 and not to the BPY.

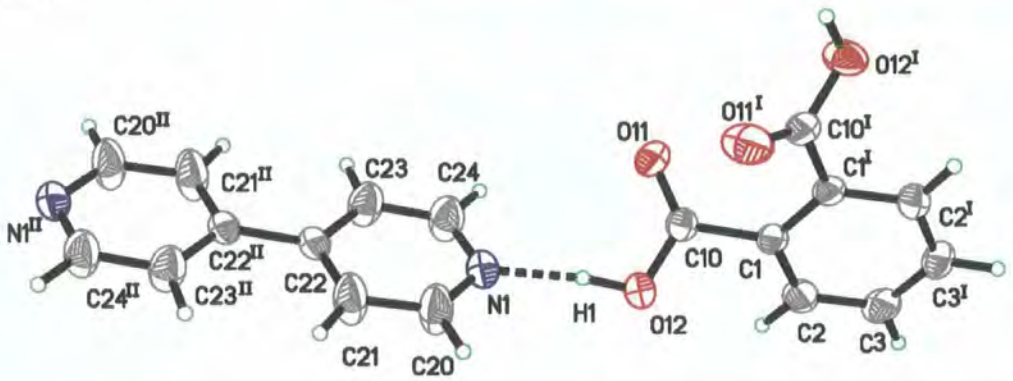


Figure 3.7.1. 50% Thermal ellipsoid plot of the PHT and BPY molecules. The dashed line indicates the O-H···N hydrogen bond and hydrogen atoms are drawn as small spheres of arbitrary radii. [Symmetry codes: (I) -x, y, 0.5-z. (II) 0.5-x, -0.5-y, -z].

The molecules are linked by a strong O-H···N hydrogen bond (O12-H1···N1) into infinite zig-zag chains along the [1 0 $\bar{1}$] direction (figure 3.7.2).

Table 3.7.1: Strong Hydrogen Bond Parameters.

| | D···A (Å) | D-H(Å) | H···A (Å) | D-H-A |
|---|---|---|---|---|
| O12-H1···N1 | 2.6299(13) | 0.97(2) | 1.67(2) | 169(2)° |

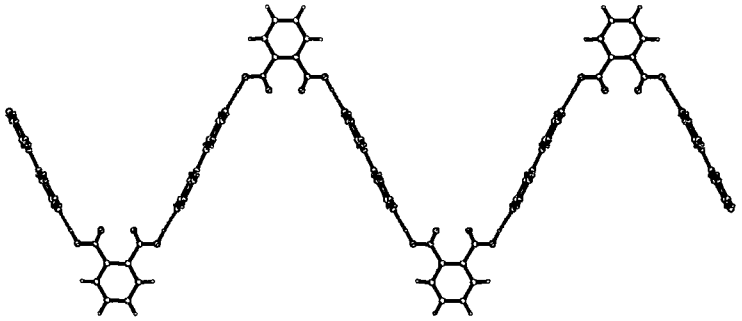

Figure 3.7.2. The PHT and BPY molecules pack in infinite zig-zag chains along the [1 0 –1] direction linked by strong O-H···N hydrogen bonds, which are indicated with dashed lines.

The zig-zag chains fit together along the b-axis, linked by weak C-H···O (C3···O11) and C-H···π (C2···pyridyl ring) hydrogen bonds to form almost planar sheets (figures 3.7.3 and 3.7.4).

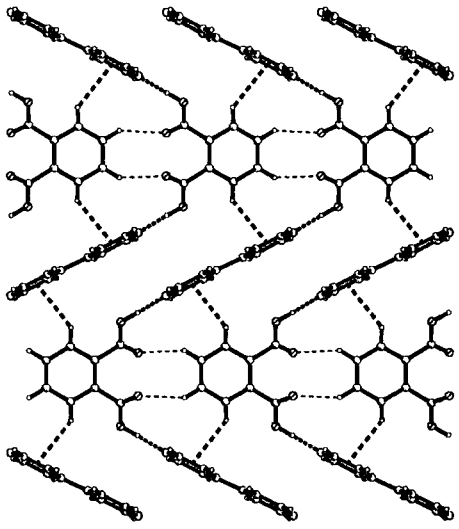

Figure 3.7.3. The intermolecular interactions actions in the planar sheets of PHT and BPY. O-H···N hydrogen bonds are indicated by the heavy dashed lines, C-H···O hydrogen bonds by thin dashed lines and C-H···π hydrogen bonds by the hollow dashed lines.

Table 3.7.2: C-H···O Hydrogen Bond Parameters.

| | D···A (Å) | C···H (Å) | H···A (Å) | D-H-A (°) |
|---|---|---|---|---|
| C3-H3···O11$^{i}$ | 3.3543(16) | 0.990(16) | 2.494(15) | 145.2(12) |
| C23-H23···O11$^{ii}$ | 3.4340(18) | 0.974(18) | 2.594(17) | 144.6(14) |

Symmetry codes: (i) x, 1+y, z. (ii) -x, -y, -z.

Table 3.7.3: C-H···π Hydrogen Bond Parameters.

| | C-Ring Centre (Å) | C-H (Å) | H-Ring Centre (Å) | C-H-Ring Centre |
|---|---|---|---|---|
| C2-H2···Ring2$^{i}$ | 3.6327(13) | 0.956(15) | 2.872(15) | 137.3(10)° |

Ring 2 = N1, C20, C21, C22, C23, C24.

Symmetry code: (i) x, 1+y, z.

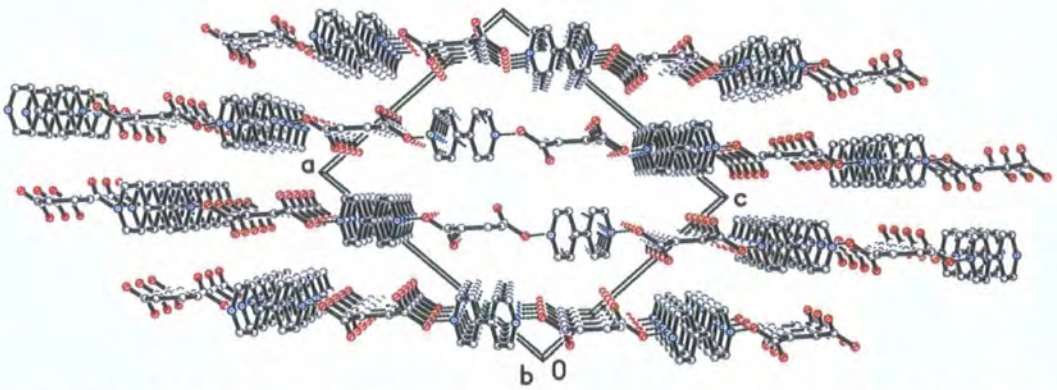


Figure 3.7.4. Packing diagram of PHT and BPY viewed parallel to the b-axis. The planar sheets pack together to form a layered structure.

Weak C-H···π and C-H···O bonds link the layers together. The C-H···π bonds from the BPY rings to the phenyl ring of the PHT seem to be directed directly at the aromatic C-C bond rather than towards the ring centres (figure 3.7.5).

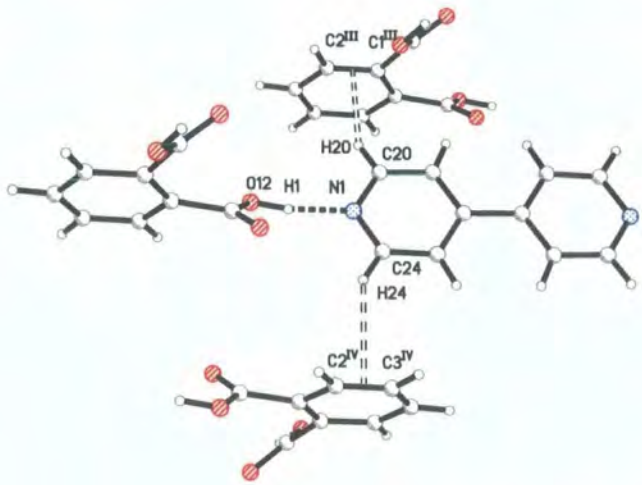


Figure 3.7.5. Weak C-H···π bonds between the pyridine and the aromatic C-C bonds in the PHT phenyl ring. The strong hydrogen bond between N1 and O12 is also indicated. Symmetry codes: (iii) 0.5-x, -0.5+y, 0.5-z. (iv) –x, 1-y, -z.

Table 3.7.4: C-H···π Hydrogen Bond Parameters.

| | C-Bond centre(Å) | C-H (Å) | H-Bond centre (Å) | C-H-Bond centre |
|---|---|---|---|---|
| C20-H20···[C1-C2][iii] | 3.8180(16) | 0.96(2) | 2.98(2) | 145.6(15)° |
| C24-H24···[C2-C3][iv] | 3.6332(16) | 0.960(18) | 2.781(19) | 148.3(14)° |

Symmetry codes: (iii) 0.5-x, -0.5+y, 0.5-z. (iv) –x, 1-y, -z.

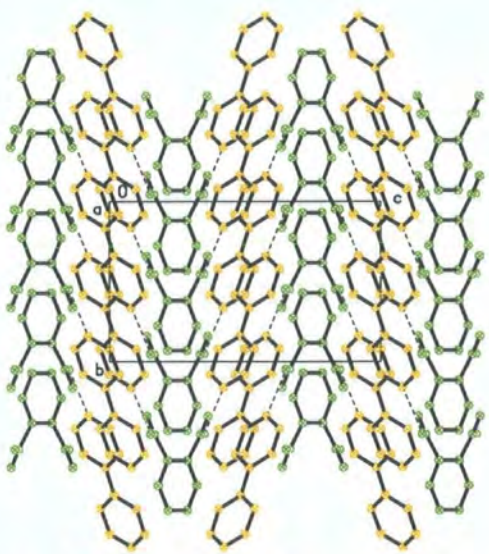


Figure 3.7.6. Packing diagram of PHT and BPY viewed parallel to the a-axis.

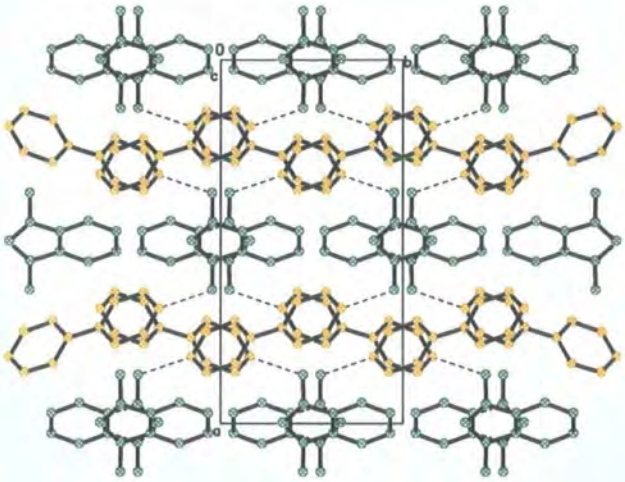

Figure 3.7.7. Packing diagram of PHT and BPY viewed parallel to the c-axis.

**Experimental details**

The data were collected at 200K as the crystal shattered at lower temperatures. Data were collected on a Bruker-SMART diffractometer using and Oxford cryosystems nitrogen flow device to cool the crystal.

Table 3.7.cry. Crystal parameters for PHT and BPY.

| Formula | $C_{10}H_8N_2 \cdot C_8H_6O_4$ | Formula Weight | 322.31 |
|---|---|---|---|
| Crystal System | Monoclinic | Space Group | C2/c |
| a (Å) | 15.7593(11) | α | 90° |
| b (Å) | 7.7580(6) | β | 98.386(3)° |
| c (Å) | 13.2466(10) | γ | 90° |
| Volume $(Å)^3$ | 1602.2(2) | Z | 4 |
| Density (Mg $m^{-3}$) | 1.336 | Colour | Colourless |
| Crystal Shape | Needle | Dimensions (mm) | 0.8*0.15*0.15 |

Table 3.7.data. Data collection details for PHT and BPY.

| Radiation | Mo Kα | λ (Å) | 0.71073 |
|---|---|---|---|
| Temperature (K) | 200 | | |
| Reflections | 9225 | Independent reflections | 2114 |
| Reflections I > 2σ(I) | 1430 | | |
| Rint | 0.0376 | Rsigma | 0.0359 |
| h | -21→20 | k | -10→10 |
| l | -17→17 | $\theta_{max}$ | 29.01 |

Table 3.7.ref. Refinement details for PHT and BPY.

| | | | |
|---|---|---|---|
| $R[F^2 > 2\sigma(F^2)]$ | 0.0420 | $wR^2(F^2)$ | 0.1181 |
| S | 0.993 | Data / Parameters | 2114 / 37 |
| $\Delta\rho_{max}$ (e Å$^{-3}$) | 0.232 | $\Delta\rho_{min}$ (e Å$^{-3}$) | -0.220 |
| $(\Delta/\sigma)_{max}$ | 0.001 | $\Delta\rho_{rms}$ (e Å$^{-3}$) | 0.043 |

Cell parameters were determined from 984strong reflections $\theta$ = 10.67 – 22.67º.
All non-hydrogen atom anisotropic thermal parameters were refined. All the hydrogen atoms were found in the difference Fourier maps and refined with isotropic thermal parameters. The X-H distances (X-H = 0.95(2)Å - 0.99(2)Å ) all refined to within standard ranges and there were no anomalous values of Uiso.

### 3.8. The X-ray Structure of the 1:2 Co-crystal of Bis-1,2-(4-pyridinium)ethane Hydrogen Phthalate at 100K.

Bis-1,2-(4-pyridyl)ethane and benzene-1,2-dicarboxylic acid (phthalic acid) crystallise in a 1:2 ratio as a molecular salt in space group C2/c. The bis-1,2-(4-pyridyl)ethane molecule has been doubly protonated to become bis-1,2-(4-pyridinium)ethane $^{+2}$ (BPA2+) and the phthalic acid has been deprotonated to become hydrogen phthalate$^{-1}$ (PHT-). The PHT- molecules are linked by strong O-H···O hydrogen bonds into one-dimensional chains. The BPA2+ molecules link the chains together by N-H···O hydrogen bonds into planar sheets perpendicular to the b-axis.

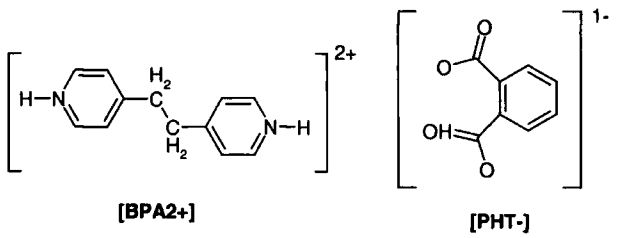


[BPA2+] [PHT-]

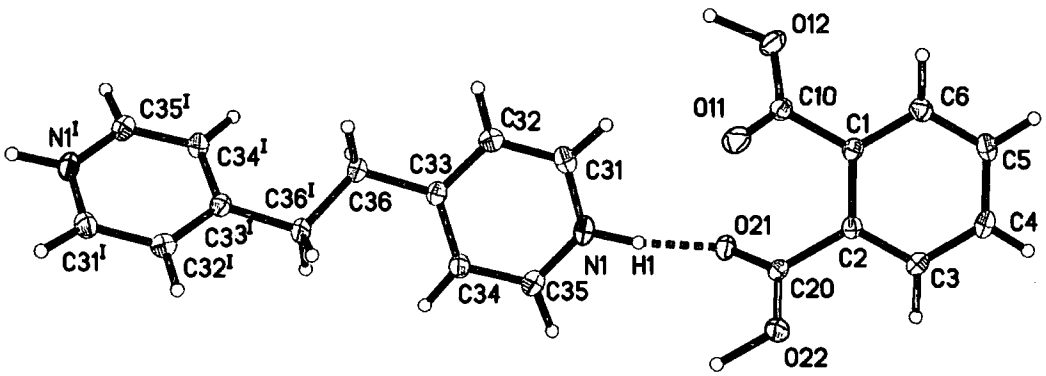


Figure 3.8.1. 50% Thermal ellipsoid plot of the PHT- and BPA2+ molecules. The dashed line indicates the N-H···O hydrogen bond and hydrogen atoms are drawn as small spheres of arbitrary radii. [Symmetry code: (I) -x, y, 2.5-z.].

The PHT- appears to be fully protonated, but both carboxylic acid hydrogen atoms lie on special positions and have occupancies of 50%.

The carboxylic acid group involving C10, O11, O12 and H12 forms a strong O-H···O hydrogen bond across a two-fold symmetry axis with the symmetry equivalent of itself. There can be only one hydrogen atom in the hydrogen bond which can be modelled in two ways. The hydrogen atom can be constrained to lie on the symmetry axis in the centre of the bond or it can be disordered over two positions either side of the centre with 50% occupancy in each position. The oxygen-oxygen separation of 2.4564(17)Å lies within the region where the

O-H bond length is expected to be significantly lengthened (graph 3.8.1). The difference Fourier map (figure 3.8.2) shows two maxima either side of the centre of the hydrogen bond suggesting that the proton is disordered over two positions. Refinement of the hydrogen atom in both situations leads to the hydrogen bond parameters in Table 3.8.1. In the disordered refinement the O-H bond length becomes much shorter than the value expected in similar hydrogen bonds of ~1.1Å and the O···O separation changes.

Table 3.8.1. O12-H12···O12' Hydrogen bond parameters.

| | D···A (Å) | D-H(Å) | H···A (Å) | D-H-A |
|---|---|---|---|---|
| Disordered refinement | 2.4612(19) | 0.85(3) | 1.63(3) | 166(2)° |
| Centred refinement | 2.4564(17) | 1.236(4)* | 1.236(4)* | 167(3)° |

* Indicates that the hydrogen atom position has been constrained.

In the crystal structure of hydrazinium hydrogen oxalate (Thomas and Liminga, 1978) an almost identical situation occurs. A short O-H···O hydrogen bond lies across a two-fold axis with an O-O separation of 2.457Å. The X-ray Fourier maps suggested that the hydrogen atom was disordered between two positions, but the more accurate neutron diffraction results placed the hydrogen in the centre of the bond. A similar situation occurs in acetamide hemihydrochloride (Speakman et al. 1981) with the X-ray results suggesting that the hydrogen atom is disordered around an inversion centre in a short O-H···O bond and the subsequent neutron diffraction results proving that the proton is infact centred.

In the present refinement the proton has been fixed on the two-fold axis (0 y 0.75), which, following the evidence of the neutron diffraction results, should give the more accurate description of the hydrogen bond.

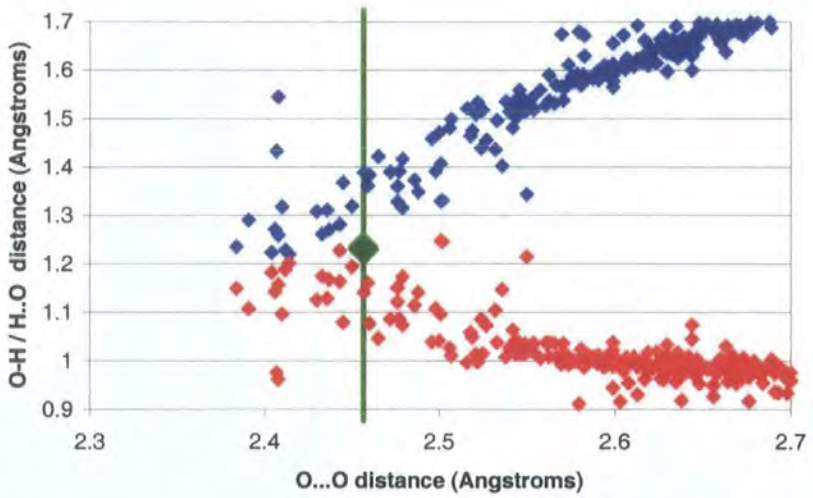


Graph 3.8.1. O-H···O hydrogen bonds measured by neutron diffraction from the Cambridge Structural Database (Allen and Kennard, 1993). The vertical green line marks an O···O distance of 2.456Å and the green points mark the O12-H12 and H22···O22 bond distances, which are overlapping.

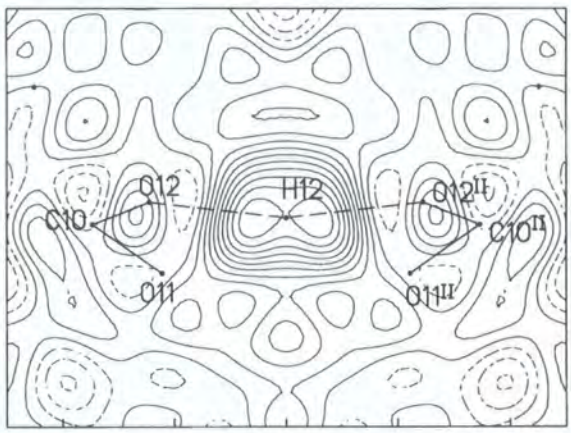


Figure 3.8.2. Difference Fourier map through the O12···O12$^{II}$ hydrogen bond calculated on omitting H12, which has been indicated in the diagram. The contours are at 0.05eÅ$^{-3}$. The two-fold axis runs vertically through H12. [Symmetry code: (II) -x, y, 1.5-z]

The carboxylic acid group C20, O21, O22, H22 is involved in two strong hydrogen bonds. O21 is a hydrogen bond acceptor in the N-H···O hydrogen bond from the BPA2+ molecule. A short O-H···O hydrogen bond is formed from O22 to its symmetry equivalent molecule across an inversion centre at (0.25, 0.25, 1). As in the O12··H12··O12 hydrogen bond the difference Fourier map (figure 3.8.3) can be interpreted to suggest that the proton is disordered over two positions either side of the inversion centre. However refinement with the proton centred leads to more likely O-H bond lengths for such a short O-H···O hydrogen bond (table A.8.2).

For the same reasons as discussed above the proton has been constrained to lie on the inversion centre.

Table 3.8.2. O22-H22···O22' Hydrogen bond parameters.

| | D···A (Å) | D-H(Å) | H···A (Å) | D-H-A |
|---|---|---|---|---|
| Disordered refinement | 2.4598(19) | 0.91(4) | 1.56(3) | 166(4)° |
| Centred refinement | 2.4568(17) | 1.2284(8)* | 1.2284(8)* | 180°* |

* The s.u's are small because the hydrogen atom position has been constrained.

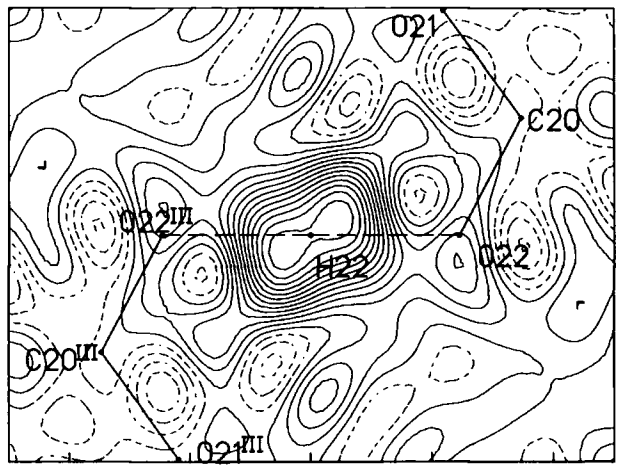


Figure 3.8.3. Difference Fourier map through the O22···O22$^{III}$ hydrogen bond calculated on omitting H22, which has been indicated in the diagram. The contours are at 0.05eÅ$^{-3}$. H22 lies on an inversion centre at (0.25 0.25 1). [Symmetry code: (III) 0.5-x, 0.5-y, 2-z]

The C-O bond lengths in the carboxylic acid groups show no evidence of disorder. The C10-O bond lengths [C10-O11 = 1.2332(14)Å and C10-O12 = 1.3009(13)Å] are close to the average values quoted in the International Tables for Crystallography (Allen at al. 1992) for a carboxylic acid group attached to a phenyl ring. The C20-O [C20-O21 = 1.2498(14)Å and C20-O22 = 1.2832(13)Å ] bond lengths are hybrid between carboxylic and carboxylate bond lengths. The C20-O21 bond is weakened and lengthened by accepting a strong hydrogen bond from the BPA2+ molecule.

A hydrogen atom, H1, was found in the difference Fourier maps bound to N1. The molecular geometry of the BPA2+ molecule agrees with this. The C31-N1-C35 angle of 121.63(11)° is characteristic of protonated pyridine molecules. From the Cambridge Structural Database (Allen and Kennard, 1993) the mean C-N-C angle in pyridinium ions is 121.9(2)°, while the C-N-C angle in pyridine molecules is 117.3(2)°. The BPA2+ molecules lies across a two-fold

axis at (0 y 1.25) and only half lies in the asymmetric unit. A strong charge-assisted N-H···O hydrogen bond links the BPA2+ and PHT- molecules.

Table 3.8.3: Strong Hydrogen Bond Parameters.

| | D···A (Å) | D-H(Å) | H···A (Å) | D-H-A |
|---|---|---|---|---|
| N1-H1···O21 | 2.6550(14) | 1.018(16) | 1.651(17) | 167.7(14)° |
| O12-H12···O12$^{II}$ | 2.4564(17) | 1.236(4)* | 1.236(4)* | 167( 3)° |
| O22-H22···O22$^{III}$ | 2.4568(17) | 1.2284(8)* | 1.2284(8)* | 180°* |

Symmetry codes: (II) -x, y, 1.5-z. (III) 0.5-x, 0.5-y, 2-z]

* Indicates that the hydrogen atom position has been constrained.

The strong O-H···O hydrogen bonds link the PHT- molecules into infinite one-dimensional zig-zag chains along the [1 0 1] direction (figure 3.8.4). The chains are linked together by the N-H···O hydrogen bonds to form planar sheets perpendicular to the b-axis (figure 3.8.5). The 'arrow head' of the BPA2+ molecule fits neatly into the cleft of the PHT- chain, held in place by the N-H···O hydrogen bond and three weak C-H···O hydrogen bonds (C31···O12, C31···O11 and C35···O22,) within the planar sheet (figure 3.8.6).

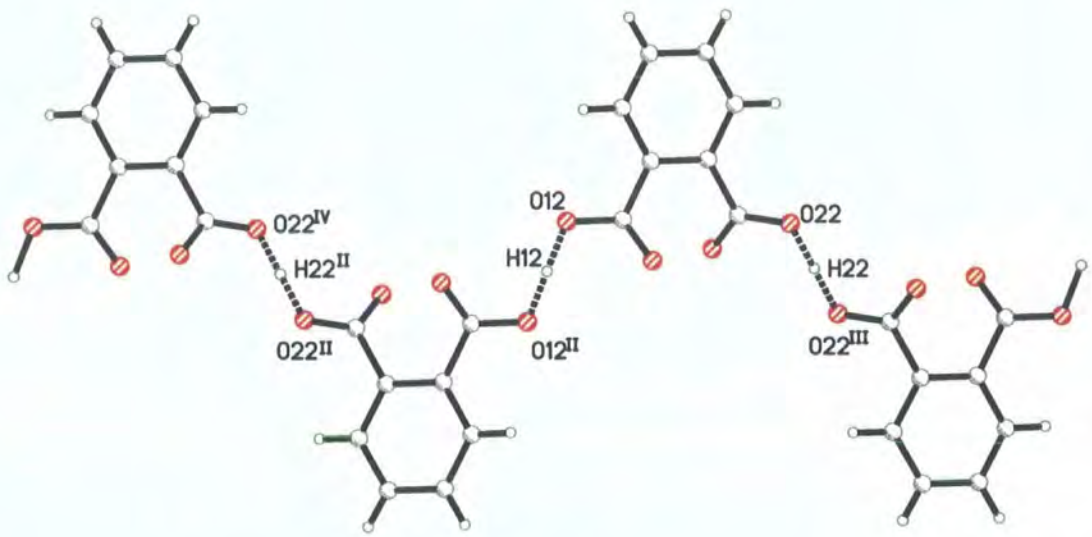


Figure 3.8.4. The PHT- molecules connected by O-H···O hydrogen bonds into zig-zag chains along the [1 0 1] direction. The dashed lines indicate the hydrogen bonds. [Symmetry codes: (II) -x, y, 1.5-z, (III) 0.5-x, 0.5-y, 2-z, (IV) –0.5+x, 0.5-y, -0.5+z.]

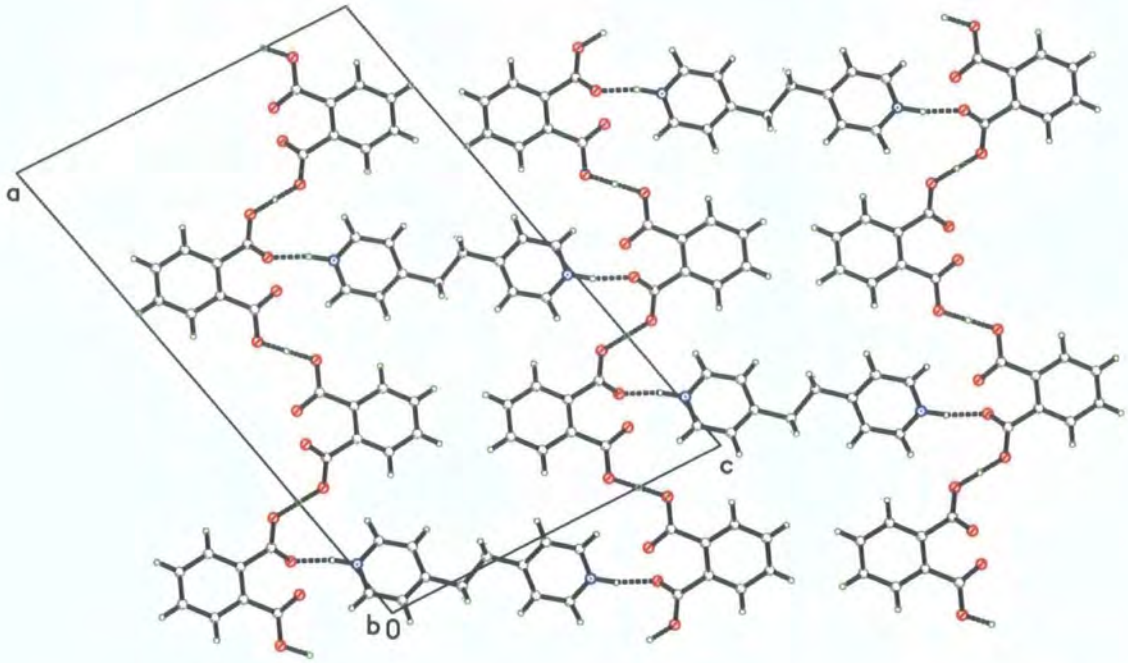


Figure 3.8.5. The PHT- chains are linked together into a planar sheet by the BPA2+ molecules. The hydrogen bonds are indicated by dashed lines.

Table 3.8.4: C-H···O Hydrogen Bond Parameters.

| | D···A (Å) | C···H (Å) | H···A (Å) | D-H-A |
|---|---|---|---|---|
| C31-H31···O12$^{II}$ | 3.2852(16) | 0.977(14) | 2.427(15) | 127.9(9)° |
| C31-H31···O11 | 3.3211(16) | 0.977(14) | 2.598(14) | 131.0(10)° |
| C34-H34···O21 $^{viii}$ | 3.5366(16) | 0.974(13) | 2.576(14) | 168.9(10)° |
| C35-H35···O22$^{III}$ | 3.1601(16) | 0.979(14) | 2.512(14) | 123.6(10)° |
| C36-H36B···O11$^{IX}$ | 3.4094(17) | 0.964(16) | 2.453(17) | 171.8(13)° |

Symmetry Codes : (II) -x, y, 1.5-z, (III) 0.5-x, 0.5-y, 2-z, (VIII) x, -y, 0.5+z (IX) -x, 1-y, 2-z.

CH-π, π-π and C-H···O weak interactions connect the planes together (figures 3.8.6 and 3.8.7). The PHT- molecules form a C-H···π bonded column along the b-axis similar to the one seen in the 2:1 co-crystal of phthalic acid and 4,4'-bipyridine (section 3.6, figure 3.6.5).

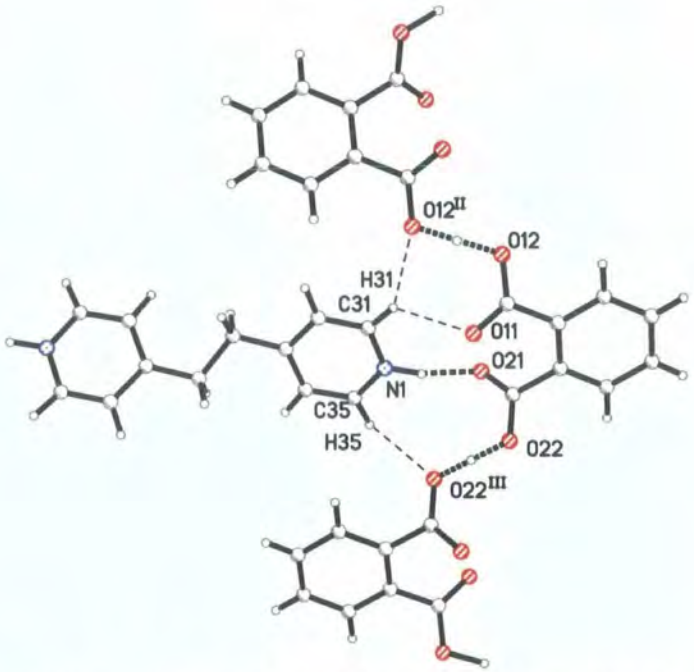


Figure 3.8.6. The BPA2+ molecule is hydrogen bonded into the cleft in the PHT- chain by an N-H···O and C-H···O hydrogen bonds. [Symmetry codes: (II) -x, y, 1.5-z, (III) 0.5-x, 0.5-y, 2-z]

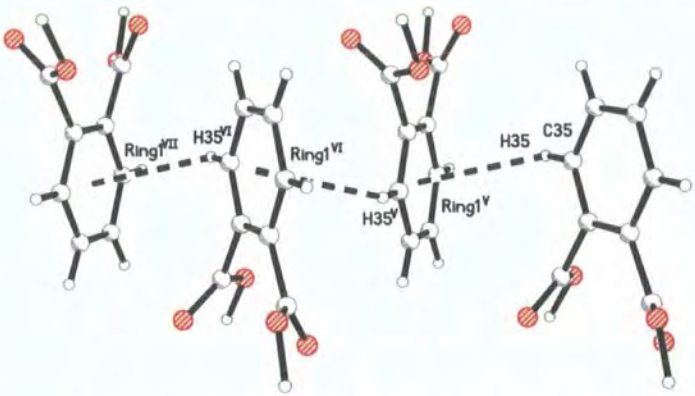


Figure 3.8.7. C-H···π hydrogen bonds forming a weakly linked chain of PHT- molecules along the [0 1 0] direction. [Symmetry codes: (V) 0.5-x, -0.5-y, 1.5-z, (VI) x, -1+y, z, (VII) 0.5-x – 1.5+y, 1.5-z]

Table 3.8.5: C-H···π Hydrogen Bond Parameters.

| | D···Ring centre (Å) | C···H (Å) | H···Ring centre (Å) | D-H-Ring centre (°) |
|---|---|---|---|---|
| C3-H3···Ring1$^{V}$ | 3.6835(15) | 0.984(13) | 2.936(13) | 133.5(9) |
| C6-H6···Ring2$^{XII}$ | 3.4937(15) | 0.973(12) | 2.829(12) | 126.2(9) |
| C35-H35···Ring1$^{VIII}$ | 3.4006(15) | 0.974(13) | 2.779(13) | 122.0(10) |

Symmetry codes: (V) 0.5-x, -0.5+y, 1.5-z, (VIII) x, -y, 0.5+z, (XII) x, 1-y, -0.5+z.

Ring 1 – C1-C2-C3-C4-C5-C6. Ring 2 – N1-C31-C32-C33-C34-C35.

Table 3.8.6. π-π Interactions.

| | Centre-to-centre distance (Å) | Angle between planes | Shortest perpendicular distance (Å) |
|---|---|---|---|
| Ring2···Ring2$^{x}$ | 4.0086(8) | 0.00(6)° | 3.3898(15) |

Symmetry code: (X) –x, -y, 2-z.

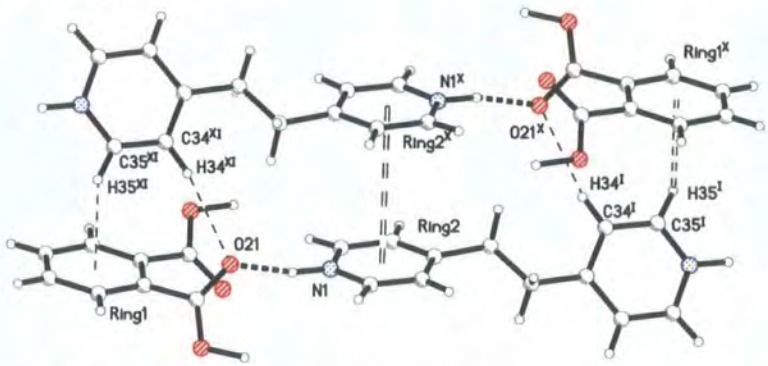


Figure 3.8.8. C-H···π, C-H···O and π···π interactions between the planes of molecules. [Symmetry codes: (I) -x, y, 2.5-z. (X) –x, -y, 2-z. (XI) x, -y, -0.5+z]

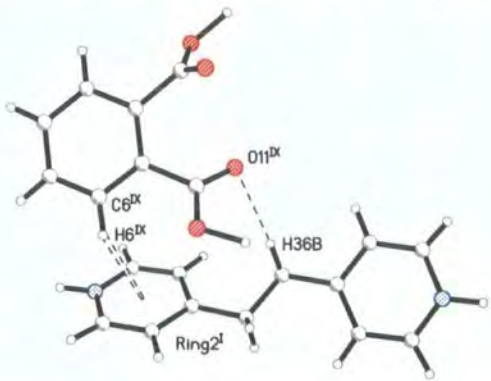


Figure 3.8.9. C-H···O and C-H···π interactions between the planes of PHT- and BPA2+ molecules. [Symmetry codes: (I) -x, y, 2.5-z. (IX) -x, 1-y, 2-z.]

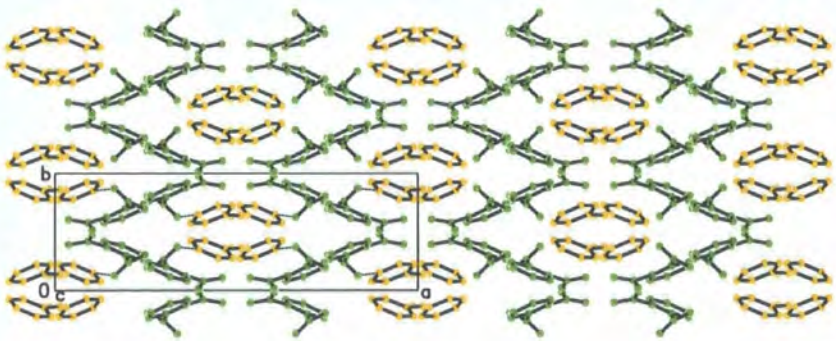


Figure 3.8.10. Packing diagram of PHT- and BPA2+ viewed along the c-axis. The PHT- molecules are green and the BPA2+ molecules are yellow. The hydrogen atoms have been omitted for clarity.

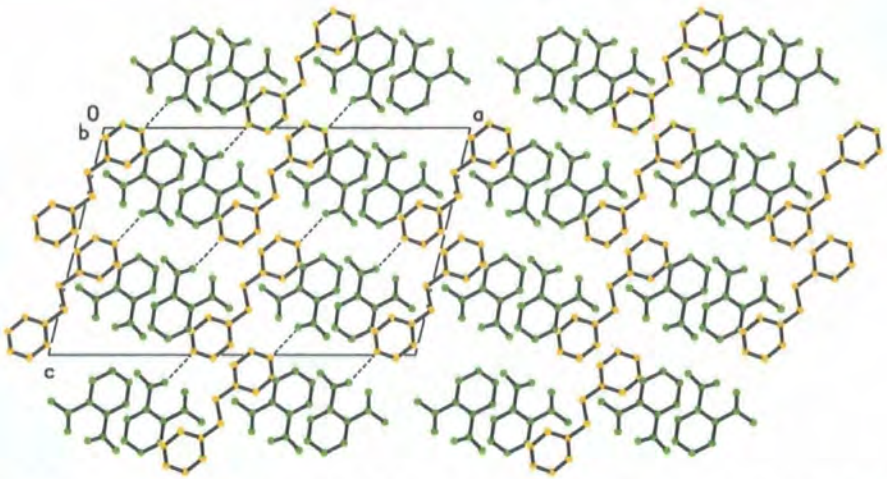


Figure 3.8.11. Packing diagram of PHT- and BPA2+ viewed along the b-axis. The PHT- molecules are green and the BPA2+ molecules are yellow. The hydrogen atoms have been omitted for clarity.

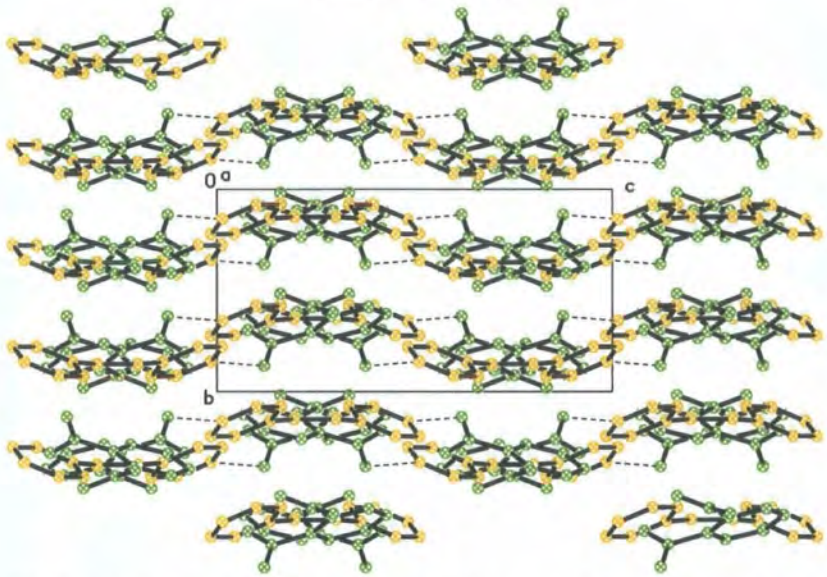


Figure 3.8.12. Packing diagram of PHT- and BPA2+ viewed along the a-axis, parallel to the planes of molecules. The hydrogen atoms have been omitted for clarity.

**Experimental Details**

The data were collected on a Bruker-SMART diffractometer using an Oxford Cryosystems nitrogen flow device to cool the crystal.

Table 3.8.cry. Crystal parameters for PHT- and BPA2+

| | | | |
|---|---|---|---|
| Formula | $2[C_8H_5O_4^-]$ $\cdot[C_{12}H_{14}N_2^{2+}]$ | Formula Weight | 516.49 |
| Crystal System | Monoclinic | Space Group | C2/c |
| a (Å) | 22.968(5) | α | 90° |
| b (Å) | 7.237(2) | β | 103.531(12)° |
| c (Å) | 14.657(3) | γ | 90° |
| Volume $(Å)^3$ | 2368.5(10) | Z | 4 |
| Density (Mg $m^{-3}$) | 1.448 | Colour | Colourless |
| Crystal Shape | Plate | Dimensions (mm) | 0.56*0.24*0.12 |

Table 3.8.data. Data collection details for PHT- and BPA2+.

| | | | |
|---|---|---|---|
| Radiation | Mo Kα | λ (Å) | 0.71073 |
| Temperature (K) | 100(2) | | |
| Reflections | 12857 | Independent reflections | 3125 |
| Reflections I > 2σ(I) | 2484 | | |
| Rint | 0.0536 | Rsigma | 0.0357 |
| h | -27→30 | K | -9→9 |
| l | -19→19 | $\theta_{max}$ | 29° |

Table 3.8.ref. Refinement details for PHT- and BPA2+.

| | | | |
|---|---|---|---|
| $R[F^2 > 2\sigma(F^2)]$ | 0.0392 | $wR^2(F^2)$ | 0.0842 |
| S | 1.749 | Data / Parameters | 3125 / 219 |
| $\Delta\rho_{max}$ (e $Å^{-3}$) | 0.337 | $\Delta\rho_{min}$ (e $Å^{-3}$) | -0.278 |
| $(\Delta/\sigma)_{max}$ | 0.001 | $\Delta\rho_{rms}$ (e $Å^{-3}$) | 0.050 |

Cell parameters were determined from 984 strong reflections θ = 12.75 – 28.72º.
All non-hydrogen atom anisotropic thermal parameters were refined. All the hydrogen atoms were found in the difference Fourier maps and refined with isotropic thermal parameters. The C-H distances (C-H = 0.964(17)Å - 1.001(17)Å ) all refined to within standard ranges and there were no anomalous values of Uiso. As we are interested in the behaviour of the hydrogen atoms with respect to any hydrogen-bonded networks, it would be artificial to add any constraints to this stable and converged refinement.

### 3.9. Comparison of Structures

In the following discussion the structures are referred to by the following convention.

Table 3.9.1: Naming Scheme

| Code | Section | Constituents |
|---|---|---|
| A | A.4 | 1 BPY + 1 PMA |
| B | A.5 | 1 BPY + 2 PMA |
| C | A.6 | 2 BPY + 1 PMA |
| D | A.7 | 1 BPY + 2 PHT |
| E | A.8 | 1 BPY + 1 PHT |
| F | A.9 | 1 BPA + 2 PHT |

#### 3.9.1. Ratio of Functional Groups

The structures can be categorised by the ratio of carboxylic acid groups to pyridyl groups in the asymmetric unit.

Table 3.9.2. Ratio of Functional Groups in the Asymmetric Unit

| Code | Constituents | Carboxylic acid groups | Pyridyl groups | Ratio |
|---|---|---|---|---|
| A | 1 BPY · 1 PMA | 2 | 1 | 2 |
| B | 1 BPY · 2 PMA | 8 | 2 | 4 |
| C | 2 BPY · 1 PMA | 2 | 2 | 1 |
| D | 1 BPY · 2 PHT | 2 | 1 | 2 |
| E | 1 BPY · 1 PHT | 1 | 1 | 1 |
| F | 1 BPA · 2 PHT | 2 | 1 | 2 |

#### 3.9.2. Similarities between A, D and F

Structures A, D and F have the same ratio of carboxylic acid groups to pyridyl groups in the asymmetric unit. It would be expected that D and F should be very closely related as the only difference between the constituent molecules is the ethane group between the two pyridyl groups.

In all the structures the protonation states are identical. The pyridyl groups have all been protonated and half of the acid groups, one in PHT and two in PMA have become deprotonated.

The strongest intermolecular interactions in A and D are almost identical (table 3.9.3.a and 3.9.3.b). A short intramolecular hydrogen bond is formed between the adjacent acid groups and an intermolecular N-H···O hydrogen bond is formed, complemented by a C-H···O hydrogen bond (diagram 3.9.1). In A the symmetry of the acid molecule means that an infinite one-dimensional chain is formed from the motif, while in D only a trimer is formed (figures 3.9.1.a and 3.9.1.b).

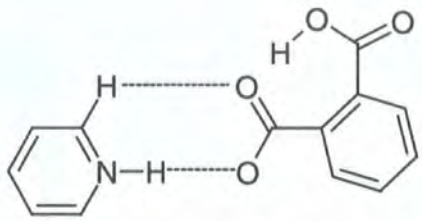


Diagram 3.9.1. The packing motif in A and D.

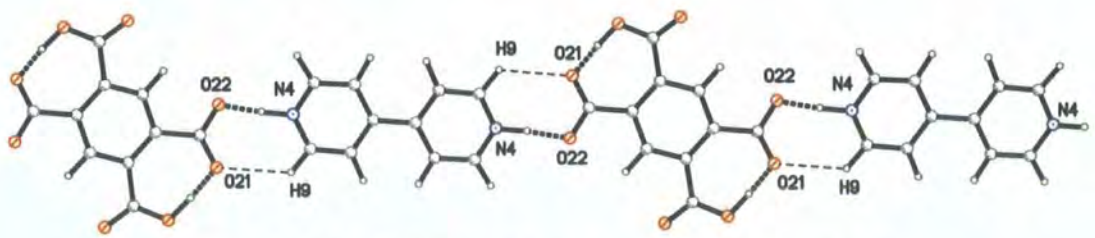


Figure 3.9.1.a. The major intermolecular packing motif in A.

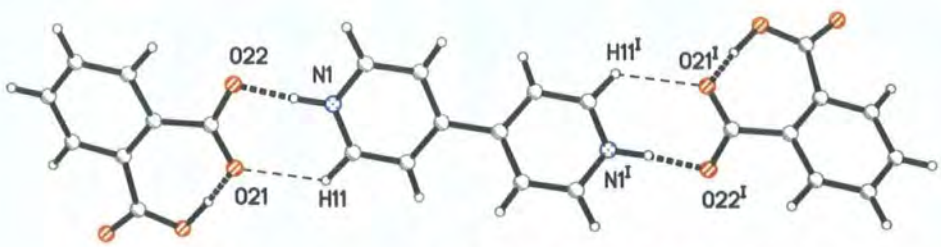


Figure 3.9.1.b. The major intermolecular packing motif in D.

Table 3.9.3.a. Selected Hydrogen Bond Parameters in A.

| | D···A (Å) | D-H(Å) | H···A (Å) | D-H-A |
|---|---|---|---|---|
| N4-H4···O22 | 2.605(2) | 1.097(3) | 1.511(3) | 174.7(3)º |
| O11-H11···O21 | 2.421(3) | 1.053(4) | 1.370(4) | 175.0(4)º |

Table 3.9.3.b. Selected Hydrogen Bond Parameters in D.

| | D···A (Å) | D-H(Å) | H···A (Å) | D-H-A |
|---|---|---|---|---|
| N1-H1···O22 | 2.6273(16) | 1.03(2) | 1.60(2) | 175(2)º |
| O11-H11···O21 | 2.4141(15) | 1.10(2) | 1.32(2) | 171(2)º |

The structure F has very different intermolecular interactions. The deprotonated acid molecules are linked into a negatively charged one-dimensional chain by intermolecular O-H···O hydrogen bonds. The BTA molecules link the supramolecular chains together with N-H···O hydrogen bonds into a two-dimensional sheet. In D and F the PHT- molecules form very similar C-H···π bonded chains parallel to the b-axis (figures 3.6.5 and 3.8.7).

Although the intermolecular interactions are different in D and F the packing diagrams are strikingly similar (figures 3.9.2.abcdef). D and F both crystallise in space group C2/c. Viewed parallel to the a-axis both structures appear to be made up of corrugated planes (figures 3.9.2.a and 3.9.2.b). Viewed parallel to the b-axis there are acid (green or red) and base (blue or yellow) stripes parallel to the c-direction (figures 3.9.2.c and 3.9.2.d). Viewed parallel to the c-axis (figures 3.9.2.e and 3.9.2.f) the PHT- chains can be seen parallel to the b-axis and the similar arrangement of the pyridyl groups surrounded by the acid groups. The packing in A is dominated by π-π stacking interactions and does not seem to be related to D or F.

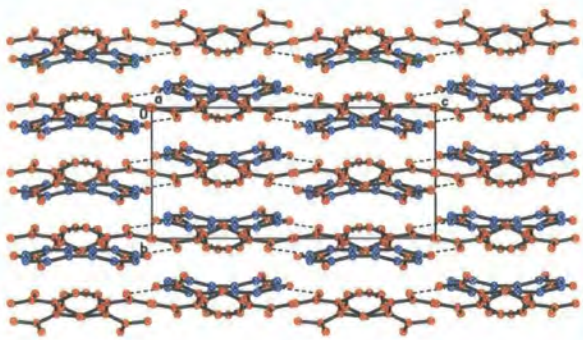

2.a.

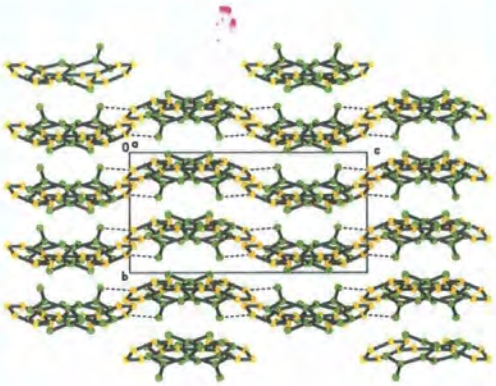

2.b.

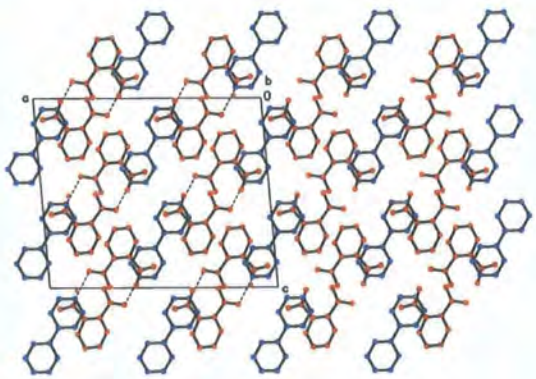

2.c.

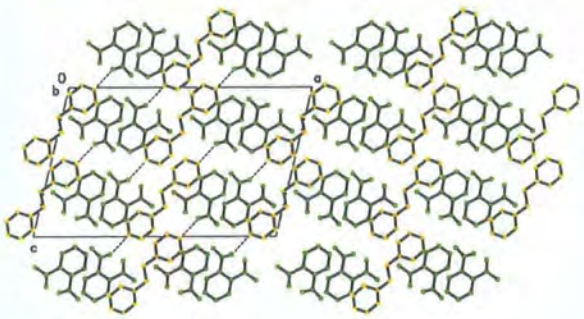

2.d.

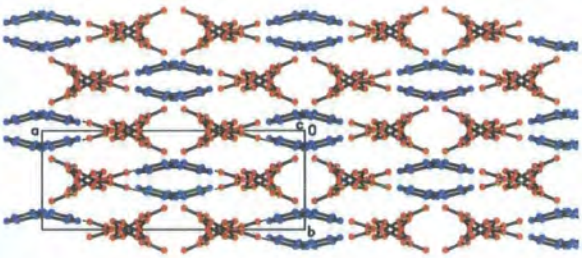

2.e

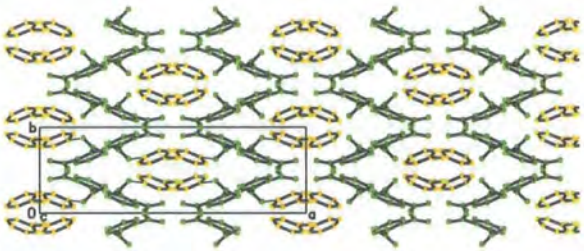

2.f.

Figures 3.9.2.abcdef. Packing diagrams from D and F. 2.a and 2.b are viewed down the a-axis. 2.c and 2.d are viewed down the b-axis. 2.e and 2.f are viewed down the c-axis. The BPY molecules are coloured blue in D and the BPA molecules are coloured yellow in F. The PTH molecules are coloured green in F and red in D.

### 3.9.3. Similarities between C and E

Structures C and E have the same ratio of carboxylic acid groups to pyridyl groups in the asymmetric unit. The strong hydrogen bonding is similar. In both structures every carboxylic acid group is involved in a strong hydrogen bond to a pyridyl group. In both structures infinite chains are formed that are held together by weak C-H···O, C-H···π and in C π···π interactions into planes (figures 3.9.3.a and 3.9.3.b).

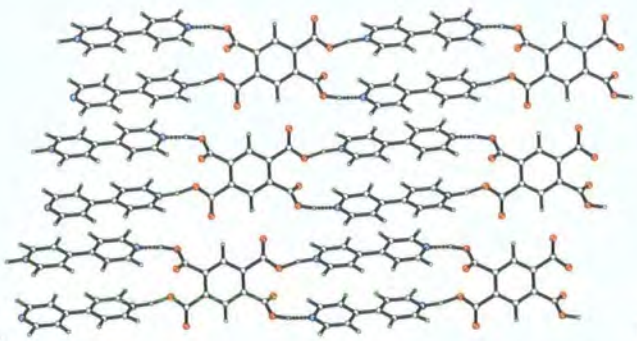

3.a.

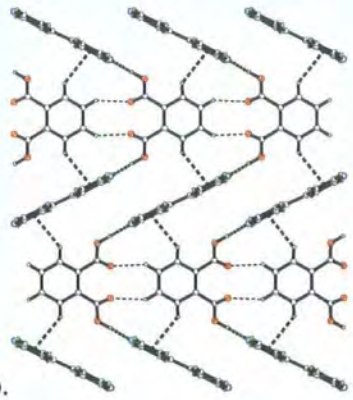

3.b.

Figures 3.9.3.a and 3.9.3.b. The chains in C and E pack into planes.

The planes explain the differences in the packing quite well. The one-dimensional chains formed in A are replaced by a trimer in D with an identical packing motif when PHT was swapped for PMA. Two molecules of PHT and two molecules of BPY could form a 'tetramer' in E with the same packing motif as in C but do not. Instead the π-π stacking interactions in C are replaced by C-H···π interactions in E as this can better utilise the extra C-H bonds of the PHT molecules.

The packing diagrams look the same viewed parallel to the molecular planes formed by the chains. The planes pack together through similar C-H···π and C-H···O hydrogen bonds.

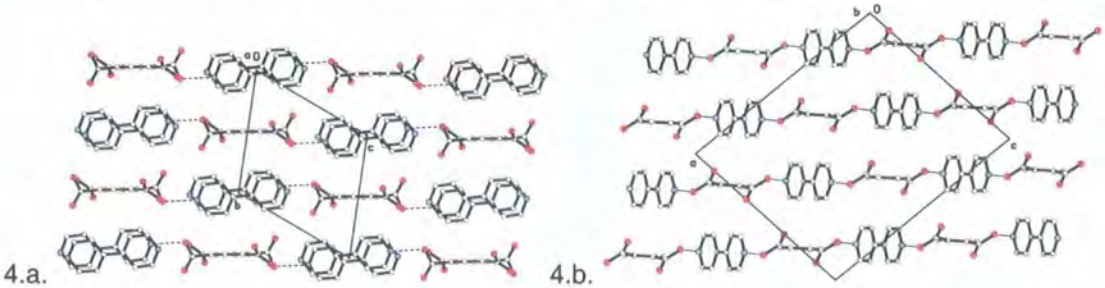

4.a. 4.b.

Figures 3.9.4.a and 3.9.4.b. Similar packing diagrams in C and E. 3.9.4.a views the plane in diagram 3.9.3.a from top to bottom. 3.9.4.b views the plane in diagram 3.9.3.b from left to right.

### 3.9.4. Similarities Between B, D and F

Structures B, D and F do not have the same ratio of carboxylic acid groups to pyridyl groups in the asymmetric unit but do have the same ratio of acid molecules to base molecules. The intermolecular interactions and the descriptions of the packing in B and F are very similar. The acid molecules have become deprotonated once and link together through O-H···O hydrogen bonds to form negatively charged supramolecular frameworks, one-dimensional chains in F and two-dimensional meshes in B. The N-H···O hydrogen bonds to the bis-pyridinium molecules link the frameworks together in two-dimensions in F and three-dimensions in B. The intermolecular interactions in D are not closely related to B or F.

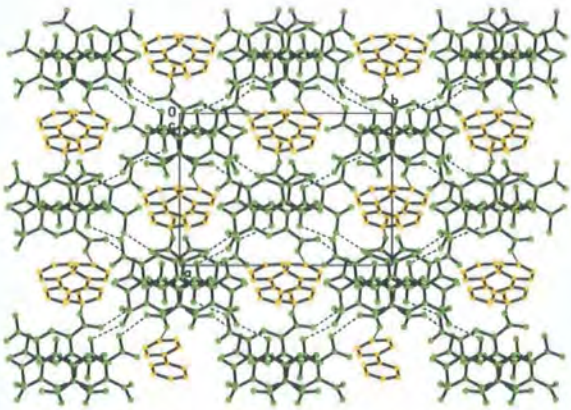

Figure 3.9.5. The packing diagram of B viewed along the c-direction shows similarities with D and F (figures 3.9.2.e and 3.9.2.f). Acid molecules surround tunnels containing BPY2+ molecules.

### 3.9.5. Similarities between A, C and E

Structures A, C and E can all be described as chains linked through N-H···O / O-H···N hydrogen bonds (figures 3.9.6.a, 3.9.6.b and 3.9.6.c) that are linked together in three-dimensions by weak C-H···O, C-H···π and π···π interactions. The chains in A are made up of almost coplanar BPY and PMA molecules, while the in C and E the phenyl ring of the acid molecules are almost perpendicular to the planes of the BPY molecules.

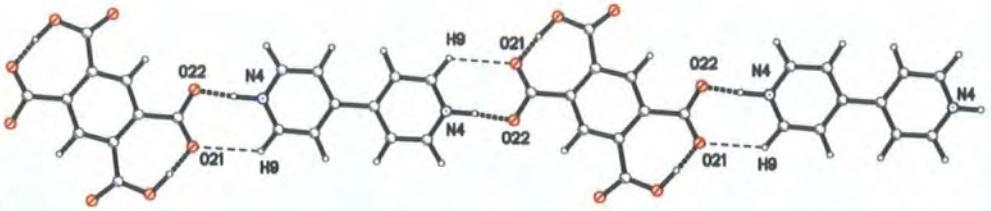


6.a.

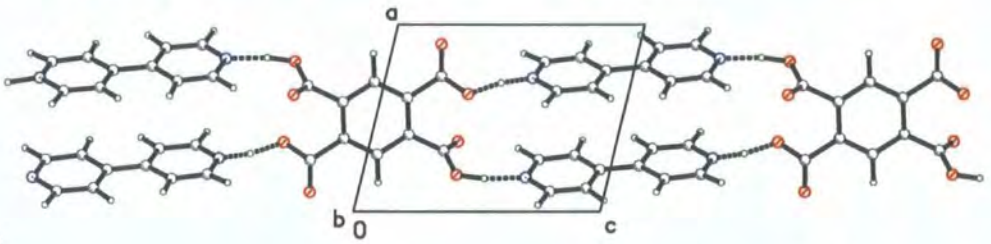


6.b.

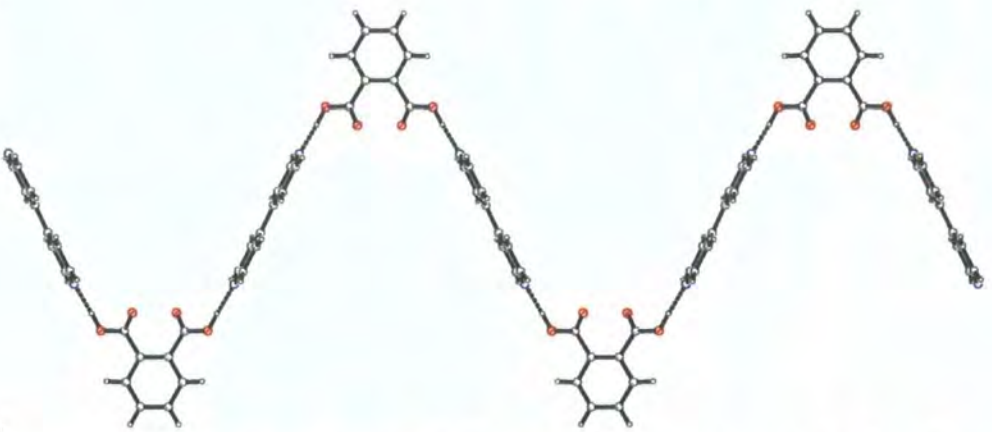

6.c.

Figures 3.9.5.a, A.9.5.b and 3.9.5.c. The hydrogen bonded chains in A, C and E respectively.

### 3.9.6. Structures Containing the Acid Molecules

There are 28 structures in the Cambridge Structural Database (Allen and Kennard, 1993) containing the benzene-1,2,4,5-tetracarboxylic acid molecule (PMA) in some form. Fourteen contain metals and fourteen are purely organic structures. Eight of the organic structures are described in a paper dedicated to PMA salts (Biradha and Zaworotko, 1998).

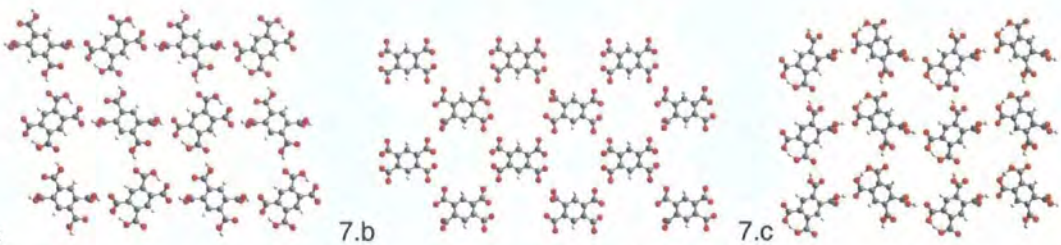

7.a 7.b 7.c

Figures 3.9.7.a, 3.9.7.b and 3.9.7.c. Two-dimensional networks formed from PMA molecules.

In the co-crystals of PMA with 2,2'-bipyridine (figure 3.9.7a, Mrvoš-Sermek et al. 1996), PMA and tetra-n-butylammonium (figure A.9.7.b, Jessen et al. 1992) and PMA and 3-methylpyridine (figure 3.9.7.c, Biradha and Zaworotko, 1998) similar two-dimensional meshes are formed to those in B. Each of the meshes are different, the meshes in B look most like those in figure 3.9.7.b with all the PMA molecules oriented in the same way, but the hydrogen bond network most resembles that in figure 3.9.7.c, with two intermolecular and one intramolecular hydrogen bond per molecule. Biradha and Zaworotko (1998) call the mesh structure of PMA and 3-methylpyridine a supramolecular rotaxane as the 3-methylpyridine molecules sit in the gaps in the mesh, this description also fits B, where the 4,4-bipyridine molecules thread through the gaps in the meshes (figure 3.9.8).

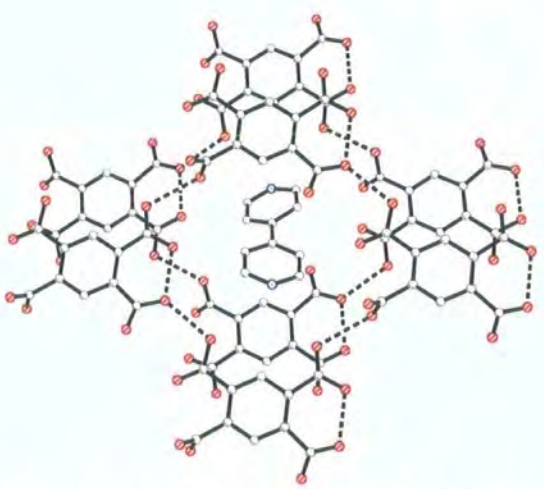

Figure 3.9.8. The supramolecular rotaxane in B. The 4,4'-bipyridine molecules thread through the mesh of PMA molecules. Hydrogen bonds are indicated by dashed lines.

Of the 14 organic PMA structures seven contain two intramolecular hydrogen bonds two contain one intramolecular bond and six contain no intramolecular bonds at all. This adds up to 15 because there are two independent molecules of PMA in the co-crystals of PMA with 2,2'-bipyridine (Mrvoš-Sermek et al. 1996), one of the molecules contains two intramolecular hydrogen bonds and the other molecule contains none.

There are 78 structures in the CSD containing phthalic acid molecules (PHT), 18 of which are purely organic, five of these contain intramolecular hydrogen bonds. In the crystal structure of PHT infinite one-dimensional chains are formed with the PHT molecules linked with classic carboxylic acid – carboxylic acid dimers (Ermer, 1981), surprisingly this is the only occurrence of these dimers in the organic structures of PHT or PMA.

In the crystal structures of ammonium hydrogen phthalate, diammonium phthalate (Smith, 1975 and 1975a), tetramethylammonium hydrogen phthalate (Jessen, 1990) and dicholine phthalate (figure A39.9, Frydenvang et al. 1994) a similar C-H···π bonded chain is observed as in D and F.

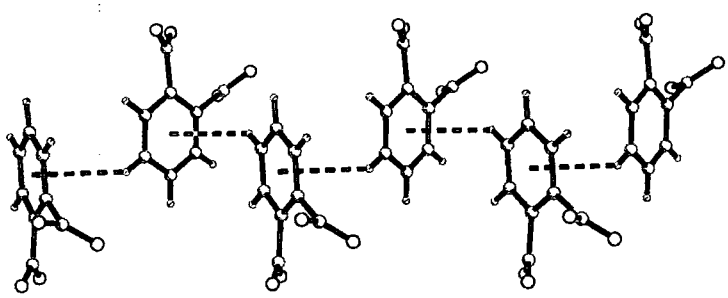

Figure 3.9.9. The C-H···π hydrogen bonded chain of PHT molecules in the structure of dicholine phthalate.

When an intramolecular hydrogen bond is formed between PHT or PMA a seven membered ring is formed which can participate in a π···pseudo-π interaction as observed in B. The most obvious example of π···pseudo-π interactions is in the crystal structure of diphthalimidodiethylamine phthalic acid hydrate (figure 3.9.10, Barrett et al. 1998). The motif also occurs in co-crystals of PMA and pyridine, PMA and 4-methylpyridine (Biradha and Zaworotko, 1998), phenylethylammonium hydrogen phthalate (Kozma et al. 1994) and bis(p-dimethylaminophenyl)phenylcarbenium hydrogen phthalate phthalic acid (Mitchell et al. 1996). This interaction could also be interpreted in some cases as a π-π interaction with a large offset between the rings. The description of π-π interactions as electrostatic interactions (Hunter et al. 2001) could include these π···pseudo-π interactions, where the attraction is between the σ-electron system of the phenyl ring and the charges in the polar C-O bonds in the hydrogen bonded ring.

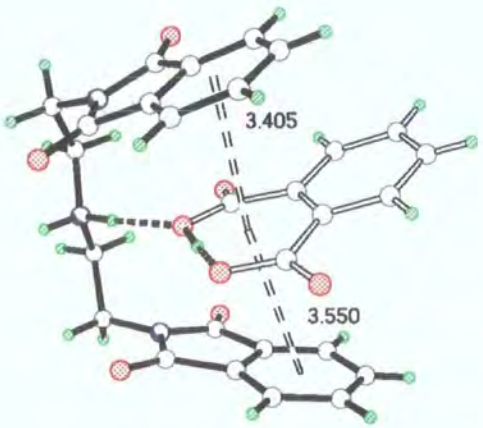


Figure 3.9.10. π···pseudo-π interactions in Diphthalimidodiethylamine phthalic acid hydrate (Barrett et al. 1998). The distances between the centroids of the rings are marked in angstroms. The π···pseudo-π interactions are indicated by the hollow dashed lines and the heavy dashed lines indicate strong hydrogen bonds.

Pseudo-π···pseudo-π interactions are also seen but are better described as electrostatic interactions between positively charged carbon atoms and the negatively charged oxygen atoms in the carboxylate groups (figure 3.9.11). These interactions occur in PMA and 4-methylpyridine, PMA and 2-ethylpyridine (Biradha and Zaworotko, 1998) and PMA and hexamethylenetetramine (Glidewell et al. 2000).

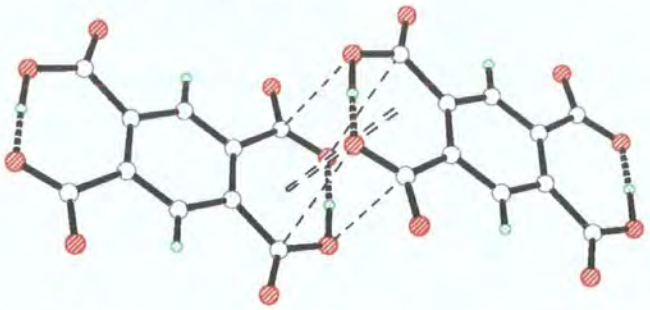

Figure 3.9.11. Pseudo-π···pseudo-π interaction in the co-crystal of PMA and 4-methylpyridine (Biradha and Zaworotko, 1998). Indicated by the hollow dashed line between the ring centres. The thin dashed lines indicate interactions between the slightly positively charged carbon atoms and the slightly negatively charged oxygen atoms in the carboxylate groups.

### 3.9.7. Structures Containing 4,4-Bipyridine Molecules

4,4-Bipyridine (BPY) is a rather rigid weak bidentate base that often occurs in crystal engineering studies because of its bridging abilities. Of the 103 BPY molecules in CSD 42 are organics the rest contain metals. There are 25 structures containing bis-1,2-(4-pyridinium)ethane, five of which are organics.

In the structures of co-crystals of BPY and molecules containing carboxylic acid groups the packing is often very similar to the packing observed in the structures in this chapter. For example the packing in 4,4-bipyridinium squarate (Reetz et al. 1994, figure 3.9.12.a) and the co-crystal of fumaric acid and BPY (Chatterjee et al. 1998, figure 3.9.12.b) is very similar to the packing in A; O-H···N / N-H···O hydrogen bonded chains held together in three dimensions by C-H···O and $\pi\cdots\pi$ interactions.

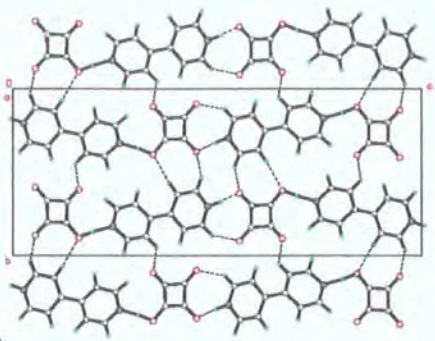

12.a.

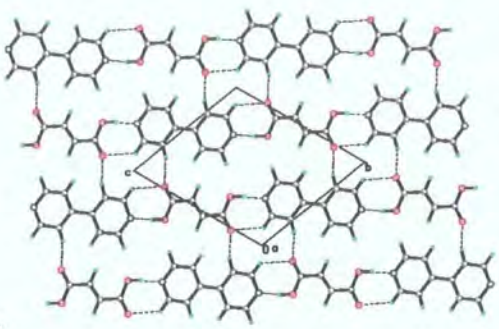

12.b.

Figures 3.9.12.a and 3.9.12.b. Packing diagrams viewed parallel to the a-axis of (a) 4,4-bipyridinium squarate and (b) fumeric acid and BPY.

The intermolecular packing motifs in C and E are also observed in other structures, which also form infinite hydrogen-bonded chains held together by weak interactions. In thiodipropionic acid, which has two carboxylic acid groups arranged at a similar angle to PHT, and BPY (Pedireddi et al. 1998) zig-zag chains similar to those observed in E are formed which pack together in three-dimensions in a similar way (figure 3.9.13.a). In tris(BPY) bis(1,3,5-trihydroxybenzene) (Coupar et al. 1996) similar packing is observed to C, again one-dimensional chains pack together through weak C-H···O and $\pi\cdots\pi$ interactions (figure A3.9.13.b).

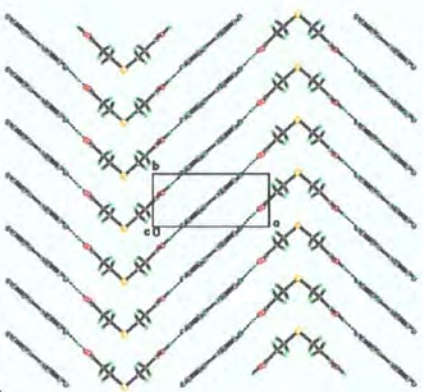

13.a.

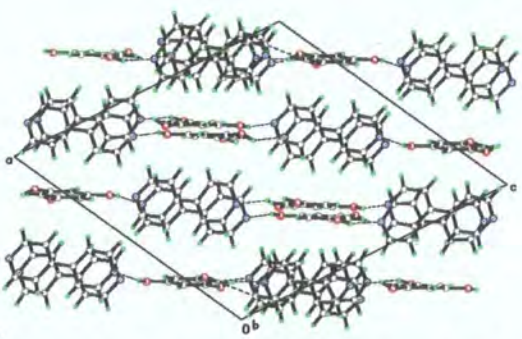

13.b.

Figures 3.9.13.a and 3.9.13.b. Packing diagrams of (a) co-crystals of thiodipropionic acid and BPY and (b) tris(BPY) bis(1,3,5-trihydroxybenzene).

In co-crystals of BPY and thiodiglycolic acid (Pedireddi et al. 1998) two BPY molecules and two thiodiglycolic acid molecules form a hydrogen bonded ring with hydrogen bonds that have similar parameters to those in C (figure 3.9.14). One hydrogen bond is O-H···N and one hydrogen bond has the hydrogen atom placed in the centre of the bond (table 3.9.4), although these are X-ray determined parameters and unreliable with respect to the hydrogen atom position.

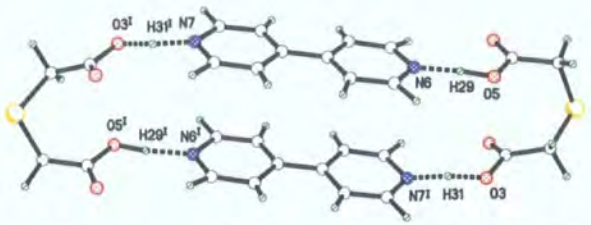


Figure 3.9.14. The hydrogen bonded ring in co-crystals of BPY and thiodiglycolic acid.

Table 3.9.4. X-ray determined hydrogen bond parameters in co-crystals of BPY and thiodiglycolic acid.

| | D···A distance (Å) | D-H distance (Å) | H-A distance (Å) | D-H-A angle (°) |
|---|---|---|---|---|
| O3··H31··N7 | 1.28(5) | 1.37(4) | 2.615(5) | 164(5) |
| O5-H29···N6 | 1.10(6) | 1.56(5) | 2.632(5) | 162(4) |

The structure of the co-crystal of bis(maleic acid) and BPY (Chatterjee et al. 1998) is very similar to D (figures 3.9.15.a and 3.9.15.b). Maleic acid replaces phthalic acid in the trimer in D (figure 3.9.16) although no C-H···O hydrogen bonds are formed.

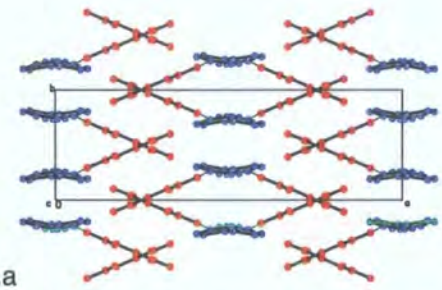

15.a

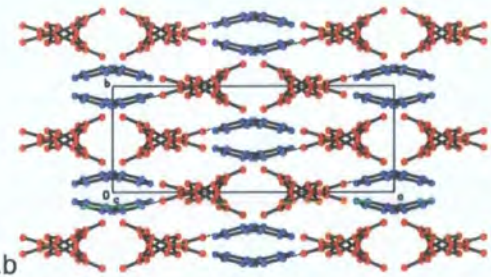

15.b

Figures 3.9.15.a and 3.9.15.b. Packing diagrams of (a) the co-crystal of bis(maleic acid) and BPY and (b) D viewed along the c-axis. The acid molecules are coloured blue and the BPY molecules are coloured red.

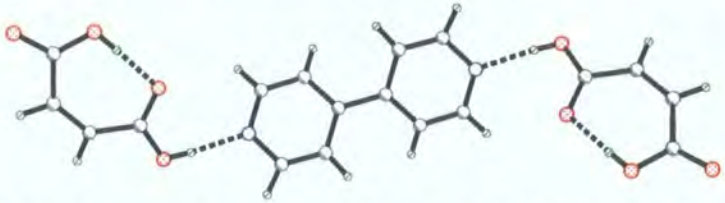

Figure 3.9.16. The molecular trimer in the co-crystal of bis(maleic acid) and BPY. The dashed lines indicate hydrogen bonds.

### 3.10. Comparison of Strong Hydrogen Bonds

One of the main aims of this study was to obtain neutron diffraction data on short N-H···O / O-H···N hydrogen bonds. All the N···O hydrogen bonds observed are between pyridyl or pyridinium groups and carboxylate groups or carboxylic acid groups, yet there are a wide range of hydrogen-bond parameters (table 3.10.1). At the same time we have observed a wide variety of O-H···O hydrogen bonds (table 3.10.2).

Table 3.10.1. Nitrogen-to-oxygen hydrogen-bond parameters

| Structure | N···O (Å) | N-H (Å) | H-O (Å) | N-H-O (°) |
|---|---|---|---|---|
| A | 2.605(2) | 1.097(3) | 1.511(3) | 174.7(3) |
| B | 2.674(2) | 1.048(4) | 1.636(4) | 169.8(4) |
| B | 2.638(2) | 1.050(4) | 1.664(4) | 152.0(3) |
| C | 2.5220(17) | 1.207(3) | 1.325(3) | 169.7(3) |
| C | 2.6104(17) | 1.551(3) | 1.068(3) | 170.2(3) |
| D* | 2.6273(16) | 1.03(2) | 1.60(2) | 175(2) |
| E* | 2.6299(13) | 1.67(2) | 0.97(2) | 169(2) |
| F* | 2.6550(14) | 1.018(16) | 1.651(17) | 167.7(14) |

* X-ray derived parameters.

Table 3.10.2. Oxygen-to-oxygen hydrogen-bond parameters.

| Structure | O···O (Å) | O-H (Å) | H-O (Å) | O-H-O (°) |
|---|---|---|---|---|
| A (I) | 2.421(3) | 1.053(4) | 1.370(4) | 175.0(4) |
| B (I) | 2.404(3) | 1.078(5) | 1.331(5) | 172.6(4) |
| B (I) | 2.419(3) | 1.076(5) | 1.347(5) | 173.2(4) |
| B | 2.613(3) | 1.011(5) | 1.612(5) | 169.8(4) |
| B | 2.717(3) | 1.002(5) | 1.718(4) | 174.4(4) |
| B | 2.630(3) | 1.009(4) | 1.636(4) | 167.2(4) |
| B | 2.739(3) | 1.002(5) | 1.741(5) | 173.2(4) |
| D (I) * | 2.4141(15) | 1.10(2) | 1.32(2) | 171(2) |
| F * | 2.4564(17) | 1.236(4) | 1.236(4) | 167(3) |
| F * | 2.4568(17) | 1.2284(8) | 1.2284(8) | 180 |

* X-ray derived parameters.

(I) Indicates an intramolecular hydrogen bond.

Every pyridyl group in the structures accepts an N···O hydrogen bond. The total number of strong hydrogen bonds in each structure is equal to the number carboxylic acid groups, which is the number of hydrogen atoms that could be expected to form strong hydrogen bonds. The number of O···O hydrogen bonds is the number of carboxylic acid groups minus the number of pyridyl groups. This follows the rule suggested by Bertolasi et al. (2001) that "All hydrogen-bond acceptors available in a molecule will be engaged in hydrogen bonding as far as there are available donors". All the pyridyl groups are acceptors and the carboxylic acid groups can act as both donors and acceptors.

Table 3.10.3. Number of hydrogen bonds, donors and acceptors.

| | Carboxylic acid groups in the A.U. | Pyridyls in the A.U. | N···O | O···O | Total Strong Hydrogen Bonds |
|---|---|---|---|---|---|
| A | 2 | 1 | 1 | 1 | 2 |
| B | 8 | 2 | 2 | 6 | 8 |
| C | 2 | 2 | 2 | 0 | 2 |
| D | 2 | 1 | 1 | 1 | 2 |
| E | 1 | 1 | 1 | 0 | 1 |
| F | 2 | 1 | 1 | 2* | 2* |

* The O···O hydrogen bonds in F are counted as halves as they lie across symmetry centres.

The strength of the hydrogen bonds must be very sensitive to the intermolecular environment. The two N···O hydrogen bonds in C are chemically very similar yet one is ~0.1A shorter than the other. The O-H···N hydrogen bonds and the N··H··O hydrogen bond occur in structures C and E where the ratio of carboxylic acid groups to pyridyl groups is 1. The longest N-H···O hydrogen bonds occur in B and F, which are the only structures to contain intermolecular O-H···O hydrogen bonds.

From the observed structures it seems that pyridyl and carboxylic acid groups prefer to form O-H···N hydrogen bonds between them in the absence of strong external influences, as is the situation in C and E. In the other structures the carboxylate or carboxylic acid groups that are part of the hydrogen bonds are also involved in another strong intermolecular hydrogen-bond as in F or intramolecular hydrogen-bond as in A and D, or both as in B.

### 3.10.1. Pyridyl···Carboxylic acid Synthons

The concept of synthons was introduced by Desiraju (1995) to describe and categorise supramolecular interactions. All the crystals herein contain an N-H···O or O-H···N hydrogen bond between a carboxylic acid and a pyridyl group. In three of the structures this is complemented by a C-H···O hydrogen bond, from the pyridyl to the other oxygen atom in the carboxylic acid, in parallel with the strong hydrogen bond. This motif occurs in structures A, C and D but not in B, E and F.

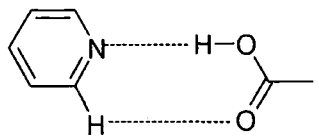


1.a.

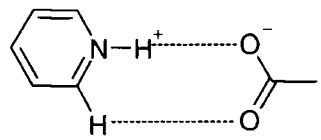


1.b.

Diagrams 3.10.1.a and 3.10.1.b. Strong N-H···O / O-H···N hydrogen bonding with a weak C-H···O hydrogen bond in parallel.

The CSD was searched to find the frequency of the motif. The number of structures that contain both groups was counted. The number of structures that contain both groups and contain a strong hydrogen-bond with a hydrogen···acceptor distance between 0.7-2.5Å were counted, and the number of structures that contained the same strong hydrogen bond and had an hydrogen···oxygen distance between 1.5-3.0Å in the C-H···O hydrogen bond were counted. Steiner (1997) suggests a cut off of around 2.8Å for the H···O distance in a C-H···O hydrogen bond.

Table 3.10.4. Occurrences of pyridyl-carboxylic acid motifs in the CSD.

| | Pyridinium-N-H···O-carboxylate | Carboxylic-O-H···N-pyridyl |
|---|---|---|
| Both constituents in the structure | 76 | 83 |
| Strong hydrogen bond | 64 | 61 |
| Strong hydrogen bond and the weak hydrogen bond | 27 | 42 |

The motif seems to be more likely to occur with a neutral hydrogen bond rather than with a charge-assisted hydrogen bond.

### 3.11. Intramolecular O-H···O Hydrogen Bonds

In the structures discussed in this section there are four short intramolecular O-H···O hydrogen bonds formed between a carboxylic acid group and an adjacent carboxylate group attached to a phenyl ring. The three that have been studied by neutron diffraction are amongst the shortest studied using this technique (graph 3.11.1). The O-H distances derived from the neutron diffraction data increase as the O···O distance decreases. The proton positions in the bonds from this chapter are quite asymmetrically placed compared with other similar hydrogen bonds. There is no evidence of disorder of the protons in the intramolecular hydrogen bonds as the anisotropic displacement parameters are not significantly elongated along the hydrogen bond direction.

Table 3.11.1. Intramolecular Hydrogen bond parameters.

| Structure | O···O distance (Å) | O-H distance (Å) | H···O distance (Å) | O-H-O angle (°) |
|---|---|---|---|---|
| A – neutron | 2.421(3) | 1.053(3) | 1.370(4) | 175.0(4) |
| B – neutron | 2.404(3) | 1.078(5) | 1.331(5) | 172.6(4) |
| B* - neutron | 2.419(3) | 1.076(5) | 1.347(5) | 173.2(4) |
| D - X-ray | 2.4141(15) | 1.10(2) | 1.32(2) | 171(2) |

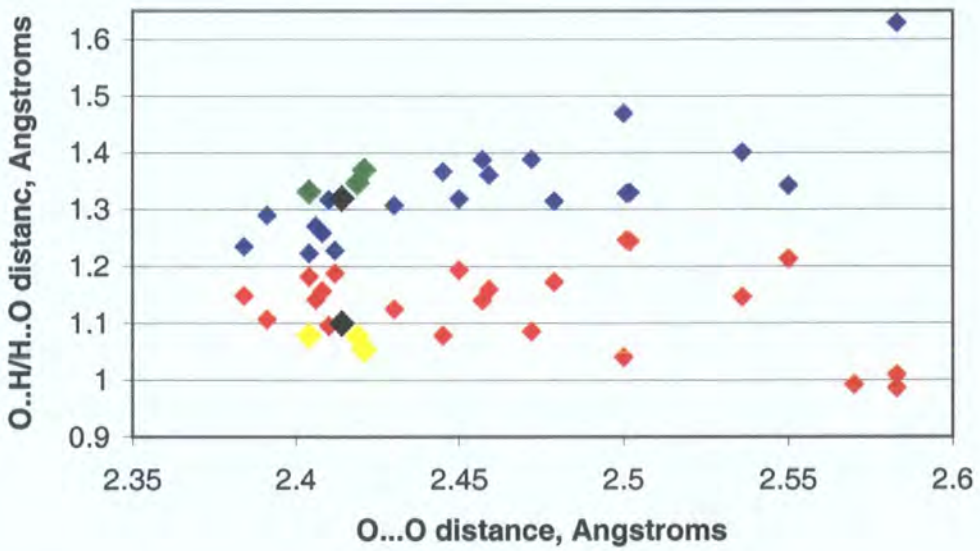


Graph 3.11.1. Short intramolecular hydrogen bonds studied by neutron diffraction. The red and yellow points indicate the O-H distance and the green and blue points indicate the H··O distance. The red and blue points are taken from the CSD the yellow and green points are taken from this chapter. The black points are X-ray results from this chapter.

In similar short intramolecular hydrogen bonds studied by neutron diffraction the hydrogen atom is rarely found to be equidistant from the oxygen atoms (Wilson, 2000). In the crystal structure of pyridine-2,3-dicarboxylic acid a short asymmetric intramolecular hydrogen bond

is formed and the asymmetry is ascribed to the nitrogen atom in the pyridyl ring (Kvick et al. 1974, Takusagawa and Koetzle, 1979). Similar short intramolecular hydrogen bonds between carboxylic acid and carboxylate groups have been studied in detail by neutron diffraction and ab-initio calculations in maleate ions (Olovsson and Olovsson, 1984, Vanhouteghem et al., 1987) and the asymmetry in the hydrogen atom position ascribed to intermolecular effects. In imidazolium hydrogen maleate (Sakhawat Hussain et al. 1980) the hydrogen atom is found to be centred, but on deuteration the deuterium atom is found to be asymmetrically placed. In the structure of lithium hydrogen phthalate (Küppers et al., 1985) there are two phthalate ions with intramolecular hydrogen bonds, in one of which the hydrogen atom is in the centre of the bond and in the other is asymmetrically placed.

Density-functional theory quantum-mechanical calculations have been performed on the phthalate anion using the program DMol$^3$ (Delley, 2000). The lowest-energy structure has been calculated beginning from an approximate structure containing an intramolecular hydrogen bond. From this structure the hydrogen-bond potential energy well has been calculated along a line connecting the oxygen atoms while keeping the rest of the structure fixed. The calculated potential well is symmetrical and the proton was calculated to lie in the centre of the hydrogen bond.

The lowest energy structure was also calculated for the phthalate anion with a pyridinium ion arranged to form an N-H···O and a C-H···O hydrogen bond in approximately the same geometry as seen in structures B and D. The hydrogen-bond potential well became significantly asymmetric and the proton position was found, by solving the one-dimensional Schrödinger equation, to be 1.075Å from one of the oxygen atoms. The calculated geometries for the phthalate anion are shown in figure 3.11.1.a and figure 3.11.1.b and the calculated hydrogen-bond potential energy wells are illustrated in graph 3.11.3.

The stretching frequencies of the O-H bond can also be calculated from the shape of the potential well and should change from around ~1850 $cm^{-1}$ in the broad symmetric well to ~2300 $cm^{-1}$ in the asymmetric well.

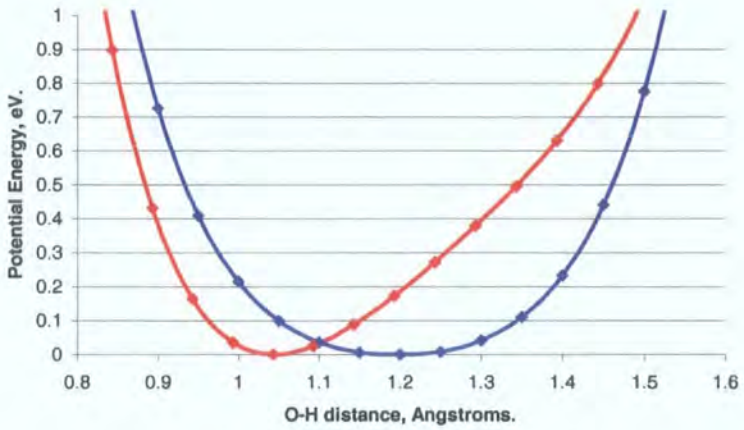


Graph 3.11.3. The hydrogen bond potential energy wells calculated using DMol[3]. The blue line indicates the well calculated from the lone phthalate anion. The red line indicates the potential energy well altered by an intermolecular hydrogen bond.

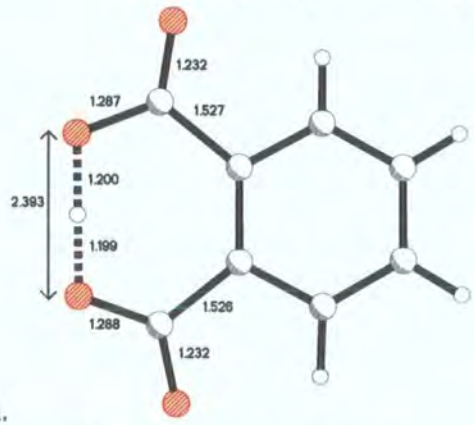


1.a.

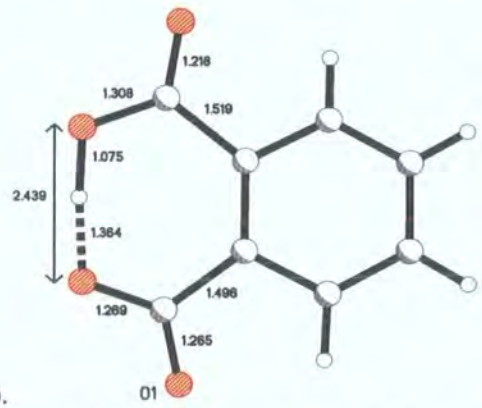


1.b.

Figures 3.11.1.a and 3.11.1.b. The calculated geometries for phthalate anion with the bond lengths in Å. 3A illustrates the free molecule. 3B illustrates the molecule that accepts an intermolecular hydrogen bond at O1.

The calculated hydrogen-bond potential well is found in the calculations to be a single-minimum potential well in both situations. The results of the calculations are not strictly applicable to molecules confined in crystals, but the quantitative agreement between the calculated and observed bond lengths, although not perfect, is good. These calculations take no account of any other intermolecular interactions such as the hydrogen bonds from the disordered water molecules in A.

The asymmetry in the intramolecular hydrogen bond is clearly caused by the intermolecular interactions in structures A, B and D. The intermolecular interactions in A and D are well modelled by the simple calculation. The situation in B is complicated by extra intermolecular O-H···O hydrogen bonding but is qualitatively similar.

### 3.12. BIPYRIDINE TWIST ANGLES

Five out of the six structures contain 4,4'-bipyridine. The torsion angle, ABCD (diagram 3.12.1), which should be very similar to the dihedral angle between the planes of the pyridyl rings, has been measured in the structures and in the Cambridge Structural Database (CSD, Allen and Kennard, 1993).

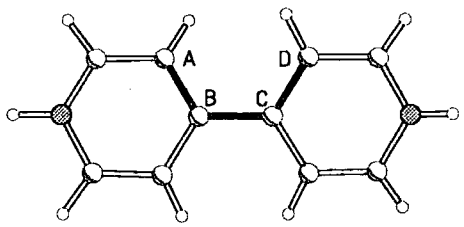


Diagram 3.12.1. The torsion angle is defined by ABCD, which is identical to the dihedral angle between the planes of the pyridyl rings if the bond BC is a subsection of a line joining the two nitrogen atoms.

Table 3.12.1. The observations in the structures in this chapter.

| | Structure | Angle between pyridyl rings | Central C-C bond length, Å. |
|---|---|---|---|
| A | 1 BPY · 1 PMA | 0°* | 1.485(2) |
| B | 1 BPY · 2 PMA | 21.36(9)° | 1.484(2) |
| C | 2 BPY · 1 PMA | 2.99(6)° | 1.4913(17) |
| D | 1 BPY · 2 PHT | 30.79(4)° | 1.483(3) |
| E | 1 BPY · 1 PHT | 0°* | 1.491(2) |

* B and E are constrained to be 0° by an inversion centre in the centre of the molecule.

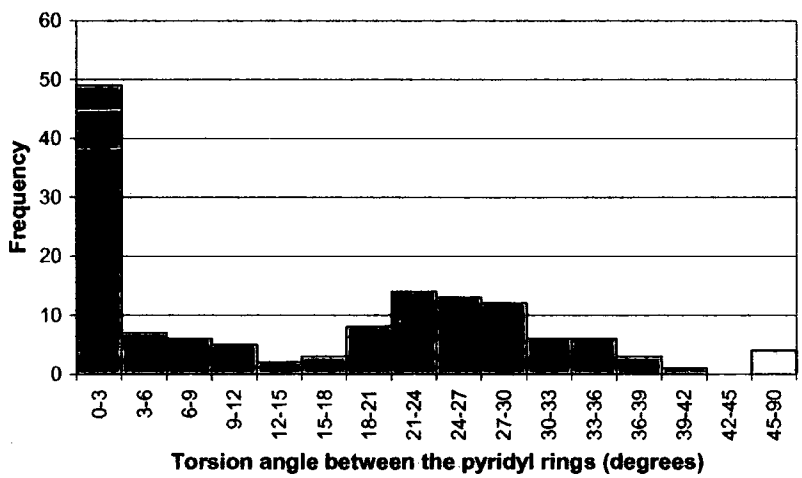


Graph 3.12.1. Torsion angles in all 4,4-bipyridine molecules from the Cambridge Structural Database.

There are two preferred conformations of 4,4'-bipyridine molecules in the solid state, either planar with a torsion angle of 0°, or twisted with an average torsion angle of ~25°. When the torsion angle is 0° the π-electron systems of the rings can interact. When the torsion angle is ~25° the steric interactions between the hydrogen atoms is reduced.

An electron-diffraction study of 4,4'-bipyridine in the gas-phase gives an angle between the pyridyl rings of 37.2° (Almenningen and Bastiansen, 1958). Ab-initio calculations give a slightly larger angle of 48° (Ould-Mussa at al. 1996). In the crystal structure of 4,4-bipyridine (Boag et al. 1999) there are two independent molecules in the asymmetric unit, with twist angles of 18.50(12)° and 34.85(10)° and in the crystal structure of the dihydrate (Näther et al. 2001) the twist angle is 41.6(1)°.

Biphenyl, a very similar molecule, in the room-temperature crystal structure is planar, but undergoes a phase transition and becomes twisted at low-temperatures (Busing, 1982), which suggests that the most stable structure is twisted and that the energy required to stabilise the flat structure is not great.

Neutral 4,4-bipyridine molecules occur in the 74 structures in the CSD, singly protonated molecules occur in nine structures and 4,4'-bipyridinium molecules occur in 21 structures. The central C-C bond in 4,4-bipyridine molecules in the CSD has an average length of 1.485(15)Å. The average bond length for molecules with twist angles less than 15° is 1.486(15)Å and the average for molecules with twist angles over 15° is 1.484(20)Å. There is a larger spread of values for the more twisted molecules. In many, but not all, of the structures in the CSD the bipyridine molecule lies across an inversion centre constraining the twist angle to be 0°.

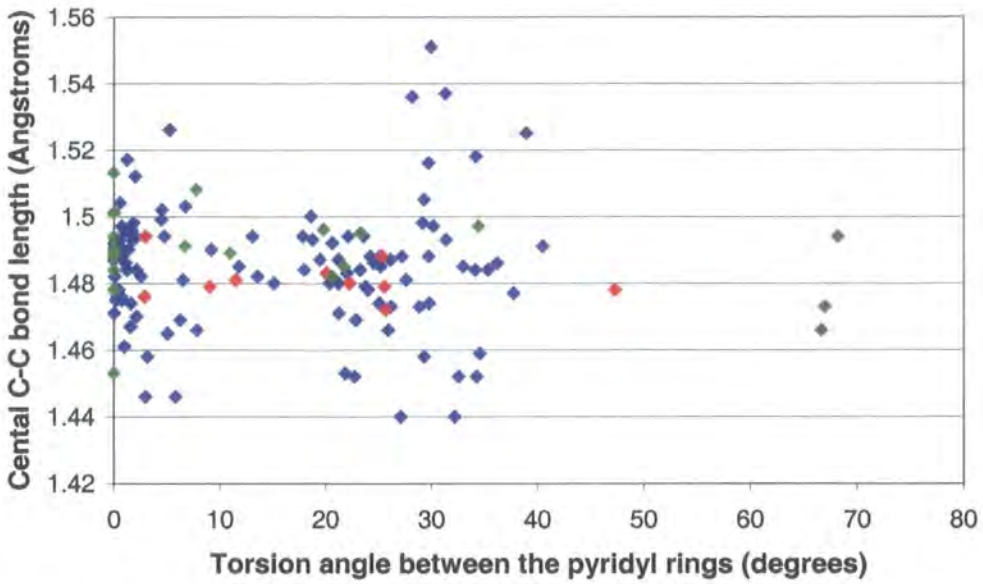


Graph 3.12.2. The Torsion angle related to the central C-C bond length. Blue points mark neutral molecules, red points mark single protonated molecules and green points mark fully protonated molecules.

Density-functional theory quantum-mechanical calculations have been performed using DMol$^3$ (Delley, 2000) to investigate the energy of 4,4'-bipyridine with different torsion angles. The energy of the structure, optimised with the torsion angle constrained, has been calculated for the fully protonated and the neutral states.

The results of the calculations do not agree with the results from the Cambridge database, although they do agree with the gas-state structures calculated and measured previously (Almenningen and Bastiansen, 1958, Ould-Mussa at al. 1996). The minimum-energy structure has a twist angle between 35°-40° for both the protonated and the neutral molecules.

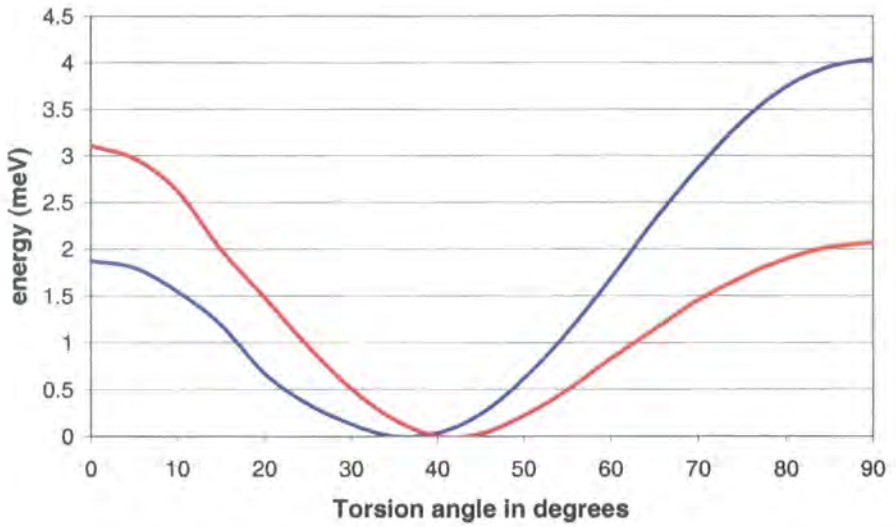


Graph 3.12.3. Results of the DMol$^3$ calculations. The red line shows the energy of the protonated molecule and the blue line shows the energy of the neutral molecule.

The energy difference between the minimum energy structure and the planar structure is 3.1meV for the protonated molecule and 1.9meV for the neutral molecule, which correspond to temperatures of 36K and 22K, close to the phase-transition temperature in biphenyl of 40K (Cailleau et al. 1979).

In this case the calculations do not adequately explain the experimental data. The twist angle is over estimated, the observed histogram from the CSD has a maximum between 21°-24° while the calculations predict that the minimum energy structure, which should be the most likely to occur, has a twist angle of 35°-40°. The planar structures are not explained at all. Perhaps the calculations underestimate energy gained by the overlap of the π-electron systems. The intermolecular environment of the molecule must explain the preference of 4,4-bipyridine. The observed structures lie at points where the gradient of the energy, which is proportional to the force, is a minimum.

### 3.13. Adjacent carboxylic acid groups attached to benzene rings

Pyromellitic acid and phthalic acid both contain carboxylic acid groups adjacent to each other attached to a phenyl ring. By surveying the Cambridge Structural Database (Allen and Kennard, 1993), performing electrostatic calculations and semi-empirical quantum-mechanical calculations the torsion angles of the carboxylic acid groups relative to the phenyl rings have been studied.

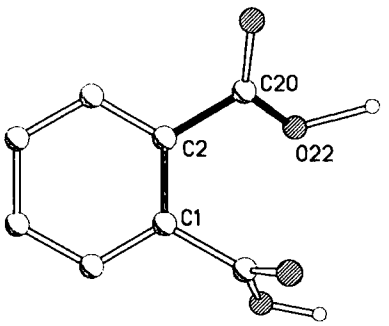


Figure 3.13.1. The torsion angle is defined between the hydroxyl group, C20-O22, and the C1-C2 bond in the phenyl ring. In this case the angle is 35.2°. If there is no hydroxyl group, i.e. a carboxylate group, then the angle could be to either oxygen atom.

#### 3.13.1. Cambridge Structural Database

Searches in the Cambridge Structural Database (CSD, Allen and Kennard, 1993) reveal definite trends in the torsion angles in adjacent carboxylic acids groups on phenyl rings. The fragment used for the search in the CSD is illustrated in diagram 3.13.1. The hydrogen atoms at positions 3 and 6 on the phenyl ring are included so that we only probe the interaction between the two carboxylic acid groups and not between any other adjacent groups. There were no restrictions on the 4 and 5 positions.

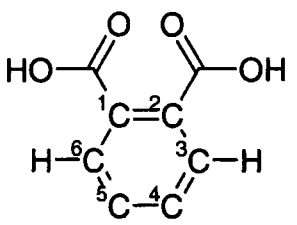


Diagram 3.13.1. The fragment used in the CSD search.

Most of the structures lie in bands where the sum of the torsion angles is either 90° or 270°. There are also clusters of points when T2 = 0° or 360° and T1 = 0°, 180° or 360°, these points correspond to intramolecular hydrogen bonds between a carboxylic acid group, with torsion angle T2, and a carboxylate group with torsion angle T1.

The graph below is slightly misleading as symmetry has been applied to the points from the database to illustrate the overall trends more clearly. When there are two carboxylic acid groups adjacent on phenyl ring, there are four equivalent sets of torsion angles, (T1, T2), (T2, T1) (2π-T1, 2π-T2) and (2π-T2, 2π-T1) (diagram 3.13.2). They may not be equivalent with respect to the rest of the molecule but they are equivalent with respect to the fragment used for the search in the CSD. Likewise two carboxylate groups have sixteen equivalent positions, and a carboxylate and a carboxylic acid group have four equivalent positions.

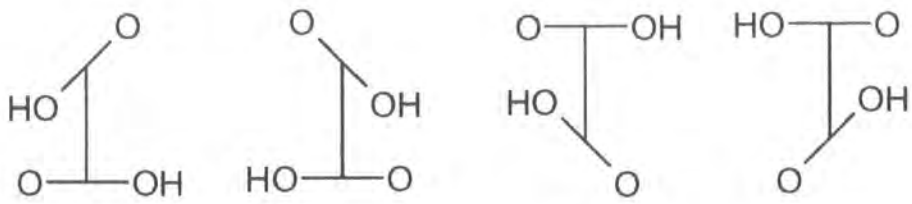


(T1, T2) (2π-T1, 2π-T2) (2π-T2, 2π-T1) (T2, T1)

Diagram 3.13.2. Four different, but equivalent, conformations for two adjacent carboxylic-acid groups.

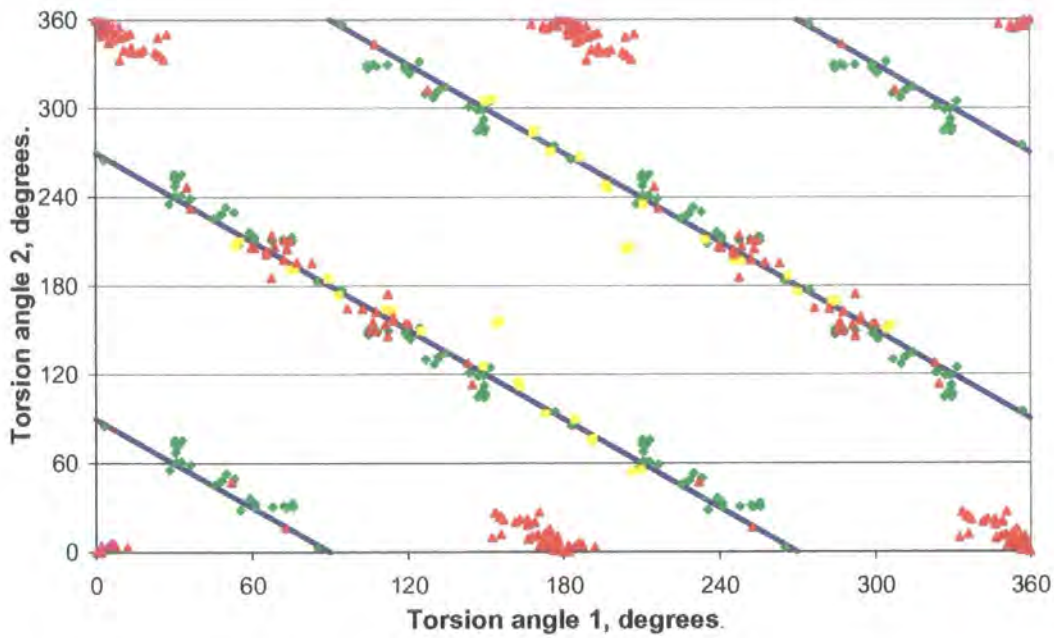


Graph 3.13.1. Torsion angles for adjacent carboxylic acids in the CSD. The yellow points indicate structures with two carboxylic acid groups, the green points indicate structures with two carboxylate groups and the red points indicate structures with one carboxylic acid and one carboxylate. The blue lines indicate where the sum of the torsion angles are 90° or 270°. The red clusters between the blue lines are intramolecular hydrogen bonds.

Table 3.13.1. Torsion angles of the structures in this chapter.

| | T1 | T2 | T1+T2 |
|---|---|---|---|
| A | 5.74(31) | 172.29(22) | 178.03 |
| B (1) | -15.93(28) | 7.95(28) | -7.98 |
| B (2) | -20.58(28) | 8.89(27) | -11.69 |
| B (3) | 143.13(18) | 126.40(18) | 269.53 |
| B (4) | 176.83(16) | 94.36(21) | 271.19 |
| D | -13.99(25) | 0.05(25) | -13.94 |
| C | -113.09 ( 0.14) | 35.37 ( 0.19) | -77.72 |
| E | -140.53(15) | -140.53(15) | -281.06 |
| F | -126.42(11) | -143.78(11) | -270.20 |

The intramolecular hydrogen bonds have torsion angles near 0 or 180 or 360 degrees or that add up to +/- 90 or +/- 270, agreeing with the observations from the CSD.

### 3.13.2. Spatial Overlap

A simple two-dimensional model has been used to estimate the overlap of the oxygen atoms depending on the torsion angles. A circle of radius 1.25Å represents an oxygen atom, this is smaller than the van der Waals radius of 1.4Å to compensate for the two-dimensional approximation. The simulation set up is illustrated in diagram 3.13.2. Two carboxylate groups with torsion angles $\theta_1$ and $\theta_2$ are separated by distance, d. The projection of the C-O bond into the plane is of length, h. The values for separation of the axes, d, of 3Å and the value for the C-O bond length, h, of 1.25Å have been taken to agree with the structures. The overlap has been calculated and the results are shown in graph 3.13.2.

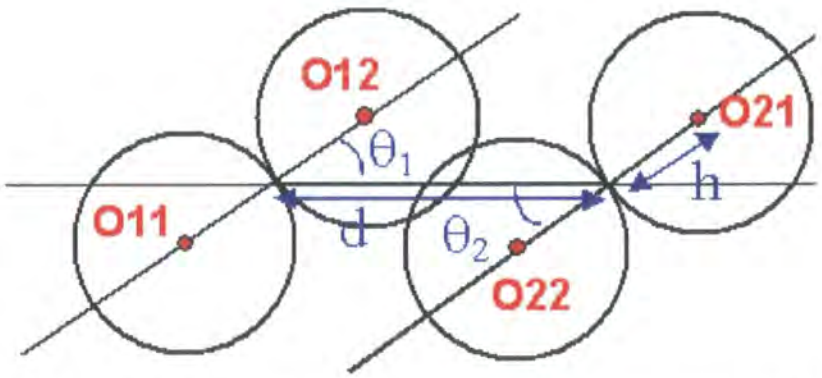


Diagram 3.13.2. The calculation of the overlap of spheres. T1=$\theta_1$, T2=$\theta_2$

The results show that although there is no overlap along a corridor close to T1+T2 = 90° or 270°, there are also large minima where the O-O vectors are parallel to each other and perpendicular to the C-C vector, i.e. (90,90), (90,270) (270, 90) and (270, 270). These points

are not observed in the CSD for any of the variations of the fragment. The intramolecular hydrogen bonds lie at points where the spatial overlap is at a maximum.

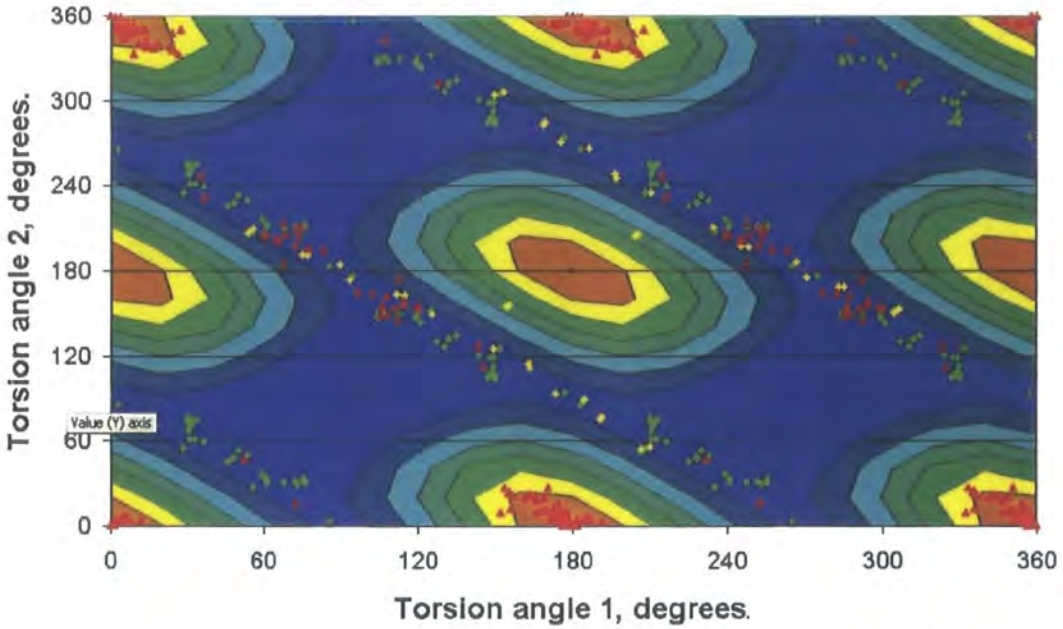


Graph 3.13.2. The amount of overlap of the circles. Blue represents no overlap and orange represents the maximum overlap. The data from the CSD have been superimposed on to the graph.

### 3.13.3. Electrostatic Calculations

The electrostatic energy between two charges is defined as:

$$E = \frac{1}{4\pi\varepsilon_0}\frac{q_1 q_2}{r}$$

where $q_1$ and $q_2$ are the charges and r is the separation of the charges. The total electrostatic energy of four charges has been calculated as they move in a plane. The positions of the charges are the same as the centres of the atoms defined in diagram 1. The energy has been calculated in three different situations:

1. All the charges equal and negative to mimic the situation where there are two carboxylate groups in the molecule.
2. One charge positive and the rest negative to mimic the situation where there is one carboxylic acid and one carboxylate.
3. Two equal dipoles to mimic the state where there are two carboxylic acid groups.

The separation between the axes and the C-O bond length of 3Å and 1.25Å have been chosen to be similar to the lengths in the measured structures and the overlap calculation above.

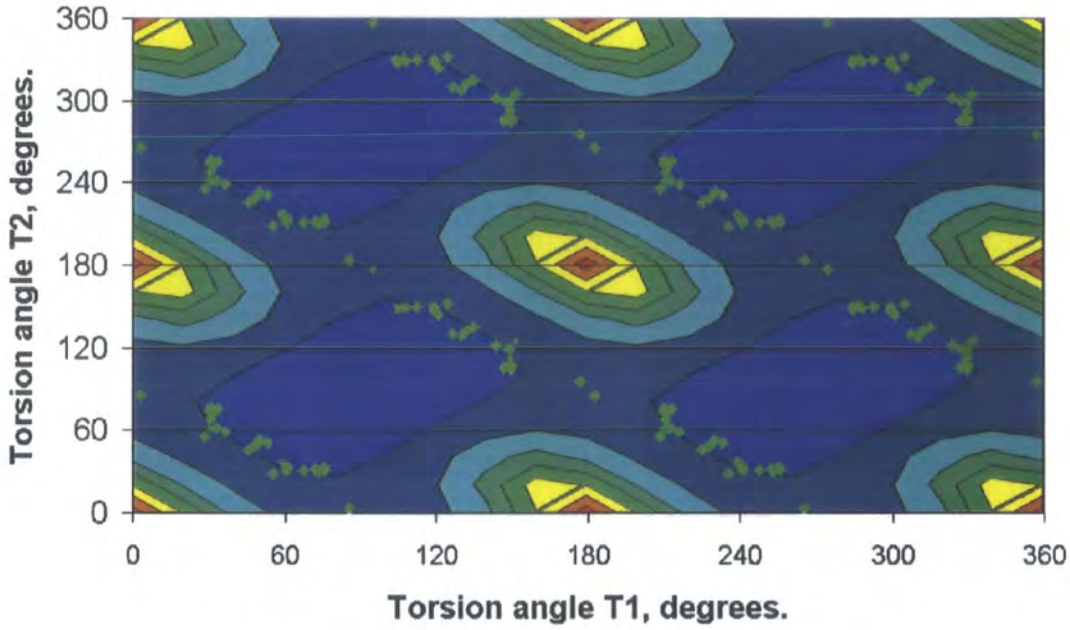


Graph 3.13.3.a. The results of the simulation for two carboxylate groups. Red marks the maxima and blue the energy minima. The data from the CSD have been superimposed.

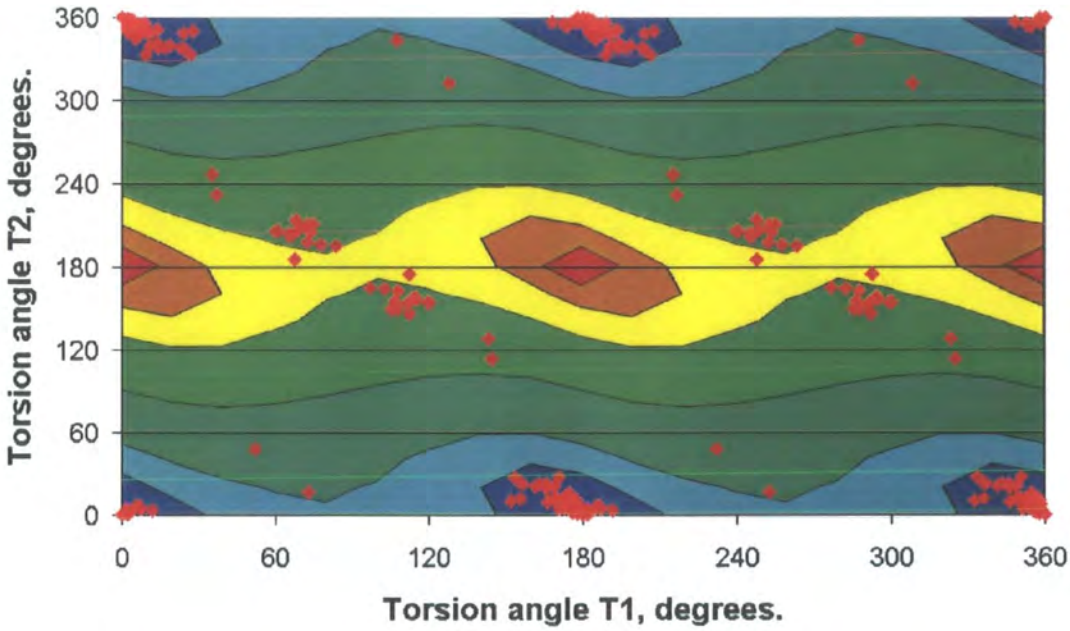


Graph 3.13.3.b. Results of the simulation for one carboxylate group, angle T1, and a carboxylic acid group, angle T2. The data from the CSD have been superimposed on the graph. Blue marks energy minima and red maxima.

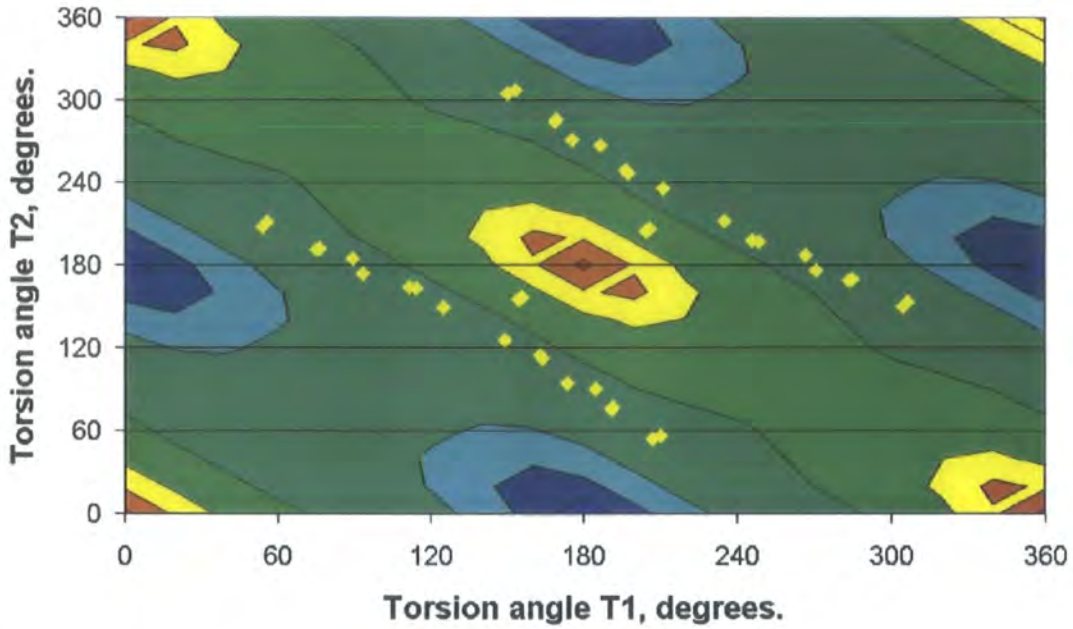


Graph 3.13.3.c. Results of the simulation for two carboxylic acid groups. The data from the CSD have been superimposed on the graph. Blue marks energy minima and red maxima.

The observed torsion angles cannot be entirely explained by the results of the electrostatic energy calculations. The results are good when there are two carboxylate groups (graph 3.13.3.a). All the points lie in the region of the minimum energy, although they all lie in a cluster at the edge of the region. No points lie near the overall minimum at T1 = 90° and T2 = 90°. The intramolecular hydrogen bonds lie at the minima in graph 3.13.3.b, but the rest of the points in graphs 13.3.b and 13.3.c are not close to minima.

### 3.13.4. Torques on the atoms

The minimum in the energy should correspond to where the forces are minimized also. The force is defined as

$$\underline{F} = \frac{1}{4\pi\varepsilon_0}\frac{q_1 q_2}{r^2}\hat{r}$$

Where $q_1$ and $q_2$ are the charges separated by distance r along unit vector $\hat{r}$. However the forces are not free to act in any direction as the relative positions of the charges are constrained and the only forces that can act are torques around the circles. The torque, $\tau$, is calculated as

$$\tau = \underline{F} \times \underline{h}$$

$\underline{F}$ is the force acting on the charge and $\underline{h}$ is the radial vector. The overall torque on each charge pair is the sum of all the torques on each charge. The single parameter that best describes the behaviour of the charges is the difference between the torques on the two

atom pairs. When the difference in the torques is zero the atom pairs do not want to change their orientation with respect to each other. In the graphs below (graphs 3.13.4.a, b and c) the magnitude of the difference between the torques is plotted depending on the torsion angles.

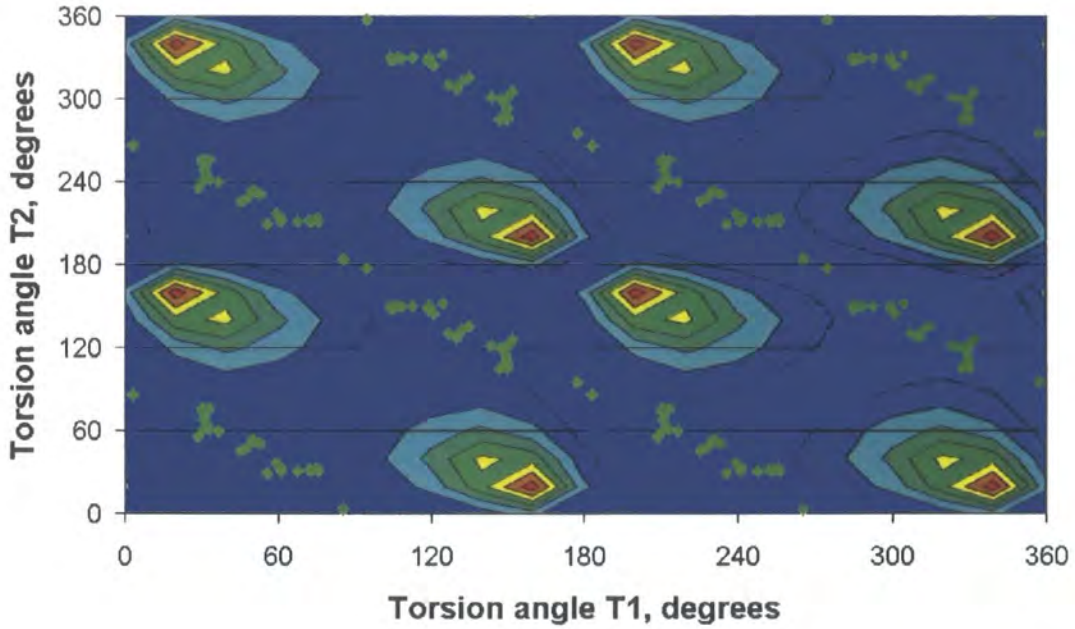


Graph 3.13.4.a. The results of the simulation for two carboxylate groups. Red marks the maximum net torque and blue the minimum. The data from the CSD have been superimposed.

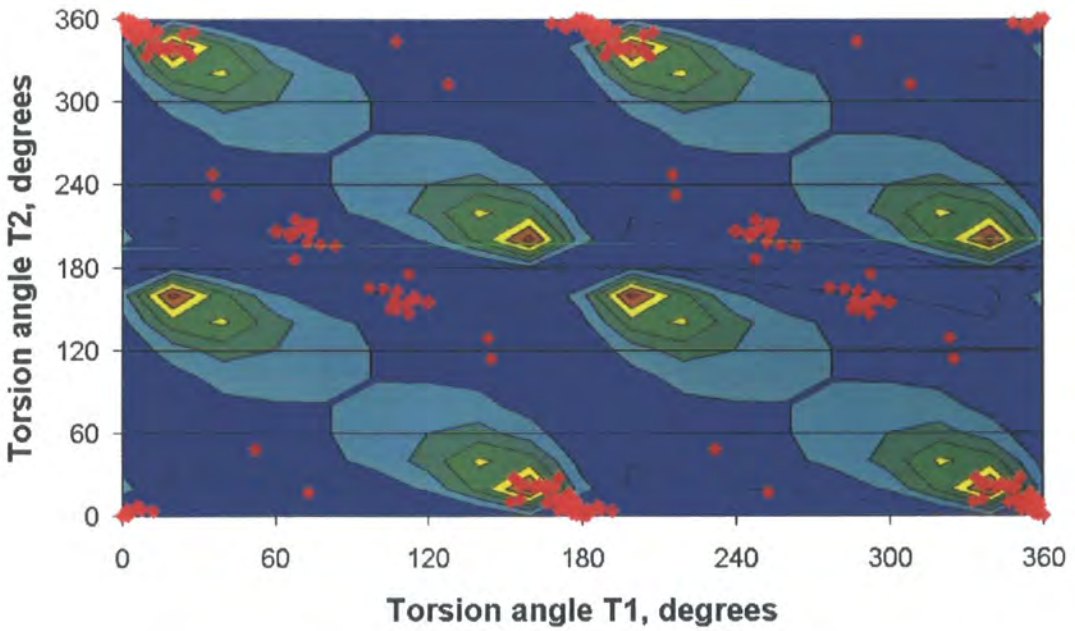


Graph 3.13.4.b. The results of the simulation for one carboxylate group, angle T1, and one carboxylic acid group, angle T2. Red marks the maximum net torque and blue the minimum. The data from the CSD have been superimposed.

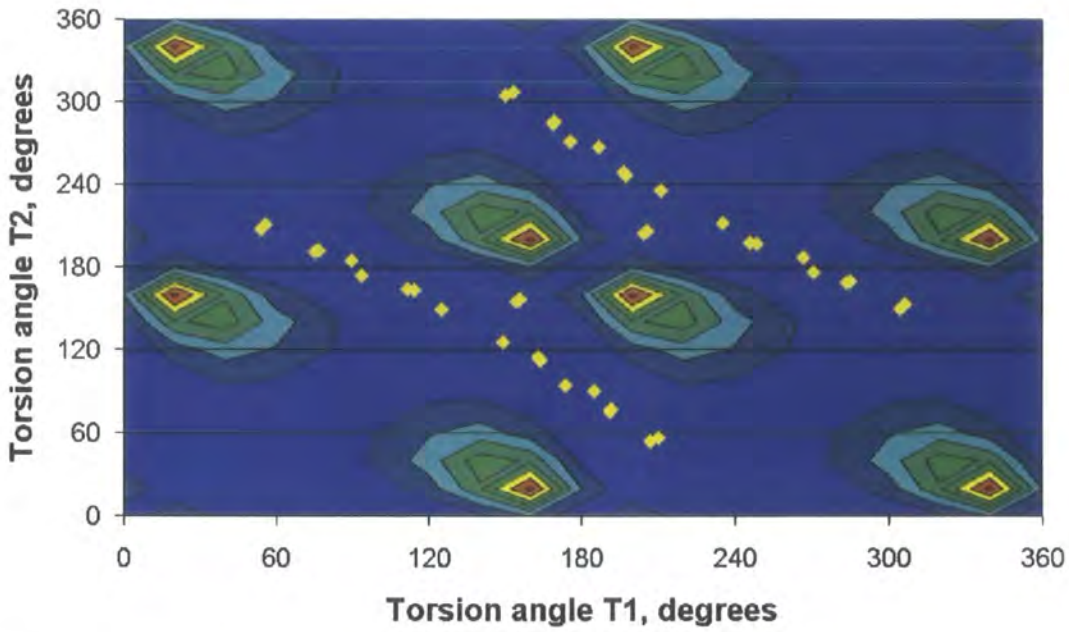


Graph 3.13.4.c. The magnitude of the difference in the torques for two carboxylic acid groups. Red marks the maximum net torque and blue the minimum. The data from the CSD have been superimposed.

The magnitude of the difference in the torques explains the observed data well. The patterns in the three graphs (3.13.4.a, b,c) are essentially the same. The difference between the three simulations is in the sign of the differences in the torques, which are not shown in the graphs. All the points in the CSD lie in regions of low net torque.

### 3.13.5. Semi-empirical Quantum Mechanical Calculations

The program MOPAC (Stewart, 1990) has been used to calculate the potential energy surface of carboxylate rotation in phthalic acid using the AM1 method (Dewar et al. 1985). Starting from an X-ray derived structure containing phthalic acid the ideal geometry was calculated with no restrictions. Then the carboxylic and carboxylate torsion angles were varied, at each angle the torsion angles were fixed and the geometry allowed to relax to a minimum of energy. The energies calculated in each case are shown in graphs 3.13.5.a, b and c.

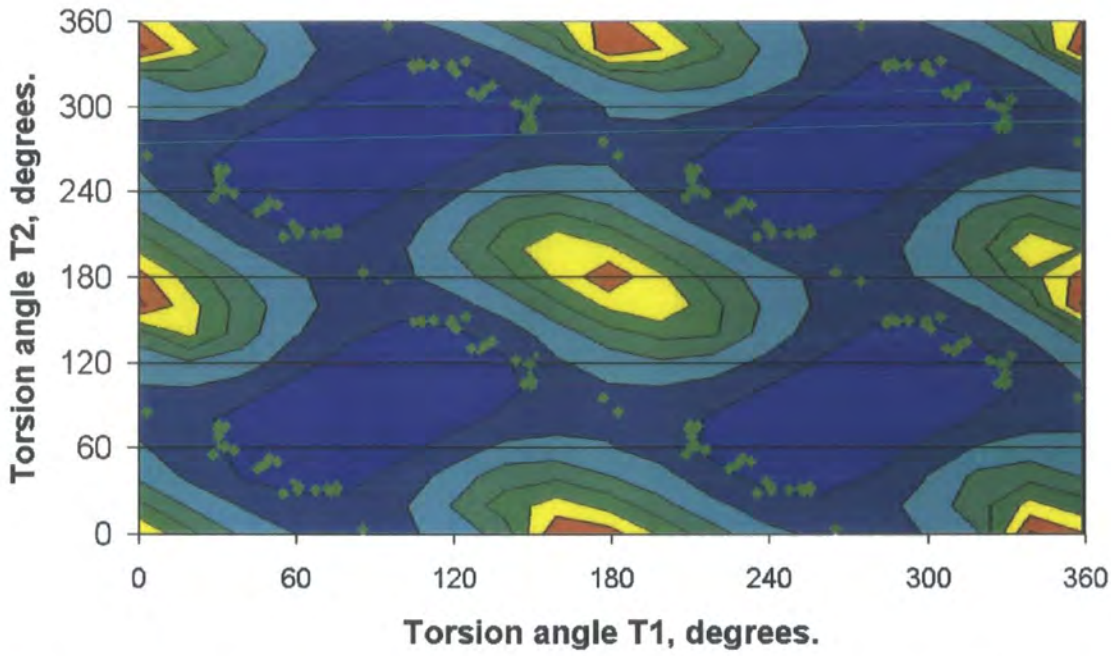


Graph 3.13.5.a. The results of the MOPAC simulation for two carboxylate groups. Red marks the maximum energy and blue the minimum. The data from the CSD have been superimposed. The graph is very similar to graph 3.13.3.a, the electrostatic energy.

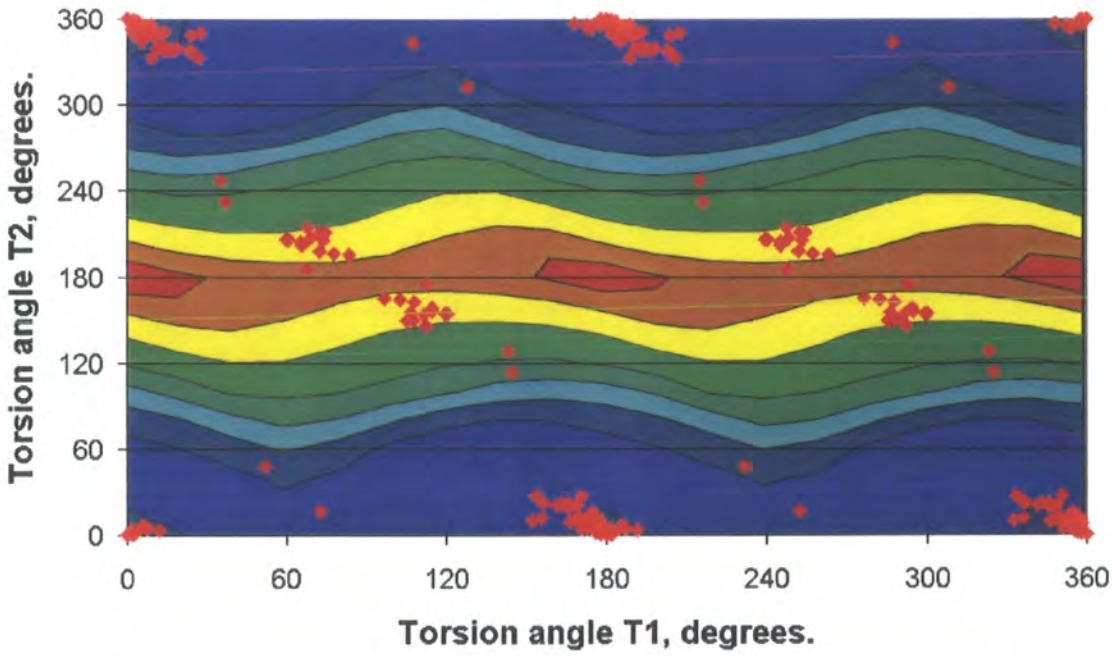


Graph 3.13.5.b. The results of the MOPAC simulation for one carboxylate group, angle T1, and one carboxylic acid group, angle T2. Red marks the maximum energy and blue the minimum. The data from the CSD have been superimposed. The graph is very similar to graph 3.13.3.b, the electrostatic energy.

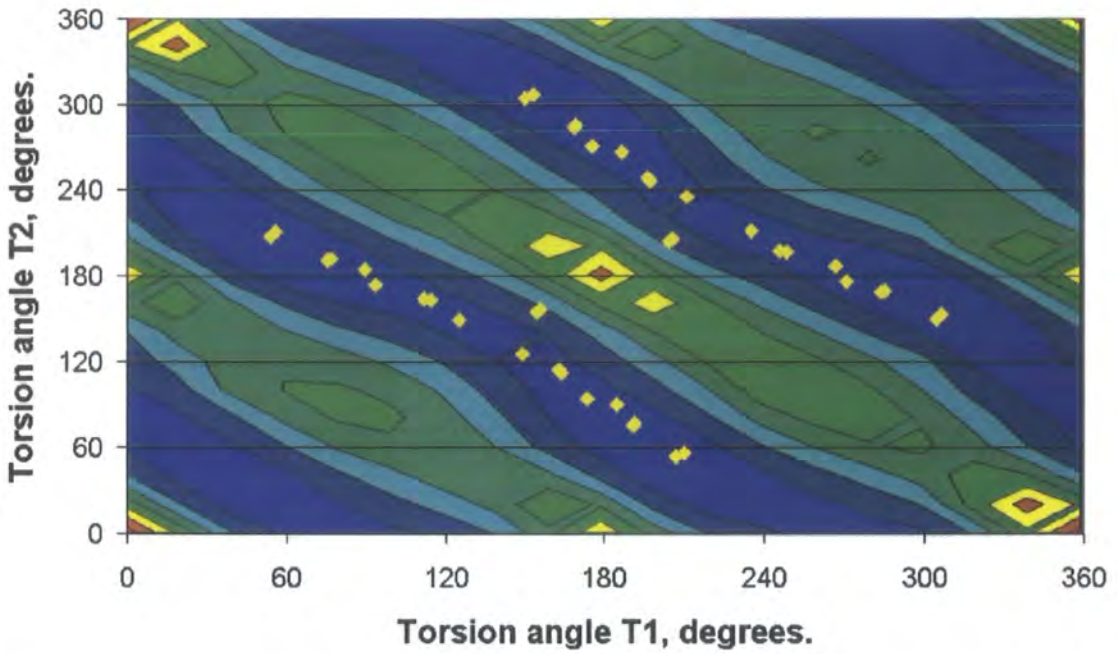


Graph 3.13.5.b. The results of the MOPAC simulation for two carboxylic acid groups. Red marks the maximum energy and blue the minimum. The data from the CSD have been superimposed.

The graphs for the energy of two carboxylate groups and for one carboxylate and one carboxylic acid group (3.13.5.a and 3.13.5.b) are very similar to the graphs of the electrostatic energy in the same cases (3.13.3.a and 3.13.3.b). This suggests that the electrostatic energy is the major contribution to the energy in these cases.

The graphs for the energy of two carboxylic groups (3.13.3.c and 3.13.5.c) are quite different which suggests that this simple electrostatic approximation does not describe this situation very well. The MOPAC graph (3.13.5.c) fits the CSD data well.

### 3.13.6. Discussion

The graphs which show the energy do not entirely explain the observations in the CSD. The approximation of free molecules therefore does not apply well to the situation in the crystal. The positions where the forces are minimised better describes the trends observed in the CSD. All the points lie on or close to equilibrium points, points where the forces are minimised. This is similar to the case in 4,4-bipyridine where the observations do not lie at minimum energy points for the free molecule but lie close to minimum force points.

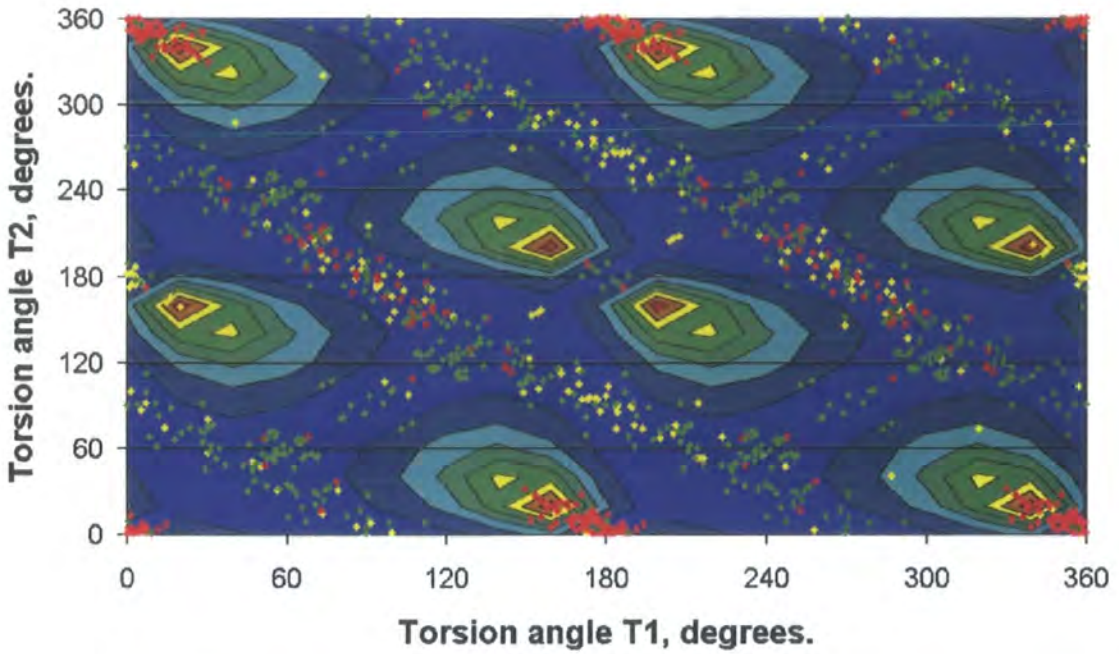


Graph 3.13.6. The CSD data for all adjacent carboxylic acid groups. The colour scheme is identical to the graphs above for the torque and the CSD data. The graph has been superimposed on the graph of the difference in the torques for two carboxylate groups.

The simple model that has been used for the electrostatic calculations and the overlap calculations is two-dimensional and allows no rearrangement of the bond lengths or changes in the charges. The quantum-mechanical simulations allow these changes but give essentially the same results in two of the three situations. Overall the simple simulations give an acceptable approximation of the important forces.

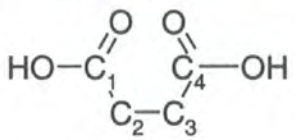


Diagram 3.13.3. The fragment used to search the CSD.

This is applicable to other systems in the CSD. Graph 3.13.6 is for carboxylic acid groups adjacent to each other (diagram 3.13.3). Only groups with T3=C1-C2-C3-C4 between –30 and 30 have been considered. The graph has more points than real data, again the symmetry has been applied. The minimum torque graph explains the data best. There are points near all the minima in the torque, intramolecular hydrogen bonds are explained as are other interaction with metals for example. This is a simple rule that could be helpful to predict the conformation, and hence the packing of molecules like phthalic acid and pyromellitic acid that contain two adjacent carboxylate groups.

### 3.14. References


Allen, F.H., Kennard, O., Watson, D.G., Brammer, L., Orpen, A.G. & Taylor, R. International Tables for Crystallography. (1992). Volume C, Table 9.5.1.1. 685-706.

Allen, F.H., Kennard. O. (1993) Chem. Des. Autom. News, **8**, 31-37.

Almenningen, A., Bastiansen, O.K. (1958) Nor. Vidensk. Selsk. Skr. **4**. 1-16.

Archer J.M. Lehmann, M.S. (1986) J. Appl. Cryst. **19**. 456-458.

Barrett, D.M.Y., Kahwa, I.A., Radüchel, B., White, A.J.P., Williams, D.J. (1998) J. Chem. Soc. Perkin Trans. 2. 1998, 1851-1856.

Baur, W.H., Kassner, D. (1992). Acta Cryst. **B48**. 356-369.

Bertolasi, V., Gilli, P., Ferretti, V., Gilli, G. (2001). Acta Cryst. **B57**, 591-598l.

Biradha, K., Zaworotko, M.J. (1998). Crystal Engineering. **1**, 67-78.

Blessing, R.H. (1995) Acta Cryst. **B51**, 816-823.

Boag, N.M., Coward, K.M., Jones, A.C., Pemble, M.E., Thompson, J.R. (1999) Acta Cryst. **C55**, 672-674.

Busing, W.R. (1982). Acta Cryst. **A39**, 340-347.

Cailleau, H., Baudour, J-L., Meinnel, J., Dworkin, A., Moussa, F., Zeyen, C.M.E. (1979). Faraday Discuss. Chem. Soc. **69**, 7-18.

Campbell, J.W., (1995). J. Appl. Cryst. **28**, 228-236.

Campbell, J.W., Habash, J., Helliwell, J.R., Moffat, K. (1996). Quarterly for Protein Crystallography, 18.

Chatterjee, S., Pedireddi, V.R., Rao, C.N.R. (1998). Tetrahedron Lett. **39**, 2843-2846.

Cipriani, F., Castagna, J.C., Lehmann, M.S., Wilkinson, C. (1995) Physica B, **213 & 214**, 975-977.

Cleland, W.W., Kreevoy, M.M. (1994). Science, **264.** 1887-1890.

Coupar, P.I., Ferguson, G., Glidewell, C. (1996). Acta Cryst. **C52**, 2524-2528.

Delley, B. (2000). J. Chem. Phys. **113**, 7756-7764.

Desiraju, G.R. (1995). Angew.Chem. Int. Ed. Engl. **34**, 2311-2327.

Dewar, M.J.S., Zoebisch, E.G., Healy, E.F., Stewart, J.J.P. (1985). J. Amer. Chem. Soc. **107**, 3902-3909.

Ermer, O. (1981). Helv. Chim. Acta. **64**, 1902-1909.

Filhol, A., (1998). RAFD19. Institut Laue Langevin, Grenoble, France.

Frydenvang, K., Hjelvang, G., Jensen, B., Rosariom S.M.M.D. (1994). Acta Cryst. **C50**, 617-623.

Gilli, P., Bertolasi, V., Ferritti, V., Gilli, G. (1994) J. Amer. Chem. Soc. **116**, 909-915.

Hibbert, F., Emsley, J. (1990). Advances in Physical Organic Chemistrym **26**. 265-379.

Hunter, C.A., Lawson, K.R., Perkins, J., Urch, C.J. (2001) J. Chem. Soc. Perkin. Trans. 2. **5**. 651-669.

Jessen, S.M., Küppers, H., Luehrs, D.C. (1992). Z. Naturforsch, Teil B, **47**, 1141-1153.

Jessen, S.M. (1990) Acta Cryst. **C46,** 1513-1515.

Kozma, D., Bocskei, Z., Simon, K., Fogassy, E. (1994). J. Chem. Soc. Perkin. Trans. 2. 1883-1886.

Küppers, H., Takusagawa, F., Koetzle T.F. (1985). J. Chem. Phys. **82**, 5636-5647.

Kvick, Å., Koetzle, T.F., Thomas, R., Takusagawa, F. (1974). J. Chem. Phys. **60**, 3866-3874.

Lough, A.J., Wheatley, P.S., Ferguson, G., Glidewell, C. (2000). Acta Cryst. **B56**, 261-272.

Marsh, R.E. (1997). Acta Cryst. **B53**. 317-322.

Matthewman, J.C., Thompson, P. & Brown, P.J. (1982). J. Appl. Cryst. **15**, 167-173.

Mitchell, C.A., Lovell, S., Thomas. K., Sazickas, P., Kahr, B. (1996). Angew. Chem. Int. Ed. Engl. **35**, 1021-1023.

Mrvoš-Sermek, D., Popvić, F., Matković-Čalogović, D. (1996). Acta Cryst. **C52**, 2538-2541.

Näther, C., Riedel, J., Jeβ, I. (2001). Acta Cryst. **C57**, 111-112.

Olovsson, G., Olovsson, I. (1984). Acta Cryst. **C40**. 1521-1526.

Ould-Mussa, L., Poizat, O., Castellà-Ventura, M., Buntinx, G., Kassab, E. (1996). J. Phy. Chem. **100**, 2072-2082.

Pedireddi, V.R., Chatterjee, S., Ranganathan, A., Rao, C.N.R. (1998). Tetrahedron. **54**, 9457-9474.

Reetz, M.T., Höger, S., Harms, K. (1994) Angew. Chem. Int. Ed. Engl. **33**, 181-183.

Sakhawat Hussain, M., Schlemper, E.O., Fair, C.K. (1980). Acta Cryst. **B36**, 1104-1108.

Sheldrick, G.M. (1997). SHELXL97 and SHELXS97. University of Göttingen, Germany.

Smith, R.A. (1975). Acta Cryst. **B31**, 1773-1775.

Smith, R.A. (1975a). Acta Cryst. **B31**, 2508-2509.

Speakman, J.C., Lehmann, M.S., Allibon, J.R., Semmingsen, D. (1981). Acta Cryst. **B37**, 2098-2100.

Spek, A.L. (1990). PLATON. Acta Cryst. **A46**, C-34.

Steiner, T. (1997). Chem. Commun. 727-734.

Steiner, T., Wilson, C.C., Majerz. I. (2000). Chem. Commun. 1231-1232.

Steiner, T., Majerz, I., Wilson, C.C. (2001). Angew. Chem. Int. Ed. **40**, 2651-2654.

Stewart, J.J.P. (1990). J. Comput.-Aided Mol. Des. **4**, 1-105.

Takusagawa, F., Koetzle, T.F. (1979). Acta Cryst. **B35**, 2126-2135.

Thomas, M., Stansfield, R.F.D., Berneron, M., Filhol, A., Greenwood, G., Jacobé, J., Feltin, D., Mason, S.A. (1983). Position Sensitive Detection of Thermal Neutrons, edited by Convert, P. and Forsyth, J.B. Academic Press, 344-350.

Thomas, J.O., Liminga, R. (1978). Acta Cryst. **B34**, 3686-3690.

Vanhouteghem, F., Lenstra, T.H., Schweiss, P. (1987). Acta Cryst. **B43**, 523-528.

Wilkinson, C., Khamis, H.W., Stansfield, R.F.D. & McIntyre, G. J. (1988). J. Appl. Cryst. **21**, 471-478.

Wilkinson, C., Lehmann, M.S. (1991). Nucl. Inst. And Meth. **A310**, 411-415.

Willis, B.T.M., Pryor, A.W. (1975) Thermal Vibrations in Crystallography, Cambridge University Press, 207-244.

Wilson, C.C. (2000) Single Crystal Neutron Diffraction From Molecular Materials. World Scientific.

## 4. Hydrogen Bonding in Pyridine-3,5-dicarboxylic Acid

In the 2:1 co-crystal of 4,4-bipyridine and benzene-1,2,4,5-tetracarboxylic acid (BPTA) we observed an extremely short N··H··O hydrogen bond in which the hydrogen atom position in the bond depends on the temperature. To investigate further this phenomenon we have performed neutron diffraction experiments on pyridine-3,5-dicarboxylic acid which contains a N··H··O hydrogen bond of a similar length.

### 4.1. Pyridine-3,5-dicarboxylic Acid

The Cambridge Structural Database (CSD, Allen and Kennard, 1993) was searched for short N-H···O / O-H···N hydrogen bonds (graph 4.1.1). One of the shortest and straightest, with the hydrogen atom found in the centre of the hydrogen bond, was in the crystal structure of pyridine-3,5-dicarboxylic acid, with an N···O separation of 2.515Å, and N-H distance of 1.289Å and O-H distance of 1.230Å (Takusagawa, 1973). Not only are the hydrogen bond parameters very similar to those in BPTA but the constituents of the hydrogen bonds, a pyridyl group and a carboxylic acid group, are identical. There are structures with shorter N···O distances in the CSD but with small N-H-O angles, or in much more complicated crystal structures. Pure PDA is readily available from chemical suppliers and the chemists in Hong Kong, who produced the crystals, were using it as a ligand in their research into organometallic polymers.

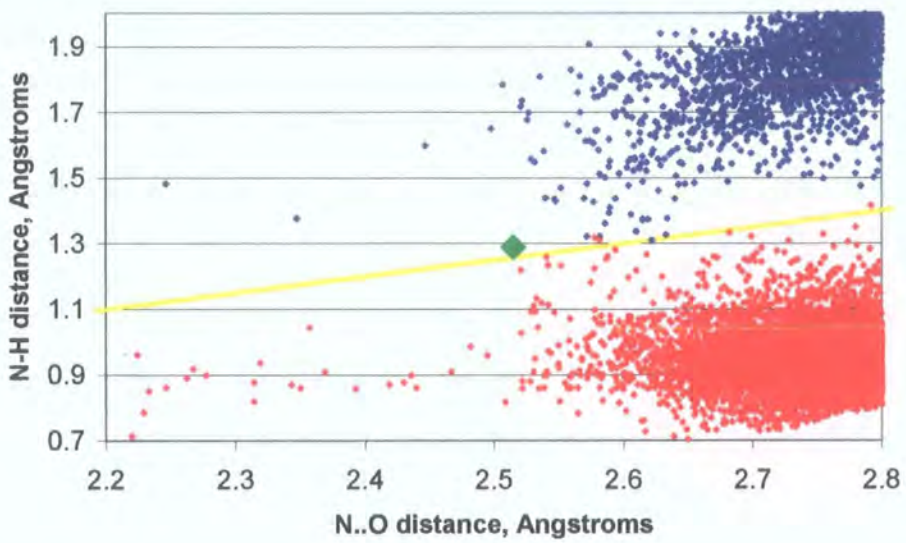


Graph 4.1.1. N···O hydrogen bonds measured by X-ray diffraction from the CSD. The red points indicate N-H···O hydrogen bonds, the blue points indicate O-H···N hydrogen bonds, the green point marks PDA. The yellow line marks where the N-H distance is half the N···O distance.

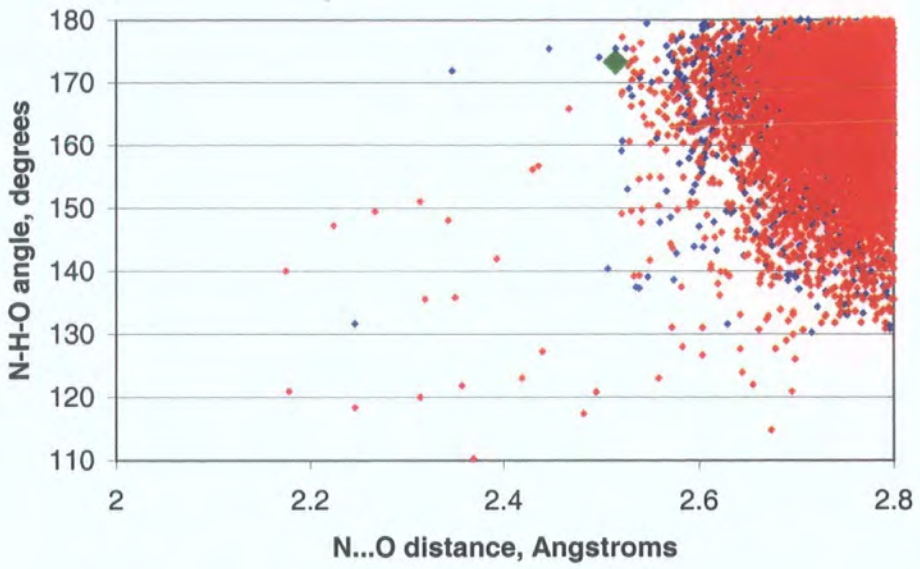


Graph 4.1.2. N···O hydrogen bonds measured by X-ray diffraction from the CSD. The red points indicate N-H···O hydrogen bonds, the blue points indicate O-H···N hydrogen bonds, the green point marks PDA. PDA is one of the shortest straightest N···O hydrogen bonds. The N···O distance decreases with decreasing N-H-O angle. The red points have been drawn second and cover many of the blue points.

## 4.2. The Crystal Structure of Pyridine-3,5-dicarboxylic acid

Pyridine-3,5-dicarboxylic acid (PDA) crystallises in space group $P2_1/c$ with four molecules in the unit cell. One strong O-H···O hydrogen bond and a strong N-H···O are formed to link the molecules in infinite two-dimensional planar sheets perpendicular to the c-axis.

PDA is an organic acid known to increase stem length in radish seedlings (Taguchi et al, 1992). The crystal structure was solved by Takusagawa et al. (1973). Neutron diffraction data have been collected at room temperature and 15K, all the parameters for the discussion are taken from the 15K data unless otherwise specified.

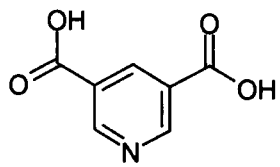


**[PDA]**

The internal geometry of the PDA molecule in the crystal conforms more closely to the zwitterionic form in which one carboxylic acid group has become deprotonated and the nitrogen atom has become protonated. This is similar to pyridine-2,3-dicarboxylic acid (quinolinic acid) which crystallises in the zwitterionic form with a strong intramolecular hydrogen bond between the adjacent carboxylic acid groups.

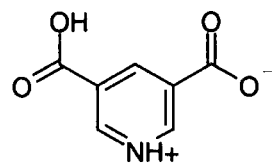


The C-O bond lengths in the carboxylic acid group [C7(=O1)-O2-H4] of C7-O1 = 1.319(2)Å and C7=O2 = 1.217(3)Å conform to the average values tabulated in the International Tables for Crystallography (Allen et al. 1992) in which C=O is 1.226(20)Å and C-O is 1.305(20)Å for a carboxylic acid group attached to an aromatic ring. This carboxylic acid group donates one strong hydrogen bond from O1 to O3. O2 is not involved in any strong hydrogen bonds.

The carboxylic acid group C8(=O3)-O4-H5 has a conformation that suggests significant carboxylate character. The C-O bond lengths of 1.245(3)Å and 1.277(3)Å are closer to carboxylate bond lengths, where both C-O bonds are expected to be 1.255(10)Å (Allen et al. 1992). The O-H bond length of 1.311(5)Å is extremely long and will be discussed in more detail. This carboxylic acid group participates in two strong hydrogen bonds, O3 accepts a hydrogen bond from O1, and O4 is part of a hydrogen bond to N1.

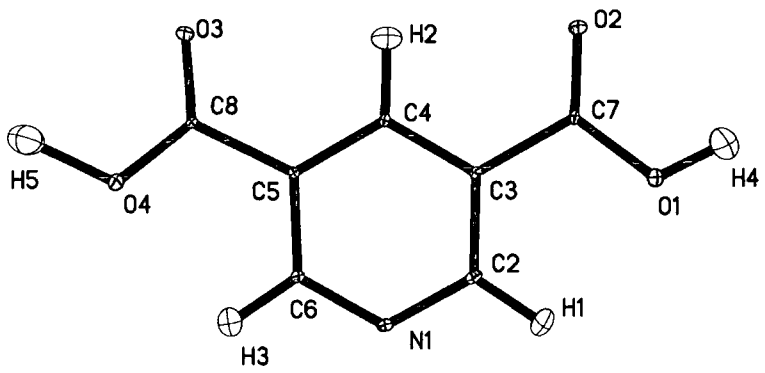


Figure 4.2.1. 50% Thermal ellipsoid plot from the 15K neutron refinement.

The average C-N-C angle in pyridyl molecules in the Cambridge Structural Database (Allen and Kennard, 1993) is 117.3(2)°, while the average for pyridinium ions is 122.0(2)°. The C2-N1-C6 angle of 121.69(14)º corresponds to the protonated conformation rather than to the unprotonated.

The most important intermolecular interactions are two strong hydrogen bonds, one O-H···O and one O··H··N. These combine with weaker C-H···O hydrogen bonds to link the molecules into planar sheets perpendicular to the c-axis.

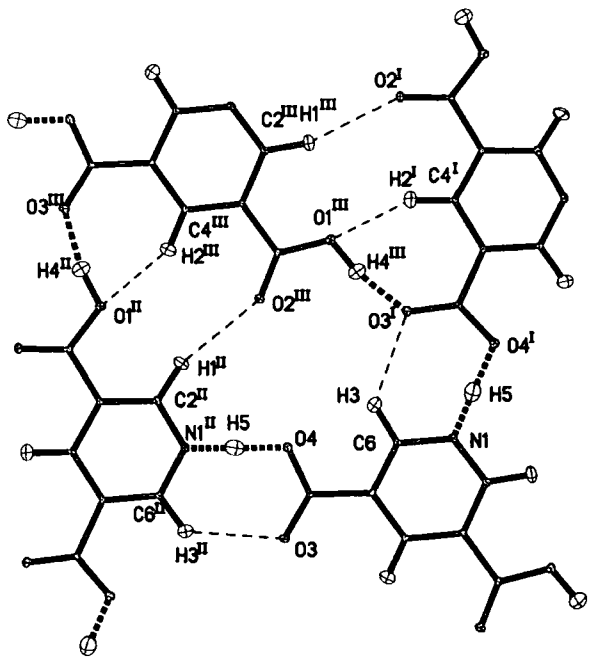


Figure 4.2.2. Co-operative intermolecular hydrogen bonding links the molecules into planar sheets. The strong hydrogen bonds are indicated by heavy dashed lines and the weak C-H···O hydrogen bonds are indicated by the thin dashed lines. [Symmetry codes: (I) = -x, -0.5+y, 0.5-z. (II) = -1-x, 0.5+y, 0.5-z. (III) = 1+x, y, z.]

The strong O-H···O hydrogen bond O1-H4···O3 is normal. The O1···O3 separation of 2.57Å is short, but not extremely short, compared with similar hydrogen bonds (Graph 4.2.1). The

O-H and H···O distances show no abnormalities compared to O-H···O hydrogen bonds of similar length.

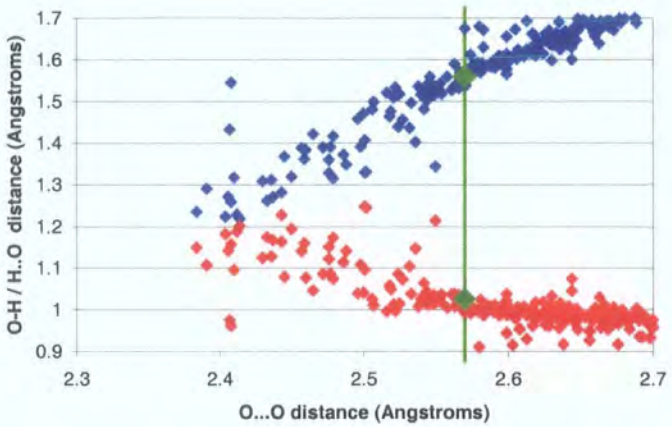


Graph 4.2.1. O-H···O hydrogen bonds measured by neutron diffraction from the Cambridge Structural Database (Allen and Kennard, 1993). The vertical green line marks an O···O distance of 2.57Å and the green points mark the O1-H4 and H4···O3 bond distances.

The N··H··O hydrogen bond, with an N···O separation of 2.523(2)Å, is one of the shortest measured by neutron diffraction (Graph 4.2.2). This hydrogen bond is chemically similar to the short N··H··O hydrogen bond in the 2:1 co-crystal of 4,4-bipyridine and benzene-1,2,4,5-tetracarboxylic acid (2BPY·PMA, Section 3.6). The N···O separations of 2.523(2)Å in PDA and 2.522(2)Å in 2BPY·PMA are essentially identical. The N···O distance of 2.523(2)Å lies in the region of Graph 4.2.2 where the proton position has been found to be near the centre of the hydrogen bond. This is also observed in this situation, the N-H distance is 1.216(5)Å and the O-H distance is 1.309(5)Å at 15K.

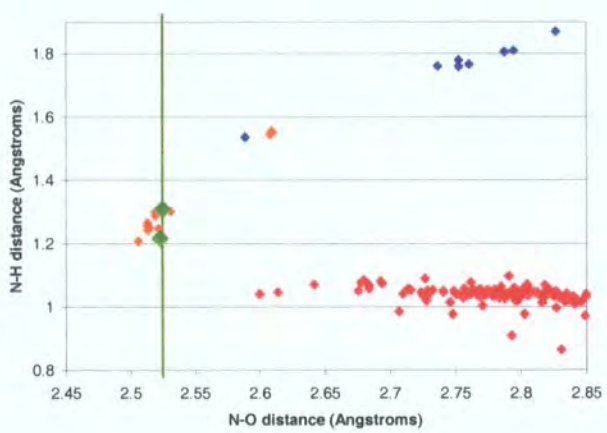


Graph 4.2.2. N-H···O / O-H···N hydrogen bonds measured by neutron diffraction from the Cambridge Structural Database (Allen and Kennard, 1993). The vertical green line marks an N···O distance of 2.523Å and the green points mark the N1-H5 and bond distances at 15K and 296K. The orange points are from the previous chapter and taken from Steiner et al (2001).

Table 4.2.1: Strong Hydrogen-Bond Parameters at 15K.

| | D···A (Å) | D-H(Å) | H···A (Å) | D-H-A |
|---|---|---|---|---|
| N1-H5···O4$^{i}$ | 2.523(2) | 1.216(5) | 1.309(5) | 176.3(5)° |
| O1-H4···O3$^{ii}$ | 2.570(3) | 1.026(4) | 1.558(5) | 167.8(4)° |

Symmetry Codes: i = -x, -0.5+y, 0.5-z. ii = -1-x, 0.5+y, 0.5-z.

Three weak C-H···O hydrogen bonds are formed in the crystal, two of which directly complement the strong hydrogen bonds. The N··H··O hydrogen bond is complemented by a C-H···O (C6-H3···O3) hydrogen bond in parallel, to form a motif seen in some of the structures in section 3 and commonly in pyridine – carboxylic acid interactions. The O-H···O hydrogen bond is also complemented by a C-H···O hydrogen bond (C4-H2···O1).

The O-H···O hydrogen bonds link the molecules in chains along the b-direction (figure 4.2.3) and the N··H··O hydrogen bonds also link the molecules in chains along the b-direction (figure 4.2.4). Combining the two chains produces strongly hydrogen-bonded two-dimensional sheets (figure 4.2.5).

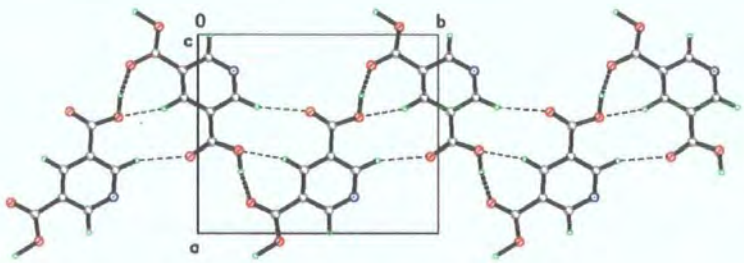


Figure 4.2.3. Chains formed along the b-axis by the O-H···O hydrogen bonds assisted by C-H···O hydrogen bonds.

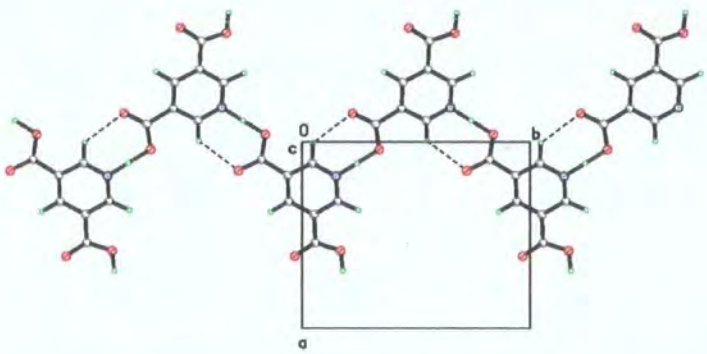


Figure 4.2.4. Chains formed along the b-axis by the N··H··O hydrogen bonds assisted by C-H···O hydrogen bonds.

Table 4.2.2: C-H···O Hydrogen Bond Parameters.

| | D···A (Å) | C···H (Å) | H···A (Å) | D-H-A |
|---|---|---|---|---|
| C2-H1···O2$^{i}$ | 3.550(3) | 1.093(4) | 2.501(4) | 160.6(3)º |
| C4-H2···O1$^{ii}$ | 3.157(3) | 1.087(4) | 2.181(4) | 148.0(4)º |
| C6-H3···O3$^{iii}$ | 3.227(3) | 1.086(4) | 2.439(4) | 128.3(3)º |

Symmetry Codes: i = -1-x, 0.5+y, 0.5-z. ii = -1-x, -0.5+y, 0.5-z. iii = -x, 0.5+y, 0.5-z.

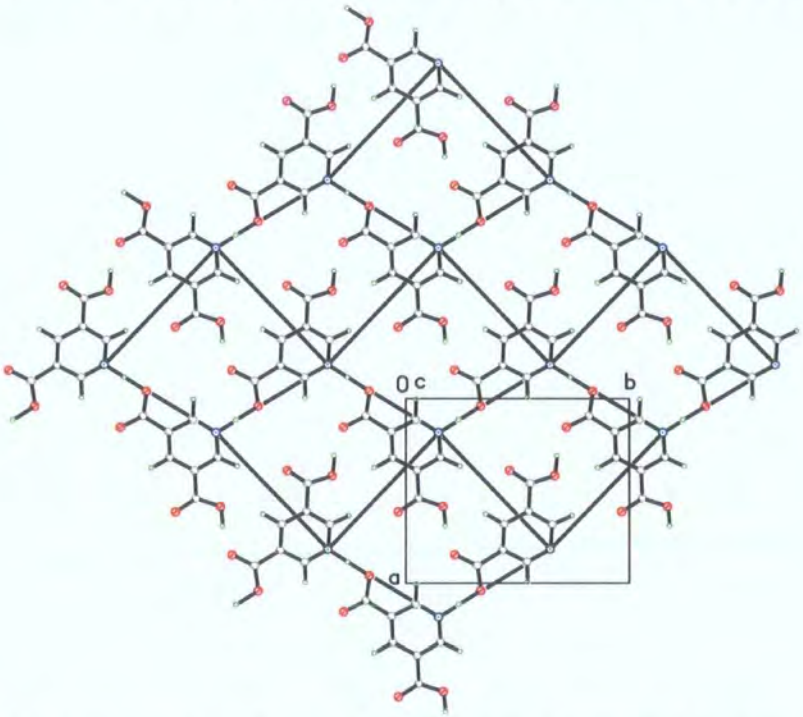


Figure 4.2.5. The molecular layer viewed along the c-axis. The hollow lines join the nitrogen atoms. Each kite contains one asymmetric unit.

Boiling points and melting points are evidence of the strength of the intermolecular interactions, the most obvious example being water. PDA has a much higher melting point than its isomers because of the strong hydrogen bond network. Quinolinic acid has the lowest melting point of the isomers as the strongest hydrogen bond is intramolecular.

Table 4.2.3. Melting points of the isomers of PDA.

| Isomer | Melting Point. °C. |
|---|---|
| Pyridine-2,3-dicarboxylic acid (quinolinic acid) | 188 |
| Pyridine-2,4-dicarboxylic acid monohydrate | 247 |
| Pyridine-2,5-dicarboxylic acid (isochinomeric acid) | 256 |
| Pyridine-2,6-dicarboxylic acid (dipicolinic acid) monohydrate | 249 |
| Pyridine-3,4-dicarboxylic acid (cinchomeric acid) | 262 |
| Pyridine-3,5-dicarboxylic acid (dinicotinic acid, PDA) | >300 |

*The melting points have been taken from the Lancaster catalogue, 1997-1999.

The mean separation between the planes of molecules is 3.221(7)Å, corresponding to half of the c-axis. There are no π-π stacking interactions in this structure. The molecules form a mesh and the molecules in the next plane lie above the gaps in the mesh (figure 4.2.7). The rings in each plane are puckered at an angle of 12.5º with respect to their neighbours.

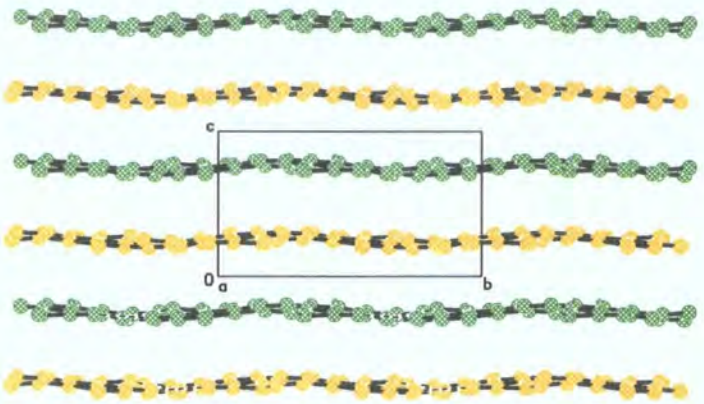


Figure 4.2.6. Packing diagram viewed along the a-axis. The layers are coloured alternately yellow and green. There are no visible strong interactions between the molecular layers.

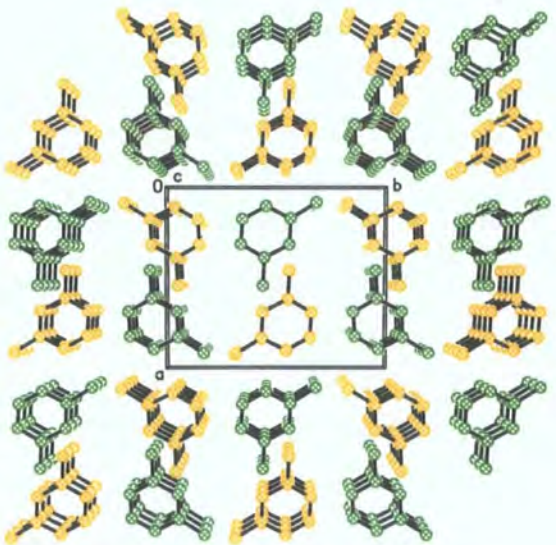


Figure 4.2.7. Packing diagram viewed along the c-axis, perpendicular to the molecular sheets. The layers are coloured in the same way as in figure 4.2.6. Hydrogen and oxygen atoms have been omitted for clarity. It can be seen how the molecules fit in the gaps left by the hydrogen-bonded rings of the layers above and below.

## 4.3. Deuteration of PDA

Pyridine-3,5-dicarboxylic acid has been crystallised hydrothermally from deuterated water to exchange the carboxylic acid protons for deuterons. Neutron diffraction data were collected on D9 at the I.L.L. at room-temperature, 150K and 15K.

### 4.3.1. Deuteration Effects

A hydrogen atom is made up of one proton and one electron and a deuterium atom is made up from one proton, one electron and one neutron. A deuterium atom has twice the mass of hydrogen atom but has the same electronic properties.

Deuteration of hydrogen bonds is used to probe different energy levels in the potential energy well. As deuterium is heavier than hydrogen it will lie lower in the potential energy well, and because the chemical properties of deuterium are the same as for hydrogen the shape of the potential energy well is assumed not to change.

On deuteration of a hydrogen bond the distance between the donor and acceptor atoms is often seen to increase (Robertson and Ubbelohde, 1939) though often by an amount smaller than the standard uncertainties of the bond lengths (Sakhawat Hussain and Schlemper, 1980). It is expected that the donor-acceptor distance should increase if the bond has a double minimum potential-well, and decrease for a single minimum potential well (Singh and Wood, 1969 and Ichikawa, 1978). In some cases deuteration has a very strong effect, for example in $KH_2PO_4$ the protonated structure has a tetragonal space group but the fully deuterated structure has a monoclinic space group (Nelmes et al. 1981). This proves that deuteration does change the hydrogen-bond potential energy well, although often only by a small amount.

The expectation value of the X-H bond length depends on the shape of the hydrogen-bond potential well. The X-D bond length is often shorter than the X-H bond length, but it depends entirely upon the shape of the potential well. In a harmonic potential well the hydrogen and deuteron should lie in exactly the same position.

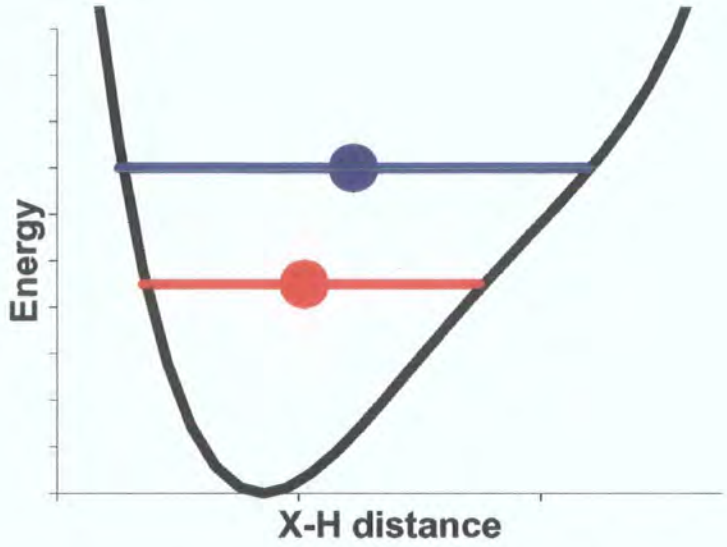


Figure 4.3.1. A hydrogen atom (blue) and a deuterium atom (red) in an asymmetric potential energy well. The deuterium atom lies lower in the well and consequently its position is closer to the minimum energy of the well, closer to the X atom.

The thermal parameters should change on substituting deuterium with hydrogen. The deuterium lies lower in the potential energy well and therefore has less room to vibrate. The change in the thermal parameters depends on the shape of the potential energy well. Hydrogen has a coherent neutron scattering length of -0.3739 fm. Deuterium has a coherent neutron scattering length of 0.6674 fm.

### 4.3.2. Changes in the structures

Pyridine-3,5-dicarboxylic acid (PDA) was recrystallised hydrothermally from deuterated water. Deuterated pyridine-3,5-dicarboxylic acid (DDA) was found to be isostructural with PDA. Upon refinement of the neutron diffraction data it was discovered that the two carboxylic acid protons had been 92% deuterated and that two of the hydrogen atoms attached to the pyridyl ring had become 49% deuterated. The hydrogen atom at the four position in the pyridyl ring had not been altered at all.

The cell parameters have increased slightly upon deuteration. The difference is much greater between the room temperature cell dimensions than the 15K cell dimensions (tables 4.3.1 and 4.3.2). The temperature dependence of the cell is larger in the deuterated structure and has opposite sign for the a-axis (table 4.3.3).

Table 4.3.1. Room Temperature Cell Dimensions.

| | a (Å) | b (Å) | c (Å) | beta (°) | Volume (Å$^3$) |
|---|---|---|---|---|---|
| Protonated | 9.6986(7) | 11.1571(8) | 6.5891(6) | 107.804(5) | 678.85(9) |
| Deuterated | 9.7614(10) | 11.2243(12) | 6.6430(8) | 108.304(2) | 691.02(13) |
| *Difference* | *+ 0.0628* | *+ 0.0672* | *+ 0.0539* | *+ 0.500* | *+ 12.17* |

Table 4.3.2. 15K Cell Dimensions

| | a (Å) | b (Å) | c (Å) | Beta (°) | Volume (Å$^3$) |
|---|---|---|---|---|---|
| Protonated | 9.7116(13) | 11.1347(17) | 6.4421(13) | 108.596(10) | 660.25(19) |
| Deuterated | 9.7196(10) | 11.1396(11) | 6.4540(6) | 108.754(8) | 661.69(11) |
| *Difference* | *+ 0.0080* | *+ 0.0049* | *+ 0.0119* | *+ 0.158* | *+ 1.44* |

Table 4.3.3. Changes in the cell parameters between 296K and 15K.

| | a (Å) | b (Å) | c (Å) | Beta (°) | Volume (Å$^3$) |
|---|---|---|---|---|---|
| Protonated | - 0.0130 | + 0.0224 | + 0.1470 | - 0.765 | + 18.6 |
| Deuterated | + 0.0418 | + 0.0847 | + 0.1890 | - 0.450 | + 29.33 |

There are no significant differences in the intramolecular bond lengths upon deuteration. The hydrogen bonds do change significantly. In both of the strong hydrogen bonds the D-H distance decreases and the H···A distance and the D···A distance increase upon deuteration.

Table 4.3.4. Changes in the strong hydrogen bonds at room temperature.

| | D···A (Å) | D-H/D (Å) | H/D···A (Å) | D-H/D-A (°) |
|---|---|---|---|---|
| O1-H4···O3 | 2.591(3) | 1.004(5) | 1.608(5) | 165.0(5) |
| O1-D4···O3 | 2.640(3) | 0.993(3) | 1.678(3) | 162.1(3) |
| *Difference* | *+ 0.049* | *- 0.011* | *+ 0. 070* | *- 2.9* |
| O4-H5···N1 | 2.525(3) | 1.218(6) | 1.308(6) | 177.9(6) |
| O4-D5···N1 | 2.564(3) | 1.108(4) | 1.457(4) | 177.6(4) |
| *Difference* | *+ 0.039* | *- 0.110* | *+ 0.149* | *- 0.3* |

The increase in the distance between the donor and acceptor atoms in the strong hydrogen bonds upon deuteration can account for the changes in the unit cell dimensions in the ab-plane.

The O···O hydrogen bond lies almost parallel to the a-axis and the N···O hydrogen bond is approximately 30° from the b-axis and both lie approximately in the ab-plane (figure 4.3.2.).

The N···O hydrogen bonds connect the molecules in series in chains along the b-direction (figure 4.3.2). The change in length of the b-axis (0.0672Å) is approximately double the projection of the change in the N···O separation onto the b-axis (2 * 0.039Å * cos30° = 0.0675Å).

The O···O hydrogen bonds connect the molecular chains in parallel. The change in the length of the b-axis (0.0628) is slightly greater than the change in the O···O separation (0.049Å).

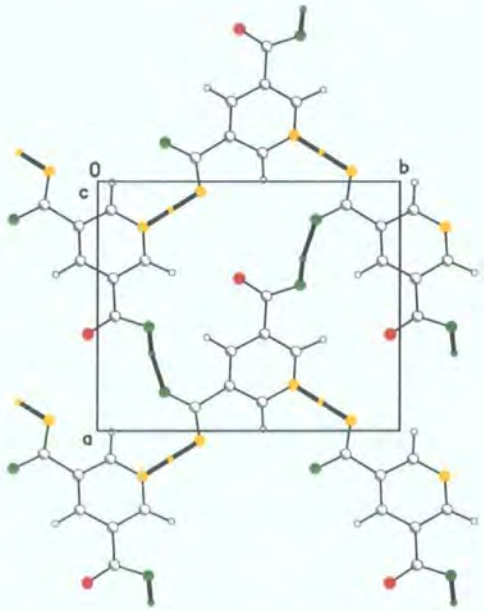


Figure 4.3.2. The strong hydrogen bonds in the unit cell. The atoms in the O-H···O hydrogen bonds are coloured yellow. The atoms in the N-H···O hydrogen bonds are coloured green.

The change in the D-H distances can be explained by an asymmetric hydrogen bond potential well (figure 4.3.1). The heavier deuterium lies lower in the potential energy well than the lighter hydrogen, therefore closer to the minimum energy of the potential well.

The C···O distances in the C-H···O hydrogen bonds have all increased slightly, this is probably due to the changes in the strong hydrogen bonds which push the molecules further apart. There are no differences in the C-H bond distances although the estimated standard deviations are large, especially on the 49% deuterated hydrogen atoms which have small net scattering-length.

## 4.4. Experimental Details

### X-ray Experiment

The X-ray diffraction experiment was performed using a Bruker-SMART diffractometer and the crystal was cooled using a Oxford Cyrosystems nitrogen flow cryostream. All non-hydrogen atom anisotropic thermal parameters were refined. All hydrogen atoms were refined with isotropic thermal parameters.

### Neutron Experiments

The neutron diffraction data were collected on the diffractometer D9 at the ILL. D9 is a four-circle diffractometer equipped with a small position sensitive detector. The incident beam was filtered using an erbium filter to remove lambda/2 contamination. A copper (220) monochromator was used to give a wavelength of 0.8404Å.

### PDA, Room Temperature

A thin transparent pale brown crystal of dimension 1.7 * 1.4 * 0.2 mm was mounted on the diffractometer D9. Data were collected at room temperature up to $\theta$=35º and some reflections up to $\theta$=40º (ILL programs HKLGEN and MAD). The data were corrected for absorption using the program DATAP (Coppens, 1970, $\mu$=0.096mm$^{-1}$, maximum transmission=0.981, minimum transmission=0.903).

### PDA, 15K

After the room temperature experiment, the crystal was cooled to 15K using a Displex cryorefrigerator whilst monitoring the strong 0 0 2 reflection. Data were collected up to $\theta$=35º. The data were corrected for absorption by the crystal ($\mu$=0.096mm$^{-1}$, maximum transmission=0.981, minimum transmission=0.906) and by the vanadium and aluminium heat shields ($\mu$=0.0251mm$^{-1}$, maximum transmission=0.9753, minimum transmission=0.9717).

### DDA, Room Temperature

A pale brown crystal of dimension 2.7 * 1.5 * 0.9 mm$^3$ was mounted on the diffractometer D9 at the ILL. Data were collected at room temperature, 150K and 15K. The wavelength used was 0.8406Å.

Data were collected up to $\theta$=35º. The data were corrected for absorption by the crystal using the program DATAP (Coppens, 1970), ($\mu$=0.054mm$^{-1}$, maximum transmission=0.9569, minimum transmission=0.9148), and by the vanadium and aluminium heat shields ($\mu$=0.0251mm$^{-1}$, maximum transmission=0.9752, minimum transmission=0.9708), which were used to prevent exchange of deuterium from the crystal with hydrogen from the atmosphere. During the data collection a piece of extra crystal was identified and indexed.

The intensity from the extra crystal was less than 10% of the intensity of the main crystal, and as it affected only a few reflections it was ignored and the affected reflections were omitted from the refinement. Structure refinement using SHELX-97 gives R1(I>4σ)=7.38% and wR2(all data)=15.30%.

Table 4.4.1. PDA Crystal Parameters

| Formula | $C_7H_5O_4N$ | Formula Weight | 167.12 |
|---|---|---|---|
| Crystal System | Monoclinic | Space Group | $P2_1/c$ |
| Z | 4 | Density | 1.634 |

**DDA, 15K**

After the structural refinement for the room temperature data was adequate the crystal was cooled to 15K using a Displex cryorefrigerator, whilst monitoring the strong 0 0 2 reflection. Data were collected up to θ=35º. The data were corrected for absorption by the crystal (maximum transmission=0.957, minimum transmission=0.9163) and the heat shields (maximum transmission=0.9752, minimum transmission=0.9700).

**DDA, 150K**

After the data collection for the 15K data was completed the crystal was warmed to 150K whilst collecting data form the 1 2 0 and 2 4 0 reflections. These reflections were chosen as the ones most sensitive to the deuterium position. Data were collected up to θ=35º. The data were corrected for absorption by the crystal (maximum transmission=0.957, minimum transmission=0.9177) and the heat shields (maximum transmission=0.9752, minimum transmission=0.9708).

At the end of the experiment the crystal was warmed to room temperature whilst collecting data on the 1 2 0 and 2 4 0 reflections.

**DDA, Refinement**

The occupation factor of the deuterium atoms D4 and D5, was refined and then fixed at 0.88% for all refinements. This is equivalent to refining the percentage deuteration. From this the H4 and H5 were found to be 92.3% deuterium and 7.7% hydrogen.
Unfortunately H1 and H3 also have become partially deuterated this is a side effect of the hydrothermal method of crystallisation. H1 and H3 refined to be 48.7% deuterium and 51.3% hydrogen, this disorder causes the s.u.'s of the bond lengths and angle to these atoms to be about 4 times larger.

Table 4.4.2. DDA Crystal Parameters

| | | | |
|---|---|---|---|
| Formula | $C_7H_{2.18}D_{2.82}O_4N$ | Formula Weight | 169.94 |
| Crystal System | Monoclinic | Space Group | $P2_1/c$ |
| Z | 4 | Density | 1.610 |

Table 4.4.data. Data collection and refinement details for PDA and DDA.

| | PDA | PDA | PDA | DDA | DDA | DDA |
|---|---|---|---|---|---|---|
| Diffractometer | Bruker SMART | D9 | D9 | D9 | D9 | D9 |
| Temperature (K) | 100 | 296 | 15 | 296 | 150 | 15 |
| Radiation | X-ray Mo-Kα | Neutron | Neutron | Neutron | Neutron | Neutron |
| Wavelength (Å) | 0.71073 | 0.8404 | 0.8404 | 0.8406 | 0.8406 | 0.8406 |
| a (Å) | 9.7368(16) | 9.6986(7) | 9.7116(13) | 9.7614(10) | 9.7210(10) | 9.7196(10) |
| b (Å) | 11.1592(18) | 11.1571(8) | 11.1347(17) | 11.2243(12) | 11.1545(13) | 11.1396(11) |
| c (Å) | 6.4908(11) | 6.5891(6) | 6.4421(13) | 6.6430(8) | 6.5112(8) | 6.4540(6) |
| beta (°) | 108.468(9) | 107.804(5) | 108.595(10) | 108.3035(19) | 108.397(9) | 108.754(8) |
| Volume ($Å^3$) | 668.94(19) | 678.85(9) | 660.25(19) | 691.02(13) | 669.94(13) | 661.69(11) |
| No. of reflections for cell parameters | 954 | 303 | 510 | 815 | 834 | 1163 |
| θ Range (°) | 12.77 – 26.27 | 4.27 – 32.75 | 4.14 – 35.06 | 3.63 – 34.91 | 3.74 – 35.14 | 3.91 – 35.93 |
| μ ($mm^{-1}$) | 0.139 | 0.096 | 0.096 | 0.054 | 0.054 | 0.054 |
| Crystal Shape | Plate | Plate | Plate | Plate | Plate | Plate |
| Crystal Colour | Colourless | Colourless | Colourless | Pale yellow | Pale yellow | Pale yellow |
| Crystal Dimensions | 0.35*0.2*0.1 | 1.7*1.5*0.2 | 1.7*1.5*0.2 | 2.7*1.5*0.9 | 2.7*1.5*0.9 | 2.7*1.5*0.9 |
| Absorption Correction | None | Integration, DATAP | Integration, DATAP. | Integration, DATAP | Integration, DATAP | Integration, DATAP |
| T min | - | 0.903 | 0.906 | 0.915 | 0.917 | 0.916 |
| T max | - | 0.981 | 0.981 | 0.957 | 0.957 | 0.957 |
| No. of reflections | 7723 | 2065 | 1812 | 1677 | 1497 | 2116 |

Table 4.4.data. *continued.*

| | PDA | PDA | PDA | DDA | DDA | DDA |
|---|---|---|---|---|---|---|
| Temperature (K) | 100 | 296 | 15 | 296 | 150 | 15 |
| Independent reflections | 1775 | 1806 | 1670 | 1503 | 1346 | 1792 |
| No. of reflections I>2σ(I) | 1581 | 1117 | 1335 | 1182 | 1189 | 1635 |
| Parameters | 129 | 155 | 155 | 156 | 156 | 156 |
| Completeness to θ max | 0.994 | 0.598 | 0.886 | 0.824 | 0.742 | 0.949 |
| R int | 0.0611 | 0.0154 | 0.0174 | 0.0141 | 0.0130 | 0.0123 |
| R sigma | 0.0322 | 0.0933 | 0.0707 | 0.0468 | 0.0400 | 0.0342 |
| θ max (°) | 29.00 | 42.96 | 35.93 | 34.85 | 35.20 | 35.96 |
| h | -13 → 13 | -13 → 12 | -13 → 12 | -7 → 13 | -7 → 13 | -7 → 13 |
| k | -14 → 15 | -15 → 7 | -15 → 7 | -10 → 15 | -10 → 15 | -15 → 15 |
| l | -8 → 8 | -8 → 8 | -8 → 8 | -8 → 8 | -8 → 8 | -8 → 8 |
| $R[F^2> 2\sigma(F^2)]$ | 0.0464 | 0.0599 | 0.0601 | 0.0738 | 0.0547 | 0.0592 |
| $wR(F^2)$ | 0.1291 | 0.1015 | 0.0992 | 0.1530 | 0.1501 | 0.1788 |
| S | 1.084 | 1.095 | 1.282 | 1.617 | 1.475 | 1.863 |
| Qmax* | 0.530 | 0.643 | 1.195 | 0.731 | 0.816 | 1.039 |
| Qmin* | -0.259 | -0.649 | -0.969 | -0.624 | -0.736 | -1.051 |
| RMS Q* | 0.070 | 0.165 | 0.230 | 0.174 | 0.183 | 0.276 |
| Shift | 0.000 | 0.000 | 0.000 | 0.000 | 0.000 | 0.000 |

* The units of Q, the residual unmodelled density, are $eÅ^{-3}$ for X-rays and fm $Å^{-3}$ for neutrons.

## 4.5. Temperature Dependence in Pyridine-3,5-dicarboxylic acid

### 4.5.1. The Unit Cell

The main change in the cell dimensions is in the c-direction. This is perpendicular to the molecular planes and the direction where there are no strong intermolecular interactions. In the fully protonated pyridine-3,5-dicarboxylic acid (PDA) the a and b cell dimensions change little, the a-axis even increases as the temperature is lowered. However the co-efficient thermal expansion of the volume is positive. In deuterated pyridine-3,5-dicarboxylic acid (DDA) the cell dimensions decrease much more, the high temperature values are much larger compared to PDA but they converge to very similar values to PDA at 15K.

Table 4.5.1. The cell dimensions in PDA.

| | a (Å) | b (Å) | c (Å) | beta (°) | Volume (Å$^3$) |
|---|---|---|---|---|---|
| 296K | 9.6986(7) | 11.1571(8) | 6.5891(6) | 107.804(5) | 678.85(9) |
| 100K – X-ray | 9.7368(16) | 11.1592(18) | 6.4908(11) | 108.468(9) | 668.94(19) |
| 15K | 9.7116(13) | 11.1347(17) | 6.4421(13) | 108.596(10) | 660.25(19) |

Table 4.5.2. The cell dimensions in DDA.

| | a (Å) | b (Å) | c (Å) | Beta (°) | Volume (Å$^3$) |
|---|---|---|---|---|---|
| 296K | 9.7614(10) | 11.2243(12) | 6.6430(8) | 108.304(2) | 691.02(13) |
| 150K | 9.7210(10) | 11.1545(13) | 6.5112(8) | 108.397(9) | 669.94(13) |
| 15K | 9.7196(10) | 11.1396(11) | 6.4540(6) | 108.754(8) | 661.69(11) |

Table 4.5.3. Changes in the cell parameters between 296K and 15K.

| | a (Å) | b (Å) | c (Å) | Beta (°) | Volume (Å$^3$) |
|---|---|---|---|---|---|
| Protonated | - 0.0130 | + 0.0224 | + 0.1470 | - 0.765 | + 18.6 |
| Deuterated | + 0.0418 | + 0.0847 | + 0.1890 | - 0.450 | + 29.33 |

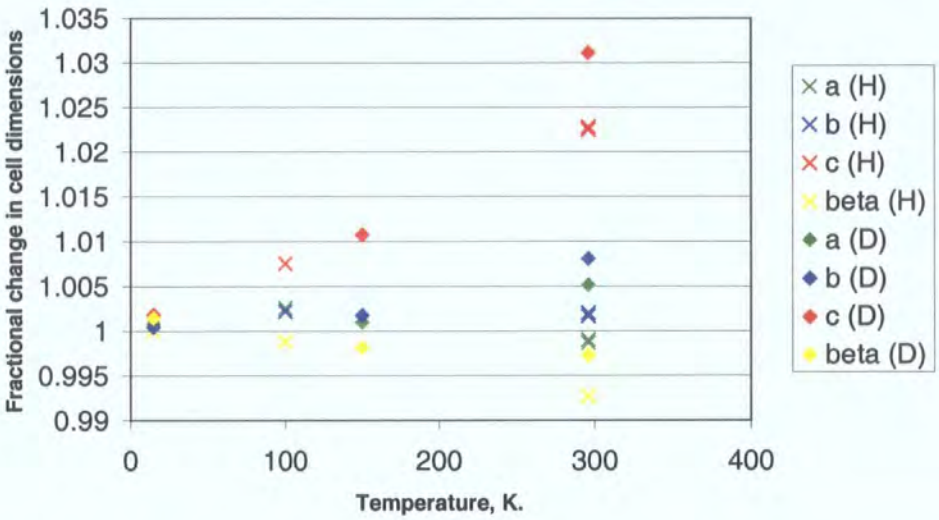


Graph 4.5.1. Fractional change in the cell dimensions from the 15K fully protonated values over the temperature range. The cell dimensions from PDA are marked by crosses and the cell dimensions in DDA are marked by diamonds.

### 4.5.2. Temperature Dependence of the Thermal Parameters

The thermal parameters of the hydrogen/deuterium atoms are slightly unreliable because of the partial deuteration. The thermal parameters decrease approximately linearly with temperature. The magnitude of the thermal parameters of an atom reflects the position of the atom in the molecule. Carbon and nitrogen in the pyridyl ring have the smallest Ueq, while oxygen and hydrogen and the ends of carboxylic acid groups have larger Ueq (graph 4.5.2).

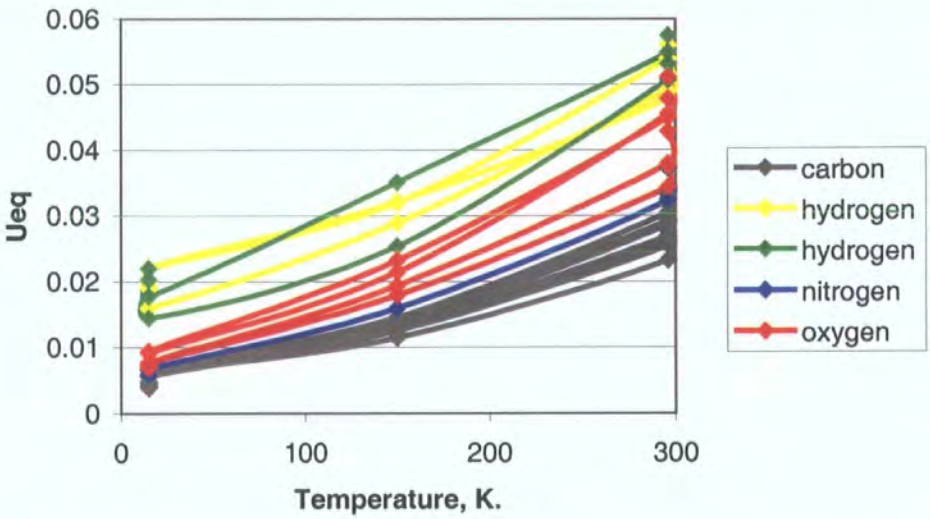


Graph 4.5.2. The temperature dependence of Ueq, measured in $Å^2$. The green line indicates the hydrogen atoms in the strong hydrogen bonds. The yellow line indicates the pyridyl hydrogen atoms.

There is good agreement between the hydrogen and deuterium thermal parameters (graph 4.5.3). There should be no change in the thermal parameters for the carbon, nitrogen and oxygen atoms upon deuteration. The thermal parameters in DDA are consistently larger than those in PDA at 296K and 15K, this could be due to the higher absorption in PDA.

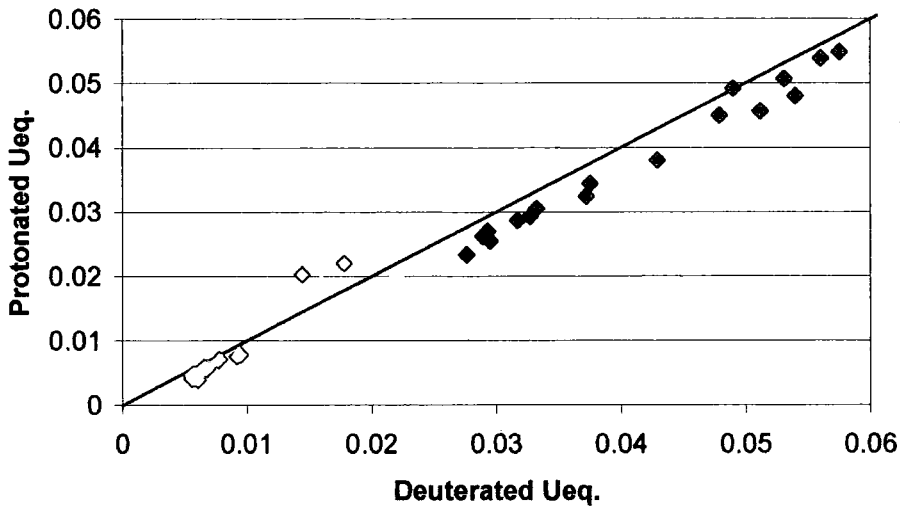


Graph 4.5.3. The differences between the thermal parameters in PDA and DDA. The blue points are the thermal parameters at 296K. The red points are the thermal parameters at 15K. The green points mark the carboxylic acid hydrogen atoms at 15K and the yellow points mark the pyridyl hydrogen atoms at 15K. The black line marks lies on x=y.

Thermal parameters of the deuterated carboxylic acid hydrogen atoms are significantly smaller at 15K. The high temperature thermal parameters are identical. At low temperature the thermal motion should be entirely dependent on the shape of the hydrogen bond potential energy well. The deuterium atom, which lies lower in the well, should have less motion. The difference in the magnitudes should provide information on the shape of the potential energy well.

Table 4.5.4. Ueq ($Å^2$) at room temperature.

| | Hydrogen | Deuterium |
|---|---|---|
| D / H4 | 0.0507(12) | 0.0531(10) |
| D / H5 | 0.0549(13) | 0.0575(10) |

Table 4.5.5. Ueq ($Å^2$) at 15K.

| | Hydrogen | Deuterium |
|---|---|---|
| D / H4 | 0.0203(8) | 0.0145(5) |
| D / H5 | 0.0220(8) | 0.0178(5) |

### 4.5.3. Hydrogen Bond Lengths and Angles

In PDA there are two short strong hydrogen bonds, one N-H···O and one O-H···O. The N-H···O hydrogen bond exhibits exactly the same behaviour as the hydrogen bond in the 2:1 co-crystal of 4,4'-bipyridine and benzene-1,2,4,5-tetracarboxylic acid (BPTA, sections 3.4 and 3.5). The hydrogen atom is seen to be 1.3Å from the nitrogen atom and 1.2Å from the oxygen atom at room temperature and 1.2Å from the nitrogen atom and 1.3Å from the oxygen atom at low temperature. The distance between the nitrogen and oxygen atoms is identical (N···O = 2.5220(17)Å at 20K in BPTA).

In PDA the N···O distance does not change over the temperature range. In the co-crystal of pentachlorophenol and 4-methylpyridine (Steiner et al. 2001), in which a similar phenomenon is observed, the N···O separation decreases by ~0.02Å between 200K and 20K, and in BPTA the N···O separation decreases by ~0.011Å between 296K and 20K.

The O···O distance in the O1-H3···O3 hydrogen bond decreases significantly with temperature. The O-H distances increases as the O···O distance decreases which is expected (Hibbert and Emsley, 1990 and Iwasaki et al. 1967) and seen in the Cambridge Structural Database (graph 4.4.4). The H···O distance consequently decreases.

Table 4.5.6. Temperature dependence in the N1··H5··O4 hydrogen bond in PDA.

| | N1···O4 | N1···H5 | H5···O4 | N1-H5-O4 |
|---|---|---|---|---|
| 296K | 2.525(3) | 1.308(6) | 1.218(6) | 177.9(6) |
| 100K (X-ray) | 2.5266(17) | 1.18(3) | 1.36(3) | 172(3) |
| 15K | 2.523(2) | 1.213(4) | 1.311(5) | 176.4(4) |

Table 4.5.7. Temperature dependence in the O1··H4··O3 hydrogen bond in PDA.

| | O1···O3 | O1-H4 | H4···O3 | O1-H4-O3 |
|---|---|---|---|---|
| 296K | 2.591(3) | 1.004(5) | 1.608(5) | 165.0(5) |
| 100K (X-ray) | 2.5799(16) | 0.91(3) | 1.67(3) | 170(3) |
| 15K | 2.569(3) | 1.025(4) | 1.558(4) | 167.7(4) |

In DDA the temperature dependent changes in both hydrogen bonds are much more pronounced. In the N1··D5··O4 hydrogen bond the N1···O4 distance decreases by 0.026Å. At room temperature the deuterium atom lies much closer to the oxygen atom than the hydrogen atom in PDA, and at lower temperature it lies much closer to the nitrogen atom. The deuterium atom moves much further ~0.29Å compared with the hydrogen atom, H5, motion of ~0.1Å in PDA over the temperature range.

In the O1-D4···O3 hydrogen bond the O1···O3 distance decreases by 0.078Å. The deuterium atom lies slightly closer to the donor oxygen atom and the increase in the O1-H4 bond length is larger (0.029Å) than the increase in PDA (0.021Å). The changes in the O-H, H···O and O···O distances follows the trends observed in the CSD (graph 4.5.4).

At 150K, approximately midway between 15K and 296K, the hydrogen bond parameters are all closer to the low temperature parameters, which suggests that the changes are not linear with respect to temperature between 15K and 296K and that the main change in the deuterated hydrogen bond occurs above 150K.

Table 4.5.8. Temperature dependence in the N1··D5··O4 hydrogen bond in DDA.

| | N1···O4 | N1···D5 | D5···O4 | N1-D5-O4 |
|---|---|---|---|---|
| 296K | 2.564(3) | 1.457(4) | 1.108(4) | 177.6(4) |
| 150K | 2.532(3) | 1.192(4) | 1.342(4) | 176.1(4) |
| 15K | 2.538(3) | 1.151(3) | 1.389(3) | 175.9(3) |

Table 4.5.9. Temperature dependence in the O1··D4··O3 hydrogen bond in DDA.

| | O1···O3 | O1-D4 | D4···O3 | O1-D4-O3 |
|---|---|---|---|---|
| 296K | 2.640(3) | 0.993(4) | 1.678(3) | 162.1(3) |
| 150K | 2.581(3) | 1.016(3) | 1.580(3) | 167.3(3) |
| 15K | 2.562(3) | 1.021(3) | 1.553(3) | 168.5(8) |

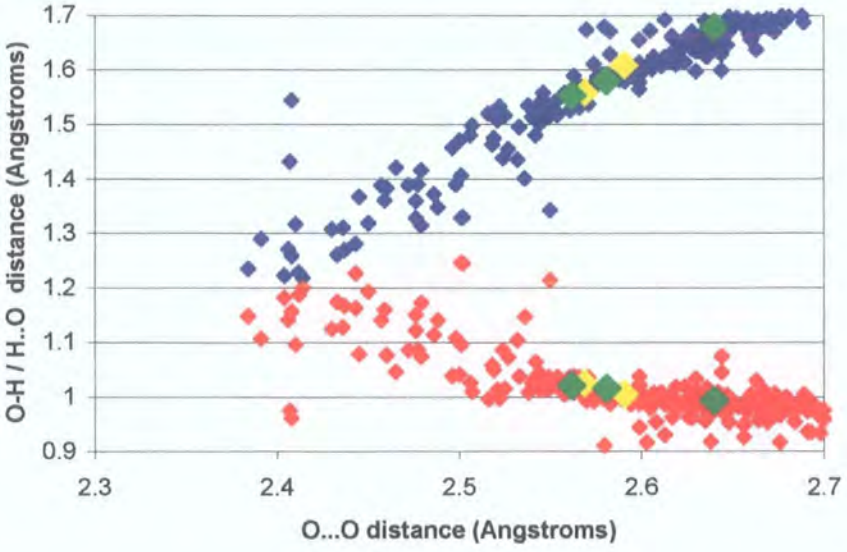


Graph 4.5.4. O-H···O hydrogen bonds from the CSD studied by neutron diffraction. The O-H distances are in red and the H···O distances are in blue. The yellow points are from PDA and the green points are from DDA.

The N··H and O··H distances in the N1··H5··O4 are unusual but they follow the general trend of observations in the CSD, although there are not very many short N···O hydrogen bonds studied by neutron diffraction in the CSD (Steiner et al, 2000).

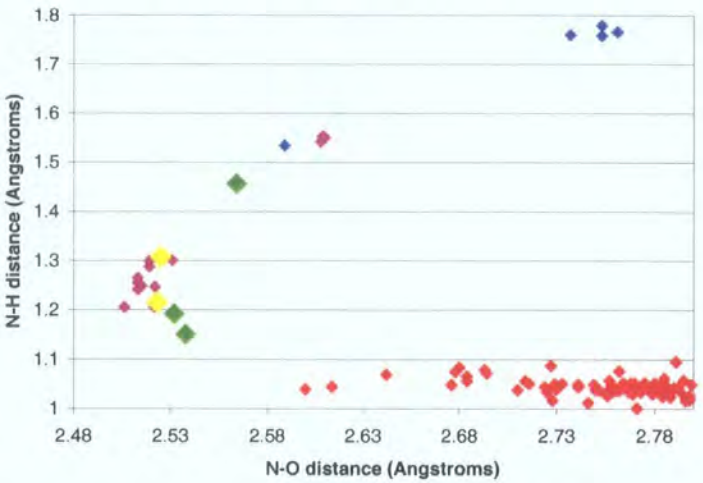


Graph 4.5.5. N-H···O and O-H···N hydrogen bonds from the CSD studied by neutron diffraction. The red points mark N-H···O hydrogen bonds and the blue points mark O-H···N hydrogen bonds. The yellow points are the measurements from PDA and the green points are the measurements from DDA. The purple points are taken from the previous chapter and Steiner et al. (2001).

### 4.5.4. X-ray Diffraction Derived Difference Fourier Map

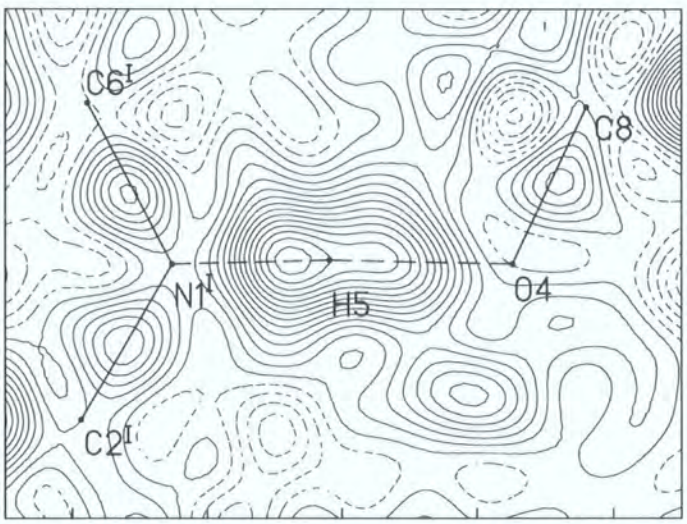


Figure 4.5.1. Difference Fourier map calculated from the 100K X-ray data. Contours are at 0.05eÅ$^{-3}$. Negative contours indicate holes. The shape of the peak is very similar to those observed in BPTA (Section 3.5).

### 4.5.5. Neutron Fourier Maps

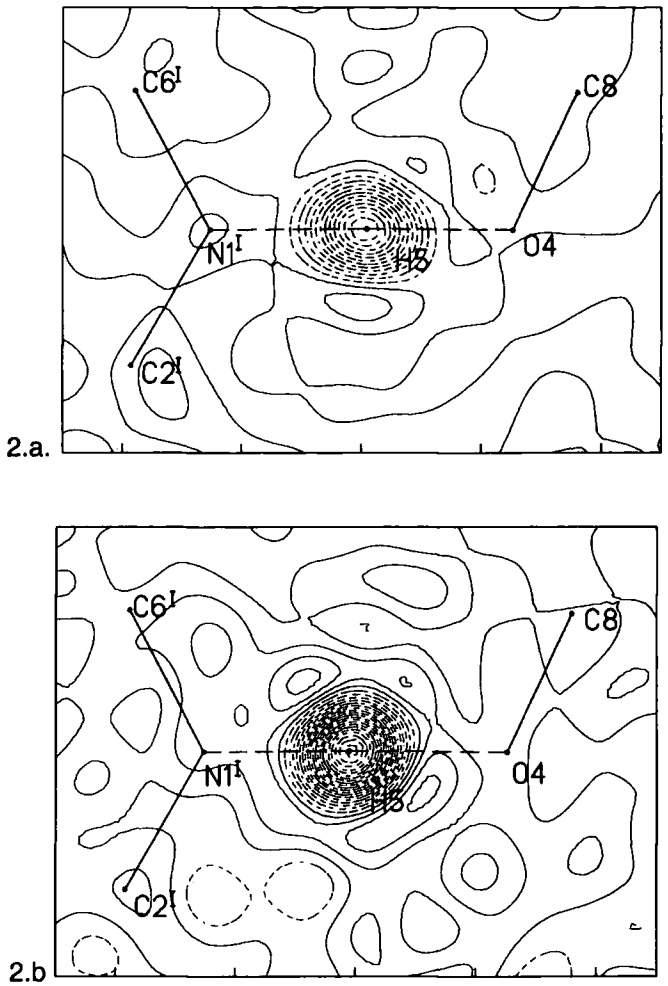


Figures 4.5.2.a and 4.5.2.b. Difference Fourier maps calculated from the neutron data on the protonated sample on omitting H5. H5 has been replaced for the diagram. The contours are at nuclear scattering density of 1 fmÅ$^{-3}$. Dashed lines indicate negative contours. The top diagram (a) is at room temperature, the lower diagram (b) is at 15K.

As in BPTA (section 3.5) disorder in the hydrogen bond, which can not be ruled out by the X-ray diffraction results, is ruled out by the neutron diffraction difference Fourier maps.

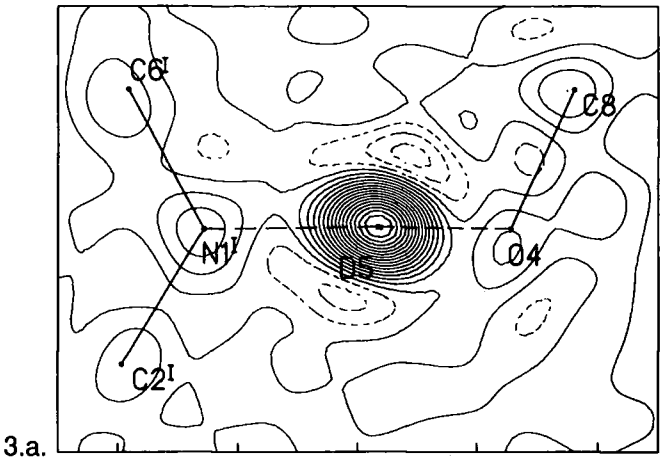


3.a.

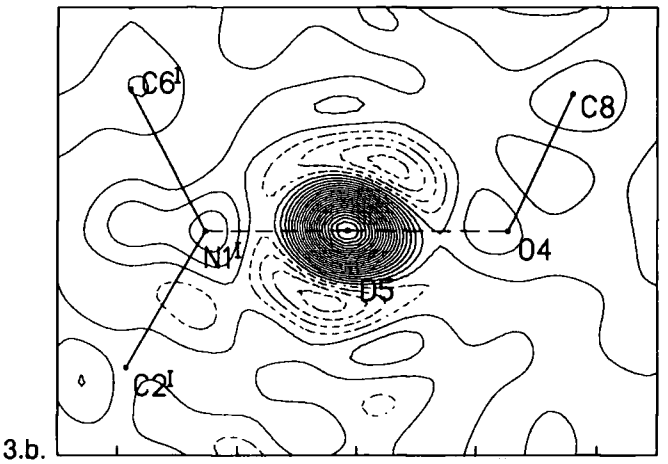


3.b.

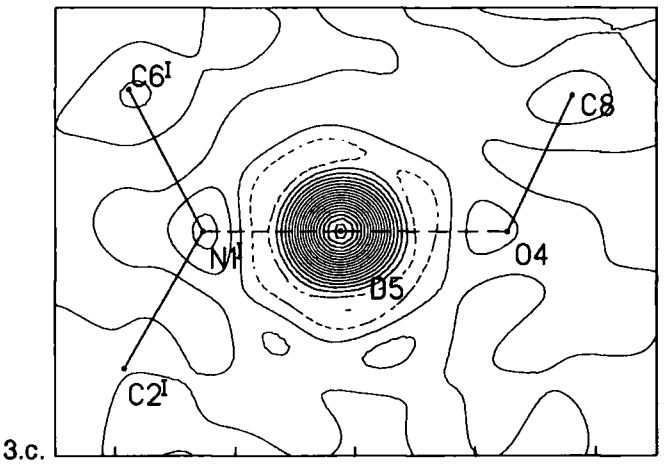


3.c.

Figures 4.5.3.a, 4.5.3.b and 4.5.3.c. Difference Fourier maps calculated from the deuterated structures on omitting D5, which has been replaced in the diagrams. The contours in a and b are at nuclear scattering density of 1 fm $Å^{-3}$ and the contours in c are at 2 fm $Å^{-3}$. (a) is from the room temperature data, (b) is from the 150K data and (c) is from the 15K data. Dashed lines indicate negative contours.

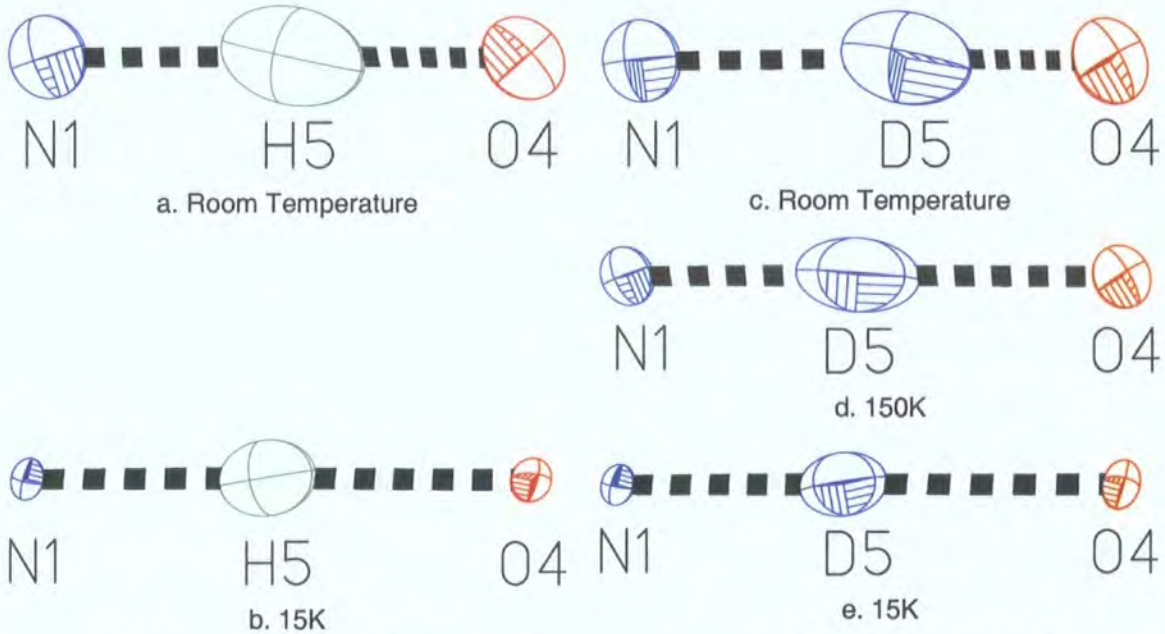


Figures 4.5.4.a, b, c, d and e. 50% thermal-ellipsoid plots of the hydrogen bond from the neutron data. (a) and (b) are taken from the PDA and (c), (d) and (e) are taken from DDA.

The thermal parameters are well defined and show no evidence of excessive distortion, which could indicate disorder, along the N···O direction.

### 4.5.6. Other Bond Lengths and Angles

The bond lengths and angles do not change significantly with temperature (graph 4.5.6). The only major change is in the O4-H5 bond length.

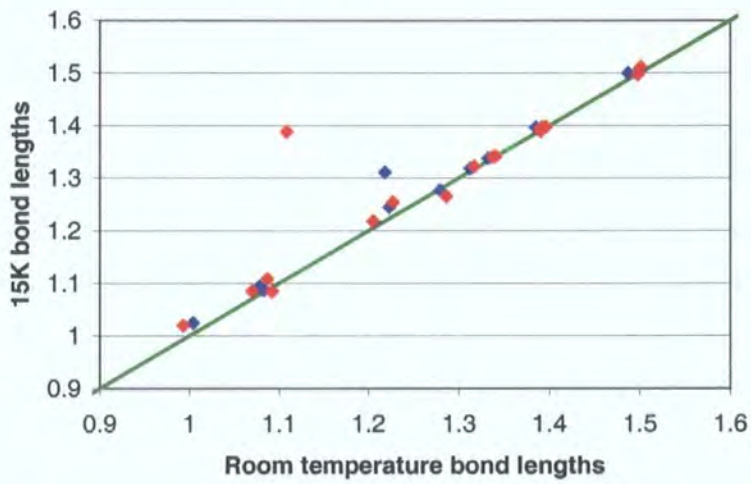


Graph 4.5.6. The bond lengths at 15K and 296K in Å. The green line corresponds to no change. The blue points are from PDA and the red points are from DDA. The two points furthest from the green line are the O4-H5 / D5 distances.

The hydrogen bond changes from an approximately O-H···N hydrogen bond between a carboxylic acid group and a pyridyl at room temperature, to an approximately $N\text{-}H^{+}\cdots O^{-}$ hydrogen bond between a carboxylate and a pyridinium at 15K. The C8-O4 distance is therefore expected to decrease with temperature and the C2-N1-C6 angle is expected to increase. The C2-N1-C6 angle and the C8-O4 bond length are parameters that should be most effected by the change in the N1··H/D5··O4 hydrogen bond. The C8-O4 bond length does not change in PDA, and the bond angle changes by 5σ. In DDA the changes are, as always, more pronounced, the C8-O4 bond angle decreases by 0.02Å (>6σ) from the room temperature value and the bond angle increases by 2.06° (>13σ). This agrees with the greater changes in the hydrogen bond in DDA.

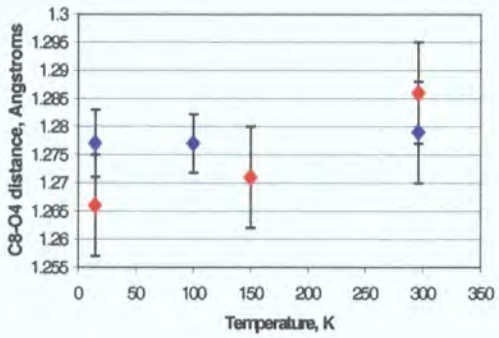


7.a

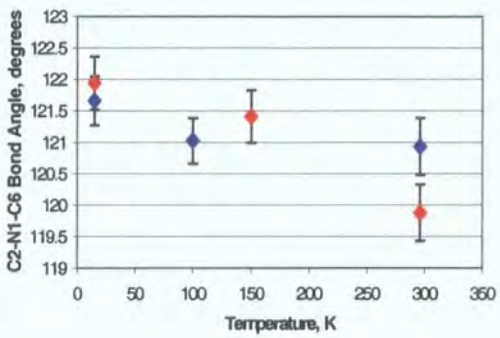


7.b

Graphs 4.5.7.a. and 4.5.7.b. Temperature dependence of (a) the C8-O4 distance and (b) the C2-N1-C6 angle. The red points are from DDA and the blue points are from PDA. The error bars are at 3 s.u's.

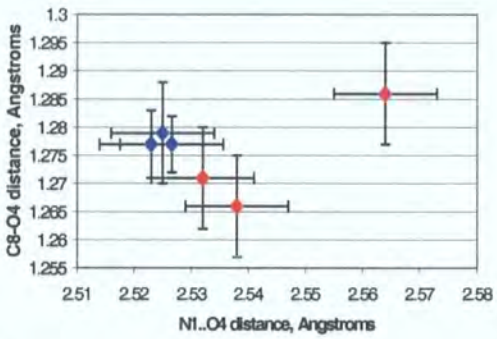


8.a

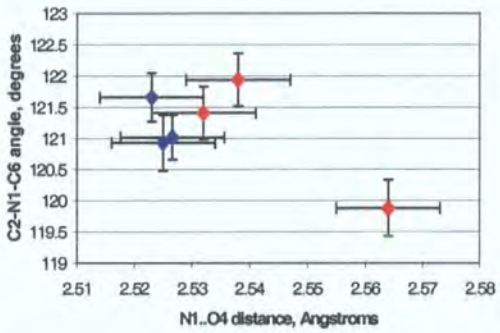


8.b

Graphs 4.5.8.a. and 4.5.8.b. The C8-O4 distance (a) and the C2-N1-C6 angle (b) compared to the N1···O4 distance. The red points are from DDA and the blue points are from PDA. The error bars are at 3 s.u's.

In the graphs comparing the N···O distance to the C8-O4 distance and the C2-N1-C6 angle (graphs 4.5.8.a and 4.5.8.b) the low temperature measurements for PDA and DDA all lie in a cluster, while the room temperature lies separately. The same trend is observed in the graph of N···O distance and N-H distance (graph 4.5.5), with the PDA points in between the room temperature DDA point and the low temperature DDA points.

## 4.6. Proton Migration in Hydrogen bonds

In two very similar short N··H··O hydrogen bonds we have observed the same temperature dependent behaviour. At high temperature the hydrogen atom is closer to the oxygen atom and on lowering the temperature the hydrogen atom moves across the hydrogen bond to lie, at low temperatures, closer to the nitrogen atom. These hydrogen bonds, along with the one between pentachlorophenol and 4-methylpyridine (PCP·4MP) studied by Steiner et al. (2001), are by far the shortest N···O hydrogen bonds studied by neutron diffraction. In PCP·4MP the hydrogen atom in the hydrogen bond is also observed to change position with temperature.

### 4.6.1. O-H··O bonds

Short O-H···O hydrogen bonds have been studied much more frequently by neutron diffraction than short N-H···O / O-H···N hydrogen bonds (Steiner et al. 2000) and the dependence of the hydrogen bond parameters on temperature and deuteration has been studied.

Pyridine-2,3-dicarboxylic acid (quinolinic acid) contains a short intramolecular hydrogen bond (Takasagawa et al. 1973a) between a carboxylic acid and a carboxylate group (similar to those discussed in section 3.11). Neutron diffraction studies of the protonated form (Takasagawa and Koetzle, 1978) and the deuterated form (Takasagawa and Koetzle, 1979) show opposite effects to those observed in PDA. Upon deuteration the O-H distance in the hydrogen bond increases by ~0.02Å and the O···O distance decreases marginally. The O-H distance increases on lowering the temperature by ~0.01Å and the O-D distance also increases but by ~0.004Å. A very similar, but slightly larger, effect has been observed in lithium hydrogen phthalate monohydrate (Küppers et al. 1985) where the hydrogen atom moves by 0.038Å and a deuterium atom by 0.028Å towards the centre of the hydrogen bond on lowering the temperature from 298K to 15K (35K for the deuterated structure).

Urea phosphoric acid, which contains a short intermolecular O-H···O hydrogen bond, has been studied at twelve different temperatures between 150K and 335K (Wilson, 2001). The hydrogen atom position is observed to change with respect to the temperature. At high-temperatures the proton is observed to lie in the centre of the hydrogen bond, and moves by 0.035Å over the temperature range to lie closer to the urea molecule at low temperature.

### 4.6.2. N··H··O Hydrogen Bonds

The 1:1 salt of 4,4'-bipyridinium and squaric acid (Reetz et al. 1994) a temperature dependent phase change, in which the colour of the crystal changes from yellow to red, is observed at 150°C. The structure is very similar to the 1:1 salt of 4,4'-bipyridinium and

benzene-1,2,4,5-tetracarboxylic acid (section A.4, figure A.9.12.a). The N···O distances of 2.613(3)Å and 2.602(3)Å are quite long, and increase by ~0.03Å upon deuteration. The phase change has been related to proton transfer across the short hydrogen bond. There are no neutron diffraction data available on this compound to confirm the hydrogen atom positions.

In the crystal structure of PCP·4MP a short N-H···O hydrogen bond is formed with a N···O separation of 2.506(2)Å at 20K (Steiner et al. 2001). From neutron diffraction data collected between 20K and 200K the proton is observed to migrate across the hydrogen bond in an identical way to that observed in the 2:1 co-crystal of 4,4'-bipyridine and benzene-1,2,4,5-tetracarboxylic acid (BPTA) and pyridine-3,5-dicarboxylic acid (PDA). At 200K the hydrogen atom is 1.228(11)Å from the oxygen atom and 1.306(11)Å from the nitrogen, and at 20K it has moved to be 1.309(7)Å from the oxygen atom and 1.206(6)Å from the oxygen.

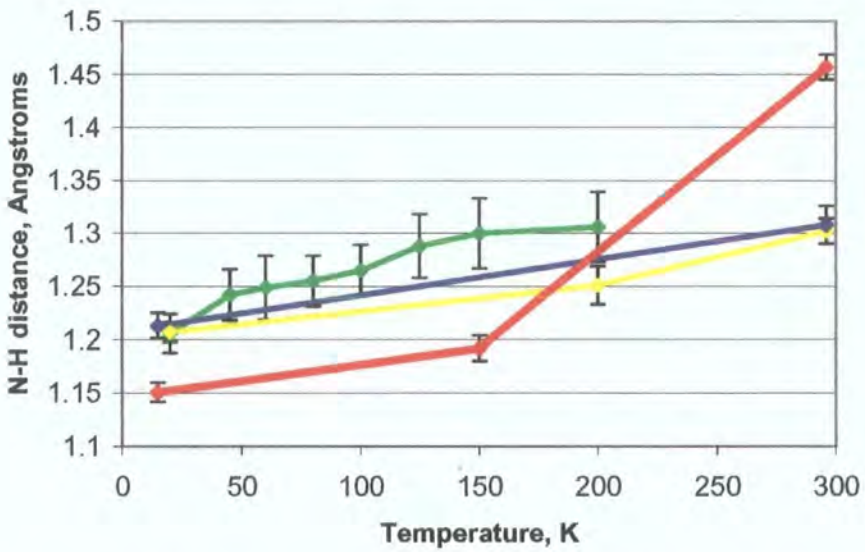


Graph 4.6.1. Temperature dependence of the N-H distance in short N··H··O hydrogen bonds. The green marks PCP·4MP, the yellow marks BPTA, the blue marks PDA and the red marks DDA. The lines are to associate the points and not to predict the intermediate values. The error bars are at 3 s.u's.

The magnitudes of the hydrogen atom migration are about ~0.1Å in PCP·4MP, PDA and BPTA. The migration takes place below 200K in PCP·4MP (green line in graph 4.6.1), with the proton lying equidistant from the nitrogen and the oxygen at ~90K. The migration seems to occur over the whole temperature range in BPTA (yellow) although there is only one measurement at an intermediate temperature. There are no intermediate temperature measurements for PDA. The deuterium atom position in DDA changes by ~0.3Å over the temperature range and most of the migration takes place above 150K.

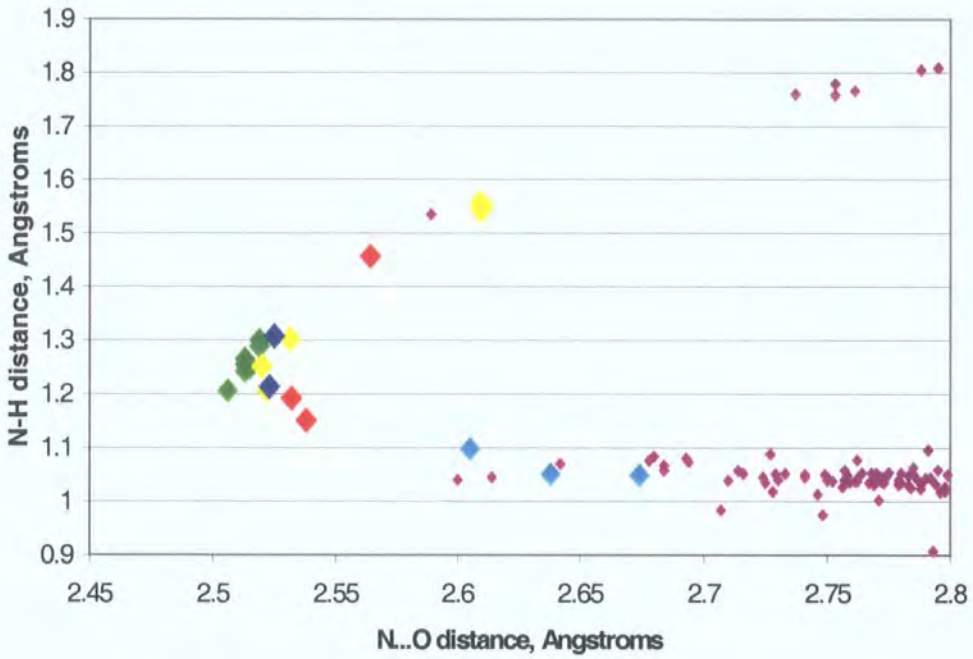


Graph 4.6.2. N···O hydrogen bonds measured by neutron diffraction from the CSD, this work and PCP·4MP. The colour coding is as in graph 4.6.1. The pale blue points are from the 1:1 and the 1:2 co-crystals of 4,4'-bipyridine and benzene-1,2,4,5-tetracarboxylic acid (sections A.2 and A.3). The small purple points are the CSD data.

The shortest intermolecular O-H···O hydrogen bonds have a O···O distance of ~2.38Å (graph 4.2.1) where the O-H and H···O distances are both ~1.2Å. Graph 4.6.2 suggests that the lower limit for straight intermolecular N···O hydrogen bonds is an N···O distance of ~2.5Å where the N··H and O··H distances are equal. This agrees with the X-ray data from CSD (graphs 4.1.1. and 4.1.2) where N···O hydrogen bonds shorter than ~2.5Å are significantly bent.

The bond valence model (Brown, 1992) has been applied to hydrogen bonds (Grabowski, 1998 and 2000, Steiner, 1998) to predict the N··H and O··H distances in hydrogen bonds. The N-H and the O-H distances in the N··H··O hydrogen bonds deviate from the curve predicted using the parameters from N-H···O and O-H···N hydrogen bonds (graph 4.6.3, Steiner, 1998).

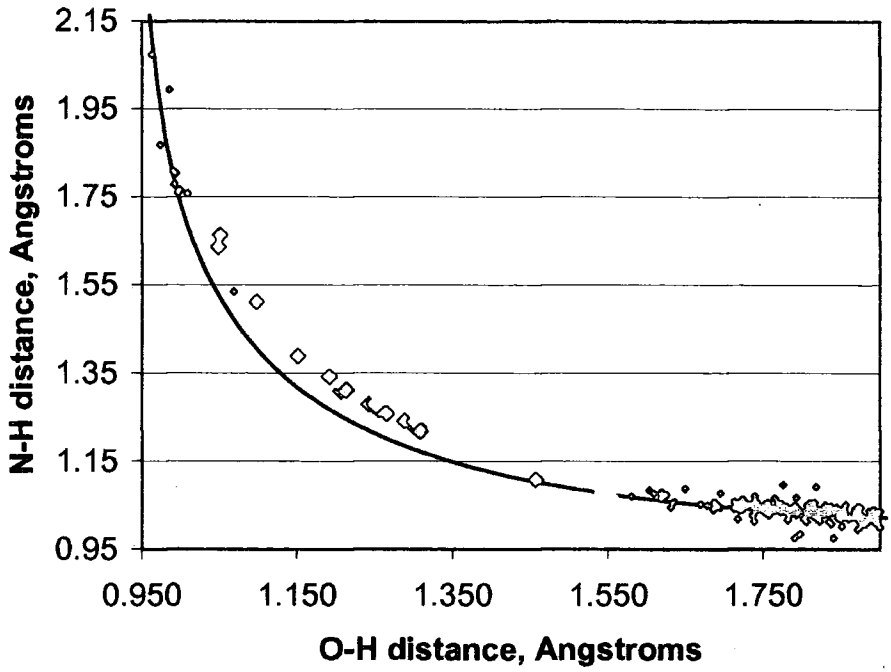


Graph 4.6.3. N-H and O-H distances in the hydrogen bonds. The colour scheme is as in graph 2. The line marks the theoretical curve predicted by the bond valence model (Steiner,1998). The curve fits the CSD data well, but not the new N··H··O data.

The apparent migration of the hydrogen atom in the hydrogen bond could be due to disorder. There may be two distinct states in the crystal, an O-H···N bond and an N-H···O bond, the crystal is disordered between the two states and the number of molecules in each state depending on the temperature. The time averaged hydrogen atom position, measured in diffraction experiments, would appear to move with temperature. This occurs in benzoic acid (Wilson et al. 1996) and is obvious in the hydrogen atom thermal ellipsoids. The hydrogen atom thermal ellipsoids in PDA, DDA, BPTA and PCP·4MP show no evidence of disorder along the N···O direction.

There may be one stable hydrogen bond potential energy well in the structure, in which the excited state has a different expectation value of position to the ground state. As the temperature increases the excited state becomes populated and the proton position appears to move.

The shape of the hydrogen bond potential energy well could change slightly due to slight changes in the local environment with temperature as suggested by Wilson (2001) for urea phosphoric acid. The low temperature well having the expectation value of the hydrogen atom position close to the nitrogen atom and close to the oxygen atom at room temperature. The systematic changes in the N···O distance, the C-O distance in the carboxylate and the pyridyl C-N-C angle suggest that the last description, the change in the shape of the

potential energy well, is the most accurate. The true situation may be a combination of all these effects. The suggestion of Steiner et al. (2001) that the "difference between the structures at room temperature and at 20K might be nothing more than an artifact caused by experimental inaccuracies." after their experiments on PCP·4MP can be ruled out by the extra experimental evidence in this work.

## 4.7. References


Allen, F.H., Kennard, O., Watson, D.G., Brammer, L., Orpen, A.G. & Taylor, R. International Tables for Crystallography. (1992) Volume C, Table 9.5.1.1. 685-706.

Allen, F.H., Kennard. O. (1993) Chem. Des. Autom. News, 8, 31-37.

Brown, I.D. (1992). Acta Cryst. B48, 553-572.

Coppens, P. (1970). Crystallographic Computing. Edited by Ahmed, F.R. Munksgaard International Booksellers and Publishers Ltd. 255-270.

Grabowski, S.J. (1998). Neutron and Numerical Methods. Edited by Johnson, M.R., Kearley, G.J., Büttner, H.G. 112-117.

Grabowski, S.J. (2000). J. Mol. Structure. 552, 153-157.

Hibbert, F., Emsley, J. (1990) Advances in Physical Organic Chemistry. 26, 255-379.

Ichikawa, M. (1978). Acta Cryst. B34, 2074-2080.

Iwasaki, F.F.,Iwasaki, H., Saito, Y. (1967). Acta Cryst. 23, 64-70.

Küppers, H., Takusagawa, F., Koetzle, T.F. (1985). J. Chem. Phys. 82, 5636-5647.

Nelmes. R.J., Meyer, G.M., Tibballs, J.E. (1982) J. Phys. C. 15, 59-75.

Reetz, M.T., Höger, S., Harms, K. (1994) Angew. Chem. Int. Ed. Engl. 33, 181-183.

Robertson, J.M., Ubbelohde, A.R. (1939) Proc. R. Soc. London. Ser. A. 170. 222.

Sakhawat Hussain, M., Schlemper, E.O. (1980) Acta. Cryst. B36, 1104-1108.

Sheldrick, G.M. (1997). SHELXL97 and SHELXS97. University of Göttingen, Germany.

Singh, T.R., Wood, J.L. (1969) J. Chem. Phys. 50, 3572-3576.

Steiner, T. (1998). J. Phys. Chem. A. 102, 7041-7052.

Steiner, T., Wilson, C.C., Majerz. I. (2000). Chem. Commun. 1231-1232.

Steiner, T., Majerz, I., Wilson, C.C. (2001) Angew. Chem. Int. Ed. 40, 2651-2654.

Taguchi, H., Maeda, M., Nishitani, H., Okumura, K., Shimahayashi, Y., Iwai, K. (1992) Bioscience Biotechnology and Biochemistry. 56. 1921-1923.

Takusagawa, F., Hirotsu, K., Shimada, S. (1973) Bull. Chem. Soc. Japan. 46. 2292 – 2294.

Takusagawa, F., Hirotsu, K., Shimada, S. (1973a) Bull. Chem. Soc. Japan. 46. 2372 – 2380.

Takusagawa, F., Koetzle, T.F. (1978). Acta Cryst. B34, 1149-1154.

Takusagawa, F., Koetzle, T.F. (1979). Acta Cryst. B35, 2126-2135.

Wilson, C.C. (2001) Acta. Cryst. B57, 435-439.

## 5. Quantum Mechanical Modelling

After observing the temperature dependent behaviour of the hydrogen and deuterium atom positions in the short N··H··O hydrogen bonds, we speculated on the explanation. To provide an insight from a different point of view we performed density functional theory calculations, which calculate the properties of the molecules from first principles.

### 5.1. Density Functional Theory Calculations

Density functional theory (Hohenberg and Kohn, 1964 and Kohn and Sham, 1965) calculates the total energy of a molecular system in the ground state, (i.e. at 0 K) as a function of the electron density. The total energy is made up of three contributions that are calculated from the electron density (equation 1): the kinetic energy of the electrons, $T_s$, the Coulomb energy from electrostatic interactions between the particles, $E_c$, and the exchange-correlation energy between the electrons, $E_{xc}$.

$$E_{total}[\rho(x)] = T_s[\rho(x)] + E_c[\rho(x)] + E_{xc}[\rho(x)] \qquad 1.$$

This equation is exact, but the function for the exchange-correlation energy is not known. The exchange correlation energy is approximated via the local density approximation (LDA), which calculates the exchange energy for a small region in the structure as if it were a homogeneous electron gas of the same electron density. The generalised gradient approximation (GGA) or gradient-corrected approximation improves upon the LDA by making a correction for the gradient of the electron density.

In general the properties of molecules depend upon the valence electrons. The influence of the electrons confined to the atomic cores is small. It is time consuming to calculate the wavefunctions for these electrons therefore pseudopotentials (Cohen and Heine, 1970) are used to model the atomic nuclei and core electrons.

One difference between density functional theory codes is the basis functions that are used to calculate the electronic wavefunctions. DMol3 (Delley, 1990) uses localised numerical atom-centred functions to model the wavefunctions, which can be used to model molecules or clusters of molecules and also can model solids using periodic boundary conditions. In CASTEP (Payne et al. 1992) and VASP (Kresse and Furthmuller. 1996) the wavefunctions are built up of plane waves analogously to the modelling of scattering density by crystallographers, which is ideal for modelling solids. As these programs use plane waves to model the electron wavefunctions they is are perfect for modelling the wavefunctions in periodic systems, i.e. crystals, therefore the calculations take into account intermolecular interactions and the space group symmetry.

### 5.2. Geometry Calculations - Single Molecule Geometry

The molecular geometry of pyridine-3,5-dicarboxylic acid (PDA) was calculated in the standard and zwitterionic forms (figures 5.2.1.a and b) using the density functional theory program DMol[3]. DMol[3] (Delley, 1990, and Delley, 1991) is a density functional theory program that uses numerical atom-centred functions as a basis set to build the electron wavefunctions. All the electrons in the molecule are accounted for in the calculation (i.e. no pseudopotentials are used to describe the core electrons). The local density approximation (Perdew-Wang, 1986) was used for the electron-electron correlation function. Calculations were carried out on a Silicon Graphics workstation within the Cerius2 package. These calculations are for a lone free molecule and do not include any intermolecular interactions. The same program has been used in the calculation of the molecular geometries in chapter 2 and chapter 3 under the same conditions.

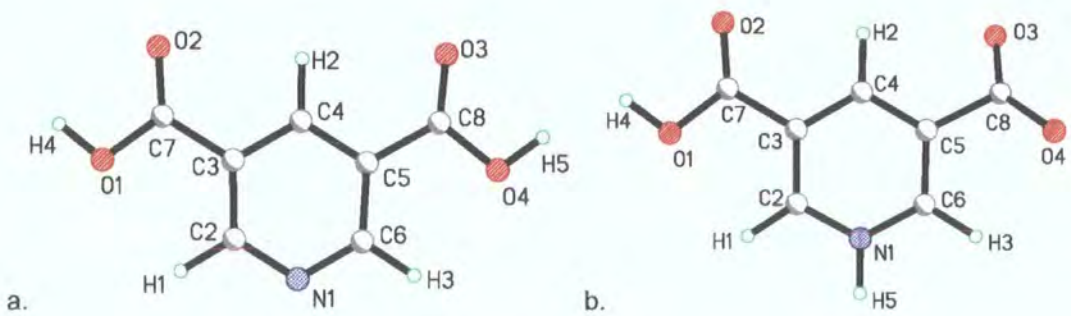


Figures 5.2.1.a and 5.2.1.b. The normal molecule of PDA (a) and the zwitterionic form (b). The geometry of the input molecules has been taken to be close to the form in the crystals.

After the geometry optimisation had converged, the maximum atomic displacement was less than $10^{-3}$Å between successive cycles of calculation.

Table. 5.2.1. Selected Bond Lengths.

| | Observed 15K, Neutron (Å) | Calculated, Normal (Å) | Difference, Obs-Calc(norm) (Å) | Calculated, Zwitterion. (Å) | Difference, Obs-Calc(zwit) (Å) |
|---|---|---|---|---|---|
| C2-N1 | 1.338(2) | 1.3268 | 0.0112 | 1.3449 | -0.0069 |
| C2-C3 | 1.397(2) | 1.3934 | 0.0036 | 1.3793 | 0.0117 |
| C3-C4 | 1.396(2) | 1.3844 | 0.0116 | 1.3954 | 0.0006 |
| C4-C5 | 1.396(2) | 1.3854 | 0.0106 | 1.3849 | 0.0111 |
| C6-N1 | 1.338(2) | 1.3267 | 0.0114 | 1.3466 | -0.0085 |
| C7-O1 | 1.319(2) | 1.3439 | -0.0249 | 1.3462 | -0.0272 |
| C7-O2 | 1.217(2) | 1.2101 | 0.0069 | 1.206 | 0.0110 |
| C8-O3 | 1.245(2) | 1.2104 | 0.0346 | 1.2396 | 0.0054 |
| C8-O4 | 1.277(2) | 1.3438 | -0.0668 | 1.2472 | 0.0298 |
| C2-H1 | 1.094(4) | 1.0977 | -0.0037 | 1.0927 | 0.0013 |
| O1-H4 | 1.025(4) | 0.9915 | 0.0335 | 0.9918 | 0.0332 |
| O4-H5 | 1.311(5) | 0.9923 | 0.3187 | - | - |
| N1-H5 | 1.213(4) | - | - | 1.0305 | 0.1825 |

Table 5.2.2. Selected Bond Angles.

| | Measurement 15K, Neutron. (º) | Calculated, Normal (º) | Difference, Obs-Calc(norm) (º) | Calculated, Zwitterion (º) | Difference, Obs-Calc(zwit) (º) |
|---|---|---|---|---|---|
| C2-N1-C6 | 121.66(13) | 117.82 | 3.84 | 123.02 | -1.36 |
| C2-C3-C4 | 119.15(14) | 118.85 | 0.58 | 119.44 | -0.29 |
| C2-C3-C7 | 120.89(14) | 122.39 | -1.50 | 120.72 | 0.17 |
| C3-C4-C5 | 119.60(14) | 118.37 | 1.23 | 119.49 | -0.11 |
| C4-C5-C8 | 123.57(14) | 118.51 | 5.06 | 122.91 | 0.66 |
| O1-C7-O2 | 125.75(18) | 123.01 | 2.74 | 123.60 | 2.15 |
| O3-C8-O4 | 124.85(17) | 122.80 | 2.05 | 134.43 | -9.58 |

Table 5.2.3. Selected Torsion Angles.

| | Measurement 15K, Neutron. | Calculated, Normal (º) | Difference, Obs-Calc(norm) (º) | Calculated, Zwitterion (º) | Difference, Obs-Calc(zwit) (º) |
|---|---|---|---|---|---|
| C2-C3-C7-O1 | -8.2(3) | 2.6 | -10.8 | -0.6 | -7.6 |
| C6-C5-C8-O4 | 13.9(3) | -6.8 | 20.7 | -26.9 | 40.8 |

The standard crystallographic R-factor for measuring the agreement between observed, $F_{obs}$, and calculated structure factors, $F_{calc}$, is defined as :-

$$R1 = \frac{\sum \left| |F_{obs}| - |F_{calc}| \right|}{\sum |F_{obs}|}$$

A similar R-factor can also be used to measure the agreement between structural parameters derived from experiment and calculated parameters, where the smaller the R-factor the better the agreement. For example an R-factor that compares bond lengths:-

$$R(\text{bond lengths}) = \frac{\sum \left| |r_{obs}| - |r_{calc}| \right|}{\sum |r_{obs}|}$$

A similar R-factor can be defined for bond angles. These factors have been calculated without including the parameters which involve H4 or H5, the hydrogen atoms involved in the strong hydrogen bonds.

Table 5.2.4. Agreement factors between calculated parameters and the parameters from the 15K neutron experiment.

| | R(bond lengths) | R(angles) |
|---|---|---|
| Normal form | 0.01426 | 0.01628 |
| Zwitterionic form | 0.01039 | 0.01581 |

The calculated binding energy of the normal structure is lower than the calculated binding energy of the zwitterionic structure and the normal structure is expected to be more stable.

Energy Normal = -103.079 eV
Energy Zwitterion = -101.826 eV

Selected bond lengths from the two calculated strutures and the measured structure at 15K are listed in table 5.2.1. The differences between the two calculated structures are predictable. The C-N bonds are longer and the C-N-C angle larger in the zwitterionic structure, in which the nitrogen atom is protonated, than in the normal structure. The C8-O bonds in the zwitterionic structure are approximately equal in length, as expected in a carboxylate group, while they are much different lengths in the normal structure.

As noted in section 4.2 and as seen in the 'R-factors' the conformation of the molecule in the crystal is closer to the zwitterionic form. The measured C-N bond lengths lie in between the lengths calculated for the zwitterionic and normal structures, marginally closer to the lengths in the zwitterionic form. The C7-O1 bond length has been overestimated and the C7-O2 bond length has been underestimated in both calculations. The C8-O3 bond length has also been underestimated in both calculations, but is much closer to the length calculated in the zwitterionic form. The observed C8-O4 bond length lies between the two calculated bond

lengths and again is closer to the length calculated in zwitterionic form. The hydrogen atoms H4 and H5 are not involved in hydrogen bonds in this single molecule calculation and therefore the calculated O-H and N-H bond lengths are shorter than the observed bond lengths.

The agreement between the observed and calculated bond angles (table 5.2.2) is worse than the agreement between bond lengths. Again the observed bond angles, except for the O3-C8-O4 bond angle, are closer to the angles calculated for the zwitterionic form.

The calculated torsion angles (table 5.2.3) for both models show poor agreement with the observed structure.

### 5.3 Geometry Calculations - Solid State Geometry

The molecular geometry of PDA in the solid state was calculated using the density functional theory program CASTEP (Cambridge Sequential Total Energy Package, Payne et al. 1992). CASTEP is a density-functional theory code that uses plane-wave functions as a basis set to model the electronic wavefunctions. The core electrons and nuclei are modelled using ultrasoft pseudopotentials (Hamann et al. 1979) and only the valence electrons are modelled in the calculation. The gradient-corrected local-density approximation (Perdew and Wang, 1992) was used for the electron-electron correlation function. Calculations were carried out on a Silicon Graphics workstation within the Cerius2 package. This procedure has produced accurate results in studies of similar molecular crystals (Plazanet et al, 2000, Nicolai and Kearley, 1999).

The lowest-energy structure has been calculated in three different circumstances

Calc 1. All atoms free and the cell dimensions free.

Calc 2. All atoms free and the cell dimensions fixed.

Calc 3. All atoms except the N and O in the hydrogen bond free and the cell dimensions fixed.

The geometry optimisations continued until the average energy change per atom was less than $0.2*10^{-4}$ eV per atom, the mean displacement of the atoms was less than $10^{-3}$ Å and the mean force on the atoms was less than 0.05 eV/Å. The basis set was made up of plane waves with energies up to 300eV.

Table. 5.3.1. Selected Bond Lengths. The differences between the calculated and measured parameters ($r_{obs}$-$r_{calc}$) are in square brackets.

| | Measurement 15K, Neutron (Å) | Calc 1. (Å) | Calc 2. (Å) | Calc 3. (Å) |
|---|---|---|---|---|
| C2-N1 | 1.338(2) | 1.3361 [0.0019] | 1.3328 [0.0052] | 1.3332 [0.0048] |
| C2-C3 | 1.397(2) | 1.3819 [0.0151] | 1.3784 [0.0186] | 1.3791 [0.0179] |
| C3-C4 | 1.396(2) | 1.3895 [0.0065] | 1.3870 [0.0090] | 1.3877 [0.0083] |
| C4-C5 | 1.396(2) | 1.3842 [0.0118] | 1.3811 [0.0149] | 1.3820 [0.0140] |
| C6-N1 | 1.338(2) | 1.3388 [-0.0007] | 1.3354 [0.0027] | 1.3354 [0.0027] |
| C7-O1 | 1.319(2) | 1.3221 [-0.0031] | 1.3184 [0.0006] | 1.3215 [-0.0025] |
| C7-O2 | 1.217(2) | 1.2245 [-0.0075] | 1.2247 [-0.0077] | 1.2241 [-0.0071] |
| C8-O3 | 1.245(2) | 1.2603 [-0.0153] | 1.2600 [-0.0150] | 1.2594 [-0.0144] |
| C8-O4 | 1.277(2) | 1.2617 [0.0153] | 1.2610 [0.0160] | 1.2664 [0.0106] |
| C2-H1 | 1.094(4) | 1.0854 [0.0086] | 1.0843 [0.0097] | 1.0848 [0.0092] |
| O1-H4 | 1.025(4) | 1.0324 [-0.0074] | 1.0331 [-0.0081] | 1.0289 [-0.0039] |
| O4-H5 | 1.311(5) | 1.4612 [-0.1502] | 1.4378 [-0.1268] | 1.4041 [-0.0931] |
| N1-H5 | 1.213(4) | 1.1161 [0.0969] | 1.1143 [0.0987] | 1.1212 [0.0918] |

Table 5.3.2. Selected Bond Angles. The differences between the calculated and measured parameters ($\theta_{obs}$-$\theta_{calc}$) are in square brackets.

| | Measurement 15K, Neutron. (º) | Calc 1. (º) | Calc 2. (º) | Calc 3. (º) |
|---|---|---|---|---|
| C2-N1-C6 | 121.66(13) | 121.90 [-0.24] | 122.36 [-0.70] | 122.18 [-0.52] |
| C2-C3-C4 | 119.15(14) | 118.75 [0.40] | 118.76 [0.39] | 118.67 [0.48] |
| C2-C3-C7 | 120.89(14) | 121.01 [-0.12] | 120.74 [0.15] | 120.74 [0.15] |
| C3-C4-C5 | 119.60(14) | 120.18 [-0.58] | 120.53 [-0.93] | 120.57 [-0.97] |
| C4-C5-C8 | 123.57(14) | 123.14 [0.43] | 123.63 [-0.06] | 123.65 [-0.08] |
| O1-C7-O2 | 125.75(18) | 125.06 [0.69] | 125.21 [0.54] | 124.93 [0.82] |
| O3-C8-O4 | 124.85(17) | 125.60 [-0.75] | 125.50 [-0.65] | 125.57 [-0.72] |

Table 5.3.3. Selected Torsion Angles. The differences between the calculated and measured parameters ($\tau_{obs}$-$\tau_{calc}$) are in square brackets.

| | Measurement 15K, Neutron. (º) | Calc 1. (º) | Calc 2. (º) | Calc 3. (º) |
|---|---|---|---|---|
| C2-C3-C7-O1 | -8.2(3) | -11.78 [3.58] | -8.27 [0.07] | -8.44 [0.24] |
| C6-C5-C8-O4 | 13.9(3) | 15.79 [-1.89] | 14.59 [-0.69] | 14.09 [-0.19] |

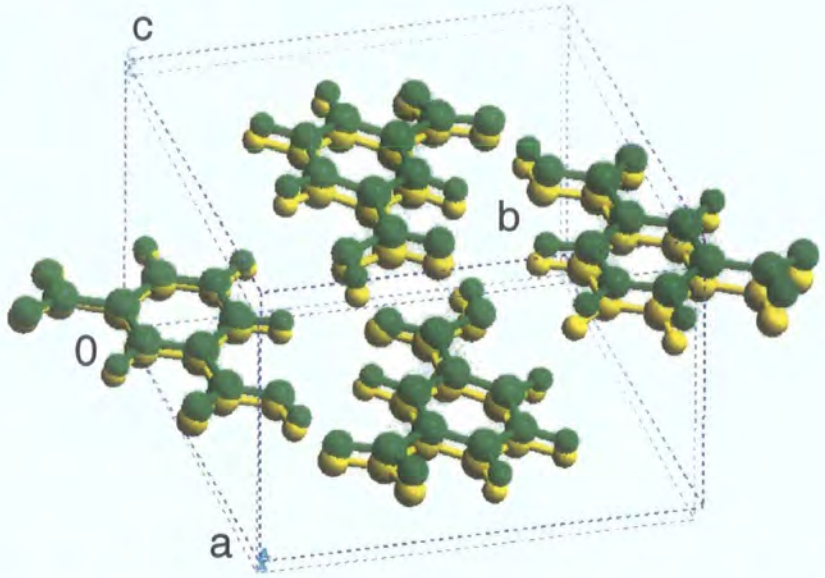


Figure 5.3.1. The structure calculated in Calc. 1. (green) and optimised (yellow) structures superimposed. A similar figure for Calcs 2 and 3 shows no appreciable difference between the calculated and measured structures.

Table 5.3.4. The calculated and measured unit cell parameters. The differences between the measured and calculated parameters are in square brackets.

| | Measurement, 15K | Calc 1. |
|---|---|---|
| a (Å) | 9.7116(13) | 9.7552 [-0.0436] |
| b (Å) | 11.1347(17) | 11.2970 [-0.1623] |
| c (Å) | 6.4421(13) | 6.8555 [-0.4134] |
| β (º) | 108.596(10) | 106.330 [2.266] |
| Vol ($Å^3$) | 660.25(19) | 725.03 [64.78] |

The expansion in the unit-cell dimensions (table 5.3.4) can be attributed to the underestimation of dispersion forces by the calculation. The largest change is in the c-direction where only dispersion forces act, whereas in the ab-plane hydrogen bonds act as well. The separation between the layers of atoms has increased by 0.24Å from 3.05Å to 3.29Å and the overall cell volume has increased by 9.8%.

Table 5.3.5. Agreement factors between the calculated parameters and the parameters from the 15K neutron experiment.

| | Calc 1. | Calc 2. | Calc 3. |
|---|---|---|---|
| R (bonds) | 0.00578 | 0.00763 | 0.00707 |
| R (angles) | 0.00357 | 0.00418 | 0.00450 |

The bond length and especially the bond angle R-factors are much smaller than those for the single molecule calculation. These again do not include the hydrogen bonded hydrogen atoms which will be discussed in more detail. Despite the volume expansion in Calc. 1 the bond lengths and angles agree most accurately with the measurement. The carboxylic acid torsion angles, which are significantly affected by the intermolecular interactions, are much more accurately predicted than in the single-molecule calculation. The carboxylic-acid torsion angles in Calc 1. are the least accurate, I suspect this is because the layers of molecules have moved further apart and allowed more freedom for the groups to rotate.

Table 5.3.6. The N1··H5··O4 Hydrogen bonds parameters.

| | N···O (Å) | N··H (Å) | H··O (Å) | N-H-O (º) |
|---|---|---|---|---|
| Measurement, 15K | 2.523(2) | 1.213(4) | 1.311(5) | 176.4(4) |
| Calc 1. | 2.575 | 1.116 | 1.461 | 175.1 |
| Calc 2. | 2.551 | 1.114 | 1.438 | 176.0 |
| Calc 3. | 2.523* | 1.121 | 1.404 | 175.2 |

* Constrained to be 2.523Å in the calculation.

Table 5.3.7. The O1-H4···O3 Hydrogen bond parameters.

| | O···O (Å) | O-H (Å) | H··O (Å) | N-H-O (º) |
|---|---|---|---|---|
| Measurement, 15K | 2.569(3) | 1.025(4) | 1.558(4) | 167.7(4) |
| Calc 1. | 2.558 | 1.032 | 1.535 | 170.1 |
| Calc 2. | 2.551 | 1.033 | 1.527 | 170.5 |
| Calc 3. | 2.571 | 1.029 | 1.552 | 169.9 |

The N-O distance in the N1··O4 hydrogen bond expanded and the O1··O3 contracted in Calc. 1 and Calc. 2. In Calc. 3 the N1···O4 distance was constrained and the O1···O3 distance did not change significantly.

The hydrogen atom position in the O1··O3 hydrogen bond corresponds well with the measured values for all the calculations. All the calculations predict the slight lengthening of the O-H distance from the calculated single-molecule value of 0.992Å.

The hydrogen atoms positions in the N1···O4 hydrogen bond are all predicted to be too close to the nitrogen atom and although the lengthening of the N-H bond from the single molecule value of 1.031Å is predicted, it is underestimated.

### 5.3.1. Pyridine-3,4-dicarboxylic Acid, Cinchomeric Acid.

The structure of pyridine-3,4-dicarboxylic acid (cinchomeric acid, CINC) has also been calculated using CASTEP, with less accuracy than the calculation for PDA, in order to compare the results qualitatively. The calculation began from the room temperature structure measured by Tagusagawa et al. (1973). The unit cell has not been optimised during the calculation and the calculation was continued until the average energy change per atom was less than $0.2*10^{-4}$ eV per atom, the mean displacement of the atoms was less than $10^{-3}$ Å and the mean force on the atoms was less than 0.05 eV/Å. The basis-set was made up of plane waves with energies below 260eV.

CINC crystallises, like PDA, in a zwitterionic form. A three-dimensional hydrogen bonded network is formed with an N-H···O hydrogen bond (N···O 2.664Å) longer than that in PDA, and one O-H···O hydrogen bond (O···O 2.514Å) shorter than the corresponding bond in PDA.

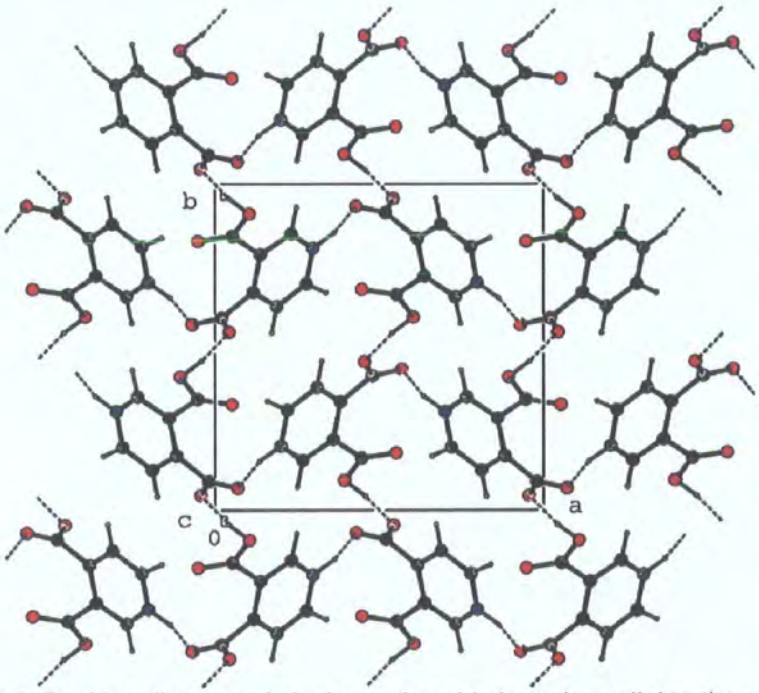


Figure 5.3.2. Packing diagram of cinchomeric acid viewed parallel to the c-direction.

Table 5.3.8. The N-H···O Hydrogen bonds parameters.

| | N···O (Å) | N··H (Å) | H··O (Å) | N-H-O (º) |
|---|---|---|---|---|
| Measurement, RT | 2.664 | 1.090 | 1.594 | 165.6 |
| Calculated | 2.637 | 1.069 | 1.603 | 160.9 |

Table 5.3.9. The O-H···O Hydrogen bond parameters.

| | O···O (Å) | O-H (Å) | H··O (Å) | N-H-O (º) |
|---|---|---|---|---|
| Measurement, RT | 2.514 | 0.941 | 1.602 | 162.1 |
| Calculated | 2.551 | 1.047 | 1.508 | 173.3 |

Table 5.3.10. Agreement factors between the calculated parameters and the parameters from the published room-temperature X-ray structure.

| | R (bonds) | R (angles) |
|---|---|---|
| No H-bonds | 0.01762 | 0.00578 |
| No H | 0.00667 | 0.00397 |

The calculated intramolecular bond distances agree with the measured parameters to within 0.02Å except the bonds involving hydrogen atoms which only agree to within ~0.1Å. The calculated bond angles all agree with the measured parameters to within ~1.2° except the angles involving hydrogen atoms which agree to within only ~2.6°. The hydrogen-bond parameters have changed significantly (tables 5.3.8 and 5.3.9), the N···O distance becoming slightly shorter and the O···O distance becoming slightly longer. The comparison of the parameters involving the hydrogen atoms is biased as the original structure was measured at room temperature using X-rays where the hydrogen atoms positions would not be measured accurately. The agreement factors between the measured and calculated parameters are approximately the same magnitude as the agreement factors between the calculated and neutron-diffraction measured parameters for PDA only when the parameters involving the hydrogen atoms are omitted.

### 5.4. Modelling the Hydrogen Bonds

Beginning from the calculated solid-state geometries the hydrogen-bond potential energy well may be calculated. To find the shape of the well the energy of the structure is calculated with the hydrogen atom in the hydrogen bond in different positions in the well, the change in energy from the minimum energy structure is the potential energy for that hydrogen atom position. No structure optimisation takes place and the calculation takes place in space group P1. The hydrogen bonds have been assumed to be linear and the proton position moved along a straight line between the donor and acceptor atoms.

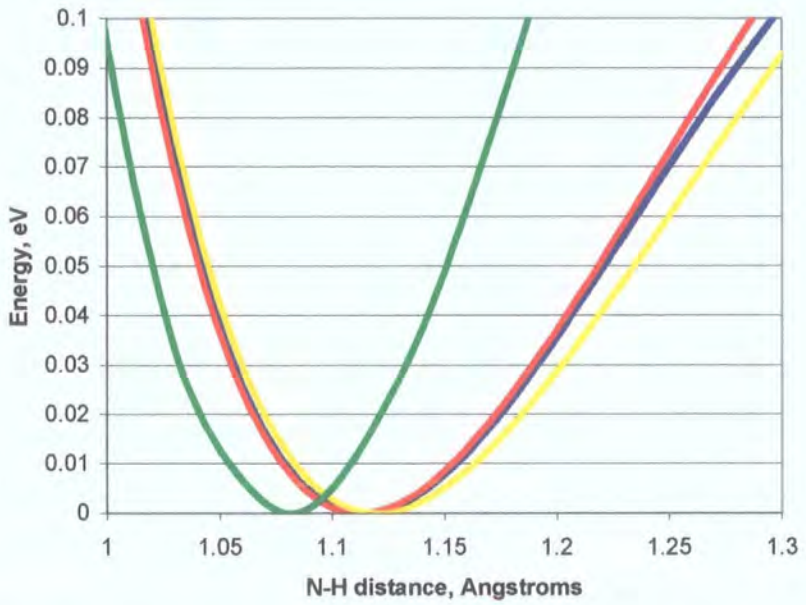


Graph 5.4.1.The calculated N1··H5··O4 hydrogen-bond potential-energy well in the region of the minima. The blue line is from calc. 1, the red line from calc. 2 and the yellow line from calc. 3. The green line is the potential energy well calculated in the N-H···O hydrogen bond in CINC.

The shapes of the calculated hydrogen-bond potential-energy wells for PDA are all very similar (graphs 5.4.1 and 5.4.2). The minima of the hydrogen bond, where the hydrogen atom is expected to lie as calculated by CASTEP, are all in approximately the same place and the gradients are quite similar.

The calculated potential-energy well for CINC is different from the calculated wells for PDA. The minimum of the well is 1.069Å from the nitrogen atom, which is close to where the hydrogen atom position would be expected to be for an N-H···O hydrogen bond with an N···O distance of 2.64Å comparing with the trend for N-H-O hydrogen bonds measured by neutron diffraction (graph 4.6.2). The gradients of the sides of the well are much steeper than those of PDA.

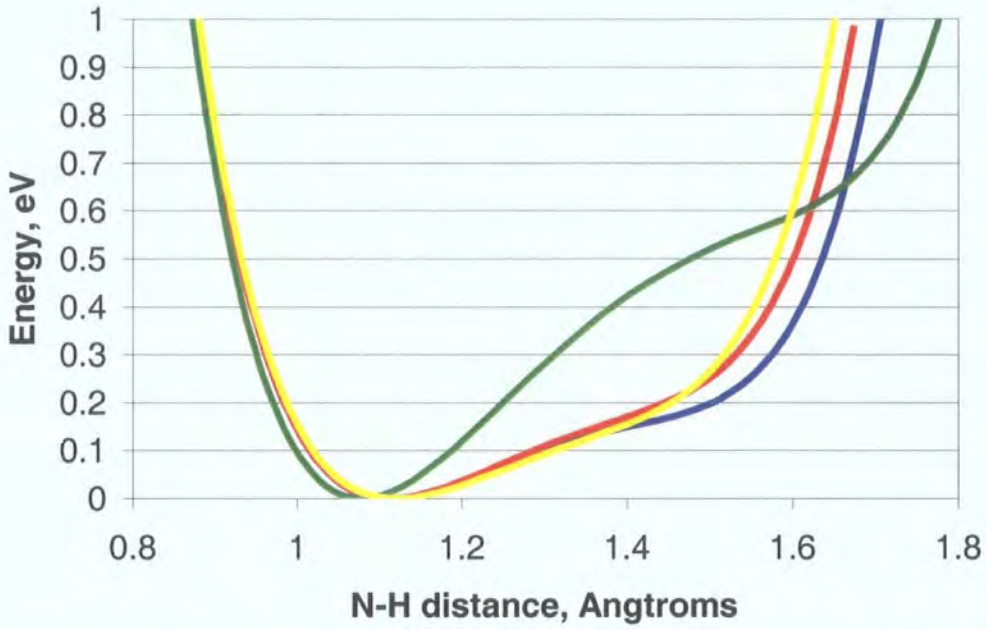


Graph 5.4.2. The hydrogen-bond potential-energy wells up to 1eV for PDA and CINC. The colour scheme is as in graph 5.4.1.

The calculated hydrogen bond potential well for CINC has a deep minimum close to the nitrogen atom. The calculated well for PDA (Calc. 1) has the overall minimum close to the nitrogen atom but is much broader. The well for CINC has a shoulder at approximately 0.5eV; this shoulder lies much lower in the potential energy well for the shorter hydrogen bond in PDA. The calculated potential energy wells for calculations 1,2 and 3 are very similar and only calc. 1 is discussed further.

The CASTEP geometry optimisation calculation treats atomic nuclei as classical particles and places them at the minimum of their potential energy well. In most cases, where the lowest energy eigenstate of a particle is in an approximately harmonic potential energy well, the expectation value of the particle position is at the minimum of the potential well. When the potential energy well is not symmetrical about the minimum energy then the particle must be treated quantum mechanically to calculate the expectation value for its position and the Schrödinger equation must be solved. The potential energy wells for PDA are clearly not symmetrical about the minimum in this region and therefore the placement of the hydrogen atom is incorrect.

### 5.4.1. The One-dimensional Schrödinger Equation

The wavefunctions and energy levels of a hydrogen atom in a three-dimensional potential-energy well are the eigenfunctions and eigenvalues of the three-dimensional Schrödinger equation (1).

$$H\Psi(\underline{r}) = E\Psi(\underline{r}) \qquad 1.$$

where the Hamiltonian,

$$H = \left[\frac{-\hbar^2}{2m}\nabla^2 + V(\underline{r})\right]$$

m is the mass of the particle, and V(r) is the potential energy. If the approximation is made that V(r) can be separated into functions that depend only on x, y or z, eg. $V(\underline{r}) = V_x(x) + V_y(y) + V_z(z)$ then the equation can be separated (2).

$$\left[\frac{-\hbar^2}{2m}\nabla^2 + V(\underline{r})\right] = \left[\frac{-\hbar^2}{2m}\frac{\delta^2}{\delta x^2} + V_x(x)\right] + \left[\frac{-\hbar^2}{2m}\frac{\delta^2}{\delta y^2} + V_y(y)\right] + \left[\frac{-\hbar^2}{2m}\frac{\delta^2}{\delta z^2} + V_z(z)\right] \qquad 2.$$

Then the Hamiltonian $H = H_x + H_y + H_z$, and the Schrödinger equation becomes:

$$H\Psi(\underline{r}) = E\Psi(\underline{r}) \qquad 3.$$

or

$$H_x\Psi(\underline{r}) + H_y\Psi(\underline{r}) + H_z\Psi(\underline{r}) = E\Psi(\underline{r}) \qquad 4.$$

Which suggests as solutions:

$$\Psi(\underline{r}) = X(x)Y(y)Z(z) \qquad 5.$$

Then substituting and dividing by Ψ gives.

$$\left[\frac{-\hbar^2}{2m}\frac{1}{X}\frac{d^2X}{dx^2} + V_x(x)\right] + \left[\frac{-\hbar^2}{2m}\frac{1}{Y}\frac{d^2Y}{dy^2} + V_y(y)\right] + \left[\frac{-\hbar^2}{2m}\frac{1}{Z}\frac{d^2Z}{dz^2} + V_z(z)\right] = E \qquad 6.$$

Separating the parts that depend on different variables leaves three equivalent equations.

$$\left[\frac{-\hbar^2}{2m}\frac{d^2X}{dx^2} + V_x(x)\right]X(x) = E_xX(x) \qquad 7.$$

$$\left[\frac{-\hbar^2}{2m}\frac{d^2Y}{dy^2} + V_y(y)\right]Y(y) = E_yY(y) \qquad 8.$$

$$\left[\frac{-\hbar^2}{2m}\frac{d^2Z}{dz^2}+V_z(z)\right]Z(z)=E_zZ(z) \qquad 9.$$

Where $E = E_x + E_y + E_z$

We are only interested in one of the variables, X, so we ignore the others and treat them as constants. Leaving the one-dimensional Schrödinger equation to solve for a one-dimensional potential well (Bransden and Joachim,1989)

### 5.4.2. Numerical Solution of the One-Dimensional Schrödinger Equation

The one-dimensional Schrödinger equation can be solved numerically to give the wavefunctions and energy levels. (Landau and Páez Mejía, 1997). The one dimensional time-independent Schrödinger equation (10) can be rearranged into equation (11).

$$-\frac{\hbar^2}{2m}\frac{d^2}{dx^2}\psi(x)+V(x)\psi(x)=E\psi(x) \qquad 10.$$

$$\psi''(x)+\frac{2m}{\hbar^2}[E-V(x)]\psi(x)=0 \qquad 11.$$

Equation (11) can be rewritten as:

$$\psi''(x)+k^2(x)\psi(x)=0 \qquad 12.$$

$$\text{Where } k^2(x)=\frac{2m}{\hbar^2}[E-V(x)] \qquad 13.$$

The function $\psi(x)$ can be obtained numerically by manipulating the Taylor expansion of $\psi(x)$. h is a small increment in x. And using an approximation for the 2nd derivative of $k^2(x)$.

$$\psi(x+h)=\frac{2\left[1-\frac{5}{12}h^2k^2(x)\right]\psi(x)-\left[1+\frac{1}{12}h^2k^2(x-h)\right]\psi(x-h)}{1+\frac{1}{12}h^2k^2(x+h)} \qquad 14.$$

This function can be calculated for any potential energy well shape at an energy E.

For a solution of the Schrödinger equation for a particle bound in a potential energy well the function, $\psi(x)$, must converge to zero at both $+\infty$ and $-\infty$ and the function must be continuous.

To find the eigenvalues and eigenfunctions of a known potential well we guess a starting value of E. Then from one side of the well we find the trial solution, and from the other side of the well also find a trial solution using equation (14). At an arbitrary point in the potential, we scale one trial solution so both functions have the same value. Then we find the difference in the gradients of the two solutions. If the gradients are equal and the magnitudes are equal, the value of E is an eigenvalue and both trial solutions are equal and an eigenfunction. The procedure is illustrated in figure 5.4.1.

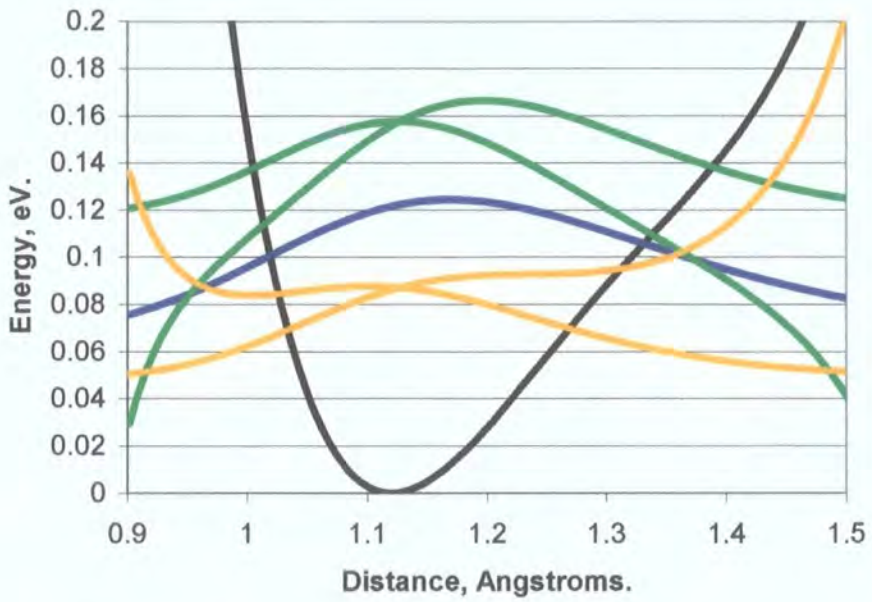


Figure 5.4.1. Solution of the one-dimensional Schrödinger equation. The potential energy well is shown in black. The trial and solution wavefunctions are shown on the same graph for illustration but the y-scale is meaningless. The first attempted solution is marked in orange. The trial solutions have been scaled to have the same magnitude at x=1.13Å. At this point the gradients of the trial solutions are too small and do not match. A higher energy was tested and is shown in the green trial solutions. At the matching point the gradients are too large and do not match. The solution, marked in blue, is where the two trial solutions have the same gradient at the matching point and are equivalent.

This procedure is used to calculate all the eigenvalues and eigenfunctions of the potential energy well.

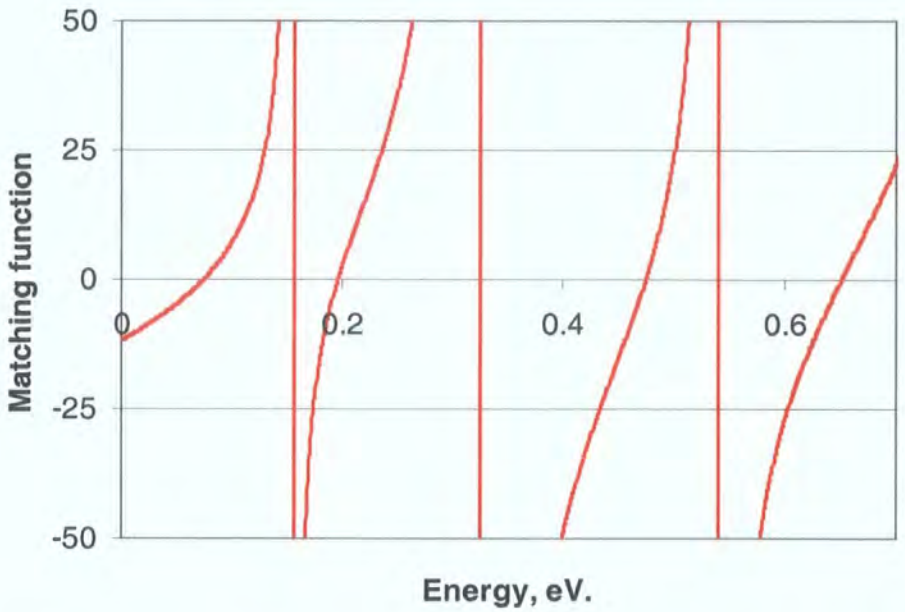


Graph 5.4.2. The matching function for a potential well. The difference in the gradients is calculated for all energies in the potential well, the solutions are at the roots of the function that are not asymptotes. The asymptotes correspond to where the trial functions change sign.

From the calculated wavefunctions the expectation value of the hydrogen atom position, <x> is calculated by.

$$\langle x \rangle = \frac{\langle \psi | x | \psi \rangle}{\langle \psi | \psi \rangle} = \frac{\int_{-\infty}^{\infty} \psi^* x \psi dx}{\int_{-\infty}^{\infty} \psi^* \psi dx} \qquad 15.$$

Which may be calculated simply by numerical integration of the wavefunction, as the wavefunction tends to zero and +∞ and -∞. <x> is at the same position as the minimum energy in a symmetric potential-energy well. In an asymmetric potential-energy well <x> is in general not at the same position as the potential-energy minimum.

In these calculation we have made a number of false assumptions that are good approximations.

The contradictory treatment of the hydrogen atom as a classical particle by CASTEP in the geometry optimisation and as a quantum mechanical particle in the Schrödinger equation introduces errors into the calculation. These errors are small as the differences between <x> calculated by CASTEP and the values calculated using the Schrödinger equation are small.

The potential energy cannot be separated into three separate orthogonal functions V(x), V(y) and V(z). The hydrogen bond is not straight (N··H··O = 176.4(4)° in hydrogenated PDA at 15K) therefore the potential-energy well must depend on at least two orthogonal coordinates. However it is a good approximation to consider the hydrogen bond as straight and one-dimensional.

### 5.4.3. Hydrogen and Deuterium Wavefunctions

The energy levels and expectation values of position have been calculated for the eigenfunctions of the potential-energy wells. The eigenvalues for deuterium lie at lower energies than the eigenvalues for hydrogen and the energy gap between these values is much smaller because of the higher deuterium mass.

Table 5.4.1.A. Eigenvalues for hydrogen in the N-H···O hydrogen bond of PDA, Calc. 1.

| Energy level | Energy (eV) | <x> (Å from N1) |
|---|---|---|
| 0 | 0.1058 | 1.186 |
| 1 | 0.2607 | 1.309 |
| 2 | 0.4334 | 1.307 |
| 3 | 0.6443 | 1.305 |

Table 5.4.1.B. Eigenvalues for deuterium in the N-H···O hydrogen bond of PDA, Calc. 1.

| Energy level | Energy (eV) | <x> (Å from N1) |
|---|---|---|
| 0 | 0.0780 | 1.163 |
| 1 | 0.1942 | 1.285 |
| 2 | 0.2990 | 1.308 |
| 3 | 0.4273 | 1.306 |

The hydrogen energy levels in PDA are much lower in the well and the energy gap between levels is smaller than in the N-H···O hydrogen bond in CINC.

Table 5.4.2. Eigenvalues for hydrogen in the N-H···O hydrogen bond in CINC.

| Energy level | Energy (eV) | <x> (Å from N) |
|---|---|---|
| 0 | 0.1551 | 1.1162 |
| 1 | 0.4111 | 1.2129 |
| 2 | 0.5994 | 1.3427 |
| 3 | 0.7610 | 1.3867 |

The calculated expectation values of the hydrogen/deuterium atom position in PDA agree reasonably well with the measurements. The hydrogen atom lies 1.213(4)Å from the nitrogen at 15K and the calculation predicts that it will lie 1.186Å from the nitrogen in the ground state. The deuterium atom lies 1.151(3)Å from the nitrogen at 15K and the calculation predicts 1.163Å from the nitrogen. The deuterium atom lies lower in the potential energy well and it 'feels' an effectively smaller potential well and lies closer to the minimum. The calculation has however underestimated the difference in the N-H and N-D bond lengths.

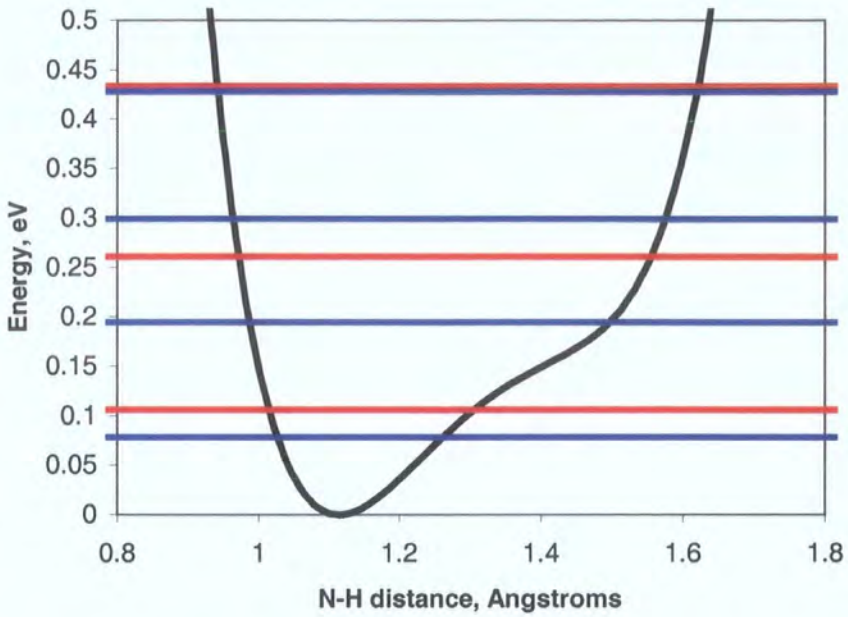


Graph 5.4.4. The calculated hydrogen (red) and deuterium (blue) energy levels for the N··H··O hydrogen bond in PDA, Calc.1.

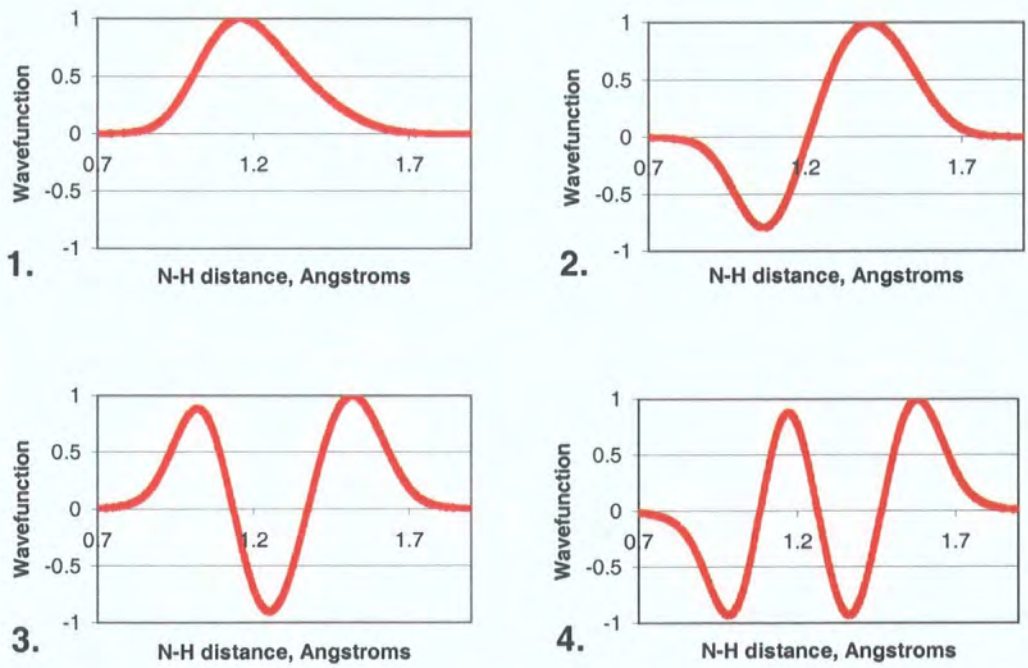


Figure. 5.4.2. The first four calculated normalised wavefunctions for a hydrogen atom in the hydrogen bond potential energy well from PDA, Calc. 1.

The calculated expectation value for the N-H distance in the hydrogen bond in CINC is longer than that predicted by CASTEP (1.069Å), and longer than the X-ray diffraction measured value (1.090Å). Neutron diffraction results are required to verify this prediction. The prediction agrees with the slight lengthening of X-H bonds when measured with neutron diffraction compared to X-ray diffraction.

The calculated O-H (1.080Å) and O-D (1.066Å) distances for PDA are overestimated compared with the measurements (O1-H4 = 1.025(4), O1-D4 = 1.021(3)Å). There is no difference between the O-H and O-D distances in the measurement, while the calculation predicts that the O-D distance is slightly shorter than the O-H distance. This may be evidence that the calculation has predicted a potential energy well which is more asymmetric than the true well.

Table 5.4.3.A. Eigenvalues for hydrogen in the O-H···O hydrogen bond in PDA from Calc 1.

| Energy level | Energy (eV) | <x> (Å from O1) |
|---|---|---|
| 0 | 0.1479 | 1.0804 |
| 1 | 0.3804 | 1.1942 |
| 2 | 0.5631 | 1.2744 |
| 3 | 0.7609 | 1.2844 |

Table 5.4.3.B. Eigenvalues for deuterium in the O-H···O hydrogen bond in PDA from Calc 1.

| Energy level | Energy (eV) | <x> (Å from O1) |
|---|---|---|
| 0 | 0.1081 | 1.0662 |
| 1 | 0.2875 | 1.1414 |
| 2 | 0.4296 | 1.2300 |
| 3 | 0.5556 | 1.2745 |

The calculated expectation value of the hydrogen atom position for the first energy level in PDA is 1.309Å from the nitrogen atom. This change from the ground state value of 1.186Å is reminiscent of the change observed in the experiment between 1.215Å at 15K to 1.308Å at 296K (section 4.5). However the calculated expectation value for the position of the deuterium atom in the first energy level is 1.285Å, a smaller change than observed for hydrogen, contrary to the change observed in the experiment of 1.151Å to 1.457Å.

We had postulated using Maxwell-Boltzmann statistics to predict the occupancies of the energy levels and deduce the temperature dependence of hydrogen and deuterium atom positions. However as the first excited state can never be more heavily populated than the ground state, and we assume that no higher energy levels are involved, this limits the motion of the hydrogen atom position to half way between the expectation values of position of the

lowest two eigenfunctions, which means a maximum change of the hydrogen atom position from 1.186Å to ~1.25Å from the nitrogen atom.

The energy difference between the ground state and the first excited state of the hydrogen atom in the N··H··O hydrogen bond potential energy well in PDA is 0.1549eV. Using the Boltzmann constant ($k = 8.617*10^{-5} eV\ T^{-1}$) and the relation E=kT, this energy gap corresponds to a temperature of ~1800K. For significant population of the first excited state of the hydrogen bond a temperature of this order must be reached. The energy gap of 0.1162eV between the lowest two deuterium energy levels corresponds to a temperature of ~1350K. The crystal is predicted to decompose above 600K. The proton migration in the crystal was observed below room temperature. Clearly using a static potential energy well and Maxwell-Boltzmann statistics is inadequate to describe the phenomena observed in the neutron diffraction experiments.

The calculated expectation values for all the lowest excited states in the hydrogen bonds would predict some, albeit maybe small, observed change of the hydrogen atom position with respect to temperature. As the energy gaps are much too large this does not occur and it has not been observed.

### 5.5. Vibrational Spectroscopy and Inelastic Neutron Scattering

The Vienna Ab-initio Simulation Package (VASP, Kresse and Furthmuller, 1996) has been used to calculate vibrational spectra of PDA in the harmonic approximation. This program was used instead of CASTEP (Payne et al. 1992) as it was available on faster, more powerful computers.

Beginning from the optimised molecular structure transformed into space group P1 each atom in turn is displaced a small amount (0.05Å in this case) in three orthogonal directions, ±x, ±y and ±z. This results, for a structure with N atoms in the unit cell, in 6N different structures. The total energy and the forces on all of the atoms are then calculated for each structure. From all the forces and the masses of the particles the dynamical matrix can be created. The vibrational frequencies and vibrational motions are the eigenvalues and eigenvectors of the dynamical matrix. This approach has produced accurate results for similar molecular crystals (Plazanet et al. 2000, Kearley et al. 2001, Plazanet et al. 2001).

#### 5.5.1. Inelastic neutron scattering.

All of the diffraction experiments have been concerned with elastic scattering, where the energy of the incoming particle and the outgoing particle is the same, only the momentum changes. Inelastic neutron scattering measures the energy change between the incident and out going neutrons. Inelastic incoherent neutron scattering measures the same phenomena as infra-red and Raman spectroscopies. The intensity of a mode in infra-red and Raman spectra depends upon the dipole moment and polarisablitity of covalent bonds respectively; the intensity of a mode in the inelastic neutron scattering spectrum depends upon the magnitude of the vibrational motion and the incoherent scattering cross section of the moving atoms and is much easier to calculate.

Table 5.5.1. Incoherent scattering cross sections for neutrons of wavelength 1.718Å (equivalent to an energy of 25.3 meV). (Sears, 1992)

| Nucleus | Incoherent scattering cross section (barns*) |
|---|---|
| Hydrogen | 80.26 |
| Deuterium | 2.05 |
| Carbon | 0.001 |
| Oxygen | 0.5 |
| Nitrogen | 0.0008 |

* 1 barn = 100 $fm^2$.

The inelastic neutron scattering is dominated by hydrogen. Selective deuteration can be used to measure the modes involving specific hydrogen atoms. The program CLIMAX (Kearley, 1995) has been used to calculate the inelastic neutron scattering spectra from the eigenvectors and eigenfrequencies calculated from VASP.

### 5.5.2. Calculated Spectra

The low-temperature incoherent inelastic neutron scattering spectra have been calculated for PDA in six different forms. Four of these forms are attainable experimentally: (a) totally hydrogenated, (b) totally deuterated, (c) deuterated with the hydrogen bonds hydrogenated and (d) hydrogenated with the hydrogen bonds deuterated.

To be able to separate more clearly the vibrations due to the hydrogen bonds the spectra have also been calculated on fully deuterated PDA with (e) only the hydrogen atom in the N··H··O hydrogen bonds hydrogenated and with (f) only the hydrogen atom in the O-H···O hydrogen bond hydrogenated. We are unlikely to be able to hydrogenate selectively the different carboxylic acid groups, which would be equivalent in solution, in order to prepare these samples.

Table 5.5.2. Selected calculated vibrational frequencies.

| Mode | Frequency region, $cm^{-1}$ |
|---|---|
| O1-H4 in-plane wag | 1431 – 1436 |
| O1-H4 out-of-plane wag | 1071 – 1108 |
| O1-H4 stretch | 2478 – 2518 |
| N1-H5 in-plane wag | 1651 – 1656 |
| N1-H5 out-of-plane wag | 1217 –1252 |
| N1-H5 stretch | 1993 – 2093 |
| C-H out-of-plane wagging | 941 – 1010 |
| C-H stretches | 3087 – 3151 |
| C7-O2 stretch | 1677 – 1696 |
| C8-O4 stretch | 1527 – 1561 |

Most of the modes below 1600 $cm^{-1}$ involve strongly coupled motions of many atoms.

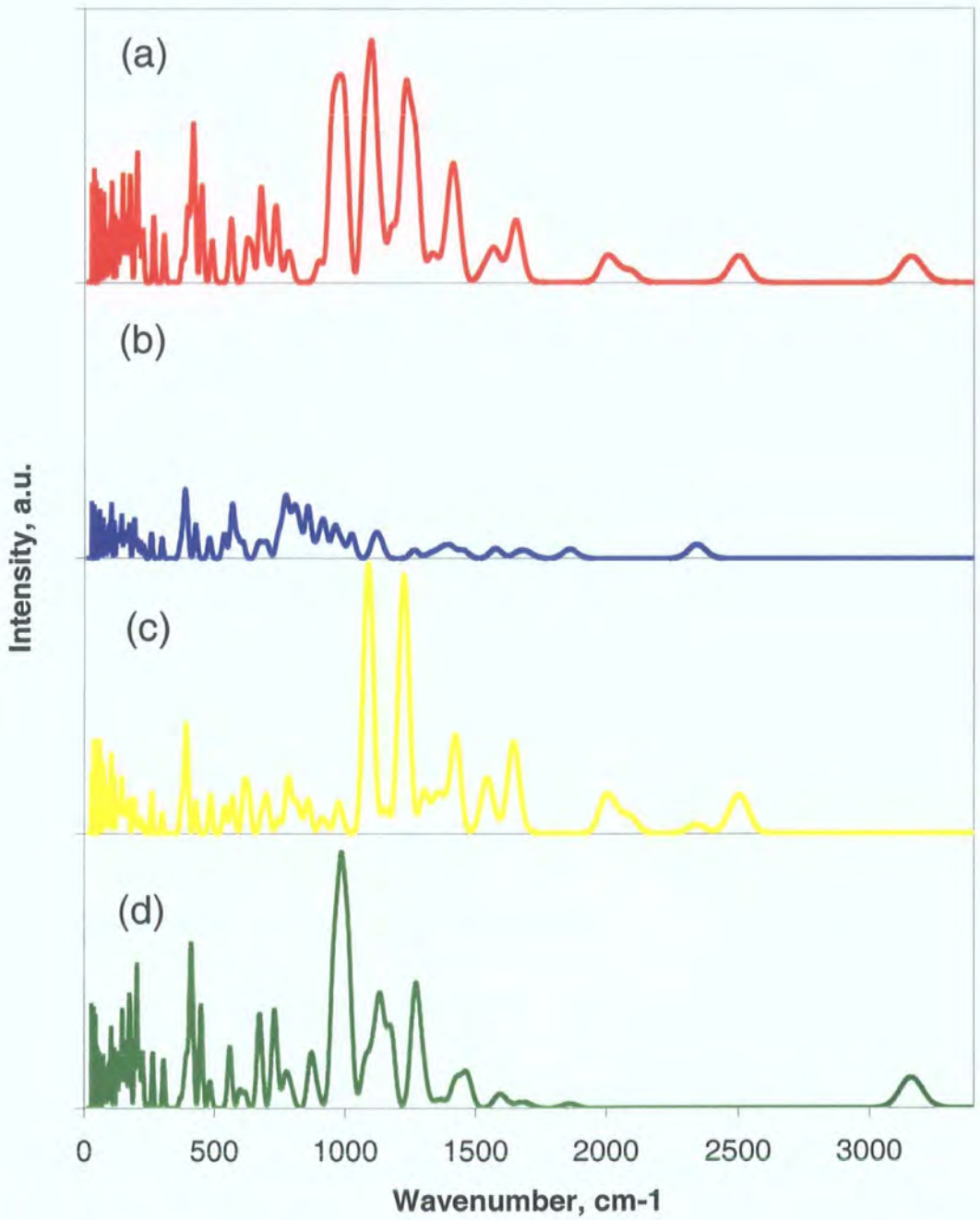


Graph. 5.5.1. Calculated inelastic neutron scattering spectra. The red spectrum (a) is calculated for the fully hydrogenated sample. The blue spectrum (b) is calculated for the fully deuterated sample. The yellow spectrum (c) is calculated for the deuterated molecule with the hydrogen bonds hydrogenated. The green spectrum (d) is calculated for the hydrogenated sample with the hydrogen bonds deuterated. The spectra have been scaled to be of approximately the correct relative magnitudes that would be observed in an experiment under the same conditions.

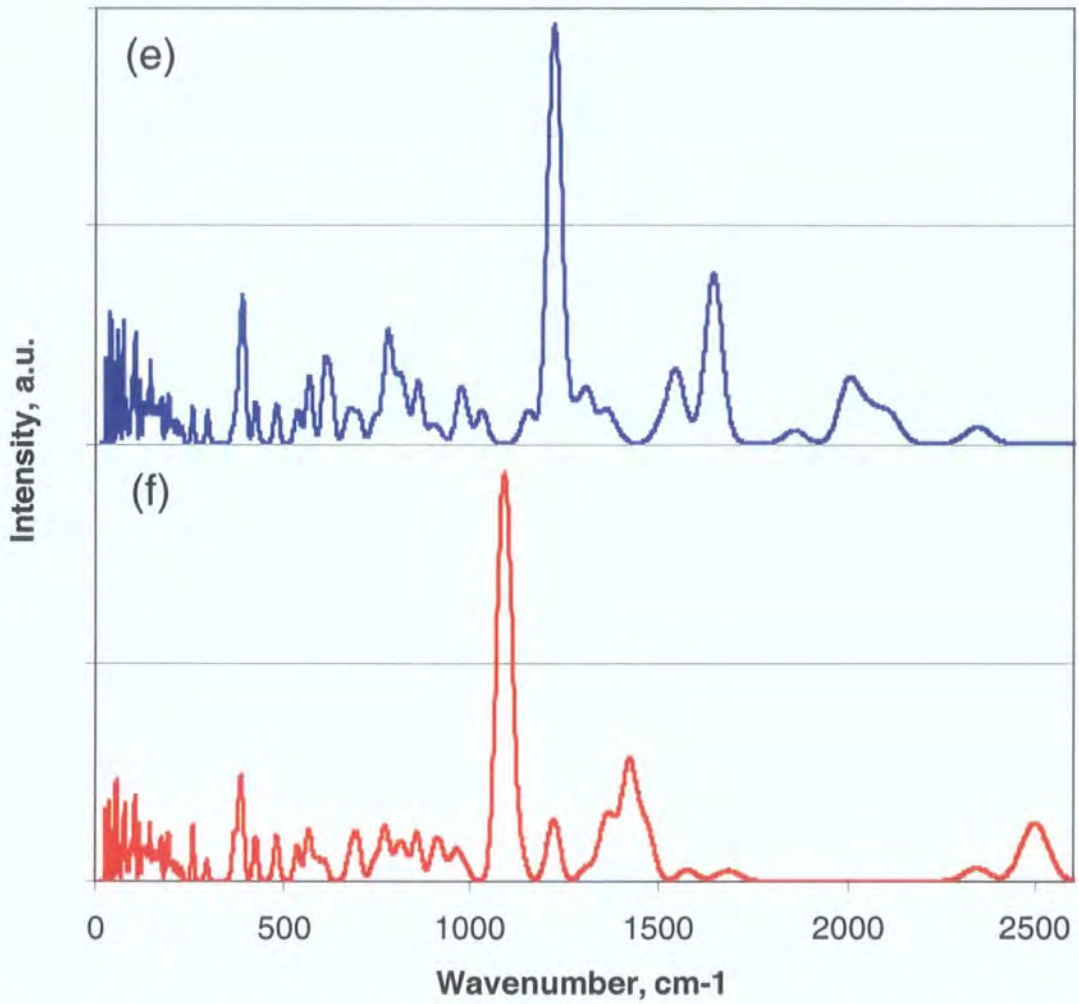


Graph 5.5.2. Calculated inelastic neutron scattering spectrum of the deuterated molecule with the N··H··O hydrogen bond protonated (blue, e) and the O-H···O hydrogen bond protonated (red, f).

The spectrum from the totally deuterated sample (b), which is much weaker than that of the hydrogenated sample (a), illustrates how much the scattering from the hydrogen atoms dominates the spectra. Even in the low-frequency region (below 900 $cm^{-1}$) where the vibrations are mainly due to motions of the carbon, nitrogen and oxygen atoms and the hydrogen atom motions are only secondary, the scattering is much reduced upon deuteration. Spectrum (b) shows similar features to (a) translated to lower frequencies because the energy levels of deuterium lie lower and closer together in potential-energy wells than the energy levels of lighter hydrogen, the frequencies corresponding to the transitions between these levels are lower.

The spectrum from PDA with only the phenyl-ring hydrogen atoms hydrogenated (d) illustrates these atom's motions. The intense peak at ~1000$cm^{-1}$ corresponds to the sum of the vibrations of the hydrogen atoms perpendicular to the plane of the phenyl ring. The two

peaks at ~1200cm$^{-1}$ and ~1300cm$^{-1}$ are due to vibrations of the hydrogen atoms in the plane of the phenyl rings. The peak at ~3100cm$^{-1}$ is due to the C-H stretching vibrations. The region below 1000cm$^{-1}$ is more intense in (d) compared with (c), where the phenyl hydrogen atoms have been deuterated, illustrating how most of the lower frequency modes are due to motions within the phenyl ring. It can be seen that spectrum (a) is essentially the sum of spectra (c) and (d).

The calculated spectrum of the N··H··O hydrogen bond (e) clearly shows the modes associated with this bond. The intense peak at ~1230cm$^{-1}$ is due to N-H bond wagging out of the plane of the phenyl ring. The peak at ~1650cm$^{-1}$ is due to N-H bond wagging in the plane of the phenyl ring. The peak at ~2000cm$^{-1}$ is due to the N-H bond stretch. The modes in the calculated spectrum due to the O-H···O hydrogen bond can be similarly assigned: O-H out-of-plane wagging at ~1100cm$^{-1}$, O-H in-plane wagging at ~1430cm$^{-1}$ and O-H stretch at ~2500cm$^{-1}$. The assignment of these modes is greatly facilitated eigenvectors being written in a form that can illustrated graphically by the Cerius$^2$ package.

The vibrational frequencies have been calculated in the harmonic approximation. The program effectively generates a harmonic potential-energy well for each atom and calculates the energy levels. The vibrational frequencies correspond to transitions between the energy levels. In most cases the harmonic approximation is adequate but the potential-energy wells for the hydrogen atoms in the short N··H··O and O-H···O hydrogen bonds (graphs 5.4.2 and 5.4.3) are significantly anharmonic in the region of the lowest energy levels and the vibrational frequencies need to be corrected.

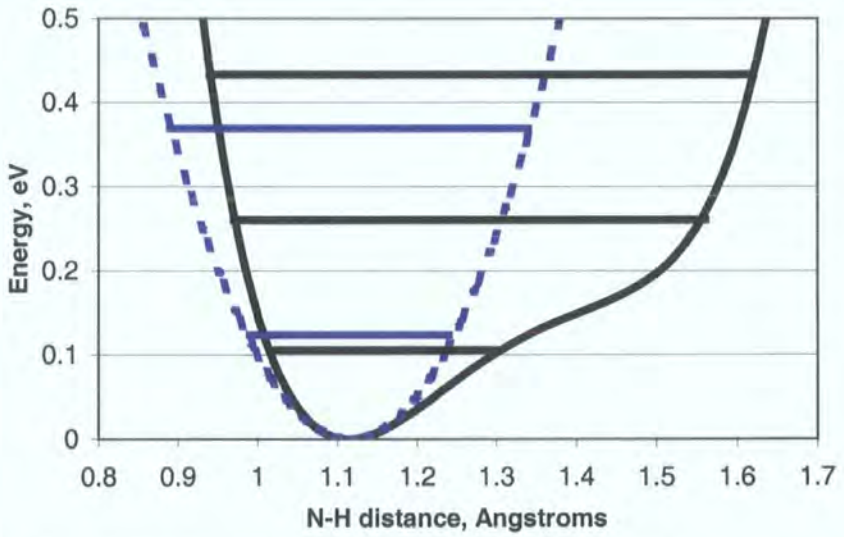


Graph 5.5.3. Harmonic potential well and energy levels (blue) and anharmonic potential well and energy levels (black) for the N··H··O hydrogen bond in PDA, Calc 1.

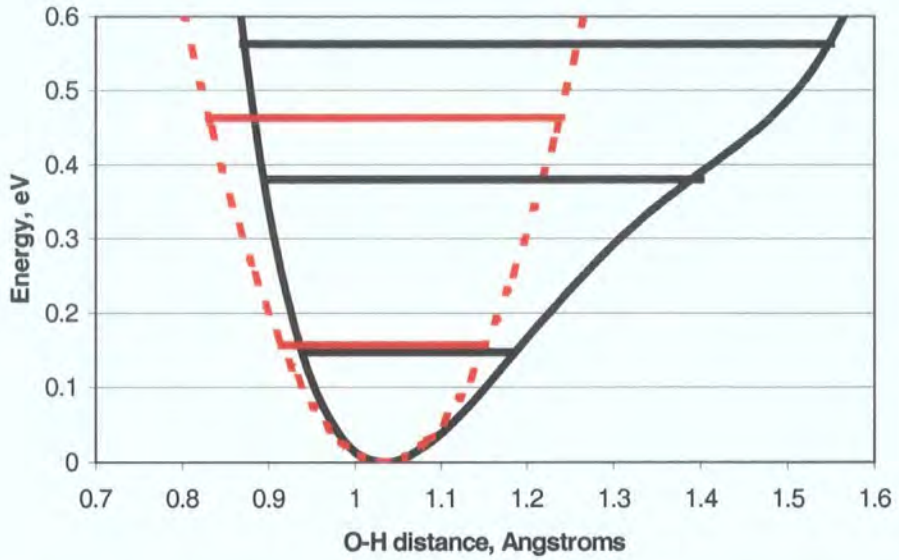


Graph 5.5.4. Harmonic potential well and energy levels (red) and anharmonic potential well and energy levels (black) for the O-H···O hydrogen bond in PDA, Calc 1.

The harmonic potential-energy wells in graphs 5.5.3 and 5.5.4 have been calculated by fitting a quadratic equation through the minimum energy and the energies calculated with the hydrogen atom displaced ±0.05Å from the minimum position along a line joining donor and acceptor atoms. This is the same displacement as in the main frequency calculation.

Using the harmonic potential-energy well in the N··H··O hydrogen bond estimates an N-H stretching frequency of ~1983cm$^{-1}$, close to the original calculated value of ~2000cm$^{-1}$. The anharmonic potential-energy well (from Calc. 1) estimates the N-H stretching frequency to be ~1240cm$^{-1}$. The harmonic potential energy well in the O-H···O hydrogen bond estimates an O-H stretching frequency of 2463cm$^{-1}$, again close to the original calculated value of ~2500cm$^{-1}$. The anharmonic potential energy (from Calc. 1) estimates the O-H stretching frequency to be ~1870cm$^{-1}$. For comparison a similar calculation for the C2-H1 stretching frequency yields 2940cm$^{-1}$ from a fully calculated potential well, 3035cm$^{-1}$ from the corresponding harmonic potential well and ~3100cm$^{-1}$ from the full dynamical matrix calculation.

In the calculated correction to the vibrational frequencies we have assumed that the hydrogen atoms in the hydrogen bonds, as they are light and weakly bonded, vibrate independently of all the other atoms in the molecule. This approximation appears reasonable given the agreement between stretching frequencies calculated from the full dynamical-matrix and the simple harmonic potential well.

The N-H stretch frequency in the N-H···O hydrogen bond (N···O distance – 2.825Å) in n-methyl acetamide (Kearley et al. 2001) is calculated, using the same procedure, to be at ~3200cm-1, much greater than that calculated for PDA. In general an N-H stretching frequency in a non-hydrogen bonded group is expected at ~3400cm$^{-1}$ and similarly a non-hydrogen-bonded O-H stretching frequency is expected to be around 3500cm$^{-1}$. The red shift in the X-H stretching frequency in X-H···Y hydrogen bonds as measured by infra-red spectroscopy has been long known and correlated with the X···Y separation (Hamilton and Ibers, 1968, and Hadži and Bratos, 1976). O-H stretching frequencies as low as 700cm$^{-1}$ have been measured in very short (O···O ~2.45Å) O-H···O hydrogen bonds.

A calculated O-H stretching frequency in an O-H···O hydrogen bond, with an O···O separation of 2.569Å at 15K, of ~2000cm$^{-1}$ fits the trend seen by Hadži and Bratos (1976). Considering the extreme shortness of the N···O separation in the N··H··O hydrogen bond and consequent weakening of the N-H bond, shown by the long N-H distance, an N-H stretching frequency of 1200-1300cm$^{-1}$ does not seem impossible. Experimental evidence is required to confirm or deny these predictions. It is claimed that broad N-H stretching bands have been seen in infrared spectra over the range between 200-1600cm$^{-1}$ in N-H···O hydrogen bonds in co-crystals of 3,5-dimethylpyridine with 3,5-dinitrobenzoic acid (N···O – 2.529Å at 80K, Jerzykiewicz et al. 1998) which does not disagree with our prediction.

### 5.5.3. Experimental Spectra

The inelastic neutron scattering spectrum of fully hydrogenaed PDA was measured on the spectrometer IN1 at the I.L.L.. IN1 can measure energy transfers between 15meV and 250meV, corresponding to between 120cm$^{-1}$ and 2000cm$^{-1}$. Approximately 5 gm of powdered PDA was encased in a rectangular aluminium sample holder and placed in a cryostat mounted on IN1. The sample was cooled to 10K where the spectrum was collected in reflection.

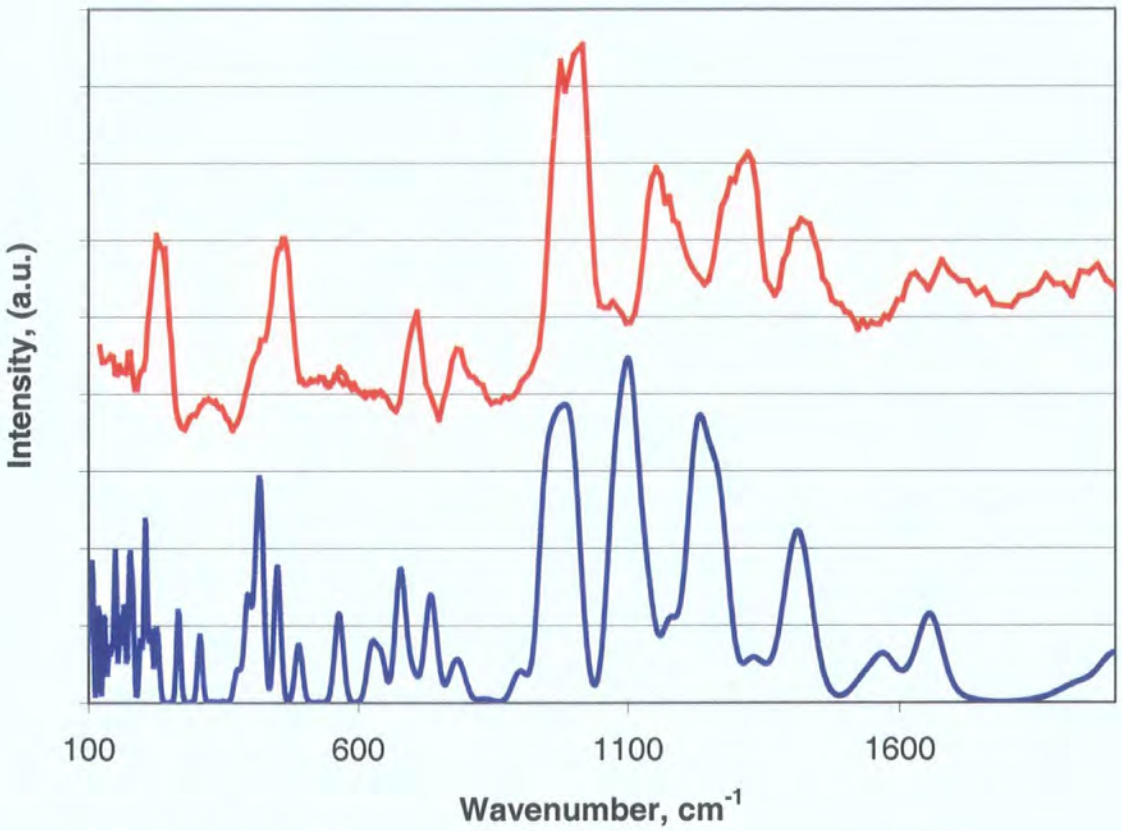


Graph 5.5.3. Calculated (blue) and measured (red) inelastic neutron scattering spectra.

The measured and calculated spectra show good agreement and it is possible to assign the important modes in the measured spectrum.

*Note.* The measurements will be completed by collecting the inelastic incoherent neutron-scattering spectra on the deuterated and partially deuterated samples using the spectrometer TOSCA at the ISIS neutron source.

### 5.6. Geometry Calculations on Expanded Unit Cells

The temperature-dependent proton migration observed in the crystals of PDA can not be explained by a static potential-energy well in which the expectation value of the proton position moves by the proton populating different energy levels in the potential well.

The calculated energy of a lone single molecule of PDA is lower in the normal form, where both carboxylic acid groups are protonated, than in the zwitterionic form, where one carboxylic acid group has become deprotonated and the nitrogen atom has become protonated (section 5.2). This suggests that the intermolecular interactions stabilise the zwitterionic form in the low-temperature crystal structure. By weakening the intermolecular interactions it should be possible to make the molecule transform to the normal form, which is the form observed in the room-temperature crystal structure.

To weaken artificially the intermolecular interactions the optimum molecular geometry has been calculated for PDA with expanded unit cells. The optimal structure has been calculated with the unit cell edges lengthened by 2%, 3% and 5% from the values measured at 15K in the fully protonated structure. The structure has also been calculated with the unit cell dimensions expanded using the measured coefficients of thermal expansion to mimic a cell at 1000K. The optimal structure has already been calculated with fixed cell dimensions (Calc. 2) and free cell dimensions (Calc. 1).

The plane wave density functional theory program CASTEP has been used for these calculations with the same conditions as the previous solid-state geometry calculations (section 5.3).

Table 5.6.1. Unit cell dimensions for the calculations.

| | a (Å) | b (Å) | c (Å) | β(°) |
|---|---|---|---|---|
| 15K, Measured | 9.7116(13) | 11.1347(17) | 6.4421(13) | 108.596(10) |
| 296K, Measured | 9.6986(7) | 11.1571(8) | 6.5891(6) | 107.804(5) |
| 2% expansion | 9.906 | 11.357 | 6.571 | 108.596 |
| 3% expansion | 10.003 | 11.469 | 6.635 | 108.596 |
| 5% expansion | 10.197 | 11.691 | 6.764 | 108.596 |
| 1000K | 9.648 | 11.188 | 6.948 | 105.716 |
| Free expansion (Calc. 1) | 9.755 | 11.297 | 6.856 | 106.330 |

Table 5.6.2. Calculated N··H··O hydrogen bond parameters.

| | N1···O4 (Å) | N1··H5 (Å) | H5··O4 (Å) | N1-H5-O4 (°) |
|---|---|---|---|---|
| No expansion (Calc. 2) | 2.551 | 1.114 | 1.438 | 176.0 |
| 2% expansion | 2.569 | 1.113 | 1.458 | 175.6 |
| 3% expansion | 2.575 | 1.505 | 1.075 | 172.5 |
| 5% expansion | 2.616 | 1.574 | 1.054 | 168.7 |
| 1000K | 2.543 | 1.120 | 1.425 | 175.8 |
| Free expansion (Calc. 1) | 2.575 | 1.116 | 1.461 | 175.1 |

* The hydrogen bond parameters have not been corrected using the potential energy well shape and the Schrödinger equation as in section 5.4.3.

Table 5.6.3. Calculated O1-H4··O3 hydrogen bond parameters.

| | O1···O3 (Å) | O1-H4 (Å) | H4···O3 (Å) | O1-H4-O3 (°) |
|---|---|---|---|---|
| No expansion (Calc. 2) | 2.551 | 1.033 | 1.527 | 170.5 |
| 2% expansion | 2.547 | 1.035 | 1.514 | 174.4 |
| 3% expansion | 2.744 | 0.999 | 1.762 | 166.8 |
| 5% expansion | 2.768 | 0.995 | 1.788 | 167.5 |
| 1000K | 2.542 | 1.034 | 1.516 | 170.9 |
| Free expansion (Calc. 1) | 2.558 | 1.032 | 1.535 | 170.1 |

The shapes of the N··H··O hydrogen bond potential energy wells have been calculated for the 3% and 5% expanded structures following the same procedure as used in section 5.4. Between the 2% expansion and the 3% expansion the potential energy wells change and the hydrogen atom jumps from the nitrogen atom to the oxygen atom.

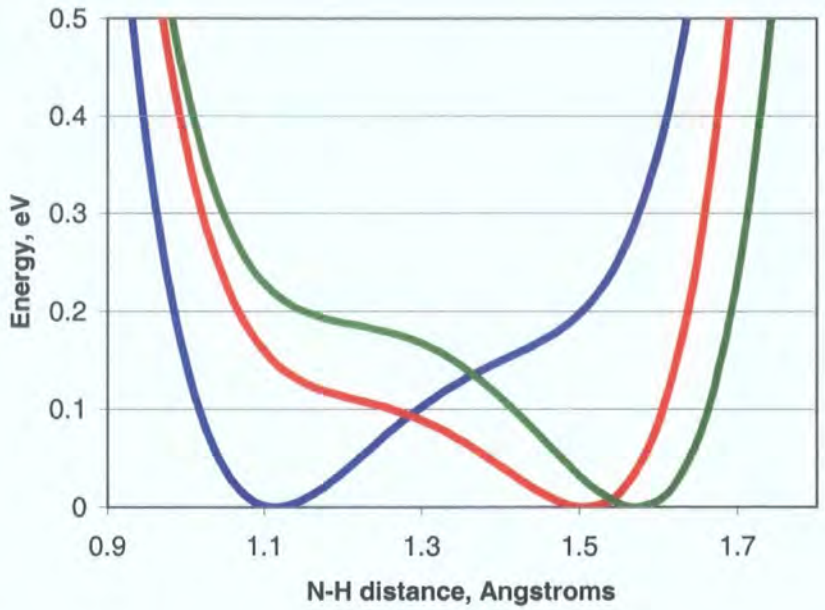


Graph 5.6.1. Calculated potential energy wells from Calc. 1 (blue), the 3% expansion (red) and the 5% expansion (green).

This theory does not agree with the real measured unit-cell expansion in hydrogenated PDA as can be seen from the calculation on the 1000K simulation and in the measured N···O distances.

However this theory does agree qualitatively with the observations of deuterated PDA, in which the cell dimensions do significantly expand, the N···O distance does significantly change and there is evidence in the diffraction data of a phase transition (graph 4.5.9). Although in deuterated PDA the O-H···O hydrogen bond shortens significantly with temperature, this calculation predicts that it should lengthen.

Table 5.6.4. Total calculated energies.

| Calculation | Total Energy, eV |
|---|---|
| Calc. 1. Free Expansion | -12800.96706 |
| 3% expansion | -12800.56298 |
| 5% expansion | -12800.65875 |

The 5% expansion has lower energy than the 3% expansion which indicates that there is a local energy minimum with an expanded unit cell. The difference between the total calculated energies of calc. 1 and the 5% expansion is ~0.3eV, which corresponds to around 3300K. This is still much too large a value for this theory to be able to explain the observed proton migration below 300K. However the extra constraints on the unit cell will have artificially increased the energy of the structure. The qualitative agreement between the

calculated results and the observed results suggests that a stable structure with the hydrogen atom closer to the oxygen atom lies in a local energy minimum close to lowest energy structure, in which the hydrogen atom lies closer to the nitrogen atom and that this structure is attainable below 300K.

From the calculations it can be concluded that the hydrogen bond potential energy well has only a single minimum not a double minimum, the proton migration is not due to populating an excited state in a static potential well and the proton migration is due to thermal evolution of the crystal structure and therefore the potential energy well.

**References**


Bransden, B.H., Joachain, C.J. (1989). Introduction to Quantum Mechanics. Longman Scientific and Technical, Harlow, Essex. 308-309.

Delley, B. (1990) J. Chem. Phys. **92**. 508-517.

Delley, B. (1991) J. Chem. Phys. **94**. 7245-7250.

Cohen, M.L., Heine, V. (1970). Solid State Physics, edited by Ehrenreich, H., Seitz, F. and Turnbull, D. Vol **24**. 38-247.

Hamann, D.R., Schlüter, M., Chiang, C. (1979). Phys. Rev. Lett. **43**, 1494-1497.

Hohenberg, P., Kohn, W. (1964). Phys. Rev. **136**, B864.

Kearley, G.J. (1995). Nucl. Insts. Meth. Phys. Res. A. **354**, 53-58.

Kearley, G.J., Johnson, M.R., Plazanet, M., Suard, E. (2001). J. Chem. Phys. **115**. 2614-2620.

Kohn, W., Sham, L.J. (1965). Phys. Rev. **140.** A1133.

Kresse, G., Furthmuller, J. (1996). Computational Materials Science, **6**, 15-50.

Nicolai, B., Kearley, G.J., (1998). Neutrons and Numerical Methods, edited by Johnson, M.R., Kearley, G.J., Büttner, H.G. 206-211.

Payne, M.C., Teter, M.P., Allan. T.C., Artas, T.A., Joannopoulos, J.D. (1992). Rev. Mod. Phys. **64**, 1045-1097

Perdew, J.P., Wang. Y. (1992). Phys Rev B. **45**, 13244-13249.

Perdew, J.P. (1986). Phys. Rev. B. **33**, 8822-8824.

Plazanet, M., Johnson, M.R., Gale, J.D., Yildrim, T., Kearley, G,J,. Fernández-Díaz, M.T., Sánchez-Portal, D., Artacho, E., Soler, J.M., Ordejón, P., Garcia, A., Tromsdorff, H.P. (2000). Chemical Physics. **261**, 189-204.

Plazanet, M., Fukushima, N., Johnson, M.R., Horsewill, A.J., Trommsdorff, H.P. (2001). J. Chem. Phys. **115,** 3241-3248.

Tagusagawa, F., Hirotsu, K., Shimada. A. (1973). Bull. Chem. Soc. Jpn. **46**, 2669-2672.

Sears, V.F. (1992). Neutron News. Vol 3. No 3. 26-37.

## 6. Conclusions

The crystal structures of DMIY have produced novel intermolecular interactions, not least the N-H···C hydrogen bond and the extremely short C-H···O hydrogen bond, which is 0.137Å shorter than any other C-H···O hydrogen previously observed. Structures using DMIY or a similar carbene-based molecule should continue to produce novel supramolecular chemistry.

The serendipitous observation of the temperature-dependent proton migration in the short N··H··O hydrogen bond in the co-crystal of benzene-1,2,4,5-tetracarboxylic acid with 4,4'-bipyridine and the hoped-for and found occurrence of the same effect in pyridine-3,5-dicarboxylic acid has proved that this phenomenon, observed only once before (Steiner et al. 2001), is not an unusual occurrence. Indeed the same behaviour may occur in all sufficiently short N···O hydrogen bonds.

Deuteration of the hydrogen bonds in pyridine-3,5-dicarboxylic acid increased the magnitude of the proton migration. The clear step in the reflection intensities and the change in the cell dimensions in the deuterated case made the phenomenon appear more like a clear-cut phase transition. More experimental evidence at a greater number of intermediate temperatures for both deuterated and protonated structures should allow an estimation of the energy gap between the O-H···N and N-H···O structures. Variable-temperature inelastic neutron-scattering spectra, infra-red or Raman spectra would also lead to a much clearer picture of what is happening in the phase transitions.

The computational work has not yet provided a convincing model for the proton transfer, although it has ruled out a static single-minimum potential-energy well with different populations in the energy levels. Increasing the volume of the unit cell managed to mimic the proton transfer effect albeit in a slightly unrealistic way, as the unit cell volume changes were of a much higher magnitude than those observed. Hopefully more complex calculations with a more realistic way to model the effects of temperature will provide a more convincing mechanism for the proton transfer with energies attainable below 300K.

Using the one-dimensional Schrödinger equation to modify the calculated inelastic neutron-scattering spectra is a simple and enticing oversimplification. Only the measured inelastic neutron-scattering spectra can confirm or deny the validity of the perhaps quite significant approximations made. A detailed investigation of the known O-H stretching frequencies using the same methodologies could perhaps be undertaken to explain the magnitudes of hydrogen-bonded red shift observed in infra-red data.

To predict a crystal structure or the conformation of a protein is extremely difficult since both rely on weak intermolecular interactions. The number of degrees of freedom can be

immense. The reduction of the degrees of freedom by calculating real or empirical potential-energy surfaces for a molecule could reduce the degrees of freedom when attempting to calculate the structure. The calculation of the minimum energies for molecules of BPY and PMA is not adequate to explain the structures observed in crystals. The Cambridge Structural database contains many examples of these molecules lying at minimum-force positions, which appear to be unstable energy states. Molecular packing must stabilise these states. The graphs in sections 3.12 and 3.13 should be helpful for crystal structure prediction although the implementation of the information in structure prediction is not obvious.

The investigation of hydrogen bonding using X-ray and neutron diffraction has yielded new insights into hydrogen bonds. Database studies and computer simulations provide complementary information and a more complete view of the chemical and physical processes in the crystals. The novel hydrogen bonds studied in this work have provided new data points for further studies.

**Supplement 2.4. Tables of Results of Refinement for 1,3-Dimesitylimidazol-2-ylidene.**

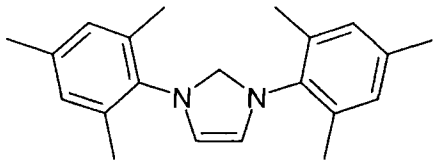

Table 2.4.xyz. Atomic coordinates ( x $10^4$) and equivalent isotropic displacement parameters ($Å^2$x $10^3$). U(eq) is defined as one third of the trace of the orthogonalized $U^{ij}$ tensor.

| | x | y | z | Ueq |
|---|---|---|---|---|
| N(1) | 879(2) | 5488(1) | 3474(2) | 21(1) |
| N(2) | -87(2) | 3958(1) | 3266(1) | 20(1) |
| C(1) | 305(2) | 4714(1) | 2358(2) | 20(1) |
| C(2) | 830(2) | 5233(1) | 4990(2) | 31(1) |
| C(3) | 219(2) | 4257(1) | 4859(2) | 29(1) |
| C(11) | 1474(2) | 6464(1) | 3076(2) | 20(1) |
| C(12) | 270(2) | 7209(1) | 2271(2) | 21(1) |
| C(13) | 867(2) | 8124(1) | 1817(2) | 23(1) |
| C(14) | 2609(2) | 8301(1) | 2157(2) | 23(1) |
| C(15) | 3765(2) | 7546(1) | 2991(2) | 24(1) |
| C(16) | 3227(2) | 6615(1) | 3464(2) | 23(1) |
| C(17) | -1619(2) | 7020(2) | 1887(2) | 31(1) |
| C(18) | 3211(3) | 9292(2) | 1633(2) | 33(1) |
| C(19) | 4498(2) | 5807(2) | 4361(2) | 32(1) |
| C(21) | -834(2) | 2991(1) | 2569(2) | 19(1) |
| C(22) | 165(2) | 2278(1) | 2093(2) | 20(1) |
| C(23) | -622(2) | 1384(1) | 1292(2) | 20(1) |
| C(24) | -2351(2) | 1190(1) | 985(2) | 21(1) |
| C(25) | -3294(2) | 1904(1) | 1508(2) | 23(1) |
| C(26) | -2568(2) | 2813(1) | 2310(2) | 21(1) |
| C(27) | 2034(2) | 2486(1) | 2391(2) | 27(1) |
| C(28) | -3161(2) | 219(1) | 115(2) | 29(1) |
| C(29) | -3623(2) | 3581(1) | 2838(2) | 30(1) |

Table 2.4.bond. Selected Bond Lengths (Å).

| | | | |
|---|---|---|---|
| N(1)-C(1) | 1.3693(19) | C(14)-C(18) | 1.507(2) |
| N(1)-C(2) | 1.390(2) | C(15)-C(16) | 1.399(2) |
| N(1)-C(11) | 1.4446(18) | C(16)-C(19) | 1.505(2) |
| N(2)-C(1) | 1.3727(19) | C(21)-C(22) | 1.401(2) |
| N(2)-C(3) | 1.3915(19) | C(21)-C(26) | 1.4027(19) |
| N(2)-C(21) | 1.4383(19) | C(22)-C(23) | 1.397(2) |
| C(2)-C(3) | 1.354(2) | C(22)-C(27) | 1.512(2) |
| C(11)-C(16) | 1.395(2) | C(23)-C(24) | 1.395(2) |
| C(11)-C(12) | 1.397(2) | C(24)-C(25) | 1.391(2) |
| C(12)-C(13) | 1.395(2) | C(24)-C(28) | 1.506(2) |
| C(12)-C(17) | 1.512(2) | C(25)-C(26) | 1.399(2) |
| C(13)-C(14) | 1.397(2) | C(26)-C(29) | 1.503(2) |
| C(14)-C(15) | 1.392(2) | | |

Table 2.4.angle. Selected Bond Angles (°).

| | | | |
|---|---|---|---|
| C(1)-N(1)-C(2) | 113.37(13) | C(14)-C(15)-C(16) | 121.88(14) |
| C(1)-N(1)-C(11) | 122.10(12) | C(11)-C(16)-C(15) | 117.69(13) |
| C(2)-N(1)-C(11) | 124.53(13) | C(11)-C(16)-C(19) | 121.25(14) |
| C(1)-N(2)-C(3) | 113.03(13) | C(15)-C(16)-C(19) | 121.06(14) |
| C(1)-N(2)-C(21) | 121.81(12) | C(22)-C(21)-C(26) | 121.92(13) |
| C(3)-N(2)-C(21) | 125.05(13) | C(22)-C(21)-N(2) | 119.15(12) |
| N(1)-C(1)-N(2) | 101.48(12) | C(26)-C(21)-N(2) | 118.85(13) |
| C(3)-C(2)-N(1) | 105.95(14) | C(23)-C(22)-C(21) | 118.28(13) |
| C(2)-C(3)-N(2) | 106.16(14) | C(23)-C(22)-C(27) | 120.79(13) |
| C(16)-C(11)-C(12) | 122.37(14) | C(21)-C(22)-C(27) | 120.91(13) |
| C(16)-C(11)-N(1) | 118.80(13) | C(24)-C(23)-C(22) | 121.39(13) |
| C(12)-C(11)-N(1) | 118.79(13) | C(25)-C(24)-C(23) | 118.73(13) |
| C(13)-C(12)-C(11) | 117.88(14) | C(25)-C(24)-C(28) | 121.22(14) |
| C(13)-C(12)-C(17) | 121.30(14) | C(23)-C(24)-C(28) | 120.04(14) |
| C(11)-C(12)-C(17) | 120.81(14) | C(24)-C(25)-C(26) | 122.10(13) |
| C(12)-C(13)-C(14) | 121.67(14) | C(25)-C(26)-C(21) | 117.55(13) |
| C(15)-C(14)-C(13) | 118.48(14) | C(25)-C(26)-C(29) | 121.04(14) |
| C(15)-C(14)-C(18) | 121.14(15) | C(21)-C(26)-C(29) | 121.40(14) |
| C(13)-C(14)-C(18) | 120.38(15) | | |

Table 2.4.anis. Anisotropic displacement parameters ($Å^2 x\ 10^3$). The anisotropic displacement factor exponent takes the form: $-2\pi^2[ h^2 a^{*2} U^{11} + ... + 2 h k a^* b^* U^{12} ]$

| | $U_{11}$ | $U_{22}$ | $U_{33}$ | $U_{23}$ | $U_{13}$ | $U_{12}$ |
|---|---|---|---|---|---|---|
| N(1) | 29(1) | 16(1) | 19(1) | 0(1) | 9(1) | -1(1) |
| N(2) | 25(1) | 18(1) | 17(1) | 0(1) | 8(1) | 0(1) |
| C(1) | 24(1) | 17(1) | 20(1) | -1(1) | 8(1) | -1(1) |
| C(2) | 49(1) | 26(1) | 19(1) | -3(1) | 13(1) | -7(1) |
| C(3) | 46(1) | 26(1) | 19(1) | 0(1) | 15(1) | -4(1) |
| C(11) | 29(1) | 14(1) | 18(1) | -3(1) | 10(1) | -1(1) |
| C(12) | 25(1) | 18(1) | 21(1) | -3(1) | 10(1) | 1(1) |
| C(13) | 29(1) | 18(1) | 22(1) | -1(1) | 9(1) | 2(1) |
| C(14) | 31(1) | 18(1) | 22(1) | -3(1) | 11(1) | -4(1) |
| C(15) | 25(1) | 23(1) | 25(1) | -3(1) | 8(1) | -3(1) |
| C(16) | 27(1) | 19(1) | 21(1) | -2(1) | 7(1) | 2(1) |
| C(17) | 25(1) | 27(1) | 40(1) | 4(1) | 13(1) | 2(1) |
| C(18) | 38(1) | 25(1) | 34(1) | 3(1) | 10(1) | -9(1) |
| C(19) | 31(1) | 26(1) | 34(1) | 2(1) | 4(1) | 5(1) |
| C(21) | 22(1) | 16(1) | 17(1) | 2(1) | 7(1) | 0(1) |
| C(22) | 19(1) | 20(1) | 20(1) | 3(1) | 8(1) | 0(1) |
| C(23) | 24(1) | 17(1) | 21(1) | 2(1) | 11(1) | 2(1) |
| C(24) | 28(1) | 19(1) | 17(1) | 3(1) | 7(1) | -3(1) |
| C(25) | 20(1) | 24(1) | 25(1) | 4(1) | 9(1) | -2(1) |
| C(26) | 24(1) | 19(1) | 22(1) | 5(1) | 10(1) | 4(1) |
| C(27) | 20(1) | 24(1) | 36(1) | -1(1) | 11(1) | -1(1) |
| C(28) | 32(1) | 25(1) | 30(1) | -4(1) | 12(1) | -9(1) |
| C(29) | 30(1) | 23(1) | 42(1) | 2(1) | 19(1) | 6(1) |

Table 2.4.H. Hydrogen coordinates ( x $10^4$) and isotropic displacement parameters ($Å^2$x $10^3$).

| | X | Y | Z | Uiso |
|---|---|---|---|---|
| H(2) | 1180(30) | 5700(20) | 5930(30) | 56(7) |
| H(3) | -130(30) | 3876(19) | 5600(30) | 38(6) |
| H(13) | 100(30) | 8682(18) | 1260(30) | 32(5) |
| H(15) | 4960(30) | 7674(18) | 3180(20) | 27(5) |
| H(17A) | -2290(30) | 7653(18) | 1440(30) | 32(5) |
| H(17B) | -1900(30) | 6870(20) | 2810(30) | 39(6) |
| H(17C) | -2020(40) | 6460(20) | 1100(40) | 55(7) |
| H(18A) | 2530(40) | 9480(30) | 540(40) | 66(9) |
| H(18B) | 4350(40) | 9300(20) | 1700(30) | 59(8) |
| H(18C) | 3070(40) | 9900(30) | 2330(40) | 78(10) |
| H(19A) | 4460(30) | 5770(20) | 5440(30) | 44(6) |
| H(19B) | 4140(30) | 5110(20) | 3870(30) | 44(7) |
| H(19C) | 5590(30) | 5970(20) | 4290(30) | 47(7) |
| H(23) | 60(20) | 921(18) | 980(20) | 25(5) |
| H(25) | -4500(30) | 1767(16) | 1320(20) | 23(5) |
| H(27A) | 2580(30) | 1870(20) | 2120(30) | 45(7) |
| H(27B) | 2610(30) | 2700(20) | 3500(30) | 43(6) |
| H(27C) | 2200(30) | 3000(20) | 1680(30) | 40(6) |
| H(28A) | -4390(30) | 320(20) | -490(30) | 47(7) |
| H(28B) | -3080(30) | -310(20) | 960(30) | 43(6) |
| H(28C) | -2560(30) | 17(18) | -590(30) | 33(6) |
| H(29A) | -3320(30) | 4300(20) | 2670(30) | 39(6) |
| H(29B) | -4830(30) | 3406(19) | 2310(30) | 33(5) |
| H(29C) | -3450(30) | 3520(20) | 4000(30) | 43(6) |

**Supplement 2.5. Tables of Results of Refinement for 2(2-hydroxyphenyl)benzoxazole and 1,3-Dimesitylimidazol-2-ylidene.**

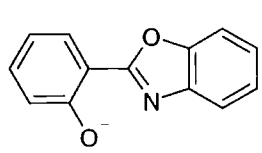


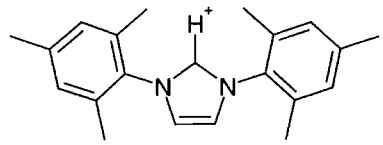


Table 2.5.xyz. Atomic coordinates ( x $10^4$) and equivalent isotropic displacement parameters ($Å^2$x $10^3$). U(eq) is defined as one third of the trace of the orthogonalized $U^{ij}$ tensor.

| | X | Y | Z | Ueq |
|---|---|---|---|---|
| N(1) | 2063(1) | 4223(1) | 5392(1) | 21(1) |
| N(2) | 1318(1) | 2897(1) | 5879(1) | 20(1) |
| C(1) | 1791(1) | 2542(2) | 5513(1) | 21(1) |
| C(3) | 1290(1) | 4872(2) | 5988(1) | 23(1) |
| C(2) | 1754(1) | 5703(2) | 5682(1) | 24(1) |
| C(11) | 2609(1) | 4458(2) | 5031(1) | 21(1) |
| C(12) | 2460(1) | 4612(2) | 4314(1) | 23(1) |
| C(13) | 2994(1) | 4885(2) | 3983(1) | 29(1) |
| C(14) | 3646(1) | 4995(2) | 4347(1) | 34(1) |
| C(15) | 3770(1) | 4813(2) | 5064(1) | 32(1) |
| C(16) | 3254(1) | 4549(2) | 5423(1) | 26(1) |
| C(17) | 1752(1) | 4502(2) | 3924(1) | 29(1) |
| C(18) | 4211(1) | 5336(3) | 3968(1) | 56(1) |
| C(19) | 3388(1) | 4392(2) | 6200(1) | 35(1) |
| C(21) | 942(1) | 1429(2) | 6157(1) | 20(1) |
| C(22) | 1290(1) | 214(2) | 6672(1) | 20(1) |
| C(23) | 918(1) | -1160(2) | 6946(1) | 22(1) |
| C(24) | 232(1) | -1371(2) | 6712(1) | 22(1) |
| C(25) | -91(1) | -151(2) | 6190(1) | 23(1) |
| C(26) | 256(1) | 1284(2) | 5911(1) | 21(1) |
| C(27) | 2035(1) | 354(2) | 6926(1) | 27(1) |
| C(28) | -149(1) | -2886(2) | 7023(1) | 33(1) |
| C(29) | -119(1) | 2611(2) | 5363(1) | 28(1) |
| C(31) | 4200(1) | -396(2) | 5729(1) | 27(1) |
| C(32) | 4868(1) | -359(3) | 6028(1) | 39(1) |
| C(33) | 5017(1) | -522(3) | 6744(1) | 44(1) |
| C(34) | 4511(1) | -710(3) | 7124(1) | 39(1) |
| C(35) | 3841(1) | -742(2) | 6808(1) | 33(1) |
| C(36) | 3685(1) | -577(2) | 6089(1) | 25(1) |

| | | | | |
|---|---|---|---|---|
| O(2) | 3920(1) | -275(1) | 5039(1) | 27(1) |
| N(3) | 3073(1) | -562(2) | 5618(1) | 24(1) |
| C(40) | 3235(1) | -386(2) | 5014(1) | 22(1) |
| O(1) | 1777(1) | -858(1) | 4660(1) | 24(1) |
| C(41) | 2833(1) | -312(2) | 4318(1) | 21(1) |
| C(42) | 3164(1) | 6(2) | 3767(1) | 27(1) |
| C(43) | 2835(1) | 21(2) | 3087(1) | 31(1) |
| C(44) | 2146(1) | -310(2) | 2943(1) | 28(1) |
| C(45) | 1806(1) | -629(2) | 3469(1) | 26(1) |
| C(46) | 2123(1) | -616(2) | 4187(1) | 21(1) |

Table 2.5.bond. Selected Bond Lengths (Å).

| | | | |
|---|---|---|---|
| N(1)-C(1) | 1.3336(16) | C(24)-C(25) | 1.3954(17) |
| N(1)-C(2) | 1.3877(16) | C(24)-C(28) | 1.5087(18) |
| N(1)-C(11) | 1.4483(15) | C(25)-C(26) | 1.3972(17) |
| N(2)-C(1) | 1.3387(15) | C(26)-C(29) | 1.5096(17) |
| N(2)-C(3) | 1.3907(16) | C(31)-O(2) | 1.3710(15) |
| N(2)-C(21) | 1.4488(15) | C(31)-C(32) | 1.3775(19) |
| C(1)-H(1) | 0.967(17) | C(31)-C(36) | 1.3863(18) |
| C(3)-C(2) | 1.3496(18) | C(32)-C(33) | 1.390(2) |
| C(11)-C(12) | 1.3924(17) | C(33)-C(34) | 1.397(2) |
| C(11)-C(16) | 1.3926(18) | C(34)-C(35) | 1.389(2) |
| C(12)-C(13) | 1.3909(18) | C(35)-C(36) | 1.3965(18) |
| C(12)-C(17) | 1.5025(19) | C(36)-N(3) | 1.4043(16) |
| C(13)-C(14) | 1.386(2) | O(2)-C(40) | 1.3932(14) |
| C(14)-C(15) | 1.394(2) | N(3)-C(40) | 1.3055(16) |
| C(14)-C(18) | 1.514(2) | C(40)-C(41) | 1.4549(17) |
| C(15)-C(16) | 1.3928(19) | O(1)-C(46) | 1.2877(15) |
| C(16)-C(19) | 1.5079(19) | C(41)-C(42) | 1.4068(17) |
| C(21)-C(26) | 1.3945(17) | C(41)-C(46) | 1.4405(17) |
| C(21)-C(22) | 1.4015(16) | C(42)-C(43) | 1.3789(19) |
| C(22)-C(23) | 1.3935(17) | C(43)-C(44) | 1.401(2) |
| C(22)-C(27) | 1.5090(17) | C(44)-C(45) | 1.3746(19) |
| C(23)-C(24) | 1.3949(17) | C(45)-C(46) | 1.4384(17) |

Table 2.5.angle. Selected Bond Angles (°).

| | | | |
|---|---|---|---|
| C(1)-N(1)-C(2) | 109.53(10) | C(23)-C(24)-C(25) | 118.65(11) |
| C(1)-N(1)-C(11) | 125.11(10) | C(23)-C(24)-C(28) | 120.28(11) |
| C(2)-N(1)-C(11) | 125.33(10) | C(25)-C(24)-C(28) | 121.07(12) |
| C(1)-N(2)-C(3) | 108.77(10) | C(24)-C(25)-C(26) | 121.36(11) |
| C(1)-N(2)-C(21) | 124.71(10) | C(21)-C(26)-C(25) | 117.90(11) |
| C(3)-N(2)-C(21) | 126.34(10) | C(21)-C(26)-C(29) | 122.59(11) |
| N(1)-C(1)-N(2) | 107.80(10) | C(25)-C(26)-C(29) | 119.51(11) |
| N(1)-C(1)-H(1) | 125.1(9) | O(2)-C(31)-C(32) | 127.54(12) |
| N(2)-C(1)-H(1) | 127.0(9) | O(2)-C(31)-C(36) | 107.76(11) |
| C(2)-C(3)-N(2) | 107.30(11) | C(32)-C(31)-C(36) | 124.70(12) |
| C(3)-C(2)-N(1) | 106.59(11) | C(31)-C(32)-C(33) | 115.76(13) |
| C(12)-C(11)-C(16) | 123.71(11) | C(32)-C(33)-C(34) | 121.10(14) |
| C(12)-C(11)-N(1) | 118.29(11) | C(35)-C(34)-C(33) | 121.91(13) |
| C(16)-C(11)-N(1) | 117.99(11) | C(34)-C(35)-C(36) | 117.50(13) |
| C(13)-C(12)-C(11) | 116.97(12) | C(31)-C(36)-C(35) | 119.02(12) |
| C(13)-C(12)-C(17) | 122.14(12) | C(31)-C(36)-N(3) | 109.07(11) |
| C(11)-C(12)-C(17) | 120.89(11) | C(35)-C(36)-N(3) | 131.91(12) |
| C(14)-C(13)-C(12) | 121.79(13) | C(31)-O(2)-C(40) | 104.60(9) |
| C(13)-C(14)-C(15) | 119.05(12) | C(40)-N(3)-C(36) | 104.61(10) |
| C(13)-C(14)-C(18) | 120.09(14) | N(3)-C(40)-O(2) | 113.97(11) |
| C(15)-C(14)-C(18) | 120.86(15) | N(3)-C(40)-C(41) | 131.93(11) |
| C(16)-C(15)-C(14) | 121.65(13) | O(2)-C(40)-C(41) | 114.09(10) |
| C(11)-C(16)-C(15) | 116.83(12) | C(42)-C(41)-C(46) | 120.40(11) |
| C(11)-C(16)-C(19) | 121.57(12) | C(42)-C(41)-C(40) | 117.85(11) |
| C(15)-C(16)-C(19) | 121.59(13) | C(46)-C(41)-C(40) | 121.71(11) |
| C(26)-C(21)-C(22) | 122.74(11) | C(43)-C(42)-C(41) | 122.55(12) |
| C(26)-C(21)-N(2) | 119.41(10) | C(42)-C(43)-C(44) | 118.25(12) |
| C(22)-C(21)-N(2) | 117.84(10) | C(45)-C(44)-C(43) | 120.78(12) |
| C(23)-C(22)-C(21) | 117.10(11) | C(44)-C(45)-C(46) | 123.18(12) |
| C(23)-C(22)-C(27) | 120.42(11) | O(1)-C(46)-C(45) | 120.65(11) |
| C(21)-C(22)-C(27) | 122.48(11) | O(1)-C(46)-C(41) | 124.56(11) |
| C(22)-C(23)-C(24) | 122.20(11) | C(45)-C(46)-C(41) | 114.79(11) |

Table 2.5.anis. Anisotropic displacement parameters ($Å^2 x\ 10^3$). The anisotropic displacement factor exponent takes the form: $-2\pi^2[ h^2 a^{*2} U^{11} + ... + 2 h k a^* b^* U^{12} ]$

| | $U_{11}$ | $U_{22}$ | $U_{33}$ | $U_{23}$ | $U_{13}$ | $U_{12}$ |
|---|---|---|---|---|---|---|
| N(1) | 24(1) | 19(1) | 21(1) | 0(1) | 7(1) | -1(1) |
| N(2) | 22(1) | 19(1) | 20(1) | 0(1) | 6(1) | 1(1) |
| C(1) | 23(1) | 19(1) | 20(1) | 0(1) | 7(1) | 0(1) |
| C(3) | 26(1) | 20(1) | 23(1) | -1(1) | 6(1) | 3(1) |
| C(2) | 28(1) | 18(1) | 25(1) | -1(1) | 6(1) | 1(1) |
| C(11) | 25(1) | 17(1) | 25(1) | 0(1) | 10(1) | -2(1) |
| C(12) | 29(1) | 17(1) | 24(1) | 0(1) | 8(1) | 0(1) |
| C(13) | 37(1) | 26(1) | 29(1) | 3(1) | 16(1) | 3(1) |
| C(14) | 32(1) | 30(1) | 45(1) | 6(1) | 20(1) | 3(1) |
| C(15) | 24(1) | 30(1) | 44(1) | 4(1) | 8(1) | 0(1) |
| C(16) | 28(1) | 22(1) | 29(1) | 2(1) | 6(1) | -1(1) |
| C(17) | 33(1) | 29(1) | 24(1) | 1(1) | 3(1) | -3(1) |
| C(18) | 43(1) | 68(1) | 68(1) | 16(1) | 35(1) | 6(1) |
| C(19) | 35(1) | 37(1) | 30(1) | 3(1) | -1(1) | -3(1) |
| C(21) | 23(1) | 18(1) | 19(1) | -1(1) | 8(1) | 1(1) |
| C(22) | 21(1) | 21(1) | 19(1) | -2(1) | 5(1) | 2(1) |
| C(23) | 26(1) | 20(1) | 20(1) | 1(1) | 5(1) | 3(1) |
| C(24) | 25(1) | 21(1) | 21(1) | -2(1) | 8(1) | -1(1) |
| C(25) | 20(1) | 25(1) | 23(1) | -2(1) | 6(1) | 0(1) |
| C(26) | 22(1) | 21(1) | 20(1) | 0(1) | 5(1) | 3(1) |
| C(27) | 22(1) | 30(1) | 28(1) | 3(1) | 2(1) | 0(1) |
| C(28) | 33(1) | 32(1) | 34(1) | 7(1) | 9(1) | -7(1) |
| C(29) | 26(1) | 30(1) | 27(1) | 7(1) | 2(1) | 3(1) |
| C(31) | 25(1) | 34(1) | 23(1) | -1(1) | 4(1) | -1(1) |
| C(32) | 22(1) | 65(1) | 31(1) | -1(1) | 6(1) | -3(1) |
| C(33) | 24(1) | 73(1) | 31(1) | -2(1) | -1(1) | 1(1) |
| C(34) | 31(1) | 62(1) | 23(1) | 0(1) | 2(1) | 5(1) |
| C(35) | 29(1) | 49(1) | 24(1) | 1(1) | 7(1) | 4(1) |
| C(36) | 22(1) | 28(1) | 25(1) | -1(1) | 5(1) | 2(1) |
| O(2) | 19(1) | 38(1) | 22(1) | 1(1) | 4(1) | -2(1) |
| N(3) | 22(1) | 29(1) | 23(1) | 0(1) | 6(1) | 2(1) |
| C(40) | 19(1) | 20(1) | 26(1) | -1(1) | 6(1) | 0(1) |
| O(1) | 22(1) | 26(1) | 27(1) | -4(1) | 9(1) | -2(1) |
| C(41) | 22(1) | 20(1) | 22(1) | -1(1) | 5(1) | 0(1) |
| C(42) | 23(1) | 31(1) | 27(1) | 1(1) | 6(1) | -3(1) |

| | | | | | | |
|---|---|---|---|---|---|---|
| C(43) | 33(1) | 36(1) | 24(1) | 2(1) | 8(1) | -5(1) |
| C(44) | 31(1) | 30(1) | 22(1) | -2(1) | 1(1) | -3(1) |
| C(45) | 23(1) | 26(1) | 27(1) | -4(1) | 1(1) | -1(1) |
| C(46) | 22(1) | 16(1) | 25(1) | -3(1) | 6(1) | 0(1) |

Table 2.5.H. Hydrogen atom coordinates ( x $10^4$) and isotropic displacement parameters ($Å^2$x 10 $^3$).

| | X | Y | Z | Uiso |
|---|---|---|---|---|
| H(1) | 1908(7) | 1310(20) | 5345(8) | 32(4) |
| H(3) | 975(8) | 5400(20) | 6241(8) | 30(4) |
| H(2) | 1884(7) | 7010(20) | 5627(8) | 32(4) |
| H(13) | 2897(8) | 5020(20) | 3476(8) | 31(4) |
| H(15) | 4231(9) | 4950(30) | 5323(9) | 45(5) |
| H(17A) | 1732(9) | 4570(30) | 3433(10) | 50(5) |
| H(17B) | 1467(10) | 5580(30) | 4073(10) | 57(6) |
| H(17C) | 1533(9) | 3270(30) | 4030(9) | 45(5) |
| H(18A) | 4053 | 6145 | 3562 | 84 |
| H(18B) | 4366 | 4098 | 3821 | 84 |
| H(18C) | 4579 | 5986 | 4276 | 84 |
| H(19A) | 3845(11) | 4390(30) | 6382(10) | 56(6) |
| H(19B) | 3185(9) | 3200(30) | 6352(9) | 47(5) |
| H(19C) | 3156(10) | 5480(30) | 6401(10) | 58(6) |
| H(23) | 1146(7) | -2000(20) | 7316(7) | 22(3) |
| H(25) | -571(8) | -280(20) | 6007(8) | 26(4) |
| H(27A) | 2166(9) | 1660(30) | 7090(9) | 46(5) |
| H(27B) | 2288(9) | 20(30) | 6558(9) | 44(5) |
| H(27C) | 2172(8) | -600(20) | 7304(8) | 30(4) |
| H(28A) | 80(11) | -3250(30) | 7478(13) | 77(7) |
| H(28B) | -225(11) | -4010(30) | 6722(11) | 70(6) |
| H(28C) | -598(12) | -2430(40) | 7071(12) | 82(7) |
| H(29A) | -564(9) | 2150(30) | 5200(9) | 43(5) |
| H(29B) | 109(8) | 2680(20) | 4968(9) | 38(4) |
| H(29C) | -136(8) | 3930(30) | 5547(9) | 41(4) |
| H(32) | 5211(9) | -220(30) | 5760(9) | 45(5) |
| H(33) | 5492(10) | -480(30) | 6983(10) | 55(5) |
| H(34) | 4632(9) | -830(30) | 7612(10) | 53(5) |

| | | | | |
|---|---|---|---|---|
| H(35) | 3480(8) | -890(20) | 7062(9) | 39(4) |
| H(42) | 3652(8) | 220(20) | 3874(8) | 31(4) |
| H(43) | 3079(8) | 290(20) | 2719(9) | 39(4) |
| H(44) | 1903(8) | -330(20) | 2459(8) | 32(4) |
| H(45) | 1327(8) | -860(20) | 3370(8) | 35(4) |

**Supplement 2.6. Tables of Results of Refinement for the Co-crystal of Diphenylamine and 1,3-Dimesitylimidizol-2-ylidene.**

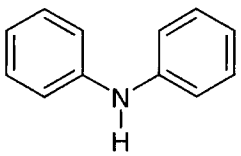


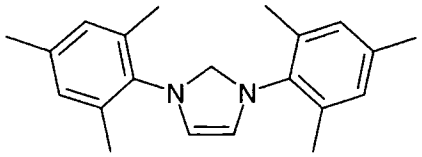


Table 2.6.xyz. Atomic coordinates ( x $10^4$) and equivalent isotropic displacement parameters ($Å^2$x $10^3$). U(eq) is defined as one third of the trace of the orthogonalized $U^{ij}$ tensor.

| | X | Y | Z | Ueq |
|---|---|---|---|---|
| C(1) | 3621(1) | -833(1) | 3200(1) | 14(1) |
| C(2) | 2016(1) | -2011(1) | 4060(1) | 15(1) |
| C(3) | 1339(1) | -1212(1) | 3407(1) | 14(1) |
| N(1) | 3396(1) | -1775(1) | 3923(1) | 13(1) |
| N(2) | 2317(1) | -500(1) | 2898(1) | 13(1) |
| C(11) | 4484(1) | -2446(1) | 4479(1) | 13(1) |
| C(12) | 5673(1) | -3696(1) | 4197(1) | 14(1) |
| C(13) | 6734(1) | -4288(1) | 4731(1) | 14(1) |
| C(14) | 6635(1) | -3679(1) | 5522(1) | 15(1) |
| C(15) | 5426(1) | -2444(1) | 5782(1) | 15(1) |
| C(16) | 4333(1) | -1806(1) | 5269(1) | 14(1) |
| C(17) | 5842(2) | -4354(1) | 3326(1) | 16(1) |
| C(18) | 7798(2) | -4346(1) | 6090(1) | 18(1) |
| C(19) | 3064(2) | -448(1) | 5548(1) | 17(1) |
| C(21) | 2073(1) | 430(1) | 2097(1) | 13(1) |
| C(22) | 2892(1) | -65(1) | 1197(1) | 13(1) |
| C(23) | 2715(1) | 856(1) | 419(1) | 14(1) |
| C(24) | 1782(1) | 2238(1) | 532(1) | 14(1) |
| C(25) | 978(1) | 2683(1) | 1444(1) | 14(1) |
| C(26) | 1087(1) | 1793(1) | 2240(1) | 14(1) |
| C(27) | 3975(2) | -1534(1) | 1081(1) | 15(1) |
| C(28) | 1672(2) | 3246(1) | -308(1) | 17(1) |
| C(29) | 189(2) | 2293(1) | 3219(1) | 17(1) |
| N(3) | 6530(1) | 108(1) | 2134(1) | 14(1) |
| C(31) | 6280(1) | 1455(1) | 1765(1) | 14(1) |
| C(32) | 4873(1) | 2203(1) | 1539(1) | 15(1) |
| C(33) | 4550(1) | 3563(1) | 1209(1) | 15(1) |
| C(34) | 5615(2) | 4212(1) | 1092(1) | 16(1) |

| | | | | |
|---|---|---|---|---|
| C(35) | 7011(2) | 3473(1) | 1316(1) | 16(1) |
| C(36) | 7351(1) | 2111(1) | 1651(1) | 15(1) |
| C(41) | 7975(1) | -945(1) | 2034(1) | 14(1) |
| C(42) | 9283(1) | -974(1) | 1269(1) | 15(1) |
| C(43) | 10661(2) | -2094(1) | 1175(1) | 17(1) |
| C(44) | 10775(2) | -3198(1) | 1833(1) | 17(1) |
| C(45) | 9484(2) | -3177(1) | 2592(1) | 16(1) |
| C(46) | 8099(1) | -2058(1) | 2698(1) | 15(1) |

Table 2.6.bond. Selected Bond Lengths (Å).

| | | | |
|---|---|---|---|
| C(1)-N(1) | 1.3700(16) | C(23)-C(24) | 1.4016(18) |
| C(1)-N(2) | 1.3730(16) | C(24)-C(25) | 1.3979(19) |
| C(2)-C(3) | 1.3446(18) | C(24)-C(28) | 1.5124(18) |
| C(2)-N(1) | 1.3954(16) | C(25)-C(26) | 1.3974(18) |
| C(3)-N(2) | 1.3935(16) | C(26)-C(29) | 1.5114(18) |
| N(1)-C(11) | 1.4460(16) | N(3)-C(41) | 1.3988(17) |
| N(2)-C(21) | 1.4413(16) | N(3)-C(31) | 1.4005(16) |
| C(11)-C(16) | 1.3986(18) | N(3)-H(1) | 0.900(18) |
| C(11)-C(12) | 1.4046(19) | C(31)-C(32) | 1.4045(18) |
| C(12)-C(13) | 1.3952(18) | C(31)-C(36) | 1.4060(18) |
| C(12)-C(17) | 1.5124(18) | C(32)-C(33) | 1.3909(18) |
| C(13)-C(14) | 1.3993(18) | C(33)-C(34) | 1.3944(18) |
| C(14)-C(15) | 1.3947(19) | C(34)-C(35) | 1.3940(19) |
| C(14)-C(18) | 1.5131(18) | C(35)-C(36) | 1.3943(18) |
| C(15)-C(16) | 1.3998(18) | C(41)-C(46) | 1.4050(18) |
| C(16)-C(19) | 1.5099(19) | C(41)-C(42) | 1.4080(18) |
| C(21)-C(22) | 1.4001(18) | C(42)-C(43) | 1.3919(19) |
| C(21)-C(26) | 1.4018(18) | C(43)-C(44) | 1.3930(19) |
| C(22)-C(23) | 1.4009(18) | C(44)-C(45) | 1.3947(19) |
| C(22)-C(27) | 1.5103(18) | C(45)-C(46) | 1.3943(19) |

Table 2.6.angle. Selected Bond Angles (°).

| | | | |
|---|---|---|---|
| N(1)-C(1)-N(2) | 101.70(10) | C(21)-C(22)-C(27) | 120.42(11) |
| C(3)-C(2)-N(1) | 106.50(11) | C(23)-C(22)-C(27) | 121.63(12) |
| C(2)-C(3)-N(2) | 106.09(11) | C(22)-C(23)-C(24) | 121.38(12) |
| C(1)-N(1)-C(2) | 112.73(10) | C(25)-C(24)-C(23) | 118.64(12) |
| C(1)-N(1)-C(11) | 123.03(10) | C(25)-C(24)-C(28) | 120.16(11) |
| C(2)-N(1)-C(11) | 124.24(10) | C(23)-C(24)-C(28) | 121.18(12) |
| C(1)-N(2)-C(3) | 112.98(10) | C(26)-C(25)-C(24) | 121.95(12) |
| C(1)-N(2)-C(21) | 122.09(10) | C(25)-C(26)-C(21) | 117.57(12) |
| C(3)-N(2)-C(21) | 124.81(10) | C(25)-C(26)-C(29) | 120.99(11) |
| C(16)-C(11)-C(12) | 122.32(12) | C(21)-C(26)-C(29) | 121.43(11) |
| C(16)-C(11)-N(1) | 118.58(11) | C(41)-N(3)-C(31) | 125.96(11) |
| C(12)-C(11)-N(1) | 119.09(11) | N(3)-C(31)-C(32) | 118.76(11) |
| C(13)-C(12)-C(11) | 117.49(12) | N(3)-C(31)-C(36) | 122.55(11) |
| C(13)-C(12)-C(17) | 120.90(11) | C(32)-C(31)-C(36) | 118.62(12) |
| C(11)-C(12)-C(17) | 121.57(11) | C(33)-C(32)-C(31) | 120.64(12) |
| C(12)-C(13)-C(14) | 122.11(12) | C(32)-C(33)-C(34) | 120.79(12) |
| C(15)-C(14)-C(13) | 118.45(12) | C(35)-C(34)-C(33) | 118.72(12) |
| C(15)-C(14)-C(18) | 120.51(12) | C(34)-C(35)-C(36) | 121.23(12) |
| C(13)-C(14)-C(18) | 121.03(12) | C(35)-C(36)-C(31) | 120.01(12) |
| C(14)-C(15)-C(16) | 121.68(12) | N(3)-C(41)-C(46) | 118.41(11) |
| C(11)-C(16)-C(15) | 117.93(12) | N(3)-C(41)-C(42) | 122.85(12) |
| C(11)-C(16)-C(19) | 121.32(12) | C(46)-C(41)-C(42) | 118.64(11) |
| C(15)-C(16)-C(19) | 120.72(12) | C(43)-C(42)-C(41) | 120.18(12) |
| C(22)-C(21)-C(26) | 122.49(12) | C(42)-C(43)-C(44) | 120.91(12) |
| C(22)-C(21)-N(2) | 117.92(11) | C(43)-C(44)-C(45) | 119.26(12) |
| C(26)-C(21)-N(2) | 119.55(11) | C(46)-C(45)-C(44) | 120.40(12) |
| C(21)-C(22)-C(23) | 117.91(11) | C(45)-C(46)-C(41) | 120.59(12) |

Table 2.6.anis. Anisotropic displacement parameters ($Å^2 x\ 10^3$). The anisotropic displacement factor exponent takes the form: $-2\pi^2[\ h^2\ a^{*2}U^{11} + ... + 2\ h\ k\ a^*\ b^*\ U^{12}\ ]$

| | $U_{11}$ | $U_{22}$ | $U_{33}$ | $U_{23}$ | $U_{13}$ | $U_{12}$ |
|---|---|---|---|---|---|---|
| C(1) | 15(1) | 13(1) | 13(1) | -2(1) | -4(1) | -4(1) |
| C(2) | 15(1) | 16(1) | 14(1) | 0(1) | -3(1) | -7(1) |
| C(3) | 14(1) | 15(1) | 15(1) | -1(1) | -3(1) | -6(1) |
| N(1) | 13(1) | 13(1) | 13(1) | -1(1) | -4(1) | -4(1) |

| | | | | | | |
|---|---|---|---|---|---|---|
| N(2) | 13(1) | 13(1) | 12(1) | -1(1) | -3(1) | -5(1) |
| C(11) | 14(1) | 15(1) | 12(1) | 3(1) | -4(1) | -7(1) |
| C(12) | 15(1) | 14(1) | 13(1) | 2(1) | -3(1) | -9(1) |
| C(13) | 13(1) | 12(1) | 15(1) | 1(1) | -3(1) | -4(1) |
| C(14) | 16(1) | 17(1) | 13(1) | 3(1) | -4(1) | -9(1) |
| C(15) | 17(1) | 17(1) | 12(1) | 0(1) | -3(1) | -9(1) |
| C(16) | 14(1) | 14(1) | 14(1) | 1(1) | -1(1) | -8(1) |
| C(17) | 18(1) | 16(1) | 15(1) | -2(1) | -5(1) | -5(1) |
| C(18) | 18(1) | 19(1) | 17(1) | 0(1) | -7(1) | -5(1) |
| C(19) | 17(1) | 16(1) | 17(1) | -2(1) | -5(1) | -5(1) |
| C(21) | 13(1) | 15(1) | 14(1) | 2(1) | -6(1) | -7(1) |
| C(22) | 12(1) | 15(1) | 15(1) | 0(1) | -5(1) | -7(1) |
| C(23) | 14(1) | 16(1) | 13(1) | -1(1) | -4(1) | -8(1) |
| C(24) | 14(1) | 17(1) | 16(1) | 2(1) | -7(1) | -8(1) |
| C(25) | 12(1) | 12(1) | 18(1) | -1(1) | -6(1) | -4(1) |
| C(26) | 12(1) | 16(1) | 16(1) | -1(1) | -5(1) | -7(1) |
| C(27) | 16(1) | 15(1) | 15(1) | 0(1) | -4(1) | -5(1) |
| C(28) | 18(1) | 16(1) | 16(1) | 1(1) | -7(1) | -6(1) |
| C(29) | 17(1) | 16(1) | 17(1) | -2(1) | -4(1) | -5(1) |
| N(3) | 12(1) | 13(1) | 17(1) | 1(1) | -4(1) | -5(1) |
| C(31) | 15(1) | 14(1) | 10(1) | -2(1) | -3(1) | -4(1) |
| C(32) | 14(1) | 16(1) | 13(1) | -3(1) | -3(1) | -5(1) |
| C(33) | 15(1) | 16(1) | 14(1) | -3(1) | -5(1) | -2(1) |
| C(34) | 20(1) | 13(1) | 14(1) | 0(1) | -5(1) | -5(1) |
| C(35) | 18(1) | 18(1) | 15(1) | -1(1) | -4(1) | -9(1) |
| C(36) | 14(1) | 17(1) | 14(1) | 0(1) | -6(1) | -5(1) |
| C(41) | 15(1) | 14(1) | 15(1) | -2(1) | -6(1) | -6(1) |
| C(42) | 17(1) | 16(1) | 14(1) | 0(1) | -6(1) | -7(1) |
| C(43) | 16(1) | 22(1) | 14(1) | -4(1) | -3(1) | -8(1) |
| C(44) | 15(1) | 15(1) | 21(1) | -5(1) | -7(1) | -2(1) |
| C(45) | 20(1) | 14(1) | 18(1) | 1(1) | -9(1) | -6(1) |
| C(46) | 17(1) | 16(1) | 14(1) | -1(1) | -5(1) | -7(1) |

Table 2.6.H. Hydrogen atom coordinates ( x $10^4$) and isotropic displacement parameters ($Å^2$x $10^3$).

| | X | Y | Z | Uiso |
|---|---|---|---|---|
| H(1) | 5710(20) | -149(17) | 2439(12) | 29(4) |
| H(2) | 1697(17) | -2670(15) | 4545(11) | 19(4) |
| H(3) | 410(17) | -1118(15) | 3268(10) | 18(4) |
| H(13) | 7596(16) | -5161(15) | 4539(10) | 14(3) |
| H(15) | 5326(17) | -2003(16) | 6345(11) | 23(4) |
| H(17A) | 4832(19) | -4310(16) | 3277(11) | 26(4) |
| H(17B) | 6530(20) | -5328(19) | 3341(12) | 36(5) |
| H(17C) | 6326(19) | -3904(17) | 2751(13) | 33(4) |
| H(18A) | 8860(20) | -4506(19) | 5689(14) | 46(5) |
| H(18B) | 7780(20) | -5252(19) | 6361(13) | 41(5) |
| H(18C) | 7600(20) | -3794(18) | 6620(13) | 37(5) |
| H(19A) | 3323(19) | 330(18) | 5155(12) | 31(4) |
| H(19B) | 2905(18) | -276(16) | 6209(12) | 29(4) |
| H(19C) | 2033(19) | -391(16) | 5482(11) | 25(4) |
| H(23) | 3297(17) | 518(15) | -229(11) | 20(4) |
| H(25) | 322(16) | 3643(15) | 1529(10) | 13(3) |
| H(27A) | 4911(18) | -1686(15) | 1291(11) | 24(4) |
| H(27B) | 4335(18) | -1761(16) | 398(12) | 26(4) |
| H(27C) | 3470(17) | -2196(16) | 1460(11) | 22(4) |
| H(28A) | 2130(20) | 3914(19) | -297(13) | 40(5) |
| H(28B) | 600(19) | 3740(16) | -309(11) | 27(4) |
| H(28C) | 2232(18) | 2788(17) | -925(12) | 28(4) |
| H(29A) | -720(20) | 2004(16) | 3462(11) | 30(4) |
| H(29B) | 866(18) | 1927(16) | 3643(11) | 26(4) |
| H(29C) | -218(18) | 3333(17) | 3208(11) | 29(4) |
| H(32) | 4139(17) | 1734(14) | 1617(10) | 16(4) |
| H(33) | 3573(17) | 4062(15) | 1046(10) | 19(4) |
| H(34) | 5377(17) | 5166(16) | 850(11) | 20(4) |
| H(35) | 7748(16) | 3915(14) | 1240(10) | 16(3) |
| H(36) | 8350(17) | 1617(15) | 1784(10) | 17(4) |
| H(42) | 9212(17) | -215(15) | 788(11) | 18(4) |
| H(43) | 11540(18) | -2087(15) | 614(11) | 21(4) |
| H(44) | 11737(18) | -3975(15) | 1764(10) | 20(4) |
| H(45) | 9555(17) | -3952(15) | 3066(11) | 20(4) |
| H(46) | 7207(17) | -2044(14) | 3231(11) | 17(4) |

**Supplement 2.7. Tables of Results of Refinements for 2,6-Di-tert-butyl-4-methylphenol and 1,3-Dimesitylimidazol-2-ylidene**

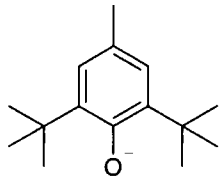

[DTPO-]

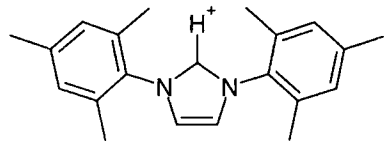

[DMI+]

Table 2.7.xyz.. Atomic coordinates ( x $10^4$) and equivalent isotropic displacement parameters ($Å^2$x $10^3$) U(eq) is defined as one third of the trace of the orthogonalized $U^{ij}$ tensor.

| | x | y | z | Ueq |
|---|---|---|---|---|
| C(1) | -1181(1) | -3276(1) | 7266(1) | 27(1) |
| N(1) | -657(1) | -2968(1) | 7550(1) | 30(1) |
| N(2) | -1223(1) | -3754(1) | 6974(1) | 27(1) |
| C(2) | -355(1) | -3254(1) | 7436(1) | 34(1) |
| C(3) | -709(1) | -3744(1) | 7079(1) | 31(1) |
| C(11) | -432(1) | -2439(1) | 7972(1) | 32(1) |
| C(12) | -639(1) | -2461(1) | 8701(1) | 29(1) |
| C(13) | -393(1) | -1951(1) | 9107(1) | 33(1) |
| C(14) | 44(1) | -1443(1) | 8813(1) | 43(1) |
| C(15) | 238(1) | -1447(1) | 8086(2) | 55(1) |
| C(16) | 5(1) | -1941(1) | 7650(1) | 48(1) |
| C(17) | -1103(1) | -3009(1) | 9034(1) | 34(1) |
| C(18) | 299(1) | -899(1) | 9272(2) | 57(1) |
| C(19) | 219(2) | -1940(1) | 6860(2) | 79(1) |
| C(21) | -1726(1) | -4212(1) | 6623(1) | 27(1) |
| C(22) | -1699(1) | -4326(1) | 5858(1) | 31(1) |
| C(23) | -2188(1) | -4778(1) | 5537(1) | 34(1) |
| C(24) | -2685(1) | -5103(1) | 5949(1) | 35(1) |
| C(25) | -2694(1) | -4966(1) | 6707(1) | 31(1) |
| C(26) | -2217(1) | -4522(1) | 7060(1) | 29(1) |
| C(27) | -1174(1) | -3960(1) | 5386(1) | 39(1) |
| C(28) | -3205(1) | -5591(1) | 5584(2) | 48(1) |
| C(29) | -2240(1) | -4376(1) | 7876(1) | 33(1) |
| C(31) | -2319(1) | -2732(1) | 7187(1) | 29(1) |
| O(1) | -2046(1) | -2997(1) | 7396(1) | 35(1) |

| | | | | |
|---|---|---|---|---|
| C(32) | -2557(1) | -2517(1) | 7738(1) | 30(1) |
| C(33) | -2879(1) | -2274(1) | 7499(1) | 33(1) |
| C(34) | -2976(1) | -2216(1) | 6741(1) | 34(1) |
| C(35) | -2721(1) | -2395(1) | 6212(1) | 32(1) |
| C(36) | -2393(1) | -2641(1) | 6402(1) | 30(1) |
| C(41) | -2451(1) | -2554(1) | 8589(1) | 33(1) |
| C(42) | -2686(1) | -3176(1) | 8832(1) | 37(1) |
| C(43) | -1806(1) | -2203(1) | 8743(1) | 42(1) |
| C(44) | -2739(1) | -2308(1) | 9094(1) | 45(1) |
| C(45) | -3338(1) | -1958(1) | 6506(1) | 44(1) |
| C(46) | -2111(1) | -2816(1) | 5779(1) | 36(1) |
| C(47) | -1457(1) | -2491(1) | 5884(1) | 47(1) |
| C(48) | -2227(1) | -2669(1) | 4982(1) | 44(1) |
| C(49) | -2355(1) | -3464(1) | 5796(1) | 41(1) |
| C(1A) | 5445(1) | -68(1) | 2698(1) | 29(1) |
| N(1A) | 5991(1) | 275(1) | 2892(1) | 29(1) |
| N(2A) | 5365(1) | -598(1) | 2636(1) | 29(1) |
| C(2A) | 6266(1) | -40(1) | 2962(1) | 33(1) |
| C(3A) | 5875(1) | -586(1) | 2798(1) | 33(1) |
| C(11A) | 6254(1) | 883(1) | 3019(1) | 31(1) |
| C(12A) | 6549(1) | 1253(1) | 2427(1) | 40(1) |
| C(13A) | 6790(1) | 1837(1) | 2567(2) | 49(1) |
| C(14A) | 6735(1) | 2040(1) | 3265(2) | 50(1) |
| C(15A) | 6445(1) | 1654(1) | 3836(2) | 45(1) |
| C(16A) | 6199(1) | 1068(1) | 3734(1) | 37(1) |
| C(17A) | 6598(1) | 1030(1) | 1664(2) | 58(1) |
| C(18A) | 6981(1) | 2677(1) | 3391(2) | 72(1) |
| C(19A) | 5866(1) | 646(1) | 4346(1) | 47(1) |
| C(21A) | 4835(1) | -1100(1) | 2425(1) | 30(1) |
| C(22A) | 4375(1) | -1320(1) | 2931(1) | 33(1) |
| C(23A) | 3877(1) | -1808(1) | 2715(1) | 36(1) |
| C(24A) | 3829(1) | -2076(1) | 2024(1) | 36(1) |
| C(25A) | 4294(1) | -1841(1) | 1536(1) | 34(1) |
| C(26A) | 4803(1) | -1344(1) | 1716(1) | 31(1) |
| C(27A) | 4411(1) | -1031(1) | 3674(1) | 42(1) |
| C(28A) | 3276(1) | -2600(1) | 1803(2) | 48(1) |
| C(29A) | 5286(1) | -1078(1) | 1157(1) | 36(1) |
| C(31A) | 4274(1) | 412(1) | 2299(1) | 27(1) |

| | | | | |
|---|---|---|---|---|
| O(1A) | 4525(1) | 156(1) | 2607(1) | 31(1) |
| C(32A) | 4191(1) | 824(1) | 2713(1) | 27(1) |
| C(33A) | 3898(1) | 1071(1) | 2376(1) | 31(1) |
| C(34A) | 3672(1) | 936(1) | 1650(1) | 35(1) |
| C(35A) | 3764(1) | 549(1) | 1243(1) | 33(1) |
| C(36A) | 4056(1) | 288(1) | 1534(1) | 29(1) |
| C(41A) | 4428(1) | 993(1) | 3523(1) | 29(1) |
| C(42A) | 4169(1) | 466(1) | 4049(1) | 34(1) |
| C(43A) | 5082(1) | 1266(1) | 3503(1) | 38(1) |
| C(44A) | 4295(1) | 1432(1) | 3880(1) | 36(1) |
| C(45A) | 3338(1) | 1199(1) | 1319(1) | 48(1) |
| C(46A) | 4149(1) | -131(1) | 1050(1) | 35(1) |
| C(47A) | 4795(1) | 109(1) | 948(1) | 46(1) |
| C(48A) | 3885(1) | -218(1) | 258(1) | 45(1) |
| C(49A) | 3872(1) | -724(1) | 1425(1) | 42(1) |
| C(0S) | 3546(2) | 5412(2) | 8630(3) | 97(1) |
| C(1S) | 3040(1) | 5281(1) | 9134(2) | 60(1) |
| C(2S) | 2741(2) | 4764(1) | 9500(2) | 64(1) |
| C(3S) | 2278(2) | 4642(2) | 9958(2) | 74(1) |
| C(4S) | 2109(2) | 5036(2) | 10058(2) | 77(1) |
| C(5S) | 2404(2) | 5554(2) | 9699(2) | 79(1) |
| C(6S) | 2864(2) | 5676(2) | 9241(2) | 71(1) |
| C(1N) | 728(14) | -230(13) | 5579(11) | 550(20) |
| C(2N) | 959(6) | -420(5) | 6221(7) | 381(16) |
| C(3N) | 1213(3) | -67(5) | 6843(6) | 277(11) |
| C(4N) | 1046(6) | 253(4) | 7315(7) | 217(7) |
| C(5N) | 631(10) | 411(12) | 7016(13) | 740(40) |
| C(6N) | 845(15) | 744(15) | 6278(14) | 640(30) |

Table 2.7.bond. Selected Bond Lengths (Å)

| | | | |
|---|---|---|---|
| C(1)-N(1) | 1.331(3) | N(2A)-C(21A) | 1.444(3) |
| C(1)-N(2) | 1.343(2) | C(2A)-C(3A) | 1.348(3) |
| C(1)-H(1) | 0.94(2) | C(11A)-C(12A) | 1.390(3) |
| N(1)-C(2) | 1.389(3) | C(11A)-C(16A) | 1.395(3) |
| N(1)-C(11) | 1.449(3) | C(12A)-C(13A) | 1.393(3) |
| N(2)-C(3) | 1.389(2) | C(12A)-C(17A) | 1.511(4) |
| N(2)-C(21) | 1.442(3) | C(13A)-C(14A) | 1.389(4) |
| C(2)-C(3) | 1.340(3) | C(14A)-C(15A) | 1.381(4) |

| | | | |
|---|---|---|---|
| C(11)-C(16) | 1.392(3) | C(14A)-C(18A) | 1.517(3) |
| C(11)-C(12) | 1.395(3) | C(15A)-C(16A) | 1.387(3) |
| C(12)-C(13) | 1.394(3) | C(16A)-C(19A) | 1.503(4) |
| C(12)-C(17) | 1.501(3) | C(21A)-C(26A) | 1.398(3) |
| C(13)-C(14) | 1.388(3) | C(21A)-C(22A) | 1.400(3) |
| C(14)-C(15) | 1.391(3) | C(22A)-C(23A) | 1.386(3) |
| C(14)-C(18) | 1.510(3) | C(22A)-C(27A) | 1.507(3) |
| C(15)-C(16) | 1.391(3) | C(23A)-C(24A) | 1.392(3) |
| C(16)-C(19) | 1.511(3) | C(24A)-C(25A) | 1.389(3) |
| C(21)-C(26) | 1.396(3) | C(24A)-C(28A) | 1.507(3) |
| C(21)-C(22) | 1.397(3) | C(25A)-C(26A) | 1.396(3) |
| C(22)-C(23) | 1.392(3) | C(26A)-C(29A) | 1.502(3) |
| C(22)-C(27) | 1.511(3) | C(31A)-O(1A) | 1.307(2) |
| C(23)-C(24) | 1.387(3) | C(31A)-C(32A) | 1.440(3) |
| C(24)-C(25) | 1.393(3) | C(31A)-C(36A) | 1.447(3) |
| C(24)-C(28) | 1.509(3) | C(32A)-C(33A) | 1.397(3) |
| C(25)-C(26) | 1.393(3) | C(32A)-C(41A) | 1.543(3) |
| C(26)-C(29) | 1.506(3) | C(33A)-C(34A) | 1.390(3) |
| C(31)-O(1) | 1.309(2) | C(34A)-C(35A) | 1.389(3) |
| C(31)-C(32) | 1.440(3) | C(34A)-C(45A) | 1.517(3) |
| C(31)-C(36) | 1.441(3) | C(35A)-C(36A) | 1.392(3) |
| C(32)-C(33) | 1.392(3) | C(36A)-C(46A) | 1.536(3) |
| C(32)-C(41) | 1.544(3) | C(41A)-C(43A) | 1.535(3) |
| C(33)-C(34) | 1.390(3) | C(41A)-C(44A) | 1.538(3) |
| C(34)-C(35) | 1.384(3) | C(41A)-C(42A) | 1.543(3) |
| C(34)-C(45) | 1.515(3) | C(46A)-C(48A) | 1.536(3) |
| C(35)-C(36) | 1.391(3) | C(46A)-C(49A) | 1.536(3) |
| C(36)-C(46) | 1.542(3) | C(46A)-C(47A) | 1.539(3) |
| C(41)-C(42) | 1.531(3) | C(0S)-C(1S) | 1.517(5) |
| C(41)-C(43) | 1.534(3) | C(1S)-C(2S) | 1.376(5) |
| C(41)-C(44) | 1.539(3) | C(1S)-C(6S) | 1.381(4) |
| C(46)-C(49) | 1.532(3) | C(2S)-C(3S) | 1.386(5) |
| C(46)-C(48) | 1.538(3) | C(3S)-C(4S) | 1.360(5) |
| C(46)-C(47) | 1.540(3) | C(4S)-C(5S) | 1.371(5) |
| C(1A)-N(1A) | 1.334(3) | C(5S)-C(6S) | 1.378(5) |
| C(1A)-N(2A) | 1.340(3) | C(1N)-C(2N) | 1.502(9) |
| C(1A)-H(1A) | 0.98(2) | C(2N)-C(3N) | 1.392(8) |
| N(1A)-C(2A) | 1.386(3) | C(3N)-C(4N) | 1.428(8) |

| | | | |
|---|---|---|---|
| N(1A)-C(11A) | 1.445(3) | C(4N)-C(5N) | 1.482(10) |
| N(2A)-C(3A) | 1.392(3) | C(5N)-C(6N) | 1.526(10) |

Table 2.7.angle. Selected Bond Angles (°).

| | | | |
|---|---|---|---|
| N(1)-C(1)-N(2) | 107.30(17) | N(1A)-C(1A)-H(1A) | 126.5(13) |
| N(1)-C(1)-H(1) | 126.2(14) | N(2A)-C(1A)-H(1A) | 126.2(13) |
| N(2)-C(1)-H(1) | 126.5(14) | C(1A)-N(1A)-C(2A) | 109.94(17) |
| C(1)-N(1)-C(2) | 109.61(17) | C(1A)-N(1A)-C(11A) | 125.07(16) |
| C(1)-N(1)-C(11) | 126.87(17) | C(2A)-N(1A)-C(11A) | 124.98(17) |
| C(2)-N(1)-C(11) | 123.34(17) | C(1A)-N(2A)-C(3A) | 109.17(17) |
| C(1)-N(2)-C(3) | 109.04(17) | C(1A)-N(2A)-C(21A) | 125.40(17) |
| C(1)-N(2)-C(21) | 125.61(16) | C(3A)-N(2A)-C(21A) | 125.43(16) |
| C(3)-N(2)-C(21) | 125.33(16) | C(3A)-C(2A)-N(1A) | 106.63(18) |
| C(3)-C(2)-N(1) | 106.86(18) | C(2A)-C(3A)-N(2A) | 107.03(18) |
| C(2)-C(3)-N(2) | 107.18(17) | C(12A)-C(11A)-C(16A) | 123.4(2) |
| C(16)-C(11)-C(12) | 123.21(19) | C(12A)-C(11A)-N(1A) | 118.69(19) |
| C(16)-C(11)-N(1) | 118.45(18) | C(16A)-C(11A)-N(1A) | 117.88(19) |
| C(12)-C(11)-N(1) | 118.21(18) | C(11A)-C(12A)-C(13A) | 117.0(2) |
| C(13)-C(12)-C(11) | 116.83(19) | C(11A)-C(12A)-C(17A) | 121.2(2) |
| C(13)-C(12)-C(17) | 121.53(18) | C(13A)-C(12A)-C(17A) | 121.8(2) |
| C(11)-C(12)-C(17) | 121.63(18) | C(14A)-C(13A)-C(12A) | 121.7(2) |
| C(14)-C(13)-C(12) | 122.3(2) | C(15A)-C(14A)-C(13A) | 118.9(2) |
| C(13)-C(14)-C(15) | 118.4(2) | C(15A)-C(14A)-C(18A) | 120.7(3) |
| C(13)-C(14)-C(18) | 120.6(2) | C(13A)-C(14A)-C(18A) | 120.4(3) |
| C(15)-C(14)-C(18) | 121.0(2) | C(14A)-C(15A)-C(16A) | 122.3(2) |
| C(15)-C(16)-C(11) | 117.3(2) | C(15A)-C(16A)-C(11A) | 116.8(2) |
| C(15)-C(16)-C(19) | 121.5(2) | C(15A)-C(16A)-C(19A) | 122.4(2) |
| C(11)-C(16)-C(19) | 121.2(2) | C(11A)-C(16A)-C(19A) | 120.8(2) |
| C(26)-C(21)-C(22) | 122.83(19) | C(26A)-C(21A)-C(22A) | 122.70(19) |
| C(26)-C(21)-N(2) | 118.73(17) | C(26A)-C(21A)-N(2A) | 118.22(18) |
| C(22)-C(21)-N(2) | 118.44(18) | C(22A)-C(21A)-N(2A) | 119.08(18) |
| C(23)-C(22)-C(21) | 117.15(19) | C(23A)-C(22A)-C(21A) | 117.5(2) |
| C(23)-C(22)-C(27) | 121.11(19) | C(23A)-C(22A)-C(27A) | 120.9(2) |
| C(21)-C(22)-C(27) | 121.67(19) | C(21A)-C(22A)-C(27A) | 121.5(2) |
| C(24)-C(23)-C(22) | 122.29(19) | C(22A)-C(23A)-C(24A) | 122.0(2) |
| C(23)-C(24)-C(25) | 118.5(2) | C(25A)-C(24A)-C(23A) | 118.6(2) |
| C(23)-C(24)-C(28) | 120.8(2) | C(25A)-C(24A)-C(28A) | 120.9(2) |
| C(25)-C(24)-C(28) | 120.7(2) | C(23A)-C(24A)-C(28A) | 120.4(2) |

| | | | |
|---|---|---|---|
| C(24)-C(25)-C(26) | 121.9(2) | C(24A)-C(25A)-C(26A) | 122.0(2) |
| C(25)-C(26)-C(21) | 117.36(18) | C(25A)-C(26A)-C(21A) | 117.17(19) |
| C(25)-C(26)-C(29) | 120.97(18) | C(25A)-C(26A)-C(29A) | 120.76(19) |
| C(21)-C(26)-C(29) | 121.65(18) | C(21A)-C(26A)-C(29A) | 122.05(19) |
| O(1)-C(31)-C(32) | 121.04(18) | O(1A)-C(31A)-C(32A) | 121.38(17) |
| O(1)-C(31)-C(36) | 121.88(17) | O(1A)-C(31A)-C(36A) | 121.75(17) |
| C(32)-C(31)-C(36) | 117.08(17) | C(32A)-C(31A)-C(36A) | 116.86(17) |
| C(33)-C(32)-C(31) | 119.70(18) | C(33A)-C(32A)-C(31A) | 119.80(18) |
| C(33)-C(32)-C(41) | 120.48(17) | C(33A)-C(32A)-C(41A) | 120.41(17) |
| C(31)-C(32)-C(41) | 119.81(17) | C(31A)-C(32A)-C(41A) | 119.79(16) |
| C(34)-C(33)-C(32) | 122.91(19) | C(34A)-C(33A)-C(32A) | 123.15(18) |
| C(35)-C(34)-C(33) | 117.28(18) | C(35A)-C(34A)-C(33A) | 117.12(18) |
| C(35)-C(34)-C(45) | 121.6(2) | C(35A)-C(34A)-C(45A) | 121.6(2) |
| C(33)-C(34)-C(45) | 121.15(19) | C(33A)-C(34A)-C(45A) | 121.27(19) |
| C(34)-C(35)-C(36) | 123.41(19) | C(34A)-C(35A)-C(36A) | 123.32(19) |
| C(35)-C(36)-C(31) | 119.40(18) | C(35A)-C(36A)-C(31A) | 119.70(17) |
| C(35)-C(36)-C(46) | 120.22(18) | C(35A)-C(36A)-C(46A) | 120.68(18) |
| C(31)-C(36)-C(46) | 120.38(17) | C(31A)-C(36A)-C(46A) | 119.62(17) |
| C(42)-C(41)-C(43) | 110.45(18) | C(43A)-C(41A)-C(44A) | 107.16(16) |
| C(42)-C(41)-C(44) | 106.82(19) | C(43A)-C(41A)-C(32A) | 109.24(17) |
| C(43)-C(41)-C(44) | 106.92(18) | C(44A)-C(41A)-C(32A) | 112.66(16) |
| C(42)-C(41)-C(32) | 110.91(17) | C(43A)-C(41A)-C(42A) | 109.83(17) |
| C(43)-C(41)-C(32) | 108.92(18) | C(44A)-C(41A)-C(42A) | 106.87(17) |
| C(44)-C(41)-C(32) | 112.73(17) | C(32A)-C(41A)-C(42A) | 110.98(16) |
| C(49)-C(46)-C(48) | 106.58(19) | C(36A)-C(46A)-C(48A) | 112.69(18) |
| C(49)-C(46)-C(47) | 111.34(19) | C(36A)-C(46A)-C(49A) | 110.70(17) |
| C(48)-C(46)-C(47) | 106.69(19) | C(48A)-C(46A)-C(49A) | 106.78(19) |
| C(49)-C(46)-C(36) | 109.84(18) | C(36A)-C(46A)-C(47A) | 108.84(18) |
| C(48)-C(46)-C(36) | 112.44(17) | C(48A)-C(46A)-C(47A) | 107.34(18) |
| C(47)-C(46)-C(36) | 109.90(18) | C(49A)-C(46A)-C(47A) | 110.43(19) |
| N(1A)-C(1A)-N(2A) | 107.22(17) | | |

Table 2.7.anis. Anisotropic displacement parameters ($Å^2 x\ 10^3$). The anisotropic displacement factor exponent takes the form: $-2p^2[\ h^2\ a^{*2}U^{11} + ... + 2\ h\ k\ a^*\ b^*\ U^{12}\ ]$

| | $U_{11}$ | $U_{22}$ | $U_{33}$ | $U_{23}$ | $U_{13}$ | $U_{12}$ |
|---|---|---|---|---|---|---|
| C(1) | 31(1) | 32(1) | 24(1) | 0(1) | 1(1) | 20(1) |
| N(1) | 31(1) | 32(1) | 29(1) | -3(1) | 2(1) | 18(1) |

| | | | | | | |
|---|---|---|---|---|---|---|
| N(2) | 29(1) | 30(1) | 26(1) | -1(1) | 1(1) | 19(1) |
| C(2) | 30(1) | 40(1) | 38(1) | -3(1) | 1(1) | 21(1) |
| C(3) | 30(1) | 35(1) | 34(1) | -1(1) | 1(1) | 21(1) |
| C(11) | 34(1) | 31(1) | 33(1) | -3(1) | 1(1) | 17(1) |
| C(12) | 27(1) | 35(1) | 29(1) | -2(1) | -3(1) | 18(1) |
| C(13) | 32(1) | 39(1) | 30(1) | -6(1) | -2(1) | 19(1) |
| C(14) | 40(1) | 37(1) | 46(1) | -9(1) | 4(1) | 14(1) |
| C(15) | 56(2) | 34(1) | 56(2) | -4(1) | 21(1) | 9(1) |
| C(16) | 53(2) | 39(1) | 43(1) | -4(1) | 18(1) | 16(1) |
| C(17) | 33(1) | 39(1) | 29(1) | 0(1) | -1(1) | 16(1) |
| C(18) | 51(2) | 43(1) | 61(2) | -18(1) | 4(1) | 11(1) |
| C(19) | 98(2) | 45(2) | 63(2) | -4(1) | 49(2) | 12(2) |
| C(21) | 30(1) | 31(1) | 28(1) | -2(1) | -2(1) | 21(1) |
| C(22) | 36(1) | 36(1) | 29(1) | 0(1) | 2(1) | 24(1) |
| C(23) | 41(1) | 42(1) | 28(1) | -7(1) | -3(1) | 27(1) |
| C(24) | 35(1) | 39(1) | 37(1) | -6(1) | -6(1) | 24(1) |
| C(25) | 30(1) | 35(1) | 35(1) | 0(1) | 2(1) | 20(1) |
| C(26) | 31(1) | 34(1) | 30(1) | 0(1) | -1(1) | 22(1) |
| C(27) | 42(1) | 46(1) | 30(1) | -2(1) | 5(1) | 24(1) |
| C(28) | 42(1) | 51(1) | 47(1) | -12(1) | -8(1) | 21(1) |
| C(29) | 33(1) | 39(1) | 29(1) | 0(1) | 3(1) | 19(1) |
| C(31) | 30(1) | 32(1) | 31(1) | -1(1) | -1(1) | 20(1) |
| O(1) | 43(1) | 49(1) | 31(1) | 1(1) | 2(1) | 36(1) |
| C(32) | 31(1) | 33(1) | 30(1) | -5(1) | -3(1) | 19(1) |
| C(33) | 37(1) | 37(1) | 35(1) | -9(1) | -3(1) | 25(1) |
| C(34) | 38(1) | 35(1) | 39(1) | -3(1) | -5(1) | 26(1) |
| C(35) | 38(1) | 33(1) | 31(1) | -1(1) | -3(1) | 22(1) |
| C(36) | 34(1) | 32(1) | 28(1) | -1(1) | 1(1) | 21(1) |
| C(41) | 37(1) | 44(1) | 28(1) | -10(1) | -5(1) | 27(1) |
| C(42) | 41(1) | 48(1) | 26(1) | -3(1) | -1(1) | 26(1) |
| C(43) | 41(1) | 48(1) | 43(1) | -10(1) | -10(1) | 26(1) |
| C(44) | 53(1) | 63(2) | 33(1) | -17(1) | -8(1) | 40(1) |
| C(45) | 56(2) | 51(1) | 46(1) | -3(1) | -5(1) | 42(1) |
| C(46) | 44(1) | 46(1) | 29(1) | 3(1) | 4(1) | 32(1) |
| C(47) | 49(1) | 66(2) | 40(1) | 10(1) | 12(1) | 39(1) |
| C(48) | 64(2) | 56(2) | 29(1) | 4(1) | 5(1) | 43(1) |
| C(49) | 60(2) | 49(1) | 32(1) | -1(1) | 3(1) | 40(1) |
| C(1A) | 34(1) | 30(1) | 27(1) | -2(1) | 0(1) | 19(1) |

| | | | | | | |
|---|---|---|---|---|---|---|
| N(1A) | 33(1) | 31(1) | 28(1) | -4(1) | -3(1) | 19(1) |
| N(2A) | 32(1) | 27(1) | 30(1) | -1(1) | 0(1) | 17(1) |
| C(2A) | 34(1) | 36(1) | 34(1) | -5(1) | -4(1) | 22(1) |
| C(3A) | 37(1) | 35(1) | 35(1) | -2(1) | -2(1) | 24(1) |
| C(11A) | 30(1) | 29(1) | 38(1) | -5(1) | -6(1) | 17(1) |
| C(12A) | 39(1) | 35(1) | 48(1) | 0(1) | -2(1) | 20(1) |
| C(13A) | 38(1) | 34(1) | 74(2) | 6(1) | -3(1) | 17(1) |
| C(14A) | 34(1) | 35(1) | 88(2) | -21(1) | -25(1) | 22(1) |
| C(15A) | 36(1) | 48(1) | 57(2) | -25(1) | -21(1) | 27(1) |
| C(16A) | 34(1) | 45(1) | 39(1) | -15(1) | -14(1) | 26(1) |
| C(17A) | 76(2) | 50(2) | 46(1) | 11(1) | 17(1) | 31(2) |
| C(18A) | 46(2) | 37(1) | 134(3) | -26(2) | -30(2) | 21(1) |
| C(19A) | 55(2) | 62(2) | 31(1) | -11(1) | -5(1) | 33(1) |
| C(21A) | 32(1) | 25(1) | 35(1) | 1(1) | -2(1) | 16(1) |
| C(22A) | 38(1) | 31(1) | 36(1) | 4(1) | 2(1) | 22(1) |
| C(23A) | 33(1) | 31(1) | 49(1) | 8(1) | 6(1) | 19(1) |
| C(24A) | 33(1) | 26(1) | 53(1) | 1(1) | -3(1) | 17(1) |
| C(25A) | 38(1) | 30(1) | 38(1) | -4(1) | -5(1) | 21(1) |
| C(26A) | 34(1) | 28(1) | 35(1) | 1(1) | -1(1) | 19(1) |
| C(27A) | 47(1) | 43(1) | 38(1) | 1(1) | 9(1) | 24(1) |
| C(28A) | 35(1) | 34(1) | 76(2) | -5(1) | -2(1) | 18(1) |
| C(29A) | 40(1) | 33(1) | 34(1) | -1(1) | 1(1) | 17(1) |
| C(31A) | 27(1) | 26(1) | 28(1) | 4(1) | 4(1) | 15(1) |
| O(1A) | 38(1) | 35(1) | 29(1) | 0(1) | 0(1) | 25(1) |
| C(32A) | 26(1) | 24(1) | 30(1) | 1(1) | 3(1) | 12(1) |
| C(33A) | 34(1) | 28(1) | 36(1) | 0(1) | 2(1) | 20(1) |
| C(34A) | 41(1) | 35(1) | 36(1) | 5(1) | 2(1) | 25(1) |
| C(35A) | 43(1) | 36(1) | 27(1) | 3(1) | -1(1) | 24(1) |
| C(36A) | 35(1) | 28(1) | 27(1) | 1(1) | 3(1) | 18(1) |
| C(41A) | 27(1) | 28(1) | 34(1) | -5(1) | -3(1) | 15(1) |
| C(42A) | 41(1) | 35(1) | 30(1) | -4(1) | -2(1) | 22(1) |
| C(43A) | 29(1) | 38(1) | 48(1) | -10(1) | -6(1) | 17(1) |
| C(44A) | 38(1) | 36(1) | 40(1) | -12(1) | -7(1) | 22(1) |
| C(45A) | 67(2) | 57(2) | 43(1) | 2(1) | -6(1) | 47(1) |
| C(46A) | 51(1) | 42(1) | 25(1) | -2(1) | -1(1) | 32(1) |
| C(47A) | 60(2) | 71(2) | 29(1) | -3(1) | 4(1) | 49(1) |
| C(48A) | 66(2) | 55(2) | 28(1) | -7(1) | -5(1) | 40(1) |
| C(49A) | 67(2) | 40(1) | 33(1) | -6(1) | -5(1) | 37(1) |

| | | | | | | |
|---|---|---|---|---|---|---|
| C(0S) | 83(3) | 94(3) | 111(3) | -35(2) | 23(2) | 43(2) |
| C(1S) | 60(2) | 67(2) | 58(2) | -22(1) | -5(1) | 36(2) |
| C(2S) | 85(2) | 67(2) | 56(2) | -16(2) | -21(2) | 50(2) |
| C(3S) | 86(2) | 76(2) | 52(2) | 1(2) | -1(2) | 35(2) |
| C(4S) | 64(2) | 111(3) | 57(2) | -8(2) | 3(2) | 45(2) |
| C(5S) | 90(3) | 106(3) | 74(2) | -2(2) | 7(2) | 74(2) |
| C(6S) | 90(2) | 64(2) | 71(2) | -1(2) | 15(2) | 47(2) |
| C(2N) | 175(12) | 304(19) | 590(40) | 290(20) | -88(17) | 66(13) |
| C(3N) | 64(4) | 350(19) | 294(16) | 259(16) | 9(7) | 11(8) |
| C(4N) | 302(15) | 153(8) | 277(14) | -111(9) | -181(12) | 174(10) |

**Supplement 2.8. Tables of Results of Refinement for Co-Crystals of Pentachlorophenol and 1,3-Dimesitylimidazol-2-ylidene**

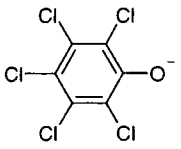


[PCPO-]

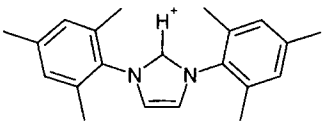


[DMI+]


[THF]

Table 2.8.xyz. Atomic coordinates ( x $10^4$) and equivalent isotropic displacement parameters ($Å^2$x $10^3$) U(eq) is defined as one third of the trace of the orthogonalized $U^{ij}$ tensor.

| | x | y | z | U(eq) |
|---|---|---|---|---|
| C(1) | 6523(4) | -1045(1) | -2221(4) | 16(1) |
| N(1) | 6392(4) | -601(1) | -1575(3) | 17(1) |
| N(2) | 5020(4) | -1326(1) | -2259(3) | 16(1) |
| C(2) | 4724(5) | -599(1) | -1202(5) | 22(1) |
| C(3) | 3862(5) | -1056(1) | -1630(4) | 20(1) |
| C(11) | 7749(4) | -190(1) | -1306(4) | 16(1) |
| C(12) | 9742(5) | -253(1) | -144(4) | 17(1) |
| C(13) | 11034(5) | 147(1) | 58(4) | 21(1) |
| C(14) | 10393(5) | 589(1) | -843(5) | 24(1) |
| C(15) | 8394(5) | 637(1) | -1981(4) | 23(1) |
| C(16) | 7034(5) | 250(1) | -2235(4) | 21(1) |
| C(17) | 10505(5) | -728(1) | 868(4) | 23(1) |
| C(18) | 11815(6) | 1020(2) | -585(6) | 38(1) |
| C(19) | 4891(5) | 315(1) | -3500(5) | 31(1) |
| C(21) | 4726(5) | -1847(1) | -2755(4) | 17(1) |
| C(22) | 5919(4) | -2200(1) | -1566(4) | 18(1) |
| C(23) | 5581(5) | -2699(1) | -2046(5) | 21(1) |
| C(24) | 4139(5) | -2843(1) | -3643(4) | 22(1) |
| C(25) | 3019(5) | -2476(1) | -4791(4) | 21(1) |
| C(26) | 3256(5) | -1976(1) | -4378(4) | 18(1) |
| C(27) | 7494(5) | -2045(1) | 170(4) | 22(1) |
| C(28) | 3819(6) | -3387(1) | -4135(6) | 33(1) |
| C(29) | 2021(5) | -1584(1) | -5616(4) | 23(1) |
| C(41) | 9738(5) | -2012(1) | -2755(4) | 15(1) |
| O(1) | 9892(3) | -1547(1) | -2440(3) | 18(1) |
| C(42) | 10913(5) | -2384(1) | -1532(4) | 17(1) |
| Cl(2) | 12612(1) | -2162(1) | 434(1) | 21(1) |
| C(43) | 10711(5) | -2889(1) | -1880(4) | 17(1) |

| | | | | |
|---|---|---|---|---|
| Cl(3) | 12178(1) | -3308(1) | -327(1) | 27(1) |
| C(44) | 9346(5) | -3068(1) | -3466(4) | 18(1) |
| Cl(4) | 9055(1) | -3701(1) | -3881(1) | 27(1) |
| C(45) | 8174(5) | -2726(1) | -4723(4) | 17(1) |
| Cl(5) | 6509(1) | -2935(1) | -6719(1) | 23(1) |
| C(46) | 8355(4) | -2220(1) | -4367(4) | 15(1) |
| Cl(6) | 6864(1) | -1792(1) | -5876(1) | 19(1) |
| C(1S) | 6793(7) | -509(2) | -6561(6) | 37(1) |
| O(1S) | 6066(5) | -74(1) | -7580(5) | 50(1) |
| C(2S) | 8827(7) | -388(2) | -5184(5) | 36(1) |
| C(3S) | 9423(6) | 76(2) | -5838(5) | 35(1) |
| C(4S) | 7466(6) | 318(2) | -6947(6) | 37(1) |

Table 2.8.bond Bond lengths (Å).

| | | | |
|---|---|---|---|
| C(1)-N(1) | 1.337(4) | C(24)-C(25) | 1.393(5) |
| C(1)-N(2) | 1.338(4) | C(24)-C(28) | 1.513(5) |
| N(1)-C(2) | 1.402(4) | C(25)-C(26) | 1.384(5) |
| N(1)-C(11) | 1.446(4) | C(26)-C(29) | 1.501(5) |
| N(2)-C(3) | 1.395(4) | C(41)-O(1) | 1.274(4) |
| N(2)-C(21) | 1.453(4) | C(41)-C(46) | 1.442(4) |
| C(2)-C(3) | 1.362(5) | C(41)-C(42) | 1.444(5) |
| C(11)-C(16) | 1.400(5) | C(42)-C(43) | 1.386(5) |
| C(11)-C(12) | 1.404(4) | C(42)-Cl(2) | 1.731(3) |
| C(12)-C(13) | 1.402(4) | C(43)-C(44) | 1.395(5) |
| C(12)-C(17) | 1.513(5) | C(43)-Cl(3) | 1.734(3) |
| C(13)-C(14) | 1.387(5) | C(44)-C(45) | 1.404(5) |
| C(14)-C(15) | 1.397(5) | C(44)-Cl(4) | 1.733(3) |
| C(14)-C(18) | 1.521(5) | C(45)-C(46) | 1.390(5) |
| C(15)-C(16) | 1.400(5) | C(45)-Cl(5) | 1.729(3) |
| C(16)-C(19) | 1.512(5) | C(46)-Cl(6) | 1.736(3) |
| C(21)-C(22) | 1.400(4) | C(1S)-O(1S) | 1.422(5) |
| C(21)-C(26) | 1.403(5) | C(1S)-C(2S) | 1.510(6) |
| C(22)-C(23) | 1.394(5) | O(1S)-C(4S) | 1.418(5) |
| C(22)-C(27) | 1.514(5) | C(2S)-C(3S) | 1.508(6) |
| C(23)-C(24) | 1.392(5) | C(3S)-C(4S) | 1.510(6) |

Table 2.8.ang. Bond Angles (°)

| | | | |
|---|---|---|---|
| N(1)-C(1)-N(2) | 108.0(3) | C(23)-C(24)-C(25) | 118.8(3) |
| C(1)-N(1)-C(2) | 108.8(3) | C(23)-C(24)-C(28) | 120.6(3) |
| C(1)-N(1)-C(11) | 125.5(3) | C(25)-C(24)-C(28) | 120.6(3) |
| C(2)-N(1)-C(11) | 125.7(3) | C(26)-C(25)-C(24) | 122.2(3) |
| C(1)-N(2)-C(3) | 109.8(3) | C(25)-C(26)-C(21) | 117.0(3) |
| C(1)-N(2)-C(21) | 125.0(2) | C(25)-C(26)-C(29) | 121.8(3) |
| C(3)-N(2)-C(21) | 125.0(3) | C(21)-C(26)-C(29) | 121.2(3) |
| C(3)-C(2)-N(1) | 107.2(3) | O(1)-C(41)-C(46) | 123.1(3) |
| C(2)-C(3)-N(2) | 106.1(3) | O(1)-C(41)-C(42) | 123.5(3) |
| C(16)-C(11)-C(12) | 122.7(3) | C(46)-C(41)-C(42) | 113.4(3) |
| C(16)-C(11)-N(1) | 118.8(3) | C(43)-C(42)-C(41) | 122.9(3) |
| C(12)-C(11)-N(1) | 118.5(3) | C(43)-C(42)-Cl(2) | 121.0(2) |
| C(13)-C(12)-C(11) | 117.2(3) | C(41)-C(42)-Cl(2) | 116.1(2) |
| C(13)-C(12)-C(17) | 120.3(3) | C(42)-C(43)-C(44) | 121.0(3) |
| C(11)-C(12)-C(17) | 122.5(3) | C(42)-C(43)-Cl(3) | 119.7(2) |
| C(14)-C(13)-C(12) | 122.1(3) | C(44)-C(43)-Cl(3) | 119.3(3) |
| C(13)-C(14)-C(15) | 118.8(3) | C(43)-C(44)-C(45) | 119.0(3) |
| C(13)-C(14)-C(18) | 121.2(3) | C(43)-C(44)-Cl(4) | 120.9(3) |
| C(15)-C(14)-C(18) | 120.0(3) | C(45)-C(44)-Cl(4) | 120.1(3) |
| C(14)-C(15)-C(16) | 121.7(3) | C(46)-C(45)-C(44) | 120.0(3) |
| C(11)-C(16)-C(15) | 117.5(3) | C(46)-C(45)-Cl(5) | 119.9(3) |
| C(11)-C(16)-C(19) | 122.5(3) | C(44)-C(45)-Cl(5) | 120.1(3) |
| C(15)-C(16)-C(19) | 120.0(3) | C(45)-C(46)-C(41) | 123.6(3) |
| C(22)-C(21)-C(26) | 123.1(3) | C(45)-C(46)-Cl(6) | 120.8(2) |
| C(22)-C(21)-N(2) | 117.9(3) | C(41)-C(46)-Cl(6) | 115.6(2) |
| C(26)-C(21)-N(2) | 119.0(3) | O(1S)-C(1S)-C(2S) | 107.5(3) |
| C(23)-C(22)-C(21) | 117.1(3) | C(4S)-O(1S)-C(1S) | 110.4(3) |
| C(23)-C(22)-C(27) | 121.5(3) | C(3S)-C(2S)-C(1S) | 103.9(3) |
| C(21)-C(22)-C(27) | 121.4(3) | C(2S)-C(3S)-C(4S) | 103.7(3) |
| C(24)-C(23)-C(22) | 121.7(3) | O(1S)-C(4S)-C(3S) | 106.0(3) |

Table 2.8.anis. Anisotropic displacement parameters ($Å^2 x\ 10^3$). The anisotropic displacement factor exponent takes the form: $-2p^2[\ h^2\ a^{*2}U^{11} + ... + 2\ h\ k\ a^*\ b^*\ U^{12}\ ]$

| | U11 | U22 | U33 | U23 | U13 | U12 |
|---|---|---|---|---|---|---|
| C(1) | 10(1) | 22(1) | 18(1) | 1(1) | 8(1) | 0(1) |
| N(1) | 11(1) | 21(1) | 23(1) | 0(1) | 11(1) | -1(1) |
| N(2) | 11(1) | 23(1) | 21(1) | -3(1) | 12(1) | 0(1) |
| C(2) | 15(2) | 28(2) | 30(2) | -4(1) | 15(1) | 1(1) |
| C(3) | 16(2) | 23(2) | 30(2) | -6(1) | 17(1) | -1(1) |
| C(11) | 11(1) | 19(1) | 19(1) | -5(1) | 9(1) | -5(1) |
| C(12) | 16(1) | 18(1) | 20(2) | -4(1) | 10(1) | -2(1) |
| C(13) | 14(1) | 26(2) | 26(2) | -6(1) | 10(1) | -3(1) |
| C(14) | 22(2) | 25(2) | 31(2) | -3(1) | 16(2) | -7(1) |
| C(15) | 26(2) | 19(1) | 25(2) | 0(1) | 11(1) | -1(1) |
| C(16) | 17(2) | 23(2) | 22(2) | -3(1) | 8(1) | 0(1) |
| C(17) | 16(2) | 28(2) | 22(2) | 2(1) | 5(1) | 1(1) |
| C(18) | 30(2) | 32(2) | 56(3) | -4(2) | 24(2) | -13(2) |
| C(19) | 19(2) | 29(2) | 35(2) | 3(2) | 4(2) | 4(1) |
| C(21) | 15(1) | 19(1) | 21(1) | -1(1) | 12(1) | -1(1) |
| C(22) | 14(1) | 24(2) | 21(1) | 2(1) | 14(1) | 0(1) |
| C(23) | 20(2) | 21(1) | 28(2) | 5(1) | 15(1) | 1(1) |
| C(24) | 21(2) | 22(2) | 29(2) | -4(1) | 17(1) | -4(1) |
| C(25) | 16(2) | 27(2) | 24(2) | -5(1) | 13(1) | -5(1) |
| C(26) | 15(2) | 24(1) | 20(1) | -1(1) | 13(1) | 0(1) |
| C(27) | 19(2) | 31(2) | 18(2) | 3(1) | 9(1) | -1(1) |
| C(28) | 33(2) | 23(2) | 48(2) | -7(2) | 23(2) | -4(2) |
| C(29) | 17(2) | 29(2) | 21(2) | 1(1) | 6(1) | 2(1) |
| C(41) | 8(1) | 24(1) | 16(1) | -2(1) | 8(1) | -2(1) |
| O(1) | 10(1) | 24(1) | 20(1) | -3(1) | 7(1) | -1(1) |
| C(42) | 8(1) | 27(2) | 14(1) | 0(1) | 4(1) | -1(1) |
| Cl(2) | 13(1) | 33(1) | 16(1) | -2(1) | 5(1) | -1(1) |
| C(43) | 10(1) | 24(1) | 17(1) | 7(1) | 4(1) | 3(1) |
| Cl(3) | 20(1) | 28(1) | 29(1) | 11(1) | 6(1) | 3(1) |
| C(44) | 16(2) | 15(1) | 25(2) | 1(1) | 10(1) | 0(1) |
| Cl(4) | 19(1) | 19(1) | 41(1) | -3(1) | 10(1) | -1(1) |
| C(45) | 10(1) | 26(1) | 15(1) | -2(1) | 6(1) | -1(1) |
| Cl(5) | 19(1) | 28(1) | 19(1) | -7(1) | 5(1) | -2(1) |
| C(46) | 10(1) | 23(1) | 14(1) | 2(1) | 7(1) | 2(1) |
| Cl(6) | 16(1) | 24(1) | 17(1) | 4(1) | 7(1) | 4(1) |

| | | | | | | |
|---|---|---|---|---|---|---|
| C(1S) | 33(2) | 35(2) | 46(2) | 3(2) | 18(2) | -6(2) |
| O(1S) | 29(2) | 31(2) | 61(2) | 2(1) | -8(2) | -2(1) |
| C(2S) | 41(2) | 35(2) | 29(2) | 4(2) | 12(2) | 16(2) |
| C(3S) | 22(2) | 43(2) | 36(2) | -2(2) | 9(2) | -1(2) |
| C(4S) | 31(2) | 27(2) | 40(2) | 4(2) | 0(2) | -5(2) |

**Supplement 2.9. Table of the Results of the Refinement for the Co-Crystal of Pentafluorophenol and 1,3-Dimesitylimidazol-2-ylidene**

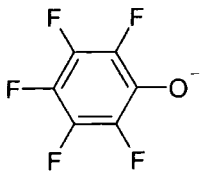


[PFPO-]

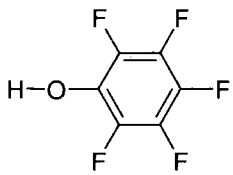


[PFP]

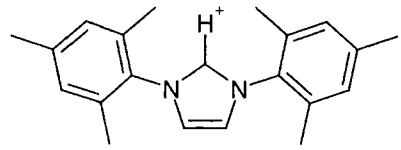


[DMI+]

Table 2.9.xyz. Atomic coordinates ( x $10^4$) and equivalent isotropic displacement parameters ($Å^2$x $10^3$). U(eq) is defined as one third of the trace of the orthogonalized $U^{ij}$ tensor.

| | x | y | z | U(eq) |
|---|---|---|---|---|
| C(1) | 5624(2) | 4817(1) | 2516(1) | 25(1) |
| N(1) | 4862(2) | 4580(1) | 2934(1) | 24(1) |
| N(2) | 5251(2) | 4160(1) | 2160(1) | 24(1) |
| C(2) | 3964(2) | 3743(1) | 2841(1) | 28(1) |
| C(3) | 4212(2) | 3479(1) | 2360(1) | 27(1) |
| C(11) | 4963(2) | 5128(1) | 3402(1) | 24(1) |
| C(12) | 5826(2) | 4743(1) | 3829(1) | 26(1) |
| C(13) | 5892(2) | 5291(1) | 4270(1) | 28(1) |
| C(14) | 5151(2) | 6190(1) | 4288(1) | 27(1) |
| C(15) | 4316(2) | 6547(1) | 3850(1) | 26(1) |
| C(16) | 4193(2) | 6023(1) | 3399(1) | 25(1) |
| C(17) | 6664(3) | 3780(1) | 3817(1) | 33(1) |
| C(18) | 5250(3) | 6772(2) | 4771(1) | 34(1) |
| C(19) | 3241(2) | 6406(1) | 2932(1) | 30(1) |
| C(21) | 5910(2) | 4150(1) | 1659(1) | 24(1) |
| C(22) | 7626(2) | 3993(1) | 1621(1) | 25(1) |
| C(23) | 8213(2) | 3986(1) | 1133(1) | 27(1) |
| C(24) | 7159(2) | 4126(1) | 701(1) | 27(1) |
| C(25) | 5461(2) | 4274(1) | 760(1) | 27(1) |
| C(26) | 4800(2) | 4299(1) | 1238(1) | 25(1) |
| C(27) | 8817(2) | 3839(2) | 2078(1) | 31(1) |
| C(28) | 7847(2) | 4122(2) | 178(1) | 36(1) |
| C(29) | 2970(2) | 4502(2) | 1291(1) | 33(1) |
| C(41) | 7922(2) | 6629(1) | 1893(1) | 25(1) |
| O(41) | 7689(2) | 6629(1) | 2383(1) | 31(1) |
| C(42) | 9490(2) | 6689(1) | 1681(1) | 27(1) |

| | | | | |
|---|---|---|---|---|
| F(42) | 10876(1) | 6745(1) | 2000(1) | 39(1) |
| C(43) | 9694(2) | 6701(1) | 1168(1) | 30(1) |
| F(43) | 11233(1) | 6758(1) | 991(1) | 43(1) |
| C(44) | 8313(2) | 6658(1) | 828(1) | 31(1) |
| F(44) | 8498(2) | 6661(1) | 323(1) | 45(1) |
| C(45) | 6745(2) | 6607(1) | 1015(1) | 28(1) |
| F(45) | 5382(1) | 6567(1) | 689(1) | 38(1) |
| C(46) | 6559(2) | 6589(1) | 1531(1) | 26(1) |
| F(46) | 4997(1) | 6527(1) | 1699(1) | 34(1) |
| C(31) | 9633(4) | 5704(3) | 3438(1) | 28(1) |
| O(31) | 9251(3) | 5535(2) | 2950(1) | 30(1) |
| C(32) | 10515(4) | 5000(2) | 3721(2) | 35(1) |
| F(32) | 10944(2) | 4178(1) | 3499(1) | 47(1) |
| C(33) | 10984(5) | 5118(3) | 4228(2) | 42(1) |
| F(33) | 11865(2) | 4444(2) | 4488(1) | 64(1) |
| C(34) | 10581(6) | 5936(4) | 4471(1) | 43(1) |
| F(34) | 11047(2) | 6089(2) | 4967(1) | 62(1) |
| C(35) | 9690(7) | 6638(3) | 4209(2) | 37(1) |
| F(35) | 9227(2) | 7452(1) | 4436(1) | 50(1) |
| C(36) | 9219(7) | 6516(2) | 3697(2) | 29(1) |
| F(36) | 8326(2) | 7208(1) | 3449(1) | 34(1) |
| C(31') | 9769(9) | 5539(5) | 3477(2) | 24(6) |
| O(31') | 9546(10) | 5169(5) | 3016(2) | 32(2) |
| C(32') | 10585(14) | 4975(5) | 3856(3) | 30(5) |
| F(32') | 11103(11) | 4087(4) | 3744(3) | 58(3) |
| C(33') | 10880(20) | 5297(7) | 4345(3) | 32(5) |
| F(33') | 11702(11) | 4754(5) | 4696(3) | 59(3) |
| C(34') | 10360(30) | 6180(8) | 4479(3) | 23(4) |
| F(34') | 10642(10) | 6533(5) | 4955(2) | 44(2) |
| C(35') | 9540(30) | 6753(8) | 4120(3) | 27(5) |
| F(35') | 8974(11) | 7627(4) | 4240(3) | 49(3) |
| C(36') | 9310(30) | 6443(9) | 3620(3) | 28(7) |
| F(36') | 8544(11) | 7033(5) | 3274(2) | 54(3) |

Table 2.9.bond. Bond lengths (Å)

| | | | |
|---|---|---|---|
| C(1)-N(1) | 1.336(2) | C(27)-H(27C) | 1.00(2) |
| C(1)-N(2) | 1.340(2) | C(29)-H(29A) | 0.96(3) |
| C(1)-H(1) | 0.98(2) | C(29)-H(29B) | 0.97(3) |
| N(1)-C(2) | 1.394(2) | C(29)-H(29C) | 0.99(3) |
| N(1)-C(11) | 1.453(2) | C(41)-O(41) | 1.318(2) |
| N(2)-C(3) | 1.393(2) | C(41)-C(42) | 1.407(2) |
| N(2)-C(21) | 1.450(2) | C(41)-C(46) | 1.413(2) |
| C(2)-C(3) | 1.349(3) | O(41)-H(100) | 1.35(4) |
| C(2)-H(2) | 0.97(2) | C(42)-F(42) | 1.358(2) |
| C(3)-H(3) | 0.97(2) | C(42)-C(43) | 1.377(3) |
| C(11)-C(16) | 1.400(2) | C(43)-F(43) | 1.346(2) |
| C(11)-C(12) | 1.400(2) | C(43)-C(44) | 1.387(3) |
| C(12)-C(13) | 1.396(3) | C(44)-F(44) | 1.352(2) |
| C(12)-C(17) | 1.513(3) | C(44)-C(45) | 1.378(3) |
| C(13)-C(14) | 1.397(3) | C(45)-F(45) | 1.354(2) |
| C(13)-H(13) | 1.00(2) | C(45)-C(46) | 1.379(2) |
| C(14)-C(15) | 1.398(2) | C(46)-F(46) | 1.356(2) |
| C(14)-C(18) | 1.513(3) | C(31)-O(31) | 1.330(3) |
| C(15)-C(16) | 1.399(2) | C(31)-C(36) | 1.382(5) |
| C(15)-H(15) | 0.98(2) | C(31)-C(32) | 1.407(5) |
| C(16)-C(19) | 1.514(2) | O(31)-H(100) | 1.12(4) |
| C(17)-H(17A) | 1.00(2) | C(32)-F(32) | 1.349(3) |
| C(17)-H(17B) | 0.98(3) | C(32)-C(33) | 1.380(5) |
| C(17)-H(17C) | 1.00(3) | C(33)-F(33) | 1.348(3) |
| C(18)-H(18A) | 0.91(3) | C(33)-C(34) | 1.363(6) |
| C(18)-H(18B) | 0.95(4) | C(34)-F(34) | 1.361(3) |
| C(18)-H(18C) | 0.98(3) | C(34)-C(35) | 1.382(6) |
| C(19)-H(19A) | 1.00(2) | C(35)-F(35) | 1.354(3) |
| C(19)-H(19B) | 1.00(2) | C(35)-C(36) | 1.393(5) |
| C(19)-H(19C) | 0.99(2) | C(36)-F(36) | 1.356(2) |
| C(21)-C(26) | 1.401(2) | C(31')-O(31') | 1.329(4) |
| C(21)-C(22) | 1.403(2) | C(31')-C(36') | 1.382(6) |
| C(22)-C(23) | 1.397(3) | C(31')-C(32') | 1.408(6) |
| C(22)-C(27) | 1.512(2) | C(32')-F(32') | 1.353(4) |
| C(23)-C(24) | 1.398(2) | C(32')-C(33') | 1.377(6) |
| C(23)-H(23) | 0.98(2) | C(33')-F(33') | 1.346(4) |
| C(24)-C(25) | 1.396(3) | C(33')-C(34') | 1.363(6) |

| | | | |
|---|---|---|---|
| C(24)-C(28) | 1.514(2) | C(34')-F(34') | 1.360(4) |
| C(25)-C(26) | 1.396(2) | C(34')-C(35') | 1.381(6) |
| C(25)-H(25) | 1.02(2) | C(35')-F(35') | 1.354(4) |
| C(26)-C(29) | 1.510(2) | C(35')-C(36') | 1.393(6) |
| C(27)-H(27A) | 0.98(2) | C(36')-F(36') | 1.357(4) |
| C(27)-H(27B) | 0.98(3) | | |

Table 2.9.angle. Bond Angles (°)

| | | | |
|---|---|---|---|
| N(1)-C(1)-N(2) | 108.34(15) | C(22)-C(27)-H(27A) | 113.2(14) |
| N(1)-C(1)-H(1) | 126.6(11) | C(22)-C(27)-H(27B) | 109.7(14) |
| N(2)-C(1)-H(1) | 125.0(11) | H(27A)-C(27)-H(27B) | 107.4(19) |
| C(1)-N(1)-C(2) | 108.67(14) | C(22)-C(27)-H(27C) | 110.6(13) |
| C(1)-N(1)-C(11) | 124.33(14) | H(27A)-C(27)-H(27C) | 106.0(18) |
| C(2)-N(1)-C(11) | 127.00(14) | H(27B)-C(27)-H(27C) | 109.8(19) |
| C(1)-N(2)-C(3) | 108.75(14) | C(26)-C(29)-H(29A) | 113.3(14) |
| C(1)-N(2)-C(21) | 124.62(14) | C(26)-C(29)-H(29B) | 112.1(15) |
| C(3)-N(2)-C(21) | 126.55(14) | H(29A)-C(29)-H(29B) | 104(2) |
| C(3)-C(2)-N(1) | 107.26(15) | C(26)-C(29)-H(29C) | 110.0(16) |
| C(3)-C(2)-H(2) | 133.1(13) | H(29A)-C(29)-H(29C) | 107(2) |
| N(1)-C(2)-H(2) | 119.6(13) | H(29B)-C(29)-H(29C) | 109(2) |
| C(2)-C(3)-N(2) | 106.98(15) | O(41)-C(41)-C(42) | 124.64(16) |
| C(2)-C(3)-H(3) | 131.1(12) | O(41)-C(41)-C(46) | 121.21(16) |
| N(2)-C(3)-H(3) | 122.0(12) | C(42)-C(41)-C(46) | 114.14(15) |
| C(16)-C(11)-C(12) | 123.30(16) | C(41)-O(41)-H(100) | 123.0(16) |
| C(16)-C(11)-N(1) | 117.98(15) | F(42)-C(42)-C(43) | 118.14(16) |
| C(12)-C(11)-N(1) | 118.72(15) | F(42)-C(42)-C(41) | 118.48(15) |
| C(13)-C(12)-C(11) | 116.95(16) | C(43)-C(42)-C(41) | 123.37(16) |
| C(13)-C(12)-C(17) | 121.05(16) | F(43)-C(43)-C(42) | 120.33(17) |
| C(11)-C(12)-C(17) | 122.00(16) | F(43)-C(43)-C(44) | 119.56(16) |
| C(12)-C(13)-C(14) | 122.13(16) | C(42)-C(43)-C(44) | 120.11(17) |
| C(12)-C(13)-H(13) | 118.4(12) | F(44)-C(44)-C(45) | 120.35(16) |
| C(14)-C(13)-H(13) | 119.4(12) | F(44)-C(44)-C(43) | 120.68(17) |
| C(13)-C(14)-C(15) | 118.75(16) | C(45)-C(44)-C(43) | 118.96(16) |
| C(13)-C(14)-C(18) | 121.06(16) | F(45)-C(45)-C(44) | 119.79(16) |
| C(15)-C(14)-C(18) | 120.20(17) | F(45)-C(45)-C(46) | 119.89(16) |
| C(14)-C(15)-C(16) | 121.53(17) | C(44)-C(45)-C(46) | 120.32(16) |
| C(14)-C(15)-H(15) | 119.6(12) | F(46)-C(46)-C(45) | 118.55(15) |
| C(16)-C(15)-H(15) | 118.9(12) | F(46)-C(46)-C(41) | 118.35(15) |

| | | | |
|---|---|---|---|
| C(15)-C(16)-C(11) | 117.34(16) | C(45)-C(46)-C(41) | 123.10(16) |
| C(15)-C(16)-C(19) | 120.99(16) | O(31)-C(31)-C(36) | 125.4(4) |
| C(11)-C(16)-C(19) | 121.66(16) | O(31)-C(31)-C(32) | 118.2(4) |
| C(12)-C(17)-H(17A) | 112.3(14) | C(36)-C(31)-C(32) | 116.4(2) |
| C(12)-C(17)-H(17B) | 110.6(15) | C(31)-O(31)-H(100) | 117.0(19) |
| H(17A)-C(17)-H(17B) | 107(2) | F(32)-C(32)-C(33) | 117.6(4) |
| C(12)-C(17)-H(17C) | 112.9(14) | F(32)-C(32)-C(31) | 120.2(4) |
| H(17A)-C(17)-H(17C) | 107(2) | C(33)-C(32)-C(31) | 122.2(3) |
| H(17B)-C(17)-H(17C) | 106(2) | F(33)-C(33)-C(34) | 118.9(4) |
| C(14)-C(18)-H(18A) | 113(2) | F(33)-C(33)-C(32) | 121.1(4) |
| C(14)-C(18)-H(18B) | 112.2(19) | C(34)-C(33)-C(32) | 119.9(2) |
| H(18A)-C(18)-H(18B) | 100(3) | F(34)-C(34)-C(33) | 121.9(4) |
| C(14)-C(18)-H(18C) | 112.4(18) | F(34)-C(34)-C(35) | 118.4(4) |
| H(18A)-C(18)-H(18C) | 110(3) | C(33)-C(34)-C(35) | 119.7(2) |
| H(18B)-C(18)-H(18C) | 109(3) | F(35)-C(35)-C(34) | 121.9(4) |
| C(16)-C(19)-H(19A) | 113.1(13) | F(35)-C(35)-C(36) | 117.9(4) |
| C(16)-C(19)-H(19B) | 109.3(12) | C(34)-C(35)-C(36) | 120.2(3) |
| H(19A)-C(19)-H(19B) | 106.7(17) | F(36)-C(36)-C(31) | 119.2(4) |
| C(16)-C(19)-H(19C) | 111.3(13) | F(36)-C(36)-C(35) | 119.3(4) |
| H(19A)-C(19)-H(19C) | 107.0(17) | C(31)-C(36)-C(35) | 121.5(3) |
| H(19B)-C(19)-H(19C) | 109.2(17) | O(31')-C(31')-C(36') | 125.9(5) |
| C(26)-C(21)-C(22) | 123.32(16) | O(31')-C(31')-C(32') | 117.7(5) |
| C(26)-C(21)-N(2) | 118.34(15) | C(36')-C(31')-C(32') | 116.4(3) |
| C(22)-C(21)-N(2) | 118.35(15) | F(32')-C(32')-C(33') | 118.0(5) |
| C(23)-C(22)-C(21) | 116.71(15) | F(32')-C(32')-C(31') | 120.1(5) |
| C(23)-C(22)-C(27) | 120.29(16) | C(33')-C(32')-C(31') | 122.0(3) |
| C(21)-C(22)-C(27) | 123.00(16) | F(33')-C(33')-C(34') | 118.9(5) |
| C(22)-C(23)-C(24) | 122.29(16) | F(33')-C(33')-C(32') | 120.8(6) |
| C(22)-C(23)-H(23) | 117.7(12) | C(34')-C(33')-C(32') | 120.3(3) |
| C(24)-C(23)-H(23) | 120.0(12) | F(34')-C(34')-C(33') | 122.3(5) |
| C(25)-C(24)-C(23) | 118.55(16) | F(34')-C(34')-C(35') | 118.1(5) |
| C(25)-C(24)-C(28) | 120.77(16) | C(33')-C(34')-C(35') | 119.6(3) |
| C(23)-C(24)-C(28) | 120.68(16) | F(35')-C(35')-C(34') | 121.5(5) |
| C(26)-C(25)-C(24) | 121.91(16) | F(35')-C(35')-C(36') | 118.4(5) |
| C(26)-C(25)-H(25) | 118.9(11) | C(34')-C(35')-C(36') | 120.1(3) |
| C(24)-C(25)-H(25) | 119.2(11) | F(36')-C(36')-C(31') | 119.7(5) |
| C(25)-C(26)-C(21) | 117.22(16) | F(36')-C(36')-C(35') | 118.7(5) |
| C(25)-C(26)-C(29) | 120.55(16) | C(31')-C(36')-C(35') | 121.5(4) |

| | | | |
|---|---|---|---|
| C(21)-C(26)-C(29) | 122.22(16) | | |

Table 2.9.anis. Anisotropic displacement parameters ($Å^2 x\ 10^3$). The anisotropic displacement factor exponent takes the form: $-2\pi^2[ h^2 a^{*2} U^{11} + ... + 2 h k a^* b^* U^{12} ]$

| | U11 | U22 | U33 | U23 | U13 | U12 |
|---|---|---|---|---|---|---|
| C(1) | 25(1) | 26(1) | 23(1) | 1(1) | 1(1) | -3(1) |
| N(1) | 26(1) | 26(1) | 22(1) | 0(1) | 2(1) | -3(1) |
| N(2) | 23(1) | 26(1) | 22(1) | -1(1) | 1(1) | -3(1) |
| C(2) | 29(1) | 26(1) | 28(1) | 1(1) | 3(1) | -5(1) |
| C(3) | 27(1) | 26(1) | 28(1) | 0(1) | 2(1) | -4(1) |
| C(11) | 25(1) | 28(1) | 21(1) | -1(1) | 3(1) | -5(1) |
| C(12) | 26(1) | 28(1) | 25(1) | 2(1) | 2(1) | -3(1) |
| C(13) | 30(1) | 30(1) | 23(1) | 4(1) | -1(1) | -4(1) |
| C(14) | 28(1) | 29(1) | 24(1) | 0(1) | 3(1) | -5(1) |
| C(15) | 27(1) | 26(1) | 27(1) | 1(1) | 3(1) | -2(1) |
| C(16) | 24(1) | 27(1) | 25(1) | 2(1) | 2(1) | -4(1) |
| C(17) | 37(1) | 30(1) | 32(1) | 0(1) | -3(1) | 3(1) |
| C(18) | 43(1) | 34(1) | 25(1) | -3(1) | -1(1) | -1(1) |
| C(19) | 31(1) | 32(1) | 27(1) | 2(1) | -1(1) | 2(1) |
| C(21) | 26(1) | 25(1) | 21(1) | -3(1) | 3(1) | -2(1) |
| C(22) | 26(1) | 26(1) | 24(1) | -3(1) | -1(1) | -2(1) |
| C(23) | 24(1) | 31(1) | 27(1) | -4(1) | 2(1) | -2(1) |
| C(24) | 30(1) | 28(1) | 25(1) | -2(1) | 2(1) | -2(1) |
| C(25) | 29(1) | 28(1) | 23(1) | 0(1) | -3(1) | -1(1) |
| C(26) | 25(1) | 24(1) | 27(1) | -1(1) | -1(1) | -1(1) |
| C(27) | 27(1) | 37(1) | 27(1) | -6(1) | -3(1) | 1(1) |
| C(28) | 36(1) | 49(1) | 24(1) | 0(1) | 4(1) | 0(1) |
| C(29) | 25(1) | 38(1) | 34(1) | 2(1) | 0(1) | 1(1) |
| C(41) | 32(1) | 23(1) | 20(1) | 1(1) | 0(1) | 0(1) |
| O(41) | 35(1) | 38(1) | 19(1) | 1(1) | 1(1) | 2(1) |
| C(42) | 28(1) | 27(1) | 25(1) | 2(1) | -4(1) | -2(1) |
| F(42) | 30(1) | 52(1) | 32(1) | 3(1) | -7(1) | -5(1) |
| C(43) | 30(1) | 31(1) | 30(1) | 4(1) | 7(1) | 1(1) |
| F(43) | 34(1) | 57(1) | 40(1) | 8(1) | 13(1) | 2(1) |
| C(44) | 44(1) | 32(1) | 16(1) | 2(1) | 4(1) | 4(1) |
| F(44) | 57(1) | 58(1) | 19(1) | 5(1) | 7(1) | 10(1) |
| C(45) | 33(1) | 27(1) | 24(1) | 2(1) | -6(1) | 1(1) |
| F(45) | 40(1) | 46(1) | 27(1) | 2(1) | -12(1) | 2(1) |

| | | | | | | |
|---|---|---|---|---|---|---|
| C(46) | 26(1) | 26(1) | 25(1) | 2(1) | 3(1) | 1(1) |
| F(46) | 27(1) | 43(1) | 32(1) | 4(1) | 3(1) | 1(1) |
| C(31) | 26(2) | 33(1) | 26(2) | 1(1) | 1(1) | -5(1) |
| O(31) | 36(1) | 29(1) | 23(1) | -6(1) | -3(1) | 2(1) |
| C(32) | 26(2) | 42(2) | 38(2) | 8(1) | 5(1) | -2(1) |
| F(32) | 41(1) | 40(1) | 61(1) | 10(1) | 13(1) | 13(1) |
| C(33) | 26(2) | 61(2) | 39(2) | 23(2) | 0(2) | 0(1) |
| F(33) | 37(1) | 94(2) | 61(1) | 48(1) | -3(1) | 12(1) |
| C(34) | 33(2) | 77(3) | 20(1) | 13(1) | -5(1) | -17(2) |
| F(34) | 50(1) | 117(2) | 19(1) | 10(1) | -9(1) | -23(1) |
| C(35) | 37(2) | 48(2) | 26(1) | -5(1) | 4(1) | -18(1) |
| F(35) | 65(1) | 56(1) | 29(1) | -17(1) | 10(1) | -23(1) |
| C(36) | 29(2) | 32(2) | 25(1) | 4(1) | -1(2) | -7(1) |
| F(36) | 48(1) | 28(1) | 26(1) | -2(1) | 2(1) | 2(1) |

Table 2.9.H. Hydrogen coordinates ( x $10^4$) and isotropic displacement parameters ($Å^2$x $10^3$).

| | x | y | z | U(eq) |
|---|---|---|---|---|
| H(1) | 6300(20) | 5388(15) | 2466(7) | 29(5) |
| H(2) | 3300(30) | 3478(15) | 3105(9) | 39(6) |
| H(3) | 3800(30) | 2933(16) | 2163(8) | 36(5) |
| H(13) | 6490(30) | 5029(15) | 4580(8) | 35(5) |
| H(15) | 3800(20) | 7180(16) | 3857(7) | 31(5) |
| H(17A) | 7340(30) | 3699(17) | 3514(9) | 49(6) |
| H(17B) | 7430(30) | 3693(18) | 4117(10) | 53(7) |
| H(17C) | 5860(30) | 3242(18) | 3818(9) | 53(7) |
| H(18A) | 4280(40) | 7080(20) | 4826(12) | 83(10) |
| H(18B) | 5970(40) | 7300(20) | 4748(12) | 88(10) |
| H(18C) | 5600(40) | 6390(20) | 5067(12) | 82(10) |
| H(19A) | 2460(30) | 5927(16) | 2766(8) | 38(6) |
| H(19B) | 2540(30) | 6961(15) | 3030(8) | 31(5) |
| H(19C) | 4010(30) | 6613(15) | 2673(8) | 36(6) |
| H(23) | 9410(30) | 3884(15) | 1101(8) | 32(5) |
| H(25) | 4680(30) | 4374(15) | 446(8) | 34(5) |
| H(27A) | 8300(30) | 3524(16) | 2360(9) | 44(6) |
| H(27B) | 9250(30) | 4456(19) | 2203(9) | 49(7) |
| H(27C) | 9770(30) | 3422(16) | 1989(8) | 40(6) |
| H(29A) | 2770(30) | 4990(18) | 1536(9) | 49(7) |

| | | | | |
|---|---|---|---|---|
| H(29B) | 2380(30) | 3954(19) | 1409(9) | 54(7) |
| H(29C) | 2450(30) | 4710(20) | 961(11) | 67(8) |
| H(100) | 8660(50) | 6130(30) | 2722(14) | 76(11) |

**Supplement 3.2. Tables of Refinement Results for the Neutron Structure of 4,4'-Bipyridinium Dihydrogen Pyromellitate (2-) Hydrate**

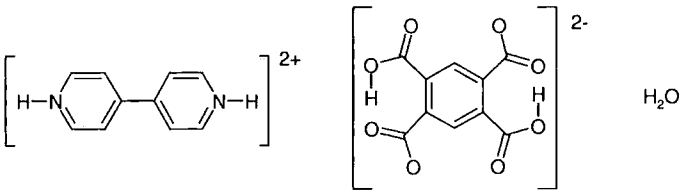


[BPY2+] [PMA2-]

Table 3.2.xyz Atomic coordinates ( x $10^4$) and equivalent isotropic displacement parameters ($Å^2$x $10^3$), U(eq) is defined as one third of the trace of the orthogonalized $U^{ij}$ tensor.

| | x | y | z | U(eq) |
|---|---|---|---|---|
| C(1) | 6150(3) | 5646(1) | 1151(1) | 18(1) |
| C(10) | 7726(4) | 6500(1) | 2290(1) | 24(1) |
| O(11) | 6904(6) | 6224(2) | 3249(1) | 37(1) |
| O(12) | 9729(5) | 7446(2) | 2291(1) | 40(1) |
| C(2) | 4121(3) | 4445(1) | 940(1) | 18(1) |
| C(20) | 2853(4) | 3714(1) | 1818(1) | 23(1) |
| O(21) | 3307(7) | 4187(2) | 2860(1) | 49(1) |
| O(22) | 1279(6) | 2629(2) | 1455(1) | 38(1) |
| C(3) | 3051(3) | 3848(1) | -202(1) | 19(1) |
| N(4) | -1427(3) | 1599(1) | 3020(1) | 26(1) |
| C(5) | -2753(4) | 388(1) | 2697(1) | 30(1) |
| C(6) | -4223(4) | -266(1) | 3460(1) | 26(1) |
| C(7) | -4251(3) | 344(1) | 4580(1) | 17(1) |
| C(8) | -2816(4) | 1611(1) | 4892(1) | 25(1) |
| C(9) | -1407(4) | 2218(1) | 4087(1) | 28(1) |
| O(1) | 1520(50) | 374(14) | -34(14) | 79(6) |
| O(2) | -1220(40) | 377(11) | -152(14) | 89(5) |
| O(3) | -3690(50) | 758(14) | -223(17) | 59(5) |
| O(4) | 4200(60) | 748(16) | -35(14) | 63(4) |

Table 3.2.bond. Bond lengths (Å).

| | | | |
|---|---|---|---|
| C(1)-C(3)#1 | 1.3954(16) | C(5)-H(5) | 1.082(3) |
| C(1)-C(2) | 1.4134(17) | C(6)-C(7) | 1.3923(17) |
| C(1)-C(10) | 1.5240(16) | C(6)-H(6) | 1.078(3) |
| C(10)-O(12) | 1.215(2) | C(7)-C(8) | 1.3989(17) |
| C(10)-O(11) | 1.300(2) | C(7)-C(7)#2 | 1.485(2) |
| O(11)-H(11) | 1.053(4) | C(8)-C(9) | 1.3875(18) |
| C(2)-C(3) | 1.3968(17) | C(8)-H(8) | 1.082(3) |
| C(2)-C(20) | 1.5171(16) | C(9)-H(9) | 1.080(3) |
| C(20)-O(21) | 1.247(2) | O(1)-H(1A) | 0.963(18) |
| C(20)-O(22) | 1.247(2) | O(1)-H(1B) | 0.985(17) |
| O(21)-H(11) | 1.370(4) | O(2)-H(2A) | 0.930(17) |
| C(3)-C(1)#1 | 1.3954(16) | O(2)-H(2B) | 1.019(18) |
| C(3)-H(3) | 1.080(3) | O(3)-H(3A) | 0.964(10) |
| N(4)-C(5) | 1.3349(17) | O(3)-H(3B) | 0.981(10) |
| N(4)-C(9) | 1.3372(17) | O(4)-H(4A) | 0.902(18) |
| N(4)-H(4) | 1.097(3) | O(4)-H(4B) | 0.946(19) |
| C(5)-C(6) | 1.3864(18) | | |

Symmetry transformations used to generate equivalent atoms:

#1 -x+1,-y+1,-z #2 -x-1,-y,-z+1

Table 3.2.angle. Bond angles (°).

| | | | |
|---|---|---|---|
| C(3)#1-C(1)-C(2) | 117.64(11) | N(4)-C(5)-C(6) | 120.60(12) |
| C(3)#1-C(1)-C(10) | 112.91(10) | N(4)-C(5)-H(5) | 116.4(2) |
| C(2)-C(1)-C(10) | 129.44(10) | C(6)-C(5)-H(5) | 123.0(2) |
| O(12)-C(10)-O(11) | 120.50(14) | C(5)-C(6)-C(7) | 119.53(11) |
| O(12)-C(10)-C(1) | 119.22(13) | C(5)-C(6)-H(6) | 117.8(2) |
| O(11)-C(10)-C(1) | 120.27(13) | C(7)-C(6)-H(6) | 122.6(2) |
| C(10)-O(11)-H(11) | 111.7(2) | C(6)-C(7)-C(8) | 118.35(11) |
| C(3)-C(2)-C(1) | 117.83(10) | C(6)-C(7)-C(7)#2 | 120.51(13) |
| C(3)-C(2)-C(20) | 114.65(10) | C(8)-C(7)-C(7)#2 | 121.13(13) |
| C(1)-C(2)-C(20) | 127.51(10) | C(9)-C(8)-C(7) | 119.48(12) |
| O(21)-C(20)-O(22) | 121.25(14) | C(9)-C(8)-H(8) | 117.97(19) |
| O(21)-C(20)-C(2) | 121.42(13) | C(7)-C(8)-H(8) | 122.53(19) |
| O(22)-C(20)-C(2) | 117.32(12) | N(4)-C(9)-C(8) | 120.38(12) |
| C(20)-O(21)-H(11) | 113.34(18) | N(4)-C(9)-H(9) | 116.0(2) |
| C(1)#1-C(3)-C(2) | 124.53(11) | C(8)-C(9)-H(9) | 123.6(2) |

| | | | |
|---|---|---|---|
| C(1)#1-C(3)-H(3) | 117.24(19) | H(1A)-O(1)-H(1B) | 108.5(19) |
| C(2)-C(3)-H(3) | 118.22(19) | H(2A)-O(2)-H(2B) | 98(2) |
| C(5)-N(4)-C(9) | 121.65(10) | H(3A)-O(3)-H(3B) | 109.3(15) |
| C(5)-N(4)-H(4) | 118.38(18) | H(4A)-O(4)-H(4B) | 118(3) |
| C(9)-N(4)-H(4) | 119.95(18) | | |

Symmetry transformations used to generate equivalent atoms:

#1 -x+1,-y+1,-z #2 -x-1,-y,-z+1

Table 3.2.anis. Anisotropic displacement parameters ($Å^2 x\ 10^3$). The anisotropic displacement factor exponent takes the form: $-2\pi^2[ h^2 a^{*2}U^{11} + ... + 2 h k a^* b^* U^{12} ]$

| | U11 | U22 | U33 | U23 | U13 | U12 |
|---|---|---|---|---|---|---|
| C(1) | 23(1) | 17(1) | 12(1) | 3(1) | 4(1) | -3(1) |
| C(10) | 31(1) | 22(1) | 16(1) | 1(1) | 3(1) | -5(1) |
| O(11) | 58(1) | 34(1) | 13(1) | -1(1) | 7(1) | -13(1) |
| H(11) | 84(2) | 47(2) | 25(1) | 6(1) | 12(2) | -18(2) |
| O(12) | 53(1) | 33(1) | 24(1) | -1(1) | 3(1) | -23(1) |
| C(2) | 23(1) | 16(1) | 14(1) | 4(1) | 5(1) | -3(1) |
| C(20) | 32(1) | 21(1) | 16(1) | 8(1) | 7(1) | -4(1) |
| O(21) | 87(2) | 39(1) | 17(1) | 4(1) | 15(1) | -25(1) |
| O(22) | 63(1) | 27(1) | 23(1) | 7(1) | 13(1) | -16(1) |
| C(3) | 25(1) | 16(1) | 14(1) | 4(1) | 5(1) | -5(1) |
| H(3) | 51(2) | 27(2) | 36(1) | 6(1) | 8(1) | -14(1) |
| N(4) | 31(1) | 28(1) | 21(1) | 12(1) | 7(1) | -4(1) |
| H(4) | 51(2) | 42(2) | 35(1) | 17(1) | 10(1) | -5(1) |
| C(5) | 43(1) | 30(1) | 16(1) | 6(1) | 10(1) | -10(1) |
| H(5) | 108(3) | 57(2) | 30(2) | 2(1) | 30(2) | -24(2) |
| C(6) | 40(1) | 22(1) | 15(1) | 1(1) | 9(1) | -10(1) |
| H(6) | 101(3) | 36(2) | 34(2) | -4(1) | 26(2) | -26(2) |
| C(7) | 21(1) | 16(1) | 13(1) | 5(1) | 4(1) | -4(1) |
| C(8) | 40(1) | 17(1) | 19(1) | 3(1) | 11(1) | -8(1) |
| H(8) | 103(3) | 37(2) | 34(2) | -4(1) | 26(2) | -21(2) |
| C(9) | 38(1) | 21(1) | 26(1) | 9(1) | 11(1) | -6(1) |
| H(9) | 95(3) | 26(2) | 52(2) | 9(1) | 21(2) | -18(2) |

Table 3.2.H. Hydrogen coordinates ( x $10^4$) and isotropic displacement parameters ($Å^2$x 10 $^3$)

| | x | y | z | U(eq) |
|---|---|---|---|---|
| H(11) | 5275(11) | 5353(3) | 3114(2) | 53(1) |
| H(3) | 1480(9) | 2933(3) | -369(2) | 39(1) |
| H(4) | -273(9) | 2082(3) | 2391(2) | 42(1) |
| H(5) | -2598(13) | -40(3) | 1822(3) | 66(1) |
| H(6) | -5321(12) | -1236(3) | 3152(3) | 59(1) |
| H(8) | -2683(12) | 2139(3) | 5752(3) | 60(1) |
| H(9) | -236(12) | 3190(3) | 4267(3) | 58(1) |
| H(1A) | 1930(80) | 1213(15) | 415(19) | 95 |
| H(1B) | 3810(60) | 10(30) | 20(20) | 95 |
| H(2A) | -380(50) | 1191(12) | 234(13) | 99(4) |
| H(2B) | 1080(50) | -20(30) | 10(20) | 73(5) |
| H(3A) | -2830(60) | 1567(14) | 252(17) | 70 |
| H(3B) | -1870(100) | 180(30) | -130(40) | 70 |
| H(4A) | 4300(80) | 1516(18) | 400(20) | 60(6) |
| H(4B) | 6120(110) | 590(40) | -450(40) | 75(15) |

**Supplement 3.3.X. Tables of Refinement Results for the X-ray Structure of 4,4'-Bipyridinium bis-Trihydrogen Pyromellitate at 30K**

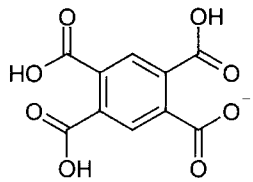

PMA-

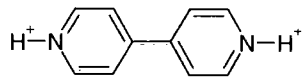

BPY2+

Table 3.3.X.xyz. Atomic coordinates ( x $10^4$) and equivalent isotropic displacement parameters ($Å^2$x $10^3$). U(eq) is defined as one third of the trace of the orthogonalized $U^{ij}$ tensor.

| | x | y | z | U(eq) |
|---|---|---|---|---|
| C(1) | -255(2) | 200(1) | 3256(1) | 10(1) |
| C(10) | -1037(2) | -514(1) | 3429(1) | 11(1) |
| O(11) | -899(1) | -1292(1) | 3212(1) | 15(1) |
| O(12) | -1786(1) | -295(1) | 3761(1) | 13(1) |
| C(2) | 818(2) | 105(1) | 3086(1) | 10(1) |
| C(20) | 1428(2) | -720(1) | 2952(1) | 11(1) |
| O(21) | 2413(1) | -677(1) | 2885(1) | 13(1) |
| O(22) | 895(1) | -1459(1) | 2883(1) | 13(1) |
| C(3) | 1442(2) | 855(1) | 3034(1) | 11(1) |
| C(4) | 1013(2) | 1678(1) | 3098(1) | 11(1) |
| C(40) | 1689(2) | 2459(1) | 2973(1) | 12(1) |
| O(41) | 1182(1) | 3083(1) | 2521(1) | 16(1) |
| O(42) | 2866(1) | 2373(1) | 3397(1) | 17(1) |
| C(5) | -82(2) | 1767(1) | 3211(1) | 11(1) |
| C(50) | -576(2) | 2647(1) | 3311(1) | 11(1) |
| O(51) | -12(1) | 3166(1) | 3899(1) | 16(1) |
| O(52) | -1688(1) | 2756(1) | 2690(1) | 14(1) |
| C(6) | -679(2) | 1034(1) | 3309(1) | 11(1) |
| C(1A) | 2618(2) | -29(1) | 448(1) | 11(1) |
| C(11) | 3389(2) | -762(1) | 303(1) | 11(1) |
| O(13) | 3291(1) | -1521(1) | 613(1) | 15(1) |
| O(14) | 4082(1) | -578(1) | -86(1) | 14(1) |
| C(2A) | 1545(2) | -82(1) | 625(1) | 10(1) |
| C(21) | 892(2) | -889(1) | 749(1) | 11(1) |
| O(23) | -103(1) | -817(1) | 795(1) | 14(1) |
| O(24) | 1393(1) | -1640(1) | 817(1) | 14(1) |

| | | | | |
|---|---|---|---|---|
| C(3A) | 963(2) | 685(1) | 672(1) | 11(1) |
| C(4A) | 1409(2) | 1496(1) | 572(1) | 11(1) |
| C(41) | 706(2) | 2298(1) | 560(1) | 11(1) |
| O(43) | 1067(1) | 3005(1) | 447(1) | 14(1) |
| O(44) | -326(1) | 2148(1) | 651(1) | 14(1) |
| C(5A) | 2489(2) | 1549(1) | 429(1) | 11(1) |
| C(51) | 3067(2) | 2387(1) | 289(1) | 12(1) |
| O(53) | 2861(1) | 2699(1) | -483(1) | 15(1) |
| O(54) | 3879(1) | 2683(1) | 1099(1) | 16(1) |
| C(6A) | 3060(2) | 793(1) | 357(1) | 11(1) |
| N(1) | 2505(2) | 5405(1) | 226(1) | 15(1) |
| C(30) | 2148(2) | 6196(1) | 373(1) | 14(1) |
| C(31) | 1618(2) | 6307(1) | 1025(1) | 13(1) |
| C(32) | 1454(2) | 5592(1) | 1527(1) | 11(1) |
| C(33) | 913(2) | 5710(1) | 2249(1) | 11(1) |
| C(34) | 939(2) | 6518(1) | 2664(1) | 12(1) |
| C(35) | 467(2) | 6613(1) | 3351(1) | 13(1) |
| N(2) | -9(2) | 5937(1) | 3629(1) | 12(1) |
| C(36) | -65(2) | 5147(1) | 3244(1) | 12(1) |
| C(37) | 386(2) | 5017(1) | 2549(1) | 12(1) |
| C(38) | 1820(2) | 4778(1) | 1341(1) | 12(1) |
| C(39) | 2337(2) | 4703(1) | 679(1) | 15(1) |

Table 3.3.X.bond. Bond lengths (Å).

| | | | |
|---|---|---|---|
| C(1)-C(6) | 1.402(2) | C(3A)-H(3A) | 0.90(2) |
| C(1)-C(2) | 1.417(3) | C(4A)-C(5A) | 1.399(3) |
| C(1)-C(10) | 1.539(2) | C(4A)-C(41) | 1.499(2) |
| C(10)-O(12) | 1.236(2) | C(41)-O(43) | 1.215(2) |
| C(10)-O(11) | 1.276(2) | C(41)-O(44) | 1.321(2) |
| O(11)-H(22) | 1.45(2) | O(44)-H(44) | 0.87(2) |
| C(2)-C(3) | 1.402(2) | C(5A)-C(6A) | 1.384(2) |
| C(2)-C(20) | 1.525(2) | C(5A)-C(51) | 1.525(2) |
| C(20)-O(21) | 1.230(2) | C(51)-O(53) | 1.206(2) |
| C(20)-O(22) | 1.296(2) | C(51)-O(54) | 1.330(2) |
| O(22)-H(22) | 0.97(2) | O(54)-H(54) | 1.00(2) |
| C(3)-C(4) | 1.391(2) | C(6A)-H(6A) | 0.96(2) |
| C(3)-H(3) | 1.02(2) | N(1)-C(39) | 1.343(3) |
| C(4)-C(5) | 1.399(2) | N(1)-C(30) | 1.345(3) |

| | | | |
|---|---|---|---|
| C(4)-C(40) | 1.510(2) | N(1)-H(1) | 0.95(2) |
| C(40)-O(41) | 1.208(2) | C(30)-C(31) | 1.379(3) |
| C(40)-O(42) | 1.321(2) | C(30)-H(30) | 0.98(2) |
| O(42)-H(42) | 0.83(2) | C(31)-C(32) | 1.402(3) |
| C(5)-C(6) | 1.382(2) | C(31)-H(31) | 0.93(2) |
| C(5)-C(50) | 1.517(2) | C(32)-C(38) | 1.399(2) |
| C(50)-O(51) | 1.202(2) | C(32)-C(33) | 1.486(2) |
| C(50)-O(52) | 1.323(2) | C(33)-C(34) | 1.395(3) |
| O(52)-H(52) | 0.89(2) | C(33)-C(37) | 1.407(2) |
| C(6)-H(6) | 0.99(2) | C(34)-C(35) | 1.373(3) |
| C(1A)-C(6A) | 1.406(2) | C(34)-H(34) | 0.97(2) |
| C(1A)-C(2A) | 1.418(3) | C(35)-N(2) | 1.337(2) |
| C(1A)-C(11) | 1.534(2) | C(35)-H(35) | 0.90(2) |
| C(11)-O(14) | 1.226(2) | N(2)-C(36) | 1.347(2) |
| C(11)-O(13) | 1.287(2) | N(2)-H(2) | 0.86(2) |
| C(2A)-C(3A) | 1.396(3) | C(36)-C(37) | 1.375(2) |
| C(2A)-C(21) | 1.526(2) | C(36)-H(36) | 0.96(2) |
| C(21)-O(23) | 1.231(2) | C(37)-H(37) | 0.94(2) |
| C(21)-O(24) | 1.295(2) | C(38)-C(39) | 1.376(2) |
| O(24)-H(24) | 0.89(3) | C(38)-H(38) | 0.94(2) |
| C(3A)-C(4A) | 1.396(3) | C(39)-H(39) | 0.98(2) |

Table 3.3.X.angle. Bond angles (°)

| | | | |
|---|---|---|---|
| C(6)-C(1)-C(2) | 118.89(15) | C(5A)-C(4A)-C(41) | 120.17(15) |
| C(6)-C(1)-C(10) | 113.03(15) | O(43)-C(41)-O(44) | 125.07(16) |
| C(2)-C(1)-C(10) | 128.05(15) | O(43)-C(41)-C(4A) | 121.21(16) |
| O(12)-C(10)-O(11) | 123.47(16) | O(44)-C(41)-C(4A) | 113.69(15) |
| O(12)-C(10)-C(1) | 117.53(15) | C(41)-O(44)-H(44) | 109.0(15) |
| O(11)-C(10)-C(1) | 118.99(15) | C(6A)-C(5A)-C(4A) | 118.78(16) |
| C(10)-O(11)-H(22) | 112.9(8) | C(6A)-C(5A)-C(51) | 116.24(15) |
| C(3)-C(2)-C(1) | 117.95(15) | C(4A)-C(5A)-C(51) | 124.89(16) |
| C(3)-C(2)-C(20) | 113.02(15) | O(53)-C(51)-O(54) | 124.81(16) |
| C(1)-C(2)-C(20) | 129.03(15) | O(53)-C(51)-C(5A) | 122.79(17) |
| O(21)-C(20)-O(22) | 120.32(15) | O(54)-C(51)-C(5A) | 112.19(15) |
| O(21)-C(20)-C(2) | 119.58(15) | C(51)-O(54)-H(54) | 107.5(14) |
| O(22)-C(20)-C(2) | 120.07(15) | C(5A)-C(6A)-C(1A) | 122.67(16) |
| C(20)-O(22)-H(22) | 111.6(12) | C(5A)-C(6A)-H(6A) | 120.4(12) |
| C(4)-C(3)-C(2) | 122.27(16) | C(1A)-C(6A)-H(6A) | 116.9(12) |

| | | | |
|---|---|---|---|
| C(4)-C(3)-H(3) | 116.2(11) | C(39)-N(1)-C(30) | 122.06(17) |
| C(2)-C(3)-H(3) | 121.4(11) | C(39)-N(1)-H(1) | 120.4(13) |
| C(3)-C(4)-C(5) | 119.42(16) | C(30)-N(1)-H(1) | 117.5(13) |
| C(3)-C(4)-C(40) | 119.50(15) | N(1)-C(30)-C(31) | 119.89(17) |
| C(5)-C(4)-C(40) | 120.94(15) | N(1)-C(30)-H(30) | 114.6(12) |
| O(41)-C(40)-O(42) | 125.05(17) | C(31)-C(30)-H(30) | 125.3(12) |
| O(41)-C(40)-C(4) | 122.21(17) | C(30)-C(31)-C(32) | 119.56(17) |
| O(42)-C(40)-C(4) | 112.74(16) | C(30)-C(31)-H(31) | 121.3(13) |
| C(40)-O(42)-H(42) | 104.3(18) | C(32)-C(31)-H(31) | 118.8(13) |
| C(6)-C(5)-C(4) | 118.94(16) | C(38)-C(32)-C(31) | 118.74(16) |
| C(6)-C(5)-C(50) | 119.24(15) | C(38)-C(32)-C(33) | 121.40(16) |
| C(4)-C(5)-C(50) | 121.63(16) | C(31)-C(32)-C(33) | 119.85(16) |
| O(51)-C(50)-O(52) | 125.28(16) | C(34)-C(33)-C(37) | 118.19(16) |
| O(51)-C(50)-C(5) | 122.89(18) | C(34)-C(33)-C(32) | 120.26(16) |
| O(52)-C(50)-C(5) | 111.82(16) | C(37)-C(33)-C(32) | 121.53(16) |
| C(50)-O(52)-H(52) | 108.0(16) | C(35)-C(34)-C(33) | 119.69(16) |
| C(5)-C(6)-C(1) | 122.36(16) | C(35)-C(34)-H(34) | 120.7(12) |
| C(5)-C(6)-H(6) | 116.0(12) | C(33)-C(34)-H(34) | 119.6(12) |
| C(1)-C(6)-H(6) | 121.7(12) | N(2)-C(35)-C(34) | 120.53(17) |
| C(6A)-C(1A)-C(2A) | 118.56(16) | N(2)-C(35)-H(35) | 115.9(14) |
| C(6A)-C(1A)-C(11) | 112.54(15) | C(34)-C(35)-H(35) | 123.5(14) |
| C(2A)-C(1A)-C(11) | 128.87(16) | C(35)-N(2)-C(36) | 121.98(16) |
| O(14)-C(11)-O(13) | 124.26(16) | C(35)-N(2)-H(2) | 121.5(14) |
| O(14)-C(11)-C(1A) | 117.12(15) | C(36)-N(2)-H(2) | 116.4(14) |
| O(13)-C(11)-C(1A) | 118.59(15) | N(2)-C(36)-C(37) | 119.89(16) |
| C(3A)-C(2A)-C(1A) | 118.12(16) | N(2)-C(36)-H(36) | 115.7(12) |
| C(3A)-C(2A)-C(21) | 113.45(15) | C(37)-C(36)-H(36) | 124.4(12) |
| C(1A)-C(2A)-C(21) | 128.41(16) | C(36)-C(37)-C(33) | 119.70(16) |
| O(23)-C(21)-O(24) | 120.67(16) | C(36)-C(37)-H(37) | 118.4(13) |
| O(23)-C(21)-C(2A) | 119.46(16) | C(33)-C(37)-H(37) | 121.9(13) |
| O(24)-C(21)-C(2A) | 119.87(16) | C(39)-C(38)-C(32) | 119.27(16) |
| C(21)-O(24)-H(24) | 111.9(14) | C(39)-C(38)-H(38) | 117.0(13) |
| C(4A)-C(3A)-C(2A) | 122.57(16) | C(32)-C(38)-H(38) | 123.7(13) |
| C(4A)-C(3A)-H(3A) | 121.4(13) | N(1)-C(39)-C(38) | 120.45(17) |
| C(2A)-C(3A)-H(3A) | 116.0(13) | N(1)-C(39)-H(39) | 115.8(13) |
| C(3A)-C(4A)-C(5A) | 119.25(16) | C(38)-C(39)-H(39) | 123.7(13) |
| C(3A)-C(4A)-C(41) | 120.48(16) | | |

Table 3.3.X.anis. Anisotropic displacement parameters ($Å^2 x\ 10^3$). The anisotropic displacement factor exponent takes the form: $-2p^2[\ h^2\ a^{*2}U^{11} + ... + 2\ h\ k\ a^*\ b^*\ U^{12}\ ]$

| | U11 | U22 | U33 | U23 | U13 | U12 |
|---|---|---|---|---|---|---|
| C(1) | 11(1) | 10(1) | 8(1) | 0(1) | 2(1) | -1(1) |
| C(10) | 9(1) | 16(1) | 8(1) | 2(1) | 2(1) | -1(1) |
| O(11) | 14(1) | 9(1) | 24(1) | 0(1) | 11(1) | -1(1) |
| O(12) | 13(1) | 13(1) | 14(1) | 1(1) | 7(1) | 0(1) |
| C(2) | 11(1) | 11(1) | 7(1) | 0(1) | 1(1) | 1(1) |
| C(20) | 10(1) | 11(1) | 9(1) | 2(1) | 2(1) | 1(1) |
| O(21) | 11(1) | 11(1) | 17(1) | -1(1) | 7(1) | 0(1) |
| O(22) | 12(1) | 10(1) | 19(1) | -2(1) | 9(1) | 0(1) |
| C(3) | 10(1) | 14(1) | 9(1) | 1(1) | 4(1) | 0(1) |
| C(4) | 11(1) | 10(1) | 9(1) | 1(1) | 3(1) | 1(1) |
| C(40) | 15(1) | 11(1) | 12(1) | -2(1) | 7(1) | 1(1) |
| O(41) | 16(1) | 12(1) | 18(1) | 3(1) | 6(1) | 1(1) |
| O(42) | 11(1) | 11(1) | 28(1) | 4(1) | 8(1) | -2(1) |
| C(5) | 10(1) | 12(1) | 8(1) | 0(1) | 1(1) | 0(1) |
| C(50) | 10(1) | 11(1) | 16(1) | 2(1) | 9(1) | 1(1) |
| O(51) | 14(1) | 12(1) | 18(1) | -4(1) | 4(1) | -2(1) |
| O(52) | 12(1) | 12(1) | 16(1) | 1(1) | 4(1) | 2(1) |
| C(6) | 10(1) | 12(1) | 10(1) | -1(1) | 3(1) | -1(1) |
| C(1A) | 12(1) | 11(1) | 9(1) | 1(1) | 3(1) | 1(1) |
| C(11) | 10(1) | 12(1) | 10(1) | 0(1) | 3(1) | 0(1) |
| O(13) | 16(1) | 11(1) | 20(1) | 2(1) | 10(1) | 3(1) |
| O(14) | 14(1) | 14(1) | 16(1) | 0(1) | 8(1) | 1(1) |
| C(2A) | 11(1) | 11(1) | 8(1) | 0(1) | 2(1) | -2(1) |
| C(21) | 11(1) | 12(1) | 10(1) | 0(1) | 3(1) | -2(1) |
| O(23) | 10(1) | 14(1) | 17(1) | 1(1) | 6(1) | 0(1) |
| O(24) | 11(1) | 10(1) | 21(1) | 0(1) | 8(1) | 1(1) |
| C(3A) | 11(1) | 13(1) | 9(1) | 1(1) | 4(1) | -1(1) |
| C(4A) | 12(1) | 11(1) | 9(1) | 0(1) | 4(1) | -1(1) |
| C(41) | 10(1) | 12(1) | 9(1) | 0(1) | 3(1) | 0(1) |
| O(43) | 15(1) | 10(1) | 16(1) | 2(1) | 7(1) | 0(1) |
| O(44) | 13(1) | 10(1) | 22(1) | 0(1) | 9(1) | 3(1) |
| C(5A) | 11(1) | 11(1) | 8(1) | 1(1) | 1(1) | 1(1) |
| C(51) | 9(1) | 12(1) | 16(1) | -1(1) | 6(1) | 1(1) |
| O(53) | 15(1) | 17(1) | 16(1) | 2(1) | 7(1) | 0(1) |
| O(54) | 15(1) | 14(1) | 16(1) | 1(1) | 4(1) | -2(1) |

| | | | | | | |
|---|---|---|---|---|---|---|
| C(6A) | 10(1) | 15(1) | 9(1) | 0(1) | 3(1) | -2(1) |
| N(1) | 11(1) | 21(1) | 13(1) | -2(1) | 6(1) | -3(1) |
| C(30) | 12(1) | 16(1) | 12(1) | 4(1) | 3(1) | -3(1) |
| C(31) | 11(1) | 11(1) | 15(1) | -1(1) | 2(1) | 0(1) |
| C(32) | 6(1) | 14(1) | 12(1) | -1(1) | 2(1) | -2(1) |
| C(33) | 8(1) | 13(1) | 10(1) | 1(1) | 2(1) | 2(1) |
| C(34) | 10(1) | 13(1) | 13(1) | 1(1) | 4(1) | -1(1) |
| C(35) | 11(1) | 13(1) | 13(1) | -2(1) | 2(1) | 2(1) |
| N(2) | 11(1) | 14(1) | 12(1) | 0(1) | 5(1) | 1(1) |
| C(36) | 9(1) | 12(1) | 14(1) | 2(1) | 3(1) | 1(1) |
| C(37) | 10(1) | 11(1) | 14(1) | -1(1) | 3(1) | 0(1) |
| C(38) | 12(1) | 12(1) | 12(1) | 1(1) | 3(1) | -1(1) |
| C(39) | 11(1) | 16(1) | 17(1) | -3(1) | 5(1) | 0(1) |

Table 3.3.X.H. Hydrogen coordinates ( x $10^4$) and isotropic displacement parameters ($Å^2$x $10^3$).

| | x | y | z | U(eq) |
|---|---|---|---|---|
| H(22) | 130(20) | -1398(13) | 2940(17) | 15 |
| H(3) | 2210(20) | 826(13) | 2904(16) | 13 |
| H(42) | 3140(20) | 2825(15) | 3271(19) | 20 |
| H(52) | -1940(20) | 3268(15) | 2796(16) | 16 |
| H(6) | -1420(20) | 1131(13) | 3428(16) | 13 |
| H(24) | 2120(20) | -1603(13) | 788(17) | 16 |
| H(3A) | 270(20) | 629(13) | 765(16) | 13 |
| H(44) | -690(20) | 2639(15) | 639(17) | 17 |
| H(54) | 4250(20) | 3216(14) | 945(17) | 19 |
| H(6A) | 3780(20) | 811(13) | 221(16) | 13 |
| H(1) | 2910(20) | 5357(14) | -207(17) | 17 |
| H(30) | 2360(20) | 6662(15) | 27(16) | 16 |
| H(31) | 1300(20) | 6835(15) | 1095(17) | 16 |
| H(34) | 1300(20) | 7002(15) | 2474(16) | 15 |
| H(35) | 490(20) | 7111(14) | 3663(17) | 16 |
| H(2) | -260(20) | 5978(13) | 4087(18) | 15 |
| H(36) | -410(20) | 4702(13) | 3498(16) | 14 |
| H(37) | 360(20) | 4458(14) | 2303(17) | 14 |
| H(38) | 1710(20) | 4267(14) | 1627(16) | 15 |
| H(39) | 2570(20) | 4152(14) | 486(17) | 17 |

**Supplement 3.3.N. Tables of Refinement Results for the Neutron Structure of 4,4'-Bipyridinium bis-Trihydrogen Pyromellitate at 20K**

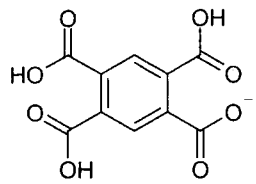

PMA-

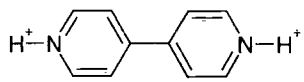

BPY2+

Table 3.3.N.xyz. Atomic coordinates ( x $10^4$) and equivalent isotropic displacement parameters ($Å^2$x $10^3$). U(eq) is defined as one third of the trace of the orthogonalized $U^{ij}$ tensor.

| | x | y | z | U(eq) |
|---|---|---|---|---|
| C(1) | -258(2) | 198(1) | 3256(1) | 4(1) |
| C(10) | -1038(2) | -510(1) | 3429(1) | 4(1) |
| O(11) | -897(2) | -1292(1) | 3216(2) | 9(1) |
| O(12) | -1785(2) | -295(1) | 3761(1) | 7(1) |
| C(2) | 819(2) | 106(1) | 3086(1) | 4(1) |
| C(20) | 1430(2) | -718(1) | 2953(1) | 5(1) |
| O(21) | 2412(2) | -671(1) | 2884(2) | 6(1) |
| O(22) | 894(2) | -1454(1) | 2882(1) | 7(1) |
| C(3) | 1442(2) | 857(1) | 3036(1) | 4(1) |
| C(4) | 1013(2) | 1683(1) | 3096(1) | 4(1) |
| C(40) | 1689(2) | 2457(1) | 2976(1) | 5(1) |
| O(41) | 1182(2) | 3086(1) | 2521(1) | 9(1) |
| O(42) | 2867(2) | 2379(1) | 3398(2) | 11(1) |
| C(5) | -80(2) | 1773(1) | 3212(1) | 4(1) |
| C(50) | -583(2) | 2645(1) | 3307(1) | 5(1) |
| O(51) | -12(2) | 3169(1) | 3901(1) | 9(1) |
| O(52) | -1694(2) | 2760(1) | 2690(1) | 7(1) |
| C(6) | -687(2) | 1036(1) | 3310(1) | 5(1) |
| C(1A) | 2619(2) | -29(1) | 447(1) | 4(1) |
| C(11) | 3382(2) | -762(1) | 306(1) | 5(1) |
| O(13) | 3294(2) | -1519(1) | 613(2) | 8(1) |
| O(14) | 4085(2) | -574(1) | -84(1) | 8(1) |
| C(2A) | 1548(2) | -84(1) | 626(1) | 5(1) |
| C(21) | 897(2) | -888(1) | 749(1) | 4(1) |
| O(23) | -104(2) | -816(1) | 797(2) | 7(1) |
| O(24) | 1397(2) | -1642(1) | 816(1) | 8(1) |

| | | | | |
|---|---|---|---|---|
| C(3A) | 959(2) | 690(1) | 672(1) | 5(1) |
| C(4A) | 1408(2) | 1499(1) | 568(1) | 5(1) |
| C(41) | 706(2) | 2295(1) | 557(1) | 5(1) |
| O(43) | 1063(2) | 3007(1) | 443(1) | 7(1) |
| O(44) | -327(2) | 2151(1) | 652(1) | 8(1) |
| C(5A) | 2494(2) | 1552(1) | 428(1) | 4(1) |
| C(51) | 3068(2) | 2383(1) | 292(1) | 5(1) |
| O(53) | 2867(2) | 2700(1) | -483(1) | 9(1) |
| O(54) | 3879(2) | 2686(1) | 1098(1) | 9(1) |
| C(6A) | 3066(2) | 791(1) | 354(1) | 5(1) |
| N(1) | 2503(1) | 5408(1) | 222(1) | 8(1) |
| C(30) | 2153(2) | 6198(1) | 375(1) | 8(1) |
| C(31) | 1617(2) | 6309(1) | 1027(1) | 7(1) |
| C(32) | 1455(2) | 5596(1) | 1530(1) | 5(1) |
| C(33) | 911(2) | 5712(1) | 2251(1) | 4(1) |
| C(34) | 940(2) | 6522(1) | 2660(1) | 6(1) |
| C(35) | 465(2) | 6620(1) | 3351(1) | 6(1) |
| N(2) | -12(1) | 5941(1) | 3627(1) | 6(1) |
| C(36) | -67(2) | 5149(1) | 3245(1) | 6(1) |
| C(37) | 385(2) | 5014(1) | 2546(1) | 5(1) |
| C(38) | 1816(2) | 4779(1) | 1343(1) | 6(1) |
| C(39) | 2344(2) | 4703(1) | 680(1) | 8(1) |

Table 3.3.N.bond. Bond lengths (Å).

| | | | |
|---|---|---|---|
| C(1)-C(6) | 1.410(2) | C(3A)-H(3A) | 1.079(4) |
| C(1)-C(2) | 1.418(3) | C(4A)-C(5A) | 1.401(3) |
| C(1)-C(10) | 1.528(2) | C(4A)-C(41) | 1.491(2) |
| C(10)-O(12) | 1.232(3) | C(41)-O(43) | 1.220(3) |
| C(10)-O(11) | 1.280(3) | C(41)-O(44) | 1.321(3) |
| O(11)-H(22) | 1.331(5) | O(44)-H(44) | 1.009(4) |
| C(2)-C(3) | 1.401(2) | C(5A)-C(6A) | 1.390(2) |
| C(2)-C(20) | 1.523(2) | C(5A)-C(51) | 1.510(2) |
| C(20)-O(21) | 1.225(3) | C(51)-O(53) | 1.214(3) |
| C(20)-O(22) | 1.293(3) | C(51)-O(54) | 1.329(3) |
| O(22)-H(22) | 1.077(5) | O(54)-H(54) | 1.002(5) |
| C(3)-C(4) | 1.395(2) | C(6A)-H(6A) | 1.090(4) |
| C(3)-H(3) | 1.094(4) | N(1)-C(30) | 1.343(2) |
| C(4)-C(5) | 1.396(2) | N(1)-C(39) | 1.347(2) |

| | | | |
|---|---|---|---|
| C(4)-C(40) | 1.498(2) | N(1)-H(1) | 1.048(4) |
| C(40)-O(41) | 1.216(3) | C(30)-C(31) | 1.383(3) |
| C(40)-O(42) | 1.319(3) | C(30)-H(30) | 1.079(4) |
| O(42)-H(42) | 1.011(5) | C(31)-C(32) | 1.399(2) |
| C(5)-C(6) | 1.392(2) | C(31)-H(31) | 1.085(4) |
| C(5)-C(50) | 1.508(2) | C(32)-C(38) | 1.401(2) |
| C(50)-O(51) | 1.215(3) | C(32)-C(33) | 1.484(2) |
| C(50)-O(52) | 1.320(3) | C(33)-C(34) | 1.396(2) |
| O(52)-H(52) | 1.002(4) | C(33)-C(37) | 1.409(2) |
| C(6)-H(6) | 1.084(4) | C(34)-C(35) | 1.381(2) |
| C(1A)-C(6A) | 1.406(2) | C(34)-H(34) | 1.080(4) |
| C(1A)-C(2A) | 1.416(3) | C(35)-N(2) | 1.338(2) |
| C(1A)-C(11) | 1.523(2) | C(35)-H(35) | 1.071(4) |
| C(11)-O(14) | 1.237(3) | N(2)-C(36) | 1.348(2) |
| C(11)-O(13) | 1.281(3) | N(2)-H(2) | 1.050(4) |
| O(13)-H(24) | 1.347(5) | C(36)-C(37) | 1.381(2) |
| C(2A)-C(3A) | 1.406(2) | C(36)-H(36) | 1.081(4) |
| C(2A)-C(21) | 1.519(2) | C(37)-H(37) | 1.083(4) |
| C(21)-O(23) | 1.236(3) | C(38)-C(39) | 1.385(2) |
| C(21)-O(24) | 1.300(3) | C(38)-H(38) | 1.082(4) |
| O(24)-H(24) | 1.076(5) | C(39)-H(39) | 1.080(4) |
| C(3A)-C(4A) | 1.396(2) | | |

Table 3.3.N.angle. Bond angles (°)

| | | | |
|---|---|---|---|
| C(6)-C(1)-C(2) | 118.74(15) | C(3A)-C(4A)-C(41) | 120.15(15) |
| C(6)-C(1)-C(10) | 112.90(15) | C(5A)-C(4A)-C(41) | 120.29(16) |
| C(2)-C(1)-C(10) | 128.33(15) | O(43)-C(41)-O(44) | 124.36(19) |
| O(12)-C(10)-O(11) | 123.10(19) | O(43)-C(41)-C(4A) | 121.43(18) |
| O(12)-C(10)-C(1) | 117.80(16) | O(44)-C(41)-C(4A) | 114.18(16) |
| O(11)-C(10)-C(1) | 119.09(17) | C(41)-O(44)-H(44) | 110.4(3) |
| C(10)-O(11)-H(22) | 113.1(2) | C(6A)-C(5A)-C(4A) | 118.59(16) |
| C(3)-C(2)-C(1) | 118.02(15) | C(6A)-C(5A)-C(51) | 116.52(15) |
| C(3)-C(2)-C(20) | 113.16(15) | C(4A)-C(5A)-C(51) | 124.80(16) |
| C(1)-C(2)-C(20) | 128.81(15) | O(53)-C(51)-O(54) | 124.04(19) |
| O(21)-C(20)-O(22) | 120.60(19) | O(53)-C(51)-C(5A) | 122.93(17) |
| O(21)-C(20)-C(2) | 119.36(17) | O(54)-C(51)-C(5A) | 112.82(15) |
| O(22)-C(20)-C(2) | 119.99(17) | C(51)-O(54)-H(54) | 110.0(3) |
| C(20)-O(22)-H(22) | 112.2(3) | C(5A)-C(6A)-C(1A) | 122.63(16) |

| | | | |
|---|---|---|---|
| C(4)-C(3)-C(2) | 122.60(16) | C(5A)-C(6A)-H(6A) | 119.6(3) |
| C(4)-C(3)-H(3) | 119.4(3) | C(1A)-C(6A)-H(6A) | 117.8(3) |
| C(2)-C(3)-H(3) | 118.0(3) | C(30)-N(1)-C(39) | 122.28(15) |
| C(3)-C(4)-C(5) | 119.27(16) | C(30)-N(1)-H(1) | 118.1(3) |
| C(3)-C(4)-C(40) | 119.66(15) | C(39)-N(1)-H(1) | 119.5(3) |
| C(5)-C(4)-C(40) | 120.96(15) | N(1)-C(30)-C(31) | 119.92(16) |
| O(41)-C(40)-O(42) | 124.28(19) | N(1)-C(30)-H(30) | 117.0(3) |
| O(41)-C(40)-C(4) | 122.21(18) | C(31)-C(30)-H(30) | 123.1(3) |
| O(42)-C(40)-C(4) | 113.50(16) | C(30)-C(31)-C(32) | 119.62(16) |
| C(40)-O(42)-H(42) | 108.9(3) | C(30)-C(31)-H(31) | 117.5(3) |
| C(6)-C(5)-C(4) | 119.11(15) | C(32)-C(31)-H(31) | 122.9(3) |
| C(6)-C(5)-C(50) | 118.64(15) | C(31)-C(32)-C(38) | 118.91(15) |
| C(4)-C(5)-C(50) | 122.09(15) | C(31)-C(32)-C(33) | 120.00(15) |
| O(51)-C(50)-O(52) | 124.95(19) | C(38)-C(32)-C(33) | 121.09(14) |
| O(51)-C(50)-C(5) | 122.38(18) | C(34)-C(33)-C(37) | 118.97(16) |
| O(52)-C(50)-C(5) | 112.67(16) | C(34)-C(33)-C(32) | 119.72(15) |
| C(50)-O(52)-H(52) | 110.0(3) | C(37)-C(33)-C(32) | 121.30(15) |
| C(5)-C(6)-C(1) | 122.09(16) | C(35)-C(34)-C(33) | 119.42(16) |
| C(5)-C(6)-H(6) | 119.7(2) | C(35)-C(34)-H(34) | 117.7(3) |
| C(1)-C(6)-H(6) | 118.2(2) | C(33)-C(34)-H(34) | 122.9(3) |
| C(6A)-C(1A)-C(2A) | 118.85(16) | N(2)-C(35)-C(34) | 120.18(15) |
| C(6A)-C(1A)-C(11) | 112.73(15) | N(2)-C(35)-H(35) | 116.9(3) |
| C(2A)-C(1A)-C(11) | 128.40(16) | C(34)-C(35)-H(35) | 122.9(3) |
| O(14)-C(11)-O(13) | 123.78(19) | C(35)-N(2)-C(36) | 122.35(14) |
| O(14)-C(11)-C(1A) | 116.66(16) | C(35)-N(2)-H(2) | 121.3(2) |
| O(13)-C(11)-C(1A) | 119.53(17) | C(36)-N(2)-H(2) | 116.3(2) |
| C(11)-O(13)-H(24) | 111.2(2) | N(2)-C(36)-C(37) | 120.06(16) |
| C(3A)-C(2A)-C(1A) | 117.98(16) | N(2)-C(36)-H(36) | 116.9(3) |
| C(3A)-C(2A)-C(21) | 113.58(15) | C(37)-C(36)-H(36) | 123.1(3) |
| C(1A)-C(2A)-C(21) | 128.41(16) | C(36)-C(37)-C(33) | 119.01(16) |
| O(23)-C(21)-O(24) | 120.47(18) | C(36)-C(37)-H(37) | 118.5(3) |
| O(23)-C(21)-C(2A) | 119.43(17) | C(33)-C(37)-H(37) | 122.4(3) |
| O(24)-C(21)-C(2A) | 120.10(17) | C(39)-C(38)-C(32) | 119.16(16) |
| C(21)-O(24)-H(24) | 112.2(3) | C(39)-C(38)-H(38) | 118.5(3) |
| C(4A)-C(3A)-C(2A) | 122.40(16) | C(32)-C(38)-H(38) | 122.4(3) |
| C(4A)-C(3A)-H(3A) | 119.5(3) | N(1)-C(39)-C(38) | 120.08(16) |
| C(2A)-C(3A)-H(3A) | 118.1(3) | N(1)-C(39)-H(39) | 117.3(3) |
| C(3A)-C(4A)-C(5A) | 119.48(16) | C(38)-C(39)-H(39) | 122.6(3) |

Table 3.3.N.anis. Anisotropic displacement parameters ($Å^2 x\ 10^3$). The anisotropic displacement factor exponent takes the form: $-2p^2[\ h^2\ a^{*2}U^{11} + ... + 2\ h\ k\ a^*\ b^*\ U^{12}\ ]$

| | U11 | U22 | U33 | U23 | U13 | U12 |
|---|---|---|---|---|---|---|
| C(1) | 2(1) | 2(1) | 6(1) | 0(1) | 1(1) | 1(1) |
| C(10) | 4(1) | 2(1) | 7(1) | 0(1) | 3(1) | 0(1) |
| O(11) | 9(1) | 3(1) | 18(1) | 0(1) | 7(1) | -1(1) |
| O(12) | 9(1) | 5(1) | 9(1) | 1(1) | 5(1) | -2(1) |
| C(2) | 3(1) | 2(1) | 6(1) | 0(1) | 2(1) | -1(1) |
| C(20) | 5(1) | 4(1) | 6(1) | 1(1) | 2(1) | 0(1) |
| O(21) | 4(1) | 4(1) | 12(1) | 0(1) | 4(1) | 0(1) |
| O(22) | 7(1) | 2(1) | 12(1) | 1(1) | 4(1) | -2(1) |
| H(22) | 19(2) | 14(2) | 26(2) | -3(1) | 10(2) | -4(2) |
| C(3) | 5(1) | 1(1) | 6(1) | 0(1) | 1(1) | 0(1) |
| H(3) | 14(2) | 15(2) | 29(2) | 1(1) | 11(2) | 0(1) |
| C(4) | 5(1) | 2(1) | 6(1) | 1(1) | 2(1) | 0(1) |
| C(40) | 5(1) | 4(1) | 7(1) | -1(1) | 2(1) | 0(1) |
| O(41) | 9(1) | 5(1) | 12(1) | 4(1) | 4(1) | 2(1) |
| O(42) | 9(1) | 5(1) | 18(1) | 4(1) | 4(1) | 2(1) |
| H(42) | 16(2) | 16(2) | 33(2) | 2(2) | 10(2) | -2(2) |
| C(5) | 3(1) | 2(1) | 6(1) | 0(1) | 1(1) | 0(1) |
| C(50) | 5(1) | 3(1) | 7(1) | -1(1) | 1(1) | 0(1) |
| O(51) | 9(1) | 4(1) | 12(1) | -3(1) | 1(1) | -1(1) |
| O(52) | 6(1) | 5(1) | 8(1) | -1(1) | 0(1) | 1(1) |
| H(52) | 16(2) | 16(2) | 20(2) | -2(1) | 5(2) | 5(2) |
| C(6) | 6(1) | 2(1) | 8(1) | 0(1) | 4(1) | 0(1) |
| H(6) | 19(2) | 14(2) | 28(2) | 0(1) | 13(2) | -1(2) |
| C(1A) | 5(1) | 3(1) | 5(1) | 0(1) | 2(1) | 1(1) |
| C(11) | 6(1) | 3(1) | 6(1) | 0(1) | 2(1) | -1(1) |
| O(13) | 10(1) | 3(1) | 14(1) | 2(1) | 7(1) | 2(1) |
| O(14) | 10(1) | 6(1) | 11(1) | 1(1) | 7(1) | 0(1) |
| C(2A) | 4(1) | 3(1) | 6(1) | 0(1) | 2(1) | 1(1) |
| C(21) | 6(1) | 1(1) | 5(1) | 1(1) | 1(1) | 0(1) |
| O(23) | 4(1) | 5(1) | 12(1) | 2(1) | 3(1) | 1(1) |
| O(24) | 10(1) | 2(1) | 12(1) | 1(1) | 5(1) | 1(1) |
| H(24) | 22(2) | 12(2) | 26(2) | 2(1) | 10(2) | 0(1) |
| C(3A) | 7(1) | 1(1) | 6(1) | 1(1) | 2(1) | 1(1) |
| H(3A) | 18(2) | 15(2) | 27(2) | 0(1) | 14(2) | 1(1) |
| C(4A) | 5(1) | 3(1) | 6(1) | 0(1) | 3(1) | 1(1) |

| | | | | | | |
|---|---|---|---|---|---|---|
| C(41) | 7(1) | 2(1) | 7(1) | 0(1) | 2(1) | 1(1) |
| O(43) | 9(1) | 2(1) | 13(1) | 1(1) | 6(1) | 0(1) |
| O(44) | 7(1) | 6(1) | 13(1) | 1(1) | 6(1) | 1(1) |
| H(44) | 20(2) | 11(2) | 29(2) | 0(1) | 15(2) | 3(2) |
| C(5A) | 5(1) | 2(1) | 7(1) | 0(1) | 3(1) | 1(1) |
| C(51) | 7(1) | 3(1) | 7(1) | 0(1) | 3(1) | 0(1) |
| O(53) | 11(1) | 9(1) | 6(1) | 3(1) | 3(1) | 0(1) |
| O(54) | 8(1) | 8(1) | 9(1) | 1(1) | 1(1) | -2(1) |
| H(54) | 21(2) | 16(2) | 24(2) | 3(2) | 6(2) | -2(2) |
| C(6A) | 7(1) | 1(1) | 7(1) | 1(1) | 2(1) | 1(1) |
| H(6A) | 22(2) | 18(2) | 29(2) | 1(2) | 14(2) | 3(2) |
| N(1) | 8(1) | 10(1) | 7(1) | -2(1) | 4(1) | -1(1) |
| H(1) | 27(2) | 22(2) | 22(2) | -2(2) | 19(2) | -2(2) |
| C(30) | 9(1) | 6(1) | 8(1) | 1(1) | 4(1) | 0(1) |
| H(30) | 38(3) | 18(2) | 26(2) | 9(2) | 21(2) | 2(2) |
| C(31) | 8(1) | 5(1) | 8(1) | 2(1) | 4(1) | 0(1) |
| H(31) | 33(2) | 12(2) | 29(2) | 0(2) | 18(2) | 4(2) |
| C(32) | 5(1) | 4(1) | 5(1) | 0(1) | 2(1) | 0(1) |
| C(33) | 4(1) | 3(1) | 6(1) | 0(1) | 3(1) | 0(1) |
| C(34) | 9(1) | 4(1) | 8(1) | -2(1) | 5(1) | -2(1) |
| H(34) | 30(2) | 10(2) | 25(2) | -2(1) | 15(2) | -8(2) |
| C(35) | 7(1) | 5(1) | 7(1) | -1(1) | 4(1) | 0(1) |
| H(35) | 34(2) | 14(2) | 24(2) | -9(2) | 17(2) | -3(2) |
| N(2) | 8(1) | 5(1) | 8(1) | -1(1) | 5(1) | 0(1) |
| H(2) | 21(2) | 20(2) | 17(2) | -3(1) | 14(2) | 1(2) |
| C(36) | 8(1) | 4(1) | 8(1) | -1(1) | 5(1) | -1(1) |
| H(36) | 29(2) | 15(2) | 25(2) | 2(1) | 17(2) | -7(2) |
| C(37) | 7(1) | 2(1) | 8(1) | 0(1) | 4(1) | -1(1) |
| H(37) | 29(2) | 11(2) | 25(2) | -6(1) | 17(2) | -3(2) |
| C(38) | 8(1) | 4(1) | 7(1) | -1(1) | 4(1) | 0(1) |
| H(38) | 34(2) | 8(2) | 29(2) | 2(2) | 19(2) | 0(2) |
| C(39) | 9(1) | 5(1) | 11(1) | -2(1) | 7(1) | 0(1) |
| H(39) | 35(2) | 16(2) | 31(2) | -4(2) | 21(2) | 2(2) |

Table 3.3.N.H. Hydrogen coordinates ( x $10^4$) and isotropic displacement parameters ($Å^2$x $10^3$)

| | x | y | z | U(eq) |
|---|---|---|---|---|
| H(22) | 55(4) | -1397(2) | 2981(3) | 19(1) |
| H(3) | 2289(4) | 785(2) | 2930(3) | 18(1) |
| H(42) | 3259(4) | 2929(3) | 3298(3) | 22(1) |
| H(52) | -2007(4) | 3332(3) | 2802(3) | 18(1) |
| H(6) | -1496(4) | 1099(2) | 3459(3) | 19(1) |
| H(24) | 2269(4) | -1603(2) | 772(3) | 20(1) |
| H(3A) | 127(4) | 648(2) | 786(3) | 18(1) |
| H(44) | -765(4) | 2712(2) | 628(3) | 19(1) |
| H(54) | 4287(4) | 3207(3) | 966(3) | 21(1) |
| H(6A) | 3881(4) | 820(3) | 202(3) | 21(1) |
| H(1) | 2872(4) | 5341(2) | -297(3) | 21(1) |
| H(30) | 2287(4) | 6721(3) | -43(3) | 25(1) |
| H(31) | 1328(4) | 6955(3) | 1116(3) | 23(1) |
| H(34) | 1350(4) | 7080(2) | 2481(3) | 21(1) |
| H(35) | 480(4) | 7221(3) | 3704(3) | 22(1) |
| H(2) | -330(4) | 5995(2) | 4180(3) | 17(1) |
| H(36) | -459(4) | 4640(3) | 3521(3) | 21(1) |
| H(37) | 345(4) | 4369(2) | 2261(3) | 20(1) |
| H(38) | 1707(4) | 4202(2) | 1704(3) | 22(1) |
| H(39) | 2623(4) | 4089(3) | 494(3) | 25(1) |

**Supplement 3.4.100X. Tables of Refinement Results for the X-ray Structure of the 2:1 Co-crystal of 4,4-bipyridine and benzene-1,2,4,5-tetracarboxylic acid at 100K**

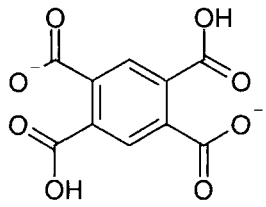

**PMA2-**

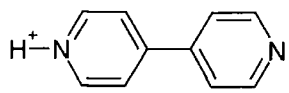

**BPY+**

Table 3.4.100X.xyz. Atomic coordinates ( x $10^4$) and equivalent isotropic displacement parameters (Å$^2$x $10^3$). U(eq) is defined as one third of the trace of the orthogonalized $U^{ij}$ tensor.

| | x | y | z | U(eq) |
|---|---|---|---|---|
| C(1) | 5860(2) | 5808(1) | -1491(1) | 14(1) |
| C(10) | 6735(2) | 6795(1) | -3078(1) | 15(1) |
| O(11) | 6247(1) | 8179(1) | -3570(1) | 22(1) |
| O(12) | 8028(1) | 6036(1) | -3821(1) | 17(1) |
| C(2) | 3921(2) | 5594(1) | -1083(1) | 14(1) |
| C(20) | 2755(2) | 6186(1) | -2253(1) | 14(1) |
| O(21) | 1049(1) | 6672(1) | -1951(1) | 21(1) |
| O(22) | 3714(1) | 6096(1) | -3508(1) | 19(1) |
| C(3) | 3068(2) | 4792(1) | 407(1) | 14(1) |
| N(1) | 2842(1) | 7742(1) | -5971(1) | 16(1) |
| C(11) | 3526(2) | 7168(1) | -7047(1) | 18(1) |
| C(12) | 3347(2) | 8049(1) | -8493(1) | 17(1) |
| C(13) | 2445(2) | 9569(1) | -8868(1) | 14(1) |
| C(14) | 1764(2) | 10139(1) | -7727(1) | 19(1) |
| C(15) | 2002(2) | 9195(1) | -6303(1) | 19(1) |
| C(21) | 2768(2) | 10907(1) | -12996(1) | 18(1) |
| C(22) | 3003(2) | 9984(1) | -11567(1) | 18(1) |
| C(23) | 2229(2) | 10540(1) | -10419(1) | 14(1) |
| C(24) | 1258(2) | 12035(1) | -10796(1) | 16(1) |
| C(25) | 1094(2) | 12885(1) | -12260(1) | 17(1) |
| N(2) | 1824(1) | 12335(1) | -13351(1) | 17(1) |

Table 3.4.100X.bond. Bond lengths (Å).

| | | | |
|---|---|---|---|
| C(1)-C(3)#1 | 1.3997(14) | C(12)-C(13) | 1.4028(15) |
| C(1)-C(2) | 1.4050(15) | C(12)-H(12) | 0.967(15) |
| C(1)-C(10) | 1.5120(15) | C(13)-C(14) | 1.4035(15) |
| C(10)-O(11) | 1.2178(13) | C(13)-C(23) | 1.4928(15) |
| C(10)-O(12) | 1.3171(13) | C(14)-C(15) | 1.3875(16) |
| O(12)-H(2) | 1.03(2) | C(14)-H(14) | 0.982(16) |
| C(2)-C(3) | 1.3966(15) | C(15)-H(15) | 0.980(16) |
| C(2)-C(20) | 1.5202(14) | C(21)-N(2) | 1.3431(14) |
| C(20)-O(21) | 1.2335(13) | C(21)-C(22) | 1.3884(16) |
| C(20)-O(22) | 1.2895(13) | C(21)-H(21) | 0.983(15) |
| O(22)-H(1) | 1.34(2) | C(22)-C(23) | 1.4028(15) |
| C(3)-C(1)#1 | 1.3997(14) | C(22)-H(22) | 0.990(15) |
| C(3)-H(3) | 0.963(14) | C(23)-C(24) | 1.4019(15) |
| N(1)-C(15) | 1.3380(14) | C(24)-C(25) | 1.3928(15) |
| N(1)-C(11) | 1.3464(14) | C(24)-H(24) | 0.956(14) |
| N(1)-H(1) | 1.20(2) | C(25)-N(2) | 1.3469(14) |
| C(11)-C(12) | 1.3844(16) | C(25)-H(25) | 0.977(14) |
| C(11)-H(11) | 0.995(16) | | |

Symmetry transformations used to generate equivalent atoms:

#1 -x+1,-y+1,-z

Table 3.4.100X.angle. Bond angles (°).

| | | | |
|---|---|---|---|
| C(3)#1-C(1)-C(2) | 120.01(10) | C(12)-C(13)-C(14) | 117.21(10) |
| C(3)#1-C(1)-C(10) | 120.23(10) | C(12)-C(13)-C(23) | 121.34(10) |
| C(2)-C(1)-C(10) | 119.58(9) | C(14)-C(13)-C(23) | 121.45(10) |
| O(11)-C(10)-O(12) | 125.21(10) | C(15)-C(14)-C(13) | 119.41(10) |
| O(11)-C(10)-C(1) | 120.25(10) | C(15)-C(14)-H(14) | 117.4(9) |
| O(12)-C(10)-C(1) | 114.54(9) | C(13)-C(14)-H(14) | 123.2(9) |
| C(10)-O(12)-H(2) | 109.3(12) | N(1)-C(15)-C(14) | 122.11(10) |
| C(3)-C(2)-C(1) | 119.70(9) | N(1)-C(15)-H(15) | 116.2(9) |
| C(3)-C(2)-C(20) | 119.58(10) | C(14)-C(15)-H(15) | 121.7(9) |
| C(1)-C(2)-C(20) | 120.70(9) | N(2)-C(21)-C(22) | 123.00(10) |
| O(21)-C(20)-O(22) | 126.22(10) | N(2)-C(21)-H(21) | 117.6(9) |
| O(21)-C(20)-C(2) | 120.17(9) | C(22)-C(21)-H(21) | 119.4(9) |
| O(22)-C(20)-C(2) | 113.60(9) | C(21)-C(22)-C(23) | 119.70(10) |
| C(20)-O(22)-H(1) | 118.8(9) | C(21)-C(22)-H(22) | 117.2(8) |
| C(2)-C(3)-C(1)#1 | 120.29(10) | C(23)-C(22)-H(22) | 123.0(8) |

| | | | |
|---|---|---|---|
| C(2)-C(3)-H(3) | 117.8(8) | C(24)-C(23)-C(22) | 117.16(10) |
| C(1)#1-C(3)-H(3) | 121.9(8) | C(24)-C(23)-C(13) | 121.94(9) |
| C(15)-N(1)-C(11) | 119.80(10) | C(22)-C(23)-C(13) | 120.90(10) |
| C(15)-N(1)-H(1) | 120.0(10) | C(25)-C(24)-C(23) | 119.39(10) |
| C(11)-N(1)-H(1) | 120.1(10) | C(25)-C(24)-H(24) | 118.6(8) |
| N(1)-C(11)-C(12) | 121.09(10) | C(23)-C(24)-H(24) | 122.0(8) |
| N(1)-C(11)-H(11) | 117.8(9) | N(2)-C(25)-C(24) | 123.03(10) |
| C(12)-C(11)-H(11) | 121.1(9) | N(2)-C(25)-H(25) | 116.7(8) |
| C(11)-C(12)-C(13) | 120.36(10) | C(24)-C(25)-H(25) | 120.3(8) |
| C(11)-C(12)-H(12) | 117.1(9) | C(21)-N(2)-C(25) | 117.72(9) |
| C(13)-C(12)-H(12) | 122.6(9) | | |

Symmetry transformations used to generate equivalent atoms:

#1 -x+1,-y+1,-z

Table 3.4.100X.anis. Anisotropic displacement parameters ($Å^2 x\ 10^3$). The anisotropic displacement factor exponent takes the form: $-2p^2[\ h^2\ a^{*2}U^{11} + ... + 2\ h\ k\ a^*\ b^*\ U^{12}\ ]$

| | U11 | U22 | U33 | U23 | U13 | U12 |
|---|---|---|---|---|---|---|
| C(1) | 18(1) | 13(1) | 10(1) | -4(1) | -3(1) | -1(1) |
| C(10) | 16(1) | 18(1) | 11(1) | -5(1) | -4(1) | -3(1) |
| O(11) | 33(1) | 16(1) | 13(1) | -3(1) | -2(1) | -2(1) |
| O(12) | 18(1) | 19(1) | 10(1) | -4(1) | -2(1) | 1(1) |
| C(2) | 17(1) | 13(1) | 11(1) | -5(1) | -5(1) | 1(1) |
| C(20) | 17(1) | 12(1) | 12(1) | -3(1) | -5(1) | -1(1) |
| O(21) | 17(1) | 26(1) | 18(1) | -8(1) | -6(1) | 3(1) |
| O(22) | 22(1) | 24(1) | 10(1) | -6(1) | -7(1) | 4(1) |
| C(3) | 14(1) | 15(1) | 12(1) | -5(1) | -3(1) | -1(1) |
| N(1) | 17(1) | 18(1) | 13(1) | -4(1) | -6(1) | -2(1) |
| C(11) | 22(1) | 16(1) | 16(1) | -4(1) | -8(1) | -1(1) |
| C(12) | 23(1) | 16(1) | 14(1) | -6(1) | -7(1) | 0(1) |
| C(13) | 13(1) | 16(1) | 12(1) | -4(1) | -4(1) | -2(1) |
| C(14) | 23(1) | 17(1) | 15(1) | -6(1) | -7(1) | 3(1) |
| C(15) | 23(1) | 21(1) | 14(1) | -7(1) | -6(1) | 2(1) |
| C(21) | 22(1) | 19(1) | 12(1) | -5(1) | -4(1) | -1(1) |
| C(22) | 21(1) | 16(1) | 13(1) | -4(1) | -5(1) | 1(1) |
| C(23) | 13(1) | 15(1) | 11(1) | -3(1) | -3(1) | -3(1) |
| C(24) | 18(1) | 18(1) | 12(1) | -5(1) | -4(1) | 0(1) |
| C(25) | 17(1) | 16(1) | 14(1) | -3(1) | -4(1) | 0(1) |
| N(2) | 18(1) | 18(1) | 12(1) | -3(1) | -4(1) | -2(1) |

Table 3.4.100X.H. Hydrogen coordinates ( x $10^4$) and isotropic displacement parameters ($Å^2$x $10^3$).

| | x | y | z | U(eq) |
|---|---|---|---|---|
| H(2) | 8200(30) | 6680(20) | -4940(20) | 69(6) |
| H(3) | 1740(20) | 4669(16) | 652(15) | 20(3) |
| H(1) | 3050(30) | 6980(20) | -4740(20) | 58(5) |
| H(11) | 4210(20) | 6105(18) | -6776(18) | 29(4) |
| H(12) | 3880(20) | 7575(17) | -9216(17) | 27(4) |
| H(14) | 1110(20) | 11184(19) | -7879(17) | 31(4) |
| H(15) | 1580(20) | 9564(18) | -5486(18) | 32(4) |
| H(21) | 3280(20) | 10501(17) | -13791(17) | 26(4) |
| H(22) | 3780(20) | 8968(17) | -11422(16) | 25(4) |
| H(24) | 660(20) | 12482(16) | -10069(15) | 19(3) |
| H(25) | 410(20) | 13926(16) | -12537(15) | 21(3) |

**Supplement 3.4.30X. Tables of Refinement Results for the X-ray Structure of the 2:1 Co-crystal of 4,4-bipyridine and benzene-1,2,4,5-tetracarboxylic acid at 30K**

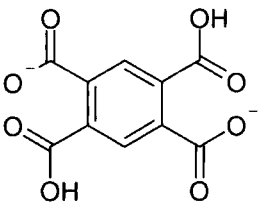

**PMA2-**

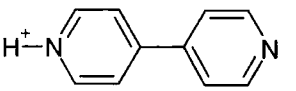

**BPY+**

Table 3.4.30X.xyz. Atomic coordinates ( x $10^4$) and equivalent isotropic displacement parameters ($Å^2$x $10^3$). U(eq) is defined as one third of the trace of the orthogonalized $U^{ij}$ tensor.

| | x | y | z | U(eq) |
|---|---|---|---|---|
| C(1) | 5863(2) | 5804(1) | -1488(1) | 11(1) |
| C(10) | 6736(2) | 6796(2) | -3073(1) | 11(1) |
| O(11) | 6254(1) | 8183(1) | -3566(1) | 14(1) |
| O(12) | 8028(1) | 6029(1) | -3818(1) | 13(1) |
| C(2) | 3916(2) | 5595(1) | -1083(1) | 12(1) |
| C(20) | 2749(2) | 6185(1) | -2259(1) | 11(1) |
| O(21) | 1039(1) | 6676(1) | -1956(1) | 15(1) |
| O(22) | 3707(1) | 6089(1) | -3507(1) | 14(1) |
| C(3) | 3066(2) | 4794(1) | 405(1) | 11(1) |
| N(1) | 2852(2) | 7740(1) | -5982(1) | 12(1) |
| C(11) | 3550(2) | 7165(2) | -7059(1) | 13(1) |
| C(12) | 3364(2) | 8049(2) | -8504(2) | 13(1) |
| C(13) | 2450(2) | 9565(2) | -8870(1) | 12(1) |
| C(14) | 1758(2) | 10133(2) | -7726(1) | 13(1) |
| C(15) | 1996(2) | 9191(2) | -6303(1) | 13(1) |
| C(21) | 2774(2) | 10909(2) | -13002(1) | 13(1) |
| C(22) | 3011(2) | 9987(2) | -11575(1) | 13(1) |
| C(23) | 2233(2) | 10540(2) | -10426(1) | 11(1) |
| C(24) | 1251(2) | 12031(2) | -10794(1) | 13(1) |
| C(25) | 1088(2) | 12884(2) | -12258(1) | 13(1) |
| N(2) | 1822(2) | 12336(1) | -13352(1) | 13(1) |

Table 3.4.30X.bond. Bond lengths (Å).

| | | | |
|---|---|---|---|
| C(1)-C(3)#1 | 1.4031(19) | C(12)-C(13) | 1.409(2) |
| C(1)-C(2) | 1.412(2) | C(12)-H(12) | 0.990(15) |
| C(1)-C(10) | 1.5205(19) | C(13)-C(14) | 1.4073(19) |
| C(10)-O(11) | 1.2244(18) | C(13)-C(23) | 1.506(2) |
| C(10)-O(12) | 1.3275(16) | C(14)-C(15) | 1.395(2) |
| O(12)-H(2) | 1.00(2) | C(14)-H(14) | 0.938(15) |
| C(2)-C(3) | 1.402(2) | C(15)-H(15) | 0.984(14) |
| C(2)-C(20) | 1.5288(19) | C(21)-N(2) | 1.3507(18) |
| C(20)-O(21) | 1.2425(17) | C(21)-C(22) | 1.394(2) |
| C(20)-O(22) | 1.2908(17) | C(21)-H(21) | 0.981(14) |
| O(22)-H(1) | 1.40(2) | C(22)-C(23) | 1.4065(19) |
| C(3)-C(1)#1 | 1.4031(19) | C(22)-H(22) | 0.967(14) |
| C(3)-H(3) | 0.964(15) | C(23)-C(24) | 1.407(2) |
| N(1)-C(15) | 1.3454(18) | C(24)-C(25) | 1.400(2) |
| N(1)-C(11) | 1.3520(18) | C(24)-H(24) | 0.960(14) |
| N(1)-H(1) | 1.15(2) | C(25)-N(2) | 1.3510(18) |
| C(11)-C(12) | 1.392(2) | C(25)-H(25) | 0.983(14) |
| C(11)-H(11) | 0.968(14) | | |

Symmetry transformations used to generate equivalent atoms:

#1 -x+1,-y+1,-z

Table 3.4.30X.angle. Bond angles (°).

| | | | |
|---|---|---|---|
| C(3)#1-C(1)-C(2) | 119.95(12) | C(14)-C(13)-C(12) | 117.35(12) |
| C(3)#1-C(1)-C(10) | 120.38(12) | C(14)-C(13)-C(23) | 121.36(12) |
| C(2)-C(1)-C(10) | 119.46(11) | C(12)-C(13)-C(23) | 121.29(12) |
| O(11)-C(10)-O(12) | 125.13(12) | C(15)-C(14)-C(13) | 119.41(13) |
| O(11)-C(10)-C(1) | 120.63(11) | C(15)-C(14)-H(14) | 118.9(9) |
| O(12)-C(10)-C(1) | 114.24(11) | C(13)-C(14)-H(14) | 121.7(9) |
| C(10)-O(12)-H(2) | 108.7(12) | N(1)-C(15)-C(14) | 121.85(12) |
| C(3)-C(2)-C(1) | 119.59(11) | N(1)-C(15)-H(15) | 115.7(8) |
| C(3)-C(2)-C(20) | 119.84(13) | C(14)-C(15)-H(15) | 122.4(8) |
| C(1)-C(2)-C(20) | 120.53(12) | N(2)-C(21)-C(22) | 123.01(12) |
| O(21)-C(20)-O(22) | 126.45(11) | N(2)-C(21)-H(21) | 115.8(8) |
| O(21)-C(20)-C(2) | 119.89(12) | C(22)-C(21)-H(21) | 121.1(8) |
| O(22)-C(20)-C(2) | 113.66(12) | C(21)-C(22)-C(23) | 119.66(13) |
| C(20)-O(22)-H(1) | 120.1(8) | C(21)-C(22)-H(22) | 116.8(8) |
| C(2)-C(3)-C(1)#1 | 120.46(13) | C(23)-C(22)-H(22) | 123.5(8) |

| | | | |
|---|---|---|---|
| C(2)-C(3)-H(3) | 118.9(8) | C(22)-C(23)-C(24) | 117.22(12) |
| C(1)#1-C(3)-H(3) | 120.7(8) | C(22)-C(23)-C(13) | 120.87(12) |
| C(15)-N(1)-C(11) | 120.18(12) | C(24)-C(23)-C(13) | 121.91(11) |
| C(15)-N(1)-H(1) | 119.9(10) | C(25)-C(24)-C(23) | 119.47(12) |
| C(11)-N(1)-H(1) | 119.8(10) | C(25)-C(24)-H(24) | 118.0(8) |
| N(1)-C(11)-C(12) | 120.72(13) | C(23)-C(24)-H(24) | 122.6(8) |
| N(1)-C(11)-H(11) | 118.4(8) | N(2)-C(25)-C(24) | 122.89(13) |
| C(12)-C(11)-H(11) | 120.9(8) | N(2)-C(25)-H(25) | 116.8(8) |
| C(11)-C(12)-C(13) | 120.47(12) | C(24)-C(25)-H(25) | 120.3(8) |
| C(11)-C(12)-H(12) | 116.4(9) | C(21)-N(2)-C(25) | 117.74(11) |
| C(13)-C(12)-H(12) | 123.2(9) | | |

Symmetry transformations used to generate equivalent atoms:

#1 -x+1,-y+1,-z

Table 3.4.30X.anis. Anisotropic displacement parameters ($Å^2 x\ 10^3$). The anisotropic displacement factor exponent takes the form: $-2p^2[\ h^2\ a^{*2}U^{11} + ... + 2\ h\ k\ a^*\ b^*\ U^{12}\ ]$

| | U11 | U22 | U33 | U23 | U13 | U12 |
|---|---|---|---|---|---|---|
| C(1) | 15(1) | 8(1) | 11(1) | -5(1) | -3(1) | 1(1) |
| C(10) | 10(1) | 13(1) | 12(1) | -5(1) | -5(1) | -2(1) |
| O(11) | 18(1) | 12(1) | 12(1) | -3(1) | -4(1) | -1(1) |
| O(12) | 13(1) | 14(1) | 9(1) | -4(1) | -2(1) | 0(1) |
| C(2) | 14(1) | 10(1) | 12(1) | -6(1) | -4(1) | 2(1) |
| C(20) | 14(1) | 8(1) | 12(1) | -3(1) | -4(1) | -2(1) |
| O(21) | 13(1) | 16(1) | 14(1) | -6(1) | -4(1) | 1(1) |
| O(22) | 15(1) | 16(1) | 10(1) | -5(1) | -4(1) | 1(1) |
| C(3) | 12(1) | 10(1) | 13(1) | -6(1) | -3(1) | -1(1) |
| N(1) | 12(1) | 13(1) | 12(1) | -4(1) | -4(1) | -2(1) |
| C(11) | 12(1) | 13(1) | 14(1) | -4(1) | -5(1) | -1(1) |
| C(12) | 12(1) | 15(1) | 13(1) | -7(1) | -3(1) | -2(1) |
| C(13) | 8(1) | 14(1) | 12(1) | -3(1) | -3(1) | -3(1) |
| C(14) | 12(1) | 12(1) | 15(1) | -5(1) | -3(1) | -1(1) |
| C(15) | 13(1) | 14(1) | 12(1) | -5(1) | -3(1) | -1(1) |
| C(21) | 13(1) | 15(1) | 11(1) | -5(1) | -3(1) | -2(1) |
| C(22) | 12(1) | 12(1) | 13(1) | -4(1) | -3(1) | -1(1) |
| C(23) | 9(1) | 14(1) | 11(1) | -4(1) | -2(1) | -4(1) |
| C(24) | 12(1) | 15(1) | 12(1) | -6(1) | -2(1) | -2(1) |
| C(25) | 11(1) | 12(1) | 14(1) | -4(1) | -3(1) | -1(1) |
| N(2) | 12(1) | 14(1) | 13(1) | -5(1) | -3(1) | -2(1) |

Table 3.4.30X.H. Hydrogen coordinates ( x $10^4$) and isotropic displacement parameters ($Å^2$x 10 $^3$).

| | x | y | z | U(eq) |
|---|---|---|---|---|
| H(2) | 8200(30) | 6660(20) | -4900(20) | 63(7) |
| H(3) | 1740(20) | 4654(16) | 667(16) | 13(4) |
| H(1) | 3090(30) | 7020(20) | -4810(20) | 58(6) |
| H(11) | 4210(20) | 6135(17) | -6807(16) | 11(3) |
| H(12) | 3910(20) | 7555(18) | -9235(17) | 18(4) |
| H(14) | 1130(20) | 11130(18) | -7894(16) | 14(4) |
| H(15) | 1590(20) | 9551(16) | -5478(16) | 13(4) |
| H(21) | 3280(20) | 10541(16) | -13818(16) | 13(4) |
| H(22) | 3760(20) | 8998(17) | -11444(15) | 10(3) |
| H(24) | 650(20) | 12487(16) | -10073(15) | 10(3) |
| H(25) | 398(19) | 13924(16) | -12530(15) | 10(3) |

**Supplement 3.4.296N. Tables of Refinement Results for the Neutron Structure of the 2:1 Co-crystal of 4,4-bipyridine and benzene-1,2,4,5-tetracarboxylic acid at 296K**

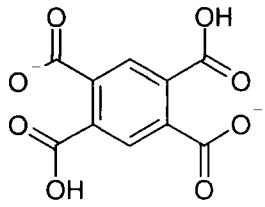

**PMA2-**

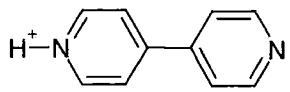

**BPY+**

Table 3.4.296N.xyz. Atomic coordinates ( x $10^4$) and equivalent isotropic displacement parameters ($Å^2$x $10^3$). U(eq) is defined as one third of the trace of the orthogonalized $U^{ij}$ tensor.

| | x | y | z | U(eq) |
|---|---|---|---|---|
| C(1) | 5842(2) | 5814(1) | -1498(1) | 25(1) |
| C(10) | 6714(2) | 6796(1) | -3081(1) | 29(1) |
| O(11) | 6216(3) | 8161(2) | -3567(2) | 53(1) |
| O(12) | 8007(2) | 6061(2) | -3819(2) | 37(1) |
| C(2) | 3933(2) | 5598(1) | -1082(1) | 24(1) |
| C(20) | 2777(2) | 6194(1) | -2237(1) | 28(1) |
| O(21) | 1093(2) | 6651(2) | -1937(2) | 49(1) |
| O(22) | 3717(2) | 6113(2) | -3490(2) | 44(1) |
| C(3) | 3097(2) | 4788(1) | 414(1) | 26(1) |
| N(1) | 2813(1) | 7757(1) | -5958(1) | 35(1) |
| C(11) | 3449(2) | 7184(2) | -7011(2) | 41(1) |
| C(12) | 3280(2) | 8057(2) | -8466(2) | 38(1) |
| C(13) | 2434(2) | 9577(1) | -8864(1) | 26(1) |
| C(14) | 1801(2) | 10157(2) | -7746(2) | 42(1) |
| C(15) | 2024(2) | 9214(2) | -6314(2) | 45(1) |
| C(21) | 2750(2) | 10899(2) | -12978(2) | 41(1) |
| C(22) | 2977(2) | 9981(2) | -11546(2) | 38(1) |
| C(23) | 2231(2) | 10544(1) | -10415(1) | 26(1) |
| C(24) | 1290(2) | 12035(2) | -10809(1) | 35(1) |
| C(25) | 1128(2) | 12884(2) | -12279(1) | 37(1) |
| N(2) | 1836(1) | 12322(1) | -13345(1) | 36(1) |

Table 3.4.296N.bond. Bond lengths (Å).

| | | | |
|---|---|---|---|
| C(1)-C(3)#1 | 1.4003(16) | C(12)-C(13) | 1.3944(18) |
| C(1)-C(2) | 1.4022(16) | C(12)-H(12) | 1.077(4) |
| C(1)-C(10) | 1.5046(16) | C(13)-C(14) | 1.3947(18) |
| C(10)-O(11) | 1.208(2) | C(13)-C(23) | 1.4849(16) |
| C(10)-O(12) | 1.301(2) | C(14)-C(15) | 1.3869(19) |
| O(12)-H(2) | 1.078(4) | C(14)-H(14) | 1.088(4) |
| C(2)-C(3) | 1.3965(16) | C(15)-H(15) | 1.080(4) |
| C(2)-C(20) | 1.5098(15) | C(21)-N(2) | 1.3334(18) |
| C(20)-O(21) | 1.218(2) | C(21)-C(22) | 1.3839(18) |
| C(20)-O(22) | 1.2804(19) | C(21)-H(21) | 1.084(3) |
| O(22)-H(1) | 1.240(4) | C(22)-C(23) | 1.3966(18) |
| C(3)-C(1)#1 | 1.4003(16) | C(22)-H(22) | 1.083(4) |
| C(3)-H(3) | 1.084(3) | C(23)-C(24) | 1.3935(18) |
| N(1)-C(11) | 1.3323(17) | C(24)-C(25) | 1.3925(18) |
| N(1)-C(15) | 1.3323(18) | C(24)-H(24) | 1.085(3) |
| N(1)-H(1) | 1.302(4) | C(25)-N(2) | 1.3372(17) |
| C(11)-C(12) | 1.3838(18) | C(25)-H(25) | 1.090(3) |
| C(11)-H(11) | 1.083(4) | | |

Symmetry transformations used to generate equivalent atoms:

#1 -x+1,-y+1,-z

Table 3.4.296N.angle. Bond angles (°).

| | | | |
|---|---|---|---|
| C(3)#1-C(1)-C(2) | 119.88(10) | C(12)-C(13)-C(14) | 117.11(11) |
| C(3)#1-C(1)-C(10) | 119.65(11) | C(12)-C(13)-C(23) | 121.50(11) |
| C(2)-C(1)-C(10) | 120.29(10) | C(14)-C(13)-C(23) | 121.38(11) |
| O(11)-C(10)-O(12) | 125.07(15) | C(15)-C(14)-C(13) | 119.41(13) |
| O(11)-C(10)-C(1) | 120.01(13) | C(15)-C(14)-H(14) | 118.5(2) |
| O(12)-C(10)-C(1) | 114.91(11) | C(13)-C(14)-H(14) | 122.1(2) |
| C(10)-O(12)-H(2) | 109.4(2) | N(1)-C(15)-C(14) | 122.26(13) |
| C(3)-C(2)-C(1) | 119.79(10) | N(1)-C(15)-H(15) | 115.8(2) |
| C(3)-C(2)-C(20) | 119.33(11) | C(14)-C(15)-H(15) | 122.0(3) |
| C(1)-C(2)-C(20) | 120.86(10) | N(2)-C(21)-C(22) | 122.91(12) |
| O(21)-C(20)-O(22) | 125.26(14) | N(2)-C(21)-H(21) | 115.9(2) |
| O(21)-C(20)-C(2) | 120.94(12) | C(22)-C(21)-H(21) | 121.2(2) |
| O(22)-C(20)-C(2) | 113.76(11) | C(21)-C(22)-C(23) | 119.71(12) |
| C(20)-O(22)-H(1) | 119.6(2) | C(21)-C(22)-H(22) | 117.7(2) |
| C(2)-C(3)-C(1)#1 | 120.33(11) | C(23)-C(22)-H(22) | 122.6(2) |

| | | | |
|---|---|---|---|
| C(2)-C(3)-H(3) | 119.53(17) | C(24)-C(23)-C(22) | 117.02(11) |
| C(1)#1-C(3)-H(3) | 120.13(18) | C(24)-C(23)-C(13) | 122.13(11) |
| C(11)-N(1)-C(15) | 119.40(11) | C(22)-C(23)-C(13) | 120.85(11) |
| C(11)-N(1)-H(1) | 119.24(17) | C(25)-C(24)-C(23) | 119.64(12) |
| C(15)-N(1)-H(1) | 121.11(17) | C(25)-C(24)-H(24) | 118.6(2) |
| N(1)-C(11)-C(12) | 121.59(12) | C(23)-C(24)-H(24) | 121.7(2) |
| N(1)-C(11)-H(11) | 116.5(2) | N(2)-C(25)-C(24) | 122.54(12) |
| C(12)-C(11)-H(11) | 121.9(2) | N(2)-C(25)-H(25) | 115.8(2) |
| C(11)-C(12)-C(13) | 120.21(12) | C(24)-C(25)-H(25) | 121.6(2) |
| C(11)-C(12)-H(12) | 118.1(2) | C(21)-N(2)-C(25) | 118.17(10) |
| C(13)-C(12)-H(12) | 121.7(2) | | |

Symmetry transformations used to generate equivalent atoms:

#1 -x+1,-y+1,-z

Table 3.4.296N.anis. Anisotropic displacement parameters ($Å^2 x\ 10^3$). The anisotropic displacement factor exponent takes the form: $-2p^2[\ h^2\ a^{*2}U^{11} + ... + 2\ h\ k\ a^*\ b^*\ U^{12}\ ]$

| | U11 | U22 | U33 | U23 | U13 | U12 |
|---|---|---|---|---|---|---|
| C(1) | 31(1) | 27(1) | 13(1) | -4(1) | -5(1) | -4(1) |
| C(10) | 40(1) | 27(1) | 14(1) | -3(1) | -5(1) | -4(1) |
| O(11) | 89(1) | 27(1) | 24(1) | -5(1) | 1(1) | -5(1) |
| O(12) | 38(1) | 39(1) | 19(1) | -6(1) | -4(1) | 4(1) |
| C(2) | 30(1) | 26(1) | 13(1) | -5(1) | -8(1) | -1(1) |
| C(20) | 33(1) | 30(1) | 18(1) | -8(1) | -12(1) | 5(1) |
| O(21) | 35(1) | 76(1) | 36(1) | -25(1) | -17(1) | 13(1) |
| O(22) | 47(1) | 57(1) | 22(1) | -17(1) | -17(1) | 16(1) |
| H(2) | 45(1) | 54(2) | 44(2) | -19(2) | 1(1) | -3(1) |
| C(3) | 30(1) | 31(1) | 14(1) | -4(1) | -6(1) | -4(1) |
| H(3) | 38(1) | 62(2) | 34(1) | -10(1) | -5(1) | -11(1) |
| N(1) | 44(1) | 38(1) | 22(1) | -7(1) | -16(1) | 0(1) |
| H(1) | 55(2) | 64(2) | 59(2) | -30(2) | -14(2) | -3(2) |
| C(11) | 63(1) | 30(1) | 26(1) | -6(1) | -20(1) | 4(1) |
| H(11) | 135(4) | 41(2) | 49(2) | -10(2) | -44(2) | 17(2) |
| C(12) | 60(1) | 29(1) | 25(1) | -10(1) | -18(1) | 6(1) |
| H(12) | 163(4) | 50(2) | 43(2) | -26(2) | -43(2) | 32(2) |
| C(13) | 31(1) | 26(1) | 18(1) | -7(1) | -9(1) | -1(1) |
| C(14) | 62(1) | 36(1) | 24(1) | -14(1) | -19(1) | 14(1) |
| H(14) | 150(4) | 51(2) | 51(2) | -28(2) | -48(2) | 41(2) |
| C(15) | 64(1) | 44(1) | 25(1) | -16(1) | -19(1) | 11(1) |

| | | | | | | |
|---|---|---|---|---|---|---|
| H(15) | 152(4) | 81(3) | 44(2) | -38(2) | -44(2) | 39(3) |
| C(21) | 57(1) | 39(1) | 19(1) | -9(1) | -10(1) | 3(1) |
| H(21) | 116(3) | 67(2) | 29(2) | -22(2) | -19(2) | 15(2) |
| C(22) | 54(1) | 32(1) | 19(1) | -8(1) | -9(1) | 4(1) |
| H(22) | 122(3) | 47(2) | 42(2) | -20(2) | -27(2) | 31(2) |
| C(23) | 32(1) | 26(1) | 18(1) | -7(1) | -8(1) | 1(1) |
| C(24) | 44(1) | 32(1) | 21(1) | -8(1) | -11(1) | 6(1) |
| H(24) | 103(3) | 48(2) | 38(2) | -22(2) | -23(2) | 23(2) |
| C(25) | 43(1) | 33(1) | 22(1) | -4(1) | -9(1) | 6(1) |
| H(25) | 96(3) | 45(2) | 44(2) | -11(2) | -25(2) | 27(2) |
| N(2) | 41(1) | 38(1) | 18(1) | -4(1) | -7(1) | -1(1) |

Table 3.4.296N.H. Hydrogen coordinates ( x $10^4$) and isotropic displacement parameters ($Å^2$x $10^3$).

| | x | y | z | U(eq) |
|---|---|---|---|---|
| H(2) | 8220(4) | 6752(4) | -4999(3) | 51(1) |
| H(3) | 1627(4) | 4608(4) | 727(3) | 48(1) |
| H(1) | 3116(5) | 6923(4) | -4631(4) | 58(1) |
| H(11) | 4100(7) | 6001(4) | -6668(4) | 78(1) |
| H(12) | 3810(8) | 7526(4) | -9265(4) | 87(2) |
| H(14) | 1129(7) | 11332(4) | -7959(4) | 86(1) |
| H(15) | 1601(8) | 9624(5) | -5423(4) | 93(2) |
| H(21) | 3339(7) | 10499(4) | -13882(3) | 74(1) |
| H(22) | 3756(7) | 8845(4) | -11357(4) | 76(1) |
| H(24) | 652(6) | 12553(4) | -9995(4) | 66(1) |
| H(25) | 406(6) | 14054(4) | -12627(4) | 69(1) |

**Supplement 3.4.200N. Tables of Refinement Results for the Neutron Structure of the 2:1 Co-crystal of 4,4-bipyridine and benzene-1,2,4,5-tetracarboxylic acid at 200K**

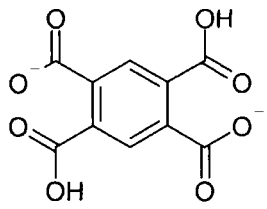

**PMA2-**

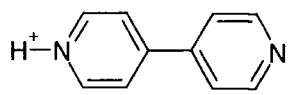

**BPY+**

Table 3.4.200N.xyz. Atomic coordinates ( x $10^4$) and equivalent isotropic displacement parameters (Å$^2$x $10^3$). U(eq) is defined as one third of the trace of the orthogonalized $U^{ij}$ tensor.

| | x | y | z | U(eq) |
|---|---|---|---|---|
| C(1) | 5851(4) | 5809(3) | -1493(2) | 18(1) |
| C(10) | 6710(4) | 6787(3) | -3075(2) | 20(1) |
| O(11) | 6218(6) | 8176(3) | -3577(3) | 36(1) |
| O(12) | 8026(5) | 6048(3) | -3822(3) | 24(1) |
| C(2) | 3934(4) | 5595(3) | -1083(2) | 17(1) |
| C(20) | 2773(4) | 6191(3) | -2248(2) | 19(1) |
| O(21) | 1072(5) | 6672(4) | -1952(3) | 30(1) |
| O(22) | 3708(5) | 6110(4) | -3500(3) | 25(1) |
| C(3) | 3086(6) | 4793(3) | 408(2) | 19(1) |
| N(1) | 2829(3) | 7743(2) | -5964(2) | 24(1) |
| C(11) | 3487(5) | 7178(3) | -7025(2) | 27(1) |
| C(12) | 3309(5) | 8047(3) | -8479(2) | 25(1) |
| C(13) | 2436(4) | 9569(3) | -8864(2) | 16(1) |
| C(14) | 1786(5) | 10150(3) | -7733(2) | 28(1) |
| C(15) | 2010(5) | 9201(3) | -6309(3) | 30(1) |
| C(21) | 2756(5) | 10900(3) | -12983(2) | 28(1) |
| C(22) | 2985(4) | 9975(3) | -11564(2) | 24(1) |
| C(23) | 2241(4) | 10542(3) | -10414(2) | 19(1) |
| C(24) | 1269(4) | 12040(3) | -10799(2) | 23(1) |
| C(25) | 1119(4) | 12894(3) | -12275(2) | 23(1) |
| N(2) | 1830(3) | 12333(2) | -13348(2) | 24(1) |

Table 3.4.200N.bond. Bond lengths (Å).

| | | | |
|---|---|---|---|
| C(1)-C(3)#1 | 1.398(4) | C(12)-C(13) | 1.400(3) |
| C(1)-C(2) | 1.400(4) | C(12)-H(12) | 1.072(6) |
| C(1)-C(10) | 1.501(3) | C(13)-C(14) | 1.403(3) |
| C(10)-O(11) | 1.225(3) | C(13)-C(23) | 1.485(3) |
| C(10)-O(12) | 1.314(3) | C(14)-C(15) | 1.382(3) |
| O(12)-H(2) | 1.062(6) | C(14)-H(14) | 1.080(5) |
| C(2)-C(3) | 1.394(3) | C(15)-H(15) | 1.083(6) |
| C(2)-C(20) | 1.516(4) | C(21)-N(2) | 1.343(3) |
| C(20)-O(21) | 1.231(4) | C(21)-C(22) | 1.375(3) |
| C(20)-O(22) | 1.278(3) | C(21)-H(21) | 1.089(6) |
| O(22)-H(1) | 1.280(6) | C(22)-C(23) | 1.412(3) |
| C(3)-C(1)#1 | 1.398(4) | C(22)-H(22) | 1.069(5) |
| C(3)-H(3) | 1.093(11) | C(23)-C(24) | 1.404(3) |
| N(1)-C(11) | 1.329(3) | C(24)-C(25) | 1.397(3) |
| N(1)-C(15) | 1.338(3) | C(24)-H(24) | 1.088(5) |
| N(1)-H(1) | 1.251(6) | C(25)-N(2) | 1.339(3) |
| C(11)-C(12) | 1.386(3) | C(25)-H(25) | 1.082(5) |
| C(11)-H(11) | 1.074(5) | | |

Symmetry transformations used to generate equivalent atoms:

#1 -x+1,-y+1,-z

Table 3.4.200N.bond. Bond angles (°).

| | | | |
|---|---|---|---|
| C(3)#1-C(1)-C(2) | 119.9(2) | C(12)-C(13)-C(14) | 117.31(19) |
| C(3)#1-C(1)-C(10) | 120.4(3) | C(12)-C(13)-C(23) | 121.41(19) |
| C(2)-C(1)-C(10) | 119.6(2) | C(14)-C(13)-C(23) | 121.26(18) |
| O(11)-C(10)-O(12) | 124.4(3) | C(15)-C(14)-C(13) | 119.1(2) |
| O(11)-C(10)-C(1) | 120.4(2) | C(15)-C(14)-H(14) | 118.7(3) |
| O(12)-C(10)-C(1) | 115.1(2) | C(13)-C(14)-H(14) | 122.2(3) |
| C(10)-O(12)-H(2) | 109.0(3) | N(1)-C(15)-C(14) | 122.5(2) |
| C(3)-C(2)-C(1) | 119.9(3) | N(1)-C(15)-H(15) | 115.8(4) |
| C(3)-C(2)-C(20) | 119.4(3) | C(14)-C(15)-H(15) | 121.8(4) |
| C(1)-C(2)-C(20) | 120.73(19) | N(2)-C(21)-C(22) | 123.4(2) |
| O(21)-C(20)-O(22) | 125.1(3) | N(2)-C(21)-H(21) | 115.9(3) |
| O(21)-C(20)-C(2) | 120.7(2) | C(22)-C(21)-H(21) | 120.7(3) |
| O(22)-C(20)-C(2) | 114.1(3) | C(21)-C(22)-C(23) | 119.5(2) |
| C(20)-O(22)-H(1) | 120.3(3) | C(21)-C(22)-H(22) | 118.5(3) |
| C(2)-C(3)-C(1)#1 | 120.3(3) | C(23)-C(22)-H(22) | 121.9(3) |

| | | | |
|---|---|---|---|
| C(2)-C(3)-H(3) | 119.7(4) | C(24)-C(23)-C(22) | 116.9(2) |
| C(1)#1-C(3)-H(3) | 120.0(4) | C(24)-C(23)-C(13) | 122.05(19) |
| C(11)-N(1)-C(15) | 119.44(18) | C(22)-C(23)-C(13) | 120.98(18) |
| C(11)-N(1)-H(1) | 119.6(3) | C(25)-C(24)-C(23) | 119.4(2) |
| C(15)-N(1)-H(1) | 120.8(3) | C(25)-C(24)-H(24) | 119.0(3) |
| N(1)-C(11)-C(12) | 121.8(2) | C(23)-C(24)-H(24) | 121.6(3) |
| N(1)-C(11)-H(11) | 117.6(4) | N(2)-C(25)-C(24) | 122.7(2) |
| C(12)-C(11)-H(11) | 120.5(4) | N(2)-C(25)-H(25) | 116.4(3) |
| C(11)-C(12)-C(13) | 119.8(2) | C(24)-C(25)-H(25) | 120.9(3) |
| C(11)-C(12)-H(12) | 118.3(3) | C(25)-N(2)-C(21) | 118.06(18) |
| C(13)-C(12)-H(12) | 121.9(3) | | |

Symmetry transformations used to generate equivalent atoms:

#1 -x+1,-y+1,-z

Table 3.4.200N.anis Anisotropic displacement parameters ($Å^2 x\ 10^3$). The anisotropic displacement factor exponent takes the form: $-2p^2[\ h^2\ a^{*2}U^{11} + ... + 2\ h\ k\ a^*\ b^*\ U^{12}\ ]$

| | U11 | U22 | U33 | U23 | U13 | U12 |
|---|---|---|---|---|---|---|
| C(1) | 19(2) | 24(1) | 9(1) | -3(1) | -4(1) | -1(1) |
| C(10) | 22(2) | 24(1) | 12(1) | -5(1) | -5(1) | -5(1) |
| O(11) | 60(3) | 18(1) | 17(1) | -2(1) | 1(1) | -5(2) |
| O(12) | 21(3) | 27(1) | 17(1) | -6(1) | -3(1) | 2(2) |
| C(2) | 23(2) | 19(1) | 10(1) | -4(1) | -7(1) | -3(1) |
| C(20) | 17(2) | 25(1) | 15(1) | -7(1) | -10(1) | 1(1) |
| O(21) | 17(3) | 50(2) | 26(1) | -16(1) | -13(1) | 4(2) |
| O(22) | 26(3) | 36(2) | 16(1) | -11(1) | -16(1) | 5(2) |
| H(2) | 38(5) | 48(3) | 31(3) | -13(2) | 1(3) | -1(3) |
| C(3) | 20(3) | 22(1) | 13(1) | -3(1) | -4(1) | -5(2) |
| H(3) | 25(6) | 52(4) | 31(3) | -11(2) | -8(3) | -4(4) |
| N(1) | 26(2) | 29(1) | 16(1) | -5(1) | -12(1) | 0(1) |
| H(1) | 26(5) | 43(3) | 45(3) | -20(2) | -10(3) | -12(3) |
| C(11) | 37(2) | 24(1) | 19(1) | -6(1) | -15(1) | 3(1) |
| H(11) | 85(6) | 24(2) | 45(3) | -12(2) | -39(3) | 13(3) |
| C(12) | 36(2) | 21(1) | 18(1) | -6(1) | -12(1) | 3(1) |
| H(12) | 105(7) | 44(3) | 29(3) | -18(2) | -20(3) | 16(4) |
| C(13) | 19(2) | 18(1) | 12(1) | -4(1) | -7(1) | -1(1) |
| C(14) | 41(2) | 26(1) | 16(1) | -9(1) | -14(1) | 10(1) |
| H(14) | 91(6) | 38(3) | 39(3) | -18(2) | -34(3) | 26(4) |
| C(15) | 41(3) | 32(1) | 17(1) | -11(1) | -16(1) | 10(2) |

| | | | | | | |
|---|---|---|---|---|---|---|
| H(15) | 95(7) | 62(4) | 31(3) | -30(3) | -26(3) | 17(4) |
| C(21) | 36(2) | 28(1) | 14(1) | -6(1) | -7(1) | 0(1) |
| H(21) | 68(6) | 49(3) | 28(2) | -19(2) | -17(3) | 10(3) |
| C(22) | 29(2) | 26(1) | 15(1) | -7(1) | -9(1) | 3(1) |
| H(22) | 73(6) | 44(3) | 30(2) | -17(2) | -19(3) | 19(3) |
| C(23) | 21(2) | 21(1) | 13(1) | -5(1) | -4(1) | 0(1) |
| C(24) | 28(2) | 22(1) | 16(1) | -6(1) | -8(1) | 2(1) |
| H(24) | 62(5) | 36(3) | 33(2) | -19(2) | -17(3) | 9(3) |
| C(25) | 25(2) | 25(1) | 15(1) | -4(1) | -7(1) | 2(1) |
| H(25) | 49(5) | 38(3) | 35(2) | -7(2) | -18(3) | 18(3) |
| N(2) | 26(2) | 29(1) | 13(1) | -5(1) | -6(1) | 0(1) |

Table 3.4.200N.H. Hydrogen coordinates ( x $10^4$) and isotropic displacement parameters ($Å^2$x 10 $^3$).

| | x | y | z | U(eq) |
|---|---|---|---|---|
| H(2) | 8218(9) | 6730(7) | -4982(5) | 43(2) |
| H(3) | 1598(12) | 4602(7) | 722(6) | 38(2) |
| H(1) | 3103(9) | 6943(6) | -4685(6) | 35(2) |
| H(11) | 4175(11) | 6014(6) | -6719(6) | 50(2) |
| H(12) | 3839(12) | 7516(7) | -9277(6) | 62(3) |
| H(14) | 1095(11) | 11311(6) | -7933(6) | 56(3) |
| H(15) | 1549(12) | 9602(7) | -5404(6) | 61(3) |
| H(21) | 3345(11) | 10495(7) | -13892(6) | 48(2) |
| H(22) | 3791(10) | 8865(6) | -11380(5) | 51(2) |
| H(24) | 642(10) | 12560(6) | -9978(5) | 43(2) |
| H(25) | 395(9) | 14055(6) | -12604(6) | 45(2) |

**Supplement 3.4.20N. Tables of Refinement Results for the Neutron Structure of the 2:1 Co-crystal of 4,4-bipyridine and benzene-1,2,4,5-tetracarboxylic acid at 20K**

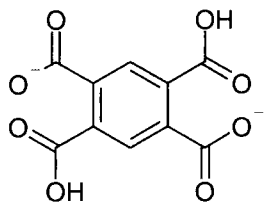

**PMA2-**

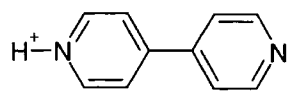

**BPY+**

Table 3.4.20N.xyz. Atomic coordinates ( x $10^4$) and equivalent isotropic displacement parameters (Å$^2$x $10^3$). U(eq) is defined as one third of the trace of the orthogonalized $U^{ij}$ tensor.

| | x | y | z | U(eq) |
|---|---|---|---|---|
| C(1) | 5866(2) | 5809(2) | -1490(1) | 4(1) |
| C(10) | 6740(2) | 6789(2) | -3073(1) | 4(1) |
| O(11) | 6249(2) | 8177(2) | -3563(2) | 8(1) |
| O(12) | 8029(2) | 6037(2) | -3821(2) | 7(1) |
| C(2) | 3914(2) | 5595(2) | -1086(1) | 4(1) |
| C(20) | 2750(2) | 6185(2) | -2257(1) | 5(1) |
| O(21) | 1040(2) | 6679(2) | -1960(2) | 8(1) |
| O(22) | 3705(2) | 6089(2) | -3507(2) | 7(1) |
| C(3) | 3056(2) | 4791(2) | 406(1) | 5(1) |
| N(1) | 2853(1) | 7739(1) | -5981(1) | 6(1) |
| C(11) | 3551(2) | 7166(2) | -7060(1) | 6(1) |
| C(12) | 3366(2) | 8050(2) | -8509(1) | 6(1) |
| C(13) | 2449(2) | 9564(1) | -8872(1) | 4(1) |
| C(14) | 1754(2) | 10132(2) | -7724(1) | 6(1) |
| C(15) | 1994(2) | 9187(2) | -6299(1) | 7(1) |
| C(21) | 2778(2) | 10908(2) | -13006(1) | 7(1) |
| C(22) | 3019(2) | 9981(2) | -11575(1) | 6(1) |
| C(23) | 2234(2) | 10538(1) | -10423(1) | 4(1) |
| C(24) | 1246(2) | 12033(2) | -10792(1) | 6(1) |
| C(25) | 1081(2) | 12889(2) | -12260(1) | 6(1) |
| N(2) | 1821(1) | 12337(1) | -13351(1) | 6(1) |

Table 3.4.20N.bond. Bond lengths (Å).

| | | | |
|---|---|---|---|
| C(1)-C(3)#1 | 1.3980(19) | C(12)-C(13) | 1.4003(17) |
| C(1)-C(2) | 1.4081(19) | C(12)-H(12) | 1.086(3) |
| C(1)-C(10) | 1.5051(16) | C(13)-C(14) | 1.4019(16) |
| C(10)-O(11) | 1.219(2) | C(13)-C(23) | 1.4913(17) |
| C(10)-O(12) | 1.3123(19) | C(14)-C(15) | 1.3876(17) |
| O(12)-H(2) | 1.068(3) | C(14)-H(14) | 1.091(3) |
| C(2)-C(3) | 1.3979(16) | C(15)-H(15) | 1.087(3) |
| C(2)-C(20) | 1.5134(17) | C(21)-N(2) | 1.3448(16) |
| C(20)-O(21) | 1.235(2) | C(21)-C(22) | 1.3897(17) |
| C(20)-O(22) | 1.2843(18) | C(21)-H(21) | 1.089(3) |
| O(22)-H(1) | 1.325(3) | C(22)-C(23) | 1.4030(16) |
| C(3)-C(1)#1 | 1.3980(19) | C(22)-H(22) | 1.080(3) |
| C(3)-H(3) | 1.093(3) | C(23)-C(24) | 1.4031(18) |
| N(1)-C(15) | 1.3362(16) | C(24)-C(25) | 1.3941(17) |
| N(1)-C(11) | 1.3441(15) | C(24)-H(24) | 1.091(3) |
| N(1)-H(1) | 1.207(3) | C(25)-N(2) | 1.3441(14) |
| C(11)-C(12) | 1.3860(17) | C(25)-H(25) | 1.089(3) |
| C(11)-H(11) | 1.091(3) | | |

Symmetry transformations used to generate equivalent atoms:

#1 -x+1,-y+1,-z

Table 3.4.20N.angle. Bond angles (°).

| | | | |
|---|---|---|---|
| C(3)#1-C(1)-C(2) | 120.11(12) | C(12)-C(13)-C(14) | 117.50(11) |
| C(3)#1-C(1)-C(10) | 120.28(12) | C(12)-C(13)-C(23) | 121.12(11) |
| C(2)-C(1)-C(10) | 119.44(11) | C(14)-C(13)-C(23) | 121.38(11) |
| O(11)-C(10)-O(12) | 124.98(13) | C(15)-C(14)-C(13) | 119.39(11) |
| O(11)-C(10)-C(1) | 119.99(12) | C(15)-C(14)-H(14) | 118.24(18) |
| O(12)-C(10)-C(1) | 115.03(11) | C(13)-C(14)-H(14) | 122.37(19) |
| C(10)-O(12)-H(2) | 109.2(2) | N(1)-C(15)-C(14) | 121.80(11) |
| C(3)-C(2)-C(1) | 119.68(12) | N(1)-C(15)-H(15) | 116.4(2) |
| C(3)-C(2)-C(20) | 119.66(12) | C(14)-C(15)-H(15) | 121.8(2) |
| C(1)-C(2)-C(20) | 120.64(11) | N(2)-C(21)-C(22) | 122.83(11) |
| O(21)-C(20)-O(22) | 126.15(14) | N(2)-C(21)-H(21) | 115.98(19) |
| O(21)-C(20)-C(2) | 120.17(12) | C(22)-C(21)-H(21) | 121.2(2) |
| O(22)-C(20)-C(2) | 113.67(12) | C(21)-C(22)-C(23) | 119.46(11) |
| C(20)-O(22)-H(1) | 120.33(17) | C(21)-C(22)-H(22) | 117.30(19) |
| C(2)-C(3)-C(1)#1 | 120.21(12) | C(23)-C(22)-H(22) | 123.24(19) |

| | | | |
|---|---|---|---|
| C(2)-C(3)-H(3) | 119.75(18) | C(22)-C(23)-C(24) | 117.37(11) |
| C(1)#1-C(3)-H(3) | 120.03(19) | C(22)-C(23)-C(13) | 120.74(11) |
| C(15)-N(1)-C(11) | 120.22(10) | C(24)-C(23)-C(13) | 121.89(11) |
| C(15)-N(1)-H(1) | 120.85(15) | C(25)-C(24)-C(23) | 119.47(11) |
| C(11)-N(1)-H(1) | 118.84(16) | C(25)-C(24)-H(24) | 118.7(2) |
| N(1)-C(11)-C(12) | 120.95(11) | C(23)-C(24)-H(24) | 121.84(19) |
| N(1)-C(11)-H(11) | 116.41(18) | N(2)-C(25)-C(24) | 122.62(11) |
| C(12)-C(11)-H(11) | 122.64(18) | N(2)-C(25)-H(25) | 116.19(18) |
| C(11)-C(12)-C(13) | 120.14(11) | C(24)-C(25)-H(25) | 121.19(19) |
| C(11)-C(12)-H(12) | 117.4(2) | C(25)-N(2)-C(21) | 118.23(10) |
| C(13)-C(12)-H(12) | 122.43(19) | | |

Symmetry transformations used to generate equivalent atoms:

#1 -x+1,-y+1,-z

Table 3.4.20N.ansi. Anisotropic displacement parameters ($Å^2 x\ 10^3$). The anisotropic displacement factor exponent takes the form: $-2p^2[\ h^2\ a^{*2}U^{11} + ... + 2\ h\ k\ a^*\ b^*\ U^{12}\ ]$

| | U11 | U22 | U33 | U23 | U13 | U12 |
|---|---|---|---|---|---|---|
| C(1) | 5(1) | 3(1) | 4(1) | -1(1) | -2(1) | -1(1) |
| C(10) | 6(1) | 3(1) | 3(1) | -1(1) | 1(1) | -3(1) |
| O(11) | 12(1) | 4(1) | 6(1) | -2(1) | 0(1) | -1(1) |
| O(12) | 7(1) | 5(1) | 6(1) | -1(1) | 0(1) | -1(1) |
| C(2) | 4(1) | 4(1) | 4(1) | -1(1) | -2(1) | -1(1) |
| C(20) | 6(1) | 5(1) | 5(1) | -2(1) | -2(1) | 0(1) |
| O(21) | 7(1) | 10(1) | 8(1) | -5(1) | -3(1) | 1(1) |
| O(22) | 8(1) | 8(1) | 4(1) | -3(1) | -2(1) | 1(1) |
| H(2) | 17(1) | 19(1) | 17(1) | -8(1) | 0(1) | -4(1) |
| C(3) | 5(1) | 7(1) | 4(1) | -2(1) | -1(1) | -2(1) |
| H(3) | 10(1) | 28(2) | 17(1) | -5(1) | -3(1) | -7(1) |
| N(1) | 7(1) | 6(1) | 6(1) | -3(1) | -2(1) | 0(1) |
| H(1) | 21(1) | 22(2) | 24(1) | -13(1) | -5(1) | -3(1) |
| C(11) | 9(1) | 4(1) | 6(1) | -2(1) | -2(1) | 0(1) |
| H(11) | 31(2) | 13(1) | 20(1) | -6(1) | -10(1) | 5(1) |
| C(12) | 9(1) | 4(1) | 5(1) | -2(1) | -3(1) | 1(1) |
| H(12) | 35(2) | 18(1) | 18(1) | -12(1) | -9(1) | 7(1) |
| C(13) | 5(1) | 4(1) | 4(1) | -2(1) | -2(1) | 0(1) |
| C(14) | 10(1) | 3(1) | 5(1) | -2(1) | -2(1) | 2(1) |
| H(14) | 33(2) | 12(1) | 21(1) | -9(1) | -8(1) | 6(1) |
| C(15) | 9(1) | 6(1) | 5(1) | -3(1) | -3(1) | 2(1) |

| | | | | | | |
|---|---|---|---|---|---|---|
| H(15) | 34(2) | 24(2) | 15(1) | -12(1) | -8(1) | 3(2) |
| C(21) | 10(1) | 6(1) | 4(1) | -3(1) | -2(1) | 0(1) |
| H(21) | 33(2) | 20(2) | 14(1) | -11(1) | -5(1) | 6(1) |
| C(22) | 9(1) | 4(1) | 5(1) | -3(1) | -1(1) | 1(1) |
| H(22) | 34(2) | 13(1) | 19(1) | -7(1) | -8(1) | 8(1) |
| C(23) | 6(1) | 4(1) | 4(1) | -2(1) | -1(1) | 0(1) |
| C(24) | 9(1) | 4(1) | 5(1) | -2(1) | -2(1) | 1(1) |
| H(24) | 31(2) | 19(1) | 16(1) | -12(1) | -6(1) | 5(1) |
| C(25) | 7(1) | 4(1) | 5(1) | -1(1) | 0(1) | -1(1) |
| H(25) | 33(2) | 14(1) | 22(1) | -9(1) | -10(1) | 7(1) |
| N(2) | 8(1) | 6(1) | 4(1) | -2(1) | -1(1) | -1(1) |

Table 3.4.20N.H. Hydrogen coordinates ( x $10^4$) and isotropic displacement parameters ($Å^2$x 10 $^3$).

| | x | y | z | U(eq) |
|---|---|---|---|---|
| H(2) | 8232(4) | 6724(3) | -4987(3) | 18(1) |
| H(3) | 1545(4) | 4613(4) | 719(3) | 19(1) |
| H(1) | 3101(4) | 6950(3) | -4746(3) | 21(1) |
| H(11) | 4249(5) | 5981(3) | -6727(3) | 22(1) |
| H(12) | 3947(5) | 7517(3) | -9328(3) | 23(1) |
| H(14) | 1036(5) | 11302(3) | -7911(3) | 22(1) |
| H(15) | 1536(5) | 9598(3) | -5390(3) | 23(1) |
| H(21) | 3383(5) | 10513(3) | -13925(3) | 23(1) |
| H(22) | 3816(5) | 8852(3) | -11411(3) | 23(1) |
| H(24) | 582(5) | 12544(3) | -9959(3) | 21(1) |
| H(25) | 341(5) | 14059(3) | -12584(3) | 23(1) |

**Supplement 3.6. Tables of Refinement Results for the X-ray Structure of the 1:2 Co-crystal of 4,4'-Bipyridinium and Hydrogen Phthalate at 153K**

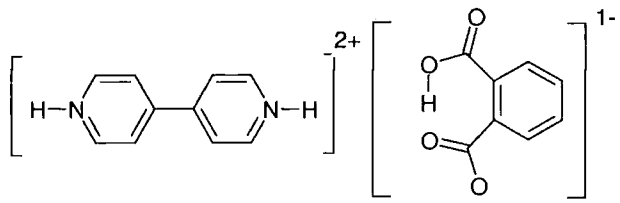

[BPY2+] [PHT-]

Table 3.6.xyz. Atomic coordinates ( x $10^4$) and equivalent isotropic displacement parameters ($Å^2$x $10^3$). U(eq) is defined as one third of the trace of the orthogonalized $U^{ij}$ tensor.

| | x | y | z | U(eq) |
|---|---|---|---|---|
| C(1) | 3607(1) | 9235(2) | 1639(1) | 21(1) |
| C(10) | 4044(1) | 8521(2) | 939(1) | 29(1) |
| O(11) | 4629(1) | 7871(2) | 1115(1) | 38(1) |
| O(12) | 3790(1) | 8670(2) | 147(1) | 51(1) |
| C(2) | 2930(1) | 10083(2) | 1573(1) | 22(1) |
| C(20) | 2416(1) | 10301(2) | 790(1) | 30(1) |
| O(21) | 2623(1) | 10024(2) | 55(1) | 52(1) |
| O(22) | 1796(1) | 10769(2) | 894(1) | 39(1) |
| C(3) | 2679(1) | 10825(2) | 2315(1) | 24(1) |
| C(4) | 3059(1) | 10690(2) | 3101(1) | 26(1) |
| C(5) | 3696(1) | 9741(2) | 3177(1) | 27(1) |
| C(6) | 3963(1) | 9042(2) | 2451(1) | 26(1) |
| N(1) | 1050(1) | 11252(2) | -568(1) | 27(1) |
| C(11) | 1340(1) | 10848(2) | -1296(1) | 27(1) |
| C(12) | 939(1) | 10901(2) | -2063(1) | 25(1) |
| C(13) | 225(1) | 11346(2) | -2092(1) | 21(1) |
| C(14) | -59(1) | 11760(2) | -1323(1) | 26(1) |
| C(15) | 365(1) | 11721(2) | -571(1) | 28(1) |

Table 3.6.bond. Bond lengths (Å).

| | | | |
|---|---|---|---|
| C(1)-C(6) | 1.404(2) | C(5)-C(6) | 1.388(2) |
| C(1)-C(2) | 1.4191(19) | C(5)-H(5) | 0.991(13) |
| C(1)-C(10) | 1.528(2) | C(6)-H(6) | 0.988(12) |
| C(10)-O(11) | 1.2158(17) | N(1)-C(15) | 1.3435(18) |
| C(10)-O(12) | 1.3060(17) | N(1)-C(11) | 1.3480(18) |

| | | | |
|---|---|---|---|
| O(12)-H(2) | 1.10(2) | N(1)-H(1) | 1.03(2) |
| C(2)-C(3) | 1.4078(19) | C(11)-C(12) | 1.376(2) |
| C(2)-C(20) | 1.5174(19) | C(11)-H(11) | 1.037(13) |
| C(20)-O(22) | 1.2470(17) | C(12)-C(13) | 1.390(2) |
| C(20)-O(21) | 1.2722(16) | C(12)-H(12) | 0.970(12) |
| O(21)-H(2) | 1.32(2) | C(13)-C(14) | 1.4020(19) |
| C(3)-C(4) | 1.384(2) | C(13)-C(13)#1 | 1.483(3) |
| C(3)-H(3) | 1.029(13) | C(14)-C(15) | 1.377(2) |
| C(4)-C(5) | 1.386(2) | C(14)-H(14) | 0.940(12) |
| C(4)-H(4) | 1.000(13) | C(15)-H(15) | 1.031(13) |

Symmetry transformations used to generate equivalent atoms:

#1 -x,y,-z-1/2

Table 3.6.angle. Bond angles (°).

| | | | |
|---|---|---|---|
| C(6)-C(1)-C(2) | 118.19(14) | C(6)-C(5)-H(5) | 120.2(7) |
| C(6)-C(1)-C(10) | 112.23(14) | C(5)-C(6)-C(1) | 122.51(16) |
| C(2)-C(1)-C(10) | 129.54(14) | C(5)-C(6)-H(6) | 118.7(7) |
| O(11)-C(10)-O(12) | 120.48(15) | C(1)-C(6)-H(6) | 118.8(7) |
| O(11)-C(10)-C(1) | 120.41(15) | C(15)-N(1)-C(11) | 121.18(15) |
| O(12)-C(10)-C(1) | 119.07(14) | C(15)-N(1)-H(1) | 121.6(10) |
| C(10)-O(12)-H(2) | 113.5(10) | C(11)-N(1)-H(1) | 117.0(10) |
| C(3)-C(2)-C(1) | 118.11(14) | N(1)-C(11)-C(12) | 120.57(15) |
| C(3)-C(2)-C(20) | 113.56(13) | N(1)-C(11)-H(11) | 116.3(7) |
| C(1)-C(2)-C(20) | 128.34(14) | C(12)-C(11)-H(11) | 123.1(7) |
| O(22)-C(20)-O(21) | 122.07(14) | C(11)-C(12)-C(13) | 120.05(15) |
| O(22)-C(20)-C(2) | 117.94(14) | C(11)-C(12)-H(12) | 117.7(8) |
| O(21)-C(20)-C(2) | 119.99(14) | C(13)-C(12)-H(12) | 122.2(8) |
| C(20)-O(21)-H(2) | 113.3(8) | C(12)-C(13)-C(14) | 117.79(14) |
| C(4)-C(3)-C(2) | 122.12(16) | C(12)-C(13)-C(13)#1 | 121.01(17) |
| C(4)-C(3)-H(3) | 121.8(7) | C(14)-C(13)-C(13)#1 | 121.19(17) |
| C(2)-C(3)-H(3) | 116.0(7) | C(15)-C(14)-C(13) | 120.22(15) |
| C(3)-C(4)-C(5) | 119.82(17) | C(15)-C(14)-H(14) | 117.5(8) |
| C(3)-C(4)-H(4) | 119.1(8) | C(13)-C(14)-H(14) | 122.2(8) |
| C(5)-C(4)-H(4) | 121.0(8) | N(1)-C(15)-C(14) | 120.16(16) |
| C(4)-C(5)-C(6) | 118.98(16) | N(1)-C(15)-H(15) | 116.6(8) |
| C(4)-C(5)-H(5) | 120.8(7) | C(14)-C(15)-H(15) | 123.2(8) |

Symmetry transformations used to generate equivalent atoms:

#1 -x,y,-z-1/2

Table 3.6.anis. Anisotropic displacement parameters ($Å^2 x\ 10^3$). The anisotropic displacement factor exponent takes the form: $-2p^2[\ h^2\ a^{*2}U^{11} + ... + 2\ h\ k\ a^*\ b^*\ U^{12}\ ]$

| | U11 | U22 | U33 | U23 | U13 | U12 |
|---|---|---|---|---|---|---|
| C(1) | 22(1) | 27(1) | 15(1) | 1(1) | 1(1) | -1(1) |
| C(10) | 33(1) | 30(1) | 24(1) | -4(1) | 6(1) | -3(1) |
| O(11) | 29(1) | 54(1) | 32(1) | -2(1) | 4(1) | 13(1) |
| O(12) | 42(1) | 93(1) | 17(1) | -3(1) | 3(1) | 20(1) |
| C(2) | 23(1) | 24(1) | 18(1) | 2(1) | -1(1) | -4(1) |
| C(20) | 34(1) | 35(1) | 19(1) | 0(1) | -3(1) | 1(1) |
| O(21) | 39(1) | 100(1) | 16(1) | -3(1) | -1(1) | 23(1) |
| O(22) | 27(1) | 63(1) | 26(1) | -4(1) | -6(1) | 12(1) |
| C(3) | 19(1) | 31(1) | 22(1) | 2(1) | 1(1) | -3(1) |
| C(4) | 30(1) | 31(1) | 18(1) | -2(1) | 4(1) | -3(1) |
| C(5) | 27(1) | 34(1) | 18(1) | 2(1) | -3(1) | -5(1) |
| C(6) | 20(1) | 31(1) | 26(1) | 0(1) | 0(1) | 0(1) |
| N(1) | 26(1) | 32(1) | 22(1) | 1(1) | -3(1) | 3(1) |
| C(11) | 23(1) | 35(1) | 25(1) | 2(1) | 1(1) | 2(1) |
| C(12) | 26(1) | 31(1) | 18(1) | -1(1) | 4(1) | 0(1) |
| C(13) | 25(1) | 21(1) | 18(1) | 1(1) | 0(1) | -1(1) |
| C(14) | 22(1) | 31(1) | 26(1) | 0(1) | 0(1) | 5(1) |
| C(15) | 28(1) | 35(1) | 21(1) | -1(1) | 1(1) | 4(1) |

Table 3.6.H. Hydrogen coordinates ( $x\ 10^4$) and isotropic displacement parameters ($Å^2 x\ 10^3$).

| | x | y | z | U(eq) |
|---|---|---|---|---|
| H(2) | 3243(12) | 9190(30) | 73(12) | 103(7) |
| H(3) | 2184(7) | 11412(17) | 2245(7) | 24(4) |
| H(4) | 2876(6) | 11320(19) | 3601(8) | 29(4) |
| H(5) | 3969(7) | 9607(17) | 3737(8) | 26(4) |
| H(6) | 4421(7) | 8384(17) | 2507(8) | 21(4) |
| H(1) | 1364(10) | 11080(30) | -10(12) | 98(7) |
| H(11) | 1870(7) | 10475(17) | -1236(8) | 28(4) |
| H(12) | 1166(7) | 10561(16) | -2568(8) | 20(4) |
| H(14) | -537(7) | 12085(17) | -1298(8) | 21(4) |
| H(15) | 185(7) | 12054(18) | 8(9) | 31(4) |

**Supplement 3.7. Tables of Refinement Results for the X-ray Structure of the 1:1 Co-crystal of 4,4'-Bipyridine and Phthalic acid at 200K**

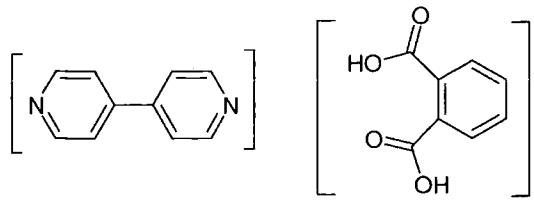


[BPY] [PHT]

Table 3.7.xyz. Atomic coordinates ( x $10^4$) and equivalent isotropic displacement parameters ($Å^2$x $10^3$). U(eq) is defined as one third of the trace of the orthogonalized $U^{ij}$ tensor.

| | x | y | z | U(eq) |
|---|---|---|---|---|
| C(1) | 278(1) | 6176(1) | 2134(1) | 31(1) |
| C(10) | 526(1) | 4541(1) | 1643(1) | 34(1) |
| O(12) | 1334(1) | 4518(1) | 1515(1) | 44(1) |
| O(11) | 19(1) | 3404(1) | 1371(1) | 61(1) |
| C(2) | 560(1) | 7744(2) | 1788(1) | 39(1) |
| C(3) | 279(1) | 9297(2) | 2146(1) | 44(1) |
| N(1) | 1838(1) | 1593(1) | 794(1) | 41(1) |
| C(20) | 2524(1) | 809(2) | 1272(1) | 63(1) |
| C(21) | 2810(1) | -777(2) | 979(2) | 66(1) |
| C(22) | 2366(1) | -1631(2) | 158(1) | 32(1) |
| C(23) | 1651(1) | -804(2) | -345(1) | 49(1) |
| C(24) | 1412(1) | 785(2) | -3(1) | 53(1) |

Table 3.7.bond. Bond lengths (Å).

| | | | |
|---|---|---|---|
| C(1)-C(2) | 1.3953(16) | N(1)-C(24) | 1.3235(18) |
| C(1)-C(1)#1 | 1.398(3) | C(20)-C(21) | 1.386(2) |
| C(1)-C(10) | 1.5031(16) | C(20)-H(20) | 0.96(2) |
| C(10)-O(11) | 1.2093(15) | C(21)-C(22) | 1.3752(19) |
| C(10)-O(12) | 1.3089(15) | C(21)-H(21) | 0.95(2) |
| O(12)-H(1) | 0.97(2) | C(22)-C(23) | 1.3811(19) |
| C(2)-C(3) | 1.3901(18) | C(22)-C(22)#2 | 1.491(2) |
| C(2)-H(2) | 0.956(15) | C(23)-C(24) | 1.3841(19) |
| C(3)-C(3)#1 | 1.375(3) | C(23)-H(23) | 0.974(18) |
| C(3)-H(3) | 0.990(16) | C(24)-H(24) | 0.960(18) |
| N(1)-C(20) | 1.3186(19) | | |

Symmetry transformations used to generate equivalent atoms:

#1 -x,y,-z+1/2 #2 -x+1/2,-y-1/2,-z

Table 3.7.angle. Bond angles (°).

| | | | |
|---|---|---|---|
| C(2)-C(1)-C(1)#1 | 119.29(8) | N(1)-C(20)-H(20) | 116.5(12) |
| C(2)-C(1)-C(10) | 118.61(12) | C(21)-C(20)-H(20) | 119.8(12) |
| C(1)#1-C(1)-C(10) | 121.92(7) | C(22)-C(21)-C(20) | 120.01(14) |
| O(11)-C(10)-O(12) | 124.38(11) | C(22)-C(21)-H(21) | 123.9(12) |
| O(11)-C(10)-C(1) | 122.85(11) | C(20)-C(21)-H(21) | 116.1(12) |
| O(12)-C(10)-C(1) | 112.73(10) | C(21)-C(22)-C(23) | 116.34(12) |
| C(10)-O(12)-H(1) | 109.4(12) | C(21)-C(22)-C(22)#2 | 121.67(14) |
| C(3)-C(2)-C(1) | 120.73(12) | C(23)-C(22)-C(22)#2 | 121.98(14) |
| C(3)-C(2)-H(2) | 122.0(8) | C(22)-C(23)-C(24) | 119.81(13) |
| C(1)-C(2)-H(2) | 117.2(8) | C(22)-C(23)-H(23) | 122.0(10) |
| C(3)#1-C(3)-C(2) | 119.97(8) | C(24)-C(23)-H(23) | 118.0(10) |
| C(3)#1-C(3)-H(3) | 120.4(9) | N(1)-C(24)-C(23) | 123.56(14) |
| C(2)-C(3)-H(3) | 119.6(9) | N(1)-C(24)-H(24) | 116.1(11) |
| C(20)-N(1)-C(24) | 116.71(12) | C(23)-C(24)-H(24) | 120.3(11) |
| N(1)-C(20)-C(21) | 123.56(14) | | |

Symmetry transformations used to generate equivalent atoms:

#1 -x,y,-z+1/2 #2 -x+1/2,-y-1/2,-z

Table 3.7.anis. Anisotropic displacement parameters ($Å^2 x\ 10^3$). The anisotropic displacement factor exponent takes the form: $-2p^2[\ h^2\ a^{*2}U^{11} + ... + 2\ h\ k\ a^*\ b^*\ U^{12}\ ]$

| | U11 | U22 | U33 | U23 | U13 | U12 |
|---|---|---|---|---|---|---|
| C(1) | 26(1) | 22(1) | 46(1) | 0(1) | 5(1) | 1(1) |
| C(10) | 33(1) | 25(1) | 46(1) | 1(1) | 7(1) | 3(1) |
| O(12) | 35(1) | 38(1) | 60(1) | -14(1) | 14(1) | 1(1) |
| O(11) | 40(1) | 33(1) | 112(1) | -23(1) | 14(1) | -4(1) |
| C(2) | 37(1) | 29(1) | 54(1) | 4(1) | 14(1) | -1(1) |
| C(3) | 44(1) | 22(1) | 65(1) | 6(1) | 8(1) | -3(1) |
| N(1) | 38(1) | 38(1) | 47(1) | -8(1) | 10(1) | 5(1) |
| C(20) | 54(1) | 61(1) | 67(1) | -34(1) | -17(1) | 22(1) |
| C(21) | 52(1) | 63(1) | 72(1) | -34(1) | -24(1) | 28(1) |
| C(22) | 29(1) | 35(1) | 35(1) | -4(1) | 10(1) | 2(1) |
| C(23) | 54(1) | 41(1) | 46(1) | -9(1) | -10(1) | 10(1) |
| C(24) | 52(1) | 43(1) | 57(1) | -7(1) | -10(1) | 15(1) |

Table 3.7.H. Hydrogen coordinates ( x $10^4$) and isotropic displacement parameters ($Å^2$x $10^3$).

| | x | y | z | U(eq) |
|---|---|---|---|---|
| H(1) | 1459(13) | 3450(30) | 1195(16) | 83(6) |
| H(2) | 940(10) | 7700(17) | 1289(12) | 43(4) |
| H(3) | 459(10) | 10396(19) | 1863(12) | 55(5) |
| H(20) | 2851(12) | 1430(30) | 1829(15) | 76(6) |
| H(21) | 3317(14) | -1200(20) | 1373(16) | 88(6) |
| H(23) | 1276(12) | -1340(20) | -906(15) | 66(5) |
| H(24) | 901(12) | 1340(20) | -328(15) | 68(5) |

**Supplement 3.8. Tables of Refinement Results for the X-ray Structure of the 1:2 Co-crystal of Bis-1,2-(4-pyridinium)ethane Hydrogen Phthalate at 100K.**

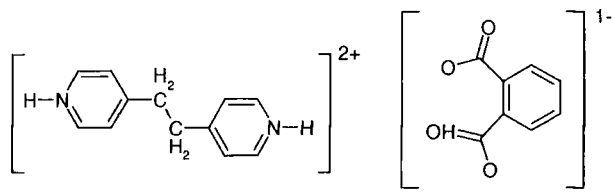

[BPA2+] [PHT-]

Table 3.8.xyz. Atomic coordinates ( x $10^4$) and equivalent isotropic displacement parameters ($Å^2$x $10^3$). U(eq) is defined as one third of the trace of the orthogonalized $U^{ij}$ tensor.

| | x | y | z | U(eq) |
|---|---|---|---|---|
| C(1) | 1419(1) | 3743(2) | 7080(1) | 15(1) |
| C(10) | 922(1) | 4204(2) | 7558(1) | 17(1) |
| O(11) | 1035(1) | 4808(1) | 8367(1) | 24(1) |
| O(12) | 385(1) | 3927(1) | 7043(1) | 27(1) |
| C(2) | 1956(1) | 2961(2) | 7596(1) | 15(1) |
| C(20) | 2012(1) | 2380(2) | 8599(1) | 15(1) |
| O(21) | 1637(1) | 1273(1) | 8782(1) | 19(1) |
| O(22) | 2462(1) | 3052(1) | 9196(1) | 21(1) |
| C(3) | 2428(1) | 2639(2) | 7160(1) | 18(1) |
| C(4) | 2367(1) | 3085(2) | 6216(1) | 20(1) |
| C(5) | 1835(1) | 3860(2) | 5701(1) | 20(1) |
| C(6) | 1363(1) | 4173(2) | 6134(1) | 18(1) |
| N(1) | 1056(1) | 1488(1) | 10146(1) | 20(1) |
| C(31) | 503(1) | 2225(2) | 9860(1) | 20(1) |
| C(32) | 119(1) | 2218(2) | 10458(1) | 19(1) |
| C(33) | 299(1) | 1458(2) | 11359(1) | 16(1) |
| C(34) | 882(1) | 751(2) | 11634(1) | 18(1) |
| C(35) | 1251(1) | 771(2) | 11013(1) | 20(1) |
| C(36) | -141(1) | 1373(2) | 11976(1) | 20(1) |

Table 3.8.bond. Bond lengths (Å).

| | | | |
|---|---|---|---|
| C(1)-C(6) | 1.3971(16) | C(6)-H(6) | 0.973(12) |
| C(1)-C(2) | 1.4069(15) | N(1)-C(35) | 1.3489(16) |
| C(1)-C(10) | 1.5104(16) | N(1)-C(31) | 1.3514(16) |
| C(10)-O(11) | 1.2332(14) | N(1)-H(1) | 1.018(16) |
| C(10)-O(12) | 1.3009(13) | C(31)-C(32) | 1.3801(17) |
| O(12)-H(12) | 1.236(4) | C(31)-H(31) | 0.977(15) |
| C(2)-C(3) | 1.4003(16) | C(32)-C(33) | 1.4015(17) |
| C(2)-C(20) | 1.5059(16) | C(32)-H(32) | 0.973(13) |
| C(20)-O(21) | 1.2498(14) | C(33)-C(34) | 1.4031(16) |
| C(20)-O(22) | 1.2832(13) | C(33)-C(36) | 1.5063(17) |
| O(22)-H(22) | 1.2284(8) | C(34)-C(35) | 1.3803(17) |
| C(3)-C(4) | 1.3952(17) | C(34)-H(34) | 0.974(13) |
| C(3)-H(3) | 0.984(13) | C(35)-H(35) | 0.979(14) |
| C(4)-C(5) | 1.3954(17) | C(36)-C(36)#1 | 1.521(2) |
| C(4)-H(4) | 0.971(16) | C(36)-H(36A) | 1.001(17) |
| C(5)-C(6) | 1.3966(17) | C(36)-H(36B) | 0.964(16) |
| C(5)-H(5) | 0.978(15) | | |

Symmetry transformations used to generate equivalent atoms:

#1 -x,y,-z+5/2

Table 3.8.angle. Bond angles (°).

| | | | |
|---|---|---|---|
| C(6)-C(1)-C(2) | 119.25(11) | C(1)-C(6)-H(6) | 118.7(7) |
| C(6)-C(1)-C(10) | 120.47(10) | C(35)-N(1)-C(31) | 121.63(11) |
| C(2)-C(1)-C(10) | 120.20(10) | C(35)-N(1)-H(1) | 120.9(8) |
| O(11)-C(10)-O(12) | 124.80(11) | C(31)-N(1)-H(1) | 117.5(8) |
| O(11)-C(10)-C(1) | 120.80(10) | N(1)-C(31)-C(32) | 119.71(11) |
| O(12)-C(10)-C(1) | 114.40(10) | N(1)-C(31)-H(31) | 116.6(8) |
| C(10)-O(12)-H(12) | 111.7(3) | C(32)-C(31)-H(31) | 123.7(8) |
| C(3)-C(2)-C(1) | 119.79(10) | C(31)-C(32)-C(33) | 120.61(11) |
| C(3)-C(2)-C(20) | 120.09(10) | C(31)-C(32)-H(32) | 119.6(8) |
| C(1)-C(2)-C(20) | 120.04(10) | C(33)-C(32)-H(32) | 119.7(8) |
| O(21)-C(20)-O(22) | 125.61(11) | C(32)-C(33)-C(34) | 117.68(11) |
| O(21)-C(20)-C(2) | 118.89(10) | C(32)-C(33)-C(36) | 119.42(10) |
| O(22)-C(20)-C(2) | 115.46(9) | C(34)-C(33)-C(36) | 122.86(10) |
| C(20)-O(22)-H(22) | 113.32(8) | C(35)-C(34)-C(33) | 119.93(11) |
| C(4)-C(3)-C(2) | 120.33(11) | C(35)-C(34)-H(34) | 118.1(7) |
| C(4)-C(3)-H(3) | 120.5(8) | C(33)-C(34)-H(34) | 121.9(7) |

| | | | |
|---|---|---|---|
| C(2)-C(3)-H(3) | 119.2(8) | N(1)-C(35)-C(34) | 120.41(11) |
| C(3)-C(4)-C(5) | 120.10(11) | N(1)-C(35)-H(35) | 115.3(8) |
| C(3)-C(4)-H(4) | 117.9(8) | C(34)-C(35)-H(35) | 124.2(8) |
| C(5)-C(4)-H(4) | 121.9(8) | C(33)-C(36)-C(36)#1 | 114.76(12) |
| C(4)-C(5)-C(6) | 119.62(11) | C(33)-C(36)-H(36A) | 106.0(9) |
| C(4)-C(5)-H(5) | 121.2(8) | C(36)#1-C(36)-H(36A) | 109.5(9) |
| C(6)-C(5)-H(5) | 119.2(8) | C(33)-C(36)-H(36B) | 110.0(10) |
| C(5)-C(6)-C(1) | 120.90(11) | C(36)#1-C(36)-H(36B) | 109.3(10) |
| C(5)-C(6)-H(6) | 120.4(7) | H(36A)-C(36)-H(36B) | 107.0(13) |

Symmetry transformations used to generate equivalent atoms:

#1 -x,y,-z+5/2

Table 3.8.anis. Anisotropic displacement parameters ($Å^2 x\ 10^3$). The anisotropic displacement factor exponent takes the form: $-2p^2[\ h^2\ a^{*2}U^{11} + ... + 2\ h\ k\ a^*\ b^*\ U^{12}\ ]$

| | U11 | U22 | U33 | U23 | U13 | U12 |
|---|---|---|---|---|---|---|
| C(1) | 14(1) | 14(1) | 17(1) | -1(1) | 5(1) | -3(1) |
| C(10) | 16(1) | 16(1) | 20(1) | 3(1) | 5(1) | 1(1) |
| O(11) | 20(1) | 32(1) | 22(1) | -6(1) | 6(1) | 4(1) |
| O(12) | 13(1) | 44(1) | 24(1) | -4(1) | 5(1) | -1(1) |
| C(2) | 15(1) | 14(1) | 15(1) | -1(1) | 4(1) | -3(1) |
| C(20) | 13(1) | 17(1) | 17(1) | 0(1) | 6(1) | 4(1) |
| O(21) | 18(1) | 22(1) | 17(1) | 0(1) | 8(1) | -1(1) |
| O(22) | 18(1) | 27(1) | 16(1) | 1(1) | 2(1) | -3(1) |
| C(3) | 15(1) | 18(1) | 21(1) | -2(1) | 6(1) | -1(1) |
| C(4) | 20(1) | 19(1) | 22(1) | -3(1) | 11(1) | -4(1) |
| C(5) | 25(1) | 20(1) | 16(1) | 1(1) | 7(1) | -5(1) |
| C(6) | 18(1) | 17(1) | 18(1) | 1(1) | 2(1) | -1(1) |
| N(1) | 23(1) | 19(1) | 21(1) | -3(1) | 12(1) | -3(1) |
| C(31) | 26(1) | 18(1) | 16(1) | 0(1) | 6(1) | -4(1) |
| C(32) | 18(1) | 17(1) | 21(1) | -1(1) | 4(1) | 0(1) |
| C(33) | 18(1) | 15(1) | 17(1) | -2(1) | 6(1) | -1(1) |
| C(34) | 20(1) | 19(1) | 18(1) | 2(1) | 7(1) | 2(1) |
| C(35) | 20(1) | 19(1) | 23(1) | -1(1) | 8(1) | 0(1) |
| C(36) | 17(1) | 28(1) | 18(1) | 0(1) | 7(1) | 2(1) |

Table 3.8.H. Hydrogen coordinates ( x $10^4$) and isotropic displacement parameters ($Å^2$x $10^3$).

| | x | y | z | U(eq) |
|---|---|---|---|---|
| H(12) | 0 | 4120(40) | 7500 | 86(9) |
| H(22) | 2500 | 2500 | 10000 | 82(9) |
| H(3) | 2801(6) | 2082(18) | 7526(10) | 23(3) |
| H(4) | 2699(7) | 2808(19) | 5933(10) | 31(4) |
| H(5) | 1790(6) | 4230(20) | 5046(11) | 32(4) |
| H(6) | 991(5) | 4724(17) | 5784(9) | 17(3) |
| H(1) | 1323(7) | 1500(20) | 9681(11) | 40(4) |
| H(31) | 403(6) | 2775(19) | 9233(10) | 29(4) |
| H(32) | -282(6) | 2726(17) | 10247(9) | 20(3) |
| H(34) | 1039(5) | 231(18) | 12256(9) | 20(3) |
| H(35) | 1657(6) | 267(18) | 11151(9) | 25(3) |
| H(36A) | -374(7) | 210(20) | 11802(11) | 47(5) |
| H(36B) | -421(7) | 2380(20) | 11829(11) | 43(4) |

**Supplement 4.100X. Tables of Refinement Results for the X-ray Structure Pyridine-3,5-dicarboxylic acid at 100K.**

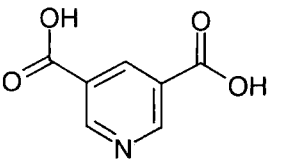


**[PDA]**

Table 4.100X.xyz. Atomic coordinates ( x $10^4$) and equivalent isotropic displacement parameters ($Å^2$x $10^3$). U(eq) is defined as one third of the trace of the orthogonalized $U^{ij}$ tensor.

| | x | y | z | U(eq) |
|---|---|---|---|---|
| C(2) | -3177(2) | -3442(1) | 2224(2) | 15(1) |
| C(3) | -3890(2) | -4477(1) | 2514(2) | 13(1) |
| C(4) | -3191(2) | -5582(1) | 2652(2) | 13(1) |
| C(5) | -1797(2) | -5629(1) | 2480(2) | 14(1) |
| C(6) | -1148(2) | -4558(1) | 2190(2) | 16(1) |
| C(7) | -5402(2) | -4424(1) | 2648(2) | 14(1) |
| C(8) | -947(2) | -6779(1) | 2634(2) | 15(1) |
| N(1) | -1832(1) | -3504(1) | 2063(2) | 15(1) |
| O(1) | -5833(1) | -3304(1) | 2729(2) | 20(1) |
| O(2) | -6122(1) | -5317(1) | 2650(2) | 17(1) |
| O(3) | -1544(1) | -7781(1) | 2485(2) | 18(1) |
| O(4) | 399(1) | -6614(1) | 2925(2) | 21(1) |

Table 4.100X.bond. Bond lengths (Å).

| | | | |
|---|---|---|---|
| C(2)-N(1) | 1.3486(18) | C(6)-N(1) | 1.3412(18) |
| C(2)-C(3) | 1.3905(19) | C(6)-H(3) | 0.94(2) |
| C(2)-H(1) | 0.97(2) | C(7)-O(2) | 1.2181(17) |
| C(3)-C(4) | 1.3980(19) | C(7)-O(1) | 1.3245(17) |
| C(3)-C(7) | 1.5035(19) | C(8)-O(3) | 1.2498(17) |
| C(4)-C(5) | 1.398(2) | C(8)-O(4) | 1.2770(18) |
| C(4)-H(2) | 0.93(3) | O(1)-H(4) | 0.91(3) |
| C(5)-C(6) | 1.3929(19) | O(4)-H(5) | 1.36(3) |
| C(5)-C(8) | 1.5127(19) | | |

Table. 4.100X.angle. Bond angles (°).

| | | | |
|---|---|---|---|
| N(1)-C(2)-C(3) | 120.48(13) | N(1)-C(6)-C(5) | 121.58(13) |
| N(1)-C(2)-H(1) | 114.7(13) | N(1)-C(6)-H(3) | 115.1(11) |
| C(3)-C(2)-H(1) | 124.8(13) | C(5)-C(6)-H(3) | 123.2(11) |
| C(2)-C(3)-C(4) | 119.17(13) | O(2)-C(7)-O(1) | 125.58(13) |
| C(2)-C(3)-C(7) | 121.01(12) | O(2)-C(7)-C(3) | 122.83(12) |
| C(4)-C(3)-C(7) | 119.81(12) | O(1)-C(7)-C(3) | 111.59(12) |
| C(5)-C(4)-C(3) | 119.58(12) | O(3)-C(8)-O(4) | 124.80(13) |
| C(5)-C(4)-H(2) | 119.6(14) | O(3)-C(8)-C(5) | 121.51(13) |
| C(3)-C(4)-H(2) | 120.8(14) | O(4)-C(8)-C(5) | 113.69(12) |
| C(6)-C(5)-C(4) | 118.17(12) | C(6)-N(1)-C(2) | 121.02(12) |
| C(6)-C(5)-C(8) | 118.37(13) | C(7)-O(1)-H(4) | 116.1(17) |
| C(4)-C(5)-C(8) | 123.45(12) | C(8)-O(4)-H(5) | 113.8(13) |

Table 4.100X.anis. Anisotropic displacement parameters ($Å^2 x\ 10^3$). The anisotropic displacement factor exponent takes the form: $-2p^2[\ h^2\ a^{*2}U^{11} + ... + 2\ h\ k\ a^*\ b^*\ U^{12}\ ]$

| | U11 | U22 | U33 | U23 | U13 | U12 |
|---|---|---|---|---|---|---|
| C(2) | 13(1) | 13(1) | 18(1) | 0(1) | 4(1) | 1(1) |
| C(3) | 12(1) | 13(1) | 15(1) | 0(1) | 4(1) | 0(1) |
| C(4) | 13(1) | 12(1) | 16(1) | 0(1) | 4(1) | 0(1) |
| C(5) | 12(1) | 13(1) | 16(1) | -1(1) | 3(1) | 1(1) |
| C(6) | 12(1) | 15(1) | 20(1) | -1(1) | 5(1) | 0(1) |
| C(7) | 13(1) | 13(1) | 15(1) | 1(1) | 5(1) | 1(1) |
| C(8) | 14(1) | 13(1) | 18(1) | -1(1) | 5(1) | 1(1) |
| N(1) | 13(1) | 13(1) | 20(1) | 0(1) | 5(1) | -1(1) |
| O(1) | 15(1) | 13(1) | 35(1) | 2(1) | 11(1) | 3(1) |
| O(2) | 15(1) | 16(1) | 20(1) | 1(1) | 6(1) | -2(1) |
| O(3) | 15(1) | 13(1) | 28(1) | -1(1) | 8(1) | 0(1) |
| O(4) | 12(1) | 14(1) | 35(1) | -2(1) | 7(1) | 1(1) |

Table 4.100X.H. Hydrogen coordinates ( $x\ 10^4$) and isotropic displacement parameters ($Å^2 x\ 10^3$).

| | x | y | z | U(eq) |
|---|---|---|---|---|
| H(1) | -3560(20) | -2640(20) | 2170(30) | 26(5) |
| H(2) | -3650(30) | -6290(20) | 2850(40) | 33(6) |
| H(3) | -190(20) | -4510(16) | 2140(30) | 14(4) |
| H(4) | -6770(30) | -3210(20) | 2710(40) | 48(7) |
| H(5) | 1160(30) | -7640(30) | 3060(50) | 71(10) |

**Supplement 4.296N. Tables of Refinement Results for the Neutron Structure Pyridine-3,5-dicarboxylic acid at 296K.**

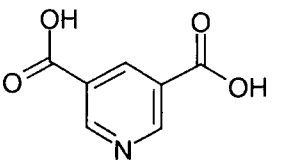


**[PDA]**

Table 4.296N.xyz. Atomic coordinates ( x $10^4$) and equivalent isotropic displacement parameters ($Å^2$x $10^3$). U(eq) is defined as one third of the trace of the orthogonalized $U^{ij}$ tensor.

| | x | y | z | U(eq) |
|---|---|---|---|---|
| C(2) | -3157(2) | -3419(2) | 2276(4) | 29(1) |
| C(3) | -3886(2) | -4457(2) | 2522(3) | 23(1) |
| C(4) | -3187(2) | -5558(2) | 2626(4) | 26(1) |
| C(5) | -1791(2) | -5594(2) | 2471(4) | 26(1) |
| C(6) | -1138(2) | -4522(2) | 2227(4) | 31(1) |
| C(7) | -5390(2) | -4408(2) | 2646(4) | 27(1) |
| C(8) | -963(2) | -6740(2) | 2573(4) | 29(1) |
| N(1) | -1815(2) | -3474(1) | 2132(3) | 32(1) |
| O(1) | -5836(3) | -3302(2) | 2715(6) | 46(1) |
| O(2) | -6109(2) | -5289(2) | 2655(5) | 34(1) |
| O(3) | -1542(2) | -7722(2) | 2466(5) | 38(1) |
| O(4) | 382(2) | -6578(2) | 2810(6) | 45(1) |
| H(1) | -3635(4) | -2541(4) | 2195(10) | 49(1) |
| H(2) | -3751(5) | -6367(4) | 2817(10) | 48(1) |
| H(3) | -31(4) | -4488(4) | 2146(10) | 54(1) |
| H(4) | -6875(5) | -3219(4) | 2674(10) | 51(1) |
| H(5) | 1072(5) | -7496(5) | 2872(10) | 55(1) |

Table 4.296N.bond. Bond lengths (Å).

| | | | |
|---|---|---|---|
| C(2)-N(1) | 1.335(2) | C(6)-N(1) | 1.333(2) |
| C(2)-C(3) | 1.392(3) | C(6)-H(3) | 1.092(4) |
| C(2)-H(1) | 1.078(4) | C(7)-O(2) | 1.206(3) |
| C(3)-C(4) | 1.393(2) | C(7)-O(1) | 1.313(3) |
| C(3)-C(7) | 1.487(2) | C(8)-O(3) | 1.223(3) |
| C(4)-C(5) | 1.390(2) | C(8)-O(4) | 1.279(3) |
| C(4)-H(2) | 1.083(4) | O(1)-H(4) | 1.004(5) |
| C(5)-C(6) | 1.385(3) | O(4)-H(5) | 1.218(6) |
| C(5)-C(8) | 1.500(3) | | |

Table 4.296N.angle. Bond angles (°).

| | | | |
|---|---|---|---|
| N(1)-C(2)-C(3) | 120.68(17) | N(1)-C(6)-C(5) | 121.80(15) |
| N(1)-C(2)-H(1) | 116.9(3) | N(1)-C(6)-H(3) | 116.4(3) |
| C(3)-C(2)-H(1) | 122.4(3) | C(5)-C(6)-H(3) | 121.8(3) |
| C(2)-C(3)-C(4) | 118.85(15) | O(2)-C(7)-O(1) | 124.6(2) |
| C(2)-C(3)-C(7) | 121.14(16) | O(2)-C(7)-C(3) | 123.3(2) |
| C(4)-C(3)-C(7) | 120.01(16) | O(1)-C(7)-C(3) | 112.08(18) |
| C(5)-C(4)-C(3) | 119.49(17) | O(3)-C(8)-O(4) | 124.5(2) |
| C(5)-C(4)-H(2) | 121.5(3) | O(3)-C(8)-C(5) | 122.07(19) |
| C(3)-C(4)-H(2) | 119.0(3) | O(4)-C(8)-C(5) | 113.40(19) |
| C(6)-C(5)-C(4) | 118.25(17) | C(6)-N(1)-C(2) | 120.93(15) |
| C(6)-C(5)-C(8) | 118.94(15) | C(7)-O(1)-H(4) | 115.1(3) |
| C(4)-C(5)-C(8) | 122.80(17) | C(8)-O(4)-H(5) | 114.5(3) |

Table 4.296N.anis. Anisotropic displacement parameters ($Å^2 x\ 10^3$). The anisotropic displacement factor exponent takes the form: $-2p^2[\ h^2\ a^{*2}U^{11} + ... + 2\ h\ k\ a^*\ b^*\ U^{12}\ ]$

| | U11 | U22 | U33 | U23 | U13 | U12 |
|---|---|---|---|---|---|---|
| C(2) | 21(1) | 17(1) | 52(1) | 4(1) | 16(1) | 1(1) |
| C(3) | 18(1) | 18(1) | 37(1) | 3(1) | 13(1) | 1(1) |
| C(4) | 20(1) | 16(1) | 44(1) | 0(1) | 14(1) | 0(1) |
| C(5) | 19(1) | 19(1) | 43(1) | -1(1) | 12(1) | 1(1) |
| C(6) | 18(1) | 20(1) | 57(1) | -1(1) | 16(1) | -1(1) |
| C(7) | 19(1) | 21(1) | 44(1) | 3(1) | 14(1) | 1(1) |
| C(8) | 19(1) | 19(1) | 54(1) | -1(1) | 16(1) | 1(1) |
| H(1) | 43(2) | 22(2) | 90(4) | 0(2) | 30(2) | 6(2) |
| H(2) | 40(2) | 25(2) | 89(4) | 7(2) | 34(2) | 1(2) |
| H(3) | 31(2) | 39(2) | 101(4) | 3(3) | 33(2) | 0(2) |
| H(4) | 37(2) | 36(2) | 87(4) | 1(2) | 31(2) | 7(2) |
| H(5) | 36(2) | 58(3) | 75(4) | -3(3) | 22(2) | -11(2) |
| N(1) | 22(1) | 19(1) | 60(1) | 0(1) | 18(1) | -2(1) |
| O(1) | 27(1) | 23(1) | 94(2) | 3(1) | 30(1) | 7(1) |
| O(2) | 25(1) | 26(1) | 56(2) | 0(1) | 18(1) | -3(1) |
| O(3) | 24(1) | 20(1) | 74(2) | -2(1) | 21(1) | 0(1) |
| O(4) | 20(1) | 23(1) | 95(2) | -5(1) | 22(1) | 1(1) |

**Supplement 4.15N. Tables of Refinement Results for the Neutron Structure of Pyridine-3,5-dicarboxylic acid at 15K.**

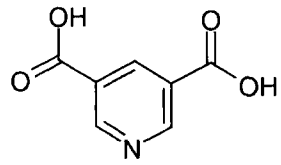


**[PDA]**

Table 4.15N.xyz. Atomic coordinates ( x $10^4$) and equivalent isotropic displacement parameters ($Å^2$x $10^3$). U(eq) is defined as one third of the trace of the orthogonalized $U^{ij}$ tensor.

| | x | y | z | U(eq) |
|---|---|---|---|---|
| C(2) | -3176(2) | -3442(2) | 2204(3) | 6(1) |
| C(3) | -3893(2) | -4482(1) | 2512(3) | 4(1) |
| C(4) | -3192(2) | -5588(1) | 2659(3) | 5(1) |
| C(5) | -1798(2) | -5638(1) | 2482(3) | 4(1) |
| C(6) | -1147(2) | -4562(1) | 2178(3) | 6(1) |
| C(7) | -5405(2) | -4423(1) | 2647(3) | 4(1) |
| C(8) | -945(2) | -6786(1) | 2645(3) | 5(1) |
| N(1) | -1838(1) | -3511(1) | 2044(2) | 6(1) |
| O(1) | -5837(2) | -3307(2) | 2730(4) | 8(1) |
| O(2) | -6118(2) | -5320(2) | 2659(4) | 7(1) |
| O(3) | -1542(2) | -7787(2) | 2495(4) | 7(1) |
| O(4) | 405(2) | -6619(2) | 2941(4) | 8(1) |
| H(1) | -3661(4) | -2548(3) | 2097(7) | 19(1) |
| H(2) | -3745(4) | -6396(3) | 2918(8) | 19(1) |
| H(3) | -55(4) | -4526(3) | 2066(8) | 20(1) |
| H(4) | -6899(4) | -3215(4) | 2673(7) | 20(1) |
| H(5) | 1152(4) | -7608(4) | 3011(7) | 22(1) |

Table 4.15N.bond. Bond lengths (Å).

| | | | |
|---|---|---|---|
| C(2)-N(1) | 1.338(2) | C(6)-N(1) | 1.3381(19) |
| C(2)-C(3) | 1.397(2) | C(6)-H(3) | 1.086(4) |
| C(2)-H(1) | 1.094(4) | C(7)-O(2) | 1.217(2) |
| C(3)-C(4) | 1.396(2) | C(7)-O(1) | 1.319(2) |
| C(3)-C(7) | 1.500(2) | C(8)-O(3) | 1.245(2) |
| C(4)-C(5) | 1.396(2) | C(8)-O(4) | 1.277(2) |
| C(4)-H(2) | 1.087(4) | O(1)-H(4) | 1.025(4) |
| C(5)-C(6) | 1.397(2) | O(4)-H(5) | 1.311(5) |
| C(5)-C(8) | 1.508(2) | | |

Table 4.15N.angle. Bond angles (°).

| | | | |
|---|---|---|---|
| N(1)-C(2)-C(3) | 120.21(14) | N(1)-C(6)-C(5) | 121.27(14) |
| N(1)-C(2)-H(1) | 117.2(2) | N(1)-C(6)-H(3) | 116.3(2) |
| C(3)-C(2)-H(1) | 122.6(2) | C(5)-C(6)-H(3) | 122.4(2) |
| C(4)-C(3)-C(2) | 119.15(14) | O(2)-C(7)-O(1) | 125.75(18) |
| C(4)-C(3)-C(7) | 119.95(14) | O(2)-C(7)-C(3) | 122.30(16) |
| C(2)-C(3)-C(7) | 120.89(14) | O(1)-C(7)-C(3) | 111.95(14) |
| C(3)-C(4)-C(5) | 119.60(14) | O(3)-C(8)-O(4) | 124.85(17) |
| C(3)-C(4)-H(2) | 119.1(2) | O(3)-C(8)-C(5) | 121.45(16) |
| C(5)-C(4)-H(2) | 121.3(2) | O(4)-C(8)-C(5) | 113.69(15) |
| C(4)-C(5)-C(6) | 118.12(14) | C(2)-N(1)-C(6) | 121.66(13) |
| C(4)-C(5)-C(8) | 123.57(14) | C(7)-O(1)-H(4) | 115.0(3) |
| C(6)-C(5)-C(8) | 118.29(13) | C(8)-O(4)-H(5) | 114.4(2) |

Table 4.15N.anis. Anisotropic displacement parameters ($Å^2 x\ 10^3$). The anisotropic displacement factor exponent takes the form: $-2p^2[\ h^2\ a^{*2}U^{11} + ... + 2\ h\ k\ a^*\ b^*\ U^{12}\ ]$

| | U11 | U22 | U33 | U23 | U13 | U12 |
|---|---|---|---|---|---|---|
| C(2) | 7(1) | 3(1) | 9(1) | 1(1) | 4(1) | 0(1) |
| C(3) | 4(1) | 2(1) | 6(1) | -1(1) | 3(1) | 0(1) |
| C(4) | 4(1) | 3(1) | 9(1) | 0(1) | 4(1) | 1(1) |
| C(5) | 3(1) | 3(1) | 8(1) | 1(1) | 3(1) | 0(1) |
| C(6) | 4(1) | 3(1) | 11(1) | 0(1) | 2(1) | 0(1) |
| C(7) | 3(1) | 3(1) | 6(1) | 0(1) | 2(1) | 1(1) |
| C(8) | 3(1) | 2(1) | 9(1) | 1(1) | 2(1) | 0(1) |
| H(1) | 18(2) | 9(2) | 33(2) | 4(1) | 13(2) | 5(1) |
| H(2) | 16(2) | 11(2) | 31(2) | 1(1) | 10(2) | -3(1) |
| H(3) | 14(2) | 15(2) | 34(2) | 2(1) | 11(2) | 2(1) |
| H(4) | 15(2) | 21(2) | 27(2) | 1(1) | 10(2) | 1(1) |
| H(5) | 20(2) | 20(2) | 26(2) | -1(2) | 8(2) | -5(1) |
| N(1) | 5(1) | 3(1) | 10(1) | 0(1) | 3(1) | -1(1) |
| O(1) | 5(1) | 6(1) | 13(1) | 0(1) | 4(1) | 1(1) |
| O(2) | 6(1) | 4(1) | 12(1) | 0(1) | 4(1) | -1(1) |
| O(3) | 5(1) | 5(1) | 12(1) | 0(1) | 3(1) | -1(1) |
| O(4) | 5(1) | 4(1) | 14(1) | 0(1) | 2(1) | 0(1) |

**Supplement 4.296D. Tables of Refinement Results for the Neutron Structure of Partially Deuterated Pyridine-3,5-dicarboxylic acid at 296K.**

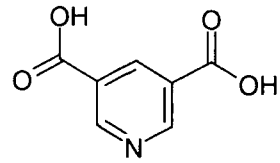


**[PDA]**

Table 4.296D.xyz. Atomic coordinates ( x $10^4$) and equivalent isotropic displacement parameters ($Å^2$x $10^3$). U(eq) is defined as one third of the trace of the orthogonalized $U^{ij}$ tensor.

| | x | y | z | U(eq) |
|---|---|---|---|---|
| C(2) | -3163(2) | -3389(2) | 2298(4) | 32(1) |
| C(3) | -3879(2) | -4427(2) | 2521(4) | 28(1) |
| C(4) | -3179(2) | -5520(2) | 2625(4) | 30(1) |
| C(5) | -1791(2) | -5542(2) | 2452(4) | 29(1) |
| C(6) | -1149(2) | -4465(2) | 2235(4) | 33(1) |
| C(7) | -5384(2) | -4389(2) | 2647(4) | 29(1) |
| C(8) | -964(2) | -6680(2) | 2550(4) | 33(1) |
| H(1) | -3653(16) | -2517(10) | 2270(30) | 49(3) |
| H(2) | -3732(5) | -6335(4) | 2832(11) | 54(2) |
| H(3) | -81(14) | -4433(12) | 2120(30) | 56(4) |
| D(4) | -6857(3) | -3225(3) | 2687(7) | 53(1) |
| D(5) | 991(3) | -7340(3) | 2814(7) | 58(1) |
| N(1) | -1827(2) | -3420(1) | 2142(3) | 37(1) |
| O(1) | -5837(3) | -3289(2) | 2713(7) | 51(1) |
| O(2) | -6091(3) | -5270(2) | 2646(5) | 38(1) |
| O(3) | -1522(3) | -7666(2) | 2456(6) | 43(1) |
| O(4) | 372(3) | -6504(2) | 2729(6) | 48(1) |

Table 4.296D.bond. Bond lengths (Å).

| | | | |
|---|---|---|---|
| C(2)-H(1) | 1.087(12) | C(6)-H(3) | 1.070(11) |
| C(2)-N(1) | 1.341(2) | C(6)-N(1) | 1.338(2) |
| C(2)-C(3) | 1.390(3) | C(7)-O(2) | 1.205(3) |
| C(3)-C(4) | 1.396(2) | C(7)-O(1) | 1.317(3) |
| C(3)-C(7) | 1.498(2) | C(8)-O(3) | 1.227(3) |
| C(4)-C(5) | 1.395(2) | C(8)-O(4) | 1.286(3) |
| C(4)-H(2) | 1.092(5) | D(4)-O(1) | 0.993(3) |
| C(5)-C(6) | 1.390(2) | D(5)-O(4) | 1.108(4) |
| C(5)-C(8) | 1.501(3) | | |

Table 4.296D.bond. Bond angles (°).

| | | | |
|---|---|---|---|
| H(1)-C(2)-N(1) | 117.1(7) | H(3)-C(6)-N(1) | 116.5(7) |
| H(1)-C(2)-C(3) | 121.6(7) | H(3)-C(6)-C(5) | 121.2(7) |
| N(1)-C(2)-C(3) | 121.33(17) | N(1)-C(6)-C(5) | 122.31(16) |
| C(2)-C(3)-C(4) | 119.18(16) | O(2)-C(7)-O(1) | 124.8(2) |
| C(2)-C(3)-C(7) | 121.11(16) | O(2)-C(7)-C(3) | 123.2(2) |
| C(4)-C(3)-C(7) | 119.71(16) | O(1)-C(7)-C(3) | 111.95(18) |
| C(5)-C(4)-C(3) | 118.97(16) | O(3)-C(8)-O(4) | 124.3(2) |
| C(5)-C(4)-H(2) | 121.8(3) | O(3)-C(8)-C(5) | 122.77(18) |
| C(3)-C(4)-H(2) | 119.2(3) | O(4)-C(8)-C(5) | 112.91(18) |
| C(6)-C(5)-C(4) | 118.31(16) | C(6)-N(1)-C(2) | 119.88(15) |
| C(6)-C(5)-C(8) | 119.36(15) | D(4)-O(1)-C(7) | 114.4(3) |
| C(4)-C(5)-C(8) | 122.31(16) | D(5)-O(4)-C(8) | 113.3(3) |

Table 4.296D.anis. Anisotropic displacement parameters ($Å^2 x\ 10^3$). The anisotropic displacement factor exponent takes the form: $-2p^2[\ h^2\ a^{*2}U^{11} + ... + 2\ h\ k\ a^*\ b^*\ U^{12}\ ]$

| | U11 | U22 | U33 | U23 | U13 | U12 |
|---|---|---|---|---|---|---|
| C(2) | 22(1) | 19(1) | 56(2) | 3(1) | 15(1) | 1(1) |
| C(3) | 20(1) | 18(1) | 47(2) | 1(1) | 14(1) | 2(1) |
| C(4) | 21(1) | 19(1) | 51(2) | 2(1) | 16(1) | 1(1) |
| C(5) | 19(1) | 19(1) | 51(2) | 1(1) | 14(1) | 2(1) |
| C(6) | 22(1) | 21(1) | 60(2) | 1(1) | 18(1) | -2(1) |
| C(7) | 20(1) | 24(1) | 47(1) | 3(1) | 14(1) | 2(1) |
| C(8) | 21(1) | 19(1) | 62(2) | -2(1) | 18(1) | 1(1) |
| H(1) | 56(7) | 23(5) | 77(11) | 7(6) | 33(7) | 3(5) |
| H(2) | 40(2) | 32(2) | 99(5) | 0(3) | 35(3) | -3(2) |
| H(3) | 31(6) | 31(6) | 113(15) | 0(7) | 30(7) | -5(4) |
| D(4) | 29(1) | 36(2) | 101(3) | 3(2) | 31(2) | 5(1) |
| D(5) | 34(1) | 51(2) | 91(3) | -9(2) | 24(2) | -11(1) |
| N(1) | 24(1) | 19(1) | 73(1) | 2(1) | 21(1) | -2(1) |
| O(1) | 30(1) | 27(1) | 106(3) | 3(2) | 33(2) | 6(1) |
| O(2) | 25(1) | 28(1) | 63(2) | 0(1) | 19(1) | -4(1) |
| O(3) | 26(1) | 23(1) | 84(2) | 2(1) | 24(1) | 0(1) |
| O(4) | 20(1) | 23(1) | 102(3) | -5(1) | 22(1) | 3(1) |

**Supplement 4.150D. Tables of Refinement Results for the Neutron Structure of Partially Deuterated Pyridine-3,5-dicarboxylic acid at 150K.**

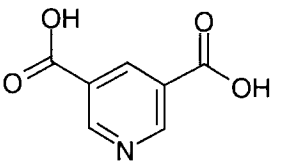


**[PDA]**

Table 4.150D.xyz. Atomic coordinates ( x $10^4$) and equivalent isotropic displacement parameters ($Å^2$x $10^3$). U(eq) is defined as one third of the trace of the orthogonalized $U^{ij}$ tensor.

| | x | y | z | U(eq) |
|---|---|---|---|---|
| C(2) | -3172(2) | -3447(2) | 2218(4) | 14(1) |
| C(3) | -3889(2) | -4480(2) | 2509(4) | 12(1) |
| C(4) | -3190(2) | -5589(2) | 2652(4) | 13(1) |
| C(5) | -1798(2) | -5636(2) | 2488(4) | 13(1) |
| C(6) | -1141(2) | -4570(2) | 2201(4) | 15(1) |
| C(7) | -5401(2) | -4428(2) | 2646(4) | 13(1) |
| C(8) | -946(2) | -6784(2) | 2648(4) | 14(1) |
| H(1) | -3661(14) | -2574(10) | 2100(30) | 29(3) |
| H(2) | -3745(5) | -6391(4) | 2905(10) | 32(1) |
| H(3) | -75(12) | -4537(10) | 2110(30) | 32(4) |
| D(4) | -6879(3) | -3222(2) | 2680(6) | 25(1) |
| D(5) | 1163(3) | -7630(3) | 3008(6) | 35(1) |
| N(1) | -1834(1) | -3514(1) | 2059(3) | 16(1) |
| O(1) | -5829(3) | -3311(2) | 2725(6) | 22(1) |
| O(2) | -6116(2) | -5317(2) | 2654(5) | 18(1) |
| O(3) | -1544(2) | -7783(2) | 2492(5) | 20(1) |
| O(4) | 397(2) | -6622(2) | 2941(6) | 23(1) |

Table 4.150D.bond. Bond lengths (Å).

| | | | |
|---|---|---|---|
| C(2)-H(1) | 1.076(11) | C(6)-H(3) | 1.056(11) |
| C(2)-N(1) | 1.340(2) | C(6)-N(1) | 1.345(2) |
| C(2)-C(3) | 1.390(2) | C(7)-O(2) | 1.212(3) |
| C(3)-C(4) | 1.400(2) | C(7)-O(1) | 1.319(3) |
| C(3)-C(7) | 1.502(2) | C(8)-O(3) | 1.246(3) |
| C(4)-C(5) | 1.392(2) | C(8)-O(4) | 1.271(3) |
| C(4)-H(2) | 1.085(4) | D(4)-O(1) | 1.016(3) |
| C(5)-C(6) | 1.390(2) | D(5)-N(1)#1 | 1.192(4) |
| C(5)-C(8) | 1.511(3) | D(5)-O(4) | 1.341(4) |

Symmetry transformations used to generate equivalent atoms:

#1 -x,y-1/2,-z+1/2 #2 -x,y+1/2,-z+1/2

Table 4.150D.angle. Bond angles (°).

| | | | |
|---|---|---|---|
| H(1)-C(2)-N(1) | 117.5(7) | N(1)-C(6)-C(5) | 121.10(16) |
| H(1)-C(2)-C(3) | 122.1(7) | O(2)-C(7)-O(1) | 125.8(2) |
| N(1)-C(2)-C(3) | 120.34(16) | O(2)-C(7)-C(3) | 122.77(19) |
| C(2)-C(3)-C(4) | 119.17(16) | O(1)-C(7)-C(3) | 111.45(17) |
| C(2)-C(3)-C(7) | 121.21(16) | O(3)-C(8)-O(4) | 124.8(2) |
| C(4)-C(3)-C(7) | 119.62(16) | O(3)-C(8)-C(5) | 121.40(17) |
| C(5)-C(4)-C(3) | 119.46(16) | O(4)-C(8)-C(5) | 113.83(18) |
| C(5)-C(4)-H(2) | 121.5(3) | N(1)#1-D(5)-O(4) | 176.1(4) |
| C(3)-C(4)-H(2) | 119.0(3) | D(5)#2-N(1)-C(2) | 120.86(18) |
| C(6)-C(5)-C(4) | 118.51(17) | D(5)#2-N(1)-C(6) | 117.35(17) |
| C(6)-C(5)-C(8) | 117.99(16) | C(2)-N(1)-C(6) | 121.41(14) |
| C(4)-C(5)-C(8) | 123.50(17) | D(4)-O(1)-C(7) | 114.6(2) |
| H(3)-C(6)-N(1) | 116.4(6) | C(8)-O(4)-D(5) | 114.7(2) |
| H(3)-C(6)-C(5) | 122.5(6) | | |

Symmetry transformations used to generate equivalent atoms:

#1 -x,y-1/2,-z+1/2 #2 -x,y+1/2,-z+1/2

Table 4.150D.anis. Anisotropic displacement parameters ($Å^2 x\ 10^3$). The anisotropic displacement factor exponent takes the form: $-2p^2[\ h^2\ a^{*2}U^{11} + ... + 2\ h\ k\ a^*\ b^*\ U^{12}\ ]$

| | U11 | U22 | U33 | U23 | U13 | U12 |
|---|---|---|---|---|---|---|
| C(2) | 11(1) | 9(1) | 23(2) | 1(1) | 7(1) | 1(1) |
| C(3) | 9(1) | 7(1) | 20(2) | 0(1) | 7(1) | 0(1) |
| C(4) | 10(1) | 7(1) | 23(2) | 1(1) | 8(1) | 0(1) |
| C(5) | 9(1) | 9(1) | 23(2) | -1(1) | 7(1) | 1(1) |
| C(6) | 10(1) | 10(1) | 26(2) | 1(1) | 9(1) | -1(1) |
| C(7) | 10(1) | 9(1) | 22(2) | 1(1) | 7(1) | 0(1) |
| C(8) | 9(1) | 8(1) | 27(2) | -2(1) | 6(1) | 1(1) |
| H(1) | 34(6) | 7(4) | 51(10) | 6(5) | 19(6) | 8(4) |
| H(2) | 22(2) | 19(2) | 59(4) | 2(2) | 18(2) | -5(2) |
| H(3) | 12(4) | 19(5) | 67(12) | -6(6) | 15(5) | -4(4) |
| D(4) | 15(1) | 19(1) | 47(2) | 1(1) | 16(1) | 3(1) |
| D(5) | 24(1) | 36(2) | 49(2) | -9(2) | 16(1) | -13(1) |
| N(1) | 10(1) | 9(1) | 31(1) | 1(1) | 10(1) | -2(1) |
| O(1) | 15(1) | 9(1) | 44(2) | 2(1) | 15(1) | 3(1) |
| O(2) | 12(1) | 12(1) | 32(2) | -2(1) | 10(1) | -3(1) |
| O(3) | 12(1) | 9(1) | 40(2) | -1(1) | 13(1) | -1(1) |
| O(4) | 10(1) | 11(1) | 49(2) | -5(1) | 11(1) | 0(1) |

**Supplement 4.15D. Tables of Refinement Results for the Neutron Structure of Partially Deuterated Pyridine-3,5-dicarboxylic acid at 15K.**

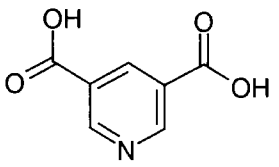


**[PDA]**

Table 4.15D.xyz. Atomic coordinates ( x $10^4$) and equivalent isotropic displacement parameters ($Å^2$x $10^3$). U(eq) is defined as one third of the trace of the orthogonalized $U^{ij}$ tensor.

| | x | y | z | U(eq) |
|---|---|---|---|---|
| C(2) | -3183(2) | -3461(2) | 2183(3) | 7(1) |
| C(3) | -3897(2) | -4495(2) | 2507(3) | 6(1) |
| C(4) | -3194(2) | -5603(2) | 2676(3) | 6(1) |
| C(5) | -1797(2) | -5659(2) | 2503(3) | 6(1) |
| C(6) | -1147(2) | -4594(2) | 2186(3) | 7(1) |
| C(7) | -5404(2) | -4435(2) | 2650(3) | 6(1) |
| C(8) | -939(2) | -6808(2) | 2688(3) | 6(1) |
| H(1) | -3654(12) | -2548(10) | 2073(18) | 16(2) |
| H(2) | -3747(5) | -6406(4) | 2938(8) | 22(1) |
| H(3) | -56(14) | -4556(10) | 2080(20) | 22(2) |
| D(4) | -6888(3) | -3220(2) | 2684(4) | 15(1) |
| D(5) | 1203(3) | -7686(2) | 3075(4) | 18(1) |
| N(1) | -1844(1) | -3541(1) | 2021(2) | 7(1) |
| O(1) | -5835(2) | -3314(2) | 2726(4) | 9(1) |
| O(2) | -6124(2) | -5329(2) | 2658(4) | 8(1) |
| O(3) | -1546(2) | -7814(2) | 2513(4) | 8(1) |
| O(4) | 406(2) | -6646(2) | 3029(4) | 10(1) |

Table 4.15D.bond. Bond lengths (Å).

| | | | |
|---|---|---|---|
| C(2)-H(1) | 1.109(11) | C(6)-H(3) | 1.086(13) |
| C(2)-N(1) | 1.342(2) | C(6)-N(1) | 1.341(2) |
| C(2)-C(3) | 1.395(3) | C(7)-O(2) | 1.219(3) |
| C(3)-C(4) | 1.398(2) | C(7)-O(1) | 1.323(3) |
| C(3)-C(7) | 1.498(3) | C(8)-O(3) | 1.255(3) |
| C(4)-C(5) | 1.398(3) | C(8)-O(4) | 1.266(3) |
| C(4)-H(2) | 1.085(4) | D(4)-O(1) | 1.021(3) |
| C(5)-C(6) | 1.390(2) | D(5)-N(1)#1 | 1.151(3) |
| C(5)-C(8) | 1.512(2) | | |

Symmetry transformations used to generate equivalent atoms:

#1 -x,y-1/2,-z+1/2 #2 -x,y+1/2,-z+1/2

Table 4.15D.angle. Bond angles (°).

| | | | |
|---|---|---|---|
| H(1)-C(2)-N(1) | 116.5(6) | H(3)-C(6)-C(5) | 122.8(6) |
| H(1)-C(2)-C(3) | 123.5(6) | N(1)-C(6)-C(5) | 121.11(16) |
| N(1)-C(2)-C(3) | 119.95(17) | O(2)-C(7)-O(1) | 125.6(2) |
| C(2)-C(3)-C(4) | 119.07(17) | O(2)-C(7)-C(3) | 122.53(18) |
| C(2)-C(3)-C(7) | 121.05(16) | O(1)-C(7)-C(3) | 111.81(16) |
| C(4)-C(3)-C(7) | 119.87(16) | O(3)-C(8)-O(4) | 125.0(2) |
| C(3)-C(4)-C(5) | 119.75(16) | O(3)-C(8)-C(5) | 121.12(18) |
| C(3)-C(4)-H(2) | 119.0(3) | O(4)-C(8)-C(5) | 113.93(17) |
| C(5)-C(4)-H(2) | 121.2(3) | D(5)#2-N(1)-C(6) | 117.43(17) |
| C(6)-C(5)-C(4) | 118.17(16) | D(5)#2-N(1)-C(2) | 120.30(18) |
| C(6)-C(5)-C(8) | 117.96(17) | C(6)-N(1)-C(2) | 121.94(14) |
| C(4)-C(5)-C(8) | 123.85(16) | D(4)-O(1)-C(7) | 115.0(2) |
| H(3)-C(6)-N(1) | 116.1(6) | | |

Symmetry transformations used to generate equivalent atoms:

#1 -x,y-1/2,-z+1/2 #2 -x,y+1/2,-z+1/2

Table 4.15D.anis. Anisotropic displacement parameters ($Å^2 x\ 10^3$). The anisotropic displacement factor exponent takes the form: $-2p^2[\ h^2\ a^{*2}U^{11} + ... + 2\ h\ k\ a^*\ b^*\ U^{12}\ ]$

| | U11 | U22 | U33 | U23 | U13 | U12 |
|---|---|---|---|---|---|---|
| C(2) | 4(1) | 4(1) | 12(1) | 1(1) | 3(1) | 0(1) |
| C(3) | 6(1) | 2(1) | 11(1) | -1(1) | 4(1) | 1(1) |
| C(4) | 5(1) | 3(1) | 10(1) | 0(1) | 3(1) | 1(1) |
| C(5) | 4(1) | 4(1) | 9(1) | 0(1) | 2(1) | 2(1) |
| C(6) | 6(1) | 4(1) | 12(1) | 0(1) | 5(1) | 0(1) |
| C(7) | 5(1) | 3(1) | 10(1) | 0(1) | 4(1) | 0(1) |
| C(8) | 4(1) | 2(1) | 11(1) | -1(1) | 3(1) | 1(1) |
| H(1) | 20(5) | 9(4) | 21(5) | 5(4) | 10(4) | 5(4) |
| H(2) | 22(2) | 10(2) | 39(2) | -1(2) | 17(2) | -2(2) |
| H(3) | 23(6) | 10(5) | 35(7) | 4(4) | 13(5) | 3(4) |
| D(4) | 11(1) | 12(1) | 22(1) | 1(1) | 8(1) | 2(1) |
| D(5) | 16(1) | 16(1) | 23(1) | -4(1) | 9(1) | -5(1) |
| N(1) | 5(1) | 3(1) | 13(1) | 0(1) | 4(1) | -1(1) |
| O(1) | 9(1) | 4(1) | 16(1) | 1(1) | 7(1) | 2(1) |
| O(2) | 8(1) | 4(1) | 12(1) | 0(1) | 4(1) | -2(1) |
| O(3) | 7(1) | 3(1) | 15(1) | 1(1) | 5(1) | -1(1) |
| O(4) | 6(1) | 4(1) | 18(1) | -2(1) | 4(1) | 1(1) |

**Conferences and Courses**

| | |
|---|---|
| 7th – 14th April 1999. | B.C.A. School, Univerity of Durham. U.K.<br>"Seventh Intensive Course in X-ray Structural Analysis" |
| 4th-13th August 1999. | IUCr Congress, Glasgow, Scotland.<br>Presented Poster – "The Interaction of N-Heterocyclic Carbenes with Organic Acids." |
| 9th-10th September, 1999. | New Perspectives in Neutron and Muon Science Meeting, Satellite to the U.K. Neutron Users Meeting, Durham, U.K.<br>Oral Presentation – "Thermal Neutron Laue Diffraction at the I.L.L" |
| 1st-4th September 1999. | European Conference on Neutron Scattering, Budapest, Hungary.<br>Presented Poster – "Complementary Neutron and X-ray Single Crystal Diffraction Studies of Potential Novel Ferroelectrics. |
| 27th February – 6th April 2000. | Hercules Course, Grenoble, France.<br>Higher European Research Course for Users of Large Experimental Systems, 10th Session. |
| 6th – 9th April 2000. | 10 Anniversary of Hercules Meeting, Grenoble, France.<br>Presented Poster – "Thermal Neutron Laue Diffraction at the I.L.L." |
| 25th-31st August 2000. | European Crystallography Meeting 19. Nancy, France.<br>Oral Presentation and Poster - "Thermal Neutron Laue Diffraction at the I.L.L." |
| 7th-10th April 2001. | B.C.A. Spring Meeting, University of Reading, U.K.<br>Presented Poster – "Thermal Neutron Laue Diffraction at the I.L.L." |
| 3rd-7th September 2001. | Horizons in Hydrogen Bond Research, XIV Conference and Workshop. Turin, Italy. |

Oral Presentation – "Proton Migration in Short Strong N-H-O Hydrogen Bonds: Neutron Diffraction and Computational Results.

**Departmental Seminars, 1998-1999.**

| | |
|---|---|
| 21st October 1998. | Dynamic electrochemistry: small is beautiful.<br>Prof. P. Unwin. |
| 26th October 1998. | Reactions of the highly electrophilic boranes $HB(C_6H_5)_3$ and $B(C_6H_5)_3$ with zirconium and tantalum based metallocenes.<br>Dr. W. Peirs. |
| 4th November 1998. | Computational adventures in d and f element chemistry.<br>Dr. N. Kaltscoyannis. |
| 20th January 1999. | Luminescence of large molecules: from conducting polymers to coral reefs.<br>Dr. A. Jones. |
| 27th January 1999. | NMR Characterisation of Multi-phase Fluid Transport in porous solids.<br>Prof K.J. Packer. |
| 10th March 1999. | Designing model magnetic materials.<br>Dr A. Harrison. |
| 12th October 1999. | Chocolate for the next millenium.<br>Dr. S. Beckett. |
| 20th October 1999. | Aspects of Complexation and Supramolecular Chemistry,<br>Prof. S. Lincoln. |